

## ABSTRACT

SHARPE, DESMOND TOVAH. Using a Hydrologic and Storm Water Model to Predict the Movement of Water Soluble Tracers via Surface Water Runoff at the Cherry Point Marine Corps Air Station. (Under the direction of Devendra Amatya and R. Wayne Skaggs.)

The purpose of the research has been to develop a storm water model to assist the officials at Cherry Point Marine Corps Air Station in responding to accidental spillage of substances into adjacent surface waters. Since the adjacent surface waters either drain directly or indirectly, into the Neuse River, preserving water quality is a major concern. Using the Cherry Point Marine Corps Air Station, North Carolina, topographic information, historical and observed rainfall datasets, streamflow measurements, subsurface conduits attributes and GPS acquired data were inserted into XPSWMM to model the downstream movement of user-defined tracer elements. The overall objective of the research was to develop a hydrologic/hydraulic model to predict pollutant movement from a spill site to subcatchment outlets on the Marine Corps Air Station. Other related research objectives were to: 1) to use spatial information gathered from the GIS to construction drainage areas in efforts to estimate catchment characteristics, 2) to evaluate the results of peak outflow rates gathered from several event-based hydrologic models and to explain the evolution from lumped parameter models to process-based, rainfall-runoff simulations and 3) to generate continuous simulations for rainfall-runoff processes using a calibrated/validated version of XPSWMM and 4) to introduce the concept of using pulse tracers to estimate travel times via surface water to understand associated reaction times.

Using a Hydrologic and Storm Water Model to Predict the Movement of Water Soluble Tracers  
via Surface Water Runoff at the Cherry Point  
Marine Corps Air Station

by  
Desmond Sharpe

A dissertation submitted to the Graduate Faculty of  
North Carolina State University  
in partial fulfillment of  
requirements for the Degree of  
Doctor of Philosophy

Biological and Agricultural Engineering

Raleigh, North Carolina

2009

APPROVED BY:

---

Dr. Devendra Amatya  
Co-chair of Advisory Committee

---

Dr. R. Wayne Skaggs  
Co-chair of Advisory Committee

---

Dr. George Chescheir

---

Dr. James Gregory

## **BIOGRAPHY**

Desmond Tovah Sharpe was born to Margaret and Willie Sharpe, in Wilmington, Delaware, in 1977. After completing his primary and secondary education at local schools, Desmond attended North Carolina Agricultural and Technical State University, in 1995, to major in Agricultural and Environmental Systems Engineering. Upon completion of his Bachelor's degree, Desmond decided to pursue further education and enrolled into the doctorate program at North Carolina State University under the direction of Dr. R. W. Skaggs. Although, not an initial fan of hydrologic modeling, he was introduced to the stormwater modeling project being completed at Cherry Point Marine Corps Air Station and eventually became the lead researcher.

Desmond is married to Shayla Sharpe and currently owns and operates Sharpe Pursuits, Incorporated, a full service events company, with his wife. They enjoy traveling, music and producing stellar events for a wide variety of clients. Although, he is not currently using his education as an engineer, education remains very important. In the near future, Desmond plans to develop self-sustained, and energy efficient, residential communities through the United States.

## TABLE OF CONTENTS

LIST OF TABLES.....	vii
LIST OF FIGURES .....	x
AN INTRODUCTION TO THE HYDROLOGIC AND STORM WATER MODELING	
STUDY AT THE CHERRY POINT MARINE CORPS AIR STATION .....	1
Introduction .....	1
General Background .....	1
Overall Research Objective .....	2
Literature Review .....	3
GIS and Hydrologic Modeling Progression .....	4
Sand Hill River Watershed District Study .....	4
City of Novi, Michigan Study .....	5
Stormwater Management Literature Review .....	6
Thesis Structure .....	7
WATERSHED CHARACTERIZATION AND FIELD HYDROLOGIC MEASUREMENTS	
AT CHERRY POINT MARINE CORPS AIR STATION	
Introduction .....	8
Background .....	8
Objectives .....	9
Methods .....	10
Site Description .....	10
MCAS-CP Major Watersheds .....	10
Schoolhouse Branch .....	13
Sandy Branch .....	14
Luke Rowes Gut .....	15
Mill Creek .....	15
Spatial Data Introduction and GIS Development .....	15
URS Consultants Incorporated Contribution .....	16
CPEC Incorporated Contributions .....	18
North Carolina State University Contributions .....	19
Source Data Challenges .....	20
Fundamentals of Stormwater Mapping and Modeling .....	21
Cherry Point MCAS GIS Introduction .....	22
Transition into ArcMAP .....	22
Watershed Delineation .....	23
Field Installation, Hydrologic Monitoring and Data Collection .....	24
Monitoring Periods and Field Note Documentation .....	24
Rainfall .....	24
Design Rainfall .....	25
Rainfall Event Data Logger .....	25
Manual Rain Gauges .....	27
Outflow Measurements .....	28
Data Acquisition - Weir 6 Program.....	30
Data Acquisition - STARFLOW Program .....	32
Data Refinement - Combined Flow Spreadsheets .....	32
Data Refinement: Flow meter Spreadsheets .....	35
Composite Flow Spreadsheets .....	36
Event Based Regression Analysis to Determine Stage-Discharge Relationships .....	37
Weather .....	38
NWS Weather Station .....	38

## TABLE OF CONTENTS - CONTINUED

NOAA Downloaded Weather .....	39
Results.....	39
Site Characteristics for Catchments K2 and K3 .....	39
Rainfall .....	42
Recorded Rainfall Amounts .....	42
Observed Storm Frequency and Rainfall Intensities .....	45
Rainfall Spatial Variations .....	46
Rainfall Distribution .....	46
Catchment Outflows .....	48
Stage-Discharge Relationships .....	48
Generalized Flow Characteristics of Observed Hydrographs .....	50
Flow Distribution .....	53
Flow Frequency-Duration .....	55
Impact of Site Characteristics on Hydrology .....	56
Discussion .....	56
Summary and Conclusions .....	58
<b>CALIBRATION AND VALIDATION OF SWMM AND XPSWMM ON TWO CATCHMENTS WITHIN THE MARINE CORPS AIR STATION AT CHERRY POINT .....</b>	<b>62</b>
Introduction .....	62
The Utilization of Spatial Data in Hydrologic Modeling .....	62
Estimating Flow Routes from Ground Topography.....	63
Objectives .....	64
Overall Objective .....	64
Chapter Objectives .....	64
Methods.....	65
Model Description .....	65
Surface Water Models Introduction .....	65
Soil Conservation Service Application of the Rational Formula for Runoff .....	66
Time of Concentration, $T_c$ .....	67
USGS Method .....	68
HEC HMS .....	69
Modeling Overview .....	73
EPA SWMM – Introduction .....	73
SWMM Adaptation and Performance .....	74
Transition into XPSWMM 9.0 .....	74
Project Application .....	77
Generic Modeling Limitations .....	79
USEPA SWMM RAIN Module .....	81
USEPA RUNOFF Module .....	81
RUNOFF Block Subroutines .....	82
RUNOFF Block Controls .....	83
Catchment Parameterization .....	83
Catchment Conceptualization .....	85
Subcatchment Surface Area .....	87
Subcatchment Slope .....	87
Infiltration .....	87
Percent Imperviousness.....	89
Storage .....	90
Evaporation .....	90

## TABLE OF CONTENTS – CONTINUED

Overland Flow .....	91
Runoff Routing .....	96
Introduction of Kinematic Wave routing .....	97
Manning's Roughness, n .....	98
Application of GIS to Parameterize XPSWMM for Two Catchments .....	99
Catchment Discretization .....	99
Importance of Catchment Discretization .....	99
Discretized Subcatchments .....	102
Area Calculation .....	106
Selected Input Parameters .....	106
Infiltration Values .....	106
Model Infiltration Inputs .....	106
Soils .....	107
Impervious Value.....	108
Surface Imperviousness .....	108
Assumptions for Overland Flow.....	109
Subcatchment Width .....	109
Slope .....	111
Assumptions for Routing.....	113
Routing .....	113
Reach Lengths .....	113
Stream Characteristics .....	114
Pipe Sizing .....	115
Rainfall Data used.....	117
User Defined Rainfall .....	117
Rainfall Variations .....	118
SWMM Evaluation .....	118
Generic Model Testing Concerns .....	118
Calibration Period and Procedures .....	120
Catchment Width and Manning's Roughness Importance .....	121
Validation Period .....	122
SWMM Event-based Storm Validation .....	122
Statistical Procedures for Evaluating Model Performance.....	122
Hydrograph Comparisons .....	122
Pearson's Product-Moment Correlation, r, & the Coefficient of Determination, R <sup>2</sup> .....	123
Coefficient of Efficiency, E .....	124
Index of Agreement, d .....	126
Sensitivity Analyses .....	126
Generic Model Sensitivities .....	126
Absolute and Relative Sensitivity .....	127
Rainfall Sensitivity Analysis .....	128
Continuous Simulations versus Event-based Simulations .....	130
Continuous Simulations .....	130
Results and Discussion.....	131
Calibration Results .....	131
Catchment K2 Single Event Calibration .....	131
Catchment K3 Single Event Calibration .....	135
Results of Statistical Analysis of SWMM Calibration Hydrographs.....	135
Z-test Results .....	135

## TABLE OF CONTENTS – CONTINUED

Single Event T-test Results .....	137
Coefficient of Efficiency, Pearson Correlation and Coefficient of Determination Results .....	139
XPSWMM 9.0 Calibration - Single Event.....	142
Continuous XPSWMM Calibration Results (2005) .....	147
XPSWMM Event-based Validation Results .....	151
XPSWMM Validation Comments.....	152
XPSWMM 9.0 Validation .....	153
Sensitivity Analyses Results .....	156
2006 XPSWMM9.0 Simulations .....	157
Updated Continuous Simulations for 2006 Simulations .....	157
XPSWMM9.0 Under-predictions .....	159
XPSWMM9.0 Over-predictions .....	162
XPSWMM9.0 K2 Overflow Routing .....	162
Summary and Conclusions .....	164
XPSWMM Continuous Simulations .....	164
<b>DETERMINING POLLUTANT TRAVEL TIMES IN TWO CATCHMENTS USING A GEOGRAPHIC INFORMATION SYSTEM .....</b>	<b>167</b>
Introduction.....	167
Background .....	167
Objectives .....	167
Overall Objective .....	167
Chapter Objectives .....	167
Literature Review .....	168
Literature review of Similar Studies .....	168
Pollutant Transport using Pulse Tracers .....	170
Methods .....	175
Travel Time Significance .....	175
Travel Time Calculations using Velocities .....	176
SWMM 3.2 Manual Travel Time Calculation Method .....	176
Simulation Setup for Design Storms .....	179
Design Storm Continuous Simulations .....	179
Comparison of Collected Rainfall to Design Storm Rainfall .....	182
Design Storm Outflows .....	183
XPSWMM Travel Times Using Pulse Tracer Results .....	186
Pulse Tracer Technique Comments .....	191
2007 XPSWMM, 5-minute Rainfall Tracer Investigation .....	191
Catchment K2, 5-minute Rainfall Travel Time Analysis .....	197
Catchment K3, 5-Minute Travel Time Analysis .....	200
Travel Time Comparison using 60-minute and 5-minute Simulation Time steps .....	204
Catchment K2 5- and 60-Minute Travel Time Comparison .....	204
Catchment K3 5- and 60-Minute Travel Time Comparison .....	205
Catchment K2 XPSWMM Travel Time Simulations using 5-minute Rainfall and Overflow Routing .....	207
Inserting XPSWMM results into ArcMAP .....	215
Summary, Conclusions and Recommendations .....	216
Overall Travel Time Comments and Limitations .....	216
XPSWMM Time Travel Discussion and Concerns .....	218
Summary and Conclusions .....	219

## TABLE OF CONTENTS – CONTINUED

Suggestions .....	220
Our Contribution and Recommendations for Future Work .....	221
REFERENCES CITED.....	223
APPENDICES.....	228
Appendix 2: Additional Chapter Two Exhibits .....	230
Appendix 2A: Chapter Two Additional Figures .....	238
Appendix 2B: Chapter Two Additional Tables .....	243
Appendix 2C: MCAS-CP Monitoring Stating Photographs .....	248
Appendix 2D: Stage Elevation Measurement Files .....	252
Appendix 2E: Flow Meter Files .....	260
Appendix 2F: Combined Flow Calculations .....	265
Appendix 2G: NOAA Weather Files .....	267
Appendix 2H: Catchments K2 and K3 Surface Data .....	288
Appendix 2I: Research Notes .....	294
Appendix 2J: Outflow Regression Graphs for Catchment K2 .....	304
Appendix 2K: Cherry Point Observed Precipitation Data .....	312
Appendix 2L: CPEC Inc. Metadata .....	327
Appendix 3A: Additional Chapter Three Figures .....	339
Appendix 3B: Additional Chapter Three Tables .....	349
Appendix 3C: HEC-HMS Materials .....	365
Appendix 3D: RAIN Module .....	372
Appendix 3E: RUNOFF Module .....	376
Appendix 3F: Catchment K2 and K3 GIS Values .....	399
Appendix 3G: XPSWMM Single Event Results .....	405
Appendix 3H: Calibration and Validation Hydrographs .....	415
Appendix 3I: XPSWMM9.0 Simulations Results .....	442
Appendix 3J: Catchment K2 Event-based Sensitivity Analyses .....	488
Appendix 4A: XPSWMM Sanitary Block Graphics .....	499
Appendix 4B: Return Period Graphics in the Runoff Block .....	504
Appendix 4C: ArcMAP Travel Time Results .....	506
Appendix 4D: Travel Time Comparison Between 60-minute and 5-minute XPSWMM simulations using Return Period Rainfall .....	525
Appendix 4E: Catchment K2 Travel Time Maps for Various Return Period Rainfall using 5-minute Precipitation and Overland Flow Elements .....	537

## LIST OF TABLES

Table 2.1	Cherry Point Precipitation Amounts in Inches from years 2000 to 2002 from Three Separate Sources .....	27
Table 2.2	Differences in Culvert Elevations for Two Catchment Outlets at Cherry Point MCAS .....	34
Table 2.3	Cherry Point MCAS Observed Flow Data for One Catchment Outlet Highlighting Overtopped Weir Conditions .....	37
Table 2.4	Land Use Percentages for Catchments K2 & K3 at Cherry Point .....	41
Table 2.5	Observed Monthly Rainfall and the Historical Precipitation Averages for the Greater Havelock Region .....	44
Table 2.6	24-hour Design Storm Intensities for Morehead City, NC .....	45
Table 2.7	Cherry Point Rainfall to Outflow Relationships for Selected Storms in Catchments K2 and K3 .....	52
Table 3.1	Catchment K3 Rational Method, USGS and HEC-HMS Results, Event 330 (Nov. 2000) .....	73
Table 3.2	Typical IMD Values for Various Soil Textures .....	88
Table 3.3	Soils Attribute Table for Catchment K2 using ArcVIEW 3.2 .....	108
Table 3.4	Selected Calibration and Validation Storms for Catchments K2 and K3 at Cherry Point .....	120
Table 3.5	Catchment K2 Single Event Peak Outflows for T-Test Analysis .....	137
Table 3.6	Catchment K2 Selected Single Event Hydrographs for T-Test Analysis .....	138
Table 3.7	Correlation Statistics for Selected Hydrographs Using XPSWMM9.0 Continuous Simulations .....	155
Table 3.8	Continuous Rainfall Validation Storm Statistics Results for Catchments K2 and K3 .....	158
Table 3.9	Catchment K2 Simulation Rainfall Intensities and Return Frequencies .....	160
Table 3.10	Catchment K3 Continuous Rainfall Intensities and Return Frequencies .....	161
Table 4.1	NRCS Type II and Type III Rainfall Distribution Chart.....	181
Table 4.2	Reported and Measured Cumulative Rainfall .....	183

## LIST OF TABLES - CONTINUED

Table 4.3	NOAA Rainfall Station Description and Statistics of Storm Events, Morehead City, N.C. (1948-2002) .....	183
Table 4.4	XPSWMM Predicted Peak Outflow Rates for Catchment K2 for 24-hour Design Storms of various Return Periods .....	184
Table 4.5	XPSWMM Predicted Peak Outflow Rates for Catchment K3 for 24-hour Design Storms of various Return Periods .....	185
Table 4.6	Catchment K2 Travel Times (minutes) using Pulse Tracers with Design Rainfall for various Return Periods .....	189
Table 4.7	Catchment K3 Travel Times (minutes) using Pulse Tracers with Design Rainfall for various Return Periods .....	190
Table 4.8	Catchment K2 Maximum, Predicted Outflow and Travel Time Estimates using 5-Minute Return Period Rainfall Data .....	192
Table 4.9	Catchment K3 Maximum, Simulated Outflow and Travel Time using 5-Minute Return Period Rainfall Data.....	193
Table 4.10	Catchment K2 Maximum, Predicted Outflow and Travel Time Estimates using 5-Minute Return Period Rainfall and Surface Overflow Routing Element .....	209
Table 4.11	Catchment K2 Percent Change in Predicted Peak Outflow Rate after Incorporating Two Overflow Elements .....	210
Table 4.12	Catchment K2 Percent Change in Estimated Travel Time after Incorporating Two Overflow Elements .....	213

## LIST OF FIGURES

Figure 2.1	Cherry Point MCAS Location Map including Portions of Eastern North Carolina .....	11
Figure 2.2	Overall Watershed Delineated for the Industrialized Section of Cherry Point .....	12
Figure 2.3	Overall Watershed for the Industrialized Section of Cherry Point Highlighting the Sandy Branch .....	14
Figure 2.4	The URS designated Drainage Area E for Cherry Point .....	17
Figure 2.5	Cherry Point Industrialized Zone Stormwater Features .....	23
Figure 2.6	Cherry Point Rain Gauge Location Map .....	26
Figure 2.7	Typical monitoring station profile for the Cherry Point Study .....	29
Figure 2.8	Sharp-Crested Weir Diagram .....	29
Figure 2.9	Location Map for Catchments K2 and K3 .....	40
Figure 2.10	Catchment K2 Normal Flow Distribution .....	54
Figure 2.11	Catchment K3 Normal Flow Distribution at Cherry Point MCAS .....	55
Figure 3.1	Cherry Point Hydrologic Study Outlet Location Map .....	65
Figure 3.2	HEC-HMS Catchment K3 Basin Model Screenshot .....	70
Figure 3.3	Catchment K2 XPSWMM Routing Schematic .....	76
Figure 3.4	Catchment K3 XPSWMM Routing Schematic .....	76
Figure 3.5	XPSWMM Results Screenshot for a Single Node .....	79
Figure 3.6	Low Level Area Conceptualization .....	85
Figure 3.7	Medium Level Area Conceptualization .....	86
Figure 3.8	High Level Area Conceptualization .....	86
Figure 3.9	Subcatchment Schematization for Overland Flow Calculation .....	92
Figure 3.10	Subcatchment Non-linear Reservoir Model .....	92
Figure 3.11	GIS Delineated Polygon representing Catchment K2 using Ground Topography .....	100
Figure 3.12	A GIS Representation of Catchment K2 Focusing on the Outlet .....	101

## LIST OF FIGURES – CONTINUED

Figure 3.13	ArcMAP Screenshot of Catchment K2 including Selected Stormwater Drainage Features .....	102
Figure 3.14	Catchment K3 Boundary with Visible Pipe and Buildings Layers.....	103
Figure 3.15	Catchment K2 Delineated Subcatchments .....	104
Figure 3.16	Catchment K3 Delineated Subcatchments .....	104
Figure 3.17	Catchment K2 Soil Coverage Map with Subcatchment Boundaries .....	107
Figure 3.18	Catchments K2 and K3 Boundaries Plus Impervious Areas .....	109
Figure 3.19	Importance of Technique when Measuring Catchment Width .....	110
Figure 3.20	Subcatchment Width and Watercourse Slope Calculation .....	112
Figure 3.21	GIS Example of a Pipe Emitting Overland Outflow to a Collector Stream in Subcatchment 12 of Catchment K2 .....	114
Figure 3.22	ArcMAP Screenshot of Several K2 Subcatchments displaying Pipes, Stormwater Features, and Surface Channels .....	116
Figure 3.23	Catchment K3 Structures Shapefile Query to Obtain Headwall/Pipe Attributes .....	117
Figure 3.24	SWMM Rainfall Sensitivity for Four Storm Events at Cherry Point .....	129
Figure 3.25	Example of Erroneous Data in the SWMM Prediction Hydrograph for Catchment K2 at Cherry Point .....	132
Figure 3.26	Event 143 Calibration Hydrograph for Catchment K2 (2001) following a Baseflow Reduction at Cherry Point MCAS .....	133
Figure 3.27	Using the Multiple Basin (Subcatchment) Option in XPSWMM for Calibration .....	143
Figure 3.28	XPSWMM output Hydrographs from Various Imperviousness, Basin Width, and Routing Methods at Cherry Point .....	145
Figure 3.29	XPSWMM Time Control Screenshot .....	147
Figure 3.30	An Excerpt of the K2 2001 Hydrograph Using XPSWMM Simulated Data and Continuous Rainfall data .....	149
Figure 3.31	Catchment K3 Event 115 Hydrograph from Continuous Rainfall .....	151
Figure 3.32	Sensitivity Analysis Plot for Catchment K2, Using Storm Event 165 in 2002 .....	157

## LIST OF FIGURES – CONTINUED

Figure 3.33	Location of Overflow Routing Elements at CPMCAS in Catchment K2 .....	163
Figure 4.1	Slug Injection Diagram as Presented by Jobson (1996) .....	172
Figure 4.2	A Typical Tracer Response Curve as Determined by Jobson .....	173
Figure 4.3	Cherry Point Catchment K2 Focus Area for Example 4.1.....	177
Figure 4.4	SCS Type II, 24-hr Design Storm Rainfall Curves for Morehead City .....	180
Figure 4.5	Typical NRCS Type II Rainfall Distribution Curve .....	182
Figure 4.6	XPSWMM Sanitary Block Flow/Concentration Input screen .....	188
Figure 4.7	Travel Time Response Map for Catchment K2 at Cherry Point using 100-yr Return Period Rainfall Amounts .....	197
Figure 4.8	Travel Time Response Map for Catchment K3 at Cherry Point using 100-yr Return Period Precipitation.....	200
Figure 4.9	Example of XPSWMM Runoff Results displaying Surcharged Conditions .....	203
Figure 4.10	SWMM Screenshot showing the Utilization of Overflow Element 111 in Catchment K2 .....	208
Figure 4.11	Catchment K2 100-yr Return Period Travel Time Map including Overland Flow Elements.....	216

# **Chapter One: An Introduction to the Hydrologic and Storm Water Modeling Study at the Cherry Point Marine Corps Air Station**

## **I Introduction**

Groundwater and surface water contamination are two national issues that deserve localized attention to reduce their overall environmental impact. In most cases, non-point sources generate harmful materials that degrade water quality. Contrarily, specific point sources may be identified, including commercial and urban generated wastes. As a global community, it is the responsibility of all American citizens to develop an environmental awareness towards pollution such that together we will be able to manage our ecological resources and guarantee their usage for future generations. Adhering to this doctrine, as a research group, we intend to implement a water quality model to assist in predicting hydrologic/hydraulic trends of stormwater movement for planning purposes. The study site is the industrialized section of Marine Corps Air Station, Cherry Point, North Carolina (MCAS-CP). We plan to calibrate and validate the U.S. EPA's Storm Water Management Model (SWMM) to display the predicted results in an effort to influence decisions pertaining to sustaining and/or improving the water quality at the air station. Macroscopically, our efforts should improve the station's existing water quality and directly influence the Neuse River estuarine system, a major river system in North Carolina.

### **A. General Background**

Receiving water bodies are generally degraded by excessive amounts of pollutants that originate from point and non-point source discharges. Non-point source (NPS) pollution is commonly described as pollution transported by storm water or snowmelt runoff from land surfaces and is generated from diffuse sources, while point source pollution usually discharges from a specific pipe (NC DEHNR, 1996). Typical examples of NPS pollution include: cropland runoff, animal feedlots, urban areas, construction sites, mining operations, logging roads, landfills and streamside vegetation removal (NC DEHNR, et al 1996). Most point sources are industrially, commercially, or municipally generated.

Urban surface runoff is a major contributor to water quality degradation, especially when associated with surface waters, such as lakes, stream or rivers (Haubner and Joeres, 1996). Urban land can be categorized as residential, commercial, industrial or recreational depending upon use, and also includes other impervious lands, i.e. roads, parking lots, and airfields. The surface runoff and subsurface drainage from these impervious areas have the potential to transport high amounts of pollutants (sediments, toxins, metals, or nutrients) depending upon topography and origination (Haubner and Joeres, 1996).

The Marine Corps Air Station (MCAS) at Cherry Point is a military installation that consists of urban areas ranging from residential parcels to paved runways. It has been determined that certain activities associated with the nature and mission of the facility tend to generate hazardous waste materials (Muhs et al., 2000). The two primary methods of pollutant transport are leachate seepage from underground water disposal and surface runoff. Both transport methods are managed under the Comprehensive Environmental Response, Compensation and Liability Act (CERCLA) and the Resource Conservation and Recovery Act (RCRA) (Goudie, 2000).

Because of the potential for contamination of subsurface waters, the air station also wished to conduct an analysis of the current surface water conditions. Accidental spillage of hazardous chemicals was not a rarity at the military installation, therefore, the officials wanted to prepare themselves for further occurrences. During the 1990's, North Carolina water quality gained attention as land developmental activities began to target the marketability of the Neuse River Basin. The related purpose of this research is to assist the air station in understanding the types of runoff situations occurring in the industrialized portion of the base, then conduct model simulations to predict the time required for runoff to travel from the point of spillage to the outlet of the basin during, various size and intensity, rain events.

## **B. Overall Research Objective**

The overall objective of the research is to develop a hydrologic/hydraulic model to predict pollutant movement from a spill site to subcatchment outlets on the Marine Corps Air Station at Cherry Point.

### **C. Literature Review**

Models that incorporated Geographic Information Systems (GIS) were becoming more accessible in the late 1990's. Likewise, the sophistication of water quality models was developing as the computer hardware needed to process larger amount of data became readily available. The art of modeling hydrology and water quality had become increasingly computational during the past decade (Tim, 1995). It had become commonplace for models once requiring large mainframe computers to be installed and executed on smaller desktop devices.

Closely related, the availability of spatial information began to explode during the late 1990's and early part of the 21<sup>st</sup> century. This proliferation generated new concerns pertaining to the source, accuracy, storage requirements and applicability of spatial data (Garbrecht et al., 2001). Combining GIS technology with hydrologic models allowed modelers to acquire, organize, analyze and display input/output data in various ways that were not previously possible. Therefore, the output data could not only be organized, but the GIS tools were able to transform the input data into formats required to model more complex simulations. Digitized stream data, drainage systems derived from digital elevation maps (DEMs), soils data, digital orthophotographic data, and remote sensing information are all examples of details that can be managed using.

In 1971, the U.S. Environmental Protection Agency (EPA) developed the Storm Water Management Model (SWMM) as a dynamic rainfall-runoff simulator for single event or long-term simulations (USEPA, 2005). Runoff generation, transportation, storage and other hydraulic activities were completed in specialized units called blocks. The main SWMM applications for this research were the generation and tracking capabilities of surface runoff via surface and subsurface conduits and the routing of water quality constituents through the drainage system. The research objective was to utilize the program to simulate runoff from typical rainfall, insert a pollutant at a given location and time, and then estimate travel times by evaluating a substance's downstream progression to any point in the drainage system.

### *GIS and Hydrologic Modeling Progression*

In 1996, D.R. Maidment presented a paper describing the progression in the application of using GIS technology to attribute hydrologic models in efforts to expedite the data acquisition process. He speculated that with the advancement of low cost and free datasets via the internet for digital elevation data, soils, land use and climatic data, the development of pre- and post-processors for surface water management models will be greatly stimulated in the next few years. The eventual automation procedure will attach existing models to GIS databases such that the model will be able to take full advantage of the GIS's data processing and management power. This task implies a reversal of the traditional priorities in hydrologic modeling where the emphasis has always been on the way that physical processes are represented, and the manner in which the parameters are to be obtained for a particular environment plays a relatively minor role (Maidment, 1996). In hydrology modeling, the digital description of the territory gains top priority and then an emphasis is placed on formulating the process model which can fit the available data.

*At present, the availability of land surface data, especially digital elevation data, has formed practicality in watershed delineation, but that greater resolution and availability would be necessary for this information to become applicable to smaller areas as opposed to restricting the relevance to fairly large watersheds only. To advance the linkage capabilities the GIS packages would need to become standardized to the point where dispersion was steadily available and the knowledge needed to operate a powerful PC-based GIS package was commonplace. It has been amazing to see the progression from GIS and hydrology models functioning independently; to the point where simulation models are using spatial information accessed from GIS databases to evaluate inputs. As technology progresses, their integration will become nearly seamless and transparent to the end user. (Maidment, 1996)*

### *Sand Hill River Watershed District Study (North Central Minnesota)*

In 1996, the Agricultural Nonpoint Source Model (AGNPS), a Geographic Information System and a relational database management system (RDBMS) were linked to investigate a nonpoint source pollution problem near Winger, Minnesota. The three units were used to create event-based simulations to generate runoff and transport sediments and pollutants from an agricultural watershed. The basic data layers were developed from USGS contour maps and SCS Soil maps. The spatial land cover/land use data was compiled from LANDSAT thematic

maps and the prepared data was inserted into an ORACLE database as separate characteristic data groups. Information from the ORACLE database and the digital base layers were georeferenced to create a spatial database of the study area where sets of programmed structured query language (SQL) were implemented to extract necessary information in a useable data format whenever a specific area was selected in GIS for AGNPS simulations (Yoon, 1996). Following simulations, the output files contained information pertaining to runoff volume, peak flowrate, erosion capabilities, sediment delivery and total sediment yields.

The Minnesota study concluded that the linkage of event-based models to GIS and relational database management systems can facilitate better data storage, manipulation and analysis than conventional methods. In addition, the automatic linkage between the resources bypasses the need to manually implement AGNPS, therefore resulting in a powerful, up-to-date tool that is capable of monitoring and instantaneously visualizing the transport of any pollutant that AGNPS can simulate (Yoon, 1996). Therefore, a bi-directional linkage exists, as opposed to the conventional one-way process used during typical input preparation, which reduces the time required to analyze model output.

#### *City of Novi, Michigan Study*

In December 2001, the City of Novi, Michigan, published a similar type of study where the objective was to demonstrate how a Geographic Information System (GIS) and related technology could be used to model the movement of a chemical spill through the city storm drainage system (Wayne County Rouge River National Wet Weather Demonstration Project). The two reasons for the Michigan study were to provide emergency personnel with incident response time and to prevent further degradation of the Rouge River. The demonstration introduced multiple chemical spill scenarios and then calculated the travel times of the substances. One spill scenario involved a 6,000 galloon tanker discharging waste in 30 minutes under varying weather conditions. The second situation involved a 12,000 galloon tanker spill discharging its entire contents in six hours under various weather conditions. Combining data from the GIS and SWMM, the movement and concentration of the substances were highlighted. Rainfall events of varying intensity and duration were inserted into SWMM and the surface features attributes were gathered from the GIS database.

The Novi research concluded that SWMM did not demonstrate substantial flows during a dry day and that spills occurring further away from the observed outlet necessitated additional time to reach the river. Basically, a pollutant discharged during a rain event would require a shorter time for containment (City of Novi, 2001). The model also identified the travel times for a spill to reach the outlet of the study area using six rainfall events. It was determined that increased spill distances from the outlet location required greater travel times. Likewise, a discharge of 6,000 gallons would travel through the system within 1.6 to 4.8 hours during a storm, while the same spill would require 2 to 12 hours to pass through the drainage network without rainfall.

Considering the success of the Michigan project, the purpose of the Cherry Point project was to utilize the newer XPSWMM 9.0 model in the coastal region of North Carolina to predict the travel times of highly soluble materials within the study area. Not only was the research goal to focus on travel times at the catchment outlets, but the modeling results would provide pollutant travel time estimates at specific points along the drainage path. Travel times calculated from design rainfall events would be completed in addition to using continuous rainfall data collected at the research site.

#### *Stormwater Management Literature Review*

Urban stormwater management, simply stated, is everything done within a catchment to remedy existing stormwater problems and to prevent the occurrence of new problems. More specifically, stormwater management includes structural and non-structural techniques to reconcile conveyance and storage functions of existing systems and uses intended details to construct best management practices to address potential problems associated with stormwater runoff (DID Malaysia, 2001).

Water quality problems have led to federal and state programs regulating combined sewer overflows, sanitary sewer overflows, and stormwater (Taylor, 2006). These concern areas are now receiving increased attention as public health and ecological preservation gain popularity. Controlling wet weather pollution is ranked high on the U.S. EPA's priority list and is considered the key to maintaining and improving the quality of the nation's waterways (Taylor, 2006). Therefore, effectively managing stormwater introduces several benefits, including increased public health, the sustainability of wetlands and other aquatic communities, the

improved quality of receiving waterbodies, the continuation of water resources conservation and effective flood control.

Environmental studies have found that areas identified as having poor environmental quality of surface water directly correspond with urban stormwater inputs from surface inlet structures, creeks, rivers and ephemeral channels (EPA Victoria, 2005). In addition, it is understood that waterbodies located adjacent to municipalities have a heightened susceptibility to stormwater quality issues. According to the U.S. EPA, urban stormwater is the second largest source of water quality damage in estuaries and a significant contributor to lake, river and bay degradation (Taylor, 2006). Therefore, stormwater should be regarded as an asset and a resource to be valued, rather than the traditional attitude of regarding it as a nuisance to be disposed of as quickly as possible (DID Malaysia, 2001).

## **II Thesis Structure**

The dissertation documenting the research completed at the Marine Corps Air Station at Cherry Point was completed using four separate chapters with exclusive purposes. Each chapter has specified goals and subject material, and therefore can stand independently. Collectively, the four chapters introduce and discuss all subject matter and procedures used to accomplish the research goal. Chapter One provides a brief description of the overall research intent and introduces some existing water quality concerns that have prompted the necessity of the study. Chapter Two is dedicated to describing the physical characteristics of the air station and more importantly the study site. The gathering of spatial information and its organization, the instrumentation of rain and flow gauging stations, and the collection of weather data are all discussed in Chapter Two. Chapter Three is solely dedicated to describing the surface water model progression, explaining the requirements needed to generate the event-based and continuous simulations using EPA's SWMM and XPSWMM, and interpreting the predicted results. The calibration and validation of the stormwater models are also presented in Chapter Three. Chapter Four displays the continuous XPSWMM simulation results and introduces a technique using water-soluble pulse tracers to estimate the travel time of chemical spills via surface waters within the study area.

## **Chapter Two: Watershed Characterization and Field Hydrologic Measurements at Cherry Point Marine Corps Air Station**

### **I Introduction**

#### **A. Background**

In 1988, the Division of Water Quality conducted an inventory of surface waters of North Carolina. As a result, all lakes, streams, and rivers were given a classification code. From the 1988 inventory, Slocum Creek received four codes: SC, C, SW and NSW (note: multiple classifications are quite common and basically reflect the best usage for a water body). Using the North Carolina-DWQ Stream Classification Descriptions legend, the above symbols are translated into: 1) Aquatic Life/Secondary Recreation, Saltwater, 2) Aquatic Life/Secondary Recreation/Freshwater, 3) Swamp Waters and 4) Nutrient Sensitive Waters, respectively. Likewise, Sandy Branch, a tributary to Slocum Creek and the location of the monitoring equipment for this project, received the C, SW, and NSW ratings. These ratings are important, since they may restrict developmental procedures and regulate discharge constituents.

On a broad scale, the Neuse River originates in the Piedmont section of central North Carolina and travels 200 miles southeast, emptying in the Pamlico Sound. The cities of Raleigh, Smithfield, Goldsboro, Kinston, New Bern and Havelock are all located along the river's path, having varying degrees of influence as urban development flourishes. Two major changes occur along the river. The Falls Lake Reservoir in Raleigh alters the flow rates due to retention, and freshwater begins mixing with saltwater in New Bern, North Carolina. Approximately two-thirds of the Neuse River basin surface area is comprised of agricultural and forested lands, thus, one-third is either wetland, urban area or open water (NCDENR, 2002).

Although the Neuse River has been the focus of increasing pollution concerns, it sustains a variety of natural habitats. For example, shad and herring migrate upstream from their saltwater homes to spawn in the freshwater areas. Approximately, 4000-acres of primary and secondary nursery areas provide excellent conditions for coastal fisheries harvesting flounder, catfish, bass, blue crabs and oysters. Government owned land such as state parks, wildlife refuges and national forests, encompass a majority of the important habitat areas.

The majority of research and management actions proposed for the Neuse River through 1988 were results of problems witnessed in the freshwater sections. National and state agencies made appointments to collect water samples for testing. The larger municipalities and point source discharge locations were the first to be introduced to new water quality legislation. The four-targeted dischargers were the Town of New Bern, the Town of Havelock, MCAS-CP, and the Phillips Plating Company. MCAS-CP is a major contributor of discharge into the Neuse River, emitting 3.5 million gallons of effluent per day. Following Slocum Creek's channel dredging, unfavorable eutrophic conditions prompted the removal of all dischargers. In 1993, the MCAS-CP relocated its discharge point to the Neuse River, installed a diffuser, and has been intermittently monitoring its effluent. (NCDENR, 2002)

Due to the air station's discharge activities, increased focus on assessing the current water quality and concerns pertaining to future surface water protection, the Cherry Point research advanced in efforts to not only address these areas, but to offer solutions.

## **B. Objectives**

The overall research objective is to predict the movement of water soluble pollutants from a spill site to various outlets on the Marine Corps Air Station at Cherry Point using a stormwater runoff model. In addition, land usage, topography, hydrology, drainage, mapped soils, imperviousness and other characteristics of the subcatchments that directly affect hydrology and pollutant movement are discussed. The field measurements of rainfall and outflow, collected at the study catchments, will be quantified and later inserted into a stormwater modeling package (SWMM) for predicting runoff, which will be compared with outflow measured at the catchment outlets. The purpose of this chapter is to describe the study site characteristics while introducing the field monitoring apparatus and explaining the acquisition of the surface water measurements to provide discussion concerning the observed hydrologic and hydraulic conditions.

The effective utilization of georeferenced data and traditional survey acquired information should prove to be adequate in characterizing the catchments and routing elements needed to simulate runoff in the Storm Water Management Model (SWMM). Flow data monitored at the catchment outlets will be used to calibrate and validate SWMM.

## II Methods

### A. Site Description

The Marine Corps Air Station at Cherry Point is the largest Marine base in the United States, situated on more than 11,000 acres and consists of various land uses. The determined land use categories include regions with residential, commercial, industrial and recreational purposes including an airfield with supporting runways. The air station is surrounded by the Croatan National Forest and is located on the coastal region of North Carolina, adjacent to the town of Havelock (the coordinates are 34.8°N and 76.9°W) , which is approximately 18 miles southeast of New Bern, NC and nearly 20 miles northwest of the Atlantic Ocean shoreline. Figure 2A.1 is a graphic displaying Cherry Point and the surrounding areas, such as Havelock and the adjacent waterbodies. The base is part of Craven County and is surrounded by surface water on three sides: 1) Slocum Creek to the west, 2) Hancock Creek to the east, and 3) the Neuse River to the north. In addition to being a major flight training facility, the air station is home to a naval aviation logistics and supply depot where more than 16,000 employees, including 11,000 stationed military officers, function daily. (MCAS Cherry Point Public Affairs Office, 2006)

*“The air station offers a temperate climate with relatively mild winters, hot and humid summers and steady annual precipitation. The average annual rainfall normally exceeds 50 inches, and snowfall occurs occasionally. The relative high water table, usually associated with coastal areas is also prevalent at this location, which provides ample baseflow for surface streams. The surface topography is mostly characterized by flat lands, at an elevation of 27 feet above sea level.”* (MCAS-Cherry Point Public Affairs Office, 2006)

#### *MCAS-CP Major Watersheds*

The vast majority of the air station is located on a peninsula formed by Slocum Creek (western side) and Hancock Creek (eastern side) and the Neuse River estuary (Muhs et al. 2000). The x-formation represents the flight line (airstrip) portion of the air station, and the industrialized zone is indicated by the red circle in Figure 2.1.

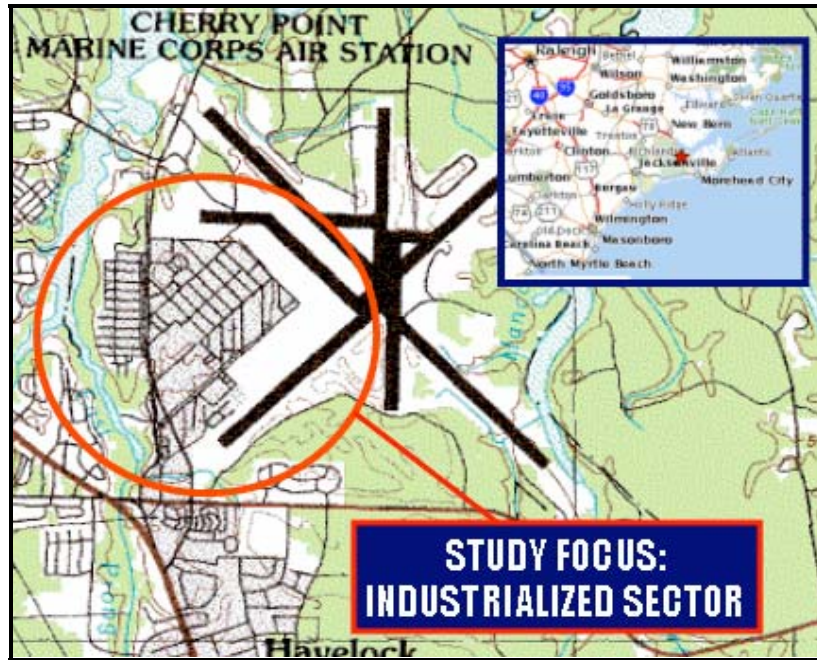


**Figure 2.1: Cherry Point MCAS Location Map including Portions of Eastern North Carolina** (adapted from [www.MapQuest.com](http://www.MapQuest.com), Inc., 2003 and [www.topozone.com](http://www.topozone.com), Maps a la carte, Inc, 2000). The air station is situated on a peninsula formed by Slocum Creek (western boundary), Hancock Creek (eastern boundary) and the Neuse River (northern boundary).

The study site was reduced to include only selected catchments within the industrialized section. The industrial portion of the base was an ecological concern which was evaluated by several environmental firms, including North Carolina State University. In 2000, an environmental consultant, CPEC Incorporated, was assigned to investigate the functionality of the existing stormwater drainage system at Cherry Point. The CPEC company concluded that the watershed outlined in Figure 2.2 drains approximately 2450 acres (993 hectare) of land, less than one-fourth of the 11,000- acre (4452 hectare) total land area dedicated to the air station (Muhs et al., 2000).

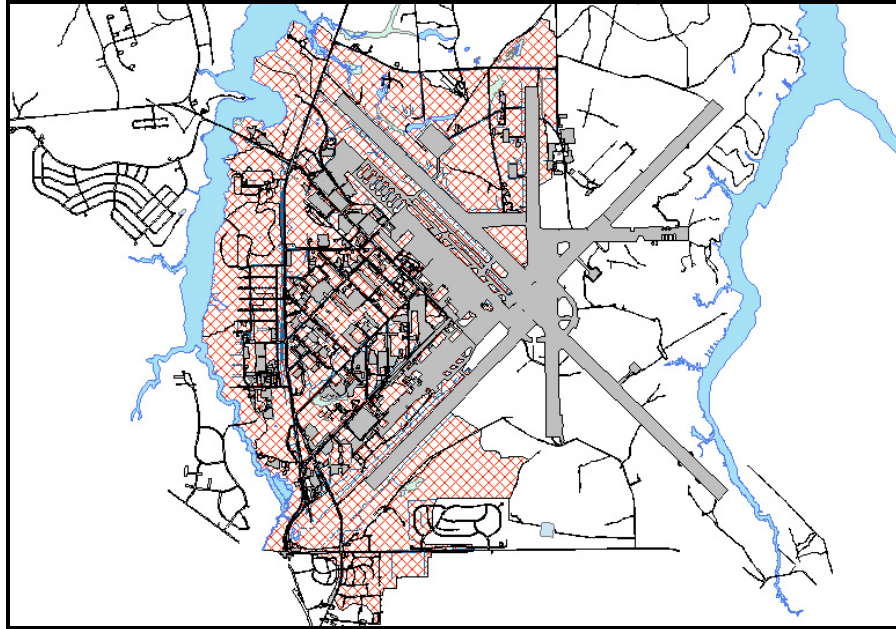


**Figure 2.2: Overall Watershed Delineated for the Industrialized Section of Cherry Point (CPEC, Inc., 2000).** The red cross-hatched region represents the estimated watershed area and the grey areas are impervious surfaces, designated prominently by the airstrip in the center.

Initially, the research staff conducted field visits with the assistance of MCAS technical personnel in efforts to document current land use, drainage network configuration and basin characteristics (Amatya, et al 2001). From these visitations, it was reported that approximately 50% of the land is occupied by loblolly pine (*Pinus taeda L.*) forests (Morgan, 1999). Table 2B.1 of Appendix 2B summarizes the area and the associated percent imperviousness per basin.

Stormwater runoff from Cherry Point drains into several watersheds prior to entering into Slocum Creek, Hancock Creek and the Neuse River estuary. The research was focused on the industrial portion of the air station that is drained by five catchments: Schoolhouse Branch, Sandy Branch, Luke Rows Gut, Turkey Gut, and Mill Creek.

The smallest basin, Turkey Gut, has a total area of almost 100 acres (40 hectare) while the largest basin, Mill Creek, has a total area of 937 acres (379 hectare). Due to its relatively small area and low imperviousness (less than 8%), Turkey Gut was not considered for further study. The remaining four basins all discharge into Slocum Creek, a tributary to the Neuse River.

### *Schoolhouse Branch*

The outlet of this catchment was designated K1 and is located near the main entrance to the air station. The outlet consists of a culvert fitted with a 72-inch arched, corrugated metal pipe (CMP) spanning approximately 100 feet beneath a railroad track (see Exhibit 2.1 under Chapter Two Exhibits). The K1 outlet drains nearly 642 acres (260 hectares) of land, including the main airstrip (runway) positioned in the southeastern section of the base. This basin borders the Sandy Branch to the northwest and a portion of Luke Rowe's Gut to the north.

A majority of the basin is pervious, open grassed lands, and is drained by surface ditches and canals. Nonetheless, an underground pipe network does drain a small fraction of this catchment. Drop inlets, situated parallel to the runway, are connected to the main stormwater piping system that discharges via surface channels. The headwaters of the main collector channel begins as a shallow ditch running parallel to the airstrip, and then passes through a double-span, gated weir installed to prevent pollutant transportation via stormwater. At a point further downstream, the stream passes through a multiple barrel, concrete culvert positioned upstream of monitoring location K1. The main channel has a fairly steep bed slope; therefore, backwater conditions rarely occur. The stream widens downstream of the railroad culvert at K1, travels for several hundred feet, passing beneath Roosevelt Boulevard, and finally empties into Slocum Creek. Stormwater monitoring station number 136 (designated as stormwater outfall #136 in Exhibit 2.2 in the Chapter Two Exhibits section) was installed at the downstream section of the arched culvert and consisted of a SIGMA water quality sampler that was maintained by air station personnel.

The outlet conditions described for the K1 basin remained applicable until November 2002 when a metallic floodgate was installed at the upstream side of the Roosevelt Boulevard culvert. Intermittently, the manually operated floodgates were closed during site visitations, causing backflow conditions and increased water retention, which possibly influenced the observed flow and stage data at monitoring station K1.

## *Sandy Branch*

The Sandy Branch watershed handles a large portion of the surface and subsurface drainage for the industrialized section of the air station. A combined system of buried pipes and surface water features, such as streams, ephemeral channels, ponds and wetland areas transfer stormwater runoff toward the outlet. Sandy Branch is approximately 539 acres in area, consisting of a compilation of mixed land types including industrial buildings, paved parking lots, open areas, streets and forested lands. This basin is 53% impervious, using a weighted average area technique.

Both catchments K2 and K3 are located in the Sandy Branch catchment. The modeling study reported in this publication is focused on subcatchments K2 and K3 exclusively. Figure 2.3 displays the location of catchments K2 and K3 and the southwest portion of Cherry Point.

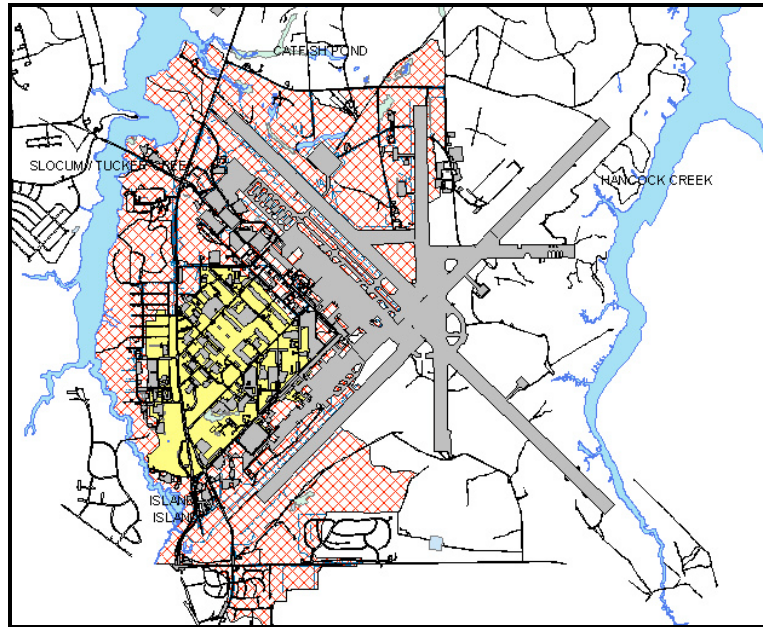


**Figure 2.3: Overall Watershed for the Industrialized Section of Cherry Point Highlighting the Sandy Branch.** The yellow region in this figure denotes the boundaries of the Sandy Branch region. The stormwater research presented in this study was confined to this specific area.

### *Luke Rowes Gut*

Luke Rowes Gut borders Sandy Branch and extends eastward to drain much of the northern part of the industrialized area (refer to Exhibit 2.3 in the Chapter Two Exhibits). Outlet K4, outfitted with a concrete box culvert, runs westward beneath Roosevelt Boulevard before discharging into Slocum Creek (see Exhibit 2.4 under the Chapter Two Exhibits section). At 41% imperviousness, this basin consists of roads, parking lots, and the flight line (runway). Outlet point K4 receives discharge from Outfall #118 through Outfall # 122 (refer to Exhibit 2.2 under the Chapter Two Exhibits section). Flows in the main channel are occasionally restricted by fallen trees and dead branches downstream of the monitoring location.

### *Mill Creek*

Part of the northern section of the industrial portion of the air station is drained by Mill Creek. This basin houses nearly one-half of the airstrip, and is 31.8% impervious. The K5 monitoring station is located at the upstream side of a four-barrel, circular, concrete pipe culvert outlet (see Exhibit 2.5 in the Chapter Two Exhibits section). The stream continues beneath the flight line before reaching Mill Creek. Another tributary to Mill Creek drains some pervious sections, but consists mostly of grassed areas and pine forests, and is located in the northern section of the basin. Together, the two tributaries empty into a large wetland located upstream of a triple-span, concrete box culvert that traverses through Mill Creek before intersecting Slocum Creek.

## **B. Spatial Data Introduction and GIS Development**

The specific research intent is to use spatial information gathered from the geographic information system to construct the drainage areas in efforts to estimate the catchment characteristics. In addition, the GIS will be used to attribute the surface features of the basins and the routing elements. The rainfall gathered from the automatic rain gauge would also be input for the stormwater model to complete the simulations on event-based and continuous time scales.

Spatial information was collected in several steps. First, the URS consultants (et al 1996) gathered land information using traditional surveying techniques. The land survey was focused on highlighting the existing surface waters and underground piping system. A global positioning system (GPS) was selected to collect additional spatial data. The location and attributes of important hydraulic elements such as headwalls, gate inlets, curb inlets and manholes were additionally noted. The second phase involved adapting the geographic information system (GIS) for Cherry Point. During the adaptation process, the research team refined the GPS data to represent the study site. The consultant used a digital terrain map (DTM) to delineate the larger watersheds. Manually, the research team divided the larger watersheds into subwatersheds using topographic maps and aerial photography. The subwatersheds were aggregated even further to the catchment and subcatchment level as necessitated by the modeling requirements. Third the GPS data was adapted to the catchments and subcatchments. The individual spatial regions and surface water attributes were applied to the conceptual model. The physical characteristics were measured using the GIS and ground truthing was conducted. Additionally, two-dimensional coordinates (x- and y- axis only) were specified for points of interest, including stream outlets and junctions.

#### *URS Consultants Incorporated Contribution*

In August 1996, the URS Consultants, Incorporated, submitted a project report entitled, "Watershed Retention Basins, Core Area". In Figure 2.4, drainage area E or the "core area" corresponds to the industrialized section of the air station.



**Figure 2.4: The URS designated Drainage Area E for Cherry Point.** Area E is indicated by the blue region. Although this delineation is similar to the watershed delineation completed by CPEC, Inc. (2000), it only incorporates a portion of the industrial area.

This action represented the beginning of the recent GIS work that evolved into the current modeling and GIS study. The purpose of the URS study was to perform an analysis of options for stormwater management in the core area of the Marine Corps Air Station, located at Cherry Point (URS Consultants, 1996). Furthermore, the project expected to complete the following tasks:

1. Define the hydrologic boundaries of the Drainage Area E using existing topographic and storm drainage maps.
2. Perform hydrologic analysis to generate runoff rates and volumes for existing and future development.
3. Determine locations for an on-site stormwater control facility.
4. Provide cost estimates for feasible engineering alternatives.

*Drainage area E was divided into sixteen hydrologic units. Each hydrologic unit was defined as the area contributing flow to a minor or major tributary during a stormwater runoff period. Using an AutoCAD file containing 0.5-foot contours and random spot elevations, a Digital Terrain Model (DTM) was generated for the area of interest. Areas having insufficient topographic coverage were supplemented. The DTM provided a three-dimensional*

*representation of the land surface and allowed the application of a hydrologic module to predict stormwater runoff flow paths. (URS Consultants, 1996)*

The URS consultants were expected to determine a best management practice (BMP) to direct storm runoff. The watershed area delineated by URS differs slightly from the CPEC region due to the fact, that URS group did not include the outflow contributions of several small roadway culverts and ephemeral streams. A stormwater control facility was selected as the BMP and potential locations were evaluated. The location was determined from the DTM in conjunction with MCAS supplied topographic information. The southwest corner of drainage area E was selected "since the area [was] undeveloped and runoff [was] conveyed here as a result of both natural topography and past land/drainage system development practices (URS Consultants, 1996). Using XPSWMM, stormwater was routed from the subcatchments into the proposed BMP location using a 10-year design storm for the Wilmington region (eastern coastal area) of North Carolina. The modeling was performed to evaluate the peak flow rates at the future BMP location following the routing of the storm hydrographs through the hydrologic units (URS Consultants, 1996).

Several alternatives were evaluated to simulate runoff and peak flow rates. According to URS, the most favorable result was to construct a wet detention pond with side bank sand filters. The reasons for selecting this alternative stemmed from state regulations involving total suspended solid constraints, land consumption, local discharge quality restraints and aesthetics.

#### *CPEC Incorporated Contributions*

In 1997, MCAS-CP hired the CPEC consultants to prepare a GIS database of the stormwater system including the open channels and closed pipe conduits. Ground truthing of archived maps and verifying existing AutoCAD documents were their two major tasks. CPEC was also expected to compile all aging maps and append them, using digital information, to create updated drainage coverages.

Simultaneously, Muhs (2000), at North Carolina State University, conducted a similar study, delineating the sub-watersheds of Slocum and Hancock Creeks, which drain the western and eastern portions of the air station, respectively. The Muhs study was considered necessary for the MCAS Environmental Affairs Division to begin its National Pollutant Discharge Elimination

System (NPDES) permit application. A NPDES permit was required for the industrial areas due to a potential for contamination of receiving surface waters. In addition, sources of contamination resulting from stormwater runoff and hazardous spills were of particular concern to the State of North Carolina since effluent from the air station discharge into the Neuse River Estuarine System (Muhs, et al., 2000). The identification of stormwater flow paths later developed into a critical water quality management component. The Muhs study involved extensive fieldwork and data processing that focused mainly on drainage features within the industrialized section of the air station. In 2001, the CPEC consultants prepared the final GIS database of the stormwater system, based on their extensive survey work at the site, including data from the Muhs research.

CPEC used a Global Positioning System (GPS) to create the GIS coverages. GPS technology allows the identification of surface position through triangulation. Triangulation involves utilizing at least three satellites and a receiver to determine terrestrial location. The GPS receiver decodes the time and positional values from the satellite and calculates the exact location of the receiver on the earth, within given limits. Using this technology, the CPEC crews were able to locate, identify and attribute stormwater structures, stream channels and other hydraulic features, including subsurface pipe inlets/outlets.

#### *North Carolina State University Contributions*

An initial step in this research was the collection of terrestrial and hydrologic information. The CPEC consultants were subcontracted to conduct a land survey using conventional instrumentation and global positioning systems to establish the study boundaries. The research team at North Carolina State University used the CPEC data to delineate prominent catchment areas. Following the catchment identification, flow-monitoring equipment was installed at each outlet point. Continuous stage, velocity, water depth, and other information were collected at the five outlets for an excess of two years (from November 2000 through December 2002).

Exhibit 2.2 (located in the Chapter Two Exhibits section) was helpful during catchment delineation by identifying existing outfall points, but no flow records were retrieved for these monitoring locations (Amatya et al 2001). Nonetheless, water quality sampling for physical and chemical parameters had been conducted at several outlets within the past few years as part of the environmental monitoring program for the National Pollutant Discharge Elimination System (NPDES) permitting process (Morgan, 1999). The research team was unable to obtain the

collected NPDES related water quality information but moved forward with the research objectives.

The initial spatial information was acquired and adapted from both the URS and CPEC information. Broad watersheds were identified but were too expansive for the research intent; therefore, the larger units were reduced to catchment areas encompassing the industrialized portion of the base. A collection of third party programs and ArcVIEW utilities were accessed to create the subcatchments needed for simulation. The delineated catchments did not match those created previously because the conduit system carrying surface and subsurface flows was not examined during earlier investigations. Thus, the finalized shape of catchments K1 through K5 resembled previously outlined areas but the regions were not identical. The attributes collected from the consultant work was then queried and attached to SWMM elements (subcatchments and routing features) accordingly. In some instances, information pertaining to shallow surface channel measurements and conduit sizes were not identified during the field survey and therefore required attribution during site visits. The North Carolina State University research team synthesized the information gathered from external sources and added pertinent information to create the SWMM input files required to properly simulate stormwater runoff from the industrial areas at Cherry Point.

#### *Source Data Challenges*

Prior to beginning a GIS project, a researcher must fully understand its intended use and collect data to support that purpose. Collected data accuracy is directly related to output quality. Managing, maintaining and updating the source data become imperative in order to generate a functional database. Following these few concerns, the generated database should prove to be worth the effort.

Getting the data into the correct format is one of the most difficult issues when forming a GIS database. This challenge encompasses transforming source data into information more suitable for a spatial database (Lutz, 2003). In many cases, map images may be digitized using a computer-aided mapping system (CMP), but attributes must be fixed to the lines and arcs. This means extracting the implied attribution from the entities as the data is imported into the spatial database, and turning them into explicit attributes on the resulting spatial database features (Lutz, 2003). Feature differentiation can be achieved with unique coloring schemes and other display options.

A GIS user must also remember that a majority of the collected data will remain static, but some features are dynamic. If dynamic features are incorporated into the source data, the modeler must remember to update values prior to running simulations. Attribute updates can normally be performed within the GIS system, if not, third-party software may be required. Once a meaningful spatial database has been created, not only are additions possible, the opportunity to export georeferenced datasets becomes feasible.

### *Fundamentals of Stormwater Mapping and Modeling*

Mapping, monitoring, modeling and maintenance are the four main areas when managing a stormwater system (Shamsi and Fletcher, 1996). The map creation software is used to compile existing data and insert field data to form a fairly accurate map. The monitoring step involves site selection and data collection. The modeling portion is used to calibrate, validate and analyze the system and to evaluate potential solutions to future problems. The maintenance area incorporates updating the GIS as changes occur and establishing areas that need attention.

Historically, GIS packages were designed for technicians who relied upon specialized workstations to complete the map production process. Therefore, the average computer user may have been overwhelmed when attempting to use some GIS software. As of 1996, some of the leading GIS products were ARC/INFO (Environmental Systems Research Institute), Geo/SQL (Generation 5 Technology), GENEMAP (Genasys) and MGE (Intergraph) (Shamsi and Fletcher). Technological advancements in micro processing capabilities now allow desktop computers to run the same type of GIS products that once required specialized workstations.

ESRI's ArcVIEW is a sophisticated desktop mapping and GIS application that promises to bring the power of GIS to the average PC user (Shamsi and Fletcher, 1996). Although paper maps cannot be directly digitized into ArcVIEW, it is best suited for data management, manipulation and modification of existing GIS coverages. Thus, if a user wishes to have existing maps converted to a format readable by ArcVIEW, these documents must be scanned using preprocessing software. Nonetheless, ESRI does publish a series of data called "ArcData". The ArcData catalogue is a compilation of digital information and includes such data as digital line graphs (road, railroads, rivers, stream, lakes, state and counties) and TIGER files (census and politically related data) (Shamsi and Fletcher, 1996).

### *Cherry Point MCAS GIS Introduction*

A GIS uses the numbers and characters from the rows and columns in the database and places them on a map (ESRI, 2003). The selected geographic information system (GIS) for this study is the ArcVIEW 3.2 package developed by the Environmental Systems Research Institute (ESRI, 2003). This Microsoft Windows based application has many functions that assisted with the compilation, organization, and analysis of the spatial data received from the CPEC, Inc. (2001) survey study. The CPEC (2001) study created a database of coordinates, and related attributes, based on the survey activities performed. Appendix 2L contains the metadata used to characterize the surface water drainage features at Cherry Point.

CPEC had created its projections in ArcVIEW and its 3.2 version supported real-time editing. Moreover, geoprocessing functions of ArcVIEW such as, clip, intersect and union permitted the research team the opportunity to create the catchments and subcatchments digitally. Once subcatchments were determined, themed layouts were created and exported into Microsoft EXCEL. Associated databases could be queried using various parameters, which allowed specific features, such as soils or impervious coverage maps to be developed per catchment. ArcVIEW also supported the importation of digital orthogonal photographs (orthos) that assisted in the correct placement of surface drainage inlet structures, the alignment of stream channels and the improved understanding of the overland flow paths.

### *Transition into ArcMAP*

The initial GIS database development began using the most current version of the Environmental Systems Research Institute's (ESRI) ArcVIEW, which was version 3.2. Until September 2002, all the GIS work completed still relied on version 3.2 (and its associated .apr file organizational scheme). Following that point, ESRI's ArcMAP, or ArcVIEW 8.0, superseded ArcVIEW. The newer version of ArcVIEW still had the geoprocessing power of its predecessor with several advanced data management features that enhanced data/map integration also allowing direct importation of SWMM information into ArcMAP via a third-party program. All recent GIS work for the Cherry Point stormwater study was completed in ArcMAP.

### *Watershed Delineation*

The CPEC, Inc., study did an excellent job of compiling the existing AutoCAD maps, ArcVIEW maps, and surveyed information to create an updated detailed map of the interest area (nearly equal to the URS Drainage Area E). Various themes (single topic map layers) were created that displayed the surface water features and piped conduits. Figure 2.5 is an example of the spatial information received from the CPEC survey.



**Figure 2.5: Cherry Point Industrialized Zone Stormwater Features.** This figure displays the geo-referenced stormwater features as received from CPEC, Inc. The red lines represent the subsurface piping system and the green points are hydraulic elements, such as drop inlets, grate inlets and headwalls.

The larger watershed boundaries were established from previous surveys. The CPEC information was the most recent resource and served as the main GIS database for this study. Using the CPEC delineated watersheds, catchments were identified within the industrialized portion of the air station. The K1 through K5 catchments drain into the five, larger basins: Schoolhouse Branch, Sandy Branch, Luke Rowes Gut, Turkey Gut and Mill Creek.

### **C. Field Installation, Hydrologic Monitoring and Data Collection**

#### *Monitoring Periods and Field Note Documentation*

Data collection began in October 2000 with the installation of the flow meters; however, the automatic rain gage was installed in November 2000. The site was visited every two to five weeks, dependent upon precipitation activity. During site visits, all instruments were downloaded and tested.

During the Cherry Point flow study, there existed circumstances when instrument malfunction occurred. The periods when the stage recorder and flow meter malfunctioned are indicated in Tables 2B.4a through 2B.4c. in Appendix 2B.

Field notes were taken during every site visit. Time, monitoring station status, rainfall, and other important observations were reported. The field notes were transposed into Microsoft Word and catalogued by download date. A sample set of the field notes is located in Appendix 2I, Exhibit 2I.1. More importantly, Exhibit 2I.2 in Appendix 2I outlines major problems experienced during the entire sampling period.

#### *Rainfall*

Accurate rainfall data is essential because SWMM uses the precipitation file to create a hyetograph that is translated into the runoff hydrographs. If the collected rainfall data does not reflect the conditions at the research site, the resulting flow simulations lack usefulness.

In order to collect continuous, uninterrupted, and accurate data, rainfall was monitored using dual methods, an automatic gauge and a manual rainfall gauge. Three manual rainfall gauges were positioned at various locations throughout the air station and one automatic gauge was installed. The tipping bucket (automatic gauge) information would eventually become the input dataset for the modeling software. The importance of rainfall accuracy and consistency in availability is discussed in Chapter Three, where the intricacies of the modeling process are explained. Appendix 2K is a collection of the observed rainfall information.

### *Design Rainfall*

Rainfall-intensity-duration information for various return periods was calculated using long-term rainfall intensity and duration data for Morehead City, North Carolina, located nearly 19 miles southeast of the study site. Initially, the model was calibrated and validated using measured rainfall-runoff data to predict the travel time of stormwater pollutants at various locations on the catchments. Then the design rainfall for a 24-hour storm duration, using 2-, 5-, 10-, 25-, 50- and 100-yr return probabilities was inserted into SWMM and XPSWMM. The purpose of the design rainfall application was to characterize the travel time responses using historical rainfall data.

### *Rainfall Event Data Logger*

The continuous rainfall data for the study area was measured using the Onset Computer Corporation's RG2 data logging rain gauge. The RG2 is an automatic, self-contained tipping bucket gauge integrated with a HOBO Event data logger (Onset 2002). One of these gauges was installed five feet above ground near the outlet of catchment K1 (Schoolhouse Branch). The orange squares in Figure 2.6 depict the location of the rain gauges. The automatic gauge referenced for the study was located at the southern-most point, adjacent to catchment K1. The red dots represent the five catchment outlet points and are labeled accordingly. The RG2 automatically records up to 80 inches of rainfall data, assigning a time and date stamp for each tip that is equivalent to one-hundredth inch of rain (Onset 2002). Therefore, cumulative rainfall volumes were initially recorded as tips. The gauges (one manual, one tipping-bucket) nearest the outlet of catchment K1 became the primary precipitation collection tools for this study.

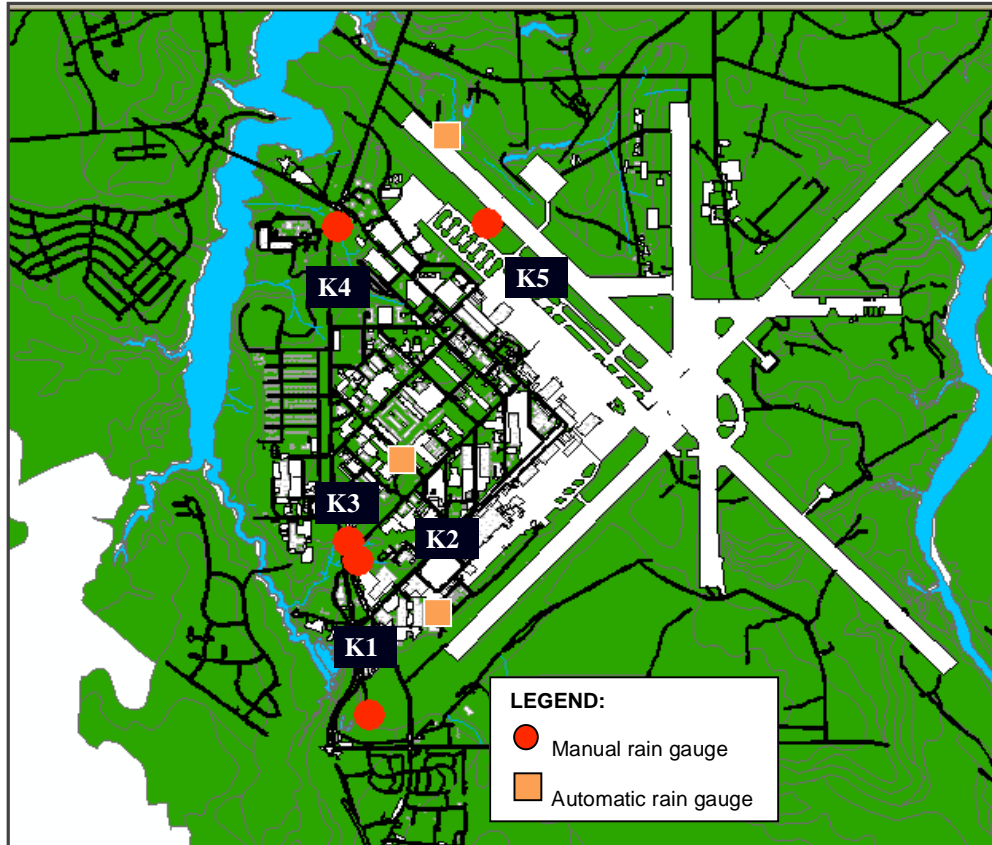


**Figure 2.6: Cherry Point Rain Gauge Location Map.** This figure indicates the spatial dispersion of the rain gauges used to collect and quantify the precipitation amounts during the Cherry Point study.

Approximately every two weeks, the HOBO gauges were downloaded using a HOBO shuttle. The shuttle transferred the data from the event logger and functioned as a temporary storage unit until the data could be downloaded to a main computer. The resulting downloads received a naming convention that specified location and download date (for example, cpr022002.txt. would be the text file for the information downloaded on February, 20, 2002). BOXCAR PRO 4.0, a Windows-based program provided by Onset, converted the downloaded material into a text format that was then exported into Microsoft Excel. Periodically the resulting spreadsheets were combined to create a cumulative spreadsheet documenting all recorded rainfall events for that particular year. Table 2.1 displays the annual, cumulative rainfall recorded by the automatic rain gauge (K1 location) and includes precipitation data from two nearby stations.

**Table 2.1: Cherry Point Precipitation Amounts in Inches from years 2000 to 2002 from Three Separate Sources.**

<b>Year</b>	<b>Unofficial Havelock Airport</b>	<b>Official NOAA download data</b>	<b>HOBO tipping Bucket</b>
<b>2000</b>	8.46	8.80	6.63
<b>2001</b>	46.80	33.58	27.37
<b>2002</b>	63.80	46.56	42.25

The precipitation reported for year 2000, in Table 2.1, is a partial collection of the annual rainfall since the study gauges were not installed until October 2000. On the other hand, years 2001 and 2002 are complete compilations. The annual precipitation averages for Morehead City during years 2001 and 2002 were 35.04 and 60.02, and the average, annual rainfall amount is 55.83 inches (State Climate Office of NC, 2006). The Official NOAA weather station for the air station is located at the control tower and the tipping bucket recorder was situated near the outlet of catchment K1.

The tipping bucket rainfall was used to generate a hyetograph which was plotted on the secondary axis of the outflow hydrographs. Exhibits 2.6 through Exhibit 2.9 (in the Chapter Two Exhibits section) are the cumulative outflow hydrographs for catchments K2 and K3, including the cumulative rainfall hyetographs, for years 2001 and 2002.

*Manual Rain Gauges*

Three manual rain gauges were installed: 1) adjacent to the tipping bucket gauge in area K1, 2) near the outlet of catchment K3, and 3) next to a retention pond located in catchment K5 (see Figure 2.6 for gauge placement). Each gauge was fastened to a post and positioned at a five-foot height. The standard rain gauge design consists of a large plastic cylinder fixed with a funnel that empties into a smaller plastic measuring tube. Once one inch of rain accumulates in the smaller tube, the overflow is collected in the larger cylinder. During field visitations precipitation amounts were documented, corresponding to the last measurement date. The reading date and accumulated rainfall amounts were also documented.

Data from the HOBO recorder was regularly verified with the manual gauges. In some instances, discrepancies did exist between the manual and automatic gauges. In addition, rainfall differences did occur between stations. Nonetheless, both sets of data, manual and automatic, were compared to document recorded rainfall patterns from the national weather station prior to beginning the modeling procedures. The examination of the various rainfall datasets also would explain the potential effects of spatial variability, if any, and its related influence on outflows predicted by the SWMM model.

#### *Outflow Measurements*

Three types of instruments were installed to measure flow rates: 1) a sharp-crested V-notch weir, 2) a stage monitoring system located upstream of the weir(s), and 3) a self-recording flow meter located downstream of the weir(s). It was essential to attempt continuous flow monitoring during the study period, therefore, the weir and the velocity meter were installed as complements. Figure 2.7 is a profile view of the monitoring station at the outlet of catchment K3.

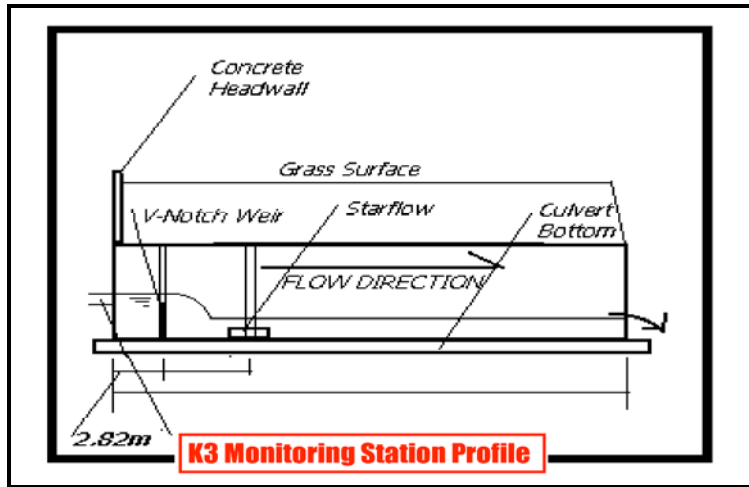


**Figure 2.7: Typical monitoring station profile for the Cherry Point Study.** This figure denotes the position of the flow meter in relationship to the upstream headwall, v-notch weir, and the culvert outlet for catchment K3.

The exact stage recording position is not indicated in Figure 2.7 but the stage was measured at the inlet headwall. The v-notch weirs were fabricated from stainless steel and built to culvert specifications. A simple diagram for a sharp-crested weir is presented in Figure 2.8.

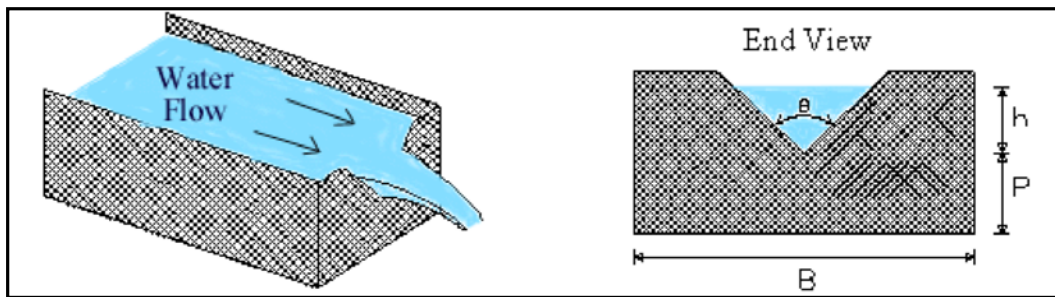


**Figure 2.8: Sharp-Crested Weir Diagram** (as viewed at: <http://www.lmnoeng.com/Weirs/vweir.htm>). V-notch weirs were used at Cherry Point to quantify low flow rates that would be difficult to describe under normal conditions.

According to Figure 2.8, the approaching channel width is designated as  $B$ . Measured head is denoted by  $h$ , while  $P$  represents the vertical distance from the crest bottom to the bottom of the channel. Pictures from the actual monitoring stations are located in Appendix 2C. Most of the weirs had 120-degree angles, but monitoring station K4 had a 135-degree weir. The weirs

were positioned inside the upstream portion of the culvert using an adjustable turnbuckle connected to a circular band. By adjusting the turnbuckle, each weir was fitted and sealed with a waterproof compound. The weirs were installed to capture periods of low flow, less than 10 cfs or 0.283 m<sup>3</sup>/s.

The stage monitoring system is what recorded the water height in relationship to the installed weir elevation. The stage system consisted of a microprocessor and a pulley-string arrangement fastened to a float, counterbalance and potentiometer. The datum for each outlet coincided with the bottom of the lowest v-notch weir. During water elevation changes, the float moved up/down accordingly, turning the pulley and shaft. As the shaft rotated, the potentiometer recorded the change in electric voltage and the microprocessor recorded the resulting electrical signals.

The ultra-Doppler flow meter, manufactured by the Unidata Corporation, continuously measures stage and average flow velocities, immediately above the meter, in ten-minute intervals. Mounted at the bottom of the culvert, the Doppler component emits sound waves in an upstream direction (Unidata, 2000). Provided the physical characteristics of the moving water (temperature and density) the apparatus calculates flow rates by measuring the time elapsed between a sound wave signal's departure and return to the sensor (Unidata, 2000).

Using the adjusted speed of sound for the current flow conditions, the meter calculates the flow velocity. The flow meter's pressure transducer measured the stream stage downstream of the weir. The collected information was transferred to the datalogger that recorded water temperature, date, time, water depth, velocity, and battery voltage. A 12-volt battery, coupled with a solar cell, supplied power to the unit. All recorded data was stored within the logger's internal memory until downloaded. During site visits, the flow meter executable program was run and an incremental download was conducted that saved the flow data as a text (.txt) file. The resultant text file was then exported into a spreadsheet and combined with other files to create a continuous dataset. A sample of a delimited flow meter data file is presented in Exhibit 2E.2 in Appendix 2E.

#### *Data Acquisition – Weir 6 Program*

A BASIC program, Weir 6, was developed in the BASIKIT compiler, specifically for instrumentation by the Department of Biological and Agricultural Engineering at North Carolina

State University. The program not only managed recorded data, but also was responsible for transferring information from the data logger to other computers (refer to Exhibit 2D.1 in Appendix 2D for the Weir 6 program). The 10 kilobyte (KB) program fits easily onto a portable computer and may be accessed using MS-DOS. In the field, a laptop or handheld computer was used to download data, via a serial port. The Weir 6 program was also used to set equipment parameters such as pulley diameters, wake-up interval, water depth, and time/date stamps.

Initially, Weir 6 was loaded onto the microprocessor and tested. Using the measured diameters of the pulley system, the program converted the electrical signals sent by the potentiometer into rotational distances. These distances were then used to determine the amount of vertical change between water level readings. The datum selected for this project was the bottom of the v-notch weir. Elevations above the datum received positive values, while numbers below this point were recorded as negative elevations.

The Weir 6 program also controlled the recording conditions for the microprocessor. A three-minute time step was selected. If a one-millimeter difference existed between readings, the new elevation was recorded, along with a time/date stamp (see Exhibit 2D.2 in Appendix 2D for a sample stage recorder download file). Following each recording period, the program then returns the microprocessor to sleep mode. During a download, the stored data on the microprocessor was saved as a .bas file in a sub-directory. Each file was given a name based upon location and date. For example a downloaded BE file from location K1 on January 11, 2002, would be named K1011102.bas.

The Weir 6 program parameters were checked following successful downloads. While in test mode, real time water stages were displayed every two seconds. A steel staff (ruler) was placed at each monitoring station and was used to insert and calibrate the water elevation reported by the program. Differences between the Weir 6 elevations and the staff readings were noted.

A 12-volt battery powered the microprocessor. Energy conservation was achieved by requesting the program to record only significant changes in water depth. To further optimize energy consumption each staging location was equipped with a photovoltaic cell (solar panel) that intermittently recharged the battery. The voltage for the system was also checked during downloads. Since the BE microprocessor becomes nonfunctional below 10.5 volts, low voltage cells were a concern and battery replacement occurred frequently.

### *Data Acquisition - STARFLOW Program*

The model 6301A STARFLOW software compliments the operation of the STARFLOW (SF) instrument by providing an easy-to-use data collection and management system (Unidata, 2000). The software may be installed onto a main computer allowing scheme development and other processes to organize data.

Each SF was programmed with the TEST1 scheme. The TEST1 scheme informed the meter to collect data every 10 minutes. During downloads, the program was initiated and the incremental unload option was selected. The incremental unload option enabled the user to retrieve data logged since the last download, preventing data repetition in consecutive download files. When the program prompted for a location identifier, a two-letter code was selected contingent upon the monitoring site, i.e. K3. The recorded data was later transferred from the SF and stored in the TEST1 sub-directory under the SCHEMES sub-directory.

The “display an unload file” option was used to convert the recorded data into a text format. The display option allows a user to select the downloaded SF file and to associate a report type. While on the “display an unload file” menu, the selected file was saved as a .prn file. By default, the program gives each file a name, i.e. test1.ug5, which was eventually edited to reflect the location and date, i.e. k1v012202.prn.

Similar to the manual check used with the BASIKIT elevations, the flow meter also has a scheme test mode. This mode allows a user to monitor the flow meter’s performance in real time. While in test mode, the battery voltage was compared to readings received from a handheld voltage meter. Velocity readings (mm/s), water depth (mm), temperature (°C), and timing were also examined while in test mode. Any discrepancies or unexplainable events were noted. See Appendix 2E for sample files related to the flow meter.

### *Data Refinement - Combined Flow Spreadsheets*

An initial step in data preparation involved synthesizing separated spreadsheets to form a continuous dataset. The stage recorder downloads consisted of information collected in two to

five week intervals. These individual download files were appended to develop a continuous, yearly dataset.

The .bas text files were later renamed using .prn file extensions. The data was sorted according to year and monitoring location and placed in corresponding directories on a central computer. Later, the raw .prn files were imported into a spreadsheet using various delimiting criteria and manually coupled based upon Julian date. Whenever a lapse, or loss, in data occurred, the time interval was recorded and the nature of the problem described. Month, day, hour, minute and stage values were placed in a tabular form and saved as an .xls (MS Excel) file. Exhibit 2F.1 in Appendix 2F contains a sample spreadsheet displaying combined flow data.

The next step involved converting the Cherry Point stage records into flow values. The stage recorder and flow meter default was metric units. Using the following 120° v-notch weir equation, the stage values were converted into flow rates (Brater, 1996).

$$Q = 2.32 H^{2.5} \quad \text{EQ. 2.1}$$

Where            Q = flow rate (m<sup>3</sup>/s)  
                      H = head measured from bottom of v-notch (m)

Equation 2.1 has been included since the flow meter recorded the measured outflow in metric units. Equation 2.2 is the English adaptation of Equation 2.1.

The weir equation applies whenever the flow is low enough as to not submerge the weir. Once weir submergence occurs, flow rates generated from the weir equation become questionable and other means of flow calculation must be utilized. For this study, it was assumed that whenever the recorded stage exceeded the top-of-weir elevation (approximately 0.30m or about 1.0 ft), that submerged weir conditions existed; therefore, Equation 2.1 becomes invalid. Likewise, the reported stages were based upon the lowest weir of the triple weir outlet (the bottom of the weirs had different elevations) so the stages for supplemental weirs (barrels) needed to be calculated individually. Table 2.2 displays the differences in height of the V-notch bottom between weirs at the monitoring stations that were used for converting the stages for the other two weirs (weirs #2 and #3). The stage readings were reported using the bottom of Weir 1 as the reference zero elevation, so negative differences reflect elevations lower than the current position of Weir 1.

**Table 2.2: Differences in Culvert Elevations for Two Catchment Outlets at Cherry Point MCAS.** This graphic is a representation of the elevation differences between individual culvert barrels at catchment outlets K2 and K3.

Catchment K2	
Weir No.	Difference In Stage
1	0m
2	-0.07m
3	-0.03m
Catchment K3	
Weir No.	Difference In Stage
1	0m
2	-0.06m
3	-0.08m

Once the height differences were known, the water stages were entered into the v-notch weir equation, and an “if-then” statement was inserted to avoid calculating negative flow rates. The total outflow rate was determined by summing the flows from all weirs at each monitoring location. The resultant flow rates were then converted to cubic meters per hour.

The same procedure was completed using English units because the final flow rates would be presented in cubic feet per second. A 3.28 factor is used to convert English stages, in feet, to metric stage values, using meters. Following the same assumptions from Equation 2.1, observed elevations exceeding the top-of-weir elevation represented weir submergence. The 120° v-notch weir equation in English units is as follows (adapted from Brater, 1996):

$$Q = 4.43 H^{2.48} \quad \text{EQ 2.2}$$

Where  $Q$  = flow rate (ft<sup>3</sup>/s)  
 $H$  = head measured from bottom of v-notch (ft)

The individual flow values were summed to create a total outflow value for that outlet. The English units, cubic feet per second (cfs), were used throughout the remaining portions of the study. The combined flow values were graphed by Julian date and flow rate, creating an annual flow summary for each monitored location.

#### *Data Refinement: Flow meter Spreadsheets*

The flow meter raw, text files were downloaded, transported to a portable computer, and eventually transferred to the main computer during data acquisition.

First, the raw files were saved to specialized folders categorized by location and year. Second, the files for a particular year were imported in Microsoft EXCEL using comma, space, and tab delimiters. Using the "date" function in EXCEL, the date stamps are converted to Julian day values. The spreadsheet is appended following each site visit, creating a continuous data set, joined by Julian date. Third, the flow velocities were converted to flow rates, in cubic meters per hour, using the VELFLO program. VELFLO is a FORTRAN program partially developed by Dr. D.M. Amatya in the Biological and Agricultural Engineering Department at NCSU to calculate flow rates exiting circular culverts (refer to Exhibit 2E.1 of Appendix 2E for the VELFLO program).

The VELFLO input structure is rather simplistic but extremely functional. To use the program, the yearly velocity file was created and saved as a .prn file. The .prn files contained time, depth, voltage and velocity information arranged in a tabular format (see Exhibit 2E.2 in Appendix 2E for a sample VELFLO .prn file). The column widths were set to 20 units to prevent numerical truncation. The .prn files were saved in a VELFLO sub-directory that also contained the VELFLO program.

When running VELFLO, the user is prompted to enter the diameter of the culvert in meters. The program then asks the user to indicate the stage-velocity file. The stage-velocity file must be located in the same directory as the VELFLO executable or the program will malfunction. The user is then prompted to name the hourly, daily and breakpoint output files. Upon completion, the program writes the three output files and stores them in the directory where the .prn data is located.

Each output file contains five columns of data. The first column is the date in a Julian format. The fifth column contains the flow rate in cubic meters per hour ( $\text{m}^3/\text{hr}$ ). Since all investigated culverts have multiple barrels, the values in the last column were multiplied times the number of barrels to estimate the total outflow for the location. The metric flow rates ( $\text{m}^3/\text{hr}$ ) were then converted to English units (cfs) by dividing the metric value by 101.30.

### *Composite Flow Spreadsheets*

The composite flow spreadsheets are complete compilations of the observed flow data. These spreadsheets incorporate flow values from both the microprocessor and the flow meter. The combined flow calculations served as the baseline during low flow conditions. Likewise, the measured flow information becomes questionable during weir submergence because the water flow across the nape of the weir does not occur; thus, the freefall conditions become a concern. Once the flow is no longer flowing freely across the weir, the calculated flow estimates increase unrealistically and other means of flow measurement should be substituted. To substitute for submerged weir conditions, the flow meter data was inserted into the combined weir spreadsheet.

To achieve integration between the SF and BE datasets, several steps were completed. First, the combined weir data (date, stage and flow rate only) was imported into a spreadsheet. Using a filter and the stage heights, records above one foot (0.3m), representing the assumed submerged weir conditions, were highlighted (refer to Table 2.3). Table 2.3 demonstrates the process of detecting when the v-notch weir was submerged, thus rendering the weir equation invalid. The yellow area highlights the weir submergence time period. During this interval, recorded data from the flow meter would be inserted into the spreadsheet to replace the weir-calculated outflow. The flow meter synthesized data created by VELFLO was also imported into EXCEL. Eventually, the breakpoint flow data replaced the highlighted stage recorder flow values. Likewise, if the stage recorder information was unusable, the flow meter data was inserted to correct for the lapse in data collection. An annual, composite flow chart for catchment K2 is presented in Exhibit 2.6 under the Chapter Two Exhibits section. In this case, “composite” refers to the application of the using the weir equation and the information from the flow meter during periods of weir submergence to create an annual hydrograph for each outlet point.

**Table 2.3: Cherry Point MCAS Observed Flow Data for One Catchment Outlet Highlighting Overtopped Weir Conditions.** The highlighted region denotes the time period when the weir was suspected to be submerged.

Julian date	Stage (m)	Flow (cfs)
20.4000	0.233	4.82737563
20.4021	0.256	6.28123288
20.4042	0.284	8.37377845
20.4063	0.307	10.3714083
20.4083	0.327	12.3220334
20.4104	0.348	14.5919163
20.4146	0.362	16.2350977
20.4167	0.362	16.2350977
20.4250	0.346	14.365744
20.4292	0.327	12.3220334
20.4333	0.311	10.745388
20.4375	0.299	9.64727643
20.4417	0.286	8.53731094
20.4583	0.275	7.66138327
20.4708	0.262	6.69919114
20.4771	0.248	5.74913837
20.4854	0.233	4.82737563
20.4917	0.22	4.1063783
20.5000	0.206	3.40798146

*Event Based Regression Analysis to Determine Stage-Discharge Relationships*

An auxiliary task was completed to develop a stage-discharge relationship for catchments K2 and K3. This action was prompted since the research team wished to develop a relationship between the stage recorder readings and the flow meter information that could compensate for missing field data. If one of the two measuring devices was inoperable, the regression equation results would fill gaps in the continuous flow data.

The regression was conducted using three steps. The first step involved plotting all flow points and creating an overall regression equation for the fitted yearly data. The next step separated the data into low flow conditions associated with less than one foot (0.3m) of head at the weir. The last step was reserved for high flow periods, when the head on the weir exceeded one foot (0.3m).

Only flow data from the year 2001 was selected for the regression investigation. Date, time and stage (ft) were imported from the combined flow dataset. Hourly flow/date combination output, generated by the VELFLO program, was imported into the same spreadsheet. Using the Microsoft AutoFilter tool, all zero values were deleted. The time values from the two devices were then manually synchronized using a 0.02-day tolerance to create equivalent sample sizes. Synchronization was needed since the recording intervals for the two devices were unequal. In addition, periods containing erroneous data due to equipment malfunction were removed. The created dataset was an annual flow spreadsheet, obtained from the microprocessor and the VELFLO program, having matching date/time stamps. Returning to the Auto filter tool, the data was then divided into three categories: 1) all data, 2) unsubmerged weir conditions with less than one foot of head and 3) submerged weir conditions with more than one foot of head.

Using the “add a trendline” function in Microsoft EXCEL, trendlines were fitted using linear, polynomial and exponential functions. The associated R-squared value was reported for each predicted line and the equation was indicated. To test the fitted equations, the stage data was inserted, as an independent variable, into each polynomial equation. The regression equation predicted flow rates were then plotted against the weir equation and flow meter outflow values (see Appendix 2J for graphs).

#### **D. Weather**

##### *NWS Weather Station*

A National Weather Service (NWS) weather station, located on the control tower at the airstation monitors hourly and daily weather data consisting of air temperature, dew point temperature, wind speed, sky cover and precipitation (NCDC, 2000). Rainfall from this weather station was inserted into the onsite rainfall dataset whenever the HOBO was malfunctioning or data was unavailable (i.e. prior to gauge installation). Not all weather information was available for the study site; therefore, potential evapotranspiration (Penman-Monteith based) parameters were estimated from a nearby research site located approximately 19 miles (30km) northeast of MCAS (Amatya et al, 2001). SWMM has the capability of accepting daily, monthly, or yearly evapotranspiration (PET) information. For Cherry Point, average, monthly PET values were inserted into the hydrologic model.

### *NOAA Downloaded Weather*

Weather information was downloaded from the National Oceanic and Atmospheric Administration (NOAA) website for years 2000 through 2003. Daily maximum and minimum temperatures were recorded in addition to documenting any precipitation that occurred, either rain or snow. Samples of the NOAA weather file are located in Appendix 2G.

Rainfall collected at Cherry Point from the manual rain gauges (catchments K1 and K3) and the automatic rain gage (catchment K1) was eventually referenced against the NOAA precipitation data. The NOAA data was collected at the air traffic control tower, located approximately 2 miles (3.2 km) east of the K2 and K3 outlets. Table 2.1 outlines the annual precipitation depths reported by both the tipping bucket recorder, located near the outlet of catchment K1, and the NOAA downloads.

## **III. Results**

### **A. Site Characteristics for Catchments K2 and K3**

Table 2.4 characterizes the current, GIS-based, land uses for the Cherry Point study area where a portion of the Sandy Branch basin was divided into two catchments, K2 and K3, with their flow monitoring stations located at the outlet positions K2 and K3, respectively. Figure 2.9 displays the spatial relationship of the catchments to the air station as a whole.

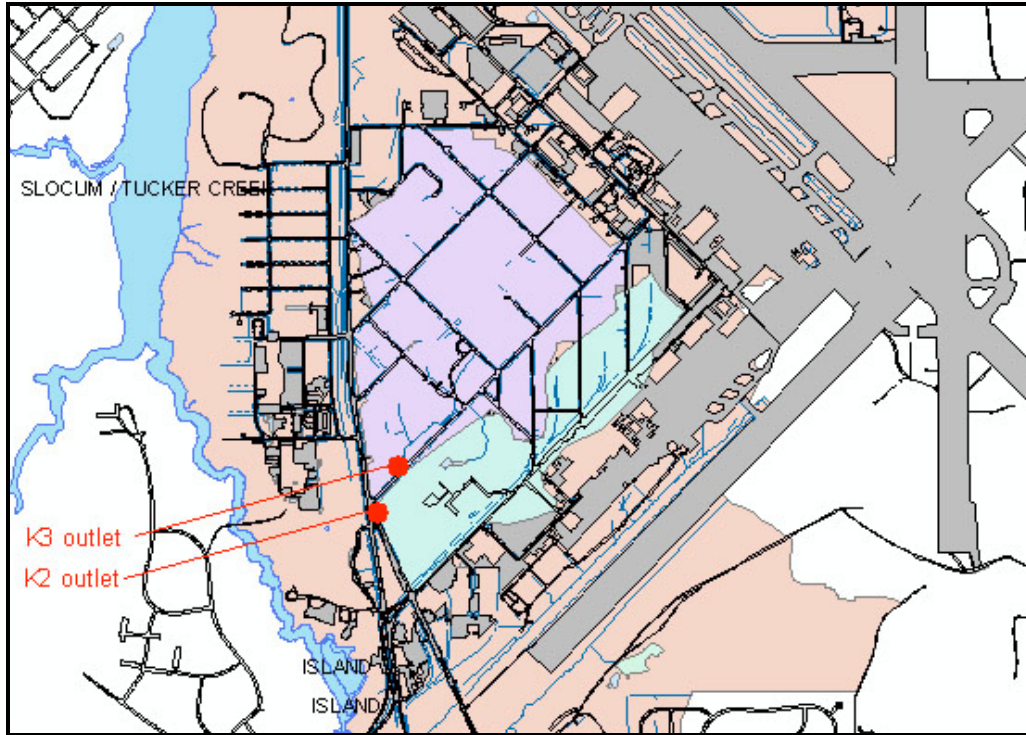


**Figure 2.9: Location Map for Catchments K2 and K3.** The above ArcMAP screenshot displays the location of catchments K2 and K3 in relationship to the industrialized section of Cherry Point MCAS (peach color).

Most of the industrial area of the military base is drained by two major tributaries of Sandy Branch that has its confluence less than one mile upstream of Slocum Creek, just west of Roosevelt Boulevard (Amatya et al 2001). Catchments K2, approximately 115 acres in area, and K3, approximately 259 acres, drain the northern and southern areas of the industrialized basin, respectively. The reported acreages are not equivalent to the values presented in Table 2B.1 (found in Appendix 2B) since the observed outlet was located upstream from the outlet point designated for CPEC's watershed delineation. Table 2.4 presents the land use types by area, for catchments K2 and K3, and displays the percent imperviousness.

**Table 2.4: Land Use Percentages for Catchments K2 & K3 at Cherry Point.**

Catchment K2	Land Use Type	Catchment K3
7.0 ac	<i>roads area</i>	14.5 ac
3.1 ac	<i>flight line area</i>	0.0 ac
40.0 ac	<i>parking lot area</i>	73.3 ac
11.8 ac	<i>buildings area</i>	27.7 ac
<b>53.8%</b>	<b>% impervious</b>	<b>44.6%</b>
115.0 ac	<i>total acreage</i>	259.0 ac

Catchment K2 is roughly 54% impervious and consists mainly of industrial buildings, parking lots, and other impervious structures. The outlet is formed by the intersection of two channels located several feet upstream of a gated, concrete culvert. The culvert travels underneath Roosevelt Boulevard and consists of three, 48-inch barrels, each equipped with a stainless steel sliding gate, manually operated by a twist-crank. Figure 2C.2 in Appendix 2C contains photographs of the K2 catchment outlet from the upstream and downstream perspectives.

Monitoring station K2 is unique because it is downstream of a wetland area with a wide floodplain, which normally results in retained water and relatively low flow rates during storm events (Amatya et al, 2001). The Division of Environmental Affairs has catalogued this discharge point as Outfall #116 (see Exhibit 2.2 in the Chapter Two Exhibits section). Due to its proximity to industrial areas, discharge from K2 has a heightened potential to transport hazardous materials via stormwater, apparently necessitating the installation of the control structure.

Catchment K3 is only 45% impervious and consists of buildings, parking lots, roads, and some vegetated areas. Exhibit 2H.1 in Appendix 2H displays a typical GIS exported attribute table highlighting several impervious regions. Maintained grassed areas surround the upstream section of the culvert, while the downstream section outlets into a wooded creek. Catchment K3 empties into the Sandy Branch Creek via a concrete culvert that consists of a triple-barrel system similar to outlet K2, but lacks the flood control structure (see Exhibit 2C.3 in Appendix C). The three 48-inch concrete barrels transport stormwater under Roosevelt Boulevard to an outlet

located several hundred feet downstream. The effluent reaches the Sandy Branch, enters Slocum Creek and eventually drains into the Neuse River.

A network of open channels and a subsurface conduit system support the catchment K3 drainage scheme. A majority of the upstream runoff travels through a piped system consisting of 18- to 36-inch concrete pipes, before reaching the main surface channel. MCAS has identified this point as Outfall #117 (see Exhibit 2.2). Initially, the URS Consultants (1996) studied the hydrology of area K3 in efforts to design retention basins to manage stormwater runoff (Amatya et al, 2001).

## **B. Rainfall**

### Recorded Rainfall Amounts

Annual rainfall amounts were calculated for the study period. The research began during September of 2000; therefore, there is only a portion of collected rainfall information for that specific year. The remaining two years, 2001 and 2002 were monitored continuously until the conclusion of the research. Table 2.1 displays the cumulative rainfall amounts from three separate sources.

One basic trend existed in the rainfall data based on the comparison of rainfall presented in Table 2.1. The unofficial, recorded precipitation from the Havelock location reported the greatest rainfall depth for all observed years and was included solely for comparative purposes. Likewise, the downloaded NOAA data was typically less than the Havelock airport amount but reflected more rainfall than the HOBO recorder. The automatic rainfall recorder recorded 6.21 more inches of rainfall than the NOAA method for 2001. Likewise, in 2002, the tipping bucket reported a cumulative, annual rainfall amount of 42.25 inches, while the NOAA dataset had an annual value of 46.56 inches. The NOAA and tipping bucket devices are approximately two miles apart and the differences in the observed rainfall depths are possibly due to spatial variability.

Table 2.5 presents the monthly precipitation recorded during the study period (excluding year 2000 since only partial data was collected) from three sources and compares the observed data to long-term monthly rainfall averages for Morehead City, North Carolina. The rainfall amounts from the 1) HOBO tipping bucket, 2) the official NOAA weather station and 3) the

unofficial Havelock airport weather station from September 2000 through December 2002 are displayed below. The tipping bucket database became the default rainfall file and would be eventually inserted into the hydrology model.

**Table 2.5: Observed Monthly Rainfall and the Historical Precipitation Averages for the Greater Havelock Region.**

Month	Morehead City, NC Monthly Rainfall Average (in)	2001			2002		
		Rainfall (in)	Rainfall (in)	Rainfall (in)	Rainfall (in)	Rainfall (in)	Rainfall (in)
		Havelock, NC	NOAA Cherry Point	HOBO Cherry Point	Havelock, NC	NOAA Cherry Point	HOBO Cherry Point
Jan	4.31	0.65	1.11	0.96	8.59	3.52	3.64
Feb	3.90	2.35	2.68	2.58	11.51	2.41	2.47
Mar	4.00	3.29	3.40	3.09	7.62	5.11	5.92
Apr	3.04	0.96	1.45	1.24	3.91	0.96	0.31
May	4.43	2.95	3.22	3.12	3.35	3.28	1.91
June	4.57	4.31	7.37	4.87	3.76	4.64	5.12
July	6.37	4.37	5.05	5.23	8.03	8.35	8.59
Aug	6.92	3.63	5.17	1.00	5.02	5.09	5.97
Sept	6.11	1.45	1.61	1.82	4.14	4.40	4.15
Oct	4.18	0.48	0.60	0.81	2.87	3.40	4.05
Nov	3.75	4.32	0.56	1.31	2.82	3.10	0.10
Dec	3.98	18.04	1.36	1.34	2.18	2.30	0.02
<b>annual total</b>	<b>55.83</b>	<b>46.80</b>	<b>33.58</b>	<b>27.37</b>	<b>63.80</b>	<b>46.56</b>	<b>42.25</b>

Historically, Cherry Point, North Carolina, annually receives more than 50 inches of rainfall; therefore, the study period represents a less than average rainfall period. The Morehead City weather station is located approximately 20 miles southeast of Cherry Point and was used to present the long-term precipitation averages for the region. The precipitation data from the Havelock airport has been included to show spatial differences in the rainfall distribution. In years 2001 and 2002, the weather station at the Havelock airport recorded substantially more rainfall than the tipping bucket gauge or the weather station at Cherry Point MCAS. Annual precipitation amounts of 46.80 and 63.80 were reported at Havelock for years 2001 and 2002. A reading of 18.04 inches of rain was reported in December 2001 and a 11.51 value was recorded for February 2002 at Havelock. The NOAA value for the same month (December 2001) was 1.36 inches and the tipping bucket reported 1.34 inches of rainfall. Likewise rainfall amounts of approximately 2.4 inches were collected by both the tipping bucket and the Cherry Point gauges in February 2002. Therefore, it is suspected that the 18.04 and 11.52 readings are false since neither of the other gauges reflected the same trend. If the 18.04 value at Havelock was reduced to 1.80, the total rainfall amount for 2001 would be decreased to 30.56 inches for 2001, which relates better to the Cherry Point data.

*Observed Storm Frequency and Rainfall Intensities*

Average, 24-hour rainfall intensities were calculated for storm events having return periods ranging from 2 to 100 years by dividing the total precipitation by the storm duration. Table 2.5 summarizes the expected rainfall intensities for several 24-hour return period storms for the Morehead region of North Carolina. This information was used to characterize the types of storm events witnessed during the study period at Cherry Point MCAS.

**Table 2.6: 24-hour Design Storm Intensities for Morehead City, NC.**

<b>Return Period</b>	<b>Average Intensity (in/hr)</b>
2 yr	0.21
5 yr	0.23
10 yr	0.31
25 yr	0.36
50 yr	0.40
100 yr	0.45

An analysis of the collected rainfall was completed to characterize the rainfall intensities and return frequency of several selected storm events. The selected storms correspond to the calibration and verification events described in Chapter Three.

A simple method was used to determine the intensities where the storm event precipitation was extracted and divided by the storm duration to calculate rainfall intensity. Only the HOBO tipping bucket intensity calculations are discussed in this section because the NOAA recorded data was only available in hourly increments, meanwhile the HOBO values were breakpoint data. The tipping bucket data recorded the actual start time of the rain event and continuing recording information until no additional rainfall occurred below the 0.01 inches of rain threshold. The NOAA data only displayed daily precipitation, so events occurring during any portion of the calendar date were summed and reported only a daily basis; thus, the storm rain depths were divided by durations that were typically longer than the actual storm duration. Since only a day time step was reported, if a storm spanned longer than 24 hours, a 48-hour storm duration was used to calculate the NOAA related intensity, resulting in a decreased, average rainfall intensity for that event.

The calculated intensities were also compared to the Morehead City design storm intensities for selected events. For catchment K2, the most intense storm was recorded on Julian day 6 in 2002, having a rainfall intensity of 0.28 in/hr which exceeded the 5-yr return period storm intensity of 0.23 in/hr. The remaining five storms, for catchment K2, all had intensities less than 0.21 in/hr which is the expected intensity for a 2-yr design storm.

Since different storm events were evaluated for catchments K2 and K3, several storms for catchment K3 had intensities greater than those for catchment K2; thus, events 175 (2001), 133 (2002) and 6 (2002) all had intensities that surpassed the 5-yr intensity rate of 0.23 in/hr. Events 175 (2001) and 133 (2002) produced 0.88 and 0.65 inches of rainfall, during 3.84 and 2.4 time spans, respectively. The remaining four storms for catchment K3 resulted in intensities failing to exceed the 2-yr intensity level or 0.21 in/hr.

Cumulative rainfall amounts for all storms were examined, particularly for the three events with return periods greater than 2 years. Storm #175, which occurred in 2001, delivered 0.88 inches of precipitation over 3.84 hours. Storm #6 (2002) contributed 0.68 inches of rainfall in a 2.4 hour time span. Also in 2002, storm # 133, produced 0.65 inches of rain over a time period of 2.4 hours.

### *Rainfall Spatial Variations*

During the research period, it became evident that rainfall monitoring position and storm movement can directly affect the amount of precipitation recorded at a given location. Therefore, the spatial distribution of the observed rainfall was examined to detect the similarities, or differences, between the three sets of precipitation data. Some research suggests (James and Huber 1999; XP Software, 2004) positioning rainfall measurement devices at each monitored outlet to combat locality differences. Further discussion regarding rainfall distribution as related to hydrologic modeling is presented in Chapter Three.

### *Rainfall Distribution*

An additional analysis was performed to characterize the measured rainfall distribution at Cherry Point. The distribution analysis was based on two sets of records: 1) the data

downloaded directly from the HOBO gage, and 2) the NOAA precipitation information collected from the NOAA website.

The SWMM user-defined rain (consisting of formatted HOBO data that was readable by SWMM) was imported into Microsoft Excel, summed on an hourly basis and graphed. Using the auto filter command, sums greater than zero were selected (since the HOBO data did not contain zero values for comparative purposes), copied, pasted into a new worksheet, and organized by year. The Analyse-it add-in software was downloaded ([www.analyse-it.com](http://www.analyse-it.com)) and used to complete the rainfall characterization.

Initially, only normal distributions were explored since Analyse-it is not capable of performing non-linear analyses. However, Analyse-it is capable of completing several variations of normality tests. Two test methods for normal distribution were used, 1) the Anderson-Darling method and 2) the Shapiro-Wilk method. According to Stephens (1974), the Anderson-Darling method is used to test if a sample comes from a specific distribution and gives more weight to the tails of the distribution than other test methods. The Shapiro-Wilk test calculates a statistic that tests whether a random sample comes specifically from a normal distribution; smaller test values represent a decreased deviation from normality (Shapiro-Wilk, 1965). Using the Analyse-it software, the Anderson-Darling and Shapiro-Wilk tests were completed. Exhibits 2K.5 through 2K.8 are the actual outputs generated using the spreadsheet extensions for the Anderson-Darling and Shapiro-Wilk investigations. These four exhibits characterize the tested sample and provide graphics that describe the distribution of the rainfall under normal analyses. Table 2B.2 in Appendix 2B summarizes the results the normal distribution findings.

The lognormal testing procedures were completed using the XLStat add-in. The XLStat extension is very similar to Analyse-it but requires correctly formatted datasets for successful program execution. Exhibits 2K.9 and 2K.10 display the spreadsheet extension calculation, using the lognormal approach. Table 2B.3 in Appendix 2B summarizes the lognormal distribution testing results.

From the results presented in Tables 2B.2 and 2B.3, the synthesized rainfall can exhibit a normal or lognormal type distribution. Most commonly, rainfall is considered to be normally distributed but a mixture of distributions is not uncommon to rainfall characterization. Due to the occurrence of raindrop particle size differences coupled with dynamic storm movement, rainfall clustering and bunching can alter localized rainfall intensities at ground level (Jameson and Kostinski, 1999).

The purpose of the rainfall distribution analysis was to first characterize the rainfall observed during the study period. Since rainfall is the sole generator or input for the model, it would be helpful to understand how this input dataset was distributed over time. The rainfall characteristics might become helpful while conducting an uncertainty analysis as a result of variability in rainfall distribution in the SWMM model. Likewise, the distribution of the rainfall can be used to represent rainfall patterns within the hydrologic model, if needed.

### C. Catchment Outflows

#### *Stage-Discharge Relationships*

The generated regression equations (fitted trendlines) were formed from the measured stage and flow data. For this study, a time span of approximately two days was used, from Julian day 48 to 50. Both catchments were examined independently and the results differed. All reference graphs are located in Appendix 2J.

Using the 2001 data for catchment K2, including all points, the following third-order polynomial equation was found as the best fitted trend line:

$$Y = -7.6137 X^3 + 31.911 X^2 - 8.7645 X + 1.0577 \quad (\text{R-squared: } 0.599) \quad \text{EQ 2.3}$$

Where Y = outflow (cfs)

X = stage (ft)

The problem was approached again after removing seemingly erroneous outliers (see Exhibit 2J.1 of Appendix 2J). The new equation was then:

$$Y = -7.495 X^3 + 31.988 X^2 - 9.338 X + 1.1621 \quad (\text{R-squared: } 0.696) \quad \text{EQ 2.4}$$

Using a threshold value equal to the height of the v-notch weir (one foot), a piecewise interpretation was considered; yielding the following equations (see graphs 2J.03 & 2J.04):

if stage < 1 ft (0.3m) then (see Exhibit 2J.2 of Appendix 2J),

$$Y = 55.544 X^3 - 52.071 X^2 + 19.51 X - 1.2132 \quad (\text{R-squared: } 0.426) \quad \text{EQ 2.5}$$

if stage  $\geq$  1 ft (0.3m) then (see Exhibit 2J.3 of Appendix 2J),

$$Y = -7.6268 X^3 + 28.909 X^2 - 4.9607 X + 6.5205 \quad (\text{R-squared: } 0.559) \quad \text{EQ 2.6}$$

The piecewise formulas, in conjunction with the weir equation values and the flow meter dataset, were used to create a comparative outflow plot (see Exhibit 2J.4 in Appendix 2J).

Catchment K3 received similar treatment and yielded the following overall equation including all points:

$$Y = 4.8738 X^3 - 9.766 X^2 + 13.702 X - 2.6929 \quad (\text{R-squared: } 0.641) \quad \text{EQ 2.7}$$

Upon removing the outliers, the equation fitted such that (see Exhibit 2J.5 in Appendix 2J):

$$Y = -0.7567 X^3 + 13.168 X^2 + 2.0203 X - 1.2084 \quad (\text{R-squared: } 0.850) \quad \text{EQ 2.8}$$

The piecewise equations are as follow:

If stage  $<$  1ft (0.3m) then (see Exhibit 2J.6 in Appendix 2J),

$$Y = -15.409 X^3 + 45.448 X^2 - 18.77 X + 2.2913 \quad (\text{R-squared: } 0.852) \quad \text{EQ 2.9}$$

If stage  $\geq$  1 ft (0.3m) then (see Exhibit 2J.7 in Appendix 2J),

$$Y = 29.051 X^3 - 191.16 X^2 + 419.16 X - 253.52 \quad (\text{R-squared: } 0.848) \quad \text{EQ 2.10}$$

Exhibit 2J.8 in Appendix 2J provides a visual comparison of the conventional weir equation results, the observed flow meter rates, and the implemented polynomial equation.

The purpose of the regression analysis was to develop a stage discharge relationship for two small catchments. The developed equations could be used to fill in missing data or to repair erroneous data. The equations developed for catchment K2 had a lower, average R-squared

value of 0.560 when compared to the average value of 0.850 for catchment K3, meaning the K3 trendlines fit the datasets better. The difference in the goodness-of-fit is possibly due to the flow meter's performance in estimating flow characteristics during low flow conditions. The observed flows for K2 are significantly less than the outflows measured at the catchment K3 outlet.

Upon graphing the solutions, the K2 predictions seemed to be over calculated (several cfs above the weir baseline) during periods of low flow (refer to Exhibit 2J.4 in Appendix 2J). The K3 results seemed statistically better, displaying a stronger relationship between the weir equation and the flow meter results (see Exhibit 2J.8 in Appendix 2J), although over-prediction during low flows was still prevalent. The process of eliminating "outliers" was completed on a visual judgment basis for stage values less than one foot, and supported by the belief that the flow meter did not record values accurately during low flow conditions, especially for flows less than 25 cfs. Outlying stage values greater than one foot were also eliminated if the corresponding flow rate seemed unrealistic provided the water stage height.

This investigation was helpful in comprehending the composite flow profile for the year 2001. Unfortunately, during some storm events, one or both instruments failed. Refining this analysis and employing the empirical equations would assist in retrofitting missing data. By combining this continuous flow database with the associated rainfall records, a better representation of rainfall-runoff conditions would be achieved.

#### *Generalized Flow Characteristics of Observed Hydrographs*

Exhibits 2.6 through 2.9 are the instantaneous hydrographs, created from the combination of the stage data using the v-notch weir equation and the downloaded information from the flow meter. The largest outflow rate of 83.9 cfs on catchment K2 occurred on Julian day 243.4, in 2001. In 2002, a maximum outflow rate of 230 cfs, for catchment K2, occurred on Julian day 207.7. The largest storm in 2001, for catchment K3, was observed on day 167 with an outflow rate greater than 238 cfs. The greatest outflow rate in 2002, for catchment K3 also occurred on Julian day 207.7. The v-notch weir equation estimated the outflow at nearly 603 cfs for this 2002 storm event. This 603 cfs value is suspected to be incorrect, since the weir was probably submerged at the recording of the peak rate, but remains reported since the flow meter was also malfunctioning. Keeping all factors constant, it can be hypothesized that the precipitation recorded in 2002 generated greater runoff volume for the study area, in comparison

to 2001. Table 2.1 supports this assumption since the annual rainfall amount for 2001, using the HOAA data, was 33.58 inches, as opposed to 46.56 inches in 2002.

The 2001 and 2002 composite hydrographs for catchment K2 displayed specific trends between the two monitored years. The largest precipitation was measured between Julian days 148 and 248 during 2001. This 101-day time span produced thirteen storm events with outflows exceeding 30 cfs. Also during 2001, two events occurring near Julian days 63 and 80 produced sufficient runoff to generate flow rates greater than 30 cfs. For 2002, days 166 through 292 in catchment K2 generated a majority of the larger precipitation events having five storm events with outflow rates greater than 30 cfs. Storms 62 and 72 from 2002 also recorded enough rainfall to create flow rates at the outlet surpassing the 30 cfs mark. A collection of erroneous data was graphed in the earlier portion of year 2002 due to incorrect stage data that was not replaced by flow meter readings during day 2. Most of the storm events had durations less than 24 hours, with intensities equal to or less than that expected from a 5-yr, 24 hour design storm. When observed at the 48-hour scale, the hydrographs for a majority of the catchment K2 storms have a slightly pointy shape, reaching the peak outflow in less than one hour, before the flow rates achieved the peak value and consequently began to subside resembling the negatively sloping portion of the typical bell-shaped curve.

Similar to catchment K2, the storm events observed at the outlet of catchment K3 had noticeable characteristics. The larger storm events for this catchment occurred during the middle of the year, for both monitored years. For year 2001, the larger precipitation depths were recorded between days 143 and 246, almost equaling the time span highlighted for catchment K2. Approximately, thirteen storms events were also recorded during this time span, each resulting in outflow rates than 30 cfs. Prior to Julian date 143, three storm events were identified having observed flow rates greater than 30 cfs during year 2001. Year 2002 demonstrated a similar trend, having a majority of the larger storm events occurring between days 166 and 253. In addition, five storms were reported prior to Julian day 136, having outflow rates greater than 30 cfs for year 2002. Exhibit 2.9 displays some seemingly high outflow rates occurring on Julian days 166, 207, and 240. These flows were calculated from the application of the v-notch weir equation using the stage measurements since the flow meter data was unavailable after day 165. It is speculated that the weir was submerged during these high flows, therefore, the flows generated from the weir equation remain questionable. To compensate for this breach in observed data, the regression analysis described previously could be implemented. Nonetheless,

Exhibit 2.9 shows only the data collected from the flow meter and the calculated outflow rates using the weir equation, which was initially reserved for low flow conditions.

The composite, annual hydrographs for catchments K2 and K3 were analyzed to discuss the trends, or potential errors, exhibited by the flow data. These outflow rates will be used later for the calibration and validation of individual and continuous storm event hydrographs. The precipitation recorded during the study period was below the 55.83 inch long term average for Morehead City, North Carolina, therefore, a “normal” annual record of rainfall data would possibly generate higher flow rates than those presented during this study. In conjunction, the research team was interested in investigating how much outflow the storm events generated, provided the amount of rainfall observed. Table 2.7 is a collection of rainfall and outflow data for several storm events from 2000 through 2002.

**Table 2.7: Cherry Point Rainfall to Outflow Relationships for Selected Storms in Catchments K2 and K3.**

<b>K2 Catchment Selected Storms</b>				
<b>Year</b>	<b>Storm Event</b>	<b>Observed Rainfall (in)</b>	<b>Observed Peak Outflow (in)</b>	<b>Outflow/Rainfall %</b>
2001	143	0.76	0.051	6.71
	327	1.14	0.021	1.84
2002	6	0.69	0.037	5.36
	72	2.25	0.104	4.62
<b>K3 Catchment Selected Storms</b>				
<b>Year</b>	<b>Storm Event</b>	<b>Observed Rainfall (in)</b>	<b>Observed Peak Outflow (in)</b>	<b>Outflow/Rainfall %</b>
2000	324	0.65	0.0096	1.48
	348	0.24	0.014	5.83
2001	115	0.6	0.0048	0.80
2002	38	1.67	0.031	1.86
	72	2.25	0.13	5.78
	150	0.95	0.006	0.63

Table 2.7 demonstrates the relationship between the rainfall and the observed outflows for several storm events in catchments K2 and K3. The table only lists the day of the event and

the maximum outflow experienced during that event only. Storm duration was not included in this presentation and has importance to the observed outflow rate due to the rainfall intensity characteristic. Nonetheless, Table 2.7 does display the overall capability of each catchment to generate runoff/outflow, based upon the measured rainfall.

From Table 2.7, the highest outflow to rainfall ratio was achieved by storm 143 of 2001, which occurred in catchment K2. The 0.76 inches of precipitation generated 0.051 inches of outflow. The average outflow to rainfall ratio for catchment K2 was 4.63. The largest ratio calculated for catchment K3 occurred during storm event 72 of 2002. The 0.24 inches of rainfall generated 0.13 inches of runoff and a corresponding outflow to rainfall percentage of 5.78. The average runoff ratio for catchment K3 during the study period was 2.73. Catchment K2 was able to generate more outflow than catchment K3 considering the observed precipitation and outflow results. These results are expected since catchment K2 is more impermeable than catchment K3 (54% imperviousness for catchment K2 versus 45% imperviousness for catchment K3), therefore, more runoff would be expected to be generated from catchment K2.

#### *Flow Distribution*

A flow distribution investigation was also conducted for catchments K2 and K3. Using the measured flow data from these two areas, and limiting the analysis to flows greater than 3 cfs, two statistical tools were employed to determine the type of distribution that best described the observed flow data. The examined flow information was collected using two different temporal situations. The stage recorder only collected changes in water surface elevations that surpassed a 0.001m threshold during three-minute intervals. Contrarily, the flow meter was programmed to record flow information in ten-minute increments. Therefore, the resulting flow distribution data had varying time intervals, ranging from 3 to 10 minutes.

The distribution investigation was based on flow estimates using the composite information. Using the Auto-filter command in Microsoft Excel, composite flows were organized and exported into a new worksheet by only selecting flow rates greater than 3 cfs. For area K3, which is larger in size than area K2, a 4 cfs minimum was established because the 3 cfs threshold was unsatisfactory; the statistical tools could not accommodate such a large dataset. The normal distribution examination was completed using the Analyse-it add-in, while the lognormal observations were completed using the XLSTAT program.

For area K2 there was little difference between the normal and lognormal distribution. Using 1513 observation points, a mean value of 20.021 cfs with a variance of 1354.04 was reported for both types of distribution. Area K3 also exhibited little differences between the two types of distribution. The normal distribution for K3 yielded a mean of 27.648 cfs with a variance of 2783.65, from 3634 points. The lognormal distribution for the same data yielded an estimated mean of 23.177 cfs with an associated variance of 2356.61. In most cases, flow exhibits a lognormal distribution. Therefore, it seems reasonable to assume that the lognormal distribution fits the K3 flow data better. For area K2, it would be safe to remark that the data is impartial to either distribution.

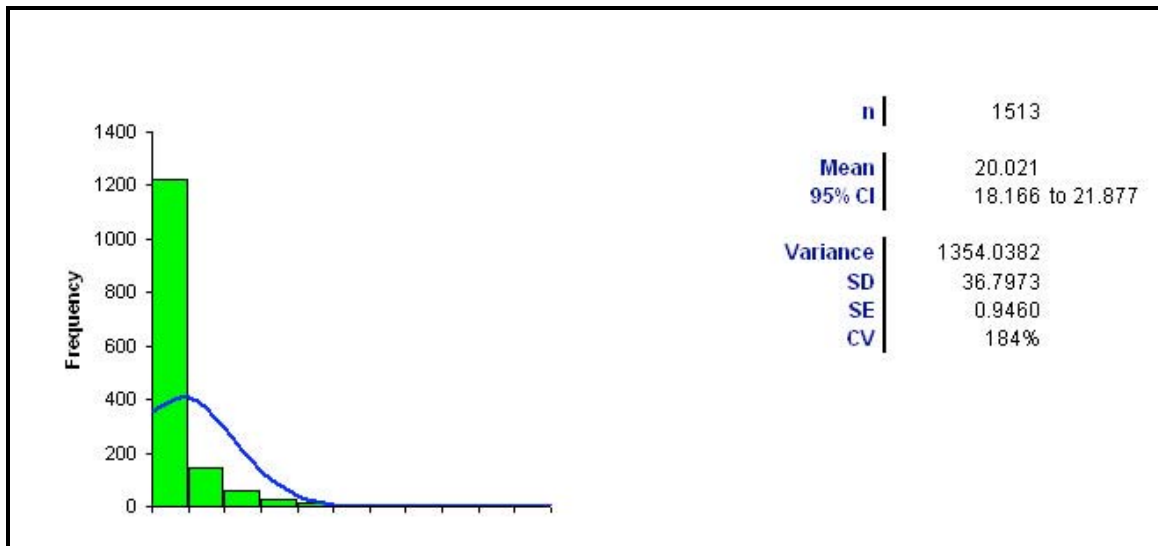


**Figure 2.10: Catchment K2 Normal Flow Distribution.** The above graphic is the flow distribution generated from the observed outflow data for catchment K2 at Cherry Point MCAS utilizing the Analyse-It software.

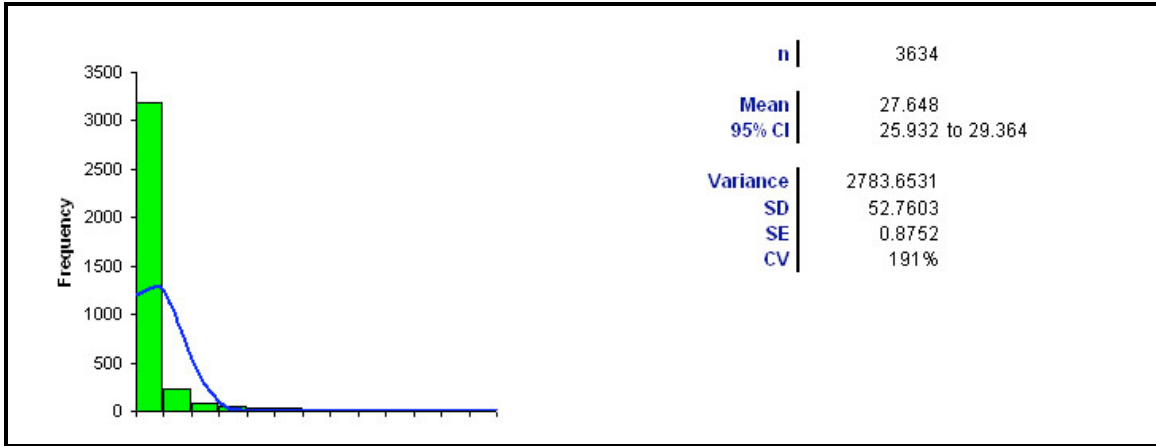


**Figure 2.11: Catchment K3 Normal Flow Distribution at Cherry Point MCAS.** The above graphic was created using the Analyse-It software and the outflows calculated from the stage recorder and flow meter at the K3 monitoring location.

#### *Flow Frequency-Duration*

Using the measured flow data from basins K2 and K3 a frequency-duration study was conducted on a uniform temporal scale. The created graphs were compared graphically and several conclusions were made based on test statistics.

The base information used for this study was a continuation of the flow distribution analysis. The Analyse-it add-in was utilized to generate a normal probability plot with confidence intervals of 95% and 99%. The flows from area K2 are once again limited to a 3 cfs minimum. Similarly a 4 cfs minimum was used for area K3.

Considering a 95% confidence interval, a value of 25cfs or less has an exceedance probability less than 25%. Meaning, flow rates greater than 25cfs should not be witnessed more than 75% of the time. The K2 peak flow rates associated with 95% and 99% confidence intervals are 18.2 cfs and 17.58cfs, respectively. The exceedance probability for flows greater than 25 cfs for area K3 is also about 25%. The peak flow rates for area K3 at the 95% and 99% testing levels are less than 25.93 cfs and 21.30 cfs, respectively.

### *Impact of Site Characteristics on Hydrology*

Noticeably, some differences exist between the two catchments. Possible reasons for the disagreement between the two basins are the runoff components of each basin and the precipitation inputs. Catchments K2 and K3 are not identical and the physical parameters such as percent imperviousness, characterize this point. Table 2.4 highlights the differences by land use area and displays the total acreage of the two study catchments. Area K2 has more wooded area than K3 and therefore, has increased water retention and retardation capabilities. Considering this, the peak rates predicted for area K2 should be less than those values estimated for K3. In addition, spatial distribution of rainfall on each catchment is a possible culprit to spatial precipitation variations. The interception effect of trees with leaves is also possible during warmer months. Nonetheless, a 3 to 4cfs fluctuation in the catchment outflow rates may prove to be negligible when considering the fact that these areas have peak outflow rates greater than 100 cfs.

In addition, the flow paths for the two catchments are uniquely different. The prominent main channel for catchment K2 is longer than 5000 feet long, having an elevation difference of about 22 feet. The flow for catchment K2 is primarily routed via surface channel, excluding the occasional culvert and short piped section. On the other hand, the main channel for catchment K3 is nearly 7000 feet in length, with a measured change in height of approximately 18 feet. A large portion of the upstream runoff for catchment K3 is conveyed via concrete pipes. The midsection of the channel is a mixture of surface channels and piped sections, while the downstream portion is mostly open channel flow. The characteristics of the conveyance method, whether open channel or piped sections, will have an effect on the travel times and the movement of pollutants via surface waters. In addition, the overall length of the main channel influences the time of concentration value. Long surface channels, with high roughness values, will ultimately reduce the time to peak, retarding the downstream progression of surface runoff, increasing the overall travel time. The subcatchment imperviousness and channel properties will be discussed in Chapter Three as related to the modeling procedures.

#### **D. Discussion**

One major concern during the data acquisition period was the recorded rainfall. Although several manual gages were scattered throughout the site, precipitation differences existed. Spatial differences in rainfall generally occur in this coastal plain region as reported by Amatya (et

al 1996). If a difference was noticed, the adjacent, manual gage was examined against the automatic rain gage. The number of over- and under-accumulation periods was nearly equal. Problems such as human interference and wildlife activities were suspected reasons for further discrepancies. Allegedly, air station employees occasionally and inappropriately emptied manual gauges located near office building before the research staff could document the accumulated rainfall depths. Also, urine and other animal waste products were noted during station visits.

An additional concern with the collected data was the unreliability of the flow meter during low flow periods. Although the flow meter was not the primary measuring device during periods of reduced flow, the values generated from the meter seemed unreasonable at times. It is arguable that some Doppler meters do not function well in clear water (Sontek, 2005). The flow rate measured by a Doppler meter is directly related to signal strength and the acoustics of the medium. The signal strength, recorded at the receiver, is a measure of the intensity of the reflected acoustic signal and the primary function of signal strength data is to verify that there is sufficient particulate matter in the water (Sontek, 2005). If the water is too clear, the return signal may not be stronger than the ambient noise level of the electronics, thus, the Doppler meter is unable to make accurate velocity measurements (Sontek, 2005). Likewise, insufficient water depth above the Doppler sensor possibly generated erroneous measurements.

Another concern deals with the outflow rates determined by the flow meter. The outflow rates calculated by the flow meter (in one barrel) were multiplied by the number of barrels present at the culvert to obtain total flow rate, but the barrels had slightly different elevations. The monitored barrel had the lowest elevation. It was assumed that the flow rates of the other barrels equaled the observed flow rate in the monitored barrel. In actuality, this probably did not occur, although eventually flow did pass through each barrel once the required stage height was achieved, which should be expected to be less than the outflow value in the monitored barrel. So, the total, summed outflow rate per outlet, using the flow meter data, will likely be higher than the outflow rates observed at the physical location. In addition, once the model simulations begin, the flow meter outflow rates that will be inserted into the composite flow spreadsheet will probably indicate larger flows than what actually occurred, so the resulting simulated outflow will over-predict the measured data.

The outflows generated from several storm events are presented in Table 2.7, also highlighting the measured rainfall during the particular storm event. Interesting enough, a person would suspect for more precipitation to generate more outflow at the catchment outlet.

Theoretically, this assumption would be correct, provided that all other variables remained constant, most importantly time. The outflow rates provided in Table 2.7 range from 8.9 cfs to 196.9 cfs. For example, in 2001, storm event 143 in catchment K2 provided .76 inches of rainfall over a time period of 12.24 hours and the a maximum outflow rate of 20.5 was observed. Storm event 6 (2002), also occurring in catchment K2, delivered .69 inches of precipitation and generated a maximum outflow rate of 25.8 cfs, having a storm duration of only 2.4 hours. By dividing the precipitation depth by the event duration, a generalized rainfall intensity can be calculated. The average intensity for the 2001 event is .062 in/hr and the intensity for the 2002 example is 0.29 in/hr. Although the amount of rainfall was nearly identical for the two events, and the outflow rates similar, the storm durations and rainfall intensities varied greatly. Therefore, only examining the outflow and precipitation values only provides a partial understanding of what occurred during each storm event. Rainfall intensity becomes extremely influential in the hydrologic and hydraulic processes experienced during the storm events, affecting such phenomena as percolation, overland flow, time to concentration and the overall travel time of soluble substances via surface waters. Rainfall intensity will continue to influence the study as the rainfall is inserted into the hydrologic model since the parameters used to describe surface runoff, percolation, and evapotranspiration are determined by the model. In addition, the time interval of the modeling sequences need to allow sufficient time for these processes to cycle completely.

#### **IV. Summary and Conclusions**

The Department of Environmental Affairs at the Cherry Point Marine Corps Air Station was interested in classifying and cataloging the effluent entering into the surrounding surface waters due to water quality concerns. Both Hancock and Slocum Creeks are tributaries to the Neuse River system, which is a major environmental concern area for the State of North Carolina. Thus, the Department of Environmental Affairs employed researchers from the North Carolina State University Biological and Agricultural Engineering department to develop a stormwater runoff model that would be capable of simulating water movement and predicting the travel time of water soluble substances at the air station.

From November 2000 to December 2002, flow and weather data was downloaded from various instruments, including flow meters, stage recorders, and rain gauges. The Schoolhouse Branch of Cherry Point became the main focus, since the all the industrial surface runoff drained into this area. Recall that the research intent is to realistically predict the movement of water

soluble pollutants exiting specific locations within the industrial portion of the Cherry Point using a stormwater hydrology model. In order to effectively accomplish this goal, information describing the topography of the study site needed to be gathered and processed. Combining the traditional surveying information completed by previous firms, and the GPS information provided by the CPEC, Inc., the research area was identified. CPEC's drainage area E was further examined, using both digital terrain maps and manual inspection, finally forging the delineation of the two interest areas, catchments K2 and K3. Catchment K2 and K3 were then aggregated into smaller subcatchments that were attributed during on-site field visitations and off-site, using geoprocessed information in ArcMAP. An expansive collection of land usage, hydrologic, drainage, soils data and weather information was compiled for insertion into SWMM and XPSWMM to characterize catchments K2 and K3 for modeling purposes, as shown in Chapter Three.

The weather collection process included gathering precipitation data from various sources, such as the Havelock airport, the HOBO tipping bucket rain gauge and the NOAA weather station located at the Cherry Point control tower. Although differences existed between the three devices, the tipping bucket data became the default rainfall database and was examined against the NOAA data to explain discrepancies between reported rainfall depths. The tipping bucket rainfall data is more suitable for modeling since the gauge recorded incremental precipitation easily integrates with the timing requirements of SWMM. Therefore, a direct data link between the hydrologic model and the recorded rainfall was created. Meaning, when the user selects the simulation time interval, the corresponding recorded rainfall depths are then referenced, instead of having SWMM interpolate rainfall over specific simulated time periods. Thus, the user-inputted rainfall database may be considered one of the most important aspects of the hydrologic model, since it contains the input which is transformed into surface runoff, which in turn dictates soluble substance movement in surface waters.

Flow measurements were completed physically and empirically. Using the ultra-Doppler flow meter, water measurements were recorded and downloaded during site visits. The microprocessor was utilized to collect water stage measurements in conjunction with installed weirs at the catchment outlets. Using the appropriate weir equation, the stage elevations were converted into flow measurements. Once weir submergence occurred, which was speculated to occur at a head value of 1 ft. (approx. 0.3m), the weir equation was abandoned, and the flow meter measurements became the default until the rise in head subsided. A collection of flow data, named "composite flow" data was developed from the combination of the stage recorder

and flow meter datasets. An additional regression analysis was conducted to demonstrate the relationship between the water stage and outflows such that when a lapse in flow data occurred, a piecewise function could be used to estimate the resulting outflows using the recorded stage elevation. Combining the “composite” flow spreadsheets with the piecewise, regression equations created a continuous outflow dataset for each observation year which would eventually be used to calibrate and evaluate the prediction capabilities of SWMM within the industrialized portion of Cherry Point.

Recall that the purpose of Chapter Two was to describe the study site characteristics while introducing the field monitoring apparatus and explaining the acquisition of the surface water measurements. The study site characteristics were analyzed and described using the GIS and field survey information. The stage recorder, flow meter and rainfall gauge data was presented and commented on earlier, highlighting anomalies. Nonetheless, upon reviewing all the collected data, several conclusions were developed.

The study period did not experience the historical rainfall average for Cherry Point which is typical more than 50 inches. The observed precipitation amounts for years 2001 and 2002 were only 27.37 and 42.25 inches, respectively. Therefore, the future model simulations, using the collected rainfall data, will possibly predict peak outflows less than the historical averages. In this situation, the incorporation of return-frequency rainfall information may be needed to successfully predict outflow reflecting historical averages. In addition, the spatial distribution of the observed rainfall could possibly become a major modeling issue since only one rain gauge was used to represent the entire study site, but recorded differences in rainfall depths were noticed across the air station.

In addition, catchments K2 and K3 have differing main channel characteristics that will effect the overall travel time and transportation of soluble substances via surface waters. The major channel associated with catchment K2 consists mostly of vegetated waterways while catchment K3 has a mixture of piped sections and natural channels. The importance of the channel attributes will be further discussed in the modeling section of this thesis.

Permeability and catchment delineation also have a strong impact on the amount of rainfall that was transformed into runoff and how the runoff is routed to the main channel. The topography was used to create ridgelines, denoting the separation between catchments and subcatchments. The created areas varied slightly from other research since this hydrologic study

incorporated the influence of roadside culverts into the runoff routing scheme. The ArcMAP data was used to determine the soil hydrologic units on the catchment and subcatchment levels using GIS extensions. From this activity it was determined that catchment K2 is more impermeable than catchment K3, therefore, more runoff is expected to be generated by catchment K2 on a percentage basis. The average outflow-to-rainfall ratios presented in Table 2.7 reinforce this point.

The site characteristics, recorded rainfall, and the quality of the observed flow data gain heightened importance once inserted into the hydrologic model for simulation. The delineated areas and the measured data must accurately reflect the natural system in order to ensure solid predictions. Chapter Three further discusses the SWMM and XPSWMM modeling efforts, focusing on the calibration and validation efforts needed to create the collection of user-selected inputs that best describes the hydrology of the Cherry Point Marine Corps Air station.

## **Chapter Three: Calibration and Validation of SWMM and XPSWMM on Two Catchments within the Marine Corps Air Station at Cherry Point**

### **I Introduction**

Prior to 1996, there was limited work to document the effects of storm water runoff on pollutant transport within the air station. No previous research had examined the natural transport capabilities of selected streams. In 1996, the Marine Corps Air Station Division of Environmental Affairs hired the URS Consultants to perform an analysis of options for regional storm water management in a core area of the air station. The URS study suggested a number of best management practices (BMP) to control or reduce pollutant movement to downstream locations. The final URS recommendation called for the construction of a wet detention pond, equipped with a filtration system. The consultant applied the EPA Storm Water Management Model (SWMM) with XP Graphical Interface (XP-SWMM) to route a 10-yr design storm and generate the corresponding runoff hydrograph for the industrial portion of the air station. These SWMM simulations were the first generation of stormwater predictions, focused mainly on the industrialized section of the base that was the forerunner to the hydrologic study discussed in this chapter.

The study focus is to predict and track stormwater and pollutant movement in the industrialized portion of the air station using a GIS-based hydrologic/hydraulic modeling approach. Such an approach requires a detailed understanding of the spatial characteristics both of the watershed as well as the pipe conduit and stream channel flow paths.

#### **A. The Utilization of Spatial Data in Hydrologic Modeling**

Geographic Information Systems (GIS) and Global Positioning Systems (GPS) are commonly used to augment traditional land surveying techniques to provide users with spatial data and a powerful array of decision-making tools within the digital realm. The global positioning systems technology allows a user to instantaneously acquire spatial coordinates in real-time. The GPS information is later embedded into a GIS, which manages the data and adds functionality.

The GIS data will be used to characterize the study basin in terms of physical attributes, including topography, soils, land use, impervious areas, and dominant flow paths such as major

channels and streams. The GPS portion of the research was used to verify the existence of stormwater features like surface inlets/outlets and pipe conduits, specify stream positions, and outline the perimeter of water bodies. In addition, the GPS database contained the attributes that would eventually be inserted into SWMM, including flow direction and channel measurements. Therefore, the GPS and GIS databases are essential for the flow routing and consequently (when coupled with the rainfall-runoff transformation) will be crucial elements in determining pollutant movement and the travel time calculated between outlet points.

### *Estimating Flow Routes from Ground Topography*

Flow routing can be derived from topographic maps, aerial photos or existing drainage system maps. Topographic maps having contour intervals of one or two feet are extremely useful for land slope interpretations, especially in flat lands like the one studied herein. Unfortunately, maps of this resolution are not always available; thus, the standard 1:24,000 scale USGS topographic quadrangles become the only practical alternative. In recent years, the availability of topographic information has dramatically increased with the introduction of online map databases. The USGS topographic information for the study site was used to delineate watershed, catchment, and subcatchment boundaries with the aid of additional tools. The techniques used to discretize the subcatchment areas will be discussed.

Once the resources have been located, data quality and reliability may become major concerns. At the time, many municipalities owned copies of the construction plans, but the majority of these cities did not possess the “as-built” drawings. Hydraulic structures indicated on older maps cannot be assumed as present and/or functional until verified. Prior to conducting a drainage study, older drawings should be field verified, indicating the current hydraulic conditions. Thus, in order to assure the most recent, available spatial data, clear study objectives and a concise plan of execution and collection is needed to create a useful database. For the Cherry Point study, the outdated, subsurface conduit maps were amended to reflect the post construction land use changes. The CPEC consultant verified two important attributes, pipe type and size.

More features of the drainage system are very important in flow routing and tracking travel time. One conservative method used to estimate travel time is adapting the peak flow rates and the cross-sectional area of each point of interest to determine travel time for each reach. The

overall travel time of the basin is then the sum of all these smaller travel times beginning at some known point to the desired end point. This method is further discussed in Chapter Four. A hydrologic/hydraulic model that can accurately predict peak flow rate is needed to perform this type of travel time calculation.

## **B. Objectives**

### *Overall Objective*

The overall research objective is to effectively utilize GIS technology to calibrate and validate the SWMM model to predict the movement of pollutants exiting from any point in a specific subcatchment to the catchment outlet (which drains the industrialized areas) at the Marine Corps Air Station at Cherry Point.

### *Chapter Objectives*

One objective of this chapter is to evaluate the results of peak outflow rates gathered from several event-based hydrologic models and to explain the evolution from lumped parameter models to process-based, rainfall-runoff simulators. The second objective of this chapter is to display the inputs gleaned from the GIS work and other referenced values in efforts to create functional SWMM input datasets using single storm events and continuous rainfall data. The third objective is to use selected storm events to calibrate SWMM.

The fulfillment of the chapter objectives will assist in achieving the broad study goal, which is to apply a validated SWMM model to predict travel times. More than one year of continuous and consistent field data is generally required to effectively calibrate and validate most surface water modeling packages. Instruments were installed in the fall of 2000 to measure rainfall and stream outflow in five catchments at MCAS-CP. From November 2000 through January 2003, rainfall, stage and flow measurements were recorded and archived.

One essential task of the study was to determine the drainage basins located within the industrialized portion of the air station. With the assistance of the Muhs (2000) study, and a GIS coverage map completed by CPEC, Inc. (2000), drainage areas were delineated for the research

site. Following delineation, five monitoring locations were selected, but only catchments K2 and K3 were used in this modeling study. The locations of the five outlet points, including the outlets of catchments K2 and K3, are displayed in Figure 3.1 and are indicated by the red circles.

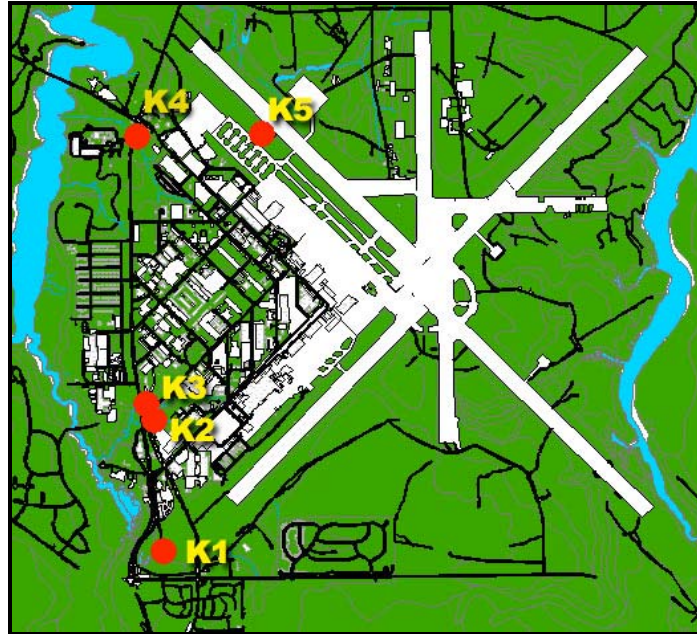


**Figure 3.1: Cherry Point Hydrologic Study Outlet Location Map.**

## II Methods

### A. Model Description

#### *Surface Water Models Introduction*

The McGraw-Hill Dictionary of Science and Technical Terms (2004) defines a model as “a mathematical or physical system, obeying certain specified conditions, whose behavior is used to understand a physical, biological or social system to which it is analogous in some way”. Simply, hydrologic models generate synthetic hydrographs from user-inputted data. Some models have sophisticated input structures, but an increased number of input variables does not necessarily guarantee improved performance. An efficient model requires minimal information to complete simulations and provides solutions that parallel physical processes.

In many instances, hydrologists attempt to predict flood events from historical information. The word prediction is selected, because probabilities have been incorporated into the simulation models. Therefore, modelers attempt to predict runoff peak flow rates in order to make future decisions concerning flow events. Two main reasons for studying runoff peaks and volumes are to quantify the runoff volume and rate of water movement and to identify critical watershed areas that demand heightened attention. (Northcott et al 2003)

*Soil Conservation Service Application of the Rational Formula for Runoff*

The Rational Formula or Rational Equation is one of the simplest rainfall-runoff methods for predicting peak flow (Bedient and Huber, 1988). The Rational Method was originally developed in the 19<sup>th</sup> century: “it is usually attributed to Kuichlang (1889) and Lloyd-Davies (1906), but Malvaney (1851) clearly outlined the procedure in a paper in Ireland” (Bedient and Huber, 1988).

In 1964, the unit hydrograph approach to estimate runoff was popularized by the Soil Conservation Service (now the Natural Resources Conservation Service), where the dimensionless unit hydrograph represented a relationship between discharge and time (Bedient and Huber, 1988). The rational method was the predecessor of the storm hydrograph concept and is an example of an uncalibrated, lumped parameter model that mathematically relates peak discharge ( $q$ ) to the drainage area ( $A$ ), the rainfall intensity ( $I$ ) and the runoff coefficient ( $C$ ) (Northcott, et al 2003). Using English units, the rational method equation may be written as follows:

$$q=CIA \qquad \text{EQ 3.1}$$

where  $q$  = design peak runoff rate ( $\text{ft}^3/\text{sec}$ , cfs)

$C$  = runoff coefficient (dimensionless)

$I$  = rainfall intensity (in/hr)

$A$  = watershed (catchment) area (ac)

When using the rational method, the modeler assumes that the rainfall intensity and duration are uniform over the entire watershed and that the storm duration is equal to the time of

concentration for the watershed (Northcott et al 2003). As an example, the peak outflow rate calculated for catchment K3 (259 acres at 44.6% imperviousness) was less than 200 cfs, for storm events having frequencies less than or equal to 5 years.

*Time of Concentration,  $T_c$*

The time of concentration,  $T_c$ , is a parameter that is defined as the time required for water to flow from the most remote point of the area to some designated outlet point. It is assumed that when the duration of the storm event equals the time of concentration, all points within the watershed are simultaneously contributing to the discharge (Northcott et al 2003). Two simple methods for calculating time of concentration are the Kirpich and the SCS lag equations. The kinematic wave and Muskingum-Cunge are two more complex transformation methods.

The Kirpich equation calculates  $T_c$  in terms of flow length and watershed gradient in the following manner (McCuen, 1997):

$$T_c = 0.0078 L^{0.77} S^{-0.385} \quad \text{EQ 3.2}$$

where  $T_c$  = time of concentration (min)

$L$  = maximum flow length (ft)

$S = \frac{\text{maximum elevation (ft)} - \text{minimum elevation (ft)}}{\text{stream length from highest to lowest point at outlet(ft)}}$

The Cherry Point study is concerned with predicting the travel times of runoff pollutants via water travel. Therefore, the values generated from the Kirpich equation were used as baseline estimates for the initial travel time figures.

The SCS lag method is similar to the Kirpich equation but incorporates a curve number (CN) parameter that describes the land cover type. The SCS (1972) equation to determine  $T_c$  in terms of CN may be written as,

$$T_c = 0.00526 L^{0.80} (1000/CN - 9)^{0.70} S^{-0.50} \quad \text{EQ 3.3}$$

where  $T_c$  = time of concentration (min)

L = watershed length (ft)  
CN = curve number (dimensionless)  
S = watershed slope (ft/ft)

The runoff curve number is an index that combines effects of rainfall conditions with soil hydrologic information and land use into a single parameter. The referenced CN values for areas K2 and K3 were weighted based on surface type and land area. Generally, the Cherry Point curve numbers ranged between 61 and 98 (see table 3B.1 in Appendix 3B)

Curve number and runoff coefficient values are documented in most hydrology/hydraulics textbooks. Watershed CN values should be selected to reflect soil and hydraulic conditions that are most dominant. McCuen's Hydrologic Analysis and Design (2<sup>nd</sup> Edition, 1997) and Schwab's Soil and Water Conservation Engineering (4<sup>th</sup> Edition, 1992) were referenced to determine CN values for the studied watersheds. Catchment K3 was categorized using four land types: 1) roads, 2) buildings 3) parking lots and 4) open areas, having runoff coefficients of 0.8, 0.8, 0.8 and 0.2, respectively.

#### *USGS Method*

During the earlier portions of the study, initial runoff estimates were generated to provide numerical guidance for future SWMM simulations. The Rational Method was used as described, but an additional method was explored for comparative purposes.

The USGS (1987) method to calculate watershed peak flow rate is based on the following regression equation for the North Carolina coastal plain watersheds:

$$Q_{10} = 225 A^{0.559} \qquad \text{EQ 3.4}$$

Q<sub>10</sub> is the peak flow (cfs) predicted for a 10-yr return period and A is the drainage area in square miles. The 10-year peak outflow for the research site, using the USGS technique, was slightly less than 280 cfs for catchment K3.

## *HEC HMS*

The U.S Army Corps of Engineer's Hydrologic Modeling Software (HEC-HMS) superseded the HEC-1 model and was designed to simulate the precipitation-runoff processes of dendritic watershed systems (HEC, 2001). The modeler creates a Data Storage System (DSS) that is utilized to complete simulations and allows the retrieval of previously inputted data. Precipitation and discharge gage information can be entered manually within the program or can be loaded from previously created DSS files (HEC 2001). HEC-HMS is available free of charge at: <http://www.hec.usace.army.mil/software/hec-hms/hechms-download.html>

HMS model was the first computer-based model used to test the MCAS-CP catchment and subcatchment discharges. The catchment area values from the Rational Method investigation were inserted into HEC HMS. The purpose of conducting the initial HEC-HMS simulations was to estimate the peak runoff rate that would be expected from the overall catchment.

The initial, uncalibrated HMS simulations for catchment K3 at Cherry Point yielded peak outflow rates greater than 496 cfs for a 10-yr, return period storm, using the lag time transformation method.

HMS does not require many input parameters, thus enabling a quick determination of the predicted peak runoff rates (using lumped parameters), per catchment area. Design storm precipitation amounts were entered from Intensity-Duration-Frequency charts developed for Morehead City, North Carolina (refer to Table 2.6 in Chapter Two). The HMS computational results were viewed from the basin model schematic. Appendix 3C is a collection of various HMS screenshots.

No reaches (linking elements) were integrated during the initial HMS simulations; rather, the focus was to examine subcatchment characterization and the individual ability to produce surface runoff. Reaches were eventually introduced as the routing scheme developed. The HMS simulations involving routing elements were completed to determine if runoff was being directed to downstream features appropriately. The elements used in this study included: subbasins

(subcatchments), reaches, and junctions. As expected, flow computation progressed from upstream elements in a downstream direction. Figure 3.2 is a screenshot of the HMS basin model for catchment K3, where rectangles, circles and lines represent the subcatchments, junctions and reaches. Unlike the XPSWMM9.0 schematics, the modeling points were not georeferenced.

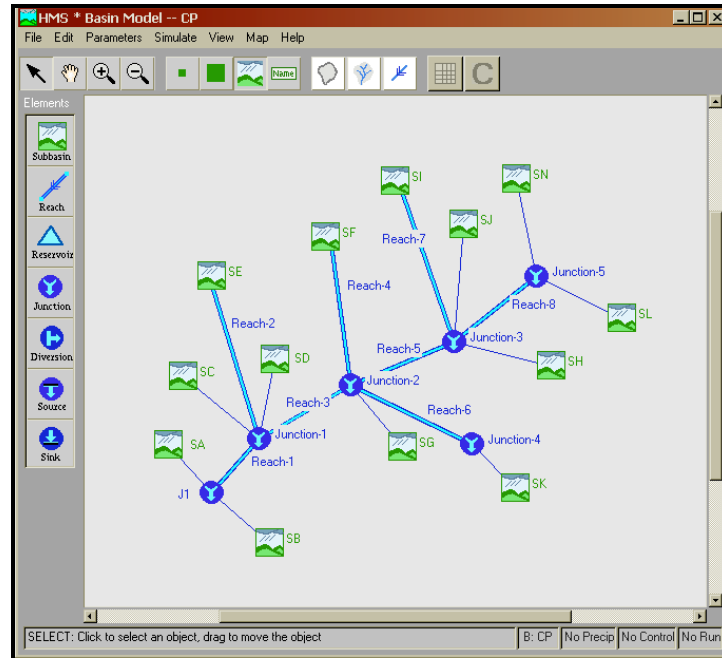


**Figure 3.2: HEC-HMS Catchment K3 Basin Model Screenshot.**

HMS includes several methods for transforming excess precipitation into surface runoff, including unit hydrograph methods (HEC 2001). The SCS curve number (CN) technique was selected due to ease of operation and time concerns. The hydrologic soil groups and the curve numbers were determined using a Soil Survey from SCS (1986) and discussions with NRCS staff (2001). Depending upon the specific soil type and land use, the CN values varied from 61 for very pervious area with high infiltration potential to a 98 for highly impervious areas with high runoff capabilities. Table 3B.1 contains a listing of the curve numbers used in HMS for catchment K3.

HMS predicts runoff volumes from precipitation depths using several different methods. For Cherry Point, the SCS Curve Number method was selected where the runoff volume, Q, is a result of a storm event with rainfall, P, and the initial loss, I<sub>a</sub>.

$$Q = \frac{(P - I_a)^2}{(P + 0.8S)} \quad \text{EQ 3.5}$$

where I<sub>a</sub> = 0.2S

The S-value is the potential abstraction in inches. The SCS method defines S in relation to curve number (CN) where S = (1000/CN) – 10. The initial loss value, I<sub>a</sub>, was assumed to be zero.

The open channel routing scenario was determined prior to running the HMS simulations. Routing with no attenuation was modeled with the lag method. Lag time is defined as the relationship between the time in hours for the center mass of rainfall excess to the peak discharge, the slope, hydraulic length and maximum retention (Sheridan, 1994). The equation used for lag time in the Cherry Point HMS simulations is,

$$L = \frac{I^{0.8} (S+I)^{0.7}}{1900 Y^{0.5}} \quad \text{EQ 3.6}$$

where L is the lag time (hrs), I is the hydraulic length of the watershed (ft) and S is the potential abstraction. S is calculated as

$$S = (1000/CN) - 10 \quad \text{EQ 3.7}$$

Where CN is the weighted runoff curve number and Y is the area slope (ft/ft).

Lag time may be estimated as 70% of the time of concentration (McCuen, 1997). Others have calculated lag time as 60% of the time of concentration (Sheridan, 1994).

The user-inputted hyetograph option allows the user to insert precipitation data in a structured format. HMS handles the evapotranspiration losses using monthly average values.

When monthly ET is determined from pan evaporation measurements, an optional pan coefficient may be used (HEC 2001).

Simulations are managed by user-designated control specifications. The control specifications include a starting date and time, ending date and time, and computation time step (HEC 2001). The combination of a basin model, a meteorological model and the controls section, forms one simulation. The lag time method was selected and simulated using the conceptual basin model. First, no lag times were computed and the model was configured, checking the routing procedures. Second, all stream elements were provided a 5-minute time lag until an appropriate time lag was calculated. Third, travel times were estimated by dividing the reach length by an estimated 1.0 feet per second (fps) stream velocity as roughly measured during field visits. The corresponding lag times were then set equal to  $0.70 T_c$ . Fourth, from the GIS data, the channel and pipe characteristics were inserted into HMS. The kinematic wave routing method was next introduced. The energy slope was assumed to be equal to the channel bed slope and the channel side slopes and lengths were measured. Manning's roughness coefficient was set equal to 0.028 for natural earth channels with grass growing on the banks (ASCE, 1996).

The meteorological information was eventually entered as user input, replacing the design storm precipitation data. As an example, consider Event 330 which occurred on day 330 (November 26, 2000). Using the user hyetograph option, gage 1 was created from rainfall measured for the storm event on day 330. The control specifications followed the storm event timing. The 24-hour simulation period began on November 26<sup>th</sup>, 2000, at 1:00am and concluded on November 27<sup>th</sup> at 1:00am.

Table 3.1 summarizes the results obtained from the rational method, the USGS equation and the HMS simulations for catchment K3. The Rational Method produced the most conservative results. The Kinematic Wave transformation in HMS produced the highest runoff of 192 cfs for a 1-yr return period storm. The USGS and Lag Time version of HMS displayed moderate results, predicting more runoff than the Rational Method but less than the Kinematic HMS runs (only the 1-yr return period storm was simulated using the kinematic wave function due to a lack of input data).

**Table 3.1: Peak Runoff rate predicted for Event 330 (Nov. 2000) on Catchment K3 using different methods.**

Return Period yr	Rational Method cfs	USGS Method cfs	HEC-HMS Model	
			Lag time cfs	Kinematic cfs
1	123.6		158.0	192.0
2	156.7	112.6	248.0	
5	192.7	206.9	358.0	
10	226.6	279.6	496.0	
25	266.4	436.1		
50	301.0	513.2		
100	339.3	586.8		

### **Modeling Overview**

#### *EPA SWMM - Introduction*

The United States Environmental Protection Agency's (USEPA) Storm Water Management Model (SWMM) is a comprehensive computer model for the analysis of quantity and quality problems associated with urban runoff (CHI, 1998). Originally, the model was developed for the USEPA between 1969 and 1971 and was the first comprehensive model of its type for urban runoff analysis (Metcalf and Eddy 1971). SWMM is capable of conducting single-event and continuous type simulations depending on the application. The simulations predict flow, stage, and calculate possible pollutant migration for catchments having storm sewers (sewersheds), or a combination of sewers with natural drainage.

SWMM is comprised of several modules or blocks that may work independently or collectively and is normally used for hydrologic and hydraulic analysis. The EXTRAN Block is capable of handling sophisticated hydraulic analysis of urban drainage networks and was used to route pollutants in this study.

For Cherry Point, runoff was generated specifically within the RUNOFF Block. For hydrologic simulation in the RUNOFF Block, data requirements include catchment area, imperviousness, slope, roughness, width, depression storage, and infiltration parameters for

either the Horton or Green-Ampt equations for up to 100 subcatchments (CHI 1998). Precipitation and evaporation are the two driving forces in SWMM.

SWMM output files are generated in tabular and graphical formats. The basic SWMM output consists of hydrographs and pollutographs for any desired location within the drainage system (CHI 1998). Summary statistics can also be generated, including depth and velocity results, as well as, summaries associated with volumes, surcharging, and continuity.

The level of calibration essential for the satisfactory simulations ranges from simple to complex depending upon the type of simulations conducted. Calibration data may consist of measured hydrographs and pollutographs for use in establishing values of input parameters for which a priori estimates are insufficient (CHI, 1998). It is often possible to obtain good agreement between predicted and measured hydrographs with little calibration; however, this is generally not true for water quality projects (Amatya, 1985). The number of events needed to adequately calibrate the model varies with application, but in most cases, six calibration and six verification events should be sufficient to reach sound conclusions (CHI 1998).

#### *SWMM Adaptation and Performance*

The Stormwater Management Model performs best in urbanized, impervious areas, although it has been adapted for further applications. The model has been used in scores of U.S. cities, as well as extensively in Canada, Europe, and Australia (Donigian 1991 and Huber 1992). Quantity simulations are enhanced by the calibration/verification process, and can be expected to agree well with measured data, if good input information is known about area, imperviousness, and rainfall. (CHI 1998)

#### *Transition into XPSWMM 9.0*

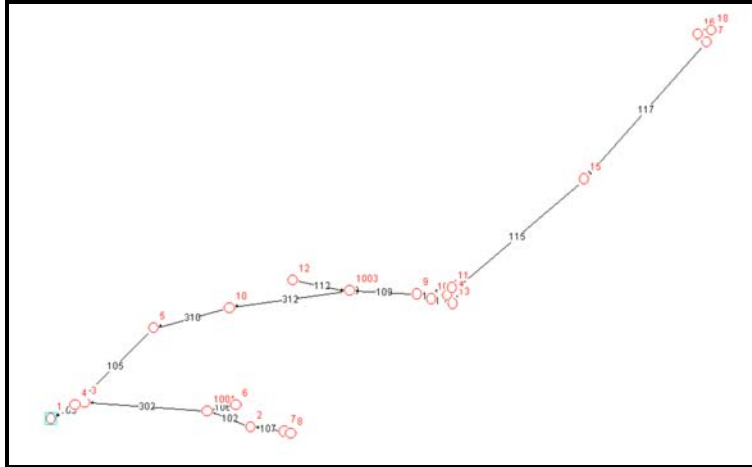
All storm input information was initially formatted using SWMM 4.02 and eventually version 4.4beta. Later, an importation utility was used to link the text version of SWMM to a more sophisticated SWMM system, XPSWMM. The XP version of the popular SWMM program is distributed by XP software. The research team purchased XPSWMM Version 9.0, including the GIS Module, in December 2004.

XPSWMM, version 9.0, is a “dynamic unsteady flow model” that is capable of “delivering results far more accurately and closer to real life than a steady state model” (XP Software, 2003). Similar to the text version, XPSWMM can operate in individual blocks. The core reason for selecting XPSWMM, for Cherry Point, was its capability of GIS interaction.

XP-GIS offers the importation of needed modeling data from GIS, and other data sources such as spreadsheets (XP Software, 2003). The GIS module is an easy method to link XPSWMM and other GIS packages while in the XPSWMM environment, through exportation and importation of spatial data. The exportation and importation features became extremely useful during the generation of hydrographs and the duplication of selected XP projects.

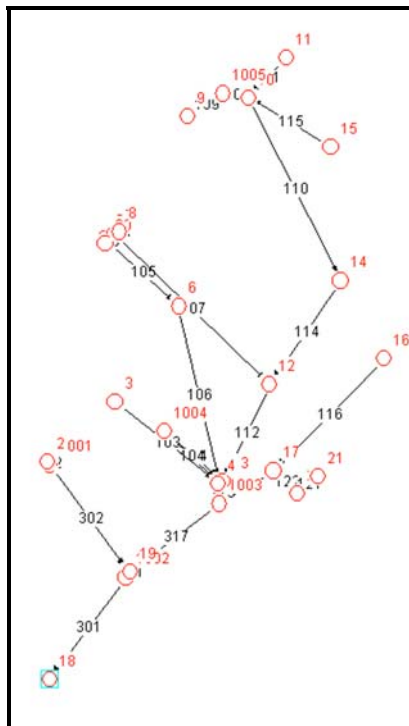
The XPSWMM files were created with the aid of the importation wizard. First, the .txt files were renamed, using a .dat file extension. The text files were then linked to XPSWMM. Next, the “Tidy Up” option was selected to create an organized network system (this option should not be selected if spatial information is already associated with nodes and/or links). Figures 3.3 and 3.4 display the resulting XPSWMM schematics for catchments K2 and K3 at Cherry Point.

Figure 3.3 is a view of the XPSWMM display detailing the nodes and routing elements used to represent catchment K2 at Cherry Point. The red circles are subcatchment outlet points that are connected via routing features, which include overland channels and subsurface piped conduits. The outlet of catchment K2 is located at the bottom left portion of this figure and is denoted by the blue rectangle. The “Tidy Up” option in XPSWMM was utilized to import the spatial information from the GPS/GIS to accurately place each node using x- and y- coordinates.



**Figure 3.3: Catchment K2 XPSWMM Routing Schematic for Cherry Point MCAS.**

Figure 3.4 was generated from a screenshot of catchment K3 as viewed in the Runoff mode of XPSWMM9.0. The red circles are subcatchment outlet and the black lines are linkage features used to route runoff between nodes and other links. The outlet of catchment K3 is located at the bottom left of the figure. Note that all nodes have been georeferenced and have corresponding x- and y- coordinates.



**Figure 3.4: Catchment K3 XPSWMM Routing Schematic at Cherry Point MCAS.**

For the Cherry Point research, numerous nodes and routing elements were used to represent the industrialized area (see Figures 3.3 and 3.4). Eighteen subcatchments were identified for catchment K2. Likewise, subcatchment K3 is comprised of twenty-two subcatchments.

### *Project Application*

The surface runoff simulations were initially completed using XPSWMM version 8.52. Later, XPSWMM9.0 was introduced and the older files were converted into the newer format. During the conversion, several SWMM controls needed updates and the rainfall data were inserted into the program in a delimited form, using the Rain Module. Additionally, the elemental attributes were scrutinized because some measurements were incorrectly transferred during the conversion from SWMM to XPSWMM. The focus of the conversion into the XPSWMM9.0 platform was to create continuous simulations using a linked, annual rainfall dataset.

The modeling approach to evaluate the expected proficiency of any management practice requires the calibration and validation of the model itself. Information pertaining to the natural systems is gathered and inserted into the program. The initial simulations remain meaningless until realistic output is generated. In order to adequately refine the model estimates, calibration involves adjusting variables to finally achieve results that parallel natural conditions. In addition, the validation procedure compares the adjusted model to measured data (for periods other than those selected for calibration) using statistical tests to quantify agreement between predicted and measured results.

For the Cherry Point project, current meters were used for measuring stream flow. The outlets of selected watersheds were equipped with a STARFLOW, ultra-Doppler, self-recording current meter. The meter collects data in 10-minute intervals, including water temperature, battery voltage, time/day information, water depth and velocity. The software provided was used to manage the in-field data collection and assist with the transfer of downloaded data. The collected stream data served as the calibration dataset for the SWMM and XPSWMM simulations.

The Runoff block was used specifically to generate watershed runoff, relying on user-defined rainfall data from manual rain gauges, a tipping-bucket gauge, and NOAA published data. The catchment surface parameters were gathered using a combination of field surveys and the geographic information system (GIS) coverages. All stream length measurements were extracted directly from the GIS using the Measuring Tool in standard units.

The input datasets for SWMM, and eventually XPSWMM, were created to allow examinations of specific points along the runoff flow path. The catchment was divided into subcatchments based upon topography and subsurface drainage. The catchments and subcatchments were individually named, having one specified outlet. Each outlet was then either routed directly into an adjacent subcatchment or connected to a pipe or channel. The dendritic network was finally complete once all subcatchment outflows were routed to reach the overall catchment outlet.

Since distinct points of interest were specified in the SWMM (XPSWMM) input dataset, various outlet points could be examined. For example, if a user wished to view the outflow generated from a particular catchment or the outflow leaving a certain routing element, that flexibility existed. The Figure 3A.1 in Appendix A is a text-based version of a SWMM input dataset.

The "GUTTER" and "NAME" columns under the "GUTTER" and "SUBCATCHMENT" sections identify specific routing elements and subcatchments. The M3 line in the output control section determines which hydrograph points will be included in the SWMM output file. For example, to review the simulation results from element 309, the user would insert the number 309 on the M3 command line (the SWMM sample file in Figure 3A.1 is configured to print the outflows for point 101 only). The generalized XPSWMM output file plots a hydrograph adhering to the user-defined print controls. To view the outflow at a specific location, simply select a node or link on the main XPSWMM screen to review the results. The resulting hydrograph points can also be manually exported into a spreadsheet to be examined more closely. Figure 3.5 demonstrates the results displaying capabilities of XPSWMM for Catchment K3. The displayed outflow hydrograph corresponds to the runoff predicted for a 10-yr return period storm for Morehead City, NC at Node 18. XPSWMM is also able to graph the hyetograph which is presented as the green graph at the top of the figure.

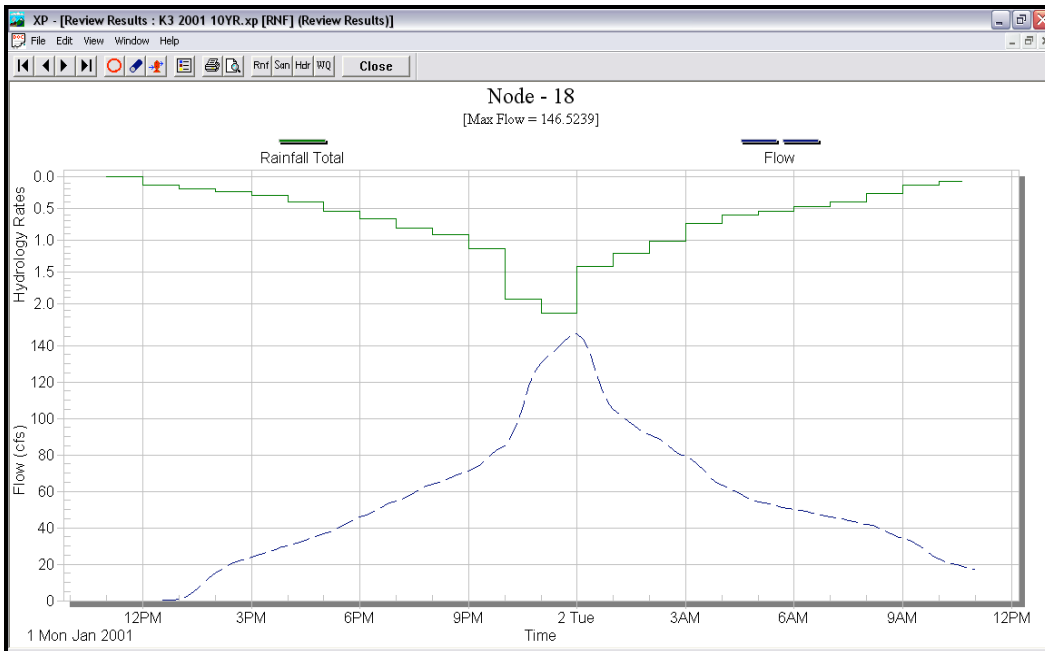


**Figure 3.5: XPSWMM Results for a 10-yr return period storm at Node 18 on Catchment K3**

*Generic Modeling Limitations*

Models are used to better understand and explain natural phenomena, and, under some conditions they provide predictions in a deterministic or probabilistic sense (Woolhiser and Brakensiek, 1982). Models attempt to represent a real system and have strengths and weaknesses depending upon the application. The user must remember that the model limitations adhere to the boundaries that are intrinsic to the specific problem as well as dependent upon user-inputted information.

Considering diversity in models themselves and diversity of their use, and in addition, considering the variability of the system(s) that the model represents, unholy errors are encountered (Shirmohammadi and Montas, 2002). In most instances, models are considered to be “magical” devices capable of predicting future trends and the results are too quickly deemed authentic without question. Output of a model may be affected by input errors as well as algorithm errors (Loague and Green, 1991). Therefore, some researcher may misinterpret model-simulated information. Simanek (2002) reinforces this point in stating that, “sometimes models breakdown when extended beyond their original scope of validity”.

Theoretical models, such as SWMM, use physical laws that govern the model's parallelism to the real system. In general, input parameters vary with space and input variables vary with space and time. In line with generalized beliefs, SWMM includes both system variables (variables describing the physical system) and state variables (variables that describe the state of the system) (Shirmohammadi and Montas, 2002). Examples of system variables include soils, slope, and surface conditions while state variables would include climatic parameters such as rainfall or evapotranspiration values. Novotny and Olem (1997) consider theoretical models to be "deterministic models" because they only provide one set of output for a given set of inputs. However, these "deterministic models" can be used with a set of input parameters described by a certain probabilistic distribution that they generally fit well to obtain a range of outputs for a variable of interest. This will provide the decision maker with a range of possibilities of outcomes for a set of inputs that can be used during modeling.

Defining the model limitations prior to conducting a study will lessen the amount of error incurred from exceeding a model's boundaries. Thus, several key points should remain prevalent during the simulation and data acquisition periods. The suggestions below may help model users to remain focused during model application (adapted from Russell's remarks regarding a participant's notes from a modeling workshop in Ekenas, Sweden, 1994)

1. Models become limited in accuracy when the appropriated field data are unavailable for comparison
2. Maintain clearly defined objectives in using the model by all participants, including model developers and regulatory agencies.
3. Avoid the misuse of the model by untrained personnel who may misinterpret modeling results
4. Models should not be used as a substitute for experimental data, but should be considered a supplemental tool.

The technical limitations as applied to this study include SWMM's difficulty of simulating depression wetlands, although damp areas may be represented using storage processes, such as the STORAGE module (CHI 1998). The biggest impediment to the application of SWMM4.0 is the lack of user-friendly menus and graphical output.

## **USEPA SWMM RAIN Module**

The RAIN module of SWMM may be used independently to simulate surface runoff for a modeled area. Basically, precipitation is the principal driving force in the SWMM package (James 1999). The purpose of the RAIN module is to read time series data containing precipitation information and generate a precipitation interface file that is accessible to the RUNOFF module. Besides handling user-generated precipitation input structures, the RAIN module is also capable of reading National Weather Service (NWS) formatted data. Good precipitation files contain consistent, meaningful information. If a rainfall dataset contains substantially lengthy periods having missing numbers or zero-values, continuous simulations should be avoided (James, 1999).

Essentially there are only three data groups required to run the RAIN module. The \$RAIN data group prompts SWMM to reference the RAIN module. The A1 data group is used for descriptive purposes and has an 80-column, two line maximum of text data. The B1 group is a general control set of commands. The B2 group is used to format user-defined precipitation information. Exhibit 3D.1 of Appendix 3D displays a sample RAIN module data file. The values selected for the B1 group should reflect the system being modeled accordingly. Table B3.3 displays the remaining parameters needed for the B1 data group.

The temporal description for the rainfall hyetograph is a function of the catchment response to rainfall input (James, 1999). Smaller, impervious catchments are expected to have shorter times of concentration. Likewise, larger, more pervious basins should demonstrate the opposite trend. In most cases, a shorter time interval will produce better SWMM simulations, but may not always be needed for larger areas.

## **USEPA RUNOFF Module**

The RUNOFF module interfaces the precipitation and runoff characteristics of the system. Its main function is to read precipitation files and generate overland flow values for the TRANSPORT and EXTRAN modules; it is capable of simulating runoff from the basin and routing the flows via the constructed drainage paths. The RUNOFF module basically represents the basin by an aggregate of idealized subcatchments and gutters or pipes (links) (James, 1999). Using the provided rainfall information, precipitation is routed as overland, canalized or pipe flows. System losses such as infiltration and depressional storage values are also calculated. The end

result of the RUNOFF module consists of output providing graphical interpretations via hydrographs and other user-selected output functionalities. Hence, the input for this module is of extreme importance.

The RUNOFF module may be simulated in single event or continuous modes. The period of interest may span from several minutes to a number of days. With the exception of snowmelt, all computations are done identically for both single and continuous mode (James, 1999). A sample, text based, RUNOFF block file for catchment K3 is located in Table 3E.7 of Appendix 3E.

#### *RUNOFF Block Subroutines*

The hydrograph created by SWMM is generated in the HYDRO subroutine. The HYDRO subroutine consists of 17 subprograms (RHYDRO, GRIN, MKRAIN, SNOWIN, QHYDRO, QINT, QSHED, BUILD, WSHED, OVRLND, GAMP, HORTON, GUTTER, GUTNR, GQUAL, MELT, AREAL, and FINDSC), which represent physical processes and are responsible for creating the information needed to plot the hyetograph and hydrographs. The HYDRO subroutine is also responsible for accessing the routing elements and ordering them in such fashion that the simulated runoff travels in a downstream direction. Following the completion of necessary preceding functions, HYDRO then creates a hydrograph for each time step. The WSHED subprogram relies upon either GAMP (Green-Ampt) or HORTON to calculate basin infiltration amounts. The GUTTER subprogram is the primary routing function of SWMM and is used to compute water depth and flow rates for each channel and pipe. Water flowing into any inlet is the sum of channel/pipe flow, direct drainage from subcatchments and direct groundwater (James, 1999). SWMM performs a continuity check during each simulation where the dispersion of rainfall in relation to runoff and other losses is completed. The error calculated during this check is presented as a percentage of the received rainfall. The HYDRO subroutine finally calls upon the HCURVE subprogram to plot the rainfall hyetograph, total infiltration, and runoff hydrograph for the entire basin.

### *RUNOFF Block Controls*

The first four data groups (B-values) of the RUNOFF module are associated with general control commands. Appendix 3E contains additional graphics concerning the RUNOFF module.

The B3 data control group handles the three available time steps: 1) WET, 2) WETDRY and 3) DRY. The WET parameter explains the length of time of the wet time step and is defined as the time step with precipitation occurring on any subcatchments (James, 1999). The WETDRY number is used to describe the transitional time step between wet and dry conditions. In addition, the transitional time step has no precipitation input on any subcatchments, but the area may have water available in depressional storage. The DRY value describes the dry time step, where no precipitation input exists, nor is the area considered to have surface storage. The B3 data group also establishes the simulation time units, and the overall simulation length.

The WET time step is inputted as a fraction of the rainfall interval, where the rainfall intensity remains constant. A smaller WET time step should be selected if the time of concentration is a fairly small fraction of the rainfall interval. In addition, the WETDRY transitional time should be substantially longer than WET. If WET has a magnitude of minutes, then WETDRY should have a magnitude of days. Likewise, the DRY time step should be greater than the WETDRY value to correctly simulate a reasonable hydrograph. The DRY value allows for the movement of groundwater flow and is used to incorporate infiltration conditions. The DRY time step should be days in wetter climates and days or weeks in very dry climates. (James, 1999)

The simulation time step depends upon the system being modeled. It should be smaller for periods of rapid change (i.e. rainfall) and longer during periods of slower changes (James, 1999).

### *Catchment Parameterization*

Depending upon the simulation objective, input data requirements can be minimal to extensive (CHI 1998). The inputs needed to simulate a complete drainage network can be accomplished in a few days by a knowledgeable field staff; larger areas may take longer to document dependent upon simulation intent. Simple data collection such as area, overland flow lengths and pipe/channel dimensions is fairly straightforward.



### Catchment Conceptualization

Conceptualization plays an important role in the output generated from the model. Moreover, the importance of watershed conceptualization is significant but relatively smaller than the impact of calibration storm event selection (Warwick and Tadepalli, 1991).

The delineated catchment areas may be simplistic or complex. In the simplest form, a watershed is assumed to have a rectangular shape. The watershed length is usually the longest distance from the outlet, adhering to a rectangular geometry. Theoretically, the effective catchment width may be computed as the total area divided by the length. In Figure 3.6, the main drainage outlet is located at the middle of width,  $w$ . The main flow path follows a leftward direction eventually entering the outlet via surface runoff only. No pipes or gutters are considered at this level of discretization and a single rain gauge provides the precipitation dataset. Therefore, Figure 3.6 demonstrates the lowest level of model conceptualization where only the one overland flow path is considered and the shape of the catchment is assumed to have simple geometry.

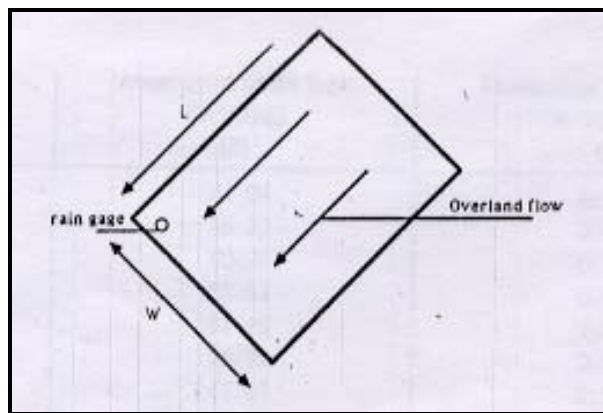


**Figure 3.6: Low Level Area Conceptualization** (adapted from Warwick and Tadepalli, 1991).

Medium level spatial conceptualization for a watershed is shown in Figure 3.7. Similar to the low level conceptualization technique, this scenario has the addition of a main collection channel. The main gutter (collection channel) travels the entire length of the watershed. The rain gauge position is maintained from the previous level. Conversely, overland flow travels in a perpendicular path before entering the main drainage channel. Additional information is needed for this type of scenario such as Manning's roughness (for the gutter), gutter length, gutter depth, right and left land slopes, bottom width, and gutter slope.

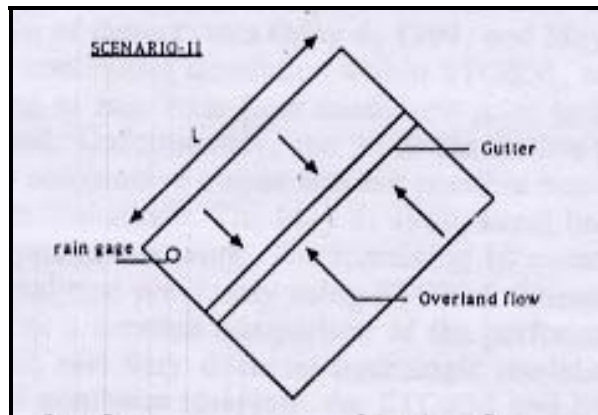


**Figure 3.7: Medium Level Area Conceptualization** (adapted from Warwick and Tadepalli, 1991).

The Cherry Point study adapted the highest-level of conceptualization, considering the contribution of subsurface drainage pipes and asymmetric catchment shapes. The catchment and subcatchment areas were delineated in ArcVIEW and the attributes were collected from the GIS database. Channel and pipe attributes were inputted from the CPEC, Inc. study (2001). Other values such as percent imperviousness, Manning's roughness, channel length and side slope values were either calculated or referenced. In special instances, measurements were acquired during site visitations, especially for channel and wetland characteristics. Figure 3.8 displays the highest type of watershed conceptualization using rectangular catchment areas.

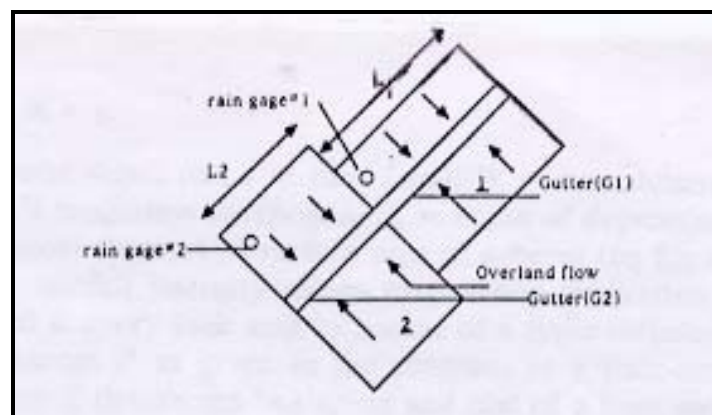


**Figure 3.8: High Level Area Conceptualization** (adapted from Warwick and Tadepalli, 1991).

### *Subcatchment Surface Area*

The GIS land coverages and topographic maps were extremely helpful in acquiring data pertaining to the study subcatchments. The areas were determined by first constructing hydraulic ridgelines that outlined a particular drainage area. The area of this region was then calculated using the XTools extension in ArcVIEW. The process was repeated for all subcatchments and a summary table was collected. Real-time changes in ArcVIEW were also possible; thus, allowing instantaneous updates to subcatchment shapes and attributes as alterations developed. Appendix 3F contains information about the physical characteristics of the K2 and K3 catchments.

### *Subcatchment Slope*

The subcatchment slope (from highest point to outlet position) was assumed to be equal to the watercourse slope. To calculate this value, the elevation difference is divided by the flow length. If the area geometry is more complex, multiple overland flow paths may be generated and an average may be constructed to best represent the overland course. On the other hand, the most dominant overland path may be used, calculating the slope of this path only.

### *Infiltration*

Infiltration is the process of surface water entering the soil matrix. Runoff occurs once the rainfall rate exceeds infiltration capacity and surface storage requirements are satisfied. SWMM is capable of handling infiltration via two methods: the Horton model (Horton, 1940) or the modified Green-Ampt model (Green and Ampt, 1911).

The Horton and Green-Ampt infiltration models were both explored during the Cherry Point research. The Horton model is empirical and probably more widely used and understood while the Green-Ampt version is physically based (James, 1999). The Horton version requires three parameters: 1) maximum initial infiltration rate (in/hr), 2) minimum infiltration rate (in/hr) and 3) decay rate of infiltration (1/sec). The Horton equation, in its normal form, is applicable only when rainfall intensity exceeds the infiltration capacity. The Mein-Larson version of the Green-Ampt equation is capable of handling instances when the rainfall intensity is less than the

infiltration capacity at the beginning of a storm (James, 1999). This equation also requires three inputs: 1) average capillary suction (in), 2) soil saturated hydraulic conductivity (in/hr) and 3) initial soil moisture deficit, a fraction calculated as the air volume divided by voids volume.

During the continuous simulations, generalized Green-Ampt parameters were inserted into XPSWMM9.0. The average capillary suction, soil saturated hydraulic conductivity and initial soil moisture deficit, were 0.16 inches, 0.04 in/hr and 0.3, respectively.

The  $f_c$ -value may be estimated as the saturated, vertical hydraulic conductivity of the surface layer of the soil profile. These values may in turn be estimated from the Soil Survey, published by the USDA for most counties in the United States. SWMM uses the HYDCON descriptor to assign a saturated hydraulic conductivity for the system.

The moisture deficit, IMD, is defined as the fraction difference between soil porosity and actual moisture content (James, 1999). Usually, sandy soils have lower porosity values than clays meaning faster drainage during periods between rain events. Therefore, IMD values for dry antecedent conditions are usually higher for sandy soils than for clay soils. This parameter is the most sensitive of the three Green-Ampt parameters for estimating runoff from pervious areas (Brakensick and Onstad, 1977). Table 3.2 displays typical values for IMD for several soil types.

**Table 3.2: Typical IMD Values for Various Soil Textures (SWMM4 User's Manual, 1999).**

Soil Texture	Typical IMD at Soil Wilting Point
Sand	0.34
Sandy Loam	0.33
Silt Loam	0.32
Loam	0.31
Sandy Clay Loam	0.26
Clay Loam	0.24
Clay	0.21

SWMM uses a piecewise function to calculate infiltration, using the Mein-Larson version of the Green-Ampt equation. The first equation predicts water volume that will infiltrate before surface saturation occurs. The second equation continues with the infiltration process until it reaches the upper limit, infiltration capacity.

The second equation is a direct application of the Green-Ampt model (1911). The first equation for infiltration prediction is as follows:

For  $F < F_s$  and  $f = i$  then,

$$F_s = \frac{S_u \text{ IMD}}{i / K_s - 1} \quad \text{for } i > K_s \quad \text{EQ. 3.8}$$

No calculation of  $F_s$  is completed when  $i > K_s$ . As stated before, the second equation is a direct adaptation of the original Green-Ampt equation and takes the following form:

For  $F \geq F_s$  and  $f = f_p$  then

$$f_p = K_s (1 + S_u \text{ IMD}/F) \quad \text{EQ. 3.9}$$

where,

$f$  = infiltration rate (ft/sec)

$f_p$  = infiltration capacity (ft/sec)

$i$  = rainfall intensity (ft/sec)

$F$  = cumulative infiltration volume for event (ft)

$F_s$  = cumulative infiltration volume required for surface saturation (ft)

$S_u$  = average capillary suction at the wetting front (ft of water)

IMD = initial moisture deficit for this event

$K_s$  = saturated hydraulic conductivity of soil (ft/sec)

### *Percent Imperviousness*

The area-weighted percent impervious values adopted for this study were collected by summing the amount of impervious area for each subcatchment and then dividing this sum by the total area. The GIS database was extremely helpful in gathering this information. The impervious areas reported in the RUNOFF module must be hydraulically significant. For example,

rooftops are impervious, but would not directly contribute to runoff unless the downspouts were directly connected to some drainage pipe. A driveway is only considered hydraulically significant if it drains directly into a nearby stormwater inlet structure. The simplification process of impervious runoff is usually caused by the fact that not all of the impervious area is directly connected in a hydraulic sense (Warwick, 1991).

Based on the land cover database, areas were divided into pervious and impervious categories. Pervious areas included open space areas, forested lands, and grassed areas. Impervious areas consisted mostly of parking lots, roads, buildings, and other paved surfaces. Percent impervious values were initially determined using the information gathered from ArcVIEW. As the research progressed, these initial values were adjusted for calibration purposes.

### *Storage*

Depressional storage is defined as the volume of water needed to fill all depressed regions of the pervious and impervious area before runoff occurs. It is a retention parameter that introduces a loss due to surface ponding, surface wetting, interception and evaporation (James, 1999). The RUNOFF module handles depression storage based upon the surface type. For impervious areas, water is stored in sunken areas and is only depleted through evaporative processes. For pervious lands, water located in depressed areas may also infiltrate into the soil.

Separate values for depressional storage are required for simulation. For Cherry Point, a depth of 0.05 inches was assumed for impervious areas with depression storage. Pervious areas having depression storage received an assumed depth of 0.10 inches. Although pervious area values are expected to exceed those for impervious areas, it must be remembered that the infiltration loss, often included as an initial abstraction in simpler models, is computed explicitly in SWMM (James, 1999). Also according to James (1999), "in certain cases, it is possible to use depressional storage as a calibration parameter to adjust runoff volumes".

### *Evaporation*

Evaporation is subtracted from rainfall depths and/or ponded water prior to calculating infiltration (James, 1999). For single event simulation, an evaporation rate is needed only during

the simulation period. For continuous simulations, rates are required for each day, but daily values are typically assumed constant on a monthly basis. The evaporation rate is subtracted from rainfall and snowmelt intensities at each time step and is also used to replenish surface depression storage and to provide an upper bound for soil moisture and groundwater evaporation (James, 1999). Evaporation gains more importance during continuous simulations since it could become a large component of the overall water balance.

The Cherry Point evaporation rates were adapted from a nearby research site. The Carteret County research site used the Penman-Monteith method to calculate monthly evapotranspiration values (Amatya et al 1995, Lu et al 2005). Initially, a single evaporation rate was selected for the entire year and then aggregated monthly. The monthly evaporation rates from the Carteret County research ranged from 0.1 in/day during the winter months to 0.5 in/day for the summer months.

#### *Overland Flow*

The SWMM approach to rainfall-runoff modeling demands a relationship between pervious and impervious areas. The overall catchment may be divided into a number of subcatchments and channels/pipes (links) plus inlets (nodes). The program does have limitations regarding inlet numbers; nonetheless, the catchment areas should be delineated prior to constructing the watershed drainage schematic.

Subcatchments may be divided into three types: 1) impervious areas with depressional storage, 2) pervious areas with depressional storage, or 3) impervious areas without depressional storage (Warwick 1991). Examples of these three types of areas are displayed in Figure 3.9. Areas A1, A2, and A3 represent the three types respectively.

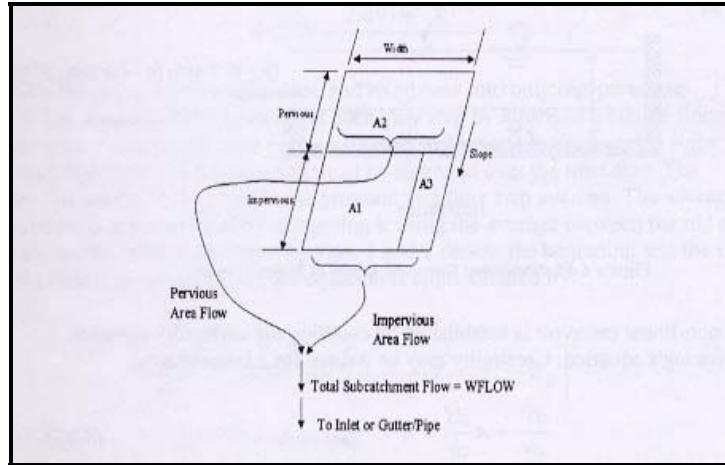


**Figure 3.9: Subcatchment Schematization for Overland Flow Calculations** (USEPA SWMM4 User's Manual, 1999).

Overland flow is generated from each of the subcatchments by approximating them as nonlinear reservoirs. (Warwick 1991). This technique does not adhere to a special basin shape but the subcatchments width,  $W$ , represents the true width of the overland flow. Therefore, the catchment is simplified to take the form of a rectangle. By default, SWMM uses the nonlinear reservoir technique to route runoff after losses have been determined. In addition, SWMM offers additional routing methods that require sophisticated hydraulics details that were not acquired during the Cherry Point study. Figure 3.10 provides a visual depiction of the non-linear reservoir technique.

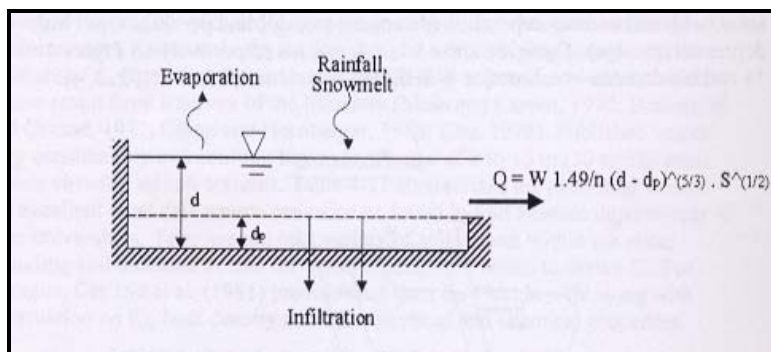


**Figure 3.10: Subcatchment Non-linear Reservoir Model** (USEPA SWMM4 User's Manual, 1999).

The continuity equation for the subcatchment is written as follows:

$$dV/dt = Add/dt = A * I - Q \quad \text{EQ. 3.10}$$

where  $V = A \times d =$  volume of water on the subcatchment ( $\text{ft}^3$ )

$d =$  water depth (ft)

$t =$  time (sec)

$A =$  surface area ( $\text{ft}^2$ )

$I =$  rainfall excess (ft/sec)

$Q =$  outflow rate (cfs)

The instantaneous outflow at the end of each time step is computed using Manning's equation in the following form (Warwick, 1991):

$$Q = W * \frac{1.49}{n} (d - d_p)^{5/3} S^{1/2} \quad \text{EQ. 3.11}$$

where  $Q =$  runoff flow rate (cfs)

$W =$  subcatchments width (ft)

$d_p =$  depression storage depth (ft)

$S =$  subcatchments slope (ft/ft)

$n =$  Manning's roughness coefficient

$d =$  water depth (ft)

The following nonlinear, reservoir equation is formed by combining the continuity equation with Manning's equation, assuming a wide channel design:

$$\frac{d(d)}{dt} = I - \frac{1.49 * W}{A * n} (d - d_p)^{5/3} S^{1/2} \quad \text{EQ. 3.12}$$

where  $d =$  water depth (ft)

$t =$  time (sec)

- W = catchment width (ft)
- n = Manning's roughness coefficient
- d<sub>p</sub> = depth of depressional storage (ft)
- S = catchment slope
- A = surface area (sq. ft)
- I = rainfall excess = rainfall intensity – evaporation-infiltration rate (ft/sec)

In SWMM, the Equation 3.12 is solved at every time step (user controlled) using a finite difference approach (Warwick, 1991). The net inflow and outflow of the equation is averaged over the time step. The I-parameter is calculated as an average during each time step. Using the subscripts 1 and 2 to denote start time and end time, equation 3.12 can be rewritten in the following form:

$$\frac{d_2 - d_1}{\Delta t} = I - \frac{1.49 * W * S^{1/2}}{A * n} [d_1 + \frac{1}{2} (d_2 - d_1) - d_p]^{5/3} \quad \text{EQ. 3.13}$$

where  $\Delta t = t_2 - t_1 =$  time step (sec)

Equation 3.13 can be solved for d<sub>2</sub> using a Newton-Raphson iteration scheme.

The Newton-Raphson method is one of the most widely used methods for finding roots that can be generalized to find solutions of a system of non-linear equations (Smith, 1998). Unlike the bisection and false prediction methods, the Newton-Raphson method requires a single initial value, x<sub>0</sub>, which is commonly called the "initial guess" (Smith, 1998). This convergence technique is based upon a Taylor series expansion, described by equation 3.14

$$f(x) = f(x_0) + f'(x_0)(x - x_0) + 0.5 f''(x_0)(x - x_0)^2 + \dots = 0 \quad \text{EQ. 3.14}$$

If the initial guess is pretty close to the actual answer, then the difference between x and x<sub>0</sub> is relatively small and fewer iterations are needed for convergence. Following this assumption, the Taylor series may be truncated to the second term involving a linear relationship with x to form the Newton-Raphson iteration formula (Smith, 1998). Equation 3.15 is the shortened form of the Taylor series. Using equation 2.23 the Newton-Raphson method finds the tangent to the function f(x) at x=x<sub>0</sub> and extrapolates it to intersect the x-axis to get x<sub>1</sub> (Smith, 1998). As with

most iterative processes, the point of intersection becomes the new approximation to the root and the procedure repeats until convergence is achieved.

$$x_1 = x_0 - ( f(x_0) / f'(x_0) ) \quad \text{EQ. 3.15}$$

The RUNOFF module treats overland flow, infiltration and groundwater flow as a coupled flow value. The catchment elements receive rainfall, account for evapotranspiration losses, and allow depression storage. Before completing the calculations, a check is performed by SWMM to see if the losses are greater than the rainfall depth and stored surface water. If the losses are greater than the addition of the rain plus depression storage, the outflow is zero. If losses alone would be sufficient to lower the depth below the depression storage, the new depth is computed on this basis only and the outflow still remains zero (James, 1999).

The Newton-Raphson technique has proven to be numerically stable. Instability issues may arise when a catchment has an area of only several square feet and the selected time step is several minutes; therefore, SWMM may generate non-convergence errors and the catchment area and/or time step values should be adjusted. (James, 1999)

XPSWMM allows a maximum of four subcatchments per node, where runoff routing is handled at the subcatchment level. The outflow to channel/pipes (links) and inlets (nodes) is computed as the product of the Manning's based velocity equation and the cross-sectional area as defined by the channel depth and width (James, 1999).

The equation representing the linear reservoir method is presented below:

$$Q = W * \frac{1.49}{n} (d - d_p)^{5/3} S^{1/2} \quad \text{EQ. 3.16}$$

where Q = WFLOW = subcatchment outflow (cfs)  
W = WW(1) = subcatchment width (ft)  
n = WW(5) or WW(6) = Manning's roughness coefficient  
d = WDEPTH = water depth (ft)  
d<sub>p</sub> = WSTORE = depression storage (ft)  
S = WSLOPE = slope (ft/ft)

The values required for Equation 3.16 are inserted into the catchment portion of the RUNOFF dataset. Equation 3.16 may also be rearranged if combined with the continuity equation and divided by the surface area. A new routing parameter, WCON, is then formed from the rearrangement and is defined for the pervious and total impervious subcatchment areas (James, 1999). WCON is then used in all subsequent calculations and is defined by Equation 3.17 where catchment width, slope and roughness parameters are combined into one parameter. It is assumed that the width and slope of the impervious and pervious areas are equal. The only parameters available for alteration are the roughness coefficient and the relative area. (James, 1999)

$$WCON = \frac{W * 1.49}{A * n} S^{1/2} \quad \text{EQ. 3.17}$$

where WCON = routing parameter used in WSHED (ft-sec)  
A = surface area of pervious or total impervious subcatchment (sq. ft)

### *Runoff Routing*

SWMM has the capacity to accept four types of surface elements or links to route runoff: 1) subcatchment elements, 2) channel elements, 3) pipe elements and 4) control structures. Overland and channelized flows are handled by the subcatchment and linkage elements, respectively. Circular channel flow is calculated using the pipe attributes. Weir and orifices are

examples of control structures. Surface flow from all elements is routed via channels, pipes, and nodes (inlet points). Subsurface drainage may also be simulated using a connected system of pipes and channels.

Similar to the overland runoff process, flow routing for linkage elements (channels and pipes) is also performed based on the combination of the continuity and Manning's equation, using the non-linear reservoir technique.

Several measurements are fundamental to correctly simulate flow. The available linkage shapes include: 1) circular pipes, 2) trapezoidal channels and 3) parabolic channels. For the Cherry Point investigation, all channels were assumed to have a trapezoidal shape. Channel depth, widths and side slopes were all extracted from the GIS. Pipe elements require diameter, slope, invert and depth values. The "depth" parameter for the pipes is actually related to the wetted perimeter and is not a true vertical distance (James, 1999). The majority of the Cherry Point channels had sandy or clay bottoms with vegetated side slopes. All pipe and culverts were constructed from reinforced concrete.

Channels serve as conduits during SWMM simulations, where the water surface created by the inflow is considered to remain parallel to the invert and the inflows are automatically distributed along the entire link length. Hence, concentration of subcatchment inflows only at the upstream end of a channel/pipe (link) may be reasonable (James, 1999). Unfortunately, this method may flatten out the resulting inflow hydrograph peak when a system of joined links is simulated. In addition, downstream activities will not affect upstream nodes since RUNOFF does not simulate backwater conditions.

#### Introduction of Kinematic Wave routing

XPSWMM is capable of using various routing techniques for catchments and conduits. The Runoff Module generates stormwater runoff using the linear reservoir technique. The Sanitary Module uses the kinematic wave technique and has been designed to simulate pollutant transport at Cherry Point. The Hydraulics Module is the most complex of the three modes and relies on the St. Venant equations to predict difficult flow patterns. Although the three modes have preset equations, it is possible to change the routing equations in each mode. For example,

although the Runoff Mode is based on the linear routing method, kinematic wave routing can be selected as an alternative routing type.

The first simulations were simplistic, using only the linear reservoir method for the all catchments and conduits. Once XPSWMM9.0 was introduced and continuous simulations became feasible, the kinematic wave function was selected for routing elements only.

#### *Manning's Roughness, $n$*

Values of Manning's roughness coefficient,  $n$ , are not as well known for overland flow as for channel flow because of the considerable variability in ground cover for the former, transitions between laminar and turbulent flow, very small depths, etc. (James, 1999). Commonly, four techniques are used to estimate a roughness value: 1) understand the factors that affect the  $n$  value and narrow the range of guesses, 2) consult a table of typical values, 3) examine and adapt values from a similar channel whose  $n$  values are known or 4) determine the  $n$  coefficient by analytical procedures (Chow, 1959). A Manning's roughness coefficient of 0.013 was assigned to all concrete conduits and a value of 0.03 was used to characterize the major channels. Table 3F.1, in Appendix 3F, presents the roughness coefficients used for the Cherry Point research as adapted from the Chow research (1959).

Commonly, a single roughness value is associated with a channel section. This simplification allows for faster simulations, but neglects dynamic processes that occur in the stream channels. According to Chow (1959), some studies have even documented that the roughness for a particular surface is inversely proportional to the depth and Reynolds number. In reality, the value of  $n$  is highly variable and depends on a number of factors including: surface roughness, vegetation, channel irregularity, channel alignment, silting and scouring, obstructions, size and shape, and stage/discharge relationships. (Chow, 1959)

## **B. Application of GIS to Parameterize XPSWMM for Two Catchments**

### **Catchment Discretization**

#### *Importance of Catchment Discretization*

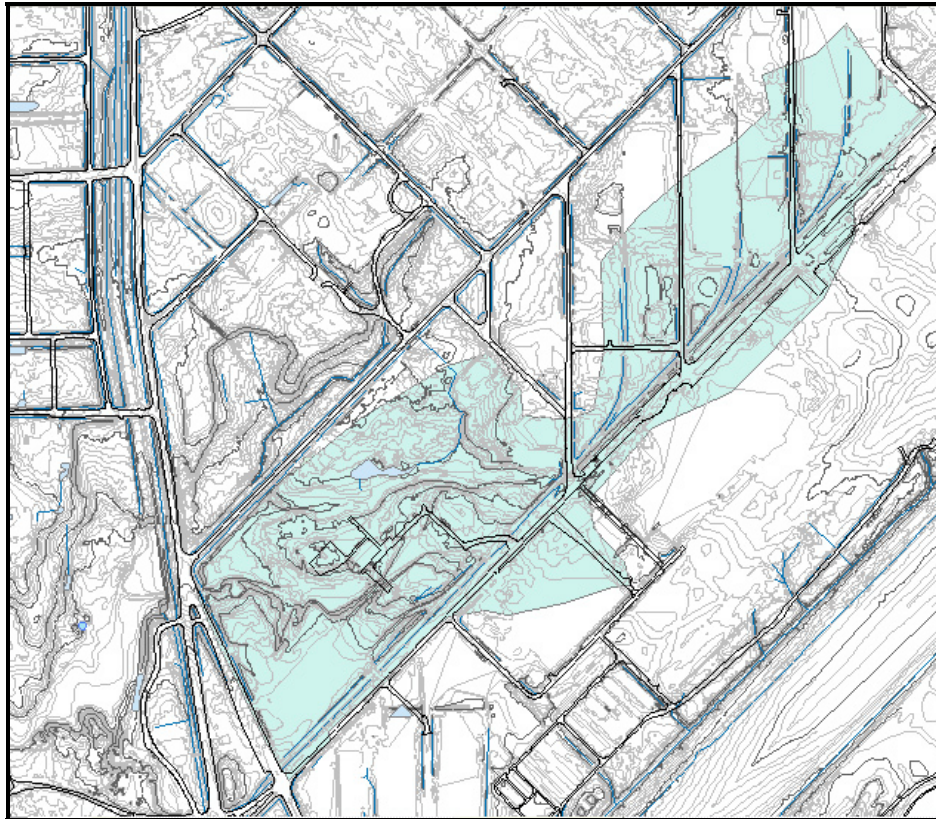
Discretization is a procedure for the mathematical abstraction of the physical drainage system (James, 1999). A network of hydraulic elements such as nodes and links may conceptually represent the drainage basin. The hydraulic properties of each element are then described by different parameters including size, slope, roughness, etc. In SWMM, the subcatchments represent runoff areas having uniform slope, roughness, and depression storage and infiltration values. For the MCAS-CP study, the discretization process began with the identification of the drainage boundaries using digital topographic information. Pipe inlets were identified from the pipe layer of ArcVIEW and the channel delineations were adapted from the surface drainage layers.

SWMM accepts 200 subcatchments and routing elements per simulation. For continuous simulations, only very coarse discretization is required. Decreasing discretization complexity could result in an increase in upland element areas and the averaging of spatial characteristics, including infiltration and rainfall variability (Miller et al, 1999). Therefore, it is desirable to represent the total catchment by as few subcatchments as possible, consistent with the needs for hydraulic detail within the catchment (James, 1999). Examining the existing surface and subsurface drainage patterns completed the subcatchment determination process. The number of subcatchments created was directly related to the physical nature of the system, and was minimized as the catchment schematization developed.

In the RUNOFF module, increasing the quantity of routing features will increase storage and ultimately attenuate a delay in the hydrograph peak. When the drainage network is removed from the simulation, subcatchment runoff feeds “instantaneous” into inlets (nodes), with consequent higher and earlier hydrograph peaks (James, 1999). Therefore, the challenge is to model the system with the least number of elements, to decrease element storage concerns.

Many subcatchments may be aggregated into single lumped or equivalent subcatchments by using spatially weighted sub-catchment parameters and by adjusting the sub-

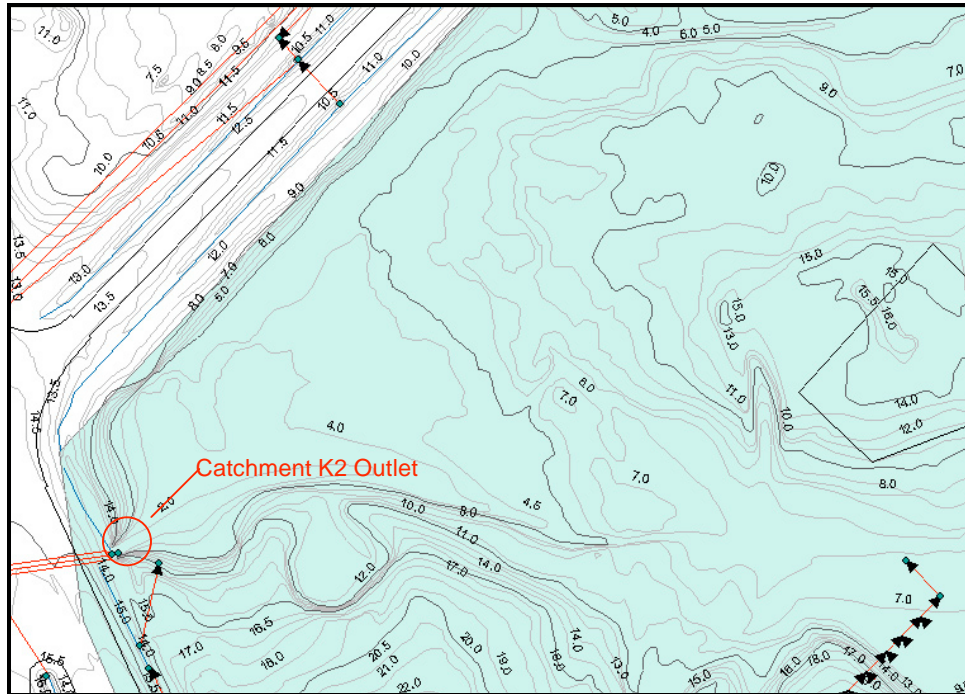
catchment width (James, 1999). Since a rectangular shape is assumed, the width should be approximately half the length of the main drainage channel. Normally, the slope of the area is measured perpendicular to the width. Figure 3.11 is an ArcMAP screenshot displaying the major and minor contours used to delineate the catchment boundaries for catchment K2. The blue region is the area designated as catchment K2 which was identified from previous survey and GIS work, in addition to manual basin delineation.



**Figure 3.11: GIS Delineated Polygon representing Catchment K2 using Ground Topography.**

Figure 3.11 is the final graphic generated from the catchment K2 delineation process and represents the area that was further discretized into subcatchments and inserted into XPSWMM. Using a combination of the land surface elevations and the reported surface/subsurface drainage systems, the boundaries of catchment K2 were eventually established. From this polygon, area measurements, and other catchment characteristics such as percent imperviousness and soil coverages were extracted by overlaying specific ArcMAP shapefiles. Two major concerns were prevalent during the delineation process: 1) connecting points of high elevation to establish the

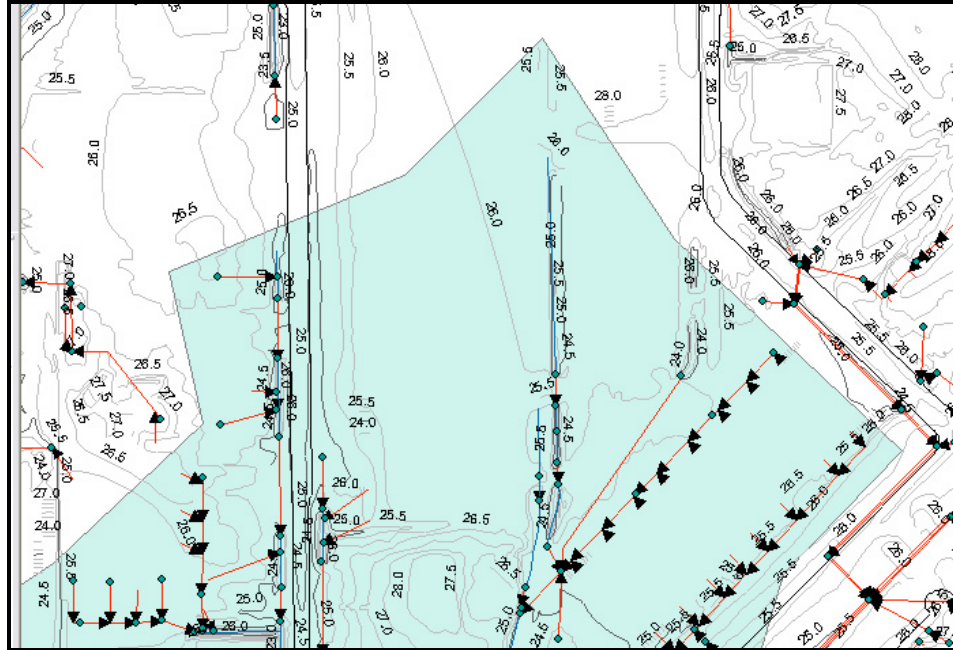
overall borders of the catchment area and 2) assuring that the roadway collector streams were included in the appropriate catchment. The following two figures displays situations of how these two focus areas were addressed.



**Figure 3.12: A GIS Representation of Catchment K2 Focusing on the Outlet.**

Figure 3.12 demonstrates how the ridge lines were determined for the catchment areas. Using the contours, boundary lines were established and the light blue region represents catchment area K2. In this particular graphic, at the top, a road has been indicated with runoff collector streams running parallel to the road surface. Note the area surrounding the roadway collection streams and its associated drainage area were not included in catchment K2 because the runoff passes beneath the road surface via a pipe to drain into the adjacent catchment.

Figure 3.13 is a graphic showing the process used to delineate the subcatchment regions. The figure below displays the topographic contours (black and grey lines) used to manually create and verify the catchment boundaries in catchment K2. The red lines indicate subsurface drainage pipes and the green circles are stormwater drainage features. The dark blue lines are surface channels and the light blue region represents the boundaries of catchment K2.



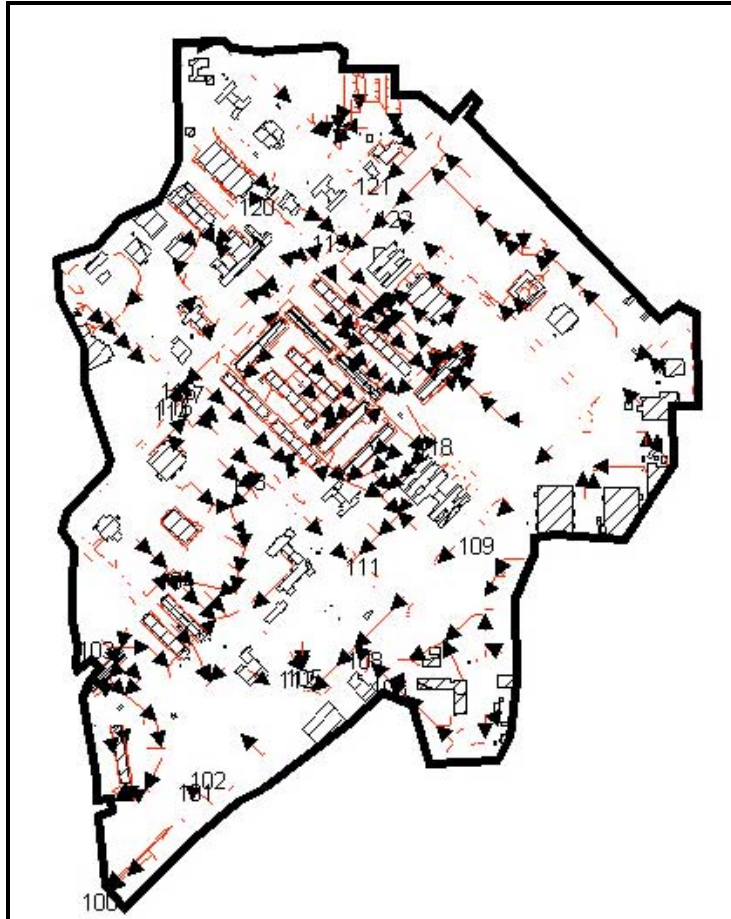
**Figure 3.13: ArcMAP Screenshot of Catchment K2 including Selected Stormwater Drainage Features.**

Figure 3.13 depicts how points of highest elevation were located and connected in the GIS platform. Manually, using the major and minor contours for the study area, ridgelines (catchment boundaries) were created. The ridgelines represent the boundaries of the catchment areas and the same technique was used to generate the subcatchment boundaries. Points of high elevation were determined and connected using the polygon function in ArcVIEW which was later used to crop important layers such as soils and impervious surface coverages.

#### *Discretized Subcatchments*

The subcatchment boundaries (subdivisions of the K2 and K3 catchments) were created using the same technique employed for the overall catchments. The outlets for K2 and K3, including surface and subsurface drainages features, were plotted in ArcVIEW. Confluence points were identified, including locations where pipes discharged into streams. The major and minor contours were then added in 5- and 10-foot increments, respectively. Using the outlet point as a base reference, the catchment boundaries were manually constructed in ArcVIEW using the “add theme” and “add polygon” functions. Figure 3.14 is an ArcMAP screenshot of the determined catchment K3 boundaries, also displaying the pipe and building layers. The boundary

determination process for catchment K3 was also conducted in ArcMAP. In Figure 3.14, the red lines represent pipes with the corresponding flow directions indicated by arrows.



**Figure 3.14: Catchment K3 Boundary with Visible Pipe and Buildings Layers.**

Using the mapped surface and subsurface drainage systems, the created subcatchment boundary was evaluated. If a point required adjustment, the “edit theme” command was used to revise polygon vertices. Since objects created in ArcVIEW have a corresponding attribute table, during editing procedures, the attribute table is updated simultaneously.

In all cases, the manually created catchment areas were compared to the processed boundaries produced using the ArcVIEW Geoprocessing extension. The only discrepancy between the two representations occurred when the outlet locations differed. Figures 3.15 and 3.16 demonstrate the constructed subcatchments for catchments K2 and K3, respectively. In Figure 3.15, the various subcatchments were created using the available GPS and topographic

information to create smaller drainage areas within catchment K2. Likewise, Figure 3.16 presents the subcatchment areas for catchment K3 based upon distinct topography.

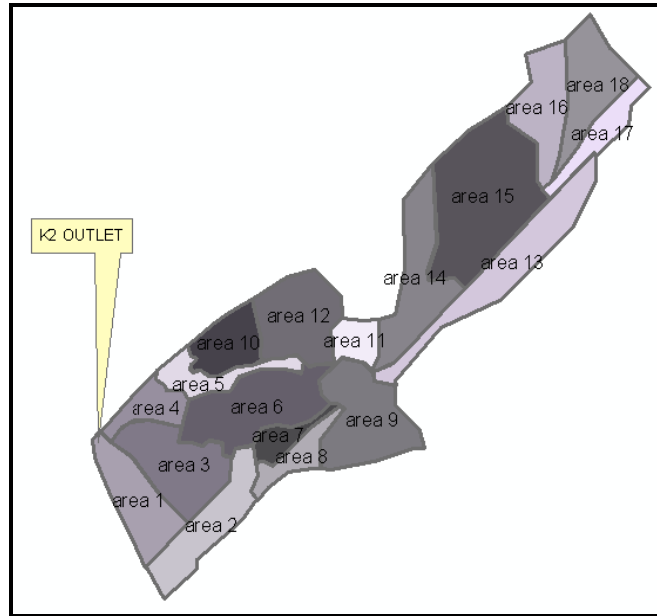


**Figure 3.15: Catchment K2 Delineated Subcatchments**

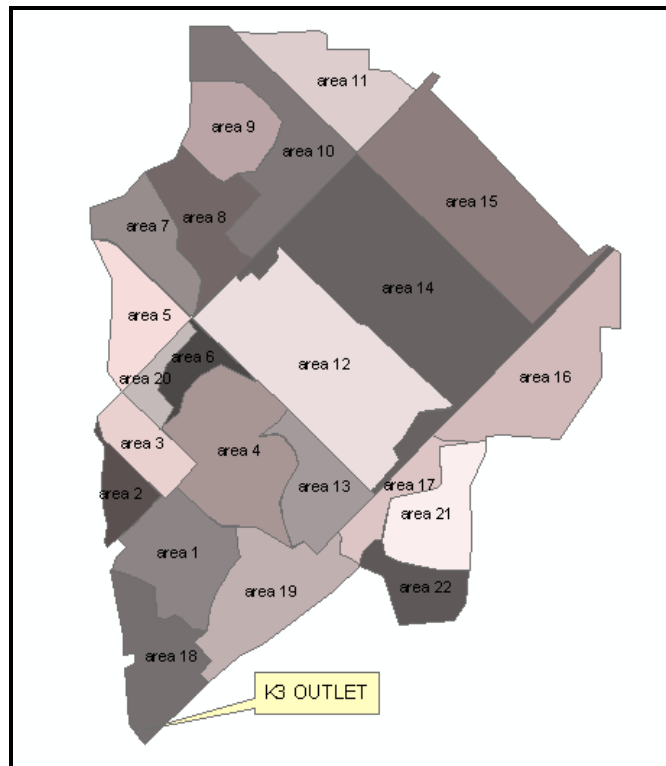


**Figure 3.16: Catchment K3 Delineated Subcatchments**

The “add theme” and “multiple-point polygon” options were revisited. The subcatchment discretization was more difficult than the catchment delineation because of the desired level of precision. Overlapping and unrealistic boundary lines were two areas of concern. In many cases, the resulting subcatchment was altered using the “edit theme” command. Increasing the number of subcatchments improved the simulation accuracy; but also required additional inputs and further increased susceptibility to user-related errors. To achieve a reasonable balance, the number of discretized subcatchments was minimized so as to represent the physical flow characteristics without compromising simulation accuracy.

Occasionally, rules governing catchment ridge lines did not apply to areas where subsurface drainage was dominant. In this situation, buried pipes were capable of dissecting hills that made “uphill” flow possible because the flow path followed a seemingly “uphill” direction. Therefore, subsurface flow directions did not always progress immediately downhill from underground stormwater structures, because constructed subsurface gradients sometimes contradicted surface topography.

From Figures 3.3 and 3.4, the XPSWMM nodes represent the subcatchment outlets. Therefore, when questioning the characteristics of a specific subcatchment, the corresponding XPSWMM node was queried, which contained the hydrologic and hydraulic information needed to appropriately represent the physical area. Note, in XPSWMM, the nodes were used to represent subcatchments solely. To query information about a routing element, that information could be directly referenced by selecting the unique routing element. ArcMAP was used to identify the node coordinates for routing purposes and delineation purposes. Whenever overland flow entered a major pipe conduit or surface channel, an outlet node was assigned. Likewise, when confluences were found, individual nodes were created. The overall discretization procedure and XPSWMM node determination process was aimed at creating sufficient model points that accurately characterized the flow regime needed to reach a specific node or outlet. Whenever major changes in surface or subsurface flow paths existed, a node point was inserted.

### *Area Calculation*

Since the subcatchments were created within ArcVIEW, area calculation was quite simple. Basically, the asymmetric polygons consisted of two-dimensional shapes. In ArcVIEW, once a polygon is created, the user may examine the polygon attribute table associated with the shapefile. All vertices are stored and the program randomly assigns names. By editing the polygon (subcatchment) attribute table, the random names were amended to reflect flow progression between subcatchments. The ArcVIEW extension XTools was used to calculate subcatchment area in square feet, acres, and hectares. The subcatchment area values ranged between 6 and 30 acres. Tables 3F.2 and 3F.3, of Appendix 3F, contain spatial information describing catchments K2 and K3.

### *Selected Input Parameters*

Table 3E.7 of Appendix 3E is an example of an event based, SWMM4.4 input dataset for catchment K3, using user defined rainfall, corresponding to Julian date 088 for the year 2001. The input parameters and controls were mostly user determined and specific to physical conditions. Table 3E.8 of Appendix 3E displays the SWMM4.4 RUNOFF Block requirements and explains the relationship between the SWMM codes to the actual measurements.

## **Infiltration Values**

### *Model Infiltration Inputs*

Both the Green-Ampt and Horton infiltration values for the SWMM and XPSWMM simulations are located in Figures 3F.4 and 3F.5 of Appendix 3F. The selected values were determined by referencing materials that provided a range of typical soil properties. The values needed to successfully complete the simulations were also dependent upon whether the Horton or Green-Ampt method was selected. The highlighted values in each figure denote the selected infiltration values per method.

## Soils

Sandy loams and fine sandy loams were present at Cherry Point, and a detailed soil map was created by the CPEC consultants (2001). The overall soils shapefile was dissected to create the soil coverage maps for the research area.

To create the categorized soils maps, the “Clip with Polygon” XTools command was used to intersect the watershed area, subcatchment boundary layer, and soils coverage shapefiles. The watershed area contained the polygon information and the soils theme possessed the raw soil data. The subcatchment boundaries were then used to crop the larger catchment soils maps. The final product was a theme entitled “clipped soils” that contained soil information on the subcatchment level. Figure 3.17 is a sample soil coverage map for catchment K2 displaying the four, mapped soil types. In Figure 3.17, each color represents a unique soil group. The corresponding name and description for any soil is accessed via the soils attribute table in ArcMAP. In addition to displaying the soil types, the attribute tables also contain area measurements for each soil. Table 3.3 is the soils attribute table for catchment K2 and was created by querying the catchment soils layer. Some of the data presented in Table 3.3 includes the soil name, area, description, texture plus some spatial data. The area and perimeter of each soil type within a subcatchment was calculated using the XTools extension.

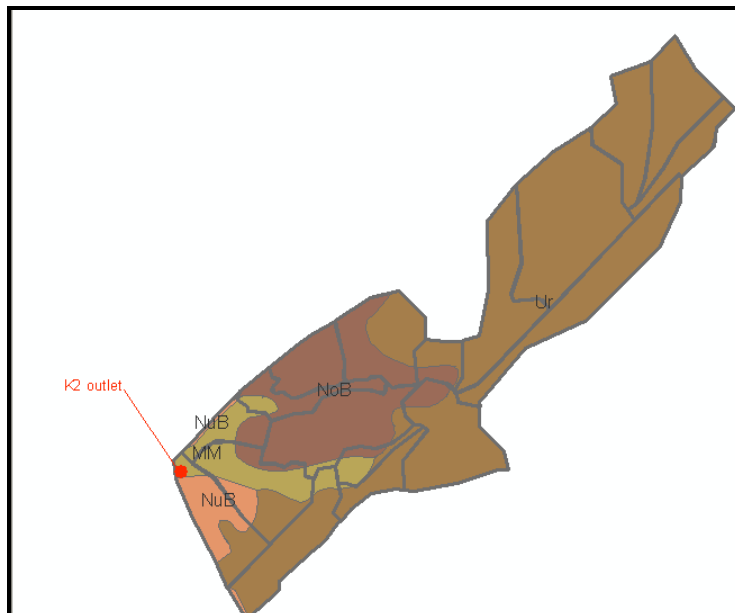


**Figure 3.17: Catchment K2 Soil Coverage Map with Subcatchment Boundaries.**

**Table 3.3: Soils Attribute Table for Catchment K2 using ArcVIEW 3.2 (MCAS study site).**

Attributes of K2_soils.shp										
Shape	Soil_type	A_texture	B_texture	A_texture2	B_texture2	Hydric	Area_Feet	Perimeter_Feet	Acres	Hectares
Polygon	NuB	loamy fine sand	sandy loam to sandy clay loam	lfs	sl-scl		12105.4	1058.420	0.278	0.112
Polygon	NoB	loamy fine sand	sandy loam to sandy clay loam	lfs	sl-scl		1050970.7	5494.778	24.127	9.764
Polygon	Ur	URBAN	URBAN	URBAN	URBAN		3362484.3	14851.421	77.192	31.239
Polygon	NuB	loamy fine sand	sandy loam to sandy clay loam	lfs	sl-scl		209137.7	2787.547	4.801	1.943
Polygon	MM	mucky fine sandy loam	fine sandy loam to silt loam	mfsl	fsl-sil	A	375036.6	4331.800	8.610	3.484

### Impervious Value

#### *Surface Imperviousness*

Surface imperviousness is a vital parameter for the SWMM model. Rainfall-runoff is directly related to percent imperviousness, which is the ratio of impermeable land area to the total catchment area. Using XTools, the subcatchment boundary theme was intersected with the impervious surface theme to create a new theme having impervious surface coverages categorized by subcatchment name. Figure 3.18 is a graphic of the impervious surfaces for the industrialized section of the air station, highlighting the K2 and K3 catchments. The supporting attribute table contains the impervious area information created by the layer intersection process.

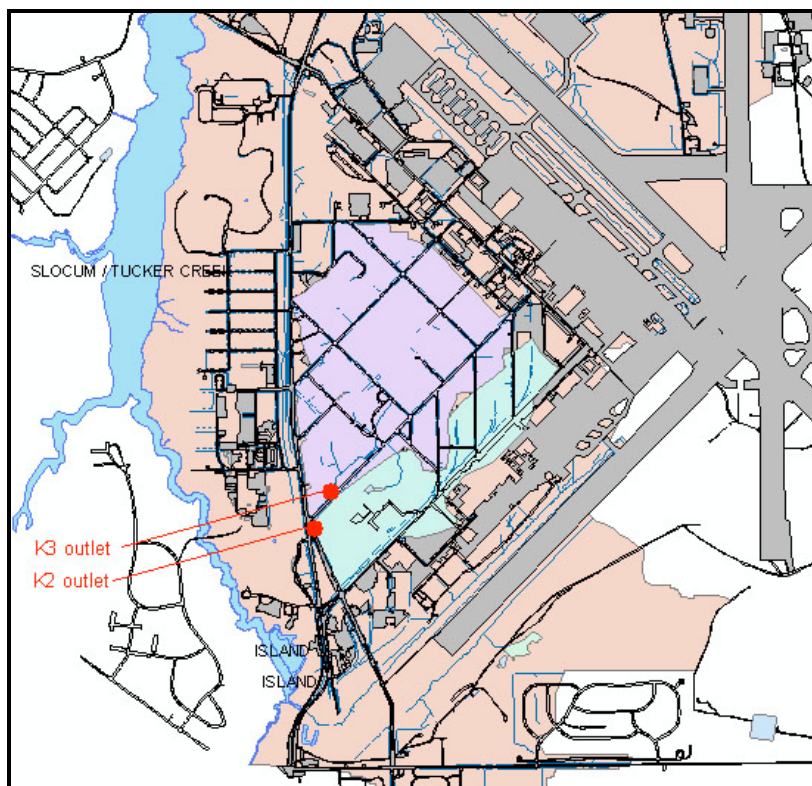


**Figure 3.18: Catchments K2 and K3 Boundaries Plus Impervious Areas for Cherry Point**

Using the subcatchment-impervious surface attribute table, the associated land areas were summed for each subcatchment. Percent impervious values for the study area ranged between 20% and 60%. Tables 3F.2 and 3F.3 of Appendix 3F are samples of the surface data information exported from ArcVIEW for catchments K2 and K3, respectively.

### **Assumptions for Overland Flow**

#### *Subcatchment Width*

Since real subcatchments are not usually rectangular with properties of symmetry and uniformity, it is necessary to adopt other procedures to obtain the width for more general cases (James, 1999). The width becomes increasingly important as a calibration parameter since the catchment slope and roughness are fixed parameters. Subcatchment shape gains importance since the modeler defines the width, which in turn either increases or decreases certain hydrologic conditions such as time of concentration.

As demonstrated in Figure 3.19, if the subcatchment width is minimized (shape E), the time of concentration increases, which would result in a retarded rising hydrograph. For shape E, more runoff is stored and less is released over time. The converse situation (shape A) would result in the fastest rising and falling limbs for the outflow hydrograph. Likewise under condition A, the runoff has the ability to reach the outlet quicker due to a lessened overland flow path. The following figure shows the difference in resultant outflow as influenced by the method used to measure the catchment width.

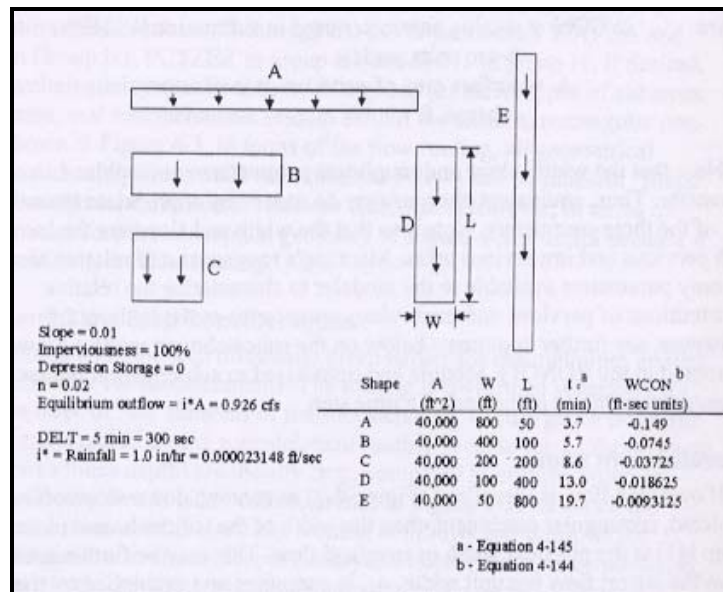


**Figure 3.19: Importance of Technique when Measuring Catchment Width (USEPA SWMM4 User's Manual, 1999).**

Obviously, the subcatchment width parameter is capable of altering the resulting outflow hydrograph. By varying the area shape, the time to peak also fluctuates. Likewise, the subcatchment width is used with other parameters to calculate WCON, the routing parameter used in WSHEd. In general, shifting hydrograph peaks in time is difficult to achieve through adjustment of RUNOFF module flow routing parameters (James, 1999). More important is the time distribution of the runoff which is directly related to the time distribution of the precipitation data.

The subcatchment widths were measured in multiple directions and recorded. The various measurements were then averaged and inserted into the hydrologic model. Multiple measurements were taken to avoid the conceptual “rectangular catchment” shape.

### *Slope*

Slope is another parameter needed to accurately route rainfall runoff in SWMM. There were two types of slopes: 1) catchment slope and 2) watercourse slope. The catchment slope reflects an average change in vertical elevation in relationship to a horizontal distance. In most cases, the subcatchments were asymmetric so measurements were taken in three directions and averaged. Figure 3.20 demonstrates the technique used to measure the subcatchment width and the watercourse length. The blue lines in the following figure represent major surface channels.

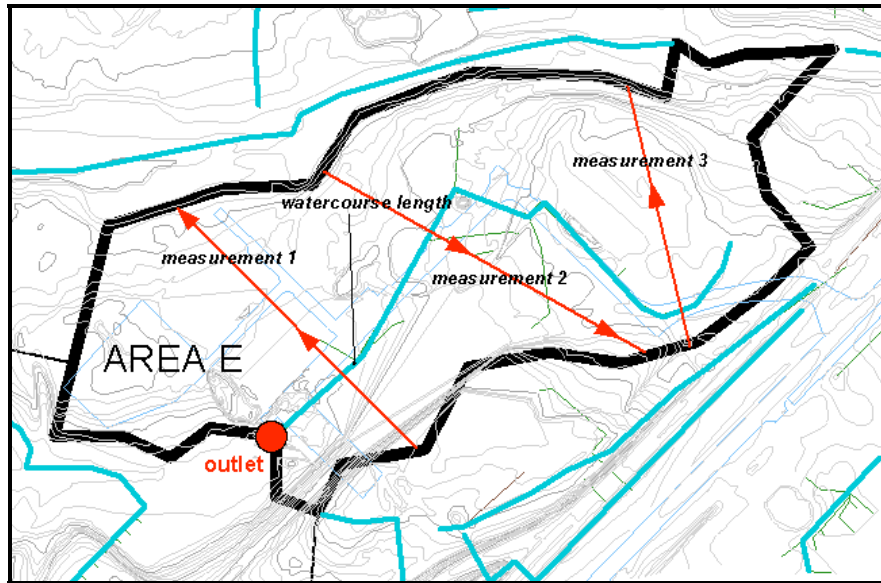


**Figure 3.20: Subcatchment Width and Watercourse Slope Calculation Technique.**

The measure tool in ArcVIEW was used to report linear distances. The average was calculated from the multiple width measurements (indicated by the red lines in Figure 3.20). Using the minor and major contour maps, the maximum elevation difference was determined. Dividing the maximum elevation difference by the average subcatchment length generated a slope value for the subcatchment.

Watercourse slope usually differs from the subcatchment slope since it follows the length of the most prominent overland flow path. First, the dominant flow path was determined using the existing topography. In most cases, the stream or channel had already been delineated by CPEC, Inc. Ephemeral streams had not been surveyed, but could be identified using surface elevation contours. The determination of the longest watercourse began with the identification of the most recognizable point upstream. Next, the flow path was followed to the outlet point. A line was digitized from the outlet point to the most upstream point designating the watercourse length (refer to the blue lines in Figure 3.20). Using the linear measurement tool in ArcVIEW, the linear distance was determined. The watercourse slope, in feet per feet, is the elevation difference divided by the watercourse length.

## **Assumptions for Routing**

### *Routing*

The main function of the GIS was to assist with the parameterization of the model inputs. Without the ArcVIEW information, it would have been extremely difficult to estimate numerous parameters prior to running the simulations. All areas, lengths, elevations, slopes, soils, and impervious ratios obtainable from GIS measurable data were calculated mainly within the ArcVIEW platform. In addition, when alterations were needed, editing procedures were facilitated while in the GIS environment.

A large majority of the information processed within the GIS also involved developing the routing scheme. The GIS allowed visualization of the watershed on a broad scale. The overland flow patterns and ephemeral channel structures were easier to comprehend when the contours were viewable. Examination of the topography further revealed an understanding of how runoff traveled downstream. Linkage features, such as reaches (overland flow channels and underground pipes), were determined in the GIS and the parameters associated with these elements were measured in ArcVIEW.

### *Reach Lengths*

Reaches are stream and channel sections that transport water. In this study, the reaches were used to route outflow from one subcatchment to a downstream subcatchment or reach. Reach lengths were determined by measuring the linear distance from one subcatchment outlet point to some downstream point. In most cases, the reaches were collector streams that exited the subcatchment. Occasionally, a subcatchment would produce runoff that was collected by a series of drop inlets. The drop inlets were connected to subsurface conduits that eventually discharged into a collector stream, where the stream would then transport water downstream and eventually intersect a channel. In this example, the (channel) collector stream would be modeled as a reach (see Figure 3.21).

The purpose of Figure 3.21 is to demonstrate that not all pipes emptied directly into a collector stream at Cherry Point. In many cases, some form of overland flow occurred before

rainfall runoff entered a surface channel. Therefore, the collector stream is considered a reach that transports runoff to the subcatchment outlet.

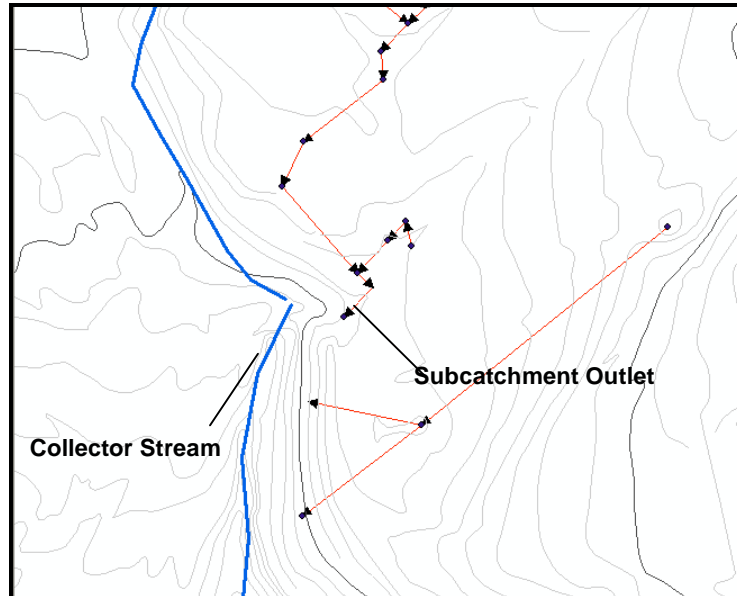


**Figure 3.21: GIS Example of a Pipe Emitting Overland Outflow to a Collector Stream in Subcatchment 12 of Catchment K2.**

Reach slopes were calculated in the same fashion as the watercourse slope values. The two main differences between a reach and a watercourse are that, 1) reaches are not necessarily located in a particular catchment, but function primarily as transport features and 2) reaches can receive and transport flows from multiple catchments

### *Stream Characteristics*

Most of the stream characterization was completed by CPEC, Inc. The surface drainage maps were particularly comprehensive in reporting the physical features of all surveyed channels. The CPEC team recorded stream data including, existing cover, erosion, vegetation, sedimentation level, top width, channel depth, bottom width and watershed association. These characteristics were accessed in ArcVIEW using the Cherry Point open drainage shapefile which was used to attribute SWMM.

One value not reported by the consultant was the channel side slope or bank slope. To compute this value an approximation was created assuming trapezoidal geometry. The top width, bottom width, and depths were already known; thus, bank slopes were determined using Equation 3.18:

$$\text{slope} = \frac{\text{vertical rise of embankment (ft.)}}{\text{horizontal distance of embankment (ft.)}} \quad \text{EQ. 3.18}$$

The calculated value for bankslope was reported in vertical feet per unit length (feet) and was assumed to remain constant along the entire reach length.

### *Pipe Sizing*

CPEC, Incorporated was not required to directly measure underground pipes/conduits, although exposed pipes sizes were verified. A 1995 study completed by MCAS and Woolpert Engineering did document the pipe sizes, but that document was unavailable; therefore, the CPEC information became the default. It was assumed that the largest pipe reported by CPEC extended indefinitely upstream, until another pipe size was reported. Therefore, all intermediate (buried) pipe sections, not directly measured, were arbitrarily assigned the same diameter as their downstream connector.

Figure 3.22 displays a typical geoprocessed, pipe coverage map created in ArcVIEW using the “Clip With Polygon” tool. Pipes located in a specific subcatchment could be investigated by clipping the initial pipe database with the subcatchment boundary layer. The clipped pipe shapefile only allowed conceptualization of the subsurface routing, because the stormwater structure shapefile actually contained the pipe attributes. In addition to showing the clipped pipes (red lines), the surveyed stormwater features (small black circles) plus the major surface channels (blue lines) are indicated in the following graphic.

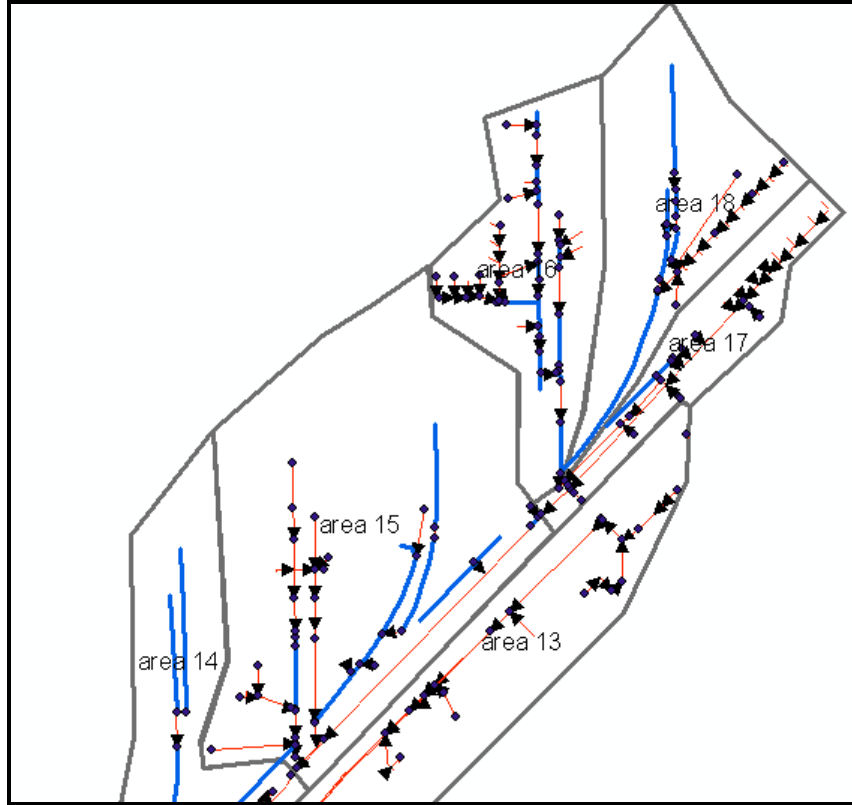


**Figure 3.22: ArcMAP Screenshot of Several K2 Subcatchments displaying Pipes, Stormwater Features, and Surface Channels.**

By querying the stormwater structure database (only headwalls), the pipe diameters were reported. Each stormwater structure shapefile contained a large amount of information but three characteristics were model essentials: 1) structure type, 2) size and 3) material. Pipe diameter (feet) and material (concrete, CMP, CPP, etc.) were the two most important values needed for modeling. Figure 3.23 displays some of the identified attributes for one headwall in the GIS database. Most importantly, the pipe diameters (labeled as “size” in the graphic) for all subsurface conduits were assigned, and eventually modeled in SWMM.

Location: [2628348.033643 426026.666420]	
Field	Value
FID	214
Shape	Point
TYPE	Headwall
X_COORD	2628346.5
Y_COORD	426021.59
CPECNUM	DHW-7L-166
SYMNUM	DHW-7L-166
CPNUM	DHW-2
RIM_ELEV	19
EFF_INV	0
D_SOURCE	CPEC
SIZE	1.5
BASAL_POS	0.10
A_CONDITION	4
C_SKIRT	0
S_GRATE	0
COMMENTS	hw
MULTIPLES	0
MATERIAL	concrete
SRVY_PRD	Y2000
STATUS	ACT
ORDERF	1320
WATERSHED_	Sandy Branch

**Figure 3.23: Catchment K3 Structures Shapefile Query to Obtain Headwall/Pipe Attributes.**

## Rainfall Data used

### *User Defined Rainfall*

A continuous rainfall dataset, including zero values, was needed for simulation. SWMM accepts precipitation input files in the form of intensity or rainfall volume. The MCAS-CP rainfall data was inserted into the RUNOFF module manually and followed the volume option. The main rainfall database was downloaded from the HOBO tipping bucket gauge located at monitoring station K1, using a constant rainfall interval. The “rainfall gap” program, transformed the breakpoint data into a continuous format. In the initial SWMM test runs, 15-minute intervals were too long and did not allow significant runoff generation. Consequently, a six-minute rainfall interval was selected.

### *Rainfall Variations*

The RUNOFF module can be very sensitive to spatial variations in rainfall. Even in smaller basins, thunderstorms may be localized and therefore result in dissimilar rainfall collection values at gages that are reasonably close. Amatya (et al 1996) reported similar rainfall distribution at the Carteret research site which is located approximately 12 miles (20km) east of the Cherry Point location. For modeling accuracy and successful SWMM calibration, it is essential that rain gages are located within and adjacent to the catchment, or that a supplemental storm model be referenced (James, 1999).

SWMM handles rainfall spatial differences by assigning gages to different catchment areas. If multiple gage data are available, it is suggested that a user use those data as opposed to attempting to create spatially averaged data. In general, if the rainfall is uniform spatially, as might be expected from cyclonic (frontal) systems, these spatial considerations are not as important, but the storm size and speed in relation to the total catchment area should be considered (James, 1999). Rainfall variations were also used to explain discrepancies between the measured and predicted hydrographs.

For the Cherry Point study, the automatic gauge located in catchment K1 became the main collector of rainfall data. The manual gauge located adjacent to the tipping bucket gauge was used to notice discrepancies and provided backup information. The other two manual gages located in catchments K3 and K5 were compared to the tipping bucket database but only the tipping bucket information was inserted in XPSWMM. Figure 2.6 (Chapter 2) displays the locations of the three precipitation monitoring stations and Table 2.1 (Chapter 2) summarizes the observed rainfall during the study period.

## **C. SWMM Evaluation**

### *Generic Model Testing Concerns*

The use of common sense, examining trends, and statistical analysis are all ways to support decisions made from modeling efforts. Before embarking on a detailed evaluation of a model, the user must first check the fundamental performance of the model (USEPA, 2005). The first level of investigation is to make sure that the collected measurements, variables, and

parameters have been appropriately inserted into the software. Then the modeler should make sure that these first level simulations are functioning properly, meaning that the input data are adequate for the purpose, and that the model is generating reasonable results. To test the validity of the simulation results, graphs of observed and simulated data should be compared. In addition, the early testing process should include generalized summaries of flow and/or loading predictions.

The initial goal of model testing is to improve the quality of the simulations. For this study, single events were simulated in SWMM to assure that 1) the rainfall data were inserted correctly, 2) that the rainfall-runoff transformation processes were occurring, and 3) that the downstream routing of surface runoff was being completed correctly. The single event results were examined against the observed flow data from catchments K2 and K3.

For this study, peak flow estimates were the major concern, because the travel time of water flow would be minimized when the flow rates are occurring at the maximum rate, thus providing conservative estimates. The observed flow data were collected for more than two years and used to evaluate the performance of the SWMM and XPSWMM results. The testing process was completed by splitting the observed data into two independent periods – calibration and validation. Ideally, these two periods are two typical time periods, not extreme conditions, with varying flow regimes (USEPA, 2005). The reliability of the validation model simulations was substantiated through the use of statistical tools.

The Cherry Point study followed the suggested, two-part, model testing technique. The calibration and validation storms were selected from various seasons of the year to evaluate XPSWMM's performance during wet and dry time periods. Return period design storms were also simulated to see what results would be generated and how these return period simulations compared to the monitored data. Maximum flow values were the most important output values simulated (serving as the objective function); therefore, observed versus predicted flow was examined. The time of peak was also critical because it is directly related to the estimated travel time for each subcatchment to some outlet point. Table 3.4 displays the dates of several storm events used to calibrate and validate the SWMM and XPSWMM runoff predictions

**Table 3.4: Selected Calibration and Validation Storms for Catchments K2 and K3 at Cherry Point.**

AREA	YEAR	CALIBRATION STORM EVENTS (JULIAN DATE)	VALIDATION STORM EVENTS (JULIAN DATE)
CATCHMENT K2	2000	319, 337	330, 352
	2001	48, 143, 185	152, 327
	2002	6	71, 165
CATCHMENT K3	2000	319, 337	330, 345, 348, 351
	2001	91, 175, 186	88, 143
	2002	6, 38	72, 90, 133, 148.5

### Calibration Period and Procedures

Several rounds of simulations were completed before satisfactory results were generated. Initially, SWMM predictions were completed using only single event precipitation. XPSWMM was then introduced and single event simulations were completed using the XP platform. Next, continuous precipitation was linked to the XP projects, allowing for continuous predictions using breakpoint rainfall for the entire year. Two sets of continuous predictions were completed: the 2005 and 2006 XPSWMM9.0 simulations. The XPSWMM9.0 calibration results generated in 2006 were the final set of model predictions.

Calibration does not need to be a complex task, but should enhance the relationship between the predicted and measured data. Therefore, the easiest solution is attempted first, followed by more complex solutions, as required.

Achieving realistic simulation results requires a comprehensive understanding of the overland flow pattern and process. Following subcatchment delineation, a schematic map was created to conceptually route runoff between areas. In most cases, outflow from one subcatchment was not direct inflow for a downstream catchment unless physical conditions required such routing. The outflows from all subcatchments were checked prior to incorporating the routing elements to make sure that SWMM was generating sufficient subcatchment runoff.

### *Catchment Width and Manning's Roughness Importance to Hydrographs*

Only two inputs were adjusted during the calibration of the XPSWMM simulations: catchment width and Manning's N. Based on the sensitivity analysis conducted, it was determined that catchment width and the Manning's roughness number were two highly sensitive input variables. The subcatchment width,  $W$ , in the non-linear reservoir routing method, is the same variable used in the numerator of Manning's flow equation (see EQ. 3.11). In the RUNOFF module, XPSWMM uses a combination of the Manning's flow equation and the continuity equation to generate outflows (see EQ. 3.12 or EQ. 3.13). Therefore, increasing the catchment width, decreases the time to concentration, and increases the hydrograph's time to peak and the maximum peak rate simulated, when all other variables are held constant. According to James (1999), the Manning's  $n$ -values (surface roughness coefficient) are "not as well known for overland flow as for channel flow because of the considerable variability in ground cover for the former, transitions between laminar and turbulent flow and very small depths, etc." Therefore, altering the  $n$ -value as compared to more measurable inputs such as depressional storage, watershed slope or catchment area seemed reasonable. An increase in the  $n$ -value results in the retardation and reduction of the flow predicted for the catchment. Most studies indicate that for a given surface cover,  $n$  varies inversely in proportion to depth, discharge or Reynolds number (James, 1999).

Additional figures and charts associated with the event-based input parameter sensitivity analyses are located in Appendix 3J of this chapter. The first, five figures demonstrate the input parameters percent change in a positive and negative magnitude and the resulting estimated peak flowrate. Likewise, the corresponding chart summarizes which parameters were most sensitive during the testing, per storm event. These observations were completed for both catchments K2 and K3, individually, and used to justify the calibration efforts.

## **Validation Period**

### *SWMM Event-based Storm Validation*

The validation storms selected in 2000, 2001 and 2002 received similar attention as the calibration storms. Each storm was input for the text version of SWMM and simulations were completed on an event basis. The next step involved importing the text database into XPSWMM version 9.0 and running the same simulations in the XP-platform as described above.

## **Statistical Procedures for Evaluating Model Performance**

### *Hydrograph Comparisons*

Calibration techniques frequently utilize statistical tests to add validity to the conclusions made from the model simulations. How well a hydrologic model reproduces a measured hydrograph is often the criterion for assessing the reliability of that model (McCuen and Snyder, 1975). Visual similarities may often lead to misinterpreted results unless some type of qualitative test is used to rank output performance. Qualitative assessments of hydrograph reproduction, however, do not provide a uniform standard for comparing the reliability of hydrograph-generating models; one needs quantitative indices of correspondence of computed and measured hydrographs (McCuen and Snyder, 1975).

Frequently, evaluations of model performance utilize a number of statistics and techniques (Legates and McCabe, 1999). These “goodness-of-fit” tests commonly measure the relative error between estimated results as compared to measured data. Likewise, the test statistics are usually bounded and yield results from -1.0 to 1.0. The resulting number describes the similarities, or differences, between the two sets of data, or in this case, hydrographs. Three such “goodness-of-fit” descriptors were used for the Cherry Point research.

*Pearson's Product-Moment Correlation, r, & the Coefficient of Determination, R<sup>2</sup>*

Pearson's product-moment correlation coefficient, r, and its square, the coefficient of determination, R<sup>2</sup>, are two commonly used correlation statistics. The Pearson correlation coefficient can be defined as (<http://www.ithaca.edu/jwiggles/stats/notes/notes8.htm>):

$$r = \frac{\sum XY - \frac{\sum X \sum Y}{N}}{\sqrt{(\sum X^2 - \frac{(\sum X)^2}{N}) (\sum Y^2 - \frac{(\sum Y)^2}{N})}}$$

EQ 3.19

Likewise the coefficient of determination takes the following form (<http://www.jsc.nasa.gov/bu2/PCEHHTML/pceh.htm>):

$$R^2 = \frac{(\sum xy - n \bar{x} \bar{y})^2}{(\sum x^2 - \bar{x} \sum x) \cdot (\sum y^2 - \bar{y} \sum y)}$$

EQ 3.20

For equations 3.19 and 3.20, X (x) and Y (y) are array points stemming from both the observed and predicted datasets and N (n) is the number of elements in the array.

The Pearson statistic describes the degree of colinearity between the observed and simulated variants. The correlation coefficient adequately measures the goodness-of-fit only when the two hydrographs being compared have nearly equal mathematical moments about a horizontal axis (McCuen and Snyder, 1975). McCuen and Snyder further explain that, "If either the mean values of the dispersions about the means of two hydrographs are dissimilar, then the correlation coefficient indicates only the similarity in the shape of the two hydrographs" (1975).

The Pearson test yields results ranging between -1.0 and 1.0. Positive values near 1.0 represent direct, positive agreement between the datasets; negative values depict an inverse relationship. Nonetheless, the correlation coefficient, r, becomes insensitive to differences in the

size of the two hydrographs. The insensitivity of  $r$  to differences in size as measured by the dispersions of two hydrographs may also be responsible for the inability of the correlation coefficient to provide an adequate quantitative indication of goodness-of-fit (McCuen and Snyder, 1975). Therefore, some hydrologists avoid calculating  $r$ -values for hydrograph analysis.

The coefficient of determination,  $R^2$ , is the square of the Pearson product-moment correlation coefficient,  $r$ . The coefficient of determination describes the proportion of the total variance in the observed data that can be explained by the model (Legates and McCabe, 1999). Unlike  $r$ ,  $R^2$  exists only in the positive realm, where values approaching 1.0 depict a strong agreement between the observed and predicted points. Two apparent limitations of  $R^2$  have been presented in literature. First,  $R^2$  is limited in that it standardizes differences between the observed and predicted means and variances since it only evaluates linear relationships between the variables (Legates and McCabe, 1999). Legates and McCabe (1999) further suggest that  $R^2$  is insensitive to additive and proportional differences between the model simulations and observations; thus, larger  $R^2$  values may result even when model-simulated values differ greatly in magnitude. Second, correlation-based measures are more sensitive to outliers than to observations near the mean (Legates and McCabe, 1999; Legates and Davis, 1997). A correlation can be greatly influenced by the number of outliers present. In most cases, removing outliers, prior to conducting the statistical analyses, improves correlation.

#### *Coefficient of Efficiency, E*

The coefficient of efficiency is another correlation measurement used to evaluate relationships between two datasets. Nash and Sutcliffe (1970) defined the coefficient of efficiency as:

$$E = 1.0 - \frac{\sum (O_i - P_i)^2}{\sum (O_i - \text{mean } O)^2} \quad \text{EQ 3.21}$$

$O$  is from the observed data and  $P$  represents the predicted values.  $N$  is the number of points in the array.

*“E ranges from negative infinity to 1.0. Values closer to 1.0, represent better agreement between the two sets of information. A value of zero for the coefficient of efficiency indicates that the observed mean is as good a predictor as the model, while negative values indicate that the observed mean is a better predictor than the model. The coefficient of efficiency is believed to outperform the coefficient of determination for model evaluation purposes because it is sensitive to differences in means and variances. However, E, is overly sensitive to extreme values.” (Legates and McCabe, 1999)*

### *Index of Agreement, d*

The coefficient of agreement, *d*, is considered one of the best correlation coefficients for evaluating model performance. Developed by Wilmot (1981), *d* overcomes insensitivity to means and variances and has the following form:

$$d = 1.0 - \frac{\sum (O_i - P_i)^2}{\sum (|P_i - \text{mean } O| + |O_i - \text{mean } O|)^2} = 1.0 - N * \frac{\text{MSE}}{\text{PE}}$$

EQ 3.22

where  $O_i$  = observed point  
 $P_i$  = predicted point  
mean  $O$  = observed mean  
  
MSE = mean square error  
PE = predicted error  
N = sample size

Similar to the coefficient of determination, *d* also ranges from 0.0 to 1.0 with higher values indicating a stronger agreement between the predicted and observed points. Wilmot (1981) argued that the index of agreement represented the ratio between the mean square error and the “potential error”, multiplied by the number of values and then subtracted from unity (Legates and McCabe, 1999). The index of agreement is believed to be a better indicator of agreement since it is sensitive to extreme values due to the squared difference (Legates and McCabe, 1999).

## **Sensitivity Analyses**

### *Generic Model Sensitivities*

The following definitions and comments regarding absolute and relative sensitivities were adapted from a PowerPoint presentation named “Sensitivity Analyses” by Terry Bahill (2003) located at: [tucson.sie.arizona.edu/sysengr/slides/sensit.ppt](http://tucson.sie.arizona.edu/sysengr/slides/sensit.ppt)

*“During a typical sensitivity analysis, input values are altered and the resulting degree of change is measured. Normally, a sensitivity analysis enhances model validation, promotes model simplification, adjusts numerical values for parameters and detects critical criteria. There are two classes of sensitivity testing: analytical and empirical. Analytical testing works best with well-defined systems. Empirical testing demonstrates sensitivities between parameters and may be used to display system changes when certain parameters are altered. Absolute and relative sensitivity tests are both examples of analytical type analyses.”*

#### *Absolute and Relative Sensitivity*

According to Bahill (2003), the absolute sensitivity of the function F to variations in the parameter  $\alpha$  is:

$$S_{\alpha}^F = \left. \frac{\partial F}{\partial \alpha} \right|_{NOP} \quad \text{EQ 3.23}$$

Equation 3.23 would be used to evaluate output errors due to changes in particular parameters or to detect when a parameter has its greatest effect on the output.

Bahill (2003) describes the relative sensitivity of the function F to variations in the parameter  $\alpha$  as:

$$\bar{S}_{\alpha}^F = \frac{\% \text{ change in } F}{\% \text{ change in } \alpha} = \frac{\partial F / F}{\partial \alpha / \alpha} \quad \text{Or} \quad \bar{S}_{\alpha}^F = \left. \frac{\partial F}{\partial \alpha} \right|_{NOP} \frac{\alpha_0}{F_0} \quad \text{EQ 3.24}$$

In most cases, relative sensitivity testing is used to compare parameters.

### *Rainfall Sensitivity Analysis*

Some runoff influencing factors include land cover type, the percent imperviousness, and the watershed slope. When analyzing the sensitivities of SWMM, these same parameters proved to be the most significant.

Rainfall transformation into runoff and the runoff flow path are two essential principles of all hydrologic models. The precipitation information is the key to the SWMM simulations, and without meaningful data, the runoff simulation results will never resemble natural processes. Thus, SWMM's sensitivity to the user-defined rainfall information was also explored. A sensitivity analysis was conducted using the rainfall input variable, where the intent was to purposely alter the input dataset to see how each variation affected the predicted runoff rates. During the analysis, two winter (Days 6 and 61) and two summer storms (Days 133 and 148) in the year 2002 were selected for catchment K3.

The original rainfall depths were adjusted from –40% to +40% in 10% increments. The newly computed rainfall depths were later inserted into SWMM and saved individually. SWMM 4.4 simulations were then conducted for each adjusted input file and the predicted peak rates were recorded and graphed. Figure 3.24 displays the incremental change in peak outflow rate from the various rainfall adjustments using the selected 2002 rainfall events.

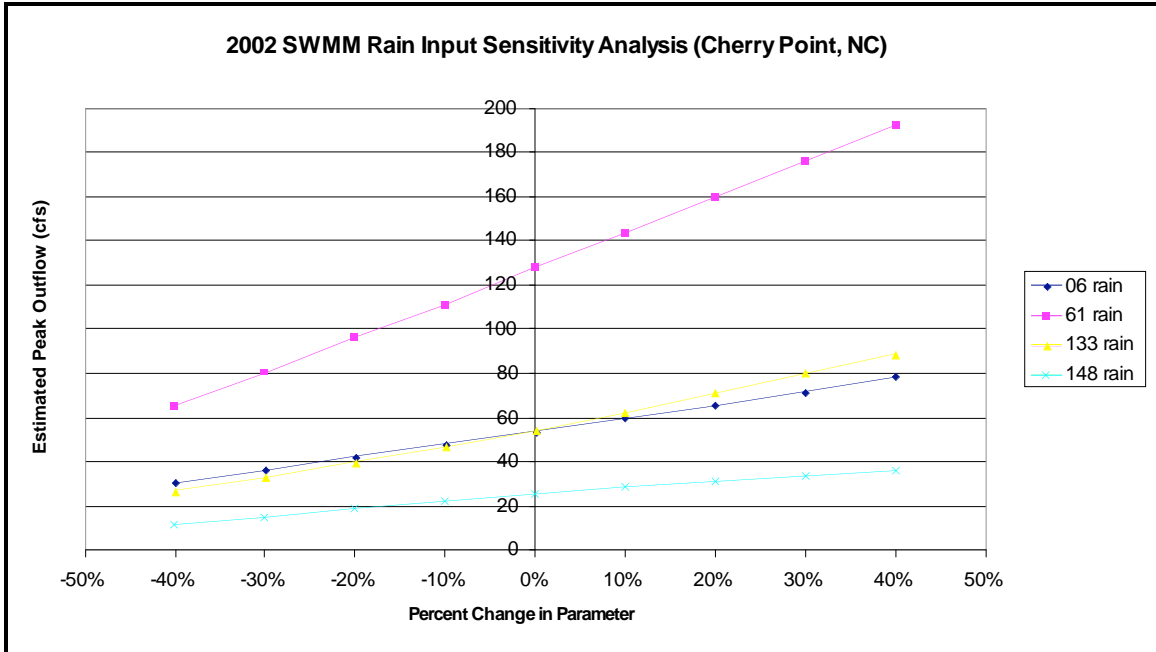


**Figure 3.24: SWMM Rainfall Sensitivity for Four Storm Events at Cherry Point (2002).**

The results from this analysis were quite interesting. For the positive direction, storm 133 (2002) demonstrated the most change, having a percent-change value of 63.8. The least affected storm, following rainfall increase, was storm 148. The negative direction yielded different results. The most effected storm was storm 148, displaying a 56.0% change, while the least effected event was storm 6, had a 43.5% change. The peak outflow base values (the peak flows predicted at 0%) for storms 6, 61, 133, and 148 were 53.8, 128.2, 54.1 and 25.7cfs, respectively.

A linear relationship exists between the rainfall amounts and peak outflows estimated by SWMM. This is reasonable since SWMM is directly accessing the user-defined rainfall to create the model input needed to simulate runoff.

For Cherry Point, the rainfall sensitivity analyses demonstrated that under and over estimations of rainfall directly influence the simulated outflow and peak flow rate proportionately. If the recorded rainfall represents a wetter than normal year, the resulting outflow will demonstrate the same trend and vice versa when compared to some baseline. Therefore, the extent of the precipitation influence can be explained by a linear relationship.

From Figure 3.24, the maximum negative difference is the difference between the 0% readings and the -40% adjustments. The maximum positive difference is the opposite. The percent change value is the calculated difference between the estimated maximum negative/positive values and the base maximum peak outflow value, reported as a fraction of the baseline value (maximum peak outflow rate). Table 3B.5, of the Chapter Three 3B Appendix, summarizes the relationship discovered during the rainfall sensitivity analysis.

### **Continuous Simulations versus Event-based Simulations**

#### *Continuous Simulations*

Initially, the SWMM simulations were completed using specific rainfall events for simplicity reasons. Continuous simulations were attempted in SWMM 4.4 where the annual rainfall data was either inserted directly into the RUNOFF file using special SWMM formatting, or an external rainfall interface file was created and linked to the project. The SWMM simulations using the rainfall interface files were unsuccessful in accessing the correct “scratch disk” and manually inserting the collected rainfall was too tedious when considering the formatting demands. Therefore, continuous simulations in SWMM 4.4 were not easily constructed. A more complete analysis of the modeling results indicated that the event-based simulations did not accurately represent the hydrology of the study site and that continuous rainfall data were needed. In addition, the predicted storm outflow rates and consequently the travel time for flows to various outlets may be affected by antecedent conditions, thus necessitating the need for continuous simulations.

The justification for converting from single event to continuous simulations stems from the fact that naturally occurring physical processes, including hydrologic activities, happen frequently and the oversimplification of only using single event simulations seemed unreasonable for the Cherry Point project. Continuous simulations allowed additional soil-water interactions to take place that would be neglected, and or minimized, during the single event application.

For the continuous XPSWMM simulations, the old SWMM files were imported into version 9.0 and the simulation dates were adjusted to reflect an annual time period. The time

controls were set to begin on January 1<sup>st</sup> and to end on December 31<sup>st</sup>. Precipitation files were saved as .txt files and imported. Using the Rain module, the measured tipping bucket rainfall for years 2001 and 2002 were connected to XPSWMM files for catchments K2 and K3. The simulation time steps were also adjusted. For XPSWMM to graph the complete annual hydrographs, the dry, transitional, and wet time steps were set to 7200, 3600, 3600 seconds, respectively.

As the simulations progressed, greater resolution was desired for the outflow hydrographs. The observed hydrographs had a ten-minute recording interval. In order to calibrate and verify the model, it was determined that the predicted hydrographs should also have the same number of points as the observed data. Therefore, the wet and transition time periods were adjusted for catchments K2 and K3 to enhance correlation. Table 3B.9 of Appendix 3B displays the final simulation time step and the corresponding number of hydrograph points for the Cherry Point data.

### **III. Results and Discussion**

#### **A. Calibration Results**

##### *Catchment K2 Single Event Calibration*

Several rounds of calibration attempts were completed. Figure 3.25 displays a collection of false, SWMM data points, from Julian date 143.00 to 143.20, which preceded storm event 143. The following outflow hydrograph was produced using the HOB0 rainfall from 2001 at the monitored outflow of catchment K2. The reason for the existence of the extra runoff was eventually discovered and corrected.

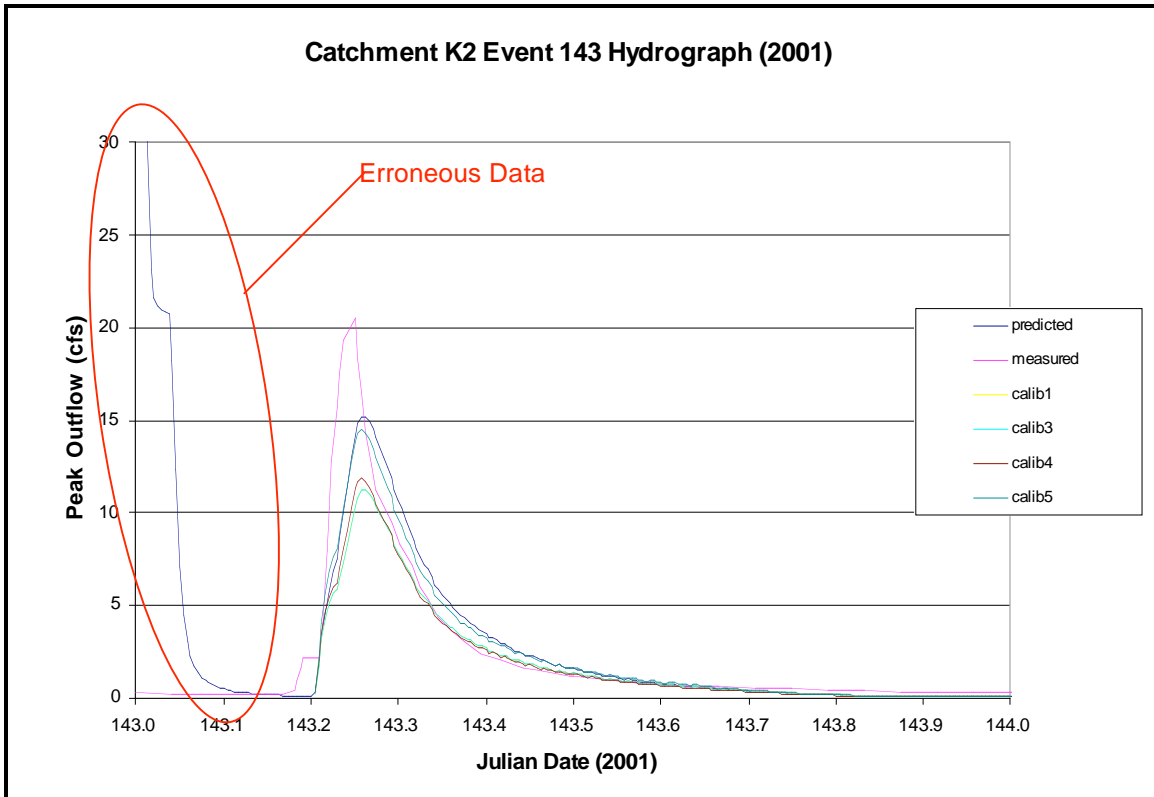


**Figure 3.25: Example of Erroneous Data in the SWMM Prediction Hydrograph for Catchment K2 at Cherry Point.**

During the first calibration attempt (calibration 1), the simulations utilized an expanded rainfall dataset that included weather information before and after the actual storm event, and the simulation length was increased from two to five days. Theoretically, increasing the simulation period should improve the overall response of the hydrograph, by incorporating antecedent rainfall conditions. Unfortunately, the “calibration 1” results did not offer an explanation to the falling limb phenomena being generated in the simulated SWMM hydrographs; however, the shape of the SWMM hydrograph began to resemble the observed curve following the “calibration 1” procedures.

The “calibration 3” simulations exposed the reason behind the falling limb prediction when the collected precipitation data did not support such a response. The routing elements, especially the wetland areas, were initially storing excess water; thus, causing large outflow at the simulation beginning. Consequently, the initial water depths were set equal to zero for all

elements, except for element 101, the physical stream equipped with the flow meter. The water depth in this element was set to one foot and the simulations were completed. Figure 3.26 is the event-based hydrograph following the baseflow reduction in several upstream routing elements that route flow into catchment K2.

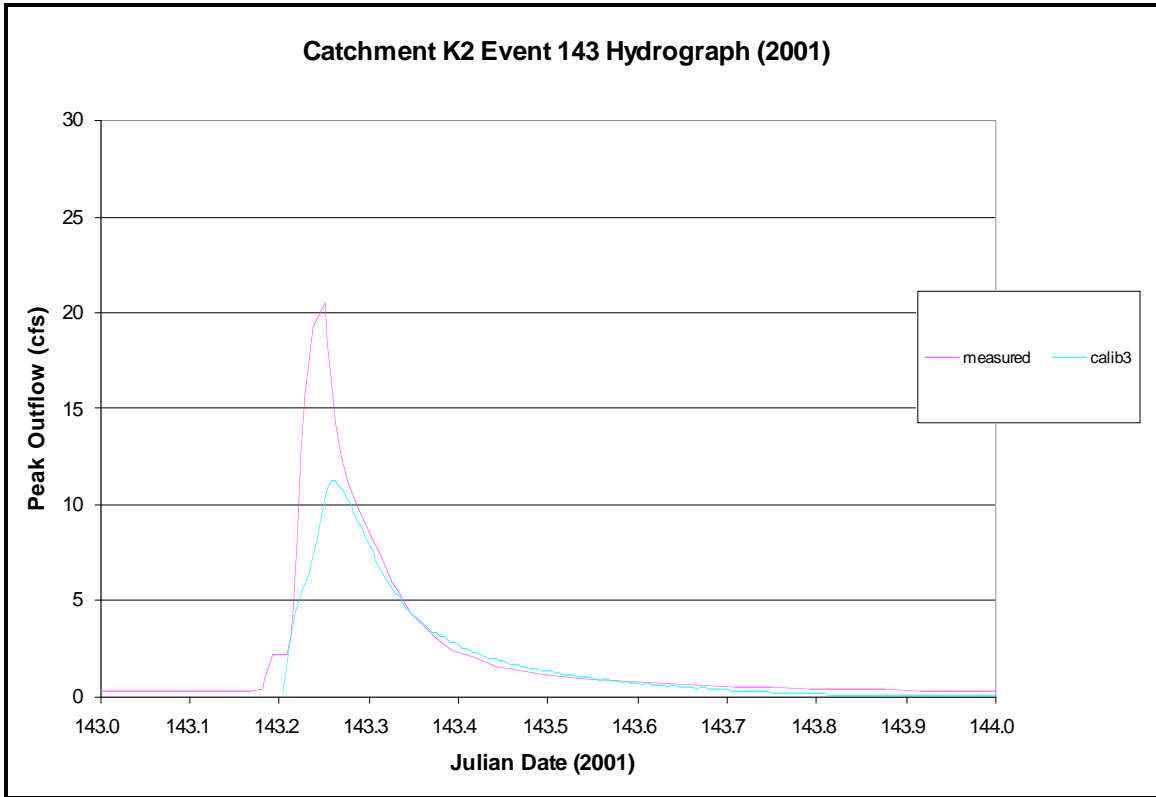


**Figure 3.26: Event 143 Calibration Hydrograph for Catchment K2 (2001) following a Baseflow Reduction at Cherry Point MCAS.**

Calibration efforts 4 and 5 were attempts to make generalized changes in the SWMM input files for area K2. Calibration 4 involved reducing Manning's roughness coefficient, N, by 25% throughout the catchment. Before the calibration 4 adjustments, the N-values used for impervious and pervious areas were 0.013 and 0.030, respectively. Following the insertion, the new N-values were decreased to 0.010 and .023, respectively. The SWMM simulations were then completed for all the K2 calibration storms using the same rainfall datasets as before. It was already determined, during the parameter sensitivity analyses that reducing the N-value resulted in an increase in the predicted peak outflow. The shape of the hydrographs remained

the same from calibration 3 to calibration 4. The fifth calibration attempt was similar to calibration 4, where generalized adjustments were made to all catchments.

For calibration 5, the percent impervious values were increased by 25% and the outflow response was examined. The calibration 5 technique generated a peak outflow greater than 24 cfs, which corresponded closely to the nearly 26 cfs outflow measured at the outlet. This study is more concerned with the time to peak than matching the volumes of the two hydrographs. Therefore, the timing of the peak outflows for both the observed and simulated hydrographs following the effects of calibration 5 are nearly equal. For example, the observed peak flowrate during storm event 143, of 2001, occurred at Julian date 143.25. Likewise, the model predicted that the peak flowrate, for the same event, would occur at 143.26. The calibrations were corrected the timing disparities, and the resulting time difference between the observed and predicted values was reduced to 0.01 days or 14.4 minutes. Recall that a time discrepancy of 14.4 minutes actually represents two time intervals, or a maximum time span of 20 minutes, since the flow meter gathered data in 10-minute increments.

In most instances, the simulated hydrographs have a rounder shape, as compared to the measured flow data, due in part to the user-defined rainfall dataset. The SWMM generated hydrograph points are heavily reliant upon rainfall data and the rainfall interval. The flow meters were also collecting information during specified intervals as well; however, the collection intervals of both the rainfall and flow meters were not synchronized. Therefore, the actual peak discharge rate (not directly recorded by the flow meter) could have happened at a point in time when the flow meter was not assigned to collect data, but the inserted rainfall amount calculated a maximum flowrate during that time span. Fewer collection points also means that the observed hydrograph would have a "sawtooth-like" shape. Since the collection period for the observed flow was longer than the modeled rainfall intervals, the predicted hydrograph would have more points (directly rainfall related), resulting in an overall smoother hydrograph shape when compared to the measured flow data.

Appendix 3H housing a collection of calibration and validation hydrographs associated with both catchments. Exhibits 3H.1 and 3H.2 display the selected, calibration hydrographs. Exhibits 3H.3 and 3H.4 focus more on the validation of the prediction model. Further explanation concerning the hydrograph trends are given in the captions for each graph.

### *Catchment K3 Single Event Calibration*

The calibration efforts for area K3 started in a manner similar to area K2. Initially, the raw flow data and the first round of SWMM simulations (calibration 1) were compared. Similarities, or differences, were noticed and recorded. Calibration 2 focused on attempting to match the peak discharge rates from storms 006 and 091. The percent imperviousness values for storm 006 were increased by 20% and yielded a peak discharge rate very similar to the measured value. For event 091, the catchment widths were decreased by 20% and resulted in a hydrograph barely over-predicting the observed data. Figures 3H2.1 through 3H2.6, located in Appendix 3H, display the hydrographs resulting from the calibration procedures for catchment K3.

### *Results of Statistical Analysis of SWMM Calibration Hydrographs*

The SWMM simulations were further examined and calibrated using traditional techniques. First, the measured and predicted datasets were correlated, meaning each dataset was synchronized by Julian date. This procedure was completed manually using the selected calibration storm event spreadsheet and observed data. Summary statistics were completed using the Data Analysis Tool and the measured and predicted sample variances were reported. The sample variances were inserted into a spreadsheet and used to calculate the z- test statistic.

### *Z-test Results*

The z-test is commonly used to test for the mean of a single normal population, of known variance. The z-statistic is a measure on a random sample (or a pair of samples) in which a mean (or pair of means) is placed in the numerator and divided by the numerator's standard deviation (Hoffman, 2002). The sample populations were the calibration 5 simulations for catchment K2, the calibration 1 curve for catchment K3, and the measured storm data at Cherry Point. The assumed hypothesis is that the two samples have equal means, conversely, the null hypothesis is that the population means differ. If the calculated z-statistic is significantly different

from zero, then the test is considered to be statistically significant. The resulting z-values from the calibration storms are presented in Table 3B.6 (see Appendix 3B). Figures 3H.1.1 through 3H.2.6 (see Appendix 3H) contain the outflow hydrographs associated with the presented statistical results in Table 3B.6.

For the catchment K2 calibration storms, event 143 (2001) and event 6 (2002) had the smallest absolute value for the z-value, reporting 0.433 and 0.248, and indicating excellent calibration results (see Figures 3H.1.5 and 3H.1.1). The smaller z-scores represent that the observed and predicted samples have similar means. Storms 48 (2001) and 185 (2001) displayed moderate deviation from zero as made evident from the plots in Figures 3H.1.4 and 3H.1.6. Event 319 (2000) had the largest z-score absolute value of 5.29, therefore, exhibiting the greatest dissimilarity between the observed and predicted means as viewed in Figure 3H.1.3

The catchment K3 z-scores were also reviewed. Events 91 (2001), 175 (2001) and 6 (2002) demonstrated the lowest absolute value of the z-test, with scores of 0.409, 0.217 and 0.75 respectively (see Figures 3H.2.2, 3H.2.3 and 3H.2.5). These three storms had the most similarities between the observed and simulated hydrographs. Events 186 (2001) and 38 (2002) received moderate z-score of 1.51 and 1.73 (see Figures 3H.2.4 and 3H.2.6). The largest z-score was received for event 319 (2000); thus, this event shows little similarity between the measured and predicted hydrographs (see Figure 3H.2.1).

The best agreement between the observed and predicted data was obtained for storm event 174 of 2001 (catchment K3), as indicated by the z-test scores. The shapes of the two hydrographs are very similar, although timing differences exist. For example the measured data peak outflow occurred at Julian date 175.19. The calibrated simulation generated peak outflow at Julian date 175.22 for a difference of .03 days or 43.2 minutes. Recall that the z-test compares the means of the two populations. The observed data has a higher peak rate (153.4 cfs), but lower values in the tail section of the curve. Conversely, the calibrated simulated outflow rate was only 109.3 but this curve has higher outflow values on the right side of the curve. Therefore, in the determination of means using the z-test, the datasets appear to be similar numerically, but visually, the timing between the peaks differs.

*Single Event T-test Results*

Since the travel time (in a conservative way) is more of a function of peak flow rate, it was suggested that the statistical t-test be explored to better explain the comparison of peak flow values for all major storms in 2001 and 2002. To complete this task, seven storm events (per catchment) were selected for the single event t-test procedures.

The mean flow rates for the selected single event storms at Cherry Point were evaluated. Exhibits 3G.1 and 3G.3 of Appendix 3G present the simulated hydrographs, by event, for catchments K2 and K3. Although the mean flow rates were of interest, the research was more concerned with determining agreement between observed and simulated peak outflows. Tables 3.5 and 3.6 contain the information used to complete the t-test statistic for catchments K2 and K3, respectively. The reported flow rates were either measured or predicted, by SWMM, at the outlet of the each catchment. The Julian date corresponding to the occurrence of the peak flow rate is also indicated.

**Table 3.5: Catchment K2 Single Event Peak Flow Rate Timing Comparison**

YEAR	EVENT NAME	MEASURED		PREDICTED		TIMING DIFFERENCE (Min)	ABS. PEAK FLOW RATE DIFFERENCE (CFS)
		TIME STAMP	PEAK FLOW RATE (CFS)	TIME STAMP	PEAK FLOW RATE (CFS)		
2000	319	319.54	10.00	319.54	12.06	0	2.06
	337	338.58	10.28	338.57	3.67	14.4	6.61
2001	143	143.25	20.53	143.27	10.07	28.8	10.46
	48	48.33	5.68	48.33	6.56	0	0.88
	185	185.19	27.80	185.20	14.69	14.4	13.11
2002	6	6.56	25.77	6.58	17.41	28.8	8.36
	71	72.33	73.53	72.32	45.55	14.4	27.98

For catchment K2, the overall event timing proved to be satisfactory. The greatest time differences occurred during events 143 (2001) and 06 (2002) having a discrepancy of 28.8 minutes between the measured and predicted peak outflows. Conversely, for events 319 (2000) and 48 (2002) these existed no difference between the timing of the peak outflow rates. The last

columns of Tables 3.5 and 3.6 were calculated to display the difference between the measured and predicted outflow rates, on an absolute scale. The smallest difference between the two rates occurred during event 48 (2001), while the largest difference was determined during event 71 (2002). The resulting t-test evaluation for these seven storms supports the conclusion that predicted and measured timing of peak outflows were in good agreement.

The null hypothesis was that no difference existed between the measured and predicted peak flow rates. A t-test was conducted using an alpha value of 0.05. Since the t-statistic, 2.39, was less than t-critical value, 2.45; thus, the null hypothesis is accepted. Meaning, at an alpha value of 0.05, there is no difference between the samples means, and the predicted and observed datasets are statistical similar.

Likewise, the catchment K2 hydrograph timing was subjected to the t-test analysis to evaluate the likeness between the two means. Using the same storm events and testing criteria, a t-statistic value of -0.89 and a t-critical value of 2.45 were generated for catchment K2. Since the test statistic was less than the critical value, the null hypothesis is accepted. Therefore, the time to peak for both the measured and simulated data, have similar means. The timing test results were very encouraging, since the modeling procedures are more focused on the timing aspects of the hydrograph as related to travel time between model points, although correctly predicting outflow peak rates is still a high priority.

**Table 3.6: Catchment K3 Selected Single Event Peak Flow Rate Timing Comparison**

YEAR	EVENT NAME	MEASURED		PREDICTED		TIMING DIFFERENCE (Min)	PEAK FLOW RATE DIFFERENCE (CFS)
		TIME STAMP	PEAK FLOW RATE (CFS)	TIME STAMP	PEAK FLOW RATE (CFS)		
2000	319	319.53	31.19	319.52	28.75	14.4	2.44
	324	324.67	23.13	324.66	8.62	14.4	14.51
2001	91	91.69	11.01	91.68	12.70	14.4	1.69
	143	143.22	47.71	143.24	22.49	28.8	25.22
	186	186.69	25.25	186.73	17.54	57.6	7.71
2002	6	6.55	55.41	6.56	40.52	14.4	14.89
	72	72.31	196.89	72.27	51.10	57.6	145.79

The timing differences displayed in Table 3.6 reports the absolute difference between the observed and simulated peak flow rate for catchment K3. Catchment K3 demonstrate larger time related discrepancies than those reported for catchment K2. For example, a 57.6-minute timing difference existed between the measured and predicted the peak outflow rates during events 186 (2001) and 72 (2002). Events 319 (2000), 324 (2001) and 91(2001) all had timing differences of 14.4 minutes. The resulting t-statistic and t-critical values for the timing application of the t-test yielded results of 0.00 and 2.45, respectively. Since the calculated test statistic is far less than the critical values, the null hypothesis of like means, as related to the timing differences, is accepted. Thus, statistically speaking, there is no difference between the sample means.

Using the t-test to analyze the peak flow rates of catchment K3, similar results were achieved. The maximum variation in peak flow rate occurred during event 72 (2002) where more than a 145 cfs difference existed. The minimum variation was recorded during event 91 (2001). The 1.52 t-statistic and 2.45 t-critical values calculated using only the peak flow rates between the observed and simulated hydrographs, for catchment K3, supports the assumption that a minimal difference exists between the two datasets.

Overall, the selected storms demonstrated a positive correlation and relationship between the peak and the timing of the peak outflows for both catchments. The test statistics calculated for the catchment K2 were numerically stronger. Therefore, SWMM was producing more statistically sound results for catchment K2 than for catchment K3. This seems reasonable, since catchment K3 had a more difficult flow pattern, involving wetlands and wide overland flow sections, which were often found to be difficult to model using SWMM.

#### *Coefficient of Efficiency, Pearson Correlation and Coefficient of Determination Results*

The governing equations for calculating the coefficient of efficiency, the Pearson product-moment correlation, and the coefficient of determination procedures were discussed previously. Equation 3.21 was directly entered into a spreadsheet and the coefficient of efficiency (N-S) values were calculated for all the calibration storms. Second, the R-square values were determined using the Data Analysis Tool. The weighted coefficients of determination calculations were performed using the Analyze-it add-in. Tables 3B.7.1 through 3B.7.3 (located in Appendix 3B) present three sets of statistical results for the catchment K2 and K3 calibrations.

The coefficient of efficiency test generates test statistics ranging between negative infinity and positive 1.0. For catchment K2, events 143 (2001) and 6 (2002) demonstrated the greatest similarities, having Nash-Sutcliffe values of 0.78 and 0.88, respectively. Events 337 (2000) and 48 (2001) reported moderate N-S results of 0.17 and 0.08. N-S values near zero mean that the observed mean is equal to the predicted mean. Events 319 (2000) and 185 (2001) demonstrated the least similarity between the datasets. Negative N-S values simply mean the observation mean was a better predictor than the model.

The results for catchment K3 were similar in distribution. Storms 324 (2000), 6 (2002) and 38 (2002) yielded the Nash-Sutcliffe values of 0.70, 0.64 and 0.75, respectively, meaning they demonstrated strong agreement between observed and predicted values. Event 91(2001) had a predicted mean that was similar to the observed mean, and reported a N-S value of 0.24. Events 319 (2000), 175 (2001), and 186 (2001) produced negative N-S values meaning that the model was not a better predictor than the mean of the observed data.

For catchment K2, the storms showing better agreement (larger R-square value) between the observed and predicted data were events 337 (2000), 48 (2001) and 6 (2002), with R-square values of 0.86, 0.81 and 0.88, respectively. Events 319 (2000) and 143 (2001) resulted in modest R-square values of 0.67 and 0.78. Storm 185 (2001) had the lowest R-square value meaning that there is little agreement between the observed and predicted means.

The catchment K3 storms also were tested using the R-square test statistic. The best R-square value was calculated for event 38 (2002), R-square=0.84, demonstrating the strongest agreement between the observed and predicted means. Events 324 (2000), 91 (2001), and 6 (2002) reported R-square values of 0.72, 0.64 and 0.69, respectively. Events 319 (2000) and 186 (2001) had the lowest R-square values (0.39 and 0.14).

For catchment K2, events 337 (2000), 48 (2001), 143 (2001), and 6 (2002) received the best Pearson values of 0.93, 0.90, 0.89 and 0.94 respectively. These four storm events had a positive agreement between the measured and continuous XPSWMM hydrographs. Event 319 (2000) reported a moderate Pearson score of 0.82, but still displayed good agreement between the predicted and observed data. Event 185 (2001) reported the lowest Pearson value of 0.51 and therefore, had the lowest level of agreement.

The Pearson results for catchment K3 were also scrutinized. Storm events 319 (2000) and 38 (2002) reported the highest Pearson values of 0.93 and 0.92. Therefore, the measured data for these two storms is positively related to the model estimates. Events 324 (2000), 91 (2001), 175 (2001) and 6 (2002) generated modest Pearson values ranging from 0.73 to 0.85. The poorest agreement between the datasets was reported for event 186 (2001), which received a Pearson value of 0.41.

An interesting observation was noticed during the interpretation of the R-square and Pearson test results for one particular storm in catchment K3. Event 319 of the year 2000, generated a R-square value of 0.39 value while the Pearson test, using the same data, produced a value of 0.93. Since such a large contradiction existed, excellent correlation versus poor agreement, involving the correlation of the observed and predicted data groups, this indicates that certain tests are definitely more sensitive than others to the arrangement of the numerical inputs when conducting a correlation analysis. Recall that the R-square test is very sensitive to extreme values (outliers) and insensitive to additive and proportional differences between model predictions and measure data (Legates, 1999). This type of situation reinforces the fact that several tests should be conducted to completely understand the agreement between the observed and forecasted hydrographs.

The calibration procedures deployed during this study involved visual analysis combined with statistical correlation testing. Individual rainfall events were selected from each catchment and analyzed individually. The purpose of the single-event evaluation was to determine the peak flow rate and timing, and to comprehend the flow volume exiting the study area. When discrepancies in a hydrograph analysis exist, Moriasi et al. (2007) describes a procedure where the hydrograph is divided into three phases (rising limb, falling limb, and baseflow) and then the statistical tests are applied directly to each phase. Once the individual phases demonstrate positive correlation, the researcher may then precede with the testing of the overall hydrograph. In addition, a good calibration procedure uses multiple statistics to test the entire hydrograph, because the utilization of a single statistic can lead to an undesirable emphasis of only matching one characteristic, or hydrograph aspect, while ignoring other important features (Moriasi et al., 2007)

Calibration at this stage was only on single events, and only thirteen storm events were selected. Although specific statistics and performance ratings have been developed for model evaluation, the researcher is free to openly conclude the model's level of acceptance until a

universal model evaluation criteria has been established (Moriassi et al, 2007). Analysis of six calibration storms for catchment K2 and seven storms events for catchment K3 resulted in the following conclusions. The Pearson Product-Moment test was the least sensitive to differences between the simulated and observed storms during the single event, SWMM calibrations. There were five events for catchment K2 and four events for catchment K3 where the Pearson Correlation Coefficient was greater than or equal to 0.70. Continuing with the arbitrarily selected 0.70 threshold, there were four events for K2 and two events for K3 that had R-square values greater than 0.70. The Nash-Sutcliffe was greater than 0.70 for only three events for K2 and two events for K3. The most sensitive test (Nash-Sutcliffe) concluded that five out of thirteen cases (39%) had agreement with values above 0.70. Better results were indicated by the Pearson Correlation Coefficient where, nine out of thirteen (69%) of the tests had values greater than 0.70. These first attempts at single event calibration provided sufficient information to proceed with using continuous datasets.

#### *XPSWMM 9.0 Calibration - Single Event*

XPSWMM version 9.0 allows users to create multiple subcatchment characteristics within a given subcatchment area. For this study, we utilized this option to create distinct subcatchment with varying characteristics. From the sensitivity analysis, it was discovered that XPSWMM was most sensitive to fluctuations in catchment width and percent imperviousness. Increasing the catchment width decreases the total amount of time needed for runoff to reach the catchment outlet, also influencing the time to peak. The percent imperviousness variable is directly associated to the amount of rainfall to calculate runoff and affects the peak outflow rate. Increasing the area of imperviousness increases the peak outflow rate, and shortens the time to peak, plus generates additional runoff, as both infiltration and evapotranspiration are reduced, meaning a larger volume of water exiting the system via stormwater features.

The research focused on percent imperviousness and catchment width, because the calibration/validation of the predicted hydrographs would be evaluated on how well they compared to the observed peak flow rates and time to peak. Likewise, the peak flow rates are directly related to the processes used to generate catchment outflows and the movement of water

(attenuation) within routing elements. The travel time estimates and tracer movement are also dependent upon the timing of the simulated peak outflow rates.

The calibrations began with the creation of template .xp files that were generated from previous .xp projects. Second, the percent imperviousness for catchment K2 was increased by 20%, and entered as subcatchment #2. As stated previously, XPSWMM allows a maximum of five variations of subcatchments at each node. Thus, at node 1 we were able to create subcatchments 1#1, 1#2, and so on (refer to Figure 3.27). The change in percent imperviousness was entered into the regional variations. Simply selecting the desired subcatchment would load the intended set of inputs. Three scenarios were introduced, 1) a 20% increase in imperviousness, 2) a 20% width increase with the percent imperviousness held at the +20% value, and 3) a 40% increase in imperviousness holding the width constant at the +20% level.

Sub-Catchments	1	2	3	4	5
Area	6.27	6.27	6.27	6.27	
Imp. (%)	57.	68.4	68.4	75.6	
Width	321.	321.	385.	385.	
Slope	.0207	.0207	.0207	.0207	

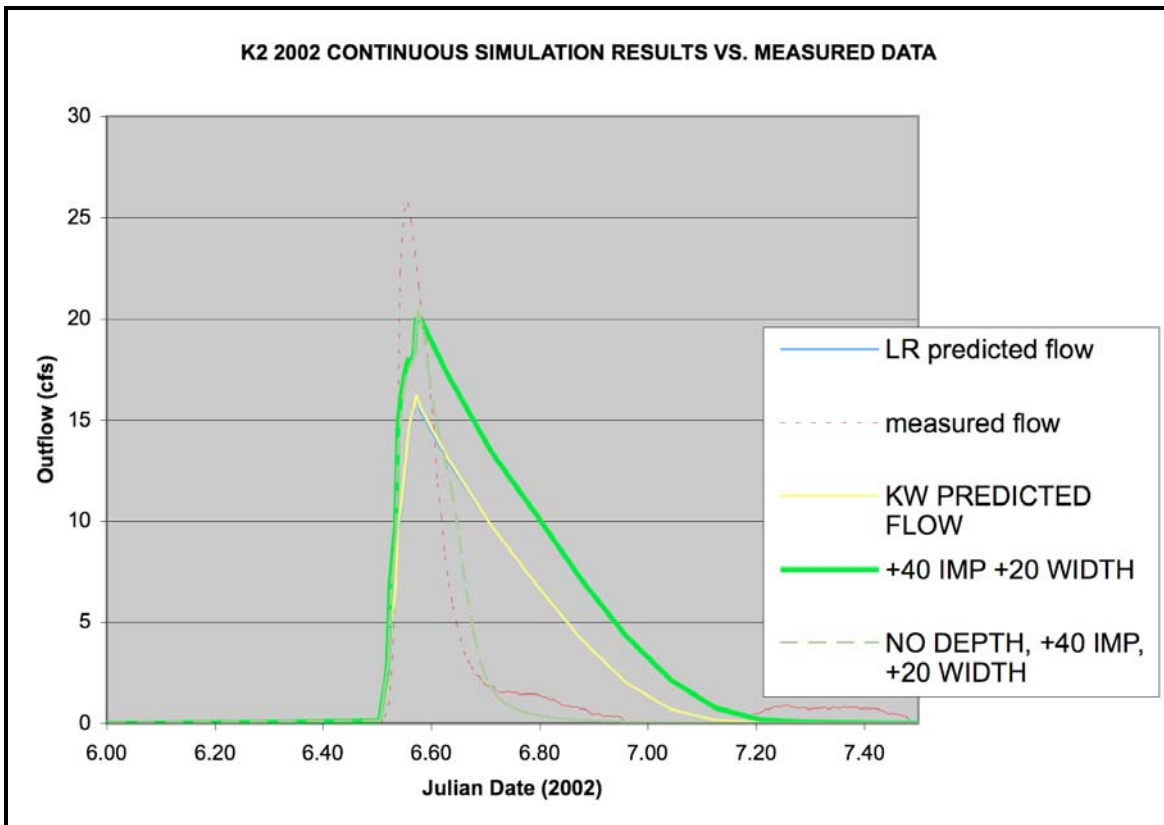
Print Flows and Concentrations  
 Save Results for Review

OK Cancel Gauged Data

**Figure 3.27: Using the Multiple Basin (Subcatchment) Option in XPSWMM for Calibration**

The screen displayed in Figure 3.27 depicts the inputs corresponding to all the subcatchment options for node 1 (in runoff mode), where subcatchment 4 has been selected. When running the simulations, only the inputs associated with the checked subcatchment are

considered. Thus this technique was utilized to create distinct subcatchments in XPSWMM, at specific node locations, and to alter the subcatchment area and imperviousness. The toggle box was used to select the appropriate set of subcatchment values.



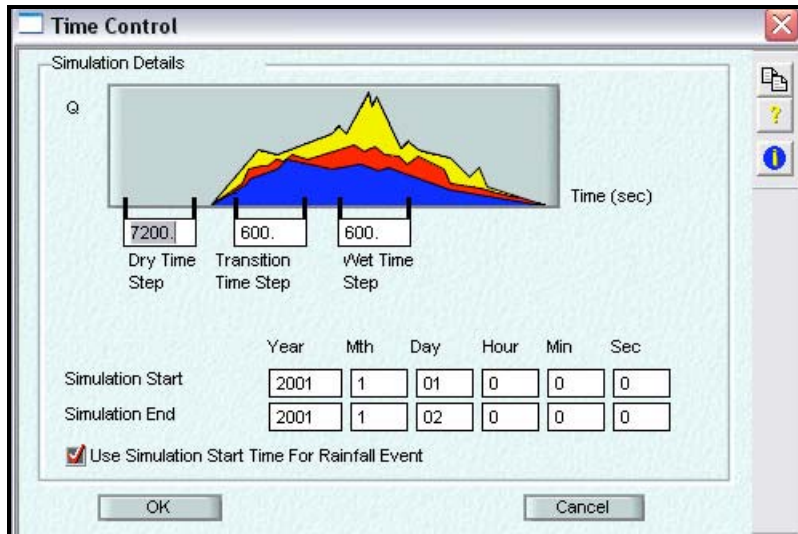
**Figure 3.28: XPSWMM output Hydrographs from Various Imperviousness, Basin Width, and Routing Methods at Cherry Point for the storm of Day 6, 2002.**

Figure 3.28 graphically displays the changes in predicted hydrographs in response to changes in imperviousness and width. As suspected, changing these two values adjusted the peak outflows simulated by the model.

Various scenarios were tested to determine which combination best represented the measured results. The “LR (Linear Reservoir) predicted flow” line is the XPSWMM hydrograph generated using the default linear reservoir routing method for the nodes and routing elements and is considered the baseline. The “measured flow” line is the field recorded flow data at the K2 outlet. The “KW (Kinematic Wave) predicted flow” line represents the XPSWMM hydrograph created after selecting the kinematic wave routing option for the routing elements. The “+40 IMP +20 WIDTH” and the “NO DEPTH +40 IMP +20 WIDTH” hydrographs are results from 1) a 40 %

increase in the percent imperviousness and a 20% increase in catchment width and, 2) deleting the initial water depth values for a majority of the routing elements and keeping the same imperviousness and width from variation 1, respectively. When altering the percent imperviousness and/or catchment width, the linear reservoir routing option was continued. There was no apparent difference between the linear reservoir and the kinematic wave routing techniques as evidenced by the almost identical hydrographs (refer to Figure 3.28). Increasing the percent imperviousness and catchment width increased the peak outflow predicted on Day 06 of 2002 to approximately 20 cfs. The observed peak flowrate for this same storm was slightly greater than 25 cfs and occurred several minutes prior to the estimated peak. The retention of water in routing elements restricted the transfer of runoff downstream, resulting in a nearly linear falling limb for the blue and yellow lines in Figure 3.28. Reducing the initial flow conditions decreased the retention effect (see the “NO DEPTH...” line in Figure 3.28) and produced a hydrograph that better resembled the observed flow data.

The next step of calibration veered from adjusting the input variables to focusing on the simulation time options. The “Use Simulation Start Time for Rainfall Event” option was selected under the time control menu (see Figure 3.29). Selecting this option enabled XPSWMM to synchronize the rainfall and simulation start dates. If this option is not selected, the simulation commences using the beginning of the rainfall database, even if the simulation start date is in the middle of the rainfall dataset. The following graphic was copied directly from the XPSWMM interface, and highlights the user-determined timing options, including the various time steps and the simulation duration.



**Figure 3.29: XPSWMM Time Control Screen (XP Software, 2005)**

*Continuous XPSWMM Calibration Results (2005)*

The dry time step is mainly utilized to update the infiltration parameters and to generate groundwater flow (XP Software, 2005). For Cherry Point, the dry time step was set to 7200 seconds. Generally, the transition time step is less than or equal to the dry time step and is used when precipitation has ceased but the subcatchment may still have water remaining in surface storage (XP Software, 2005). During the transitional time step, the subcatchment continues to lose water via infiltration, evaporation and surface water outflows (Huber, 1999). The wet time step must be greater than or equal to the transition time step and is used during times of precipitation (XP Software, 2005). The transition and wet time steps were then set to 600 seconds each. The simulation start and end options were adjusted to span approximately 180 days per simulation as not to exceed the number of hydrograph points viewable in XPSWMM. Once the default limit (number of hydrograph data points) is surpassed, only a portion of the hydrograph is displayed and saved in XPSWMM. Thus, one set of start/end dates were from January 1 to May 31 while the next simulation period began on June 1 and ended on December 31. Since the entire annual hydrograph could not be graphed while in XPSWMM, the piecewise information was opened in a spreadsheet and joined to plot the annual predicted hydrographs.

There still existed erroneous, predicted values at the beginning of the XPSWMM hydrographs. In efforts to correct this simulated outflow error, the initial depths of all K2 conduits were reduced by 50%. The downstream elements were selected by examining the output results per node and recording where the occurrence of the false hydrograph points began. The reduction of the baseflow depths slightly reduced the spike in the hydrograph. Being unsatisfied with the results, the initial depths of all routing elements were set equal to zero and the simulations were completed. Refer to Figure 3.25 which highlights incorrect runoff predictions at the beginning of a continuous hydrograph.

The final, continuous simulation, calibration efforts involved alterations to the routing techniques. At first, the linear reservoir method was selected as the default. Next, the kinematic wave equation, allowing backwater conditions, was implemented. The last step involved removing the kinematic wave equation from the subcatchments (nodes) because there was insufficient information to fully complete the method requirements. The final calibration also included adjusted increases in percent imperviousness and catchment width, plus the updated time controls for the simulations.

The calibration of K2 for 2002 followed the same procedures as the 2001 calibration. The percent imperviousness was increased by 40% and the catchment width was adjusted by +20%. The downstream baseflow depths were set equal to zero. The time steps were also adjusted and the kinematic wave function was used to route runoff exiting all subcatchments. Appendix 3I is a collection of continuous calibration hydrographs for the Cherry Point project. The XPSWMM calibrations were completed using the observed continuous rainfall, and measured flow, dataset for 2001.

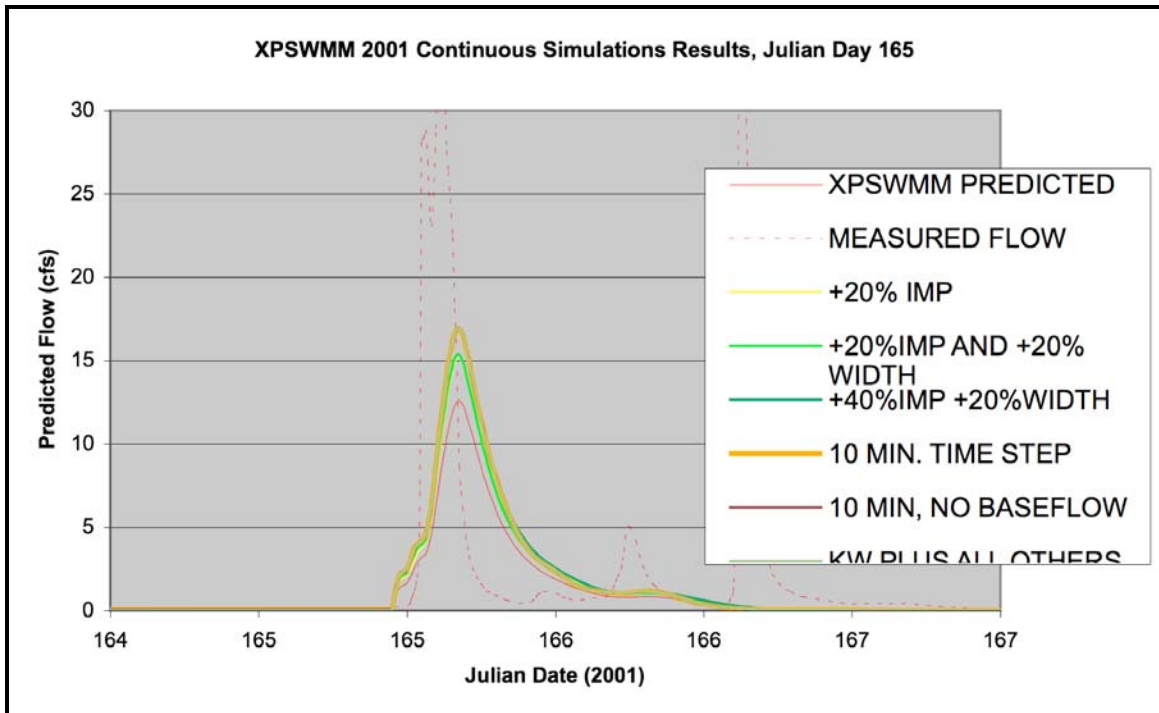


**Figure 3.30: An Excerpt of the K2 2001 Hydrograph Using XPSWMM Simulated Data and Continuous Rainfall data.**

From Figure 3.30, the initial XPSWMM predicted hydrograph, for Julian day 165 (2001), has a peak flow rate of nearly 13 cfs, using the linear reservoir routing technique. Increasing the percent imperviousness and catchment width increased the peak flow rate to a maximum value of more than 15 cfs. In addition to increasing the peak flow rate, the changes in imperviousness and the area width increased the volume of runoff generated during this particular storm event. Altering the simulation time step to 600 seconds improved the precision of the hydrographs and increased the maximum predicted flow rate to nearly 17 cfs. Instituting the kinematic wave function also produced a maximum flow rate of approximately 17 cfs. The final set of calibration variables incorporated changes in the percent imperviousness, stimulation time step, catchment width and routing technique. The final collection of inputs used to create the XPSWMM simulations involved the “KW PLUS ALL OTHERS” heading as described above. For the final predictions, the percent imperviousness for all subcatchments was increased by 40%, subsequently; the catchment width was also increased by 20%. The simulation time step was set equal to 600 seconds and the initial baseflow for all routing elements was set equal to zero. Lastly, the kinematic wave routing formula was selected as the primary transformation equation

for the conduits only, meaning the linear reservoir method became the default function for overland flow regime.

Area K3 calibration also followed the trends set forth from the K2 continuous simulation procedures. The dry, transition and wet time steps were adjusted to 7200, 300, 300, respectively. However, unlike catchment K2, no adjustments were made to the downstream baseflow depths or any catchment variables. The “Use Simulation Start...for Rainfall...” option was also selected in XPSWMM, the simulations were completed for years 2001, 2002 and then the results were exported into Microsoft Excel.

Various storms were selected from the continuous dataset to evaluate the performance of the model. Initially, correlation statistics were completed on the entire predicted dataset. The existence of outliers and missing data collection periods (situations when the field instruments were not recording the measured flow data properly) greatly decreased the agreement between the two datasets. It was also noticed that if the complete rainfall dataset was linked to XPSWMM and the simulation dates were altered to focus on a shorter simulation period, the resulting hydrograph matched the observed data better. Figure 3.31 is an example of a continuous hydrograph simulated using a shorter time period. Although XPSWMM is slightly over predicting the peak rates and rushing the time-to-peak slightly (later than measured), Figure 3.31 is an improvement in the hydrograph shape and timing as compared to the event-based simulation results presented earlier. The following hydrograph was generated using XPSWMM and utilized the continuous predictions options in 2001 at the Cherry Point research site. The associated R-square value for Figure 3.31 is 0.89.

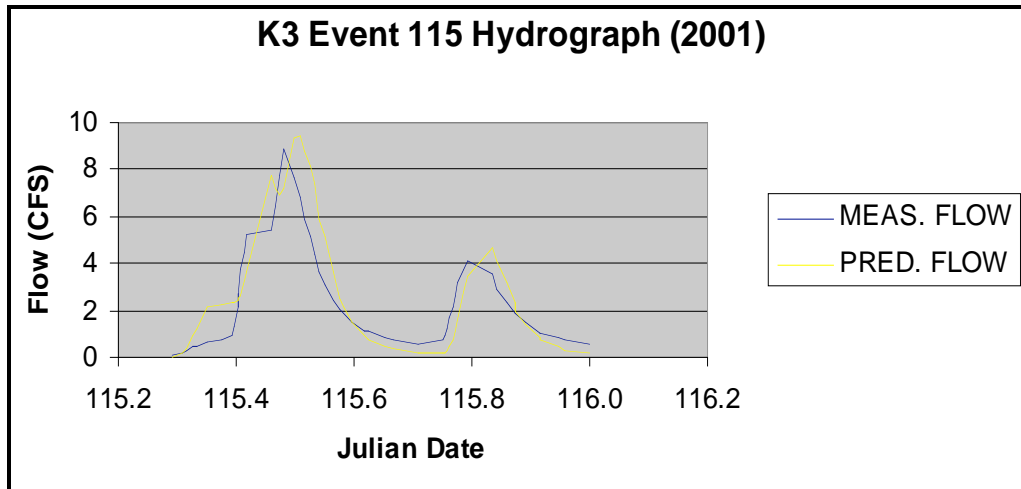


Figure 3.31: *Catchment K3 Event 115 Hydrograph from Continuous Rainfall*

#### B. XPSWMM Event-based Validation Results

Test statistics, comparing the observed and predicted, outflow hydrographs were completed for the validation storms. All validation storm hydrograph results were completed using the imported XPSWMM datasets and eventually compared to the measured data.

The results of the Nash-Sutcliffe (N-S) tests were encouraging (see Table 3H.9b). For catchment K2, the best results were achieved during storm event 327 (2001), which reported an N-S value of 0.82. Events 352 (2000), 71 (2002) and 165 (2002) received N-S values of 0.40, 0.65 and 0.58, respectively. Events 330 (2000) and 152 (2001) received the lowest N-S scores, with resulting values of -0.0059 and -1.94, respectively.

Catchment K3 had less favorable results. The best storm events were storms 348 (2000) and 72 (2002), where the N-S values were 0.43 and 0.49. Events 330 (2000), 345 (2000), 88 (2001), 143 (2001) received N-S values ranging from 0.16 to 0.30. Events 351 (2000), 90 (2002) and 133 (2002), had negative N-S values, so XPSWMM was having difficulties in catchment K3.

The final test statistic computed for the validation storms was the R-square test (see Table 3H.9c). For catchment K2, event 327 (2001) reported the highest R-square value of 0.90,

indicating a strong agreement between the observed and predicted means. Events 352 (2000), 71 (2002), and 165 (2002) presented mediocre results, having R-square values of 0.68, 0.72, and 0.60, respectively. Events 330 (2000) and 168 (2002) generated the worst results and; therefore, have the least agreement between the sample means.

Catchment K3 also was subjected to the R-square test statistic evaluation. The best R-square value was calculated for event 348 (2000), with R-square of 0.87. Events 351 (2000) and 72 (2002) reported reasonable values. Events 330 (2000), 345 (2000), 88 (2001), 143 (2001), 90 (2002) and 133 (2002), had the lowest R-square values, reaching a minimum of 0.20. R-square values near zero represent poor agreement between measured and predicted results.

#### *XPSWMM Validation Comments*

The validation storm hydrograph statistics varied tremendously, depending upon the subcatchment and storm event. The R-squared tests yielded the best results but this method is not totally suitable for event hydrograph evaluations. Nonetheless, the coefficient of efficiency, a better indicator of correlation, reported a maximum value of 0.82 for one event, indicating decent correlation. On the other hand, the negative values for the Nash-Sutcliffe tests displayed that there was no correlation, or apparently an inverse relationship, between the predicted and measured datasets. Note that the simulations generally looked fairly good, but the scattered nature of the measured data, and the influence of outliers, is what altered the statistical results. The outliers probably should have been removed prior to completing the test statistics because particular tests, especially the coefficient of efficiency, are highly sensitive to outlying points. Also, some of the measured data seemed a bit suspicious, indicating higher peaks than expected from relatively small storm events.

In several cases, XPSWMM did create false baseflow. It was determined that the large initial baseflow phenomenon was due to the initial conditions established in SWMM and by altering the initial water depths of selected routing elements, effects of the baseflow were minimized.

Several important conclusions were made following the validation test statistics procedure. Apparently, XPSWMM was not treating the input parameters in the same manner as

the older version of SWMM. Therefore, the calibration procedures used to calibrate SWMM 4.4 were conceivably invalid for the XPSWMM simulations and the older datasets could not be directly imported into XPSWMM. Thus, the peak rates generated by XPSWMM varied, depending on which storm was examined. To correct this error, the SWMM calibration storm hydrographs were simulated in XPSWMM. Efforts were made to calibrate this set of storms for XPSWMM instead of SWMM and then the validation process was revisited.

#### *XPSWMM 9.0 Validation*

The time controls in XPSWMM allow the user to customize the simulation timing during the dry, transitional, and wet time zones. Table 3H.10 summarizes the final time controls used during the XPSWMM 9.0 hydrograph validation and the accompanying number of points. Taking this into consideration, and the simulation time controls were updated to produce approximately the same number of hydrograph points as the observed dataset. Each predicted and its related measured dataset were manually correlated using a .002- or .003-day (3 or 4 minute) tolerance. Points not meeting this tolerance level were eliminated until the measured and predicted samples were numerically equal. The continuous rainfall information was used for the simulations but particular events of interest were selected and the observed/predicted hydrographs were extracted from the annual data. Therefore, true event hydrographs were not created; simply detailed enlargements of the continuous data were evaluated.

XLStat was used to complete the descriptive and Pearson's Product Moment correlative statistic. The descriptive statistics were accomplished first because information describing the datasets was needed to calculate the coefficient of efficiency, E, and the index of agreement, d. Table 3B.10 summarizes the correlation statistical results.

Prior to continuing with the analysis, it was discovered that discrepancies existed between the original SWMM and the XPSWMM files. For some reason, link attributes had not been imported entirely when updating to XPSWMM 9.0. Routing element slopes, pipe diameters, roughness coefficients and channel measurements were corrected where needed. In addition, catchment K2 was retaining too much water during the simulations. To combat this error, the wetland area of K2 was not incorporated into the newer simulations. The test statistics presented

in Table 3.7 are the results of the correlation of the observed and predicted outflow rates for catchments K2 and K3 at Cherry Point.

**Table 3.7: Correlation Statistics for Selected Hydrographs Using XPSWMM9.0 Continuous Simulations.**

Area	Event	Year	Statistical Test Method	
			Pearson	Product Moment
K2		2001		
	48		0.85	
	143		0.93	
	328		0.95	
		2002		
	6		0.97	
	71		0.84	
	91		0.91	
243		0.91		
K3		2001		
	20		0.73	
	115		0.89	
	175		0.88	
	243		0.85	
		2002		
	134		0.93	
	150		0.95	
269		0.85		

Occasionally, local conditions introduced problems into the validation process. Ongoing development and the modification of hydraulic features altered the natural processes being modeled. For example, the flood gates installed at the catchment K2 outlet were sometimes closed during site visits. Closing the flood gates in whatever capacity greatly reduced the outflow released from this monitoring site. Sometimes all the floodgates were closed. Essentially no flow would be released until they were opened, which would then appear as a large storm event to the flow meter and stage recorder, although it was artificial. The actual time of the floodgate operation was not known but could be retrospectively interpolated by comparing the rainfall data to the flow data. As a result, seemingly large flow rates without corresponding rainfall input were

detected. The XPSWMM simulations were not affected by the floodgate operations because they only generated runoff when the appropriate rainfall file indicated a storm event. During the calibration/validation process, these events were not selected for analysis, because from visual observations it was decided that the agreement between the observed and predicted data would not be advantageous.

### **C. Sensitivity Analyses Results**

A sensitivity analysis test was completed for major input parameters like Manning roughness, percent imperviousness, pervious and impervious depression storage, width and slope of subbasins, and maximum infiltration rate using the SWMM model. Two winter and two summer events (2002) were selected for catchments K2 and K3. The two storm events representing summer precipitation for catchment K2 were Julian days 165 and 168. The two selected winter storms were events, as days, 006 and 061. The four storms selected for catchment K3 were, as days, 06, 61, 133, and 148.

To complete the sensitivity analyses, parameters were adjusted positively and negatively. Saturated hydraulic conductivity was substituted for the maximum infiltration rate. The resulting variations in peak outflow estimates were evaluated based upon the magnitude of difference from the baseline value (the 0% adjustment value). The absolute values for maximum differences in both the positive and negative directions were calculated and ranked based on parameter.

Overall, predictions seemed to be the most sensitive in both the positive and negative directions, to three parameters. The Manning's roughness coefficient, percent imperviousness, and catchment width were the most sensitive parameters. Generally speaking, the least sensitive parameters were saturated hydraulic conductivity, catchment slope, impervious depression storage and pervious depression storage. Figure 3.32 demonstrates the peak outflow rate response to positive and negative parameter changes for storm event 165 in catchment K2.

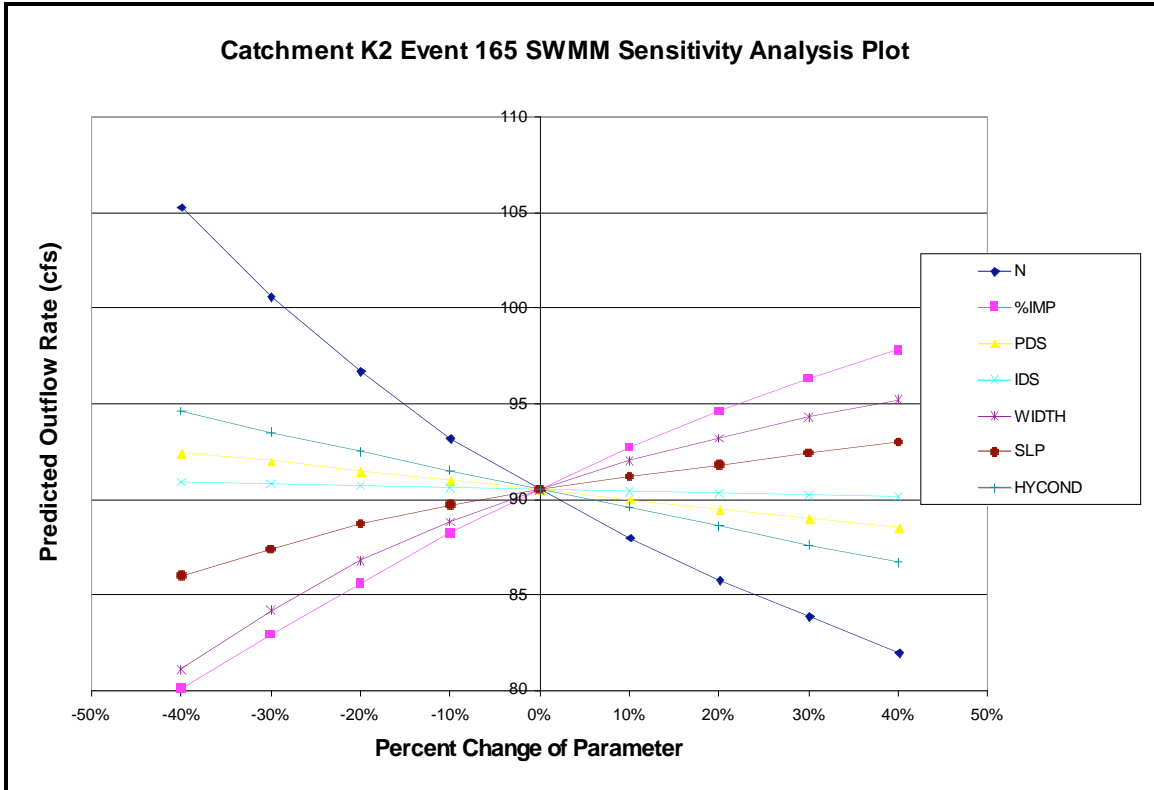


Figure 3.32: Sensitivity Analysis Plot for Catchment K2, Using Storm Event 165 in 2002.

#### D. 2006 XPSWMM9.0 Simulations

##### *Updated Continuous Simulations for 2006 Simulations*

Upon further examination of the results, it was of interest to rerun the XPSWMM9.0 simulations, excluding the retention capabilities of the flat, wetland area in catchment K2. Although the effects of the wetland were reduced previously, the research team intended to completely remove the flat area of catchment K2. Apparently, XPSWMM was retaining too much water during the simulations, resulting in flattened, elongated peaks of the outflow hydrograph. To complete this task, the original variables used prior to attempting to route water through the wetland area were inserted in XPSWMM (from the SWMM4.4 text files) and the corresponding simulations were classified as “2006 XPSWMM” projects and completed on a continuous basis.

It was discovered that removing the wetlands areas in catchment K2, returning to the original input variables that did not include routing runoff through wetland areas, improved the overall response of the simulated, continuous hydrographs. No longer was an erroneous, predicted storage unit, releasing large amounts of runoff at the beginning of the hydrograph. Thus, the simulated and actual hydrographs were in better correlation. Several storms simulated in catchment K2 received fairly high coefficients of determination. Event 328 (2001) had a calculated R-squared value of 0.95 and event 6 (2002) had a determination coefficient value of 0.97. Similar test statistics were completed for catchment K3 and the resulting determination coefficients for events 115 (2001) and 150 (2002) were 0.89 and 0.95, respectively. Considering the fact that the calibration storms from both catchments K2 and K3 only achieved a maximum determination coefficient value of 0.84 and the validation storms generated a maximum R-squared value of 0.90, it was concluded that the wetland removal process positively impacted the correlation between the predicted and observed runoff hydrographs. Table 3.8 presents the Pearson Product statistics results from the continuous rainfall simulations, following the removal of the wetland areas in catchment K2.

**Table 3.8: Continuous Rainfall Validation Storm Statistics Results for Catchments K2 and K3.**

Area	Event	Year	Statistical Test Method
			Pearson Product Moment
K2	48 143 328	2001	0.85
			0.93
			0.95
	6 71 91 243	2002	0.97
			0.84
			0.91
			0.91
	K3	20 115 175 243	2001
0.89			
0.88			
0.85			
134 150 269		2002	0.93
			0.95
			0.95
			0.85

The following two sections deal with the over- and underestimations of the predicted hydrographs and adhere to one major assumption: the outflows in each barrel were the same as flows through the monitored barrel. The calculated outflows at the catchment outlets were manually tabulated. The combined information from the STARFLOW and Blue Earth stage readings were placed into a spreadsheet and using differences in the barrel elevations, it was assumed that the flows in the non-monitored barrels behaved in a similar manner to the lowest barrel. The assumptions pertaining to water elevations in the non-monitored barrels were not field verified; therefore, there were possible errors in the measured data.

#### **E. XPSWMM9.0 Under-predictions**

The continuous hydrographs for both catchments demonstrate fairly good correlation between the measured and predicted outflow values. The top three Pearson correlation values for catchment K2 were 0.85, 0.93 and 0.95 for year 2001. For year 2002 the top two correlation values were 0.91 and 0.97, for catchment K2. Catchment K3 had calculated correlation values of 0.88 and 0.90 for year 2001, and the best correlation values reported in 2002 were 0.85, 0.92 and 0.95. The reported Pearson correlation values were collected from the XPSWMM simulations of selected storms, completed in the year 2006.

In most cases, when the observed flow rate was less than 50 cfs, observed and simulated flows were in good agreement. For years 2001 and 2002 the largest rainfall event occurred between Julian date 200 and 250. Accordingly, the largest runoff was predicted and observed during that same period. For year 2001, the installed flow equipment measured a maximum flow of 83.4 cfs on Julian day 243.4. On this day, the flow meter data were inserted into the composite flow hydrograph for catchment K2 because the weir was submerged. For year 2002, in catchment K2, the recorded flow event was 245 cfs on Julian day 207.8. The 245 cfs value is probably an outlier and represents an error in the measured data since the observed rainfall amount of approximately 3.7 inches was recorded in less than 24 hours, which was atypical for the study area. According to the historical records at Morehead City, NC, only 8.04 inches of precipitation were recorded for the entire month of July during 2002.

The peak flow rates from the observed data were further compared to the historical outflow trends for the region, using the design storms for Morehead City, NC. It was determined that the measured rainfall intensities during the 2000 to 2002 monitoring period only included

storm events with a maximum return period of 5 yr. The corresponding rainfall intensity for a 5-yr storm at Morehead City, NC, is 0.23 in/hr. An average 2-yr return period storm for the same region has an associated intensity of 0.21 in/hr. The 100-yr return period intensity for this area is 0.45 in/hr. Tables 3.9 and 3.10 display the calculated rainfall intensities for several rainfall events in catchment K2 and K3 and then categorize the storms by return frequency.

**Table 3.9: Catchment K2 Simulation Rainfall Intensities and Return Frequencies**

Catchment Name	Year	Event Name	Tipping Bucket (HOBO) Rainfall Intensity (in/hr)	Storm Duration (hr)	Return Frequency
<b>Calibration Storms</b>					
K2	2000	319	0.19	2.6	< 2-year
		337	0.03	22.8	< 2-year
	2001	48	0.01	21.6	< 2-year
		143	0.06	12.2	< 2-year
		186	0.03	13.9	< 2-year
	2002	6	0.28	2.4	5-year
<b>Validation Storms</b>					
K2	2000	330	0.11	24.0	< 2-year
		352	0.02	19.9	< 2-year
	2001	152	0.12	7.2	< 2-year
		327	0.07	16.3	< 2-year
	2002	71	0.07	30.2	< 2-year
		165	0.13	13.7	< 2-year

**Table 3.10: Catchment K3 Continuous Rainfall Intensities and Return Frequencies**

Catchment Name	Year	Event Name	Tipping Bucket (HOBO) Rainfall Intensity (in/hr)	Storm Duration (hr)	Return Frequency
<b>Calibration Storms</b>					
K3	2000	319	0.19	2.6	< 2-year
		337	0.03	22.8	< 2-year
	2001	91	0.04	6.0	< 2-year
		175	0.23	3.8	5-year
		186	0.03	13.9	< 2-year
	2002	6	0.28	2.4	5-year
		38	0.03	62.6	< 2-year
<b>Validation Storms</b>					
K3	2000	330	0.11	24.0	< 2-year
		345	0.02	14.6	< 2-year
		348	0.03	8.4	< 2-year
		351	0.01	20.6	< 2-year
	2001	88	0.02	26.2	< 2-year
		143	0.06	12.2	< 2-year
	2002	61	0.16	12.7	< 2-year
		72	0.11	20.0	< 2-year
		90	0.11	5.8	< 2-year
		133	0.27	2.4	5-year
		148.5	0.03	33.4	< 2-year

Using the Rational Equation, setting the catchment runoff coefficient equal to the percent imperviousness, and using a 1.25 adjustment factor to transform the estimated runoff to correspond to a 100-yr return period storm, the following outflows could be expected for catchment K2 and K3. Q100 for catchment K2, with an area of 115 acres, is approximately 38 cfs while catchment K3 would generate over 58 cfs. Since the measured rainfall data did not demonstrate the heightened intensities reflecting a large design storm (100-yr return period), the large outflow values presented in the previous paragraph are questionable.

#### **F. XPSWMM9.0 Over-predictions**

In some instances, the XPSWMM generated outflows were greater than the values measured directly by the weir or the flow meter. For example, in catchment K2, on Julian day 211 (2001), the XPSWMM program estimated an outflow rate of approximately 211 cfs. The STARFLOW reported a value of 67.7 cfs for the same date in 2001. The outflows presented were extracted from the 2006 XPSWMM simulations where the wetland areas were removed. Removing the wetlands allowed for water that had been retained or retarded during storm events to flow uninhibited. Therefore, the predicted summation effect of water reaching downstream points from upstream subcatchments was increased because the upstream outflows were now unrestricted and flowed faster. Therefore, the maximum outflow predicted at the outlet of K2 is probably greater than the observed data since the observed data still included the wetland. The predicted outflow for Julian Day 211 (2001) prior to removing the wetland was approximately 50 cfs.

#### **G. XPSWMM9.0 K2 Overflow Routing**

The runoff routing for catchment K2 was revisited, when it was observed that the XPSWMM model was having difficulties passing runoff through modeling points during pipe surcharged conditions. Two specific pipe sections, elements 111 and 115, were restricting the passage of the hydrograph peak flow during rain events. The locations of the overflow pipes are displayed in Figure 3.33. The dashed lines represent instances where subsurface pipes and surface swales are both transporting surface runoff.

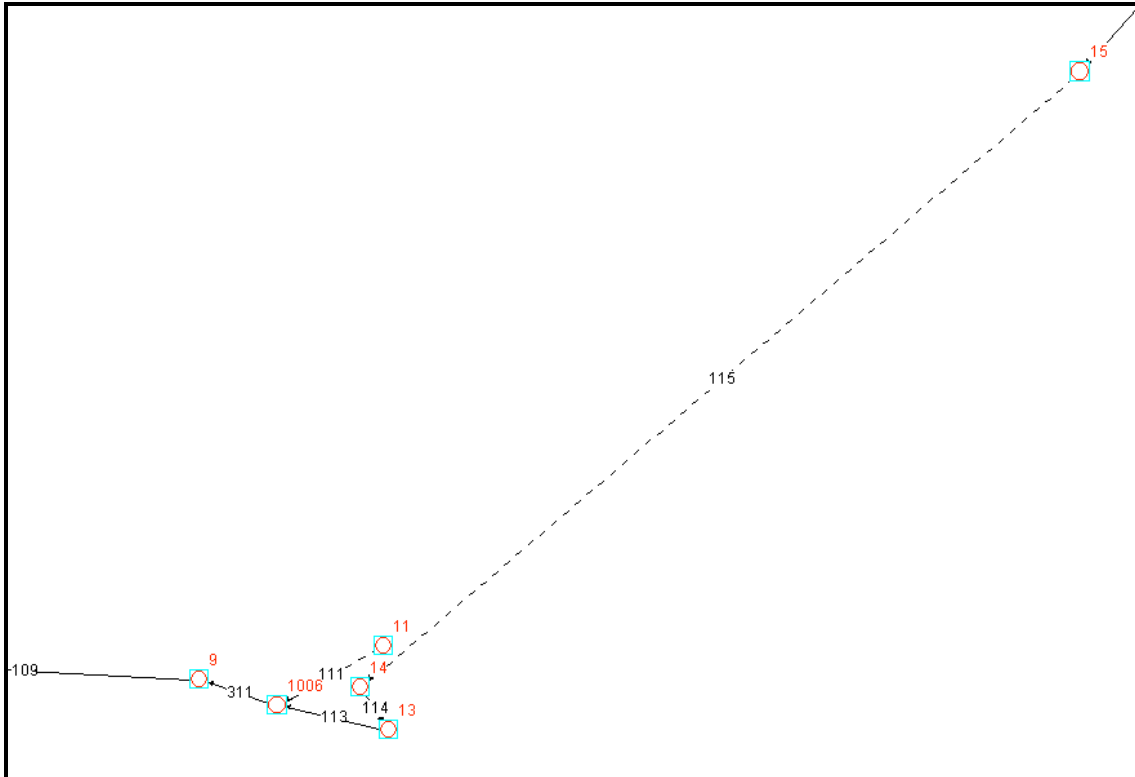


**Figure 3.33: Location of Overflow Routing Elements at CPMCAS in Catchment K2**

It was understood that both pipe sections, 111 and 115, were under pressure flow situations during a majority of precipitation events, as were predicted by the model. However, although the pipe conduits were designed to handle a large percentage of the runoff, a surface component existed. Failure to model the surface flow component yielded simulations results that failed to predict observed flows. To incorporate the surface flow interaction, overflow channels were added to two regions. The dimensions of the overflow channels were determined by examining the area's topography. The first overflow channel, named "overflow 115", directed surface water between catchments 15 and 14. "Overflow 115" was assigned a trapezoidal shape with an overall length of 933 ft. The channel had an initial depth of zero, with a maximum depth of 2 ft. and 12:1 side slopes. Similarly, "overflow 111" routed excess runoff between catchment 11 and modeling point 1006, respectively. The 111 overflow channel, was also a trapezoidal feature with an overall length of 33 ft. The side slopes associated with this element were 10:1, the channel was determined to be 1 ft. deep with no initial water depth. The roughness coefficient for both overflow channels was 0.03.

The predicted, peak runoff rate results utilizing the introduction of the overflow channel sections will be further discussed in Chapter Four.

#### **IV. Summary and Conclusions**

Three manual rain gages were installed at Cherry Point, along with a recording tipping bucket gage within catchment K1. From the rainfall analysis, it was found that SWWM outflow predictions were directly related to rainfall, as expected. During the period of data collection, precipitation was less than average; therefore, smaller outflows should be expected.

##### *XPSWMM Continuous Simulations*

The XPSWMM simulations incorporated continuous datasets and replaced the event based predictions. Under the event based simulations, a 2-day time period was selected. This 48-hour simulation duration may not have allowed sufficient time for all hydrologic processes (infiltration, percolation, ET, etc.) to function fully and properly. Continuous simulations proved to be extremely useful in the tracer study, where travel times, conduit hydraulics, and more complex routing equations required more time than the event-based simulations provided.

Continuous XPSWMM simulations with recorded rainfall allowed inclusion of effects of antecedent soil moisture and its effects on infiltration, evaporation and transpiration. Depressional storage depths could also be considered as rainfall satisfied initial conditions before being routed as surface runoff. Although groundwater was not included in this study, the continuous simulations would also provide the necessary time and inputs for rainfall to percolate into groundwater aquifers. In addition, the time needed for evapotranspiration to occur, during and after the rain period, was considered in continuous simulations. This included time between storm events; it did not require estimation of antecedent conditions as was necessary with single event simulations.

The results of SWMM and XPSWMM calibration and validation simulations indicated that the continuous XPSWMM runs provided the best set of predicted hydrographs. However, as with most modeling applications, there is room for improvement, and further work can ultimately enhance the model's prediction capabilities.

At one point, the kinematic wave routing method was selected for the routing elements and time controls were adjusted to generate more hydrograph points. Unfortunately, the field phase of this study did not provide enough information concerning hydraulics of subsurface conduits to fully capitalize on the prediction capabilities of the kinematic wave functions available in XPSWMM. Likewise, the time control adjustment did not have visible impacts on the resulting hydrographs. The importance of altering the time controls was manifested during the correlation procedures, when the observed and predicted samples sizes needed to be equal.

Examination of the hydrographs from catchment K2 indicates that XPSWMM continually under-predicted runoff for events with outflows greater than 50 cfs. This seems to be due partly to the simplification of the hydraulics of the pipe conduit system and to the use of potentially erroneous flow data during weir submergence. Analysis of the measured rain data indicated no storm events during the monitoring period that surpassed the 5-yr return period level. This indicates that the every large observed flows are probably incorrect. Nonetheless, this study did not measure or acquire all the needed information regarding subsurface conduits to accurately model the system at the most sophisticated level. Although XPSWMM is capable of handling pressure flows and backwater conditions, the field measurements needed to model these hydraulic processes were not collected. Thus, the XPSWMM simulations depended on the user-inputted rainfall and the transformation equations used to create runoff in the RUNOFF Module. Once again, since less sophisticated methods were used, the importance of topographic conditions, catchments shapes, rainfall, and baseflow values were heightened.

The XPSWMM accurately modeled the hydraulics of the system for moderate and lower flows. The assumptions and calibrations used to adjust the model resulted in hydrographs that match measured data fairly well. Three out of six selected events for catchment K2, in 2001, had Pearson correlation values greater than 0.84. In 2002, five out of the selected eight storms had correlation values of at least 0.84 or higher. Catchment K3 demonstrated similar results, and in 2001, two of the six storms reported correlation values of 0.88 or more; where three out of seven

storms had a Pearson correlation value of at least 0.85 in 2002. Measurement errors may have accounted for disagreement during higher flows.

The velocity meter outflow rates were incorporated into the composite flow hydrograph when either the stage data were not available or the weir was submerged. A possible reason for the higher velocity meters flows for larger storm events may be due to pressurized flow situations, where higher heads at the culvert inlet would create a pressurized system increasing the flow velocity. In XPSWMM, pressurized systems (surcharged conditions) were indicated but not modeled accurately due to the lack of available hydraulics data.

Within limits, the XPSWMM over-predictions are acceptable because of the overall scope of the study. The retention capabilities of the wetland areas were working too well conceptually, retarding the downstream movement of runoff to the outlet, therefore, creating a plateau in the outflow hydrograph for that subcatchment. The retained runoff was eventually reaching the catchment outlet, but elongating the overall hydrograph and flattening its peak section.

The introduction of the two overflow channels corrected the flattened hydrograph peak, by increasing the passage of surface runoff. Initially, only the subsurface routing elements were modeled. In such instances where a corresponding surface component existed, the runoff volume simulation generated errors in the flow transport functions. Although runoff was being routed downstream, the model was unable to handle the excess. The combined transport capacity of the surface and subsurface routing elements, allowed the model to route runoff more effectively downstream. More effective routing would eventually mean better simulations which in turn, would assist in better determining the travel times of potential pollutants.

The XPSWMM simulations were generated to calculate response times for contaminants entering surface waters. The over-predictions resulted in shorter estimates for time of travel than would actually occur. While more accurate predictions are desirable, the errors are conservative, requiring air station personnel to respond to accidental spills somewhat faster than necessary.

## **Chapter Four: Determining Pollutant Travel Times in Two Catchments Using a Geographic Information System**

### **I. Introduction**

#### **A. Background**

More than fifty percent of the pollution entering the nation's waters came from non-point sources in 1992 (Tyler, 1992). Effective stormwater management requires an accurate representation of the physical system. In most cases, the natural processes occurring are highly complex, and would require extensive attention to simulate completely. Evaluating alternative management strategies through experiments and a limited amount of field measurements is usually not feasible, and a modeling study is often the only viable means of providing input to management decisions (Yoon, 1996).

#### **B. Objectives**

##### *Overall Objective*

The overall research objective is to develop a GIS-based stormwater management model to predict the movements of potential pollutants from one specific spill location in a subcatchment to other downstream points, including the subcatchment outlet, on the Marine Corps Air Station at Cherry Point, North Carolina.

##### *Chapter Objectives*

The purpose of Chapter Four is 1) to document the earlier results generated from the continuous simulations of rainfall-runoff processes using a calibrated/validated version of XPSWMM at the study site, 2) to introduce the concept of using pulse tracers to estimate travel times and 3) to generate corresponding GIS maps highlighting the calculated time estimates. Considering each tracer as a potential point source, the travel time from the insertion location to the catchment outlet would be used to generate a reaction time matrix. The reported reaction times are based upon the 24-hr design storm XPSWMM simulations. The corresponding travel

times are the elapsed times needed for runoff to be observed at the main outlets of catchments K2 and K3 at Cherry Point.

### **C. Literature Review**

Water pollution may lead to negative impacts on the environment, including disease transmission, poisoning of human and/or animals, generation of unwanted odors, degradation of water quality, and a decrease in aquatic organisms (Goudie, 2000). Usually water pollutants are classified according to their source. Point source pollution and non-point source pollution are the two broad pollution categories. Pollution emitted from a point source is usually identifiable and may include sewage discharge pipes and industrially generated effluent. Non-point source pollution is generally harder to assess since the source is diffuse. Agricultural fields and some urban runoff situations are examples of non-point source pollution.

*“Pollution trends are not always easily identifiable since long term monitoring data is unavailable and fluctuations in water quality may be due to natural factors, such as climatic changes. Nonetheless, a majority of the water quality problems experienced globally are produced by human activity. In 1979, Meybeck concluded that about 500 million tons of dissolved salts reach the oceans each year as a result of human activity. Likewise in 1991, Peierls demonstrated that the quantity of nitrates in World Rivers now appears to be closely correlated to human population density.” (Goudie, 2000)*

#### *Literature review of Similar Studies*

The coupling of a GIS and a selected modeling package has been explored many times in various subject areas within the scientific community. The basic function of the software union is to aid the user in determining the necessary spatial parameters, minimizing the preparation requirements.

A logical step in improving the quality of hydrologic modeling would be the integration of spatially distributed parameter models with practical data management schemes such as the geographic information system and database management system (DBMS)(Yoon, 1996). The

GIS system is used to organize the spatially referenced data collected from various sources, such as topographic maps, digitized aerial photographs, digital terrain maps and field surveys. During the 1960's, the first generation of GIS-automated drafting programs was applied to create conventional maps using a computer (Yoon, 1996). The first GIS-data management integration gained popularity during the 1970's, having a large influence on the management and analysis of digital geographic information (Yoon, 1996). Nonetheless, a database management system is not always spatially oriented, but is introduced to allow quick referencing. For example, if updates occur in a particular area, the database management system is accessed to retrieve the old map files and then used to append the older data with more current information. No spatial information is required for such an update.

The distributed parameter aspect of modeling is most appropriate to preserve the spatial characteristics of the watershed and to obtain more accurate results. XPSWMM is a model that can be data-intensive should the user decide to model at higher resolutions. Barber, Lage and Carolan (1994) applied the integration of SWMM4.0 and GIS for the purpose of stormwater master planning at Kansas City, Missouri. The goals of their study were to 1) organize and input data describing the drainage basin, 2) create the SWMM model data files, and 3) display the SWMM results graphically within GIS. (Barber, 1994). Likewise, Wolfe and Neale (1988) had to manually process the data to meet data format requirements when integrating GIS with the finite element storm hydrograph model (FESHM) (Yoon, 1996). Likewise, researchers in Michigan (2001) published a study demonstrating how a Geographic Information System could be used to model the movement of a chemical spill through the city's stormwater drainage system. The Michigan study concluded that SWMM did not simulate substantial flows during relatively dry periods and that chemical spills occurring further away from the observed outlet demonstrated longer travel times than spills simulated near the outlet.

The first step in achieving GIS and model integration deals with gathering the information that will be managed by the GIS. There are several steps that must be considered prior to actually acquiring the spatial data (Lutz, 2003). First, identify and describe the type of data needed to make the integration work correctly. Second, define a specific process that will be used to transform the source data into a usable GIS database. Third, specify what expectations the end-user might desire and attempt to meet those expectations throughout data collection. Fourth, be conscious of data integrity and perform qualitative checks during collection. Fifth, set

up an export procedure. Following these few steps will then allow a user to progress to the second stage in automation. (Lutz, 2003)

The second level of GIS and model integration involves extracting acquired data from the GIS, formatting the data to meet model standards, inserting the information into the model, and then completing the simulations. In most cases, manual data preprocessing is performed prior to running the model, or all necessary data manipulation functions such as altering data formats and the extraction of usable data for existing models are provided by specially written software (Fisher, 1989, Piwowar and LeDrew, 1990). Linking problems still exist when integrating models with a large amount of spatial data in unorganized formats (Yoon, 1996). Researchers continue to search for the optimal format type needed to facilitate a direct linkage.

In the past, the main focus in the GIS-model linkage involved inserting the spatial data into the model only. Therefore, the data transition was in a single direction. A true linkage should also manage bi-directional informational transfers. It is imperative to develop data handling procedures to prepare inputs to the model, and then inflict changes to the watersheds, and procedures, to analyze and display corresponding model results within the GIS environment (Yong, 1996). A bi-directional linkage allows researchers to monitor changes in real time. Alterations in input parameters can be viewed instantaneously, decreasing the time needed to analyze simulation results. This would allow managers to watch time-dependent data like runoff and sediment yield at particular outlets and quickly assess the situation to make better management decisions. Furthermore, the graphical display could provide an indication of problems due to erosion and pollutant movement on a watershed and help pinpoint critical locations for further study and/or control action (Yoon and Padmanabhan, 1995).

#### *Pollutant Transport using Pulse Tracers*

One of the most important physical factors affecting movement of pollutants within natural open channel systems is water flow; however, water movement does not directly reflect transport of even dissolved substances (Bowers and Dirnberger, 2000). Bowers and Dirnberger (2000) further explain that there are two differences in channel flow. First, for uniform open channels, disturbances can create translatory (Pickford, 1969) or kinematic (Runkel et al., 1998; Nolan &

Hill, 1989; Lee & Yen, 1997; Leopold et al., 1964) waves where “old” water is displaced because certain waves are moving faster than the stream current. Second, a zone exists where an interaction occurs between the channel water (flow) and the streambed (load). The kinematic wave effect has been observed to cause increases in water height prior to changes in water quality (Bowers & Dirnberger, 2000), while the hyporheic zone phenomena may retain solutes and delay pollutant transport downstream (Bowers & Dirnberger, 2000; Fortner & White, 1988).

Rainfall is the main input source for most runoff models. Other parameters include catchment attributes and routing system variables. The availability of reliable input information is usually the weakest link in the chain of events needed to predict the rate of movement, dilution, and mixing of contaminants in rivers and streams (Jobson et al., 1996). Likewise, rainfall runoff is also subject to spatial differences due to topography. As a result, it is usually difficult to attribute a particular change in flow and concentration to a specific rainfall event (Bowers & Dirnberger, 2000).

During an urban stream-monitoring project, Bowers and Dirnberger (2000) used ion concentrations to characterize stream flow fluctuations. The project was established to compare travel times based on spatial changes in stream height and ion concentration against current velocity measurements. The study evaluated ion concentration at varying stream depths to evaluate the hyporheic zone’s capability to retard pollutant transport. The investigators identified an “asynchronous relationship between stream height peaks and maximum dissolved ion concentration [which may] be explained by translation of energy...” (Bowers and Dirnberger, 2000). Pickford (1969) hints that any disturbance within a water body introduces translatory waves that can displace the energy of the disturbance causing lags between predicted and measured peak flow rates.

Another common method used to measure pollutant transport in streams is the tracer method. Soluble tracers are normally selected because they possess physical characteristics similar to water. Following experimentation, a response curve may be generated to evaluate a pollutant’s downstream travel path. Knowing the travel times and stream mixing rates would allow water-resources managers to predict pollutant movement and dilution rates of various substances.

The measured tracer-response curves produced from the injection of a known quantity of soluble tracer provide an efficient method for obtaining stream flow values (Jobson, 1996). To

create such a curve, the water-soluble tracer is injected into a stream, usually at the center of flow, and the concentration changes are observed as the tracer flows downstream. Evaluation of the created curves allows a researcher to 1) estimate the rate of movement of the contaminant, 2) evaluate the attenuation rate of the peak concentration and 3) determine the amount of time required for the pollutant plume to pass a given point. The general shape of a slug-injection is demonstrated in Figure 4.1.

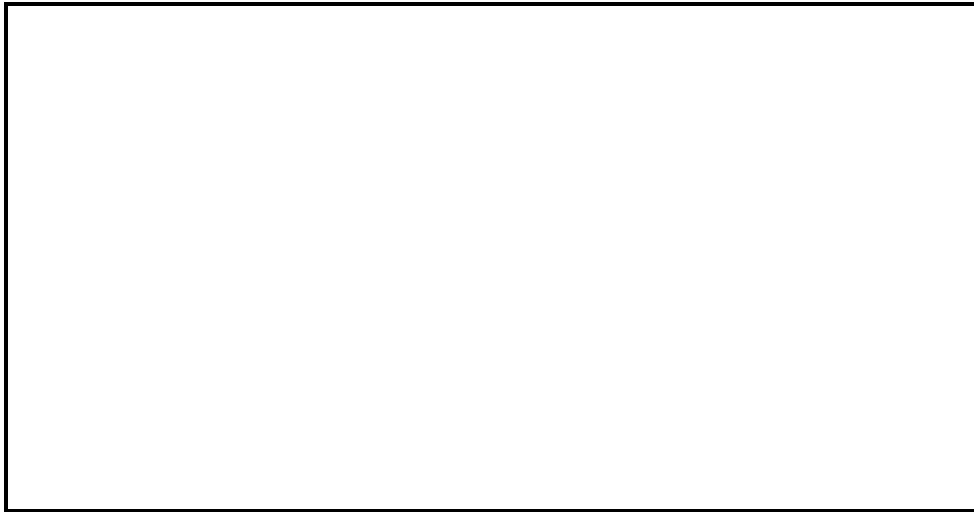


**Figure 4.1: *Slug Injection Diagram as Presented by Jobson (1996).*** Imaginary tracers were simulated at Cherry Point to model the movement of water-soluble pollutants.

Following the slug injection, the dispersion and mixing of the tracer occurs in three planes. For simplicity, Jobson (1996) refers to the vertical and lateral diffusion of the tracer as mixing, while the elongation of the trace cloud is termed longitudinal dispersion. Jobson (1996) goes further to explain that the vertical mixing occurs rapidly, but the lateral mixing is much slower and may require kilometers to diffuse completely. The longitudinal dispersion continues indefinitely, since the conceptual stream length could continue forever.

Normally, if the tracer is inserted at the midpoint of the stream, the tracer cloud moves faster than the average stream velocity because a majority of the tracer is located in the high velocity section of the stream cross section (Jobson, 1996). After insertion, a researcher should also make sure that the stream monitoring locations are at least near (or beyond) the optimum distance. The optimum distance is the physical point where the vertical and lateral dispersions are the main mixing processes. Point III in Figure 4.1 displays the theoretical location of the

optimum distance. Points at or beyond the optimum distance should be situated far enough from the initial point such that longitudinal dispersion is the dominant mixing component.

A tracer-response curve is a collection of concentrations measured at various points along the stream channel at given intervals. Using two or more cross sections, a tracer-response curve may be constructed. When plotted against time, the curve serves as the basis for determining time-of-travel and dispersion characteristics for a particular stream. Figure 4.2 is an example of a tracer-response curve.

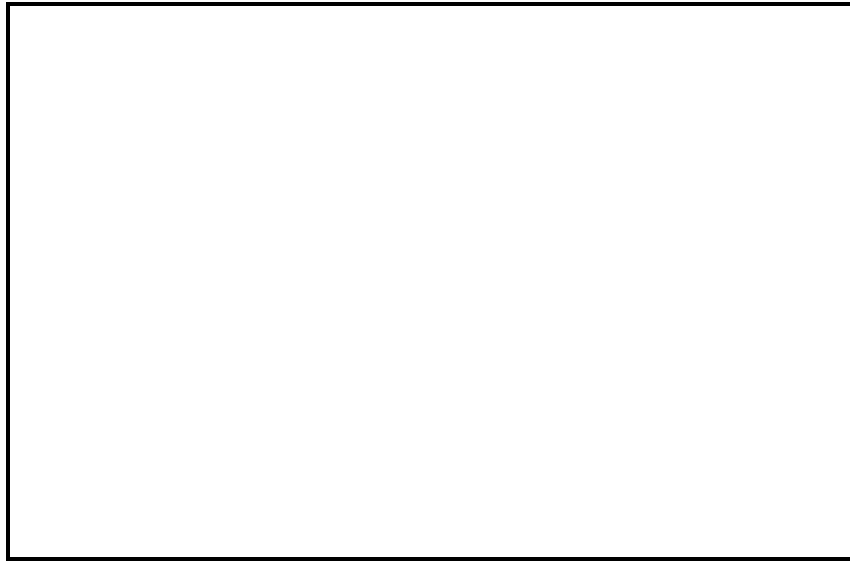


**Figure 4.2: A Typical Tracer Response Curve as Determined by Jobson (1996).**

The following values are the important features of the trace-response curve (Jobson, 1996):

- $C_p$  = peak concentration of the tracer cloud
- $T_l$  = elapsed time of the arrival of the leading edge of the tracer cloud
- $T_p$  = elapsed time to the peak concentration of the tracer cloud
- $T_t$  = elapsed time to the trailing edge of the tracer cloud
- $T_d$  = duration of the tracer cloud
- $T_{10d}$  = duration from leading edge until tracer concentration has reduced to within 10% of the peak concentration
- $n$  = number of downstream sampling sites

The quantity of the tracer injected, the degree of tracer conserved, the average stream discharge and the longitudinal dispersion are four factors that influence the tracer-response curve formation (Jobson, 1996). The magnitude of the tracer concentration is directly proportional to the injected mass. Some tracers are lost due to adhesion and other chemical reactions. For example, fluorescent dyes can be absorbed on fine clay sediments and Rhodamine WT decays photochemically (Scott, 1969; Hetling & O'Connell, 1966, Tai and Rathbun, 1988). The factor that inversely affects the magnitude of the response curve is the stream discharge. As related to average discharge, Kilpatrick (1993) discovered accelerated decay rates for rivers (about 5% per day) as compared to estuaries (3% per day). Note that velocity usually increases and travel time decreases as the discharge increases, plus stream reaches with significant pools may have a slower velocity than reaches with uniform depths (Reed & Stuckey, 2002). Therefore, as stream discharge rates increase, the magnitude of the response curve should decrease accordingly.

If the ion concentration or water-soluble tracer methods for collecting stream velocities are not feasible, some other collection methods include:

1. Float method
2. Velocity Head Rod
3. Current Meter method
4. Weirs
5. Measuring Flumes

Each method has its advantages and disadvantages depending upon the application. It is up to the researcher to determine which level of precision is applicable to the given situation and choose a measuring method that satisfies those requirements and the study objectives.

## **II. Methods**

### *Travel Time Significance*

The significance of the pulse tracer study is of great benefit to air station and the surrounding environment. The officials from Cherry Point Marine Corps Air Station were concerned about the length of time allotted for responses to accidental spills at various locations. The region of greatest concern was the industrialized portion of the air base, including the airfield. Due to the nature of the industrial sector and the airfield, accidents occur more frequently in those regions and the MCAS Environmental Affairs Unit needs to be able to respond to substances entering surface waters in an expedited manner. More than two years of hydrologic and hydraulic information was collected and the research focus was concentrated on the most populated portions of the industrialized section (catchments K2 and K3).

The XPSWMM9.0 projects used a combination of collected information and educated assumptions to complete continuous simulations at the air station. The subcatchment peak outflow rates generated from the Runoff Block were entered into the Sanitary Block and continuous simulations were conducted to predict the movement of hypothetical, soluble tracers. The soluble tracers were linked to individual subcatchments and the results were analyzed. Although the Cherry Point research only focused on water-soluble substances, the movement and fate of other materials could have been simulated.

The calculated travel times simulated by XPSWMM are the times needed for a water-soluble substance to reach a designated outlet from a given subcatchment or routing element. Therefore, if a substance was spilled directly on a modeling element (node or link), the model could be used to predict how much time would elapse before the pollutant reached an outlet, or other known point, due to the precipitation that occurred before, during or after the spill. Once the simulations have been completed for varying scenarios, results can be analyzed to determine approximate response time, given the magnitude of the runoff. If a return period storm does not fit the rainfall observed during the spillage, XPSWMM has the capability of accepting recorded

rainfall data or observed flow information, which can be manually inserted or linked to a corresponding precipitation or flow file that is XPSWMM compatible.

The overall goal is to provide air station personnel with a management tool that would accurately estimate travel time of a substance from the spillage point to a point of interest on the subcatchment, for given rainfall and storm flow conditions. Following the completion of the XPSWMM simulations, a matrix of travel times, pertaining to spillage location and storm frequency was formed. Using the predicted times, staff charged with preventing further contamination of the surrounding surface waters would be able to take the necessary precautions to reduce or eliminate the movement of hazardous substances into nearby water bodies including the Neuse River.

#### **A. Travel Time Calculations using Velocities**

##### *SWMM 3.2 Manual Travel Time Calculation Method*

The original calculations used simple mathematics to calculate travel times from points within a subcatchment to the catchment outlet. Two equations were applied. One equation handled calculating travel times associated with subcatchments, while the second equation generated times of travel for routing elements. Example 4.1 was calculated utilizing a SWMM dataset and predicted outflows from subcatchments 7 and 8 in catchment K2. Figure 4.3 is the associated graphic for Example 4.1 where the orange lines represent watercourses and the purple areas are impervious regions. Subcatchments 7 and 8 drain to model points 107 and 108, respectively. Stream section 108 is an ephemeral stream that conveys water from subcatchment 108 to outlet point 107, the outlet of subcatchment 7.

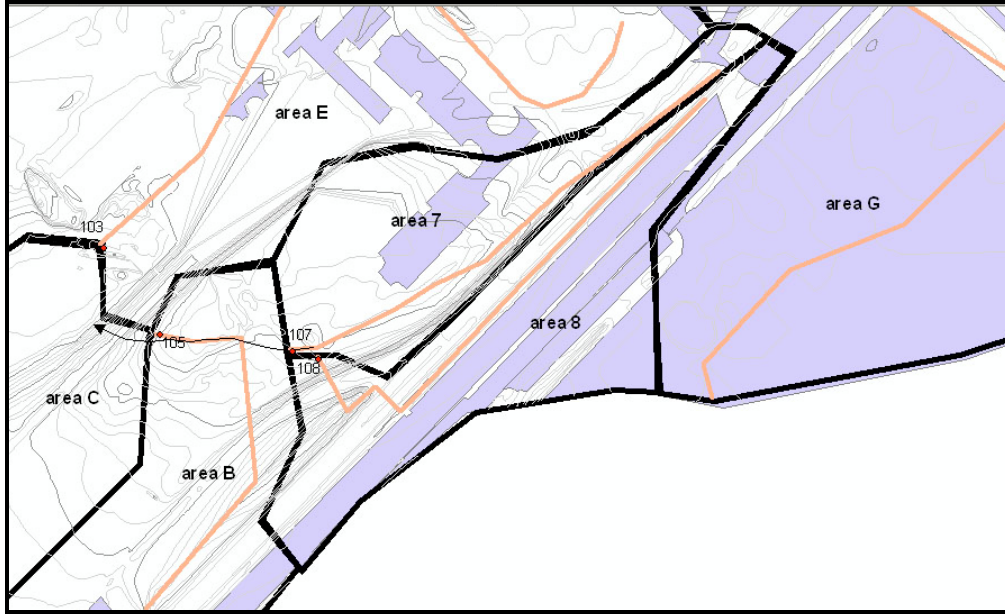


**Figure 4.3: Cherry Point Catchment K2 Focus Area for Example 4.1.** This graphic displays the stormwater features and their locations as described in the manual travel time calculation example provided below.

*Example 4.1: Travel Time Calculations Using SWMM Output Data from Storm 006 (2002)*

Manual Travel Time Equations:

1. Watershed Travel Time (WTT) Equation:

$$\frac{\text{watercourse area (ft}^2\text{)} \times \text{watercourse length (ft)}}{\text{peak flowrate (cfs)} \times 60} \quad \text{EQ 4.1}$$

where, WTT is in minutes.

2. Conduit Travel Time (CTT) Equation:

$$\frac{\text{element length (ft)}}{\text{peak velocity (fps)} \times 60} \quad \text{EQ 4.2}$$

where CTT is in minutes

Required information:

**Subcatchment 7**

*Watercourse length=665 ft*

*Channel top width=13 ft*

*Channel bottom Width=4.0 ft*

*Channel depth=1.0 ft*

*Cross sectional area of channel = 8.5 sq. ft*

*Peak flowrate=1.77 cfs*

**Subcatchment 8**

*Watercourse length=732 ft*

*Channel top width=8 ft*

*Channel bottom Width= 1.0 ft*

*Channel depth=1.0 ft*

*Cross sectional area of channel = 4.0 sq. ft*

*Peak flowrate=2.43 cfs*

**Stream section 108**

*Element length=26 ft.*

*Peak velocity=2.49 fps*

**Situation 1:** travel time to catchment 8 outlet

$$\text{WTT} = \frac{(4.0 \text{ sq. ft}) \times (732 \text{ ft})}{2.43 \text{ cfs} \times 60} = 20.0 \text{ min.}$$

**Situation 2:** travel time at end of stream section 108

$$\text{CTT} = \frac{26 \text{ ft}}{2.49 \text{ fps} \times 60} = 0.17 \text{ min}$$

**Situation 3:** travel time from catchment 8 to catchment 7 outlet

$$\text{Total TT} = \text{catchment 8 TT} + \text{stream 108 TT}$$

$$= 20 \text{ min} + 0.17 \text{ min.}$$

$$= 20.17 \text{ min}$$

Example 4.1 is highly oversimplified but displays one of the more complex routing situations. Runoff must first travel via overland flow before entering the catchment watercourse. Once in the watercourse, the flow is routed downstream to the subcatchment outlet. The outlet is where the outflows can either become inflow for an adjacent subcatchment or continue to flow downstream via additional routing elements. In Example 4.1, the outflow from subcatchment 8 reached the subcatchment 8 outlet before intersecting the 107 watercourse twenty-six feet upstream of the subcatchment 7 outlet point.

## **B. Simulation Setup for Design Storms**

### *Design Storm Continuous Simulations*

The Marine Corps air station intends to use results from this study to determine reaction times at various locations throughout the industrialized portion of the base. Thus far, the simulations completed were based on information gathered from flow and stage devices, located at the catchment outlets, during the course of several years. A more effective use of XPSWMM, for planning and management purposes, would be to apply the validated model using return period rainfall. Figure 4.4 displays the rainfall amounts corresponding to 2-, 5-, 10-, 25-, 50- and 100-year return period storm events for Morehead City, North Carolina, the US Weather Bureau long-term station nearest to the study site. Morehead City is located approximately 20 miles southeast of Cherry Point, at the confluence of the Newport River and Bogue Sound.

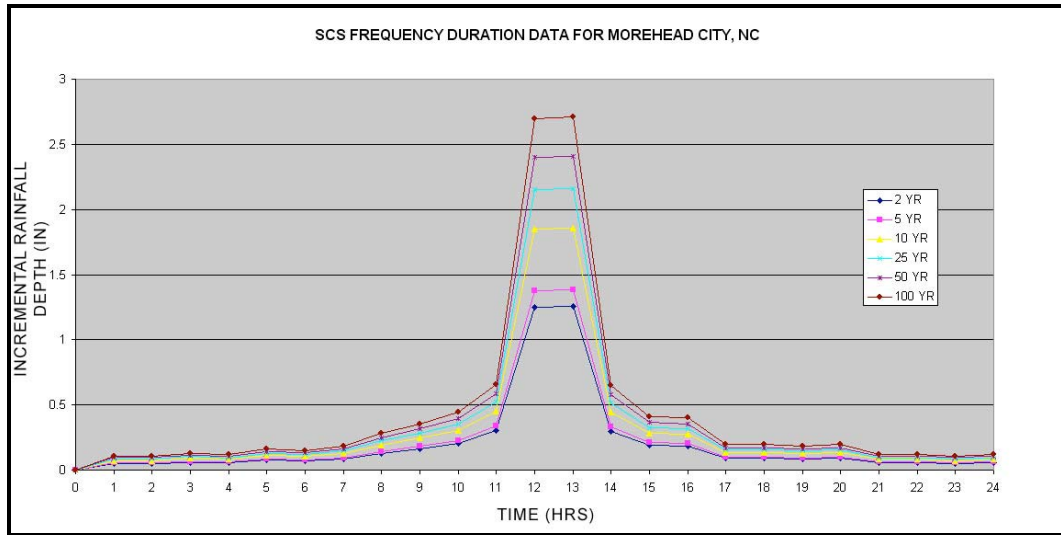


**Figure 4.4: SCS Type II, 24-hr Design Storm Rainfall Curves for Morehead City.**

The 24-hour hyetograph was created using incremental rainfall depths at 60-minute intervals and the National Resources Conservation Service, or NRCS (formerly SCS), type II rainfall distribution curve. Figure 4.5 displays the NRCS type II distribution curve and Table 4.1 is the collection of the incremental values used to generate Figure 4.5. Cherry Point was assumed to demonstrate similar precipitation characteristics as exhibited by the generalized NRCS Type II distribution curve.

**Table 4.1: NRCS Type II and Type III Rainfall Distribution Chart (Texas DOT, 2002).** This table displays the rainfall fractions used to generate the typical Type II and Type III rainfall distribution curves.

<b>NRCS 24-Hour Rainfall Distributions</b>		
<b>Time, t (hours)</b>	<b>Fraction of 24-hour Rainfall</b>	
	<b>Type II</b>	<b>Type III</b>
0	0.000	0.000
2	0.022	0.020
4	0.048	0.043
6	0.080	0.072
7	0.098	0.089
8	0.120	0.115
8.5	0.133	0.130
9	0.147	0.148
9.5	0.163	0.167
9.75	0.172	0.178
10	0.181	0.189
10.5	0.204	0.216
11	0.235	0.250
11.5	0.283	0.298
11.75	0.357	0.339
12	0.663	0.500
12.5	0.735	0.702
13	0.772	0.751
13.5	0.799	0.785
14	0.820	0.811
16	0.880	0.886
20	0.952	0.957
24	1.000	1.000

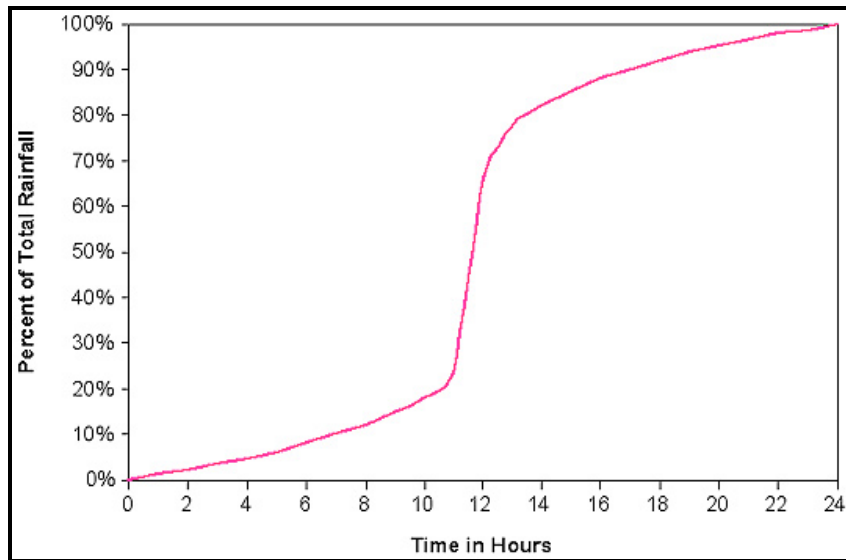


**Figure 4.5: Typical NRCS Type II Rainfall Distribution Curve.**

The return period, 24-hour, rainfall amounts were distributed using the NRCS type-II curve and placed in a spreadsheet. Hourly, cumulative rainfall amounts for each return period were entered into XPSWMM using the constant rainfall option and a steady time interval. The appropriate rainfall was linked to each XPSWMM node, organized by return period. The created global database (.xpx) enabled the exportation of the return period rainfall data and controls; thus, the precipitation information for each return period storm was only entered into XPSWMM once. The corresponding .xpx files transferred the information into sequential XPSWMM projects. Each return period storm was then simulated, in the Runoff Block, using a 24-hour time interval. Appendix 4B contains screenshots of the return period rainfall insertion process.

### **C. Comparison of Collected Rainfall to Design Storm Rainfall**

It was of interest to analyze how the collected rainfall compared to the historical values inserted into XPSWMM from the Morehead City location. From year 2000 to year 2002, all of the collected rainfall had a return period less than 2 years. The maximum, cumulative rainfall for a 24-hour period at the study site, did not exceed 4 inches, which is less than the 5-inch precipitation depth expected for a 2-yr design storm. During the study period, the maximum,

cumulative rainfall values reported by the NOAA weather station at Morehead City did not exceed the 5-yr design storm. Table 4.2 displays the three largest storm events during the study period and compares the NOAA cumulative depths to the rainfall depth collected by the automatic rain gauge. Table 4.3 demonstrates the historical averages of storm events for Morehead City, NC.

**Table 4.2: Reported and Measured Cumulative Rainfall during the Cherry Point study period.**

NOAA Cumulative Rain (in.)	Year	Day	Measured Cumulative Rain (in.)
3.51	2000	330	2.69
1.81	2001	165	1.69
2.33	2002	240	3.14

**Table 4.3: NOAA Rainfall Station Description and Statistics of Storm Events, Morehead City, N.C. (1948-2002).** The following data was adapted from a Duke University water resources laboratory assignment exploring the statistical analysis of time-series rainfall data.

Station No. 315830	Morehead City 2 WNW, Carteret County; Hourly rainfall	Lat: N 34:44:00
		Long: W 76:44:00
		Elevation: 10 ft
Storm Event Variable		<b>Mean</b>
No. of Storms <sup>1</sup> per year <sup>2</sup>		72.58
Depth, inches		0.550
Intensity, in./hr		0.119
Duration, hours		5.475
Time Between Events, hours		91.072

#### D. Design Storm Outflows

The design return period storms were evaluated for several reasons. Knowing the expected frequencies of the observed rainfall, the research team planned to examine how efficiently the stormwater system accommodated the expected rainfall runoff during the study period. Second, the results generated from the return period rainfall would be inserted into the Sanitary Block for analyzing pollutant travel time from the point of spillage to various locations. This would provide Cherry Point officials with a set of predicted response times for accidental

spills as a result of various return period storms, where the response time is defined as the time needed to treat or isolate the polluted water. Upon completing the importation of the design rainfall from the NRCS resource manual, the hydrology model was used to determine the return period maximum outflows. Tables 4.4 and 4.5 display the simulated peak runoff rates at each node in catchments K2 and K3, respectively.

**Table 4.4: XPSWMM Predicted Peak Outflow Rates for Catchment K2 for 24-hour Design Storms of various Return Periods.**

ELEMENT NUMBER	PREDICTED FLOWRATE (CFS) FOR INDICATED PERIOD					
	2 YR	5 YR	10 YR	25 YR	50 YR	100 YR
<b>1 (OUTLET)</b>	<b>83.3</b>	<b>94.2</b>	<b>125.4</b>	<b>144.9</b>	<b>161.1</b>	<b>180.5</b>
2	9.9	10.8	14.6	16.9	18.9	21.2
3	80.0	88.7	117.7	135.1	150.2	168.4
4	54.9	62.9	82.9	95.3	105.6	117.9
5	55.6	63.6	83.5	95.9	106.2	118.5
6	7.0	7.7	10.3	12.0	13.4	15.0
7	3.7	4.1	5.5	6.4	7.1	8.0
8	2.4	2.7	3.6	4.2	4.6	5.2
9	43.4	50.1	64.5	73.4	80.9	89.7
10	54.9	62.9	82.3	94.4	104.5	116.4
11		3.2	4.3	5.0	5.6	6.3
12						
13	33.3	35.7	44.6	50.0	54.6	60.0
14	26.2	26.2	26.2	26.2	26.2	26.2
15	32.1	34.3	43.1	48.6	53.2	58.7
16	15.1	16.5	22.3	25.8	28.8	32.4
17	13.2	13.6	15.2	16.1	17.0	17.9
18						

**Table 4.5: XPSWMM Predicted Peak Outflow Rates for Catchment K3 for 24-hour Design Storms of various Return Periods.**

ELEMENT NUMBER	PREDICTED FLOWRATE (CFS) FOR INDICATED PERIOD					
	2 YR	5 YR	10 YR	25 YR	50 YR	100 YR
1	7.8	8.5	11.5	13.3	14.9	16.7
2	1.5	1.7	2.2	2.6	2.9	3.3
3	3.2	3.5	4.8	5.5	6.2	6.9
4	20.9	22.9	30.9	35.9	40.0	45.0
5	4.4	4.8	6.5	7.5	8.4	9.4
6	6.8	7.4	10.0	11.6	13.0	14.6
7	11.1	11.6	13.5	14.8	15.8	17.0
8	7.4	8.1	11.0	12.7	14.2	16.0
9	5.2	5.8	7.8	9.0	10.0	11.3
10	29.7	32.2	42.5	46.8	49.8	53.5
11	6.0	6.6	8.9	10.3	11.5	12.9
12	39.5	41.6	50.0	55.3	59.7	65.0
13	63.3	67.6	85.2	96.1	105.3	116.2
14	30.6	32.8	41.6	47.1	51.7	57.3
15	11.7	12.8	17.2	20.0	22.3	25.1
16	9.2	10.1	13.7	15.9	17.7	19.9
17	15.1	16.5	22.3	25.9	28.9	32.5
<b>18 (OUTLET)</b>	<b>93.3</b>	<b>100.5</b>	<b>129.6</b>	<b>147.7</b>	<b>162.8</b>	<b>181.0</b>
19	83.2	89.5	114.6	130.3	143.4	159.1
20	0.2	0.2	0.3	0.4	0.4	0.5
21	3.7	4.1	5.5	6.4	7.2	8.1
22	5.0	5.5	7.4	8.6	9.6	10.8
1001	1.5	1.65	2.23	2.59	2.89	3.25
1002	90.9	97.9	126.1	143.6	158.3	175.9
1003	78.3	84.2	107.5	122	134.1	148.7
1004	20.9	22.9	30.9	35.9	40	45
1005	2.7	2.74	2.74	2.73	2.74	2.74

The outlet of catchment K2 is node #1 and the outlet of catchment K3 is node #18. These two nodes have the largest runoff rates since all stormwater runoff drains to these two locations that coincide with the monitored outlets referenced in Chapter Three.

The XPSWMM blocks are capable of working independently. However, by combining the outputs from two blocks, additional analysis of runoff trends could be evaluated. For example, since the Runoff module had been created for the return period storms, maximum runoff rates were generated for each node. The Sanitary module is capable of routing user-inserted pollutants through the system, determining the path and time for each tracked pollutant, and requires only pollutant concentration, time of insertion, decay rate, and the flowrate for successful transport. Combining the strengths and capabilities of the two modules, the study was extended to use the Runoff Block's predicted flow rates, in conjunction with the Sanitary Block, to simulate the movement of distinct pollutants downstream and to track the travel times.

### **III. XPSWMM Travel Times Using Pulse Tracer Results**

The analyzed travel time estimates were computed in XPSWMM. The tracer study was adapted to create imaginary tracers that were water soluble and resisted decay. Individual tracers were created for each subcatchment, therefore a tracer named "tracer 18" in catchment K2 corresponded to runoff departing subcatchment 18. The creation of distinct tracers allowed the capability of viewing each tracer's route individually. Single tracers could then be examined at any point of the routing scheme.

The Sanitary Block of XPSWMM was used to run independent water quality simulations using user-defined pollutants. These imaginary tracers were constructed solely to function as very soluble substances and progressed moved downstream as runoff was routed through the system. Initially, the tracers were inserted over one-hour period. The insertion time of the tracer was then altered to reflect the occurrence of an accidental spill and a pulse technique was introduced.

To generate the pulse effect, the beginning and ending tracer concentrations were set equal to zero and reached a maximum value of 100 dimensionless units at 12 noon. At 11.99 hours, the tracer concentration was inserted as 0 units. At 12.00 hours, the tracer concentration was inserted as 100 units and then returned to 0 at 12.01 hours. The pollutant concentration graph (pollutograph) formed a triangular shape when graphed against time. The pollutant insertion time was governed by the distribution of the NRCS type-II design storm rainfall.

When inserting the return period rainfall amounts into XPSWMM, the maximum rainfall depth in the NRCS Type II distribution occurred near 12 noon. The outflows for each subcatchment were manually inserted into XPSWMM. At 11.99, 12.00 and 12.01 hours, the maximum predicted outflows (from the Runoff Block), corresponding to each return period storm, were inserted into the Sanitary Block. No temporal variations were selected for the tracer, meaning that no additional amounts of the tracer were introduced to the system after the initial pulse (Note: Temporal variations can be used to vary concentration amounts by using multipliers as opposed to entering separate concentrations for a time series). The time controls in the Sanitary Block were then set to run a 12- or 24-hour simulation. In some instances, a longer simulation period was needed in the Sanitary Block for specific tracers to be detected at the catchment outlet. Figure 4.6 is an illustration of the Sanitary Block flow input screen, displaying the time and concentration relationship. From Figure 4.6, the maximum predicted outflow rates were inserted into the flow column and the tracer concentrations were placed beneath the tracer name at the appropriate time value. Appendix 4A contains further graphics of the Sanitary Block input screens.

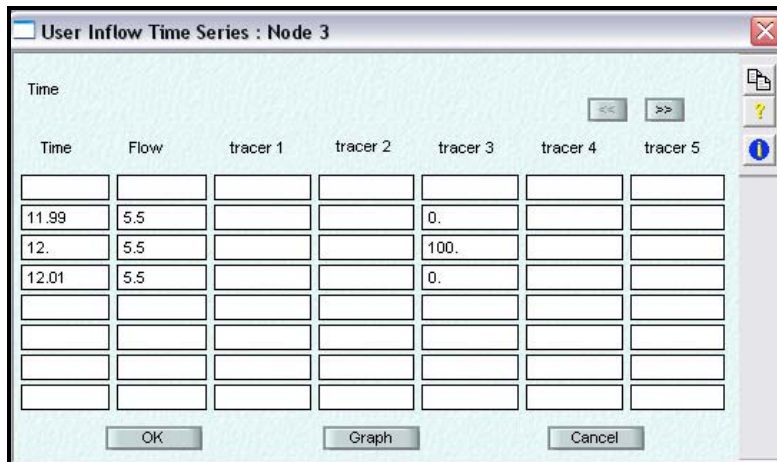


**Figure 4.6: XPSWMM Sanitary Block Flow/Concentration Input screen.** This XPSWMM input screen was used to insert concentration, flow rates and time stamps for the modeled pollutants for the Cherry Point research.

The XPSWMM simulations completed using the maximum predicted outflows from each design storm and the Sanitary Block were saved individually and named according to the return period. The text output files were then opened in a spreadsheet, recording the maximum concentration and corresponding times. Tables 4.6 and 4.7 are compilations of XPSWMM travel time estimates using return period rainfall and the pulse tracer technique.

**Table 4.6: Catchment K2 Travel Times (minutes) using Pulse Tracers with Design Rainfall for various Return Periods. .**

TRACER NO.	2 YR	5YR	10 YR	25 YR	50 YR	100 YR
	TRAVEL TIMES (MINUTES) AFTER TRACER INSERTION					
<b>1 (outlet)</b>	:00	:00	:00	:00	:00	:00
2	:05	:03	:04	:04	:05	:03
3	:01	:01	:01	:01	:01	:01
4	:03	:02	:04	:03	:02	:03
5	:07	:07	:08	:08	:07	:08
6	N/A	N/A	:04	:06	:05	:06
7	:07	:06	:06	:18	:07	:08
8	:07	:06	:06	:06	:07	:08
9	:24	:22	:08	1:39	:30	:34
10	:11	:09	:09	:09	:09	:08
11	N/A	:24	:29	1:39	:31	:35
12	N/A	N/A	N/A	N/A	N/A	N/A
13	:24	:24	:30	1:40	:30	:35
14	:24	:28	:30	1:41	:33	:38
15	:52	:56	1:11	3:20	1:27	:38
16	:20	1:31	2:22	3:29	3:00	:30
17	:56	1:03	1:21	3:27	1:30	>5:00
18	N/A	N/A	N/A	N/A	N/A	N/A

**Table 4.7: Catchment K3 Travel Times (minutes) using Pulse Tracers with Design Rainfall for various Return Periods.**

TRACER NO.	2 YR	5YR	10 YR	25 YR	50 YR	100 YR
	TRAVEL TIMES (MINUTES) AFTER TRACER INSERTION					
1	:02	:02	:02	:02	:02	:02
2	:09	:08	:06	:02	:06	:07
3	:07	:07	:06	:06	:06	:07
4	:06	:07	:06	:06	:06	:05
5	:10	:10	:10	:09	:10	:09
6	:08	:08	:07	:07	:07	:07
7	:10	:11	:10	:10	:09	:08
8	:15	:19	:23	:23	:25	:25
9	1:37	1:45	2:18	2:27	:58	UNSTABLE
10	1:00	1:03	1:02	1:02	1:04	UNSTABLE
11	1:07	1:09	1:09	1:13	1:10	1:10
12	:06	:05	:05	:05	:06	:05
13	:04	:04	:04	:04	:03	:03
14	:21	:20	:20	:19	:20	:20
15	1:01	1:02	1:09	1:11	1:16	UNSTABLE
16	:05	:05	:05	:05	:05	:05
17	:04	:04	:04	:04	:04	:03
<b>18 (outlet)</b>	<b>:00</b>	<b>:00</b>	<b>:00</b>	<b>:00</b>	<b>:00</b>	<b>:00</b>
19	:06	:02	:02	:01	:02	:01
20	:13	:12	:11	:10	:12	:10
21	:06	:05	:05	:05	:05	:05
22	:05	:05	:05	:04	:04	:04

The outlet for catchment K2 is located in subcatchment 1. Therefore, the corresponding time values for subcatchment 1 are zero, reflecting an instantaneous appearance of tracer 1 at the catchment K2 outlet.

At this simulation level, notice that the 50- and 100-year period storms were generating longer travel times than the shorter return period incidents. This seems a bit odd, since higher return period storms should generate more runoff volume, which would result in increased flow rates. Wetland regions of the catchment apparently stored water and impeded the downstream movement of runoff.

The outlet for catchment K3 is located in subcatchment 18. The tracer travel times predicted for subcatchment 18 all equal zero, therefore, tracer 18 was instantaneously detected at the subcatchment 18, and catchment K3, outlet. Similar to catchment K2, the 25-year return period storm is generating travel times that fail to fit the result trends. Meaning, as the return period increases, the travel times should decrease accordingly. Subcatchments 9, 10, 11 and 15 are the four regions that produced conflicting results.

#### *Pulse Tracer Travel Time Comments*

Various simulations were conducted in order to strengthen the predictive power of the stormwater model. The following section outlines the progression and refinement processes used during our investigation. There is a definite relationship between the modeling elements, the inserting data, the inserted rainfall depths, and the generated outflow data. Likewise, there were speculations regarding the tracer movement, providing the amount of rainfall observed and resulting runoff generated. In certain cases, the predicted data displayed expected outcomes. During other instances, anomalies existed. The results section will explain the conditions resulting in anomalies and the corrective actions employed.

#### **A. 2007 XPSWMM, 5-minute Rainfall Tracer Investigation**

Since XPSWMM shares information between modules, the associated travel times are directly influenced by any changes in both the Sanitary and Runoff Blocks. Alterations conducted in either block ultimately affect runoff generation, routing and tracer movement. The inserted rainfall used to generate outflow in the Runoff Block was apparently not performing correctly.

The 60-minute rainfall data produced unsatisfactory results, since it was discovered that the majority of the tracers were moving at rates requiring several minutes, not hours. Thus, the flow routines at Cherry Point demanded a shorter simulation period, which in turned required precipitation information with increased resolution. Therefore, using HEC-HMS, 5-minute rainfall data was exported into XPSWMM and simulated for return period storms ranging from 2 to 100 years. The intent of completing the new XPSWMM simulations was to complete the modeling procedures in order to accurately predict the movement of the tracer with a decreased simulation time period. Tables 4.8 and 4.9 present the findings from the second pulse tracer investigation using a shorter rainfall interval.

**Table 4.8: Catchment K2 Maximum, Predicted Outflow and Travel Time Estimates using 5-Minute Return Period Rainfall Data**

Area	XPSWMM Predicted Maximum Runoff Rates and Travel Time for Indicated Return Period											
	2 YR		5 YR		10 YR		25 YR		50 YR		100 YR	
	Runoff (CFS)	Travel time (min)	Runoff (CFS)	Travel time (min)	Runoff (CFS)	Travel time (min)	Runoff (CFS)	Travel time (min)	Runoff (CFS)	Travel time (min)	Runoff (CFS)	Travel time (min)
1 (outlet)	135.55	0	148.62	0	199.49	0	232.63	0	256.6	0	282.52	0
2	30.74	2	33.11	2	41.37	2	46.74	3	50.89	2	56.22	2
3	125.18	1	137.61	1	183.64	1	213.97	1	235.2	1	257.87	1
4	82.78	3	89.2	3	112.89	3	122.54	>1HR	129.59	2	138.36	4
5	84.32	12	90.59	12	114.01	11	123.27	>1HR	128.49	12	137.73	11
6	23.39	2	26.08	2	35.5	3	41.56	4	46.26	2	52.29	3
7	12.15	16	13.56	16	18.55	16	21.79	>1HR	24.29	16	27.52	17
8	8.16	16	9.09	16	12.36	17	14.46	>1HR	16.09	15	18.18	17
9	77.22	>1HR	84.68	>1HR	112.75	>1HR	130.85	>1HR	145.08	>1HR	162.07	>1HR
10	83.97	13	90.33	13	114.12	12	121.81	>1HR	123.77	13	134.53	13
11	9.99	>1HR	11.11	>1HR	15.01	>1HR	17.52	>1HR	19.47	>1HR	21.97	UNST
12	26.97	>1HR	30.16	>1HR	41.40	>1HR	48.68	>1HR	54.32	>1HR	61.54	>1HR
13	45.22	>1HR	49.41	>1HR	65.81	>1HR	76.59	>1HR	84.84	>1HR	94.67	UNST
14	47.68	>1HR	50.43	>1HR	60.46	>1HR	67.13	>1HR	72.34	>1HR	78.93	UNST
15	71.09	>1HR	79	>1HR	107.74	>1HR	126.84	>1HR	141.75	>1HR	160.6	>1HR
16	22.1	>1HR	24.33	>1HR	32.45	>1HR	37.86	>1HR	42.1	>1HR	47.46	>1HR
17	19.38	>1HR	20.73	>1HR	25.71	>1HR	29.05	>1HR	31.67	>1HR	34.98	>1HR
18	22.90	>1HR	25.84	>1HR	36.56	>1HR	43.68	>1HR	49.25	>1HR	56.30	>1HR

**Table 4.9: Catchment K3 Maximum, Simulated Outflow and Travel Time using 5-Minute Return Period Rainfall Data**

Element Number	XPSWMM Predicted Maximum Runoff Rates and Travel Time for Indicated Return Period											
	2 YR		5 YR		10 YR		25 YR		50 YR		100 YR	
	Runoff (CFS)	Travel time (min)	Runoff (CFS)	Travel time (min)	Runoff (CFS)	Travel time (min)	Runoff (CFS)	Travel time (min)	Runoff (CFS)	Travel time (min)	Runoff (CFS)	Travel time (min)
1	25.65	1	28.56	1	38.77	1	45.38	1	50.49	1	57.03	1
2	5.17	7	5.75	6	7.77	5	9.08	5	10.09	5	11.39	4
3	9.69	7	10.88	6	15.14	6	17.94	6	20.1	5	22.86	5
4	62.44	5	69.95	5	95.67	5	111.62	5	122.67	5	136.8	5
5	14.59	9	16.27	8	22.17	16	25.97	18	28.91	18	32.69	19
6	21.53	7	24.03	7	30.85	6	32.95	6	34.57	6	36.66	6
7	22.37	9	24.33	8	31.29	7	35.81	7	39.31	7	43.79	6
8	23.1	43	25.9	42	35.82	45	42.29	42	47.3	48	53.71	39
9	17.55	>1HR	19.57	>1HR	26.64	>1HR	31.2	>1HR	34.74	>1HR	39.27	>1HR
10	64.69	>1HR	70.17	>1HR	89.88	>1HR	102.87	>1HR	112.97	>1HR	125.82	>1HR
11	19.88	>1HR	22.18	>1HR	30.27	>1HR	35.49	>1HR	39.53	>1HR	44.71	>1HR
12	75.72	5	83.3	5	110.73	5	128.96	5	143.15	5	161.1	4
13	136.07	3	150.22	3	200.66	3	233.51	3	257.34	3	287.31	3
14	69.09	30	77.04	29	106	29	125.28	29	140.36	33	159.44	28
15	33.4	>1HR	37.6	>1HR	52.73	>1HR	62.72	>1HR	70.48	>1HR	80.36	>1HR
16	26.79	5	30.14	8	42.19	44	50.13	>1HR	56.3	>1HR	64.15	>1HR
17	41.27	4	46.12	8	56.88	11	58.69	8	60.1	7	61.91	7
18 (outlet)	189.38	0	209.36	0	276.4	0	317.16	0	347.6	0	384.46	0
19	178.62	1	197.7	1	259.34	1	294.3	1	319.74	1	351.24	1
20	0.72	10	0.8	10	1.08	17	1.26	18	1.4	19	1.58	19
21	12.57	5	14.01	12	19.06	51	22.31	>1HR	24.84	>1HR	28.07	>1HR
22	16.35	5	18.25	8	20	11	21.1	8	21.96	8	23.06	8

The first observed difference between the two simulations, using 60-minute and 5-minute rainfall data, was the increase in predicted peak runoff rates for the 5-minute rainfall case. The second set of results (5-minute rainfall simulations) not only generated more runoff than the previous predictions, but all subcatchments were now contributing runoff. Previously, in catchment K2, subcatchments 12 and 18 failed to produce runoff at any return storm level. Likewise, subcatchment 11 did not simulate runoff at the 2-yr storm level. It was later discovered that the runoff generated from subcatchments 12 and 18 was being redirected into nodes 1003 and 16, respectively; therefore, the model failed to report runoff exiting subcatchments 12 and 18. In most cases, the flow redirection option would not be selected, however it is useful when

needed to pass flow through noncontributing model points, such as manholes. The flow redirection option was disabled during the second phase of tracer testing.

Table 4.8 offers the best synopsis of the pulse tracer study results for catchment K2. Using the 5-minute rainfall, and the updated flow routing scheme, resulted in the following observations. First, the minimum and maximum predicted outflows for this catchment were 8.16 and 279.70 cfs, respectively. Predicted travel time of the pulse tracers typically ranged between 1 and 60 minutes, although there were periods with travel times greater than 60 minutes. Instabilities in the numerical solution had prevented definitive conclusions, at the 25-year storm level. Once the two overflow channels were incorporated, the model was able to achieve improved convergence and predicted slightly higher outflows in catchments directly affected by routing elements 111 and 115. This alleviated the problem of numerical instability. Third, the typical difference between the estimated travel times across the six design storms only varied approximately 1 to 3 minutes, excluding the instances that required longer than 60 minutes. Fourth, the travel time numbers for a 100-year return period storm produced the most instances of 60 minutes or greater results.

Table 4.9 resulted from the combination of the Runoff Block and Sanitary output files following the completion of the 2007 XPSWMM simulations using 5-minute design rainfall data. Table 4.9 is similar to Table 4.8, but highlights the finding for catchment K3. The following observations were recorded for this catchment. First, the minimum predicted runoff was 0.72 cfs, and the maximum value was observed at the catchment outlet, having a value of 384.46 cfs. Similar to catchment K2, the overall range of travel times ranged between 1 minute and 1 hour, having a difference across storm events of approximately 4 minutes. Likewise, the 25-year return period storm results presented the most deviance from the normal observations, reporting the most occurrences of instability and the difference between selected travel times exceeded 4 minutes.

Results of the XPSWMM simulations presented in Tables 4.8 and 4.9 demonstrated that travel time was not only affected by flow rate, but the interactions between the subcatchments and routing elements. The spatial relationship of the subcatchment outlet to the catchment outlet also played a significant role in the resulting travel time estimates. Apparently, the combination of the rainfall and routing chosen during the 25-year return period simulations introduced additional complications, which in several instances, prevented the model from reaching a numerically stable solution. As a result, we were unable to determine a maximum travel time because the

predicted times fluctuated and never reached a stable number by the conclusion of simulation period. Even when the simulation period was extended to 24 hours, the numerical instability still existed. It was later discovered that pipe surcharge conditions existed in routing elements 111 and 115, where excess runoff was not being routed through the system efficiently. It was finally understood that the surface flows were just as important as the subsurface pipe routing, therefore, the interaction of the surface drainage was revisited. Additional explanation regarding this situation is discussed in Section E, "Catchment K2 XPSWMM Travel Time Simulations using 5-minute Rainfall and Overflow Routing".

There were two situations when the specific travel time results were not included in Tables 4.8 and 4.9. The first situation occurred when the travel time was greater than one hour. Since the scale of the typical time results was confined to several minutes, including the larger times did not seem reasonable, because the response time application is dependent upon the shortest time scenario. For this reason, travel times of several hours were not explicitly reported in the results table, but given the generic label of "greater than one hour". The other numerical situation that occurred was instability in the iterative process. The number of iterations in XPSWMM is user-defined. For the 5-minute rainfall simulations, the routing time step was set to 60 seconds, the number of iterations equaled four and the tolerance was defined as 0.001. Increasing the number of iterations and reducing the tolerance level is one way to solve instability issues. We attempted adjusting the number of iteration and tolerance, but discovered that the program defaults generated the most stable solutions. The typical XPSWMM SANITARY block simulation required between 1000 and 2000 attempts to reach convergence. Unstable conditions usually occurred in 5000 or more attempts without reaching a solution that satisfied the tolerance requirement. The "unstable" label does not mean that a solution was not determined. This label means that the model generated output but the results were unstable and it was not possible to determine when the maximum tracer concentration was achieved.

The overall time travel trends for catchments K2 and K3 seemed fairly realistic. More intense storms (higher return period rainfall events, i.e. 50- and 100-year storms) would deliver more rainfall, greater runoff rates and faster travel times. Tables 4.8 and 4.9 partially reflect this assumption by reporting decreasing travel time estimate as the storm return frequency decreases for higher return periods. For example, subcatchment 2 of catchment K3 generated very predictable travel time results. The timing sequence across the six storms was 7, 6, 5, 5, 5, and 4 minutes respectively. At the 2-year storm level it was determined that 7 minutes were needed for tracer 2 to reach a maximum concentration level at the outlet of catchment K3. Conversely, at

the 100-year level, only 4 minutes were needed for tracer 2 to be detected at the same location. In most situations, when the travel time estimates failed to follow the reduced travel time trend, for storms of higher return periods, increased travel times predicted were due to the routing elements inability to handle excess water, not the model's capabilities for predicting flow rates.

Theoretically, one would expect that a higher flow rate would produce a smaller travel time, since the water soluble tracer is dependent upon the element's flow rate for downstream movement. This statement also assumes that all portions of the flow are moving at the same velocity and that the pollutant does not disperse or travel at a different velocity than the water. In a limitless situation (very large conduits) this hypothesis would prove to be valid, since the area of the flow conduit (routing element or catchment) could be assumed large and velocity increases with flow rate. In nature, limits exist: the Manning equation was used to calculate the inflow velocity, at each node and time step, which is limited by the element's width, slope and roughness. Width was considered to be a user defined parameter, dependent upon area delineation and was not assumed to have fixed conditions. Therefore, once these physical limits are reached, either over bank flow conditions exists or pipes enter into a pressure flow situation. The majority of the unstable and longer travel time results came from the catchments where pipe flow was the main transport function.

Another important consideration is the function of the time of concentration and the rainfall. In XPSWMM, it is assumed that the time of concentration equals the rainfall duration. In addition, the movement of the particular storm is not modeled unless multiple rainfall gauges are incorporated into the simulation. The resulting situation is the time of concentration being defined as the time of equilibrium. Moreover, the time of equilibrium is the time required for water to travel from the most remote point in the catchment, to the designated outlet location. This definition for time of concentration is very close to the application of the pulse tracer study, where the point of insertion is considered the most remote point at some point in time. The travel time study then relies on the modeling sequence to determine the elapsed length of time needed for the point tracer to be viewed at the outlet of the inserted subcatchment, routing element, or catchment outlet.

In most cases, excess rainfall and the time of concentration are directly proportional. When applied to the travel time interpretations, one would suspect that as the rainfall events increase in total delivered rain that the amount of runoff would increase, if all other variables are held constant. Therefore, a 100-year return period storm would be expected to create more

runoff than a 25-yr storm. As stated previously, this linear relationship would prove to be valid in all situations, if the importance of physical limitations were ignored. So, not only is surface water travel time a function on excess rainfall, but under certain conditions, it also becomes a function of watershed and routing element characteristics. Therefore, increased excess rainfall during the travel time study, does not necessarily guarantee a shorter travel time, although an increased time of concentration does result.

### B. Catchment K2, 5-minute Rainfall Travel Time Analysis

At the 2-, 5- and 10- year return period levels, two distinct observations summarize the results from the XPSWMM trace pulse application. First, all of the areas surrounding the catchment outlet had travel times less than 10 minutes. Second, the majority of the upstream areas had travel time estimates greater than 50 minutes. One example of the 5-minute travel time results for catchment K2 are presented in Figure 4.6

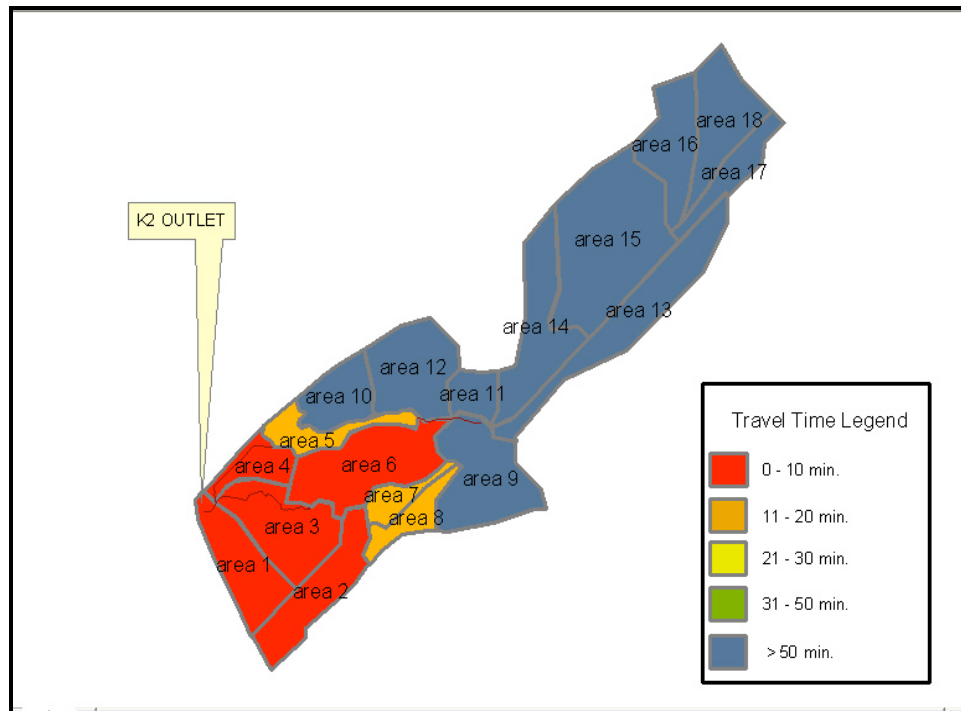


**Figure 4.7: Travel Time Response Map for Catchment K2 at Cherry Point using 100-yr Return Period Rainfall Amounts (5-Minute Rainfall Interval).**

The shortest travel times for catchment K2 were reported for subcatchments 3 and 4. Runoff travels from subcatchments 2 and 6 via overland flow (through subcatchment 3) for approximately 794 ft before entering channel 101 that drains subcatchment 1. Consequently, subcatchment 1 has a travel time of zero since it is the catchment outlet. The travel time estimates for subcatchments 2, 3, 4 and 6, using a 10-year return period rainfall event, are 2, 1, 3 and 3 minutes, respectively. These estimates simply reflect the time required for the maximum pulse tracer concentration to be observed at the catchment outlet. The short travel times for these sections seem reasonable since the outlets of the four subcatchments are located near one another.

Subcatchments 5, 7, 8, and 10 all had travel times that ranged between 11 and 20 minutes. At the upstream section of catchment K2, the response times ranged from 4 to 11 hours depending on the interest area. The upland areas of catchment K2 consist of subcatchments 9, 11, 12, and 13 through 18. In most cases the longer travel times associated with these subcatchments were subject to convergence issues.

The similarities between the three shorter return period storms is probably due to the amount of precipitation delivered to the study area during each level, the process of the transforming rainfall into runoff, and the simulation time step. The maximum 24-hour rainfall produced for a 2-, 5-, and 10-year rain event for this region of North Carolina is 5, 5.5 and 7.4 inches, respectively. One would suspect close results from the 2- and 5-year storms because the difference between the storm precipitation depths is only 0.5 inches. On the other hand, a difference of 2.4 inches exists between the 2- and 10-year amounts.

The 50- and 100- year return period, travel time simulations, also produced results similar to those received from the higher probability rainfall events, such as the 2-year through 25-year storms. The majority of the downstream subcatchments in catchment K2 still had travel time estimates that ranged between 0 and 10 minutes. The upstream results remained fairly consistent as well.

Lengthy travel times might simply be due to computational error. The 5-minute rainfall and model settings were chosen to optimize the prediction performance. Nonetheless, when viewing the sanitary output file for the 50-year return period, K2, tracer study simulation, it appears the XPSWMM was having difficulties achieving convergence. For example, the typical total number of iterations that corresponded with minimal error ranged between 1000 and 2000.

For link element 105, more than 5000 attempts were made to achieve convergence, having a XPSWMM maximum error of 0.242. The error of convergence associated with runoff routing is a dimensionless figure, used to quantify the stormwater model's ability to reach a finite conclusion. Therefore, the maximum error is a value that simply assists in understanding the error associated with reaching numerical convergence. The convergence threshold value is inserted in decimal form, but is probably better suited for analysis if converted into a percentage. The error value and the number of iterations are directly proportional. The normal error range did not surpass 0.01 in most situations. The same situation holds true at the 100-year level. A total of 5701 attempts were made at solving the flow equation for element 105, with a maximum error of 0.238. Therefore, an increase in travel time seems reasonable since the model results oscillated about a range in numbers and not one particular value. Logically, if convergence were an issue, the associated travel time would probably be longer rather than shorter, since the model is constantly attempting to reach a convergence at each increasing simulation time step.

Examining the percentage of the subcatchment that is impervious offers a different interpretation of the XPSWMM travel time results for catchment K2. Subcatchments 5, 7, 8, and 10 all had estimated travel times between 11 and 20 minutes; however, the individual travel times for the unique areas, using the 5-minute rainfall data for a 10-year rainfall event were 11, 16, 17 and 12 minutes respectively. The imperviousness for these same subcatchments is 28%, 50.1%, 71.5% and 83.2%. The outlets of subcatchment 7 and 8 are very close in proximity, and the tracer study reflects this fact. In addition, the outlets of subcatchments 5 and 10 are connected by a 403 ft. circular pipe section and the effluent leaving subcatchment 10 should only lag behind that water leaving subcatchments 5 as determined by the flow velocity. Noticeably, the subcatchment percent imperviousness had little effect on the travel time analysis, because the tracer was inserted at the subcatchment outlet and then routed to the catchment outlet. Therefore, the imperviousness of the subcatchment was not considered in the Sanitary Block nor the travel times estimates. However, the subcatchment roughness and imperviousness were critical components in the Runoff Block and would affect the predicted outflow velocities. Thus, the time required for the tracer to reach the subcatchment outlet is not considered. XPSWMM is only capable of estimating runoff and travel times from the model points designated. In order to simulate the time needed for a tracer to reach a given position, which has not been already included in the simulation, an additional model point is needed.

### C. Catchment K3, 5-Minute Travel Time Analysis

Catchment K3 yielded similar results to those concluded for catchment K2 regarding the travel times estimated for upstream and downstream subcatchments. In most cases, the downstream subcatchments had travel times less than 20 minutes at all six storm levels. On the other hand, the most remote subcatchments had the greatest travel times that, under normal conditions, exceeded 60 minutes. Nonetheless, there existed situations when the simulated travel times fluctuated between 21 and 59 minutes, and generally speaking, these instances occurred in subcatchments that were located in the middle region of the catchment. Figure 4.7 is one example of the travel time results using the 5-minute rainfall for catchment K3.

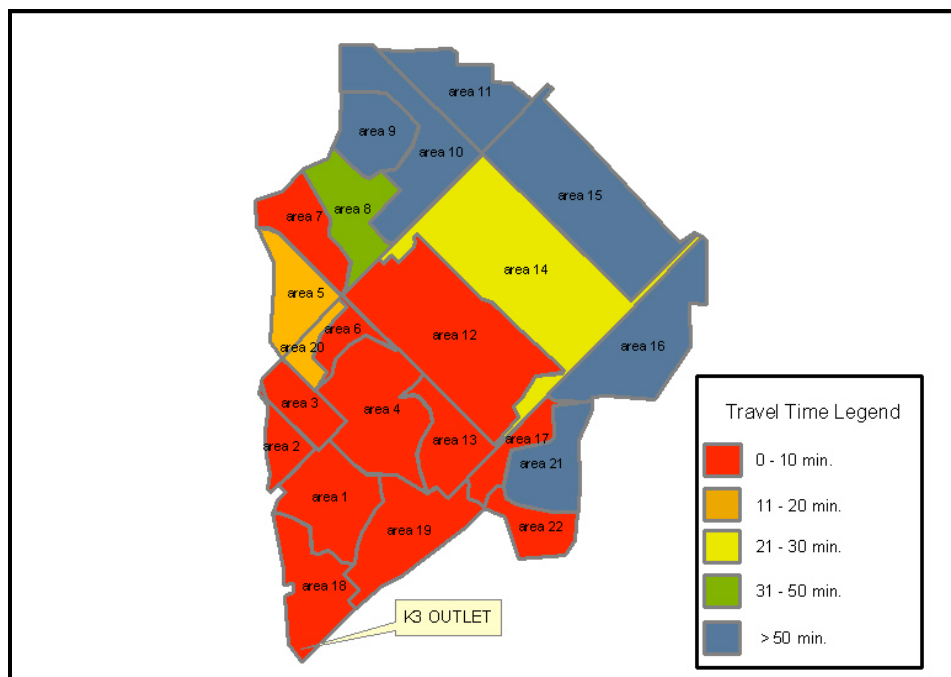


**Figure 4.8: Travel Time Response Map for Catchment K3 at Cherry Point using 100-yr Return Period Precipitation (5-minute Rainfall Interval).**

At the 2- and 5-yr rainfall levels, the model predicted closely related travel times. Using the 2-yr design rainfall only, subcatchments located near the catchment outlet, subcatchment 18, had travel times, which were less than 10 minutes. This prediction seems reasonable since the distances to the catchment outlet, for these areas only, would be the shortest lengths, which would require the least amount of time to traverse. Numerically, the model suggests a similar conclusion. At the catchment outlet, a maximum outflow of approximately 189 cfs was

generated, for the 2-yr rainfall event, having a related travel time value of zero minutes. The three areas directly adjacent to the outlet, subcatchments 1, 2 and 19, had travel time values of 1, 7 and 1 minutes, respectively. The second tier consists of subcatchments 3, 4, 13, 17 and 22. The travel times corresponding to these areas are 7, 5, 3, and 4 minutes. The last group of subcatchments having 10 minute travel times, or less, is comprised of subcatchments 5, 6, 7, 12, 16, 20 and 21 which were estimated to have travel times of 9, 7, 9, 5, 10 and 5 minutes, respectively. Subcatchment 14, with a travel time of 30 minutes, was the only area having a travel time ranging between 21 and 30 minutes. Likewise, tracers leaving subcatchment 8 required an estimated 43 minutes to reach a maximum level at the catchment outlet. Lastly, subcatchments 9, 10, 11 and 15 all had travel times greater than one hour. The difference in travel time between the 2- and 5-yr storm events usually differed between 1 and 3 minutes. The greatest disparity between the two simulations occurred in subcatchments 17 and 21 where the time differences increased by 4 and 7 minutes, respectively.

At the 2- and 5-yr year rainfall levels, the model seemingly reached convergence without much difficulty. The average number of iterations ranged between one and four attempts adhering to the user-defined 0.001 convergence error. Only five elements had a greater computational error value. Elements 108, 109, 120, 121 and 301 had relative errors of 0.19, 0.18, 0.13, 0.037 and 0.24 as opposed to the 0.001 to 0.003 range calculated for the remaining regions for the 2-yr storm event. Of these five elements, only pipes 108 and 109 underwent surcharged conditions during the 2-yr rainfall simulation, using 5-minute time steps. Routing element 120 drains subcatchment 20 and is a 30-inch concrete pipe with a 0.05% slope. Likewise, pipe number 21 was assumed to have a continuous 24-inch diameters and a slope of 0.26%. Elements 108 and 109 are also pipes with diameters of 24 and 18 inches. Element 301 is a 21-foot wide surface channel with a 0.05% bed slope. The error related to element 301 seems typical since XPSWMM might have difficulty simulating overland flow during over-bank conditions and does not route flow well through wetland areas. Although one would suspect that the system was designed to handle runoff from a 2-yr rainfall event, the natural channels “adjust” to overflow conditions, meaning that during intense runoff situations the assumed channel dimensions change; thus resulting in a higher flow error due to the original conduit parameters. During the 5-yr results, subcatchments 108, 109, 119, 120 and 301 still generated the highest error values.

The four remaining storms from the 5-minute rainfall investigation of catchment K3 displayed fairly consistent similarities despite their differing return periods. The model was able

to simulate the increasing amount of rainfall and runoff as expected. Likewise, the travel times generated from the pulse tracer study during the 10-, 25-, 50- and 100-yr storms for catchment K3 could be grouped into three categories.

The first category, dealt with travel times, where the pulse tracers were able to reach the K3 outlet within 20 minutes or less. These shorter travel times corresponded to the downstream subcatchments of catchment K3, such as subcatchments 1 through 7, 12, 13, 17 through 20, and 22. Although these estimates seem reasonable, sometimes the model demonstrated difficulties in calculating a solution. For example, the iteration errors associated with subcatchments 1, 19 and 20 were elevated beginning with the 10-yr results. Routing elements 301, 120 and 119 had computational errors of 0.276, 0.138 and 0.034, respectively. In most cases the error associated with convergence ranged between 0.001 and 0.008, for catchment K3. Despite higher computational errors, the distance to the catchment outlet was not lengthy and thus, the estimated travel times only fluctuated 1 to 3 minutes for the lower subcatchments.

The second category had travel times greater than one hour and contained most of the upstream areas. These upstream regions are drained mostly by pipes and include subcatchments 9 through 11, 15 and 21. During the larger storm events, these subcatchments always required more than 50 minutes for runoff to be transported to the catchment outlet. Subcatchments 9 through 11 and 15 consistently required more than one hour to route their outflow downstream, despite the inserted rainfall. This consistency leads to the assumption that the time required for outflows to reach the catchment outlet for these subcatchments is due mostly to traversed distance. However, surcharged pipe situations did exist which limited the flow handling capabilities of the routing elements. The runoff from subcatchments 9, 11 and 15 are routed into subcatchment 10 before continuing downstream. At the 10-yr rainfall level, pipes 109, 110 and 115 (the 18-inch, 24-inch and 24-inch pipes handling outflow for subcatchments 9, 10 and 15) were surcharged for a majority of the simulation period that could lead to increased travel time values due to flow restrictions. Likewise, pipe 116, which is routed through subcatchment 17, was surcharged for nearly 58% percent of the 10-yr rainfall simulation period.

Figure 4.9 displays the runoff simulation results for routing element 115 in catchment K3, which drains subcatchment 115. Rainfall is not reported, because it was inserted at the subcatchment level, transformed to runoff, and then routed. The surcharge, or pressure flow, condition results in a flattened hydrograph peak due to pipe capacity limits.

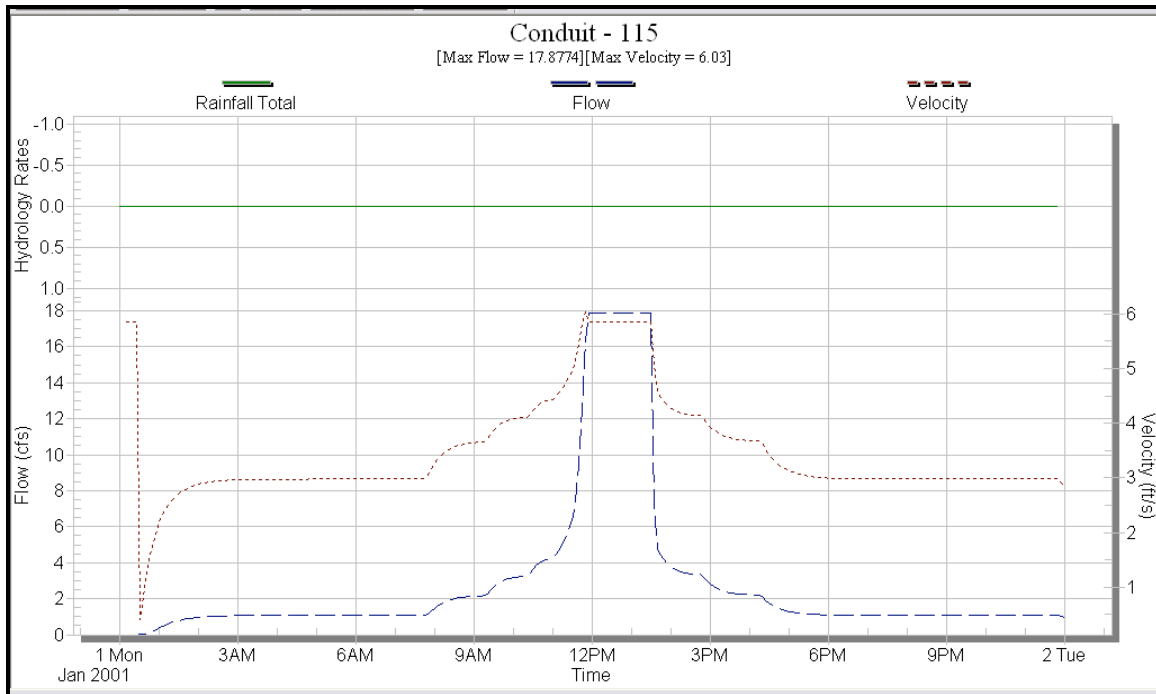


**Figure 4.9: Example of XPSWMM Runoff Results displaying Surcharged Conditions**

The third category deals with the subcatchments, whose travel times fluctuated during the 10-, 25-, 50- and 100-yr storm events and ranged between 21 minutes and 49 minutes. Subcatchments 14 and 16 form this last group. During the 50-year rainfall level, subcatchment 14 had a travel time of 33 minutes, while at the 10-, 25-, and 100-yr levels the simulated travel time was approximately 29 minutes. Due to the arbitrary grouping of the travel times, graphically, it seems as though the model was having difficulties in simulating runoff from subcatchment 14. Numerically, the subcatchment 14 estimates only had a difference of 4 minutes and seemed quite reasonable. The subcatchment 16 results are a bit more decisive. For example, during the 10-yr rainfall event, the travel time required for tracer 16 to reach the catchment outlet is 44 minutes. At the 25-, 50- and 100- storm levels, the time value for tracer 16 increases to more than one hour. This deviates from normal. From the model routing schematic, effluent from 16 is directly routed through subcatchment 17 that is first drained by pipe 117 before being routed downstream via surface channel 317. Element 117 was under pressure flow for at least 65% of the simulation duration, for the 25-yr, and higher, rainfall events and therefore restricted the movement of subcatchment 16's outflow which resulted in a lengthier travel time for tracer 16.

#### **D. Travel Time Comparison using 60-minute and 5-minute Simulation Time steps**

The Sanitary Block of XPSWMM, using return period rainfall data with a 60-minute simulation time step, simulated the initial pulse tracer travel times. Upon further inspection of the study area's observed flow patterns, it was determined that a 60-minute simulation interval probably was not sufficient to accurately generate and route runoff. Therefore, an additional set of simulations was conducted, where the simulation time period was reduced to 5 minutes. Keeping all other inputs constant, the travel time results from both sets of simulations were gathered into a spreadsheet and examined. Appendix 4D is a collection of the findings from the comparative activities concerning travel time for catchments K2 and K3 at Cherry Point MCAS. The following two sections describe the interaction of the reducing the simulation time step and the resulting runoff responses.

##### *Catchment K2 5- and 60-Minute Travel Time Comparison*

Several trends were noticed during the evaluation of the 5- and 60-minute rainfall interval simulations for catchment K2. Reducing the rainfall interval increased the estimated runoff. For example, the 2-yr storm values demonstrated an 88.8% increase in runoff between the 60- and 5-minute simulations. Meaning, that the 5-minute simulations generated nearly twice the runoff (outflow wise) as compared for the first set of predictions. This trend continued throughout all the testing levels with the 100-year, 5-minute results, having a calculated runoff increase of 109.5%. This finding seemed reasonable since the reduction of the simulation time step minimized the effects of system losses, including evapotranspiration, depression storage regeneration, and infiltration. Although reducing the rainfall interval did not increase the runoff uniformly across catchment K3, the occurrence of a sizeable increase was consistent.

Reducing the simulation time period also affected the travel time results but failed to display a consistent trend. Although, 5 out of 6 of the return period storm simulations resulted in an increase in travel time, during the 5-minute simulation interval, the magnitude of that increase lacked a noticeable pattern. The results reported increases in estimated travel time, between the 5- and 60-minute scenarios, that ranged from 13.3% to 25.9%. However, at the 25-year storm level, a 3.2% decrease in time was calculated. The 60-minute scenario results represented a free flowing stormwater system, where the restrictive processes had been minimized due to the systems ability to recover from flow losses as related to a longer simulation time step. Likewise,

during the 5-minute scenario there were greater occurrences of numerical instability and travel times in excess of one hour, because the simulation time step was small enough to incorporate flow congestion (the presence of pipes under pressure flow and backwater conditions). Therefore, the travel times generated from the 5-minute simulations represented more realistic flow situations.

The time of travel for catchment K2 could be grouped into two broad categories: 1) 0 to 20 minutes and those results 2) greater than one hour. Although fluctuations did occur, in most cases, the computed travel time for both sets of simulations fit into these two categories. The downstream subcatchments, 1, 2, 3, 4, and 6 usually corresponded to the shortest travel time which is due mainly to their close proximity to the catchment outlet. The longer times were related to the upstream subcatchments, such as 9, and 11 through 18. Therefore, subcatchments 5, 7, 8, and 10 were labeled “transitional”, with respect to travel time, since the associated time values fluctuated between the lower and higher extremities and altered as the simulated rainfall was adjusted. The travel time results for catchment K3 also displayed similarities to those concluded for catchment K2.

#### *Catchment K3 5- and 60-Minute Travel Time Comparison*

Catchment K3 displayed more consistencies than catchment K2, which is probably due to better topographic and flow information collection. Nonetheless, several conclusions were discovered during the comparison of the 5- and 60-minute rainfall datasets. The first observation between the two simulation types was that reducing the rainfall interval to 5 minutes, in catchment K3, increased the predicted runoff by approximately 190%. Therefore, simply reducing the simulation interval by 55 minutes almost tripled the amount of simulated surface runoff. This occurrence, once again, is probably due to the model's inability to fully integrate the effects of system losses such as evapotranspiration, infiltration and the replenishment of water stored in surface depressional areas.

Second, the travel time estimates that resulted from the simulation time step reduction failed to display a noticeable pattern. Reducing the simulation time step did not always result in a travel time increase. Nonetheless, in most cases, the travel time did increase to some degree. During the 5-, 50- and 100-yr return period storms, the travel time increased by 12.2%, 12.1% and 16.8%, respectively. The 10- and 25-yr results for travel time demonstrated slightly higher

increases of 113.8% and 24.1%, uniquely. On the other hand, at the 2-yr level the results reflected a 3.1% decrease in travel time. At the lower return period levels (i.e. 2- and 5-yr), one would suspect minimal flow constrictions since it was assumed that the stormwater system was designed to handle runoff amounts at this frequency. This assumption only remains valid during the time of initial construction and becomes questionable during land use changes, or if the system is not properly maintained. Therefore, little fluctuation should exist in the travel time estimates and small increases and/or decreases in the travel times seem reasonable. Once larger differences in travel time were reported, such as at the 10- and 25-yr levels, the systems flow routing capabilities become challenged. Pressure flow situations, overflowing banks and flow restriction are issues that probably exist at this simulation level. From the study, the 60-minute simulations handled excess flow better than the 5-minute simulations, but that is expected since the summation effect of additional outflow is reduced and the system has more time to recover.

Third, results from the travel time study for catchment K3 demonstrated more stability than those from catchment K2. During the 2- to 10-yr test levels, only subcatchments 9, 10, 11 and 15 had travel times greater than one hour. These subcatchments are located in the most remote portions of the catchment and are drained mainly by piped conduits. However, travel time was observed at the catchment outlet, so downstream interactions, such as overland flow in ephemeral channels, could increase the overall travel time for a pollutant. At the 25- to 100-yr rainfall level, subcatchments 16 and 21 increased their travel time values to greater than one hour during the 5-minute simulations. The 60-minute simulations failed to demonstrate the same increase at the 25- to 100-yr test levels for subcatchments 16 and 21 and remained fairly consistent throughout all simulated storm types.

Fourth, the travel times from both simulations, for catchment K3, can be categorized into two basic groups, 1) those travel time ranging between 0 and 20 minutes and 2) simulated travel times greater than one hour. Although some slight variation did occur during the study, this basic generalization holds true for the majority. In addition, the only occurrence of numerical instability occurred during the 100-yr storm level. Within subcatchments 9, 10 and 15, using a 60-minute simulation time step, the model was unable to calculate a numerical solution which fit the tolerance and iterative criteria.

## **E. Catchment K2 XPSWMM Travel Time Simulations using 5-minute Rainfall and Overflow Routing**

The final set of simulations completed at Cherry Point combined several changes that resulted in predictions that not only seemed numerical stable, but followed noticeable patterns across varying return storm periods. During the 5-minute rainfall simulations, one particular set of data generated results that failed to follow the travel time trends for catchment K2 (refer to Table 4.8). The 25-year storm, as associated with catchment K2, resulted in only four reasonable travel times for four respective subcatchments. Subcatchments 1, 2, 3, and 6 had predicted travel times of 0, 3, 1 and 4 minutes. All other travel time values for this return period storm were greater than 1 hour or oscillated about a series of values. Apparently, model predictions for transporting runoff downstream via the current routing system were in error.

The problem appeared to be that several pipe sections were retarding the release of runoff water and elongating the hydrograph peak. At first, the likely culprit seemed to be the 25-yr return period rainfall dataset; however, after scrutinizing the information, it was concluded that was not the problem. The next step involved checking the Manning roughness, and catchment width, but those parameters seemed reasonable. The next step involved understanding why the continuous simulations results from the RUNOFF module were not translating into more reasonable travel time predictions in the SANITARY block.

The first thought was that the runoff velocity was slowing to a point where the water soluble, pollutant was falling out of suspension. However, since the pollutant was inserted as 100% soluble, that hypothesis proved to be invalid. Second, it was believed that the RUNOFF block was having difficulties creating surface runoff at the 25-yr level. This theory was also rejected once the 25-yr XPSWMM project was recreated and rerun, yielding the same results. It was finally determined that the runoff amount were correct but the routing needed improvement.

The model nodes and routing elements were adapted from the field survey and topographic information. Only subsurface pipe conduits and larger open channels were modeled. Apparently, beginning with the 25-yr return period storm, the interaction of smaller surface channels was large enough to become influential. Runoff exiting subcatchments 11 and 15 now had a surface flow component that utilized shallow channels to convey overflow, once pipe sections reached capacity. Overflow element 111 was modeled as a trapezoidal, grassed channel, having no initial water depth, a maximum depth of 1 ft, and 10:1 side slopes. Overflow

element 115 is also a trapezoidal surface feature, with 12:1 side slopes, no initial water depth and an average depth of 2 ft. Incorporating these two surface flow elements now handled the excess runoff exiting two subcatchments, which in turn, improved the overall simulation results. Only two additional surface channels were introduced, in efforts to minimize their influence with the previous work completed. Figure 4.10 displays the application of an overflow routing element, for area 11, in catchment K2. The same technique was applied to area 15.

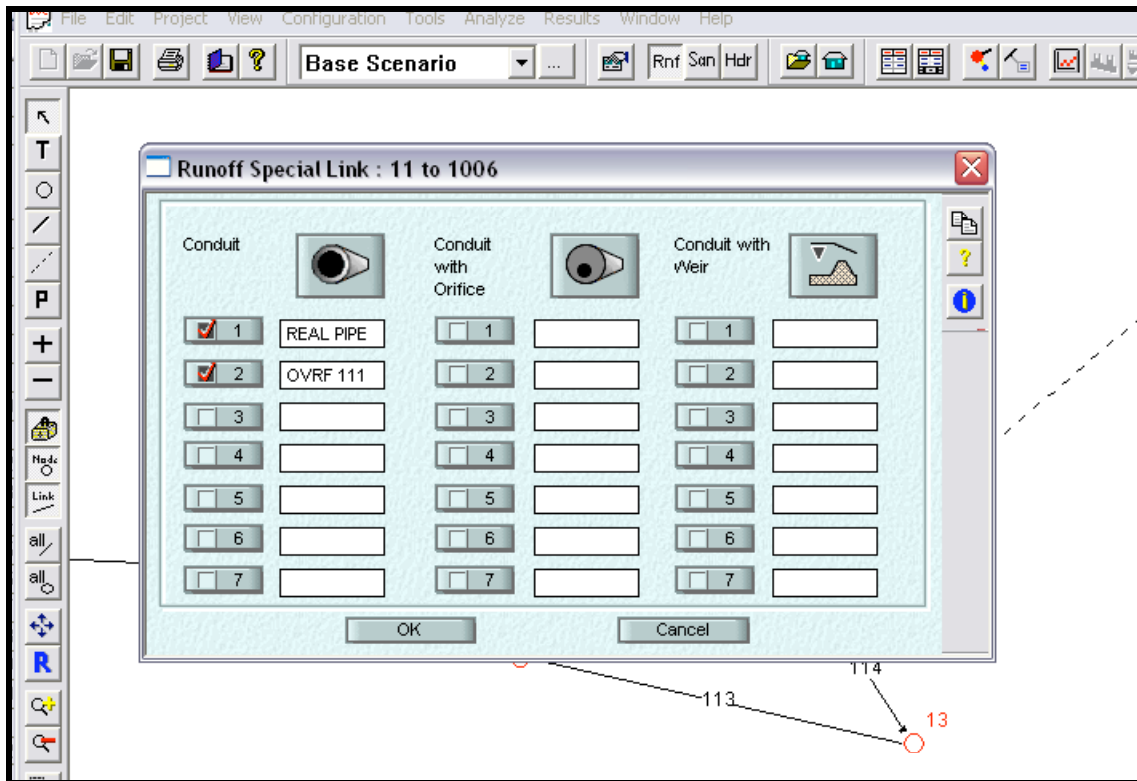


**Figure 4.10: SWMM Screenshot showing the Utilization of Overflow Element 111 in Catchment K2**

Table 4.10 presents the predicted outflow rates and associated travel times following the introduction of the overflow routing elements. Likewise, Table 4.11 displays the percentage change in predicted, peak outflow rate as compared to simulations not utilizing the overflow elements.

**Table 4.10: Catchment K2 Maximum, Predicted Outflow and Travel Time Estimates using 5-Minute Return Period Rainfall and Surface Overflow Routing Element**

Area												
	2 YR		5 YR		10 YR		25 YR		50 YR		100 YR	
	Peak Runoff Rate (CFS)	Travel time (min)	Peak Runoff Rate (CFS)	Travel time (min)	Peak Runoff Rate (CFS)	Travel time (min)	Peak Runoff Rate (CFS)	Travel time (min)	Peak Runoff Rate (CFS)	Travel time (min)	Peak Runoff Rate (CFS)	Travel time (min)
1	128.87	0	143.36	0	191.80	0	225.85	0	251.93	0	279.70	0
2	30.77	2	33.11	2	41.37	2	46.74	2	50.89	2	56.22	9
3	119.97	1	132.87	1	178.34	1	208.64	1	231.99	1	257.57	1
4	82.73	3	91.07	2	123.72	3	146.27	2	162.23	3	181.63	>1HR
5	84.35	13	93.04	11	125.86	11	148.79	>1HR	164.83	>1HR	184.55	>1HR
6	23.39	2	26.08	2	35.50	3	41.56	2	46.26	2	52.29	12
7	12.17	15	13.57	17	18.51	17	21.70	18	24.18	16	27.36	>1HR
8	8.16	16	9.09	17	12.36	17	14.46	17	16.09	15	18.18	>1HR
9	77.81	>1HR	86.52	>1HR	119.23	>1HR	143.69	>1HR	157.49	>1HR	177.60	>1HR
10	84.13	14	92.51	13	124.37	12	147.10	>1HR	162.36	>1HR	182.19	>1HR
11	9.99	>1HR	11.11	>1HR	15.00	>1HR	17.34	>1HR	19.47	>1HR	21.97	>1HR
12	26.97	>1HR	30.16	>1HR	41.40	>1HR	48.68	>1HR	54.32	>1HR	61.54	>1HR
13	50.26	>1HR	54.84	>1HR	72.71	>1HR	84.24	>1HR	93.42	>1HR	104.58	>1HR
14	74.91	>1HR	83.05	>1HR	112.52	>1HR	130.76	>1HR	142.16	>1HR	152.63	>1HR
15	71.09	>1HR	78.99	>1HR	107.74	>1HR	126.84	>1HR	141.75	>1HR	160.60	>1HR
16	22.10	>1HR	24.33	>1HR	32.44	>1HR	37.86	>1HR	42.10	>1HR	47.46	>1HR
17	19.38	>1HR	20.73	>1HR	25.71	>1HR	29.05	>1HR	31.67	>1HR	34.98	>1HR
18	22.90	>1HR	25.84	>1HR	36.56	>1HR	43.68	>1HR	49.25	>1HR	56.30	>1HR

**Table 4.11: Catchment K2 Percent Change in Predicted Peak Outflow Rate after Incorporating Two Overflow Elements**

Element Number	2 YR Peak Runoff Rate (CFS)	5 YR Peak Runoff Rate (CFS)	10 YR Peak Runoff Rate (CFS)	25 YR Peak Runoff Rate (CFS)	50 YR Peak Runoff Rate (CFS)	100 YR Peak Runoff Rate (CFS)
	% change	% change	% change	% change	% change	% change
1(outlet)	-5.2	-3.67	-4.0	-3.0	-1.9	-1.0
2	0.10	0.0	0.0	0.0	0.0	0.0
3	-4.3	-3.6	-2.9	-2.6	-1.4	-0.12
4	-0.06	2.1	8.8	16.2	20.1	23.8
5	0.04	2.6	9.4	17.2	22.1	25.4
6	0.00	0.0	0.0	0.0	0.0	0.0
7	0.16	0.07	-0.22	-0.41	-0.45	-0.58
8	0.0	0.0	0.0	0.00	0.0	0.0
9	0.76	2.1	5.4	8.9	7.9	8.7
10	0.19	2.4	8.2	17.2	23.8	26.2
11	0.0	0.0	-0.07	-1.0	0.0	0.0
12	0.0	0.0	0.0	0.0	0.0	0.0
13	10.0	9.9	9.5	9.1	9.2	9.5
14	36.3	39.3	46.3	48.7	49.1	48.3
15	0.0	-0.01	0.0	0.0	0.0	0.0
16	0.0	0.0	-0.03	0.0	0.0	0.0
17	0.0	0.0	0.0	0.0	0.0	0.0
18	0.0	0.0	0.0	0.0	0.0	0.0

The introduction of the overflow elements resulted in mixed outcomes on the maximum runoff generated at the subcatchment level. Theoretically, one would suspect that implementing additional routing element could introduce increased flow capacity and possibly introduce delays as related to longer conduits. However, with this study, runoff was only generated at the subcatchment level; therefore, the system runoff volume did not change with the introduction of the overflow components. Evaluating the percent change in simulated runoff in Table 4.11, yielded four basic observations: 1) increase in runoff, 2) decrease in runoff, 3) no change detected and 4) mixed results.

Increases in runoff following the addition of the overflow elements were observed in areas 5, 9, 10, 13 and 14. Area 14 yielded the highest increase in runoff, with a 49.1% change during the 50-yr return period rainfall input. Area 13 also displayed a fairly consistent increase in runoff across all storm types, ranging from 10.0%, at the 2-yr level, to 9.5% at the 100-year return period storm type. Areas 5, 9 and 10 all had gradually increasing runoff amounts directly

proportional to the year return period, eventually achieving maximum levels at the 100-year storm type. The maximum percent change increase in runoff for areas 5, 9, and 10 were 25.4%, 8.7% and 26.2%, respectively.

Only two areas demonstrated a decrease in runoff rate when the overflow elements were introduced into the XPSWMM simulations. The K2 catchment outlet, area 1, demonstrated the most negative response, reporting a 5.2% reduction in runoff at the 2-yr return period level. The remaining five storms, at the catchment outlet, also yielded negative changes in runoff, that ranged between -1.0% and -4.0%. Area 3 demonstrated a similar response to the overland elements as area 1, however, the runoff rates for area 3 gradually decreased as the rainfall return period increased. At the 2-yr level, a maximum decrease of 4.3% was reported for area 3 and the minimum value of -0.12% was received from the 100-yr rainfall data.

The most upstream areas of catchment K2, areas 15 through 18, demonstrated little (less than 0.03%) or no change in runoff volume when the overflow elements were added. This is expected seems they are located upstream on the inserted overflow channels. Likewise, areas 2, 6, 8, and 12 almost remained unchanged this time. A slight increase of 0.10% at the 2-yr return period level was reported for area 2.

The final collection of areas demonstrated a mixture of increasing and decreasing runoff rates as a result of including the overflow elements into the routing scheme. Area 11, which is directly connected to the overflow element 111, initially showed no changes at the 2- and 5-yr return period levels. However, during the 10- and 25-yr rainfall events, a slight decrease of 0.07% and 1.0% were observed. At the 50- and 100-yr return period levels, the results once again demonstrated no influence by the overflow element addition. Area 7 only had an increase in runoff during the 2-yr and 5-yr return period storms, with corresponding percentages of 0.16 and 0.07, respectively. At the 10-yr level, for area 7, a minimal decrease of 0.22% was generated and steadily increased negatively, reaching a maximum negative value of 0.58% at the 100-yr return period level. Area 4 probably demonstrated that most erratic behavior, as a result of the overflow element addition. At the 2-yr return period storm level, area 4 had a slight decrease of runoff, corresponding to a -0.06% change. However, for the remaining 5 storms, the change in runoff rate for area 4, increased from 2.1%, during the 5-yr return period storm, to a maximum value of 23.8% at the 100-yr rainfall event.

The most obvious reason to explain the changes in maximum, predicted runoff at the subcatchment level, due to the implementation of the overflow elements, is system capacity. Previously, outflow was being retarded because certain pipe sections were under pressure flow conditions. Once the overflow routing elements were introduced, the capacity, especially for routing elements 111 and 115 was increased, allowing most runoff to be transported onto downstream subcatchments. The occurrence now created a new situation. The new concern would be whether or not the downstream elements could handle the increased routed runoff from the element 111 and 115, in addition to the upstream elements whose flows were now able to pass freely through the increased capacity system. Interesting enough, a negative change in runoff, probably means that the downstream elements now fell into the same situation as elements 111 and 115, meaning they were either under pressure flow, or in overbank conditions. Although negative situations did occur, we believe that a -5.2% change in runoff is an acceptable level. Likewise for the opposite, an increase in runoff probably meant that runoff was being routed more efficiently through the system and that the system was able to accommodate that added capacity. More interesting than the maximum runoff rate at the subcatchment level is the timing of the peak and its interaction with the travel time. Table 4.12 displays the changes in travel time as associated with the introduction of the overflow elements at areas 111 and 115.

**Table 4.12: Catchment K2 Percent Change in Estimated Travel Time after Incorporating Two Overflow Routing Elements**

Element Number	2 YR Travel Time (min)	5 YR Travel Time (min)	10 YR Travel Time (min)	25 YR Travel Time (min)	50 YR Travel Time (min)	100 YR Travel Time (min)
	% change	% change	% change	% change	% change	% change
<b>1(outlet)</b>	0.0	0.0	0.0	0.0	0.0	0.0
<b>2</b>	0.0	0.0	0.0	-50.0	0.0	77.8
<b>3</b>	0.0	0.0	0.0	0.0	0.0	0.0
<b>4</b>	0.00	-50.0	0.0	N/A	33.3	N/A
<b>5</b>	7.7	-9.1	0.0	0.0	N/A	N/A
<b>6</b>	0.0	0.0	0.0	-100.0	0.0	75.0
<b>7</b>	-6.7	5.9	5.9	N/A	0.0	N/A
<b>8</b>	0.0	5.9	0.0	N/A	0.0	N/A
<b>9</b>	0.0	0.0	0.0	0.0	0.0	0.0
<b>10</b>	7.1	0.0	0.0	0.0	N/A	N/A
<b>11</b>	0.0	0.0	0.0	0.0	0.0	N/A
<b>12</b>	0.0	0.0	0.0	0.0	0.0	0.0
<b>13</b>	0.0	0.0	0.0	0.0	0.0	N/A
<b>14</b>	0.0	0.0	0.0	0.0	0.0	N/A
<b>15</b>	0.0	0.0	0.0	0.0	0.0	0.0
<b>16</b>	0.0	0.0	0.0	0.0	0.0	0.0
<b>17</b>	0.0	0.0	0.0	0.0	0.0	0.0
<b>18</b>	0.0	0.0	0.0	0.0	0.0	0.0

Note: The not applicable value (N/A) was generated when unequal units of time were compared (i.e. inequalities versus a numerical value).

A majority of the calculated travel times, using the pulse tracers, remained unaffected when the overflow elements were added into the routing scheme in catchment K2. The purpose of inserting the overflow components was to assist in the movement of excess runoff downstream using the existing routing elements.

8 out of the 19 areas (subcatchments 1, 3, 9, 12, 15, 16, 17, 18) displayed neither an increase nor decrease in travel time when the overflow elements were added. Most importantly, area 1 is the K2 catchment outlet, so the changes in peak runoff discussed in the preceding sections had minimal effects on the travel time estimates. An additional three areas, subcatchments 11, 13 and 14, were almost uniform in reflecting no change in time as well, except at the 100-yr return period level. During the 100-yr rainfall event, oscillations in numerical convergence prevented the calculation of a single peak runoff rate. Areas 8 and 10 reflected

increases in travel time. Subcatchment 8 reported a 5.9% increased in travel time during the 5-yr rainfall event. Likewise area 10 yielded a 7.1% increase in observed travel time at the 2-yr return period level. The remaining five areas produced results that showed both signs of increase and decrease in travel times.

Subcatchment 2 had no change in travel time during the 2-, 5-, 10- and 50-yr return period events. However, this same area displayed a 50.0% decrease in travel time during the 25-yr rainfall event and reported a 77.8% increase in travel time for the 100-yr return period data. Area 6 also demonstrated similar results, presenting a decrease and increase pattern during the same two return periods. The associated percent changes for area 6 were, -100.0% and 75.0%, respectively. Area 4 had varying results as well. At the 5-yr rainfall return period level, the travel time for area 4 was decreased by 50.0%, while an increase of 33.3% occurred during the 50-yr rainfall level. The remaining storms for area 4 either displayed no change or the change was immeasurable. A 7.7% increase in travel time was simulated for area 5 during the 2-yr return period storm, and a negative 9.1% change was calculated using the 5-yr rainfall data. The remaining four travel times, for area 5, displayed no charge or yielded inconclusive results. Area 7 demonstrated the most sporadic results. At the 2-yr rainfall level, a negative 6.7% change was simulated. During the 5-yr and 10-yr return periods, for area 7, a 5.9% increase in travel time was calculated. The 25- and 100-yr storm events, for area 7, yielded inclusive results, while the 50-yr storm data resulted in no travel time change.

The purpose of the study is to use the combination of the peak runoff and pulse tracers, to simulate the movement of soluble pollutants via surface water. Therefore, the travel time analysis is one of the most important observations. The introduction of the overflow elements seemed to have minimal effects on the travel times, with some exceptions. The exceptions included scenarios when the travel time either increase or decreased. A 10%, positive or negative, change in travel time seems fairly reasonable. Likewise, the conclusive results were accepted, since the refined routing system was not calculating a value, which previously had problems reaching a numerically stable solution. However changes in magnitudes, ranging between 50% and 100%, needed further explanation.

At first glimpse, a 50% or 100% change in travel time seems unrealistic until the corresponding numbers are revealed. For example, the 50.0% decrease in travel time for area 4, at the 5-yr return period scenario, is associated in a travel time reduction from 3 to 2 minutes. In

fact, the difference in travel times between all of these situations only varied between 1 and 7 minutes.

The final process of this study was to transfer the updated travel time values into ArcMAP, for visual recognition, in quantifying, and displaying spatially, response times provided any given amount of rainfall and a specified duration.

#### **F. Inserting XPSWMM results into ArcMAP**

All simulations for various rainfall return periods were completed in XPSWMM with the GIS module. Although XPSWMM advertised the GIS functionality of exporting aspects of the simulations results into a GIS package, we were not successful in correctly forming the linkage. Therefore, the simulation results were manually correlated and inserted in ArcMAP to display the relative response times corresponding to storms with varying return periods. Response time intervals were created and a unique coloring scheme was developed (see Figure 4.11). By viewing the GIS maps, with spatial distribution of simulated travel times, the Cherry Point officials would be able to determine the amount of time required for a water-soluble pollutant exiting any subcatchment to reach the catchment outlet. Appendix 4E contains additional GIS maps created from the pulse tracer investigation.

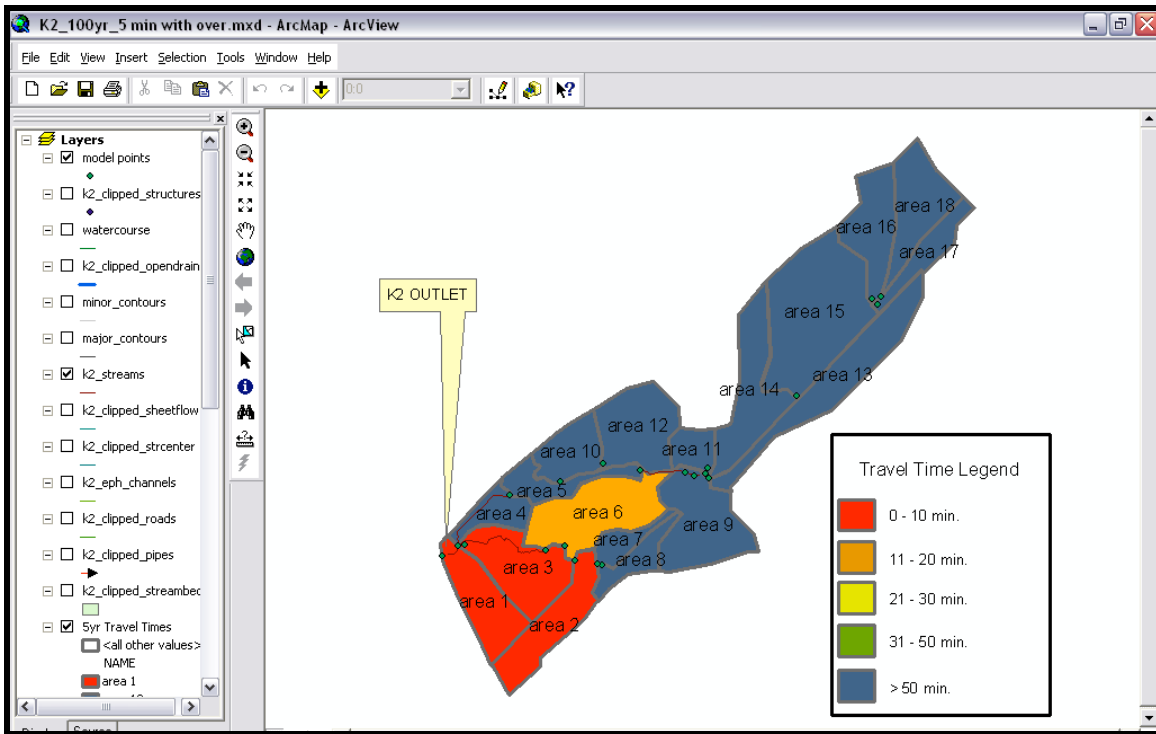


**Figure 4.11: Catchment K2 100-yr Return Period Travel Time Map including Overland Flow Elements.**

#### **IV. Summary, Conclusions and Recommendations**

##### **A. Overall Travel Time Comments and Limitations**

Recall that it is difficult to attribute a specific change in flow to a certain rainfall event (Bowers & Dimberger, 2000). Thus, several important assumptions were made in calculating (modeling) travel times. First, the modeler assumes that the pollutant is water-soluble or at least that water is capable of transporting the materials. Materials that possess decaying properties or altering physical characteristics would not demonstrate the intended transport functions. Adhesion to clay particles or the concrete pipes or non-buoyant substances are three examples. Second, the modeler assumes that each pollutant enters the stream at a specific location at a single point in time. This is probably incorrect; unless the contaminant was instantaneously poured directly into the channel. Some time elapses between the time of spillage and the time the pollutant enters the water. Also, the pollutant may become less concentrated as it travels towards the main channel because of downward seepage, dilution, storage, adsorption and

possible plant uptake. Third, the modeler considers only uniform flow throughout the entire flow regime. This is an oversimplification of the natural system, since pools, wetlands, and other flow retardants, are present within the stream and it is understood that water flows at varying velocities. Water located near the center of the channel has a higher flow rate than water located near the edge due to friction and tension forces. Fourth, the calculated travel time, based on peak flow rates, would represent the shortest amount of time needed for the substance to reach the outlet under ideal conditions. For example, the peak discharge rate is sustained for a few minutes, a rather short time span, when compared to the entire storm duration. Even the inserted return periods had durations lasting 24 hours, with the majority of the rainfall concentrated into a 2-hour time span. Temporary flow surges from tributary inflow and fluctuations in rainfall would alter the actual travel time to some degree. Fifth, the last major assumption made was that all underground, routing elements retained a constant shape throughout their length. All pipe size measurements were obtained by querying measured headwalls at entry and exit points within the GIS. If a headwall was not present at the point of interest, the next attributed upstream headwall's information was used. Therefore, from the headwall providing the information to the outlet point, it was assumed that the pipe maintained a constant diameter. Likewise, for streams, most measurements were made near the outlet of the stream element. The calculated and observed parameters for each stream section were attributed assuming that the entire stream element demonstrated similar geometry.

There is more confidence pertaining to the model's ability to estimate the routing element time of travel as compared to the time predictions associated with overland flow within the subcatchments. One reason for the difference is the fact that the subcatchment did not receive as much attention during the field surveys as the streams and pipes. The survey crew was not aware of the eventual catchment discretization that would occur, nor did the individual subcatchment boundaries physically exist (they are purely conceptual). Likewise, the travel time equation for the catchments is sensitive to channel measurements. For example, the calculated travel times are proportional to some channel measurements, such as length. For Cherry Point, the survey consultant provided a range of values to describe channel top width, bottom width, and depth. The channel length was measured in ArcMAP.

Routing element travel time estimates are probably more accurate because SWMM is structured as an urban, stormwater runoff-modeling program. Once the input data are in the correct format, the program runs algorithms to eventually route runoff generated from subcatchments to some designated outlet. The process of the runoff reaching the catchment

outlet relies upon the limitations of the user-selected routing method. For Cherry Point, surface runoff was modeled using the linear reservoir technique. There were not many situations where flow is routed through another catchment; therefore, the stream/pipe network is basically independent of catchment interference. Upon reaching a stream or pipe, the flow is routed, adhering to element parameters, such as conduit dimensions, slope and Manning's roughness coefficient. The measurements for the streams, and pipe sizes, were based on the field survey information as inputted into the GIS. It is easy to quantify pipe sizes and channel attributes for a routing element, as opposed to explaining the surface runoff processes involved as water travels, as overland runoff, towards the catchment outlet.

## **B. XPSWMM Time Travel Discussion and Concerns**

In theory, as the return period storm size (amount of rainfall produced) increases, the travel time required for the tracer to reach the outlet should decrease given that the flow rate increases within limits. It was discovered that flow relates inversely to concentration. As expected, the travel times decreased as the return period storm size increased in most cases. Occasionally, XPSWMM predicted travel times that increased when the return period increased, although the resulting time difference had only a magnitude of several minutes. Other situations occurred where the travel time neither increased nor decreased for the various storms. Usually when no change in travel time occurred two situations prevailed, 1) the subcatchment was the catchment outlet point, or 2) the subcatchment generated small outflows.

Another concern regarding the travel time analysis was water retention. XPSWMM was only provided sufficient information to complete basic simulations. More challenging attributes pertaining to the conduit systems and the nature of the imaginary tracers were not included, and not all inputs were known or measured. In certain cases, the model would generate warning messages, stating that certain aspects of the simulation did not seem correct (i.e. underground culvert size, conduit slopes and inverts). It is also suspected that since accurate conduit size information was not measured during the GPS survey that potential water movement was retarded in smaller pipes. In catchment K2, a large wetland was retaining and slowly releasing water, which was not apparent in the observed data. To combat this issue, the modeling technique involving simulating a wetland as a storage unit was abandoned and replaced by the actual physical measurements.

In some instances XPSWMM had difficulty reaching a convergence point. The Sanitary Block allows the user to specify the number of iterations and a numerical tolerance associated with solving the iterative, convergence equation. The default settings for the number of iterations and the convergence criteria are 4.0 and 0.001 (dimensionless), respectively. During the travel time analysis, both the number of iterations and the tolerance were adjusted to see how the model responded. When the number of iterations was increased, the model had difficulty reaching numerical stability. Therefore, it was difficult to extract a maximum point and time value since the results oscillated about a given time period never reaching a distinct peak. Likewise, increasing the convergence tolerance level altered the results to the point where determining the maximum tracer concentration was ambiguous. The default values were then replaced. One option that increased the precision of the XPSWMM was the simulation time step. Having the model print each time step greatly improved the capability of extracting needed information. Also, the initial travel time simulations were completed using a 120-second time step. By the conclusion of the study, a 60-second time step was preferred and the 5-minute rainfall data were inserted into the Runoff Block that yielded desirable outputs that were presented earlier.

### **C. Summary and Conclusions**

The purpose of the Cherry Point study was to characterize the study area with spatial catchment attributes, collect rainfall data, calibrate/validate a rainfall runoff simulation model (SWMM) and use the model to estimate soluble, pollutant transport travel time via surface water. In order to complete the travel time portion of the objectives several other areas needed to be addressed and completed. First, the Runoff Block was used to generate the maximum outflow for the routing elements. Variables and parameters were assigned in the Runoff Block that would ultimately affect the performance of SWMM and XPSWMM in estimating travel times. Very little information was gathered about the impervious area, especially the wetland areas in catchment K2, where the occurrence of surface depressional storage became an important factor in the water balance. In addition, some of the values inserted into the Runoff Block were simplified due to a lack of collected data.

A compromise of complexity and utility resulted in conceptualizing the study area into unique, manageable subcatchments while implementing a functional routing scenario for surface runoff. The underground piping system was not attributed and only exposed headwalls were

used to determine pipe sizing. The linear reservoir method was selected as the primary routing technique. Runoff was assumed to only occur at the upstream portion of the link, and was equally distributed along the entire element. Therefore, to simulate better flow routing, additional channels or pipes would be required (Conversely, the introduction of additional drainage elements may add unwanted storage and delay the hydrograph peaks). The model predicted outflows were calculated by Manning's flow equation, and become instantaneous inflow at the end of each time step. By shortening the time step, the overall losses were minimized which reduced the occurrence of a zero net water situation. Thus, inserting historically derived rainfall data for various return periods, for the specific region, the best normalized storm situations were routed during the travel time investigations.

The tracer study utilized the functionality of the SANITARY Block to route and track pollutant movement using the simulation results from the runoff analysis. The objective of the pulse tracer study was to insert a surrogate, non-decaying, highly soluble substance into the runoff waters, and to track its downstream progression. A single tracer, having a maximum concentration of 100 units, was inserted during the occurrence of the peak runoff rate. Ideally, hydraulic tracers should be inexpensive, having low adsorption rates to most soil particulates and minimal decay. The imaginary tracers used in the Cherry Point study had no decay rates. Unfortunately chemicals decay, especially in direct sunlight, therefore, the decay process and other complex processes were not considered during the tracer study. This over-simplification may have caused the travel times calculated to be somewhat less than actual travel times for some pollutants, but, in terms of developing methods for responses to spills, the error would be on the safe side.

#### **D. Suggestions**

Model predictions are only as good as the data used to create the simulations, and simulations cannot replicate natural conditions perfectly. Acknowledging the limitations of the results presented based on input data uncertainty, the XPSWMM predicted trends in stormwater runoff patterns and relative magnitudes. Following the calibration and validation processes completed for this study, the SWMM outflow estimates are the best predictions given the limitations of the input data. The travel time estimates are somewhat simplistic since basic dispersion assumptions were followed, meaning the tracers were considered to be completely soluble in water and their movement was restricted to follow the movement of the runoff waters

within the subsurface pipes and streams only, and chemical transformations were neglected. Nonetheless, the predicted travel times, using the peak outflow rates, should provide the Cherry Point officials a basic, conservative, response time window for the operation and management of flow control gates. If more accurate estimates of travel time are desired, a detailed flow analysis is recommended using detailed hydraulic parameters of the entire drainage system.

Chapter Three comments on the stormwater modeling process as a whole, including understanding what information is required to optimize the simulations for the study site. The GIS and field data were collected in efforts to simply characterize the current surface water conduits and the current water quantity at Cherry Point as a requirement for NPDES permitting. The consultant was unaware at the time of execution that the attributed information would be applied to a stormwater management model to predict pollutant movement. If the modeling intent had been known at the time of data collection, then possibly better attributes could have been provided for the subsurface conduits, including verifying all pipe sizes and inverts, and thoroughly examining the surface water conditions. However, the Cherry Point project progressed with the available information (as an adaptive management approach), making assumptions when needed, to provide the best results possible, using a calibrated and validated XPSWMM.

#### **E. Our Contribution and Recommendations for Future Work**

The overall research intent was multiple faceted. The goal was to deliver the Environmental Affairs Department at Cherry Point Marine Corps Air Station with a functioning hydrologic and hydraulic model that they could utilize to assess the amount of time required to respond to accidental spills that entered surface waters on the study area. The research study was restricted to the industrialized portion of the air station, and was further refined to include only two catchments. Based upon the field data and GIS map creations, the watersheds draining the industrial area were dissected into smaller catchments and eventually subcatchments. Flow monitoring devices were installed and the rainfall data was collected for an excess of two years. The observed hydrographs were created from the measured flow data, which were then simulated using lumped parameters models and checked before the EPA's Stormwater Management Model (SWMM) was ever introduced. Following the addition of SWMM, the first event-based simulations were created, eventually progressing from single events to the continuous simulations completed by XPSWMM. The continuous simulations opened the gateway to use design storms, with varying return periods, and a combination of the Runoff and

Sanitary Blocks for the creation and routing of imaginary tracers. The tracers then became inputs to the model, as water-soluble pollutants, that allowed the generation of travel time estimates for all subcatchments.

The pulse tracers now provided the air station with travel time estimates in a distinct section of the air station. Since the tracers were attached to particular subcatchments the travel times are related to spills leaving only particular subcatchment outlets and are not capable of estimating travel times at other points within the subcatchment. Likewise, the travel times associated with the routing elements are only useful at the most downstream point because XPSWMM distributes flows along the entire reach element.

Nonetheless, we believe that we have achieved the research goal in developing a technology that uses a GIS database and tools to parameterize the widely used EPA stormwater management model (SWMM), and then use the model predictions to estimate pollutant travel times. Generalized, highly soluble, pollutants were simulated, but specific substances could be inserted. This research helped develop an application displaying the options of combining a GIS tool with a water quantity/quality model effectively. Our contribution to the scientific community is that we developed a useable combination that does predict travel times, including the complete hydrographs, and pollutographs, resulting from various storm events, and the output is viewable in a GIS package. As research in this area continues, the linkage between the two applications will allow easier database information, such that a majority of the work will be automated, in a bi-directional format.

## REFERENCES CITED

- Amatya, D.M. and R.W. Skaggs. 2001. Hydrologic modeling of pine plantations on poorly drained soils. *Forest Science* 47(1): 103-114.
- Amatya, D.M. 1985. *Statistical Evaluation of Parameters in Deterministic Water Quality Modeling*. M.S. Thesis. Duke University, Durham, N.C. (unpublished)
- ASCE, 1996. *Hydrology Handbook, 2<sup>nd</sup> Edition*. ASCE Manuals and Reports on Engineering Practice, Number 28, American Society of Civil Engineers, New York, NY.
- Barber, J.L., K.L. Lage, and P.T. Carolan. 1994. *Stormwater Management and Modeling Integrating SWMM and GIS*. Urban and Regional Information Association, 5, 310.
- Bendient, P.B. and W.C. Huber. 1988. *Hydrology and Floodplain Analysis*. Addison-Wesley Publishing Company, New York, NY.
- Berry, J.K. 1994. *What Does Your Computer Really Think of Your Map*. *GIS World*, 7(11), pp. 30.
- Bowers, R. and J.M. Dirnberger. 2000. *Using Temporal Changes in Water Quality in Noonday Creek to Describe Pollutant Transport and Pinpoint Sources*. National Water Quality Monitoring Council, 2000 Conference Proceedings.  
[http://www.nwqmc.org/2000proceeding/papers/pap\\_bowers.pdf](http://www.nwqmc.org/2000proceeding/papers/pap_bowers.pdf)
- Brakensiek, D.L. and C.A. Onstad. 1977. *Parameter Estimation of the Green-Ampt Equations*. *Water Resources Research*, Vol 13, No. 6, December 1977. Paper no. 10091012.
- Brater, E.F., H.W. King, J.E. Lindell and C.Y. Wei. 1996. *Handbook of Hydraulics for the Solution of Hydraulic Engineering Problems, Seventh Edition*, pp. 5.15-5.21
- Chow, V.T. 1959. *Open Channel Hydraulics*. McGraw-Hill: New York, pp. 101-112.
- City of Novi, Michigan. 2001. GIS/Public Awareness Project. As published in the Wayne County Rouge River National Wet Weather Demonstration Project.
- Computer Online Dictionary, 2004. <http://www.computer-dictionary-online.org/>
- Department of Irrigation and Drainage Malaysia. 2001. *Urban Stormwater Management Manual for Malaysia*. <http://agrolink.moa.my/did/river/stormwater>
- Dueker, K.J. 1987. *Geographic Information Systems and Computer-Aided Mapping*. *APA Journal*, Summer, pp: 383-390.
- EPA Victoria. 2005. *Victoria's Water Environment – Urban Stormwater Management Plans*. [http://www.epa.vic.gov.au/Water/Programs/stormwater\\_management.asp](http://www.epa.vic.gov.au/Water/Programs/stormwater_management.asp)
- Fisher, G.T. 1989. *Geographic Information System/Watershed Model Interface*. Proceedings from the 1989 National Conference on Hydraulic Engineering, ASCE, Hydraulics Division, New Orleans, Louisiana, pp. 851-856.
- Fortner, S.H. and D.S. White. 1988. *Interstitial Water Patterns: A Factor Influencing the Distributions of some Lotic Aquatic Vascular Macrophytes*. *Aquatic Botany*, 31: 1-12.

## REFERENCES - CONTINUED

- Garbrecht, J., F.L. Ogden, P.A. DeBarry and D.R. Maidment. 2001. *GIS and Watershed Models: Data Coverages and Sources*. Journal of Hydrologic Engineering, ASCE, November/December.
- Goudie, Andrew. 2000. *The Human Impact on the Natural Environment, Fifth Edition*. pp 253-238.
- Haan, C.T. 1977. *Statistical Methods in Hydrology*. The Iowa State University Press.
- Hetling, L.J. and R.L. O'Connell. 1966. *A Study of Tidal Dispersion in the Potomac River*. Water Resources Research, v. 2, no. 4, p.825-841.
- Hillel, D. 1998. *Environmental Soil Physics*. Academic Press: New York, pp. 118, 183-185.
- Hoffman, Russell D. 2002. *The Statistic Z from the Internet Glossary of Statistical Terms*. [http://www.animatedsoftware.com/statglos/sgstat\\_z.htm](http://www.animatedsoftware.com/statglos/sgstat_z.htm).
- Huber W., R. E. Dickinson and W. R. C. James. (1999) *Hydrology: A Guide to the Rain, Temperature and Runoff Modules of the USEPA SWMM4*. Based on the U.S. EPA SWMM4 User's Manual.
- Hydrologic Engineering Center (HEC), 2001. *U.S. Army Corps of Engineers, Hydrologic Modeling System HEC-HMS User's Manual, Version 2.1*.
- Jameson, A.R. and A.B. Konstinski. 1999. *Fluctuation Properties of Precipitation. Part V: Distribution of Rain Rates—Theory and Observations in Clustered Rain*. American Metrological Society Journal of the Atmospheric Sciences. Volume 56, Issue 22: pp. 3920-3932.
- Jobson, H.E. 1996. *Prediction of Traveltime and Longitudinal Dispersion in Rivers and Streams*. U.S. Geological Survey, Water Resources Investigations Report 96-4013.
- Korte, G.B. 1994. *GIS Book*. Third Edition, Onword Press, Santa Fe, New Mexico. pp.213
- Lee, K.T. and B.C. Yen. 1997. *Geomorphology and Kinematic-wave-based Hydrograph Derivation*. Journal of Hydraulic Engineering, 123 (1): 73-80.
- Legates, D.R. and R.E. Davis. 1997. *The Continuing Search for an Anthropogenic Climate Change Signal: Limitations of Correlation-based Approaches*. Geophysical Research Letters, Vol. 24, pp. 2319-2322.
- Legates, D.R. and G.J. McCabe. 1999. *Evaluating the Use of "Goodness-of-Fit" Measures in Hydrologic and Hydroclimatic Model Validation*. Water Resources Research, Vol. 35, no. 1, pp. 233-241, January 1999.
- Leopold, L.B., M.G. Wolman, and J.P. Miller. 1992. *Fluvial Processes in Geomorphology*. Dover Publications, Inc., New York.
- LMNO Engineering. 1998. *Manning's N Values*. [www.lmnoeng.com/manningn.htm](http://www.lmnoeng.com/manningn.htm)

## REFERENCES - CONTINUED

- Loague, K.M. and R.E. Green. 1991. *Statistical and Graphical Methods for Evaluating Solute Transport Models: Overview and Application*. Journal of Contaminant Hydrology, 7, 51.
- Lutz, D. 2003. *Take Advantage of that Spatial Database: Users should know their data resources, needs and expectations to maximize the benefits of an enterprise wide resource*. [www.geoplace.com/gw/2000/0008/0800es.asp](http://www.geoplace.com/gw/2000/0008/0800es.asp).
- Maidment, D.R. 1996. *GIS and Hydrologic Modeling – an Assessment of Progress*. The Third International Conference on GIS and Environmental Modeling, January 22-26.
- MCAS-Cherry Point, Office of Public Affairs, 2005. <http://www.cherrypoint.usmc.mil/>
- McCuen, R.H. and W.M. Snyder. 1975. *A Proposed Index for Comparing Hydrographs*. Water Resources Research, Vol. 11, no.6, December 1975.
- McCuen, R.H. and W.M. Snyder. 1986. *Hydrologic Modeling: Statistical Methods and Applications*. Prentice-Hall: New Jersey.
- McCuen, R.H. 1997. *Hydrologic Analysis and Design, 2<sup>nd</sup> Edition*. Prentice Hall.
- Medina, 2002. *Laboratory Exercise No. 2 - Synoptic Precipitation Analysis, CE 123: Water Resources Engineering*. Duke University. <http://ceeweb.egr.duke.edu/~medina/CE123/ce123.lb2.pdf>
- Meijerink A.M., H.A. de Bouwer, C.M. Mannaerts and C.R. Valenzuela. 1994. *Introduction to the use of Geographic Information Systems for Practical Hydrology*. International Institute for Aerospace Survey and Earth Sciences, Publication no. 23.
- Meybeck, M. 1979. *Concentration des eaux fluviales en elements majeurs et apports en solution aux ocean*. Revue de geographie physique et geologie dynamique, 21a, 215-46.
- Miller, S.N., J.J. Stone, J.G. Martinez and D.P. Guertin. 1999. *Influence of GIS-Based Watershed Characterization on the Prediction of Runoff from Southwest Rangelands*. Proceedings from the 1999 Annual Summer Specialty Conference, AWRA, Bozeman, Montana.
- Moriasi, D.N., J.G. Arnold, M.W. Van Liew, R.L. Bingner, R.D. Harmel, and T.L. Veith. 2007. *Model evaluation guidelines for systematic quantification of accuracy in watershed simulations*. Transactions of ASABE. 50(3):885-900.
- Nolan, K.M. and B.R. Hill. 1990. *Storm-runoff Generation in the Permanente Creek Drainage Basin, West Central California-an example of Flood-wave Effects on Runoff Composition*. Journal of Hydrology, 113: 343-367.
- North Carolina Department of Environment and Natural Resources (NCDENR), 2002. Division of Water Quality. <http://h2o.enr.state.nc.us/index.html>
- Novotny, V. and H. Olem. 1993. *Water Quality: Prevention, Identification, and Management of Diffuse Pollution*. John Wiley & Sons, Inc.
- Peierls, B. L., N.F. Caraco, M.L. Pace and J.J. Cole. 1991. *Human Influence on River Nitrogen*. Nature, 350, 386.

## REFERENCES - CONTINUED

- Pickford, J.A. 1969. *Analysis of Water Surge*. Gordon and Breach Science Publishers, New York.
- Piowar, J.M. and E.F. LeDrew. 1990. *Integrating Spatial Data. A User's Perspective*, Photogrammetric Engineering and Remote Sensing, 56(11):1497-1502.
- Reed, L.A. and M.H. Stuckey. 2002. *Prediction of Velocities for a Range of Streamflow Condition in Pennsylvania*. U.S. Geological Survey, Water Resources Investigations Report 01-4214.
- Rossman, Lewis. 2005. Wet Weather Flow Research: Storm Water Management Model Redevelopment Project. [www.epa.gov/ednrmrl/swmm/index.htm](http://www.epa.gov/ednrmrl/swmm/index.htm)
- Runkel, R.L., D.M. McKnight, E.D. Andrews. 1998. *Analysis of Transient Storage Subject to Unsteady Flow and Flow Variation in an Antarctic Stream*. Journal of North American Benthologic Society, 17 (2): 143-154.
- Russel, M.H., R.J. Layton, and P.M. Tillotson. 1994. *The Use of Pesticide Models in a Regulatory Setting: an Industrial Perspective*. Journal of Environmental Science and Health, A29 (6), 1105.
- Schwab, G.O., R.K. Frevert, W. J. Elliot, D. D. Fangmeier. 1992. *Soil and Water Conservation Engineering, 4<sup>th</sup> Edition*. John Wiley & Sons, Inc.
- Scott, C.H., V.W. Norman, and F.K. Fields. 1969. *Reduction of Fluorescence of Two Tracer Dyes by contact with a Fine Sediment*. Geological Research, 1969: U.S. Geological Survey Professional Paper 650-B, p. B164-B168.
- Shapiro, S. S. and M. B. Wilk. 1965. *An analysis of variance test for normality (complete samples)*, Biometrika, 52, 3 and 4, pages 591-611.
- Sheridan, J.M., 1994. *Hydrograph Time Parameters for Flatland Watersheds*. 1994. Transactions of the ASAE, 37 (1): 103-113.
- Shimohammadi, A. and H. Montas. 2002. *Using Hydrologic and Water Quality Models Beyond Their Boundaries*. Proceedings of the American Society for Engineering in Agricultural, Food and Biological Systems, Chicago, Illinois, July 28-31, 2002. ASAE paper no. 022090.
- Simanek, D. 2002. [www.1hup.edu/~dsimanek/logic.htm](http://www.1hup.edu/~dsimanek/logic.htm)
- Smith, M.D. 1998. *Newton-Raphson Technique*. [web.mit.edu/10.001/web/course\\_notes/nlae/node6.html](http://web.mit.edu/10.001/web/course_notes/nlae/node6.html)
- Sontek. 2005. *Ocean Principles of Operation*. <http://www.sontek.com/princop/advo/advopo.htm>
- Stephens, M. A. 1974. *EDF Statistics for Goodness of Fit and Some Comparisons*, Journal of the American Statistical Association, Vol. 69, pp. 730-737.

## REFERENCES - CONTINUED

- Tai, D.Y. and R.E. Rathburn. 1988. *Photoanalysis of Rhodamine-WT dye*: Chemosphere, v.17, no.3, pp. 559-573.
- Taylor, R.B. 2005. *Stormwater Management*.  
[http://hazenandsawyer.com/services/services\\_sm.htm](http://hazenandsawyer.com/services/services_sm.htm)
- Tim, U. Sunday. 1995. *Emerging Issues in Hydrology and Water Quality Modeling*. ASAE International Symposium proceedings, April 2-5, 1995, Orlando, Florida. ASAE publication 5-95, pp. 358-373.
- Tyler, E.L. 1992. *Re-Authorization of the Clean Water Act*, The Universities Council on Water Resources, Water Resources update, Spring 1992. Issue No.88, pp:7-15.
- U.S. Department of Agriculture-Natural Resources Conservation Service. 2002. *Detailed County Soils - Craven County*, North Carolina.
- U.S. Geological Survey. 1987. *Magnitude and Frequency of Floods in Rural and Urban Basins of North Carolina*. USGS Water Resources Inventory Report 87-4096, Raleigh, NC.
- U.S. Environmental Protection Agency. 2005. *Handbook for Developing Watershed Plans to Restore and Protect Our Waters (Draft)*, Chapter 8: Estimate Pollutant Loads.
- Warwick, J.J. and P. Tadepalli. 1991. *Efficacy of SWMM Application*. Journal of Water Resources Planning and Management, Vol. 117, No.3, May/June 1991. ASCE paper no. 25819.
- Willmott, C.J. 1981. *On the Validation of Models*. Physical Geography v 2, n 2, pp. 184-194.
- Woolhiser, D.A. and D.L. Brakensiek. 1982. *Hydrologic System Synthesis*. In: Haan, C.T., H.P. Johnson, and D.L. Brakensiek (eds.) Hydrologic Modeling of Small Watershed. ASAE Nomograph Number 5, publish by Am. Soc. Of Ag. Eng, 3.
- XP Software, 2003. [www.xpsoftware.com/products/xpswmm/htm](http://www.xpsoftware.com/products/xpswmm/htm).
- XP Software, 2005. XP-SWMM Reference Manual.
- Yoon, J. and G. Padmanabhan. 1995. *Multiobjective Agricultural Nonpoint Source Pollution Management on Water Quality*. Proceedings in Soil Conservation and Water Quality Symposium, the Minnesota Academy of Science, Morris, Minnesota, April 27-28.
- Yoon, Jaewan. *Watershed-Scale Nonpoint Source Pollution Modeling and Decision Support System Based on a Model-GIS-RDBMS Linkage*. American Water Resources Association. AWRA Symposium on GIS and Water Resources, Ft. Lauderdale, Florida, Sept 22-26, 1996.

## APPENDICES

## Chapter Two Appendix

## Appendix 2: Additional Chapter Two Exhibits

This section contains the tables and figures referenced in the body text of Chapter Two.

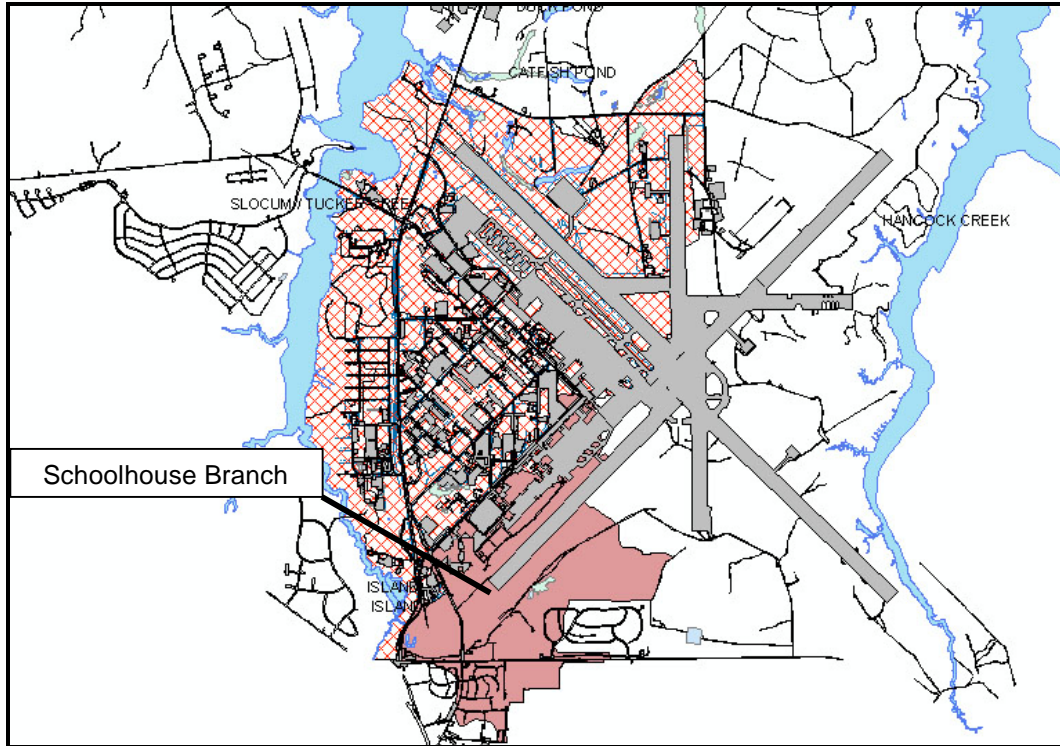


**Exhibit 2.1: Schoolhouse Branch Watershed.** The Schoolhouse Branch is located at the southern region of the airstation and is drained by a culvert that empties into Slocum Creek.

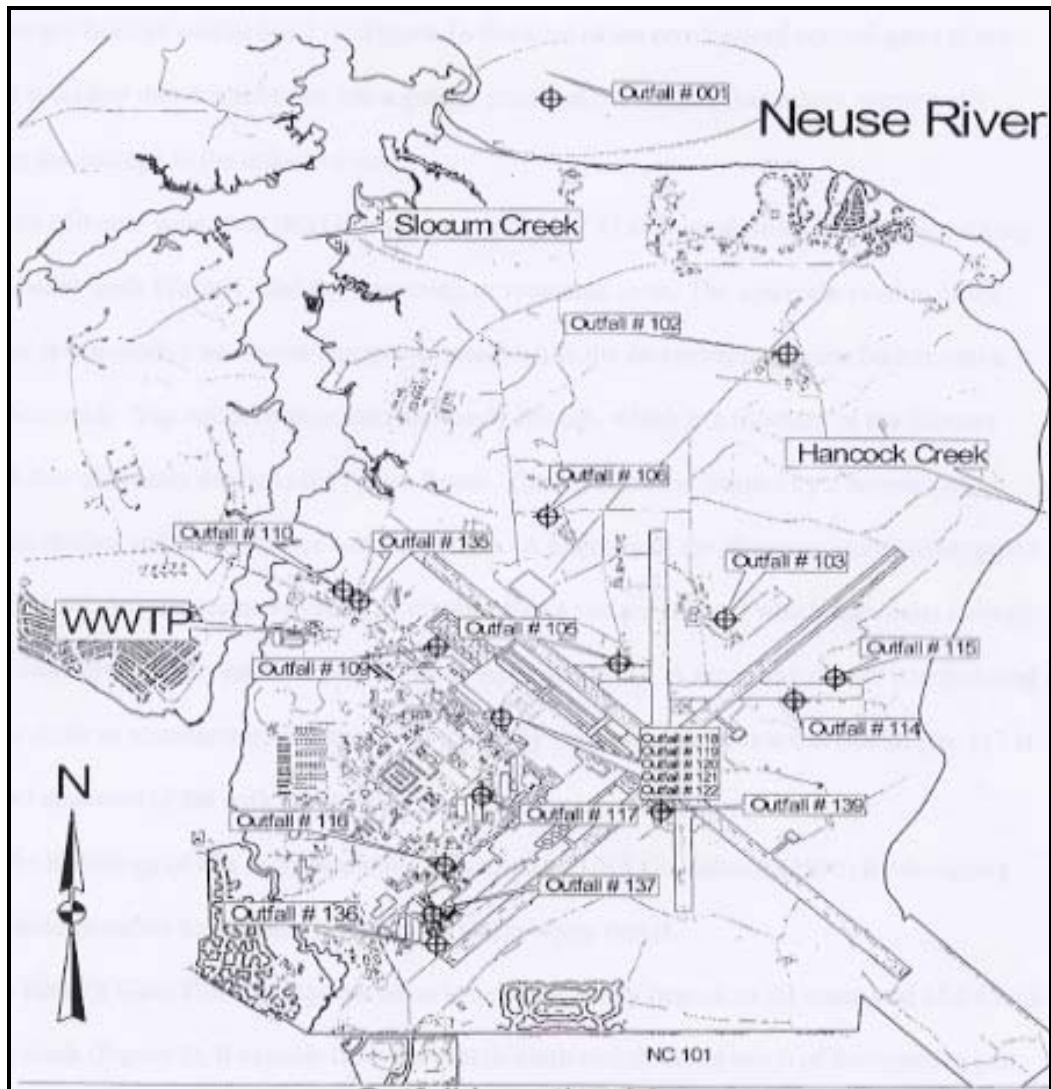


**Exhibit 2.2: Stormwater Outfall locations for the Cherry Point Marine Corps Air Station, Cherry Point, NC, as described by Morgan (1999).** Various devices including weirs, dams, flood gates, flow meters and water samplers are located throughout the base and used to describe and manage the stormwater runoff at Cherry Point.

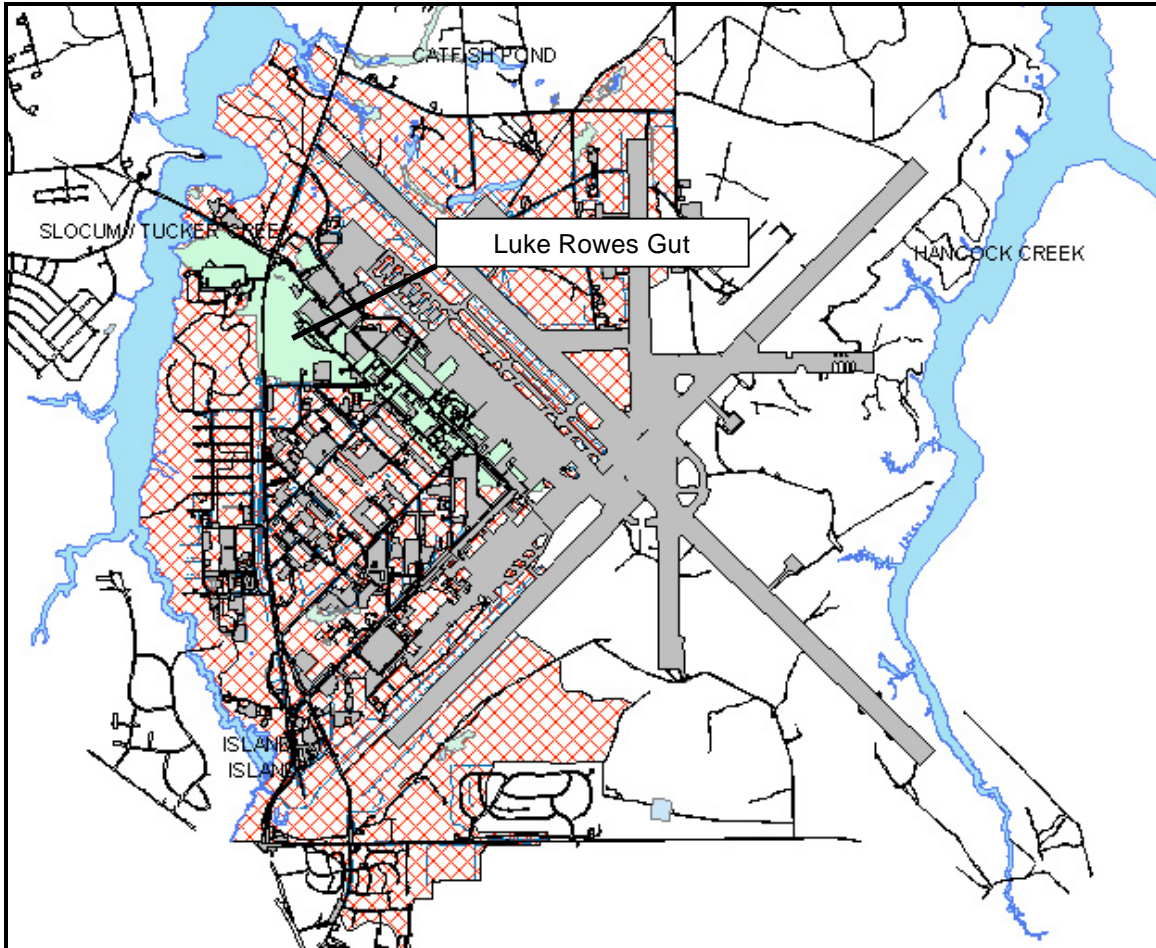


**Exhibit 2.3: Luke Rows Gut.** The graphic displays the location of the Luke Rows Gut in relationship to the overall watershed for the industrialized section of Cherry Point MCAS, Cherry Point, NC. Luke Rows Gut drains into Slocum Creek.

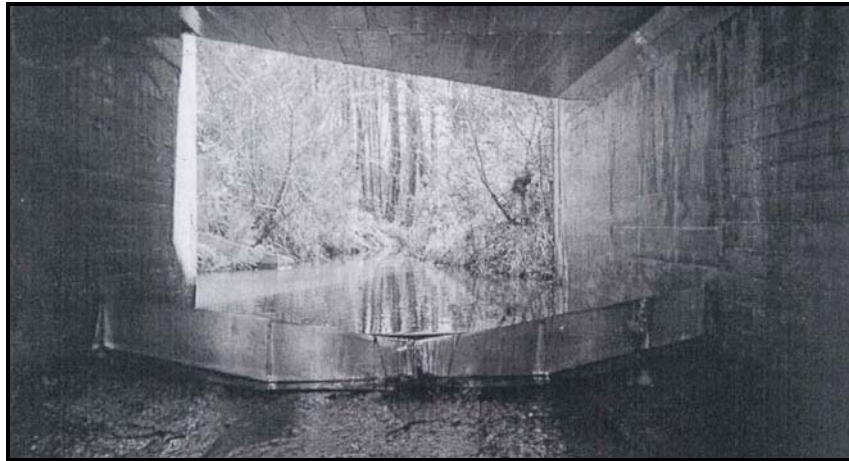


**Exhibit 2.4: Study Catchment K3 Control Weir.** This picture depicts the concrete box culvert outlet for catchment K4 looking upstream. The 160-degree metal weir retains water during low flows.

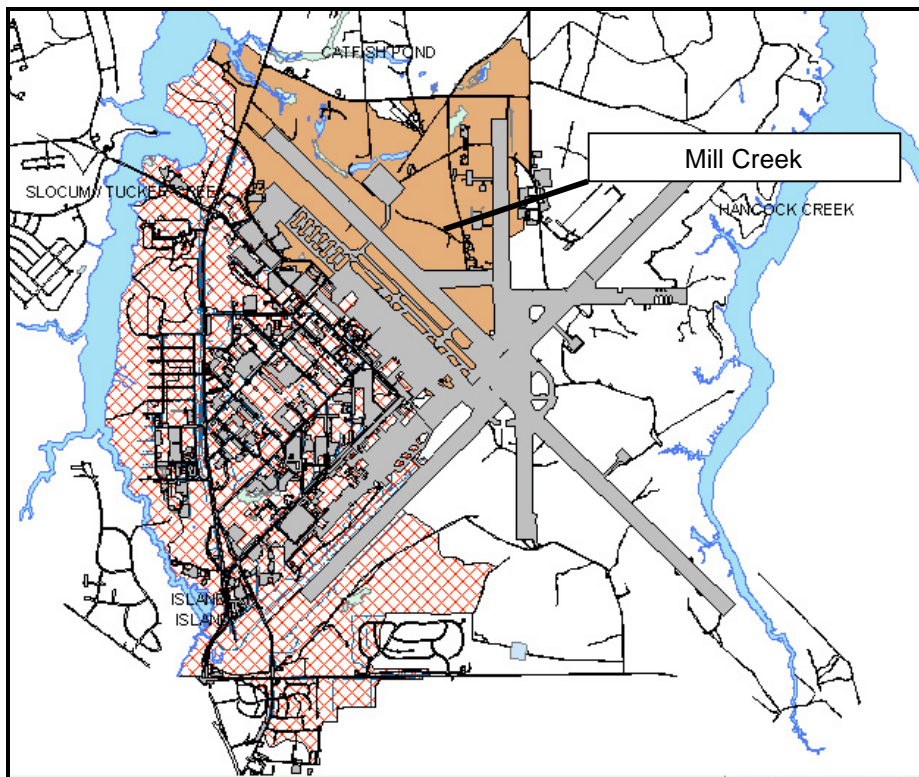


**Exhibit 2.5: Mill Creek Basin at Cherry Point MCAS.** The above graphic displays the location of basin Mill Creek in relationship to the overall watershed for the industrialized section of Cherry Point MCAS, Cherry Point, NC.

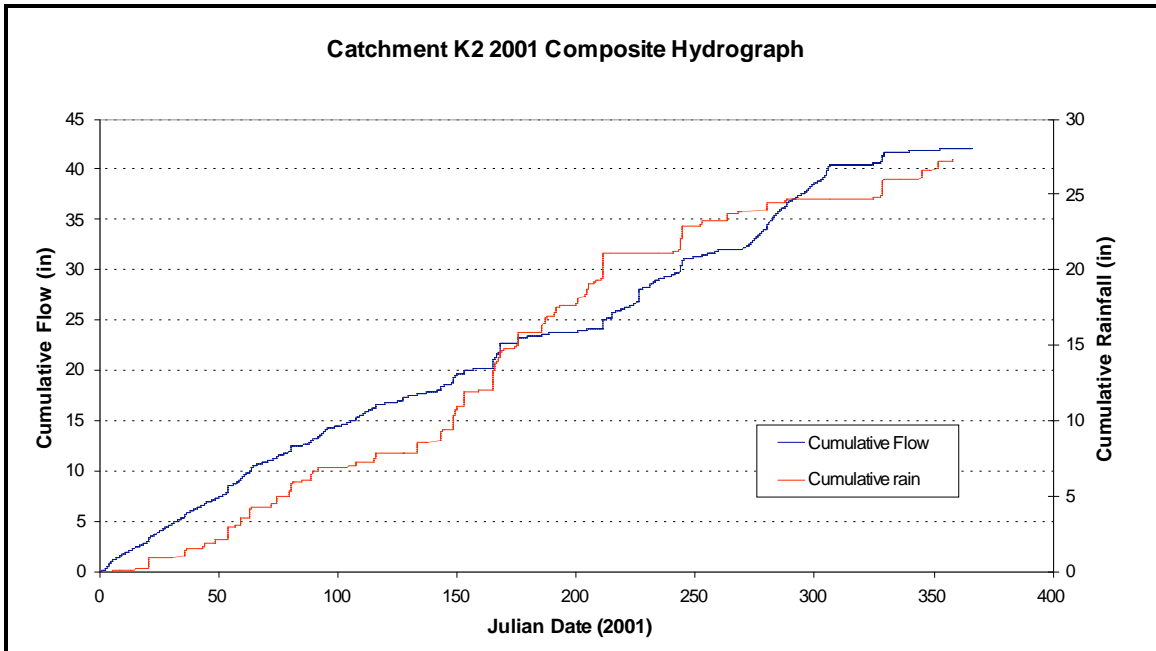


**Exhibit 2.6: Outflow Hydrograph for Catchment K2 in 2001 at Cherry Point, MCAS.** The red lines represent the rainfall hyetograph and the blue graph is the cumulative outflow data for catchment K2.

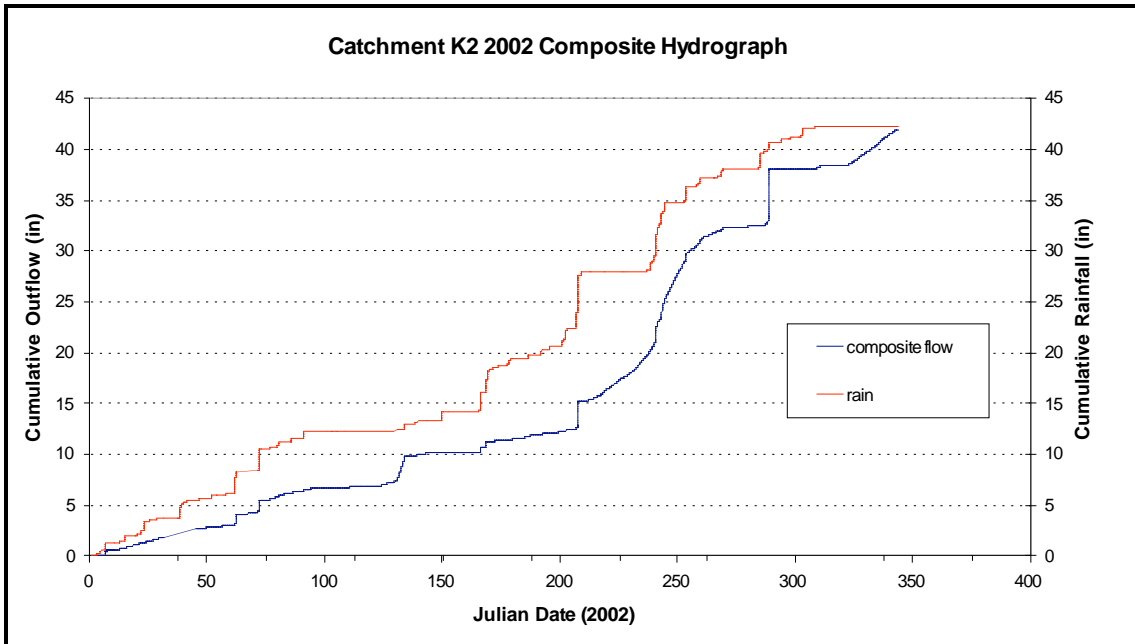


**Exhibit 2.7: Outflow Hydrograph (2002) for Catchment K2 at Cherry Point, MCAS.** The cumulative precipitation data has been graphed in red and the cumulative, observed outflow is presented in blue.

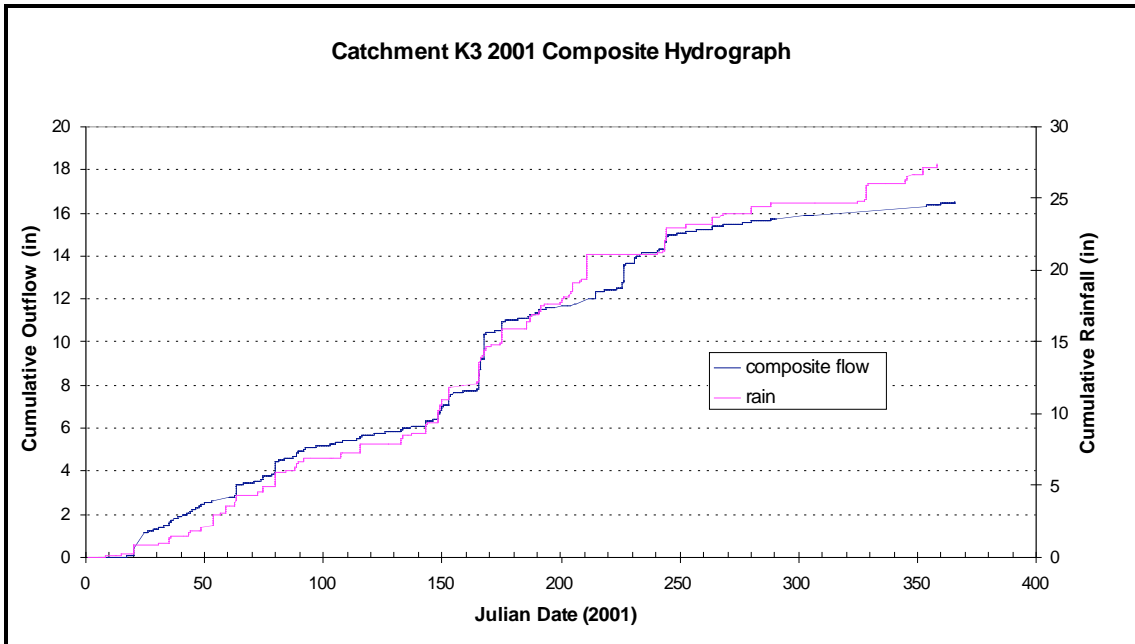


**Exhibit 2.8: Catchment K3 2001 Composite Hydrograph for Cherry Point, MCAS.** The purple line represents the cumulative rainfall and the blue line is the measured outflow at the catchment outlet.

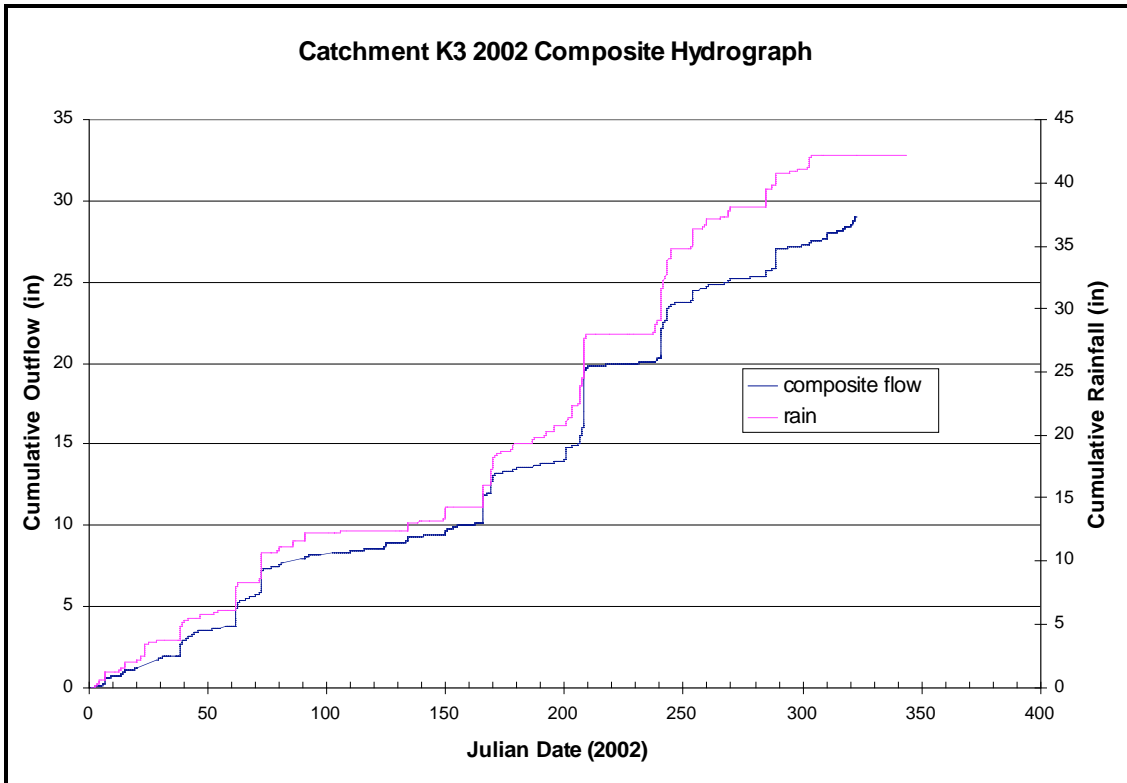


**Exhibit 2.9: Catchment K3 2002 Composite Hydrograph for Cherry Point, MCAS.** The purple line reports the cumulative rainfall and the blue line represents the cumulative, measured flow at the catchment K3 outlet.

**Appendix 2A:** Chapter Two Additional Figures



**Figure 2A.1: Cherry Point and Surrounding Area Topographic Map, 1:200,000 scale** (adapted from [www.topozone.com](http://www.topozone.com), Maps a la carte, Inc., 2000). This figure displays the orientation of the air station in relationship to several major surface water bodies in eastern North Carolina. The study area is denoted by the dashed rectangle.

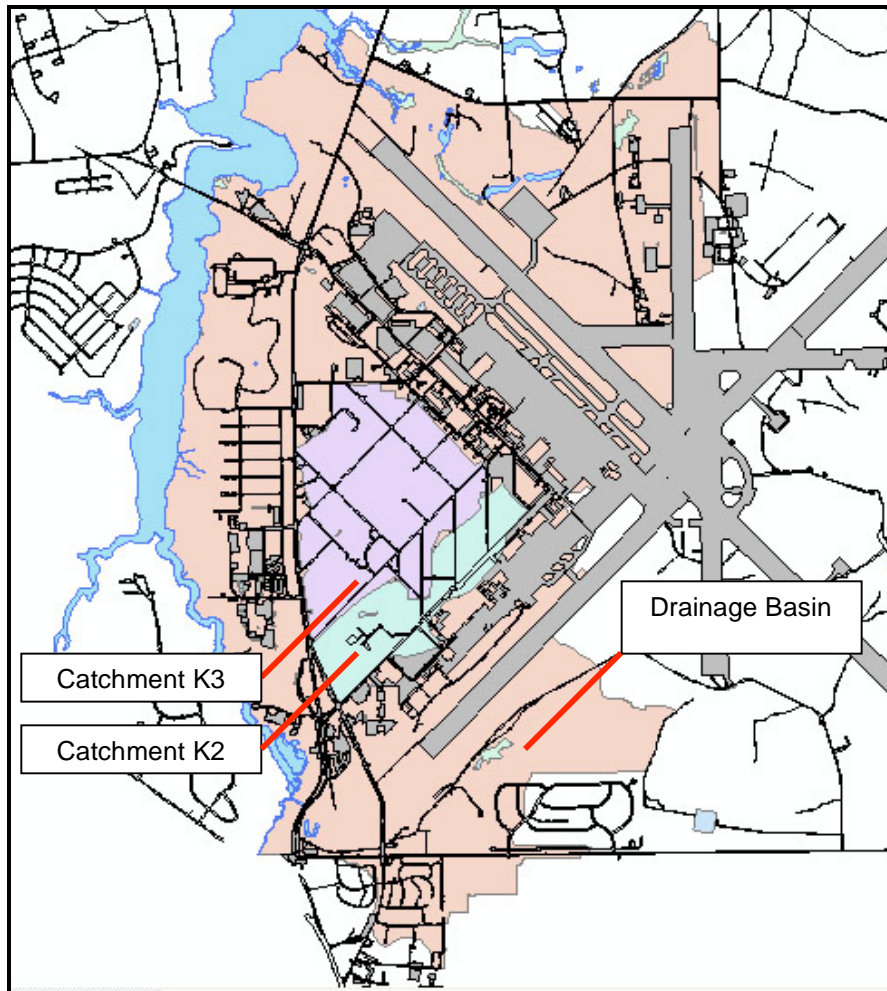


**Figure 2A.2: The Delineated Drainage Basin at Cherry Point Marine Corps Air Station.** The light red color presents the boundaries of the watershed that was surveyed during the research period. Catchment K2 has been colored teal and catchment K3 is shaded light purple.

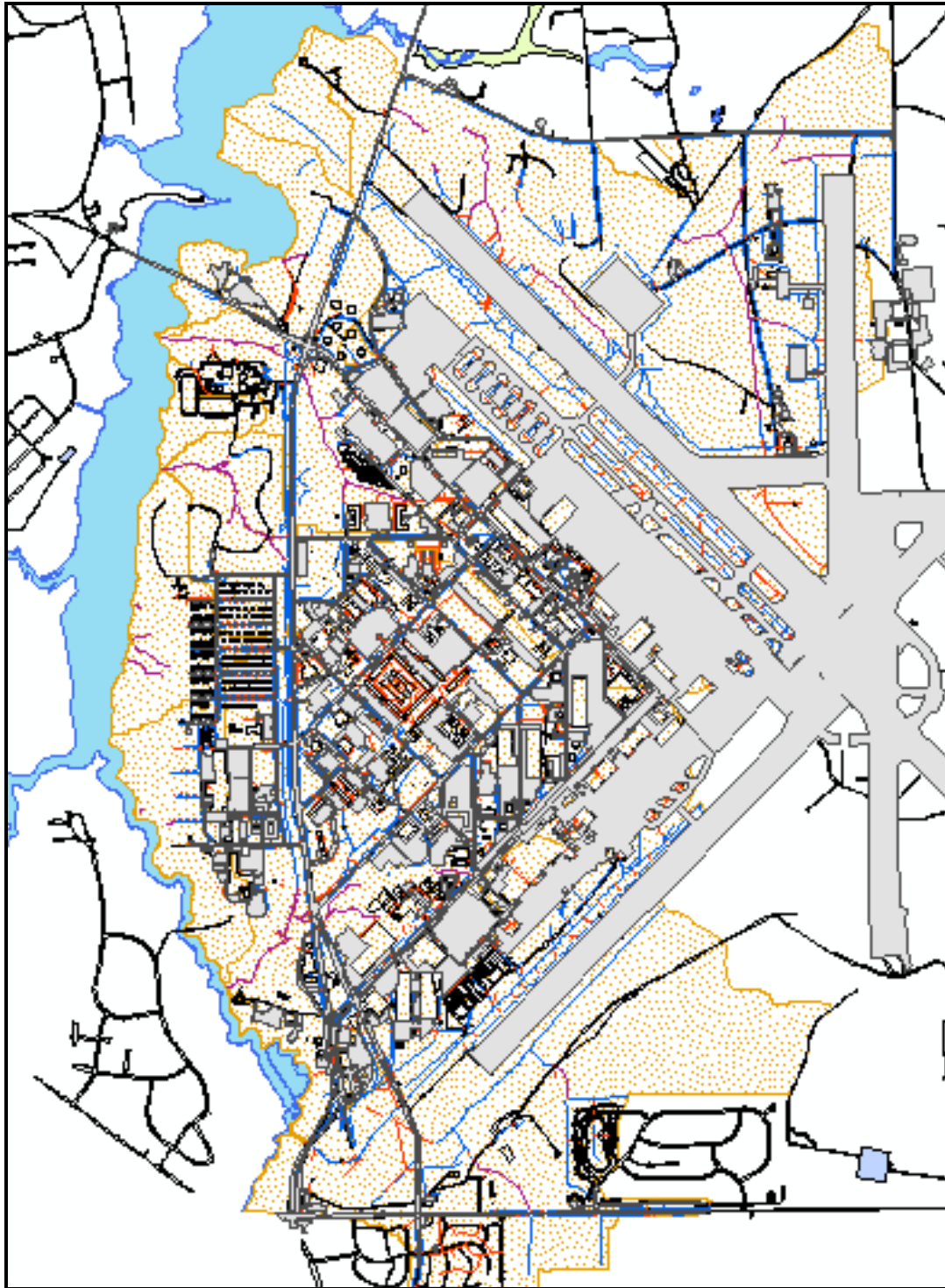


**Figure 2A.3: Cherry Point Industrialized Area GIS Map.** This figure is an ArcVIEW screenshot of the study area. The grey areas represent impervious areas, such as parking lots, buildings, runways and roads. The purple and smaller blue lines are surface runoff channels.

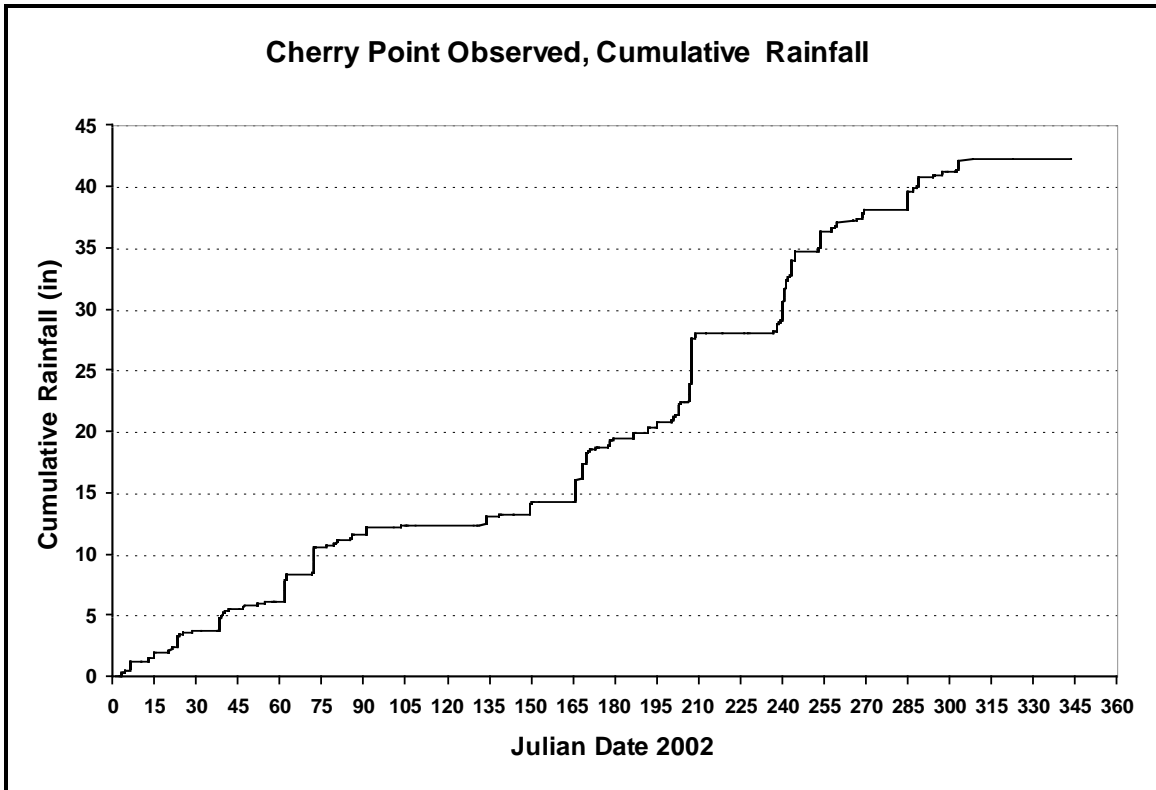


**Figure 2A.4: 2002 Cherry Point Cumulative Rainfall Spreadsheet.** This figure displays the collected tipping bucket cumulative rainfall for 2002 near the K1 catchment outlet. The long-term average rainfall for the Havelock region of North Carolina is nearly 56 inches.

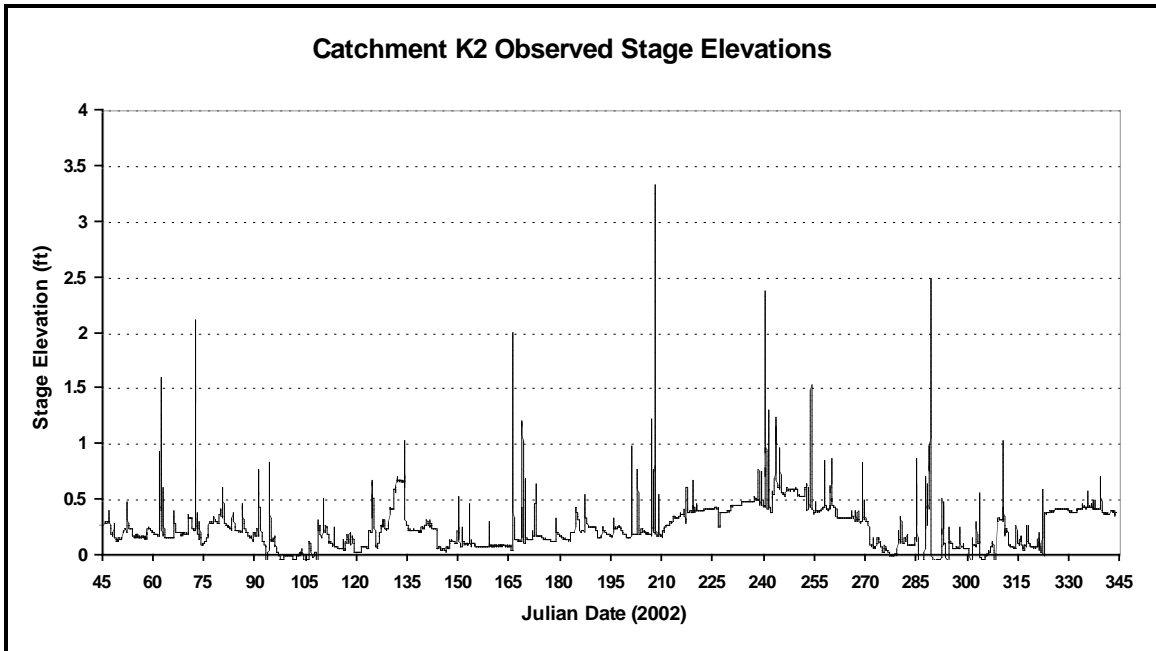


**Figure 2A.5: 2002 Observed Stage Elevation Graph for Catchment K2.** This figure is the water stage graph for 2002, following the combination of the separate, observed elevation files.

**Appendix 2B:** Chapter Two Additional Tables

**Table 2B.1: Imperviousness values for Five Basins at Cherry Point.** The below table is a representation of the surveyed Cherry Point watershed presented on a basin level.

<b>Basin Name</b>	<b>Area (ac.)</b>	<b>Total % Imperviousness</b>
Schoolhouse	642	20.4
Sandy Branch	539	53.4
Luke Rowes	281	41.3
Mill Creek	937	31.8
Turkey Gut	100	7.9

**Table 2B.2: Rainfall Normal Distribution Results (Anderson-Darling and Shapiro-Wilk methods) for Cherry Point MCAS, years 2000 through 2002.**

<b>Rain Year</b>	<b>Method</b>	<b>Mean</b>	<b>Variance</b>
2000	Anderson-Darling	5.619	145.7764
	Shapiro-Wilk	5.619	145.7764
2001	Anderson-Darling	5.954	92.7905
	Shapiro-Wilk	5.954	95.7905
2002	Anderson-Darling	8.566	299.3514
	Shapiro-Wilk	8.566	299.3514

**Table 2B.3: Rainfall Lognormal Distribution Results for Cherry Point MCAS for years 2000 through 2002.**

<b>Rain Year</b>	<b>Method</b>	<b>Mean</b>	<b>Variance</b>
2000	Log-normal	5.619	145.776
2001	Log-normal	5.954	92.790
2002	Log-normal	8.566	299.3514

**Table 2B.4a: Observed Stage Elevations Missing Data Gaps for Cherry Point MCAS years 2000 to 2002.** The following three tables present the time intervals where either data was not available from the stage elevation microprocessor and/or the flow meter.

Catchment K2 Missing Stage Elevations Intervals					
2000		2001		2002	
<i>start day</i>	<i>end day</i>	<i>start day</i>	<i>end day</i>	<i>start day</i>	<i>end day</i>
319.5417	same	20.4063	20.4333	1.0000	10.5833
330.7042	330.9042	53.4708	53.5000	62.0625	62.1667
338.5833	same	53.5875	53.6104	72.2750	72.3938
352.3208	352.3333	63.2354	63.2729	133.9792	same
		79.9583	79.9771	165.9521	166.0188
		143.2188	143.2875	168.6937	168.7354
		148.5062	148.5521	200.6667	same
		152.9542	152.9938	206.6604	206.6917
		165.0458	165.1708	207.7271	207.8104
		166.1167	166.1708	240.3229	240.4396
		167.7188	167.8104	241.1250	241.1750
		175.1896	175.2438	243.1188	243.4250
		185.1813	185.2083	253.6563	253.7562
		203.5000	same	271.6667	273.0000
		211.0146	211.1042	274.3333	274.8333
		214.6563	214.7104	277.5833	278.4167
		225.9583	226.0146	287.3917	287.6792
		226.3333	226.4146	288.775	289.1438
		231.1417	231.1708	310.4458	366.0000
		243.3667	243.4146		
		244.5500	244.5979		
		285.4021	285.4333		
		306.4167	366.0000		

**Table 2B.4b: Downloads with Missing Stage Elevation Data in Catchment K3 during years 2000 to 2002 at Cherry Point MCAS.**

Catchment K3 Missing Stage Elevation Intervals					
2000		2001		2002	
<i>start day</i>	<i>end day</i>	<i>start day</i>	<i>end day</i>	<i>start day</i>	<i>end day</i>
237.8854	238.7917	20.3125	20.3333	6.5479	6.6458
241.2021	241.2813	20.4020	24.5833	38.2021	38.8479
242.4833	242.5000	35.3880	35.4104	61.7646	61.9229
243.0167	243.0417	48.3000	48.3438	62.0500	62.2063
243.0979	255.3333	63.1479	63.1833	62.7292	62.7625
262.4771	262.8083	63.2167	63.3063	72.1542	72.2479
262.9771	263.0417	74.5229	74.5625	72.2562	72.4354
266.8958	266.9167	79.7354	79.7562	72.8229	72.8333
267.2312	267.3750	79.9396	80.1104	91.0021	91.0417
267.5313	267.5833	88.4104	88.4271	109.9187	109.9375
268.7375	268.7667	91.6813	91.7042	124.4250	124.5396
319.5229	319.5354	103.6000	103.6021	133.9563	134.0500
324.6667	same	115.4792	same	149.5396	149.9500
330.6896	330.9437	132.8833	same	150.7688	150.8208
336.6750	366.0000	133.0646	133.0813	152.8562	152.8958
		143.2125	143.2979	165.9458	166.0458
		148.4979	148.5667	168.6854	168.7667
		148.6083	148.6312	169.5313	169.5917
		148.6563	148.6813	170.6917	170.7167
		149.3167	149.3625	178.4896	178.5583
		152.9417	153.0458	186.8458	186.8875
		153.1937	153.2146	195.3187	195.3458
		165.0313	165.1875	200.6333	200.7208
		165.7104	165.7729	206.6125	206.7125
		166.1062	166.1979	207.2708	207.3313
		167.7125	167.8458	207.6333	207.7125
		175.1896	175.2542	207.7208	207.8500
		186.6875	186.7208	208.7875	208.8542
		190.8083	190.8333	238.2792	239.1500
		190.9187	190.9625	240.1958	240.2333
		214.6541	214.7208	240.2479	240.5042
		225.9520	226.0229	240.5188	240.5542
		226.3210	226.4396	240.5604	240.6104
		231.1310	231.1896	241.1104	241.1896
		240.6708	240.6917	243.0979	243.4375
		243.3650	243.4333	244.5687	244.5875

Table 2B.4b Continued

		244.5500	244.6146	253.6542	253.7667
		263.5000	263.5229	257.0000	257.7125
				259.5875	259.6167
				268.8396	268.8833
				284.7604	284.8250
				284.9313	284.9812
				288.6875	289.0979
				303.2354	303.3063
				310.4167	310.5104
				317.5333	317.5521
				320.6500	320.6813
				321.7854	321.8417

**Table 2B.4c: Downloads with Missing Flow Meter Data from Catchments K2 and K3 at MCAS-CP during the Study Period**

Catchment K2 Missing Flow Meter Intervals					
2000		2001		2002	
<i>start day</i>	<i>end day</i>	<i>start day</i>	<i>end day</i>	<i>start day</i>	<i>end day</i>
269.368	308.532	1.000	47.618	178.000	365.000
319.588	366.000				

Catchment K3 Missing Flow Meter Intervals					
2000		2001		2002	
<i>start day</i>	<i>end day</i>	<i>start day</i>	<i>end day</i>	<i>start day</i>	<i>end day</i>
0.000	235.521	None		96.813	143.451
				165.438	365.000

**Appendix 2C: MCAS-CP Monitoring Station Photographs**

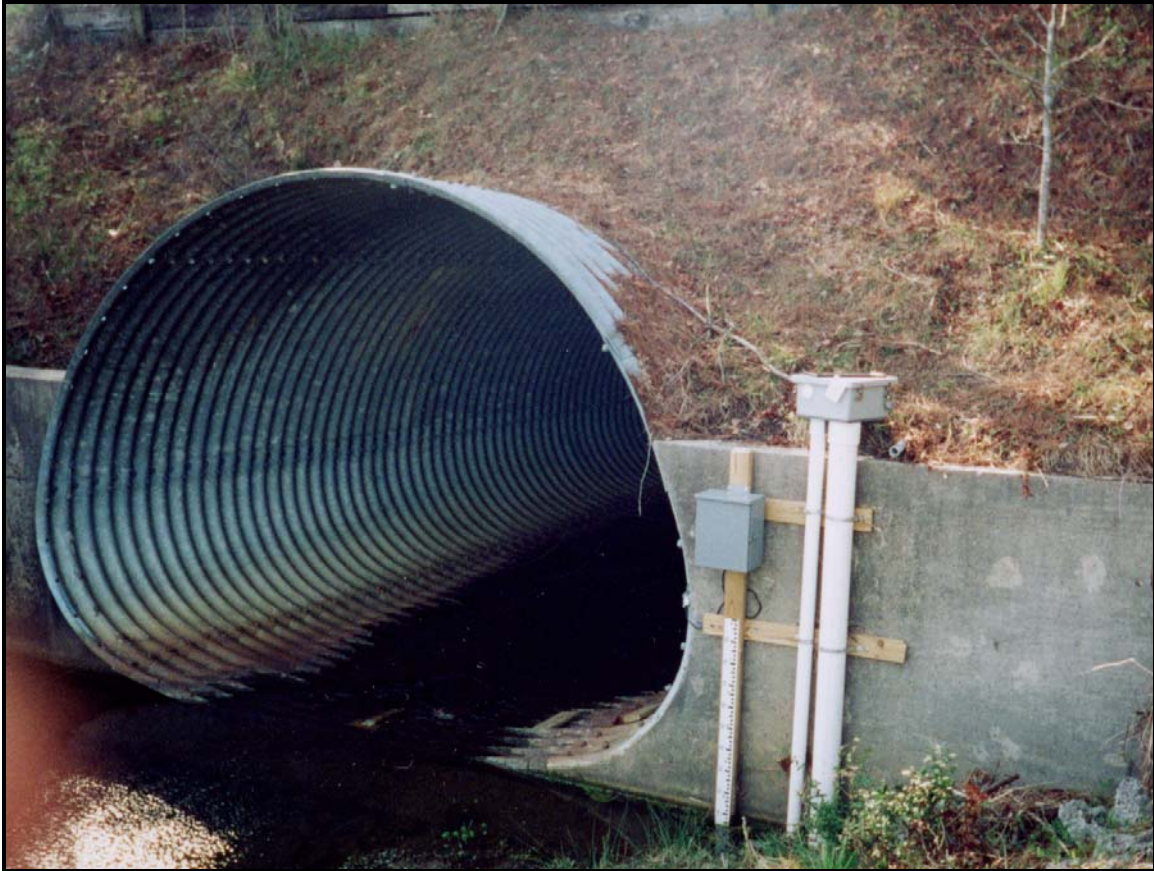


**Figure 2C.1: K1 Monitoring Station looking Downstream.** This picture was taken following the installation of the flow monitoring devices at outlet K1. The staff has been affixed to the upstream headwall. In addition, the float/pulley system used to record water stage is located in the two white pipes on the right. Likewise, the Blue Earth microprocessor is housed in the light grey box to the right, and the flow meter is fastened to the bottom of the culvert (not visible). No weir was installed at this location.

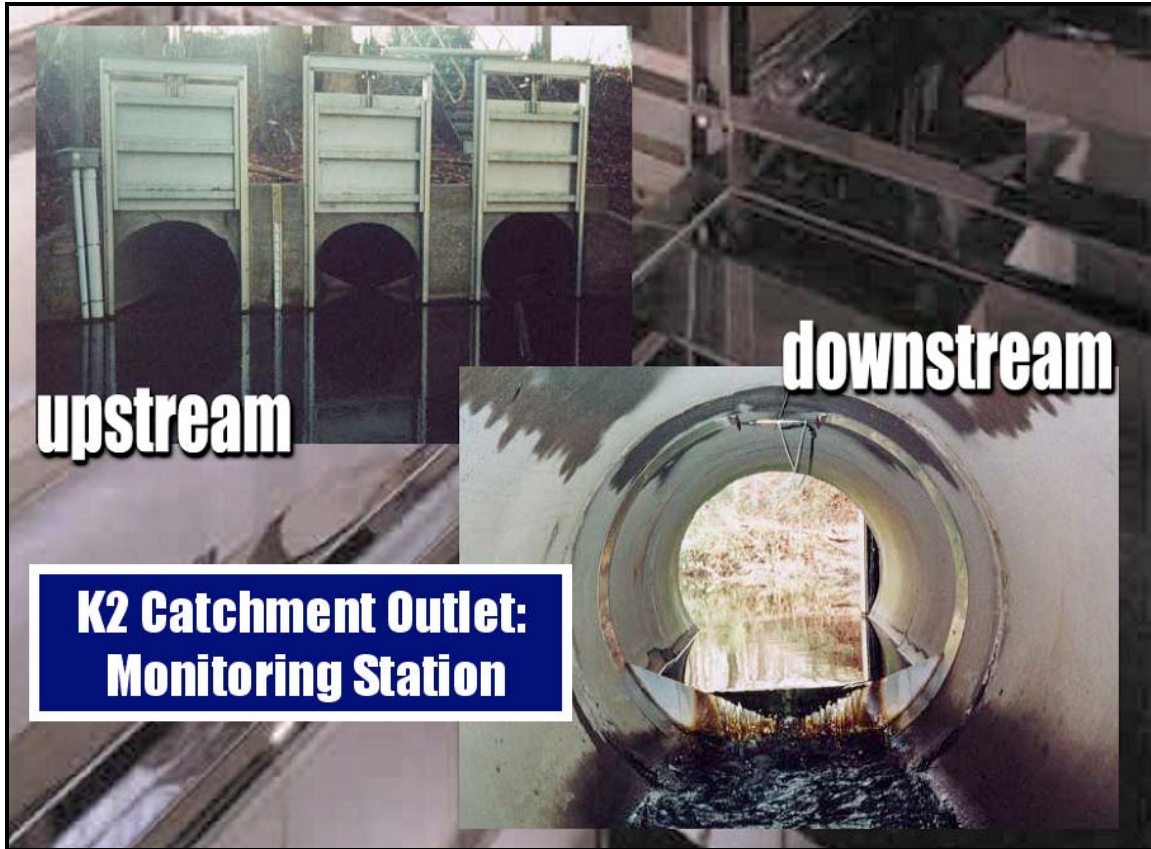


**Figure 2C.2: Catchment K2 Outlet at CPMCAS from two Viewpoints.** This figure presents views of the K2 catchment outlet displaying the floodgates, v-notch weir, and stage recording apparatus. The flow meter was installed in the far left barrel (top left picture) and downstream of the weir.



**Figure 2C.3: Catchment K3 Outlet at CPMCAS looking Downstream.** The outlet of the K3 catchment is similar to that of K2, having three barrels, three weirs, water stage elevation monitoring equipment and the one flow meter. The flow meter is located in the far left culvert barrel, downstream of the installed weir.

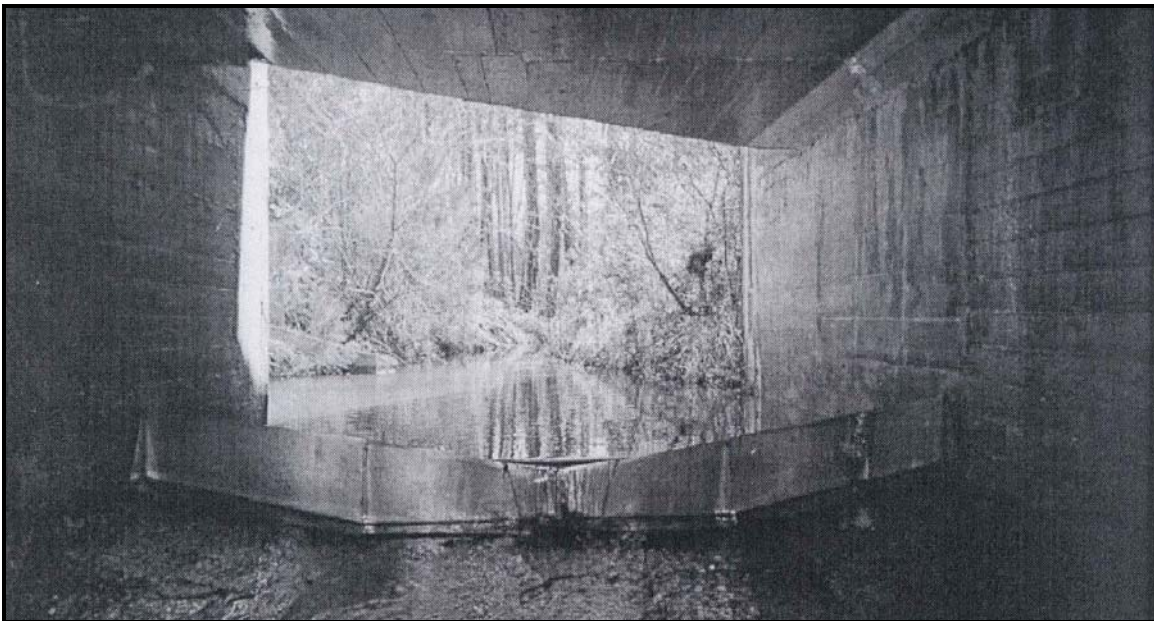


**Figure 2C.4: Catchment K4 Outlet at Cherry Point MCAS looking upstream.** This picture displays the 160-degree v-notch weir that was installed at the concrete, box culvert near the K4 monitoring station. The weir was positioned to retain low flows such that the stage recorder had sufficient water depth for measurement. The flow meter was installed downstream of the weir.



**Figure 2C.5: K5 Monitoring Station at MCAS-CP looking downstream.** The outlet of catchment K5 is located along the airstrip and conveys a majority of its stormwater runoff. This location is equipped with manually operated floodgates and this picture was taken prior to the installation of the flow monitoring equipment.

## Appendix 2D: Stage Elevation Measurement Files

**Exhibit 2D.1: Weir 6 Program source code in BASIC.** The following BASIC program was used by the research staff to collect the stage elevations at the Cherry Point flow monitoring locations based upon the pulley diameters and other physical characteristics. The program was loaded onto the microprocessor and downloaded in two to four week increments.

```
1  REM  ** Uruguay wells & flumes *
5  CLEAR S : CLEAR I
10  GOSUB 200
20  GOSUB 300
30  SW=XBY(PC).AND.1 : TB=XBY(MB)
40  IF TB<>55H THEN GOSUB 1300 : GOTO 60
50  GOSUB 500
60  IF SW=1 THEN GOSUB 100
62  IF HR=20 THEN 65 ELSE 66
65  DT=3 : GOSUB 2260 : REM 60 min wakeup
66  IF HR>7.OR.HR<20 THEN 68 ELSE 70
68  DT=3 : GOSUB 2260 : REM 3 min wakeup
70  GOSUB 5000
90  XBY(F)=0 : G=XBY(E) : END
100 PRINT : PRINT
102 PRINT " MAIN MENU "
104 PRINT "-----"
108 PRINT "1 DOWNLOAD DATA", TAB (32),"# of saved blocks=",NB
110 PRINT "2 TEST", TAB (40),INT(100*(LM-FML)/(64767-FML)),"% of mem."
112 PRINT "3 SET PARAMETERS"
114 PRINT "4 SET READ POINT "
116 PRINT "5 CONTINUE"
118 PRINT "6 QUIT"
119 PRINT
120 PRINT : INPUT " enter your choice: ",KY1
125 PRINT
130 IF KY1<1.OR.KY1>6 PRINT "wrong key, try again" : GOTO 120
135 IF KY1=5 RETURN
140 IF KY1=6 END
145 ON KY1-1 GOSUB 3000,4000,2000,1800
150 GOTO 100
200 RTC=0FE00H : B=0FEB0H : D=B+20H : E=D+10H : F=E+10H
230 HBE_H=0FF01H : BOTH_H=0FF03H : ADC=0FF00H
240 PA=0FD00H : PB=PA+1 : PC=PB+1 : MD=PC+1
260 FML=8100H : LML=0FCFFH
270 MB=8000H
280 FOR I=1 TO 200 : NEXT I
285 XBY(MD)=89H : XBY(PB)=6
295 RETURN
300 NC=XBY(MB+2) : DT=XBY(MB+3)
310 DR=XBY(MB+6) : TP=XBY(MB+8) : S1=XBY(MB+9)
317 DV=(XBY(MB+0FH)*256+XBY(MB+0EH))*10
320 LS1=XBY(MB+11H)*256+XBY(MB+10H)
325 LS2=XBY(MB+13H)*256+XBY(MB+12H)
335 HLM=XBY(MB+2FH)*256+XBY(MB+2EH) : HLM=HLM/1000
340 WS=XBY(MB+18H) : PC1=XBY(MB+19H)
345 PC2=XBY(MB+1BH)*256+XBY(MB+1AH)
350 HB3=XBY(MB+1DH)*256+XBY(MB+1CH) : HB3=HB3/1000
355 HB4=XBY(MB+1FH)*256+XBY(MB+1EH) : HB4=HB4/1000
360 LM=XBY(MB+21H)*256+XBY(MB+20H)
365 NB=XBY(MB+23H)*256+XBY(MB+22H)
370 AM=XBY(MB+24H) : AH=XBY(MB+25H) : WSN=XBY(MB+26H)
375 HB1=XBY(MB+29H)*256+XBY(MB+28H) : HB1=HB1/1000
380 HB2=XBY(MB+2BH)*256+XBY(MB+2AH) : HB2=HB2/1000
382 SN=XBY(MB+0DH)
383 M1=XBY(MB+2DH)*256+XBY(MB+2CH)
384 M2=XBY(MB+2FH)*256+XBY(MB+2EH)
```

## Exhibit 2D.1 Continued

```
386 TTS=XBY(MB+31H)*256+XBY(MB+30H)
395 VOL=(XBY(MB+37H)*256+XBY(MB+36H))*256+XBY(MB+35H)
398 RETURN
500 GOSUB 550
510 GOSUB 600
520 GOSUB 700
530 RETURN
550 XBY(F)=0 : DO : RDY=1.AND.XBY(F) : UNTIL RDY
560 MO=(XBY(RTC+090H).AND.15)*10+(XBY(RTC+080H).AND.15)
565 DAY=(XBY(RTC+070H).AND.15)*10+(XBY(RTC+060H).AND.15)
570 HR=(XBY(RTC+050H).AND.15)*10+(XBY(RTC+040H).AND.15)
575 MN=(XBY(RTC+030H).AND.15)*10+(XBY(RTC+020H).AND.15)
580 IF 1.AND.XBY(F) THEN 550
590 RETURN
600 XBY(BOTH_H)=2 : REM sample in latched output mode
610 FOR KK=1 TO 3
615 J=KK-1 : SUM=0
620 FOR I=1 TO 30
622 JHI=0
625 XBY(ADC)=J
626 JHB=XBY(HBE_H)
628 IF JHB>16.AND.JHI<10 THEN JHI=JHI+1 : GOTO 626
630 SUM=SUM+XBY(ADC)+256*JHB
640 NEXT I
660 NR(KK)=SUM/30
665 NEXT KK
672 REM VG=0
674 REM FOR N=0 TO 7
676 REM VG=N+1 : G=3 : PORT1=N
678 REM FOR Z=0 TO 250 : NEXT Z
680 REM SUM=0
682 REM FOR IK=1 TO 10 : XBY(ADC)=G
684 REM ZX=XBY(ADC)+256*XBY(HBE_H)
685 REM SUM=SUM+ZX : NEXT IK
686 REM RSLT=SUM/10 : TEM(VG)=RSLT/16 : REM in deg F
688 REM NEXT N
690 RETURN
700 SF=0
705 PC1=PC1-1
710 GOSUB 1100
715 PC1=INT(3*60/DT)
720 D1=ABS(NR(1)-LS1)*1.221
721 IF D1>=DR.OR.MN=0 THEN SF=1
870 IF SF=1 THEN GOSUB 930
890 RETURN
930 FA=MB+10H : NB=NB+1
940 XBY(LM)=MO : LM=LM+1 : XBY(LM)=DAY : LM=LM+1
945 XBY(LM)=HR : LM=LM+1 : XBY(LM)=MN : LM=LM+1
950 FOR I=1 TO 2
955 II=2*(I-1)
960 HNR=INT(NR(II)/256) : LNR=INT(NR(II))-256*HNR
965 XBY(LM)=LNR : LM=LM+1 : XBY(LM)=HNR : LM=LM+1
970 XBY(FA+II)=LNR : XBY(FA+II+1)=HNR
971 NEXT I
972 REM XBY(LM)=TEM(1) : LM=LM+1 : XBY(LM)=TEM(2) : LM=LM+1
974 REM XBY(LM)=TEM(3) : LM=LM+1 : XBY(LM)=TEM(4) : LM=LM+1
976 REM XBY(LM)=TEM(5) : LM=LM+1 : XBY(LM)=TEM(6) : LM=LM+1
978 REM XBY(LM)=TEM(7) : LM=LM+1 : XBY(LM)=TEM(8) : LM=LM+1
980 GOSUB 1450
990 RETURN
```

## Exhibit 2D.1 Continued

```
1100 H1=(NR(1)/819*M1/1000)-HB1 : H2=(NR(2)/819*M2/1000)-HB2
1110 RETURN
1300 SW=1
1307 PRINT "-----"
1310 IF TB=15H THEN PRINT "| GO SET WELL READ POINT |"
1312 IF TB<>15H THEN PRINT "| SYSTEM NOT INITIALIZED |"
1315 PRINT "-----"
1320 PRINT : PRINT "press <S.B.> to continue"
1325 DO : G=GET
1330 UNTIL G=20H
1380 GOSUB 1400
1390 RETURN
1400 LM=FML : NB=0
1410 GOSUB 1450
1420 RETURN
1450 HNB=INT(NB/256) : LNB=NB-HNB*256
1455 LMH=INT(LM/256) : LML=LM-LMH*256
1460 XBY(MB+23H)=HNB : XBY(MB+22H)=LNB
1465 XBY(MB+21H)=LMH : XBY(MB+20H)=LML
1470 RETURN
1700 IF TTS=TS2 THEN TTS=INT(TP*60/12)
1720 IF TTS=TS3 THEN TTS=INT(TP*60/2)
1750 XBY(MB+31H)=INT(TTS/256) : XBY(MB+30H)=TTS.AND.255
1760 RETURN
1800 PRINT "To avoid <Enter>, to proceed hit <space-bar>"
1805 DO : G=GET : IF G=13 THEN RETURN
1810 UNTIL G=32
1812 INPUT "Enter location #:",SN
1815 INPUT "Enter reading for Well 1 (mm):",Y1
1816 INPUT "Enter reading for Well 2 (mm):",Y2
1825 GOSUB 600
1830 HB1=INT(NR(1)/819*M1-Y1) : HB2=INT(NR(2)/819*M2-Y2)
1831 YY1=HB1+Y1 : YY2=HB2+Y2 : YC1=YY1-Y1 : YC2=YY2-Y2
1832 YR1=YC1/(M1/2) : YR2=YC2/(M2/2)
1833 IF HB1<0 PRINT "set Well 1 down",Y1,YR1 : GOTO 1815
1834 IF HB2<0 PRINT "set Well 2 down",Y2,YR2 : GOTO 1816
1835 XBY(MB+29H)=INT(HB1/256) : XBY(MB+28H)=HB1.AND.255
1840 XBY(MB+2BH)=INT(HB2/256) : XBY(MB+2AH)=HB2.AND.255
1841 XBY(MB+1DH)=INT(HB3/256) : XBY(MB+1CH)=HB3.AND.255
1842 XBY(MB+1FH)=INT(HB4/256) : XBY(MB+1EH)=HB4.AND.255
1845 XBY(MB+0DH)=SN
1850 HB1=HB1/1000 : HB2=HB2/1000 : HB3=HB3/1000 : HB4=HB4/1000
1860 TB=TB.OR.40H : XBY(MB)=TB
1870 RETURN
2000 PRINT " PARAMETERS"
2010 PRINT "-----" : PRINT
2014 PRINT "1 station location", TAB (39),"sn=",SN
2018 PRINT "2 wake-up interval (min)", TAB (39),"dt=",DT
2020 PRINT "3 m1 coefficient", TAB (39),"m1=",
2025 PRINT USING(####),M1
2057 PRINT "4 m2 coefficient", TAB (39),"m2=",
2058 PRINT USING(####),M2
2059 PRINT "5 return to main menu"
2060 PRINT : INPUT "Enter choice: ",KY2
2070 PRINT : PRINT
2075 IF KY2<1.OR.KY2>5 THEN PRINT "wrong key" : GOTO 2060
2080 IF KY2=5 THEN RETURN
2085 IF KY2=1 THEN GOSUB 2199
2087 IF KY2=2 THEN GOSUB 2250
2090 IF KY2=3 THEN GOSUB 2300
2092 IF KY2=4 THEN GOSUB 2400
2100 GOTO 2000
2150 LLT=1
```

## Exhibit 2D.1 Continued

```
2152 IF KY2=1 THEN ULT=255
2154 IF KY2=3 THEN ULT=1000
2160 IF KY2=4 THEN ULT=1000
2170 DO : PRINT "Enter value between ",LLT,"and ",ULT,
2175 INPUT " ",Q
2180 UNTIL (Q>=LLT.AND.Q<=ULT)
2185 RETURN
2199 GOSUB 2150
2200 SN=Q : XBY(MB+0DH)=SN
2240 RETURN
2250 PRINT
2255 PRINT "option not available" : PRINT
2260 XBY(MB+3)=DT
2265 GOSUB 1700
2290 RETURN
2300 GOSUB 2150
2305 M1=Q
2310 XBY(MB+2DH)=INT(M1/256) : XBY(MB+2CH)=M1.AND.255
2315 RETURN
2400 GOSUB 2150
2405 M2=Q
2410 XBY(MB+2FH)=INT(M2/256) : XBY(MB+2EH)=M2.AND.255
2415 RETURN
3000 PRINT "press <F8> to save file"
3010 DO : G=GET
3020 UNTIL G=20H
3065 PNT=FML
3066 PRINT SN : PRINT
3070 FOR I=1 TO NB
3080 GOSUB 3300
3090 GOSUB 4100
3100 NEXT I
3110 DO : G=GET
3120 UNTIL G=20H
3125 INPUT "Did you get that? (0=N/1=Y)",KY4
3126 IF KY4=0 THEN GOTO 3000
3130 GOSUB 1400
3140 WS=1 : WSN=1
3150 XBY(MB+18H)=WS : XBY(MB+26H)=WSN
3160 FOR I=1 TO 20 : PRINT : NEXT I
3200 RETURN
3300 REM prepare data for down loading
3310 MO=XBY(PNT) : PNT=PNT+1 : DAY=XBY(PNT) : PNT=PNT+1
3315 HR=XBY(PNT) : PNT=PNT+1 : MN=XBY(PNT) : PNT=PNT+1
3320 FOR J=1 TO 2
3330 NR(J)=XBY(PNT)+256*XBY(PNT+1) : PNT=PNT+2
3335 NEXT J
3337 REM TEM(1)=XBY(PNT) : PNT=PNT+1 : TEM(2)=XBY(PNT) : PNT=PNT+1
3339 REM TEM(3)=XBY(PNT) : PNT=PNT+1 : TEM(4)=XBY(PNT) : PNT=PNT+1
3342 REM TEM(5)=XBY(PNT) : PNT=PNT+1 : TEM(6)=XBY(PNT) : PNT=PNT+1
3344 REM TEM(7)=XBY(PNT) : PNT=PNT+1 : TEM(8)=XBY(PNT) : PNT=PNT+1
3350 RETURN
4000 PRINT "*** PRESS SPACE BAR TO EXIT ***"
4010 DO
4020 GOSUB 550
4030 GOSUB 600
4040 GOSUB 4100
4060 G=GET
4070 UNTIL G=20H
4080 RETURN
4100 GOSUB 1100
4110 PRINT USING(##),MO,DAY,HR,MN,
4120 PRINT USING(##.###),H1,H2
4125 REM PRINT USING(###),TEM(1),TEM(2),TEM(3),TEM(4),
```

## Exhibit 2D.1 Continued

```
4130 REM PRINT USING(###),TEM(5),TEM(6),TEM(7),TEM(8)
4200 RETURN
5000 IF SW=0 GOTO 5055
5008 PRINT " Press <S.B.> to continue"
5015 DO : G=GET
5018 UNTIL G=20H
5020 GOSUB 550 : AM=MN : AH=HR
5025 SHR=(INT(HR/3)+1)*3
5030 FRC=0
5035 NF=INT((60-MN)/DT) : DTMP=60-MN-NF*DT
5040 IF DTMP>0 THEN FRC=1 : DT=DTMP
5045 PC1=INT(((SHR-HR)*60-MN)/DT)+FRC
5050 XBY(MB+19H)=PC1
5055 PRINT AH,AM : AM=AM+DT
5070 IF AM>59 THEN AM=AM-60 : AH=AH+1 : GOTO 5070
5075 IF AH>23 THEN AH=AH-24
5078 PRINT AH,AM
5080 A10H=INT(AH/10) : A1H=AH-10*A10H
5090 A10M=INT(AM/10) : A1M=AM-10*A10M
5100 XBY(MB+24H)=AM : XBY(MB+25H)=AH
5120 XBY(F)=8 : XBY(E)=6 : DO : DP=XBY(E) : WHILE 1.AND.DP
5130 XBY(B)=6
5140 XBY(RTC)=0 : XBY(RTC+10H)=0
5150 XBY(RTC+20H)=A1M : XBY(RTC+30H)=A10M
5155 XBY(RTC+40H)=A1H : XBY(RTC+50H)=A10H
5160 XBY(F)=0 : XBY(D)=9 : XBY(F)=8 : XBY(E)=7 : XBY(F)=0
5190 RETURN
```

**Exhibit 2D.2: A Raw Stage Elevation Text file, showing a Single Storm Event (Catchment K3), from 12/17/01 to 12/19/01 at Cherry Point MCAS.** The following text is an actual Blue Earth downloaded file from catchment K3 for a two day period. The file contains information about the date, time and water elevation.

1<sup>st</sup> column: month  
 2<sup>nd</sup> column: day  
 3<sup>rd</sup> column: hour  
 4<sup>th</sup> column: N/A  
 5<sup>th</sup> column: stage (m)

12	17	1	0	0.063
12	17	2	0	0.063
12	17	3	0	0.063
12	17	4	0	0.063
12	17	5	0	0.063
12	17	6	0	0.063
12	17	7	0	0.063
12	17	8	0	0.063
12	17	9	0	0.063
12	17	10	0	0.063
12	17	11	0	0.063
12	17	12	0	0.063
12	17	13	0	0.062
12	17	14	0	0.062
12	17	15	0	0.06
12	17	16	0	0.061
12	17	17	0	0.062
12	17	18	0	0.063
12	17	19	0	0.062
12	17	20	0	0.062
12	17	21	0	0.062
12	17	22	0	0.06
12	17	23	0	0.062
12	18	0	0	0.062
12	18	1	0	0.061
12	18	2	0	0.063
12	18	2	51	0.076
12	18	2	54	0.095
12	18	2	57	0.111
12	18	3	0	0.165
12	18	3	3	0.29
12	18	3	6	0.416
12	18	3	9	0.498
12	18	3	12	0.542
12	18	3	15	0.574

**Exhibit 2D.2 Continued**

12	18	3	18	0.588
12	18	3	24	0.563
12	18	3	27	0.547
12	18	3	30	0.52
12	18	3	33	0.502
12	18	3	36	0.485
12	18	3	39	0.461
12	18	3	42	0.447
12	18	3	45	0.428
12	18	3	48	0.408
12	18	3	51	0.391
12	18	3	54	0.377
12	18	3	57	0.364
12	18	4	0	0.352
12	18	4	6	0.33
12	18	4	12	0.314
12	18	4	18	0.301
12	18	4	24	0.288
12	18	4	33	0.273
12	18	4	42	0.26
12	18	4	51	0.246
12	18	5	0	0.236
12	18	5	12	0.224
12	18	5	24	0.21
12	18	5	45	0.197
12	18	6	0	0.186
12	18	6	27	0.172
12	18	6	54	0.159
12	18	7	0	0.158
12	18	7	39	0.144
12	18	8	0	0.142
12	18	8	45	0.13
12	18	9	0	0.125
12	18	10	0	0.114
12	18	11	0	0.11
12	18	12	0	0.111
12	18	13	0	0.108
12	18	14	0	0.108
12	18	15	0	0.108
12	18	16	0	0.109
12	18	17	0	0.109
12	18	18	0	0.108
12	18	19	0	0.108
12	18	20	0	0.108

**Exhibit 2D.2 Continued**

12	18	21	0	0.108
12	18	22	0	0.108
12	18	23	0	0.108
12	19	0	0	0.108
12	19	1	0	0.108
12	19	2	0	0.108
12	19	3	0	0.109
12	19	4	0	0.108
12	19	5	0	0.108
12	19	6	0	0.108
12	19	7	0	0.108
12	19	8	0	0.108
12	19	9	0	0.108
12	19	10	0	0.108
12	19	11	0	0.108
12	19	12	0	0.108
12	19	12	9	0.062

## Appendix 2E: Flow Meter Files

**Exhibit 2E.1: VELFLO FORTRAN Source Code.** *The following source code was utilized by the Cherry Point research team to transform the information recorded by the flow meter into useable flow measurements.*

```
program VELFLOW
c
c This program reads complete data set of Julian day in decimal format, stage,
c water temperature, Battery Voltage, Adjusted velocity, and raw measured
c velocity from STARFLOW velocity meter. The input file is actually the output
c file obtained by running "nospikev" program to smoothen the raw velocity
c from STARFLOW meter (program written on May 06, 1998).
c
  character*40 infile, outfile1, outfile2
  integer bday, no
  real day, stage, temp, battv, adjvel, rawvel
  real avhrstg(24), avhrvel(24), flo(24), dflo(366)
  real hrstg, hrvel, hrday(24),areaf(24)
  real flow, area
  real diam, rad, hrarea, avhrarea(24)
c
c stage is stage measured by STARFLOW in "mm";
c temp is water temperature in "deg F";
c battv is Battery voltage
c adjvel is adjusted velocity in "mm/sec" obtained from "nospikev" program;
c rawvel is raw velocity in "mm/sec";

c parameters for Single &ft diameter CMP pipe Culvert:

  write(*,*)'Enter culvert internal diameter in meters'
  read(*,*) diam
  rad = diam/2.

  write(*,*)'Enter input file with stage velocity data'
  read(*,'(A)')infile
  open(unit = 1,file=infile,status='old')
c
  write(*,*) 'Enter output file to write hourly data'
  read(*,'(a)')outfile1
  open(unit=2,file=outfile1,status='unknown')
c
  write(*,*) 'Enter output file to write daily data'
  read(*,'(a)')outfile2
  open(unit=3,file=outfile2,status='unknown')
```

### Exhibit 2E.1 Continued

```
write(*,*)'Enter the Beginning Day'
read(*,1)bday
1  format(i3)

dflo(bday) = 0.

5  do 10 i = 1,24
    hrstg = 0.
    hrvel = 0.
    hrarea = 0.
    do 20 j = 1,6
        read(1,*,end=99)day,stage,temp,battv,rawvel

        if (stage .ge. diam*1000) then
            stage = diam*1000
        endif
c
        area = rad**2 * acos((rad-(stage/1000))/rad) -
&    sqrt((2*rad-(stage/1000))*(stage/1000)) * (rad-(stage/1000))

        hrstg = hrstg+stage
        hrvel = hrvel+rawvel
        hrarea = hrarea+area
20  continue

        hrday(i) = day
        avhrstg(i) = (hrstg/6)/1000.    ! stage in meters
        avhrvel(i) = (hrvel/6)/1000.    ! measured velocity in meters/sec
        avhrarea(i) = hrarea/6.

c
c if velocity -stage data by velocity meter is available use the measured
c data to calculate flow rates as given below
c
        flo(i) = (avhrarea(i) * avhrvel(i)) * 3600
c
        write(2,35)hrday(i),avhrstg(i),avhrvel(i),avhrarea(i),flo(i)
35  format(2x,f8.4,3x,f5.3,3x,f5.3,3x,f7.4,3x,f8.2)
c
        dflo (bday) = dflo(bday) + flo(i)

10  continue
```

**Exhibit 2E.1 Continued**

```
write(3,40)bday, dflo(bday)  
40 format(2x,l3,4x,f10.1)
```

```
bday = bday + 1  
dflo (bday) = 0.
```

```
go to 5
```

```
99 close(1)  
stop  
end
```

**Exhibit 2E.2: 2001 K2 VELFLO Input File in .prn format for Julian Day 48.** The below collection is the delimited .prn file that was downloaded from the flow meter. This file would then be inserted in the VELFLO program to calculate the flow rates for Julian Day 48 in 2001. The columns represent the Julian date, water temperature, water depth, battery voltage and flow velocity, respectively.

48	72	19.09	12.44	426
48.00694	72	19.09	12.44	290
48.01389	69	19.04	12.44	257
48.02083	68	19.03	12.44	394
48.02778	68	19.03	12.44	394
48.03472	67	19	12.44	394
48.04167	67	18.96	12.44	394
48.04861	68	18.96	12.44	394
48.05556	69	18.96	12.44	394
48.0625	68	18.93	12.44	394
48.06944	69	18.92	12.44	359
48.07639	68	18.9	12.44	223
48.08333	69	18.9	12.44	223
48.09028	69	18.9	12.44	223
48.09722	70	18.9	12.44	223
48.10417	70	18.9	12.44	223
48.11111	71	18.84	12.44	245
48.11806	71	18.83	12.44	245
48.125	71	18.83	12.44	245
48.13194	72	18.83	12.44	245
48.13889	72	18.83	12.44	457
48.14583	70	18.83	12.44	417
48.15278	71	18.8	12.44	433
48.15972	72	18.77	12.44	514
48.16667	72	18.77	12.44	501
48.17361	72	18.76	12.44	483
48.18056	72	18.77	12.44	382
48.1875	72	18.76	12.44	232
48.19444	72	18.76	12.44	232
48.20139	72	18.76	12.44	232
48.20833	74	18.76	12.44	414
48.21528	77	18.72	12.44	317
48.22222	81	18.72	12.44	198
48.22917	86	18.7	12.44	309
48.23611	82	18.72	12.44	562
48.24306	82	18.76	12.44	910
48.25	83	18.76	12.44	1012
48.25694	84	18.76	12.44	1058
48.26389	85	18.8	12.44	1025

**Exhibit 2E.2 Continued**

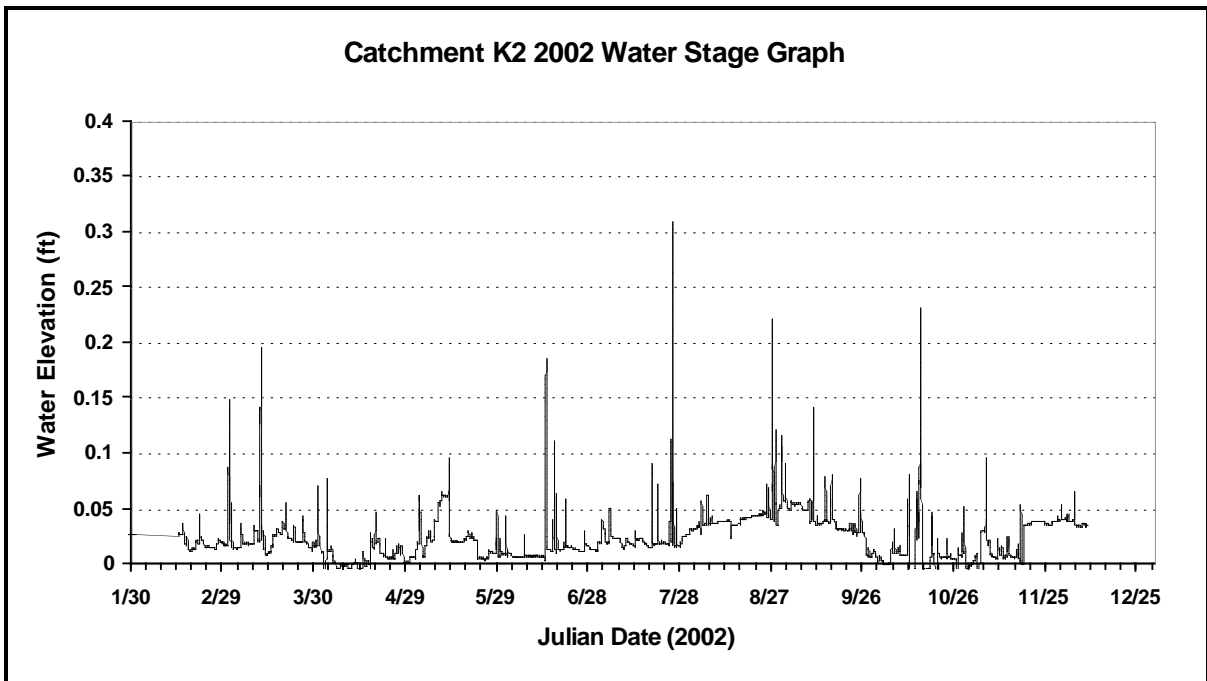
48.27083	84	18.81	12.44	980
48.27778	89	18.77	12.44	1070
48.28472	99	18.59	12.44	1072
48.29167	105	18.14	12.44	1300
48.29861	107	17.97	12.44	1603
48.30556	134	17.98	12.44	1866
48.3125	167	18.1	12.44	1796
48.31944	169	18.26	12.44	1835
48.32639	154	18.34	12.44	1836
48.33333	145	18.37	12.44	1868
48.34028	134	18.3	12.44	1771
48.34722	125	18.22	12.44	1739
48.35417	117	18.14	12.44	1608
48.36111	110	18.07	12.44	1516
48.36806	109	18.02	12.44	1381
48.375	108	17.97	12.44	1254
48.38194	106	17.97	12.44	1294
48.38889	102	17.94	12.44	1277
48.39583	102	17.92	12.44	1103
48.40278	99	17.91	12.44	1132
48.40972	97	17.91	12.44	1085
48.41667	95	17.91	12.44	1021
48.42361	93	17.91	12.44	1009
48.43056	91	17.91	12.44	1126
48.4375	89	17.91	12.44	1068
48.44444	90	17.95	12.44	1062
48.45139	86	17.97	12.44	1041
48.45833	85	17.97	12.44	1006
48.46528	84	17.97	12.44	1035
48.47222	81	17.97	12.44	1029
48.47917	79	18.02	12.44	1010
48.48611	79	18.04	12.44	1059
48.49306	77	18.04	12.44	1024
48.5	77	18.04	12.44	854

**Appendix 2F: Combined Flow Calculations**

**Exhibit 2F.1: Excerpt of the Combined Weir Spreadsheet for Catchment K2 (2000).** The below table is a collection of hydraulics data that describes the water stage elevation and calculated flow rates using the weir equation at the K2 outlet.

Julian Date (2000)	weir1_stg (m)	weir2_stg (m)	weir3_stg (m)	Estimated Weir Flow Rates			Combined weir Flow rate	
				weir1 (cum/sec)	weir2 (cum/sec)	weir3 (cum/sec)	(cum/sec)	(cum/hr)
270.0000	0.131	0.061	0.101	0.01441	0.002132	0.007521	0.024063	86.62850332
270.0417	0.131	0.061	0.101	0.01441	0.002132	0.007521	0.024063	86.62850332
270.0833	0.131	0.061	0.101	0.01441	0.002132	0.007521	0.024063	86.62850332
270.1250	0.131	0.061	0.101	0.01441	0.002132	0.007521	0.024063	86.62850332
270.1667	0.131	0.061	0.101	0.01441	0.002132	0.007521	0.024063	86.62850332
270.2083	0.132	0.062	0.102	0.014687	0.002221	0.007709	0.024616	88.61783522
270.2354	0.154	0.084	0.124	0.021592	0.004744	0.012562	0.038898	140.0321531
270.2500	0.167	0.097	0.137	0.026441	0.006799	0.016117	0.049357	177.684614
270.2917	0.155	0.085	0.125	0.021944	0.004887	0.012816	0.039647	142.7302935
270.3333	0.145	0.075	0.115	0.018574	0.003574	0.010405	0.032553	117.1899761
270.3750	0.140	0.070	0.110	0.017014	0.003008	0.00931	0.029332	105.5958612
270.4167	0.138	0.068	0.108	0.016413	0.002797	0.008893	0.028103	101.1719957
270.4583	0.136	0.066	0.106	0.015825	0.002596	0.008487	0.026908	96.86850881
270.5000	0.135	0.065	0.105	0.015535	0.002499	0.008288	0.026323	94.76153114
270.5417	0.132	0.062	0.102	0.014687	0.002221	0.007709	0.024616	88.61783522
270.5833	0.132	0.062	0.102	0.014687	0.002221	0.007709	0.024616	88.61783522
270.6250	0.132	0.062	0.102	0.014687	0.002221	0.007709	0.024616	88.61783522
270.6667	0.132	0.062	0.102	0.014687	0.002221	0.007709	0.024616	88.61783522
270.7083	0.132	0.062	0.102	0.014687	0.002221	0.007709	0.024616	88.61783522
270.7500	0.132	0.062	0.102	0.014687	0.002221	0.007709	0.024616	88.61783522
270.7917	0.131	0.061	0.101	0.01441	0.002132	0.007521	0.024063	86.62850332
270.8333	0.131	0.061	0.101	0.01441	0.002132	0.007521	0.024063	86.62850332
270.8750	0.131	0.061	0.101	0.01441	0.002132	0.007521	0.024063	86.62850332
270.9167	0.131	0.061	0.101	0.01441	0.002132	0.007521	0.024063	86.62850332
270.9583	0.131	0.061	0.101	0.01441	0.002132	0.007521	0.024063	86.62850332
271.0000	0.131	0.061	0.101	0.01441	0.002132	0.007521	0.024063	86.62850332

**Exhibit 2F.2: Measured Water Elevation Graph for Catchment K2 (2002) at Cherry Point MCAS.** The following graphic is the observed stage data from the catchment K2 monitoring station.



**Appendix 2G: NOAA Weather Files**

**Exhibit 2G.1: NOAA Weather Download (2000).** *The following table presents the information downloaded from the NOAA database for Cherry Point, NC. The columns represent Julian date, maximum and minimum daily temperature, observed temperature, precipitation depth and snowfall amount..*

<b>Julian date (2000)</b>	<b>Tmax (°F)</b>	<b>Tmin (°F)</b>	<b>Tobs (°F)</b>	<b>Precip (in.)</b>	<b>Snow (in.)</b>
245.00	88	73		0.43	0
246.00	89	72		0	0
247.00	86	73		0.12	0
248.00	82	72		0.32	0
249.00	74	68		0.8	0
250.00	99999	67		0.03	0
251.00	81	66		0	0
252.00	82	66		0	0
253.00	83	66		0	0
254.00	82	63		0	0
255.00	84	68		0	0
256.00	86	69		T	0
257.00	88	70		0	0
258.00	86	69		0	0
259.00	86	69		0	0
260.00	75	55		0	0
261.00	72	55		0	0
262.00	74	68		3.88	0
263.00	83	69		0	0
264.00	85	66		0	0
265.00	86	74		T	0
266.00	81	72		0.49	0
267.00	76	71		1.62	0
268.00	88	70		0.22	0
269.00	88	71		0.01	0
270.00	79	56		0.02	0
271.00	70	57		0	0
272.00	74	57		0	0
273.00	77	60		0	0
274.00	77	63		0	0
275.00	73	65		0.07	0
276.00	99999	99999		0	9999.9
277.00	99999	99999		0	9999.9
278.00	99999	99999		0	9999.9
279.00	99999	99999		0	9999.9
280.00	99999	99999		0	9999.9

Exhibit 2G.1 Continued

281.00	99999	99999		0	9999.9
282.00	99999	99999		0	9999.9
283.00	99999	99999		0	9999.9
284.00	99999	99999		0	9999.9
285.00	99999	99999		0	9999.9
286.00	99999	99999		0	9999.9
287.00	99999	99999		0	9999.9
288.00	99999	99999		0	9999.9
289.00	99999	99999		0	9999.9
290.00	99999	99999		0	9999.9
291.00	99999	99999		0	9999.9
292.00	99999	99999		0	9999.9
293.00	99999	99999		0	9999.9
294.00	99999	99999		0	9999.9
295.00	99999	99999		0	9999.9
296.00	99999	99999		0	9999.9
297.00	99999	99999		0	9999.9
298.00	99999	99999		0	9999.9
299.00	99999	99999		0	9999.9
300.00	99999	99999		0	9999.9
301.00	99999	99999		0	9999.9
302.00	99999	99999		0	9999.9
303.00	99999	99999		0	9999.9
304.00	99999	99999		0	9999.9
305.00	99999	99999		0	9999.9
306.00	68	37		0	0
307.00	70	38		0	0
308.00	74	35		0	0
309.00	75	43		0.03	0
310.00	64	41		0.39	0
311.00	63	37		0	0
312.00	70	43		0	0
313.00	76	56		0	0
314.00	78	58		T	0
315.00	75	55		T	0
316.00	63	46		0	0
317.00	58	41		0	0
318.00	67	37		0	0
319.00	66	44		0.54	0
320.00	53	35		0	0
321.00	60	31		0.18	0
322.00	56	46		0.07	0
323.00	50	38		0.01	0

**Exhibit 2G.1 Continued**

324.00	44	40		1	0
325.00	53	33		T	0
326.00	45	30		0	0
327.00	45	23		0	0
328.00	47	26		0	0
329.00	54	33		0	0
330.00	68	48		3.51	0
331.00	67	48		0	0
332.00	67	44		0	0
333.00	62	41		0	0
334.00	61	40		0	0
335.00	57	32		0	0
336.00	53	32		0	0
337.00	52	33		0.32	T
338.00	37	33		1.07	T
339.00	45	28		0	0
340.00	53	24		0	0
341.00	48	32		0	0
342.00	53	34		0	0
343.00	63	30		0	0
344.00	51	36		T	0
345.00	52	40		0.4	0
346.00	65	42		0	0
347.00	67	41		0.04	0
348.00	50	35		0.08	0
349.00	75	50		0.26	0
350.00	54	44		0	0
351.00	69	46		0.26	0
352.00	71	38		0.32	0
353.00	50	27		0	0
354.00	54	30		0.01	0
355.00	38	25		0	0
356.00	49	24		0	0
357.00	49	29		T	T
358.00	36	23		0	0
359.00	48	24		0	0
360.00	38	26		0	0
361.00	37	21		0	0
362.00	43	26		0.13	0
363.00	40	31		0.11	0
364.00	44	27		0	0
365.00	44	25		0	0
366.00	39	23		0	0
			sum =	<b>16.74 (in.)</b>	

**Exhibit 2G.2: Cherry Point NOAA Weather Download (2001).** This weather data was downloaded from the NOAA website and contains the annual precipitation/weather data for Cherry Point during the year 2001.

Julian date (2001)	Tmax (°F)	Tmin (°F)	Tobs (°F)	Precip. (in.)
1.00	41	20		0
2.00	41	24		0
3.00	39	19		0
4.00	45	17		0
5.00	51	18		0
6.00	52	26		0
7.00	59	25		0
8.00	55	34		0.07
9.00	43	30		T
10.00	53	26		0
11.00	64	24		0
12.00	56	43		0.07
13.00	61	43		0
14.00	58	42		0.1
15.00	67	50		T
16.00	62	45		0
17.00	52	43		0
18.00	59	45		T
19.00	72	48		0.03
20.00	69	43		0.75
21.00	44	28		T
22.00	49	25		0
23.00	50	36		0
24.00	54	33		0
25.00	48	33		T
26.00	45	27		0
27.00	61	38		0
28.00	52	29		0
29.00	61	28		0
30.00	66	53		0.09
31.00	67	48		0
32.00	58	47		0
33.00	52	42		T
34.00	46	33		0
35.00	51	34		0.48
36.00	56	41		0.06
37.00	57	30		0
38.00	59	31		0

Exhibit 2G.2 Continued

39.00	69	36		0
40.00	73	39		0
41.00	68	45		0.01
42.00	49	36		0
43.00	57	36		0.31
44.00	59	40		0.13
45.00	64	47		0.01
46.00	76	57		0
47.00	77	56		0
48.00	64	42		0.29
49.00	43	26		0
50.00	56	23		0
51.00	70	33		0
52.00	75	48		0
53.00	48	34		0.81
54.00	56	33		0
55.00	55	31		0
56.00	71	46		0.14
57.00	74	47		0
58.00	59	43		0
59.00	51	35		0.44
60.00	61	32		0
61.00	70	46		0
62.00	57	50		0.34
63.00	63	49		0.5
64.00	61	42		T
65.00	42	29		T
66.00	51	31		0
67.00	57	29		0
68.00	57	33		T
69.00	52	30		0
70.00	66	27		0
71.00	65	45		0.02
72.00	78	58		0.18
73.00	74	44		0
74.00	67	50		0.47
75.00	65	50		0
76.00	70	50		0
77.00	56	45		0
78.00	53	39		0
79.00	61	45		0.78
80.00	62	49		0.13
81.00	64	47		0.07

Exhibit 2G.2 Continued

82.00	66	42		0
83.00	70	36		0
84.00	57	36		0.07
85.00	53	32		0
86.00	50	33		0
87.00	52	27		0
88.00	67	47		0.58
89.00	73	56		0.25
90.00	73	52		0.01
91.00	60	44		0.29
92.00	61	39		0
93.00	61	42		0.01
94.00	62	46		0
95.00	61	38		0
96.00	74	42		0
97.00	87	60		0
98.00	86	64		0
99.00	86	60		0
100.00	86	60		0
101.00	81	62		0
102.00	80	63		0
103.00	85	66		0.21
104.00	74	57		0
105.00	78	54		0
106.00	71	50		0
107.00	58	36		0.26
108.00	54	34		0
109.00	64	30		0
110.00	72	39		0
111.00	76	58		0
112.00	78	51		0
113.00	79	54		0
114.00	81	62		0
115.00	68	49		0.68
116.00	66	46		0
117.00	77	38		0
118.00	79	54		0
119.00	70	48		0
120.00	76	40		0
121.00	77	48		0
122.00	78	49		0
123.00	80	50		0
124.00	84	53		0

Exhibit 2G.2 Continued

125.00	87	54		0
126.00	74	58		0.01
127.00	73	55		0
128.00	74	57		0
129.00	80	51		0
130.00	83	49		0
131.00	85	56		0
132.00	85	64		0.43
133.00	75	54		0.21
134.00	76	47		0
135.00	71	49		0.04
136.00	73	58		0.01
137.00	62	56		0.08
138.00	85	59		0
139.00	94	69		0
140.00	87	62		T
141.00	82	67		T
142.00	85	74		0
143.00	76	62		0.78
144.00	75	58		0
145.00	83	57		0
146.00	82	64		0.01
147.00	85	55		T
148.00	82	63		1.04
149.00	73	59		0.61
150.00	83	54		0
151.00	75	63		0
152.00	82	45		0.65
153.00	82	68		0.07
154.00	88	65		0
155.00	81	69		0
156.00	92	73		0
157.00	88	69		T
158.00	89	72		0.21
159.00	78	71		0.01
160.00	82	67		T
161.00	84	67		T
162.00	85	64		0
163.00	90	71		0
164.00	87	73		0.39
165.00	77	73		1.81
166.00	80	73		0.51
167.00	88	70		2.02

Exhibit 2G.2 Continued

168.00	78	67		0
169.00	87	62		0
170.00	85	66		0
171.00	84	67		0
172.00	85	69		T
173.00	85	66		0
174.00	82	70		0.69
175.00	84	70		1.01
176.00	82	70		0
177.00	85	69		0
178.00	89	68		0
179.00	89	71		0
180.00	90	73		0
181.00	87	72		0
182.00	87	73		T
183.00	83	70		0.23
184.00	81	68		0.04
185.00	84	72		0.51
186.00	83	72		0.42
187.00	83	67		0.04
188.00	81	64		0
189.00	79	61		0.03
190.00	91	69		0.43
191.00	94	72		0.05
192.00	90	75		0.02
193.00	85	73		0
194.00	81	66		0.04
195.00	83	63		0
196.00	87	61		0
197.00	86	63		0
198.00	86	66		0
199.00	87	65		0.01
200.00	83	71		0.29
201.00	82	68		0
202.00	83	66		0
203.00	83	71		0.57
204.00	84	71		0.7
205.00	86	76		0.03
206.00	88	77		0
207.00	86	77		0.06
208.00	82	71		T
209.00	80	69		T
210.00	83	72		0.67

Exhibit 2G.2 Continued

211.00	78	69		0.91
212.00	81	67		0
213.00	81	64		T
214.00	82	67		0.84
215.00	83	65		0.01
216.00	85	65		T
217.00	87	66		T
218.00	87	70		0.16
219.00	89	72		0
220.00	91	77		0
221.00	92	77		0
222.00	89	78		0
223.00	88	79		T
224.00	88	73		0.37
225.00	88	73		0.84
226.00	84	73		1.01
227.00	86	69		0
228.00	87	66		0
229.00	89	67		0
230.00	89	73		T
231.00	87	74		0.33
232.00	87	69		0.36
233.00	83	69		0.14
234.00	85	69		0
235.00	87	63		0
236.00	82	68		T
237.00	86	70		0
238.00	85	67		0
239.00	89	65		0
240.00	92	71		0.26
241.00	84	71		0.03
242.00	84	70		0.02
243.00	89	72		0.8
244.00	84	71		0.66
245.00	83	70		0
246.00	83	67		T
247.00	80	70		T
248.00	85	68		T
249.00	82	69		0
250.00	85	67		0
251.00	86	67		T
252.00	86	70		0.15
253.00	87	68		T

Exhibit 2G.2 Continued

254.00	84	68		0
255.00	83	60		0
256.00	80	63		0
257.00	81	64		0
258.00	75	61		0
259.00	78	63		0
260.00	80	61		0
261.00	81	54		0
262.00	82	57		0.01
263.00	80	68		0.62
264.00	84	55		0
265.00	87	67		0
266.00	86	66		T
267.00	83	66		0.14
268.00	76	62		0.03
269.00	69	54		0
270.00	77	50		0
271.00	75	51		0
272.00	70	54		0
273.00	70	54		0
274.00	73	49		0
275.00	79	45		0
276.00	83	50		0
277.00	83	54		0
278.00	83	57		0
279.00	85	56		0.41
280.00	66	46		T
281.00	64	42		0
282.00	67	49		0
283.00	76	55		0
284.00	79	52		0
285.00	79	51		0
286.00	79	52		0
287.00	81	57		0.19
288.00	77	54		T
289.00	81	54		0
290.00	66	44		0
291.00	65	46		0
292.00	74	48		0
293.00	80	55		0
294.00	82	57		0
295.00	84	59		0
296.00	83	58		0

Exhibit 2G.2 Continued

297.00	87	64		0
298.00	86	61		T
299.00	70	47		0
300.00	56	41		0
301.00	58	39		0
302.00	62	35		0
303.00	70	33		0
304.00	72	47		0
305.00	75	50		T
306.00	81	54		0
307.00	82	53		0
308.00	71	46		0
309.00	65	44		0
310.00	60	37		0
311.00	74	32		0
312.00	76	41		0
313.00	70	41		0
314.00	71	32		0
315.00	70	50		0
316.00	61	46		0
317.00	64	42		0
318.00	70	51		0
319.00	71	54		T
320.00	77	57		0
321.00	72	52		0
322.00	66	50		0
323.00	71	51		0
324.00	70	48		0.07
325.00	56	34		0
326.00	64	30		T
327.00	64	48		0.02
328.00	72	62		0.35
329.00	73	63		0.12
330.00	80	64		T
331.00	72	58		0
332.00	80	55		0
333.00	77	54		T
334.00	78	58		0
335.00	79	60		0
336.00	66	54		0.02
337.00	67	49		0
338.00	67	45		0
339.00	73	38		0

**Exhibit 2G.2 Continued**

340.00	76	47		0
341.00	77	51		0
342.00	76	56		0
343.00	71	49		0.01
344.00	64	47		0.11
345.00	64	57		0.53
346.00	65	57		T
347.00	70	56		0.01
348.00	71	64		0.05
349.00	67	50		0
350.00	59	45		0
351.00	72	48		T
352.00	70	48		0.46
353.00	65	35		0
354.00	57	39		0
355.00	54	31		0
356.00	51	29		0
357.00	66	25		T
358.00	66	41		0.17
359.00	47	32		0
360.00	53	31		0
361.00	48	27		0
362.00	57	25		0
363.00	63	45		0
364.00	45	26		0
365.00	49	25		0
averages=	<b>73.03288</b>	<b>52.80274</b>	sum =	<b>33.58</b>

**Exhibit 2G.3: NOAA Weather Download (2002).** The below table is the collection of weather information downloaded from the NOAA website for Cherry Point in 2002. The columns represent daily maximum and minimum temperatures, plus precipitation.

Julian Date (2002)	Tmax (°F)	Tmin (°F)	Tobs (°F)	Prcp (in.)
1.00	47	32		0
2.00	40	31		0.07
3.00	35	29		0.45
4.00	36	25		0.1
5.00	50	21		0
6.00	64	29		0.6
7.00	48	32		0
8.00	45	26		0
9.00	55	25		0
10.00	67	44		0
11.00	68	37		0
12.00	61	33		0.04
13.00	55	30		0.22
14.00	59	26		0.24
15.00	63	38		0.14
16.00	50	34		0
17.00	63	37		0
18.00	57	42		0
19.00	68	41		0.17
20.00	49	40		0.06
21.00	62	40		0.28
22.00	58	41		0
23.00	64	42		0.98
24.00	76	58		0
25.00	65	38		0.14
26.00	62	38		0
27.00	70	37		0
28.00	75	44		0.03
29.00	76	45		0
30.00	79	51		0
31.00	77	62		0
32.00	76	63		0
33.00	65	41		T
34.00	50	39		0
35.00	53	32		T
36.00	43	28		0
37.00	99999	32		0.09
38.00	63	38		1.41
39.00	61	40		0.09

Exhibit 2G.3 Continued

40.00	63	35		0
41.00	66	45		0.17
42.00	61	36	T	
43.00	62	32		0
44.00	57	37		0
45.00	53	39		0
46.00	67	37		0.25
47.00	65	47		0
48.00	55	40		0
49.00	51	30		0
50.00	61	25		0
51.00	71	42	T	
52.00	71	48		0.22
53.00	63	38		0
54.00	53	43		0.09
55.00	56	40		0
56.00	62	37		0
57.00	70	38		0
58.00	60	30		0.09
59.00	46	24		0
60.00	53	20		0
61.00	66	43		0.87
62.00	69	60		0.67
63.00	60	32	T	
64.00	49	29		0
65.00	61	26		0
66.00	69	36		0
67.00	71	44		0
68.00	75	50		0
69.00	67	45		0.02
70.00	55	42		0
71.00	70	48		0.08
72.00	69	57		2.02
73.00	71	52		0
74.00	77	51		0
75.00	80	60		0
76.00	66	52		0.1
77.00	69	51	T	
78.00	60	51	T	
79.00	77	54		0.14
80.00	67	46		0.3
81.00	50	31		0
82.00	56	28		0

**Exhibit 2G.3 Continued**

83.00	70	32		0
84.00	77	43		0
85.00	76	53		0.05
86.00	69	50		0.34
87.00	60	41		0
88.00	72	40		0
89.00	76	66		0
90.00	79	67		0.52
91.00	71	51		0.13
92.00	74	46		0
93.00	80	56	T	
94.00	56	50	T	
95.00	60	42	T	
96.00	58	37		0
97.00	59	38		0
98.00	71	37		0
99.00	78	62	T	
100.00	71	57		0.02
101.00	76	52		0
102.00	78	58		0.01
103.00	72	55		0.18
104.00	80	57		0
105.00	82	68		0.14
106.00	86	63		0
107.00	88	65		0
108.00	89	67	T	
109.00	85	66		0.36
110.00	86	67		0.03
111.00	86	67		0.01
112.00	90	65		0
113.00	69	50		0
114.00	71	46		0.01
115.00	73	57		0.07
116.00	68	56		0
117.00	71	58	T	
118.00	87	68		0
119.00	88	59		0
120.00	71	54		0
121.00	78	56		0.12
122.00	85	67		0
123.00	83	63	T	
124.00	67	57		0.92
125.00	64	56	T	

Exhibit 2G.3 Continued

126.00	79	54		0
127.00	81	66		0
128.00	87	69	T	
129.00	86	67		0
130.00	90	72		0.03
131.00	76	66		0
132.00	88	63		0
133.00	85	69		0.67
134.00	72	53		0.09
135.00	76	48		0
136.00	79	50		0
137.00	84	59		0
138.00	88	57		0.18
139.00	62	55		0.05
140.00	69	46		0
141.00	70	44	T	
142.00	70	55		0.01
143.00	75	51		0
144.00	86	50		0
145.00	93	60		0
146.00	85	58		0
147.00	85	59		0
148.00	86	62		0
149.00	79	70		0.97
150.00	81	70		0.24
151.00	86	65	T	
152.00	94	70		0.49
153.00	95	70		0
154.00	87	69		0.01
155.00	86	65		0
156.00	85	68		0
157.00	86	67		0
158.00	81	66		0.07
159.00	78	62		0
160.00	85	59		0
161.00	89	56		0
162.00	86	59		0
163.00	92	69		0
164.00	97	73		0
165.00	91	70		1.65
166.00	88	69		0
167.00	88	64		0
168.00	85	66		0.76

**Exhibit 2G.3 Continued**

169.00	80	69		0.38
170.00	78	69		0.1
171.00	79	70		0.1
172.00	81	71		0.1
173.00	82	70		0.14
174.00	86	68		0.01
175.00	87	68		0
176.00	88	71		0
177.00	86	72		0.12
178.00	82	75		0.64
179.00	90	73		0.07
180.00	90	72	T	
181.00	86	69		0
182.00	87	64		0
183.00	90	67		0
184.00	89	71		0
185.00	90	74		0
186.00	95	71		0.07
187.00	88	70		0
188.00	87	64		0
189.00	88	61		0
190.00	91	67		0
191.00	94	74		0.17
192.00	82	72		0.23
193.00	81	69		0
194.00	84	72		0.03
195.00	84	70		0.49
196.00	89	75	T	
197.00	95	76		0
198.00	95	75		0
199.00	94	72		0
200.00	93	76		0.83
201.00	95	73		0.17
202.00	89	73		1.13
203.00	89	72		0.06
204.00	85	76		0.04
205.00	85	73		0.15
206.00	88	73		0.82
207.00	89	73		3.5
208.00	90	74		0.66
209.00	94	75		0
210.00	95	78		0
211.00	96	79		0

**Exhibit 2G.3 Continued**

212.00	93	74		T
213.00	92	74		0
214.00	89	71		T
215.00	90	72		0
216.00	89	75		0
217.00	89	72		0
218.00	91	68		T
219.00	84	68		0
220.00	84	65		0
221.00	85	60		0
222.00	85	61		0
223.00	88	59		0
224.00	91	66		0
225.00	92	72		0
226.00	89	71		0
227.00	88	73		T
228.00	89	72		T
229.00	94	75		T
230.00	94	75		0
231.00	95	74		T
232.00	92	74		T
233.00	91	73		0
234.00	93	68		0
235.00	101	75		0
236.00	99	74		0.01
237.00	94	74		T
238.00	84	72		0.43
239.00	87	73		0.3
240.00	76	72		2.33
241.00	86	72		0.77
242.00	79	74		0.08
243.00	84	72		1.17
244.00	85	74		0.56
245.00	79	69		T
246.00	88	70		0
247.00	90	70		0
248.00	88	75		0
249.00	84	66		0
250.00	84	70		T
251.00	87	73		T
252.00	83	73		0.24
253.00	80	75		0.88
254.00	93	69		0

Exhibit 2G.3 Continued

255.00	80	65		0
256.00	82	62		0
257.00	84	69		0.72
258.00	85	69		0.13
259.00	82	73		0.73
260.00	86	72		0
261.00	81	67		0
262.00	84	67		0
263.00	85	66		0
264.00	86	66		0
265.00	86	67		0.05
266.00	85	69		0.05
267.00	77	70		0.05
268.00	79	70		0.63
269.00	83	74		0.36
270.00	85	74		0
271.00	89	73	T	
272.00	80	70		0
273.00	82	67		0
274.00	85	67		0
275.00	88	65		0
276.00	90	67		0
277.00	87	70		0
278.00	90	65		0
279.00	82	69		0
280.00	85	65		0
281.00	78	66		0
282.00	79	65		0
283.00	81	69	T	
284.00	81	70		1.22
285.00	76	68		0.01
286.00	81	61		0.14
287.00	71	59		0.08
288.00	69	60		0.77
289.00	76	60	T	
290.00	74	57		0
291.00	65	45		0
292.00	73	44		0
293.00	76	53		0
294.00	67	56		0.18
295.00	67	54	T	
296.00	70	52		0
297.00	64	56		0.13

Exhibit 2G.3 Continued

298.00	71	61		0.03
299.00	75	59		0
300.00	71	57		0
301.00	74	62		0.04
302.00	65	59		0.24
303.00	61	50		0.56
304.00	57	46		0
305.00	60	37		0
306.00	59	39		0
307.00	59	41		0
308.00	59	47		0.06
309.00	73	50		0.05
310.00	74	48		0.73
311.00	58	38		0
312.00	66	35		0
313.00	74	40		0
314.00	77	62		0.29
315.00	82	63		0.1
316.00	77	58		0.08
317.00	58	44		0.47
318.00	61	37		0
319.00	68	36		0.07
320.00	68	58		0.62
321.00	67	49		0.6
322.00	54	36		0.01
323.00	64	34		0
324.00	61	40		0
325.00	62	52		0.02
326.00	68	42		0
327.00	53	35		0
328.00	65	34		0
329.00	72	36		0
330.00	61	40		0
331.00	53	38		0
332.00	47	26		0
333.00	53	24		0
334.00	64	49		0
335.00	49	26		0
336.00	57	22		T
337.00	54	29		0
338.00	43	29		0.13
339.00	45	35		0.3
340.00	47	32		0

**Exhibit 2G.3 Continued**

341.00	48	25		0
342.00	56	24		0
343.00	48	38	T	
344.00	49	41		0.6
345.00	50	44		0.01
346.00	55	42		0
347.00	67	44		0.53
348.00	57	44		0
349.00	55	35		0
350.00	64	36		0
351.00	50	35		0
352.00	54	36		0
353.00	69	45		0.05
354.00	70	49		0.15
355.00	60	35		0
356.00	65	30		0
357.00	62	39		0
358.00	52	36		0.45

359.00	58	38	T	
360.00	49	30		0
361.00	50	24		0
362.00	50	24		0
363.00	64	37		0
364.00	71	33		0
365.00	72	46		0.08
			sum =	<b>46.56</b>

**Appendix 2H: Catchments K2 and K3 Surface Data**

**Exhibit 2H.1: Partial Impervious Surface Attribute Table for Catchment K2.** This table was created by selecting the ArcVIEW shapefiles and exporting the attribute information in order to determine the percent imperviousness of this catchment.

<b>Catchment K3 Impervious Surface Shapefile</b>						
<b>ID</b>	<b>TYPE</b>	<b>ID</b>	<b>NAME</b>	<b>AREA_FEET</b>	<b>PERIMETER_</b>	<b>ACRES</b>
2	flight line	10	area J	81.806	154.835	0.002
2	flight line	10	area J	82.691	38.188	0.002
2	flight line	10	area J	33.383	37.994	0.001
2	flight line	10	area J	159.015	530.703	0.004
2	flight line	10	area J	282.089	345.738	0.006
2	flight line	10	area J	76.297	35.224	0.002
2	flight line	10	area J	126.047	46.122	0.003
2	flight line	10	area J	29.929	25.416	0.001
2	flight line	10	area J	216.183	58.892	0.005
2	flight line	10	area J	709.037	1040.309	0.016
2	flight line	10	area J	81.350	44.223	0.002
2	flight line	10	area J	64.426	33.398	0.001
2	flight line	10	area J	427.258	82.749	0.010
2	flight line	10	area J	153.507	284.460	0.004
2	flight line	10	area J	49.031	28.329	0.001
2	flight line	10	area J	196.563	56.393	0.005
2	flight line	10	area J	12.520	14.238	0.000
2	flight line	10	area J	15.406	16.231	0.000
2	flight line	10	area J	291.993	403.889	0.007
2	flight line	10	area J	17.277	17.739	0.000
2	flight line	10	area J	131408.300	5296.372	3.017
3	parking lots	1	area A	2086.885	556.731	0.048
3	parking lots	1	area A	575.794	108.091	0.013
3	parking lots	1	area A	560.008	105.510	0.013
3	parking lots	1	area A	244.111	93.904	0.006
3	parking lots	1	area A	113113.977	2035.103	2.597
3	parking lots	2	area B	80.660	86.431	0.002
3	parking lots	2	area B	93172.247	3888.764	2.139
3	parking lots	3	area C	491.927	179.536	0.011
3	parking lots	3	area C	3603.203	240.107	0.083
3	parking lots	3	area C	383.768	81.739	0.009
3	parking lots	3	area C	24133.616	1127.198	0.554
3	parking lots	4	area D	0.041	1.042	0.000
3	parking lots	5	area E	1400.576	169.442	0.032
3	parking lots	5	area E	633.063	102.624	0.015
3	parking lots	5	area E	210.308	82.683	0.005

Exhibit 2H.1 Continued

3	Parking lots	5	area E	51.457	29.349	0.001
3	Parking lots	5	area E	34.566	21.088	0.001
3	Parking lots	5	area E	62.219	39.038	0.001
3	Parking lots	5	area E	11.736	155.159	0.000
3	Parking lots	5	area E	184.178	58.693	0.004
3	Parking lots	5	area E	34988.358	3005.645	0.803
3	Parking lots	6	area F	971.220	140.157	0.022
3	Parking lots	6	area F	260.561	79.529	0.006
3	Parking lots	6	area F	57880.837	3799.128	1.329
3	parking lots	7	area G	563.660	854.265	0.013
3	parking lots	7	area G	897.019	118.453	0.021
3	parking lots	7	area G	0.101	1.822	0.000
3	parking lots	7	area G	562.306	126.302	0.013
3	parking lots	7	area G	60.786	120.926	0.001
3	parking lots	7	area G	8.571	14.170	0.000
3	parking lots	7	area G	23.010	32.734	0.001
3	parking lots	7	area G	41.183	78.200	0.001
3	parking lots	7	area G	78931.530	1771.295	1.812
3	parking lots	7	area G	17.176	15.116	0.000
3	parking lots	7	area G	81.457	130.620	0.002
3	parking lots	7	area G	400.594	80.616	0.009
3	parking lots	7	area G	191.867	58.691	0.004
3	parking lots	7	area G	244.523	65.426	0.006
3	parking lots	7	area G	128.750	41.330	0.003
3	parking lots	7	area G	1462.667	180.191	0.034
3	parking lots	7	area G	161413.714	6194.288	3.706
3	parking lots	8	area H	123007.476	2331.745	2.824
3	parking lots	9	area I	31.250	22.368	0.001
3	parking lots	9	area I	16.808	149.724	0.000
3	parking lots	9	area I	322.125	88.134	0.007
3	parking lots	9	area I	338.383	88.914	0.008
3	parking lots	9	area I	4.640	92.438	0.000
3	parking lots	9	area I	223317.604	5128.393	5.127
3	parking lots	10	area J	2.370	13.194	0.000
3	parking lots	10	area J	21.606	63.892	0.000
3	parking lots	10	area J	47.039	27.624	0.001
3	parking lots	10	area J	195.445	65.368	0.004
3	parking lots	10	area J	44.279	55.781	0.001
3	parking lots	10	area J	105.210	42.147	0.002
3	parking lots	10	area J	104.316	40.885	0.002
3	parking lots	10	area J	81.215	192.333	0.002
3	parking lots	10	area J	20.958	45.086	0.000
3	parking lots	10	area J	48.109	27.983	0.001
3	parking lots	10	area J	27.998	44.313	0.001
3	parking lots	10	area J	27933.979	1942.551	0.641

Exhibit 2H.1 Continued

3	parking lots	11	area K	220.012	62.126	0.005
3	parking lots	11	area K	351.139	86.246	0.008
3	parking lots	11	area K	356.453	89.760	0.008
3	parking lots	11	area K	1829.141	219.271	0.042
3	parking lots	11	area K	1410.641	151.260	0.032
3	parking lots	11	area K	6.727	10.524	0.000
3	parking lots	11	area K	104.965	49.693	0.002
3	parking lots	11	area K	145245.590	5510.087	3.334
3	parking lots	12	area L	4.572	17.468	0.000
3	parking lots	12	area L	719.462	670.122	0.017
3	parking lots	12	area L	461.281	105.169	0.011
3	parking lots	12	area L	146.191	48.378	0.003
3	parking lots	12	area L	233.570	63.255	0.005
3	parking lots	12	area L	84.479	56.711	0.002
3	parking lots	12	area L	145.716	312.392	0.003
3	parking lots	12	area L	65.957	79.143	0.002
3	parking lots	12	area L	11.044	13.784	0.000
3	parking lots	12	area L	213.622	61.016	0.005
3	parking lots	12	area L	0.911	27.236	0.000
3	parking lots	12	area L	17.602	15.275	0.000
3	parking lots	12	area L	9133.156	376.999	0.210
3	parking lots	12	area L	1631.738	183.857	0.037
3	parking lots	12	area L	4648.961	285.236	0.107
3	parking lots	12	area L	281686.860	9861.444	6.467
3	parking lots	13	area M	569.618	119.472	0.013
3	parking lots	13	area M	365.003	1395.354	0.008
3	parking lots	13	area M	15.989	18.127	0.000
3	parking lots	13	area M	12.840	14.489	0.000
3	parking lots	13	area M	88.359	52.192	0.002
3	parking lots	13	area M	79.161	50.601	0.002
3	parking lots	13	area M	28575.080	738.127	0.656
3	parking lots	13	area M	85.813	51.573	0.002
3	parking lots	13	area M	286.852	70.130	0.007
3	parking lots	13	area M	77.758	51.441	0.002
3	parking lots	13	area M	47811.283	1033.980	1.098
3	parking lots	13	area M	295.620	70.953	0.007
3	parking lots	13	area M	159.000	55.688	0.004
3	parking lots	13	area M	156.363	55.289	0.004
3	parking lots	13	area M	164.242	56.581	0.004
3	parking lots	13	area M	8.848	25.215	0.000
3	parking lots	13	area M	157.563	55.914	0.004
3	parking lots	13	area M	38.390	108.496	0.001
3	parking lots	13	area M	158.250	55.649	0.004
3	parking lots	13	area M	134.105	50.261	0.003
3	parking lots	13	area M	259.395	68.032	0.006

**Exhibit 2H.1 Continued**

3	parking lots	13	area M	140.344	52.157	0.003
3	parking lots	13	area M	150.652	53.576	0.003
3	parking lots	13	area M	142.465	53.484	0.003
3	parking lots	13	area M	139.148	52.069	0.003
3	parking lots	13	area M	119.566	52.065	0.003
3	parking lots	13	area M	163.316	55.957	0.004
3	parking lots	13	area M	140.031	53.760	0.003
3	parking lots	13	area M	20.688	43.041	0.000
3	parking lots	13	area M	5.938	16.070	0.000
3	parking lots	13	area M	7.172	30.309	0.000
3	parking lots	13	area M	5959.352	318.554	0.137
3	parking lots	13	area M	9.091	12.214	0.000
3	parking lots	13	area M	44.818	65.966	0.001
3	parking lots	13	area M	232458.865	10226.255	5.337
4	roads	1	area A	18070.933	1915.443	0.415
4	roads	2	area B	8969.013	1723.110	0.206
4	roads	6	area F	12177.998	1431.785	0.280
4	roads	7	area G	13024.015	1259.158	0.299
4	roads	9	area I	6526.260	696.453	0.150
4	roads	10	area J	88.412	42.372	0.002
4	roads	10	area J	8.151	13.835	0.000
4	roads	10	area J	145445.755	5000.679	3.339
4	roads	11	area K	27724.344	2906.904	0.636
4	roads	12	area L	65.909	67.921	0.002
4	roads	12	area L	71.949	68.977	0.002
4	roads	12	area L	41902.784	4572.602	0.962
4	roads	13	area M	69.893	71.146	0.002
4	roads	13	area M	66.812	70.548	0.002
4	roads	13	area M	35921.787	3885.394	0.825

**Exhibit 2H.2: Impervious Surface Attribute Table for Catchment K3.** This figure was created by selecting the ArcVIEW shapefiles of interest and then exporting their attributes into Microsoft Excel. The area information was then utilized to effectively characterize the catchments in SWMM and XPSWMM.

<b>Catchment K3 Impervious Surface Shapefile</b>							
<b>Shape</b>	<b>Id</b>	<b>Type</b>	<b>Source</b>	<b>Area (sq. ft)</b>	<b>Perimeter (ft.)</b>	<b>Acres</b>	<b>Hectares</b>
Shape	4	Roads	S0_area.shp	45768.645	2679.044	1.051	0.425
Shape	3	parking lots	S0_area.shp	49053.474	2354.038	1.126	0.456
Shape	3	parking lots	S1_area.shp	29028.616	1622.321	0.666	0.27
Shape	4	roads	S10_area.shp	43514.729	3763.877	0.999	0.404
Shape	3	parking lots	S10_area.shp	147866.637	6476.869	3.395	1.374
Shape	4	roads	S11_area.shp	12168.639	2676.481	0.279	0.113
Shape	3	parking lots	S11_area.shp	118568.304	4368.851	2.722	1.102
Shape	4	roads	S12_area.shp	22277.768	2960.069	0.511	0.207
Shape	3	parking lots	S12_area.shp	100724.623	2341.483	2.312	0.936
Shape	4	roads	S13_area.shp	7927.725	1665.129	0.182	0.074
Shape	3	parking lots	S13_area.shp	399293.672	6440.398	9.167	3.71
Shape	4	roads	S14_area.shp	20443.424	2996.43	0.469	0.19
Shape	3	parking lots	S14_area.shp	134346.933	4125.266	3.084	1.248
Shape	4	roads	S15_area.shp	16440.215	1687.244	0.377	0.153
Shape	3	parking lots	S15_area.shp	121954.248	4517.839	2.8	1.133
Shape	4	roads	S16_area.shp	31386.773	3422.345	0.721	0.292
Shape	3	parking lots	S16_area.shp	195298.291	4864.895	4.483	1.814
Shape	4	roads	S2_area.shp	18462.846	1322.448	0.424	0.172
Shape	3	parking lots	S2_area.shp	53510.941	1921.525	1.228	0.497
Shape	3	parking lots	S3_area.shp	80543.734	2733.898	1.849	0.748
Shape	4	roads	S4_area.shp	15513.313	1207.795	0.356	0.144
Shape	3	parking lots	S4_area.shp	47080.624	2729.398	1.081	0.437
Shape	4	roads	S5_area.shp	140810.233	8796.012	3.233	1.308
Shape	3	parking lots	S5_area.shp	392453.957	10621.197	9.01	3.646
Shape	4	roads	S6_area.shp	62088.973	5381.339	1.425	0.577
Shape	3	parking lots	S6_area.shp	208202.076	7165.354	4.78	1.934

**Exhibit 2H.2 Continued**

Shape	4	roads	S7_area.shp	64204.461	4864.624	1.474	0.596
Shape	3	parking lots	S7_area.shp	441505.061	12595.619	10.136	4.102
Shape	4	roads	S8_area.shp	85306.282	6340.073	1.958	0.793
Shape	3	parking lots	S8_area.shp	418026.124	12492.782	9.597	3.884
Shape	4	roads	S9_area.shp	50272.191	4249.929	1.154	0.467
Shape	3	parking lots	S9_area.shp	255621.557	9817.533	5.868	2.375

## Appendix 2I: Research Notes

**Exhibit 2I.1: Cherry Point Field Notes Samples.** The following information is a collection of notes that document download times and dates, problems with water measurement devices and other observations relevant to the Cherry Point stormwater runoff research. The label "BE" refers to the Blue Earth microprocessor and the "SF" was used to identify the STARFLOW water meter.

### Field Notes from Cherry Point MCAS visit, dated 09/26/2001

---

**Area K1:** railroad culvert  
Real time: 940  
BE time: 907  
Staff reading: 0.045m  
BE reading: .040  
SF file name: \*.u6o  
Voltage BE: 13.3  
Voltage SF: 14.0

*SF velocity reading: 0mm/s@3mm*  
SF time: 842

Comments: R1 reading: 3.07 in. (4 weeks)  
1. Algal buildup on SF  
2. Replaced desiccant

---

**Area K2:** woods  
Real time: 1008  
BE time: 936  
Staff reading: 0.10m  
BE reading: -.01m (incorrect)  
SF file name: \*.u6p (40 KB)  
Voltage BE: 12.2  
Voltage SF: 11.8

*Velocity SF: 137 mm/s @16mm*  
SF time: 910

Comments:

1. Heavy debris at weir, removed as much as possible
2. Reset well read point
3. NOTE: possibly should readjust weir setup: the counterweight was maxed out at the highest height, therefore it was touching the pulley and exposed from the tubing....no further upward movement for the weight is possible under these conditions.

## Exhibit 2I.1 Continued

---

**Area K3:** open field  
Real time: 1030  
BE time: 955  
Staff reading: .065m  
BE reading: .066  
SF file name: \*.u6q (40 KB)  
Voltage BE: 12.58  
Voltage SF: 13.64  
Velocity SF: 36mm/s @ 51mm  
SF time: 930

Comments: R2: 3.16 in (4 weeks)  
1.

Note time differences in BE and SF

---

**Area K4:** *convenience store*  
  
*Real time: 1047*  
BE time: 1007  
  
*Staff reading: too low*  
BE reading: **-0.105**  
  
*SF file name: \*.u6r*  
Voltage BE: 3.8 (dead battery)  
Voltage SF: 13.8  
Velocity SF: 0 mm/s @ 0mm  
SF time: 948

Comments:

1. water level too low for accurate staff measurement and SF
2. BE battery was dead, only 61 saved blocks of data
3. Replaced BE battery and checked to see if now working properly

---

**Area K5:** runway  
Real time: 1127  
BE time: 1040  
  
*Staff reading: 0.09m*  
BE reading: .089m  
SF file name: \*.u6s  
Voltage BE: 14.0  
Voltage SF: 12.8  
Velocity SF: 0 mm/s @ 19mm  
Time SF: 1028

**Exhibit 2I.1 Continued**

Comments: R3: 2.82 in (4 weeks)

1. SF and BE times seem to be off considerably

**Exhibit 21.2: Field Notes Compilation Indicating Field Problems at Cherry Point MCAS.**  
 This exhibit was created to summarize the problems that were introduced during the research period, including the problem description and any actions taken to alleviate the predicament.

<b>Cherry Point Compiled FN Problems and Actions Spreadsheet (created 8.20.02)</b>			
<b>BE=Blue Earth SF=STARFLOW</b>			
<b>Date</b>	<b>location</b>	<b>problem description</b>	<b>Actions</b>
<b>9.28.00</b>	P4	SF dislodged	
<b>10.11.00</b>	K4	no weir installed yet no weir yet	
<b>11.03.00</b>	K1 K2 K5	staff not set no weir installed SF clock resetting back to 1.12.80 BE time adjusted by one hour	
<b>11.22.00</b>	K3  K1  K2 K1	BE no returning to sleep mode since 11.02.00 SF clock off by 45 minutes  all BE elevations are negative  leak in culvert so SF not capturing all flow (was downstream then) SF problems...wont convert data to ASCII format frozen R1 contents	unplugged and checked reinitialized test1 scheme reset well read point moved SF upstream
<b>12.15.00</b>	K2  K3 K4 K5 K1	SF date resetting back to 1.1.80 SF velocity, large flow...are units reasonable check SF data...low flow visually, compare to other values condensation found in box high flow have passed....debris on weir buckles pulley tangled around potentiometer shaft	
	K2	incorrect stage measurements since late November dislodged SF wire...no download available no SF download available	

Exhibit 2I.2 Continued

1.5.01	K3	SF date still malfunctioning resetting to 1.1.80 BE showing signs of rust BE battery dead...only 315 data points...stopped 12.1.00 changed BE battery. now unable to establish communication...disconnected	brought back to lab
	K5	initially SF error while downloading	attempted again..ok
	K1	water frozen in manual gauge	estimated volume
	K2	newer HOBO top available  SF detached timeout on SF prompt...unable to download	replaced with update SF removed swapped SF and loaded test1 scheme
	K3	BE replaced...fixed in lab and tested...ok? pulley stuck	set read point and parameters Detangled
2.16.01	K4	incorrect SF date...12.31.00	
	K1	incorrect BE read point	reset well read point
3.01.01	K4	inspected new SF location...not submerged weir is leaking BF apparatus too low	move SF downstream  raise location with pipe
	K3	BE already awake since 2.22.01	
4.12.01	K4	not SF velocity reading during test mode Weir leaking note SF velocity reading	plugged with Oakum
	all sites	note time...daylight savings time shift	leave alone, will adjust by itself
5.07.01	K4	unable to download SF. "time out prompt"	
	K1	SF velocity incorrect	

Exhibit 2I.2 Continued

5.24.01	K2	floodgate 90% closed in barrel #1	contacted dept. of env.affairs...no response
	K4	BE has little data...only 688 saved blocks SF not working properly	reloaded scheme and returned to check
	K1	SF velocity incorrect	replaced SF and programmed with test1 scheme
6.19.01	K2 K3 K4	floodgate 90% closed in barrel #1 strong smell of urine in rain gauge 2 low water depth over SF SF dislodged	
	K2	floodgate 90% closed in barrel #1	
7.03.01	K3	barrel #1 entrance clogged with debris	Unclog
	K4	SF malfunctioning...time/date discrepancies SF completely dislodged incorrect stage measurements	reprogrammed scheme
	K5	SF completely dislodged	reset well read point
	K1	BE red light on...only 108 saved blocks...dead battery	Reattach reloaded Des2.bas program and checked later
7.12.01		Be no longer working properly...will not return from sleep mode even if forced to wake	pulled and brought to lab
	K2 K3	floodgate 90% closed in barrel #1 SF relaunched automatically	check downloaded file
	K4	weir dislodged and downstream no ponded water...stage levels not recorded	remount next visit
	K1	replaced BE. Set weir factor and read point	
	K2 K3	floodgate 90% closed in barrel #1 rainfall difference from other gauges SF time off	

Exhibit 2I.2 Continued

	K4	BE red light already on...4 saved blocks reattached weir and secured with nails reattached SF mounting bracket	replaced battery
	K5	differences in all rain gauges	
<b>8.02.01</b>	K1	pulley stuck...incorrect stage readings SF un-side-down low BE battery...BE not waking up	untangled strings SF flipped over and secured attempted to force awake...did not work
	K2	floodgate 90% closed in barrel #1 SF recording high velocities BE initially not waking up after download	manually reset
	K3	BE did not wake without manual boost...only 38 blocks of saved data	
	K4	lowered staff because did not replace weir reattached potentiometer to pulley shaft	reset well read point
	K5	Downloaded BE data very noisy...negative numbers?	
<b>8.22.01</b>	K1	SF not recording velocity	
		BE recording elevation changes every3 min. regardless to difference	reset read parameter to make measurements for 10mm changes. then checked
	K2	opened floodgate on barrel #1 SF facing downstream reattached SF but needs new hardware and mounting plate	check data since floodgate closed
	K4	weir washed downstream again SF battery reading incorrect...reporting 16.13V	
<b>9.26.01</b>	K2	BE reading off	reset well read point

Exhibit 2I.2 Continued

		counterweight maxed out	adjusted string situation
	K4	time differences in SF and BE water level too low for measurement for staff or SF	
	K5	BE battery dead..61 saved blocks	replaced BE battery
<b>11.02.01</b>	K1	SF and BE times off SF not submerged	
	K2	SF date incorrect SF stage readings are low when compared to previous readings	
	K3	SF date incorrect incorrect SF date	
	K4	water level too low for measurement for staff or SF	
	K5	SF and BE times off rain gauge #3 seems off as compared to other gauges area under construction	need adjustment?  remove equipment in 3 weeks...see how construction effected data
<b>12.19.01</b>	K2	weir full...blocked with debris	
	K3	BE time incorrect	
	K4	water level too low for measurement for staff or SF	
<b>1.10.02</b>	K2	BE stuck since last download...depth of 2.225m	reset well read point
		debris clogging barrel #1	
	K3	BE awake upon arrival BE seemed to be stuck at a .113m	check data
<b>1.31.02</b>	K2	constant BE values of .090ms since last download	
		BE not responding to pulley changes SF not recording any velocity BE readings no good...pulley stuck at .131m	pulled BE and replace
<b>2.14.02</b>	K3		
	K2	loose wire on BE circuit board	replaced BE. reset well read point
		No BE data available for download	

Exhibit 2I.2 Continued

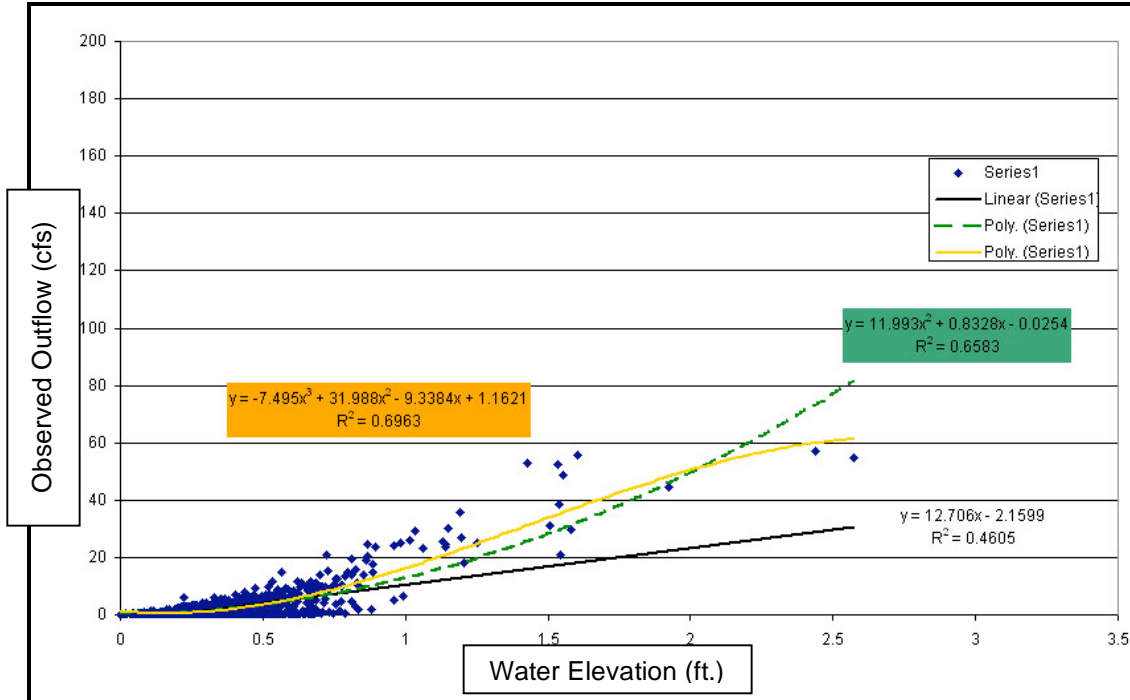
<b>2.26.02</b>	K3	SF dislodged. pointing backwards pulley stuck at .145m mark	replaced bolts review data to see where stuck
	K2	evidence of beaver activity	check data for this period
<b>4.18.02</b>	K3	BE awake upon arrival. stopped recording on 2.24.02	
	K1	SF dislodged	reattached with nail gun
<b>5.23.02</b>		inserting dual stainless steel floodgates downstream R1 rain seems low compared to other areas	
	K2	BE reading off	reset well read point
	K3 K1	SF date incorrect...reporting 4.06.02 SF depth incorrect	probably ok since low flow
<b>6.14.02</b>	K2	BE reading off	reset well read point...problem is recurring
	K3	SF time off SF date still incorrect...reporting 4.06.02	reloaded scheme and returned to check
<b>7.12.02</b>	K1	no problems to report	
<b>7.12.02</b>	K1	lost BE data...exited program prematurely	
<b>8.14.02</b>		SF dislodged	reattached with nail gun
	K2 K3	SF depth seems high SF depth seems high here also SF not working properly...unable to download	look at data left SF in place...no replacement available
	K1	R3 has been tampered with entire location has been submerged...all equipment malfunctioned	possibly due to downstream floodgate closure
	K2	SF damaged...hole in sensor pulled ALL equipment except staff SF battery dead	pull and return to lab replaced battery

Exhibit 2I.2 Continued

09.09.02	K3	SF date incorrect...depth off...program not reading voltage correctly BE read off	reset well read point
	K1	SF not working again. unable to download...powered down message Replaced BE, set pulley parameters, set well read point	viewed red light...seems okay
09.23.02	K2	downloaded HOBO removed extra solar panel swapped BE battery reset well read point to 0.120m large dataset for SF...	
	K3	SF date incorrect attempted SF download	same power down failure message
	K1	changed desiccant SF was removed at last visit	
10.15.02	K2	pulled extra solar panel SF still malfunctioning	
	K3	SF download failure	same power down failure message
	K1	HOBO recorder not responding properly	removed and brought to lab
11.18.02	K2	Replaced the HOBO recorder with a spare logger during last visit, discovered that a beaver dam existed upstream from the logging station...officials plan to implode the dam soon	
	K3	R3 gauge is reporting a larger rainfall depth as compared to the other stations.	
	K1	HOBO problems...spider webs in tipping bucket	Possibly recorded number of tips is incorrect, so compare to manual gauge value.
	K2	reset well read point to 120 mm BE timing is off slightly	
	K3	heavy condensation inside box R3 gauge is reporting a larger rainfall depths	

**Appendix 2J:** Outflow Regression Graphs for Catchment K2 at Cherry Point

**Exhibit 2J.1: Catchment K2 Regression Graph Excluding Outliers (2001).** This graph includes all stage elevations and flow rates used to establish a mathematical relationship between these two numbers, excluding outliers. The color boxes contain equations that describe the trend lines using linear, polynomial and exponential functions.



**Exhibit 2J.2: Piecewise Catchment K2 Regression Graph (2001).** The accompanying figure is a collection of hydrologic data for catchment K2 excluding water stages below 1 ft.

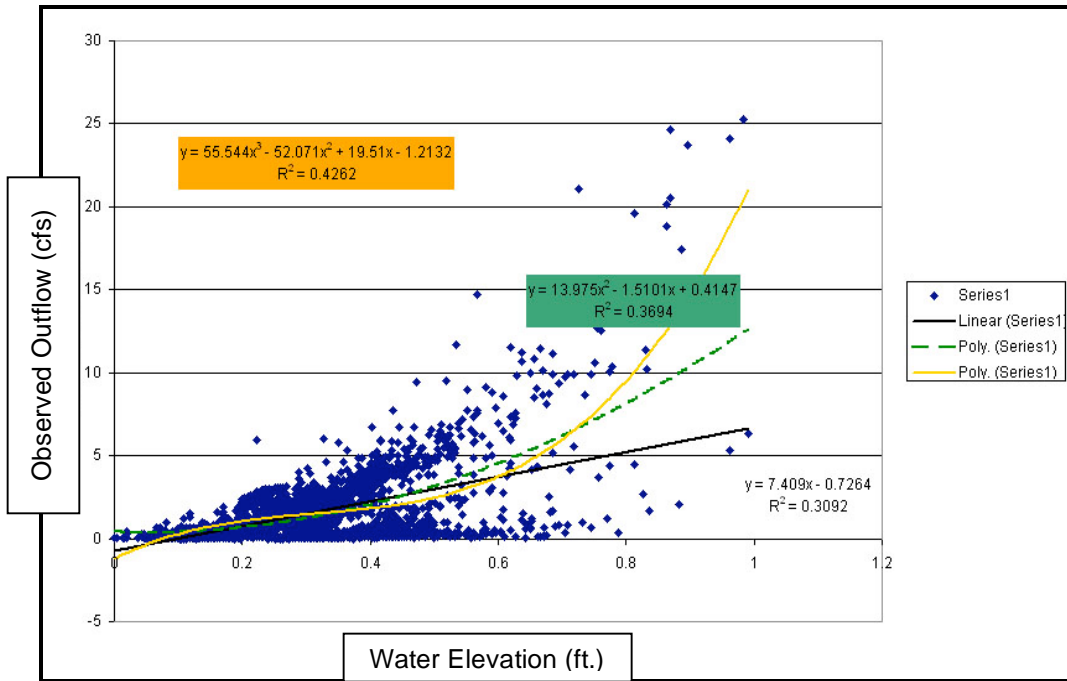


**Exhibit 2J.3: Piecewise Catchment K2 Regression Graph (2001).** The accompanying figure is a collection of hydrologic data for catchment K2 including water stages above 1 ft. The colored lines represent three sets of the equations used to mathematically describe the data points.

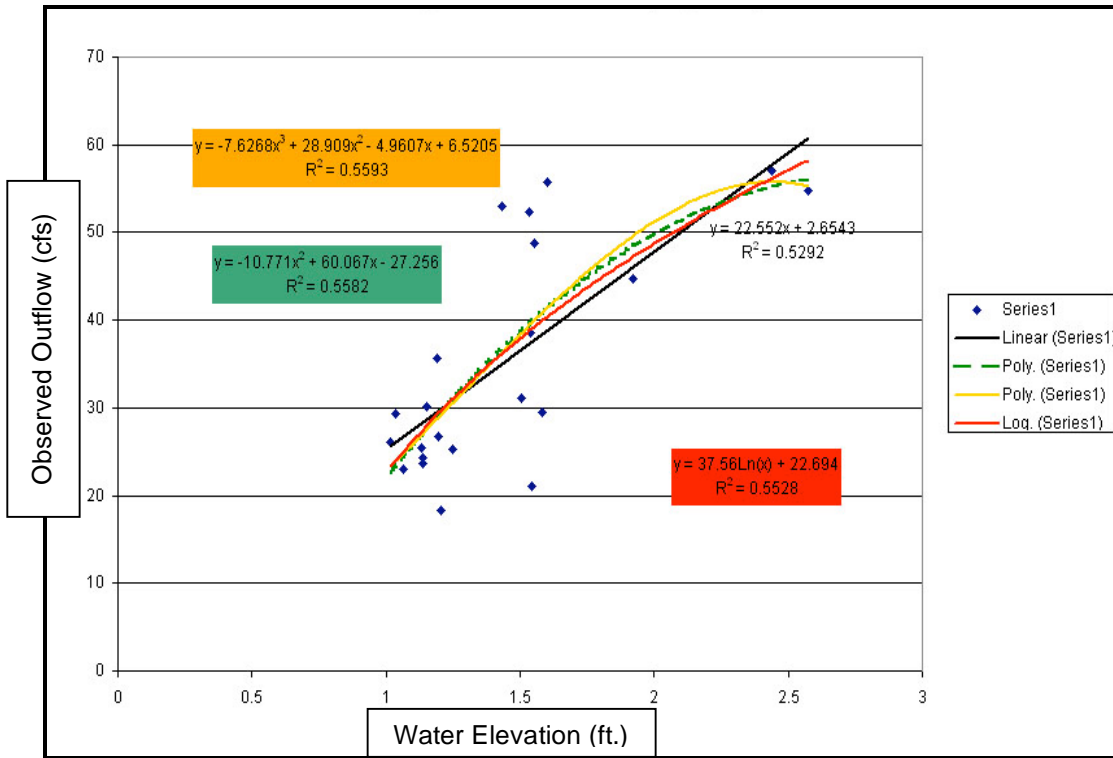


**Exhibit 2J.4: Catchment K2 Observed and Regression Predicted Flows.** The purpose of this diagram is to demonstrate the performance of the piecewise, regression equations in relationship to the measured data.

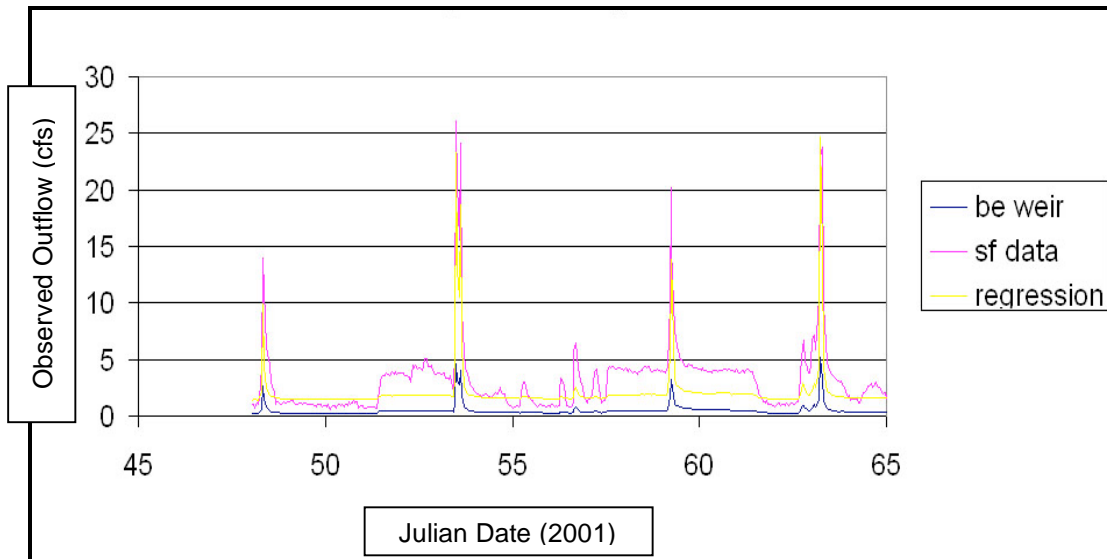


**Exhibit 2J.5: Catchment K3 Regression Graph Excluding Outliers (2001).** This graph includes all stage elevations and flow rates used to establish a mathematical relationship between these two figures, excluding outliers. Three types of regression equations were used to identify the relationship between the two datasets.

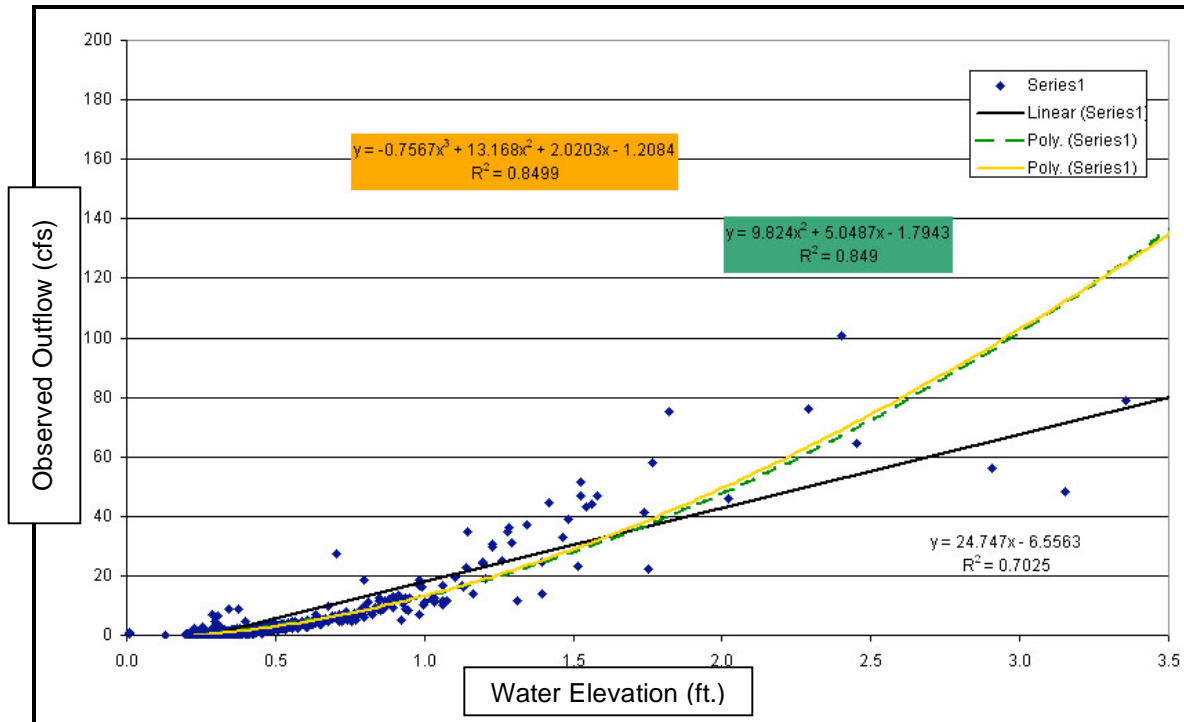


**Exhibit 2J.6: 2001 Catchment K3 Regression Graph for Water Elevations Below 1ft.** The below presentation shows the regression equations generated for the K3 catchment following the removal of the stage elevations greater than 1 ft.

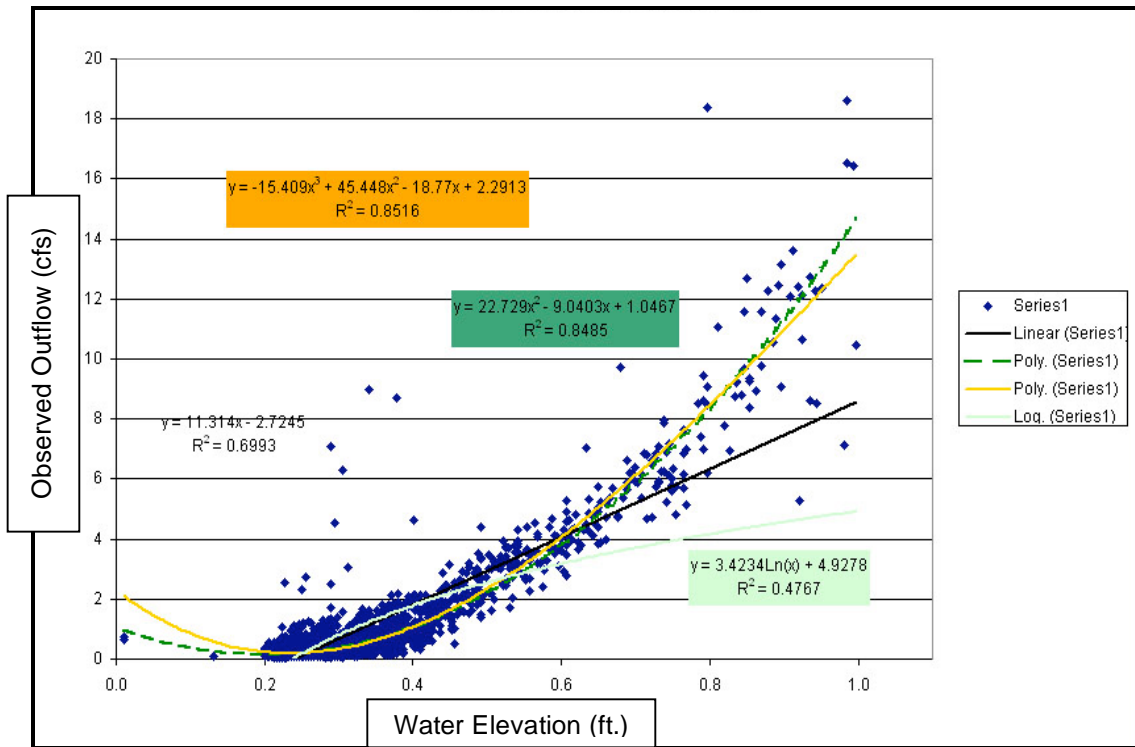


**Exhibit 2J.7: Catchment K3 Regression Graph for Water Elevations Greater Than 1 Ft.**  
 This exhibit focuses on establishing a relationship between the BE stage values and the SF flow measurements when the recorded water elevation was greater than or equal to 1 ft. The resulting three equations describe the shape of the colored trendlines.

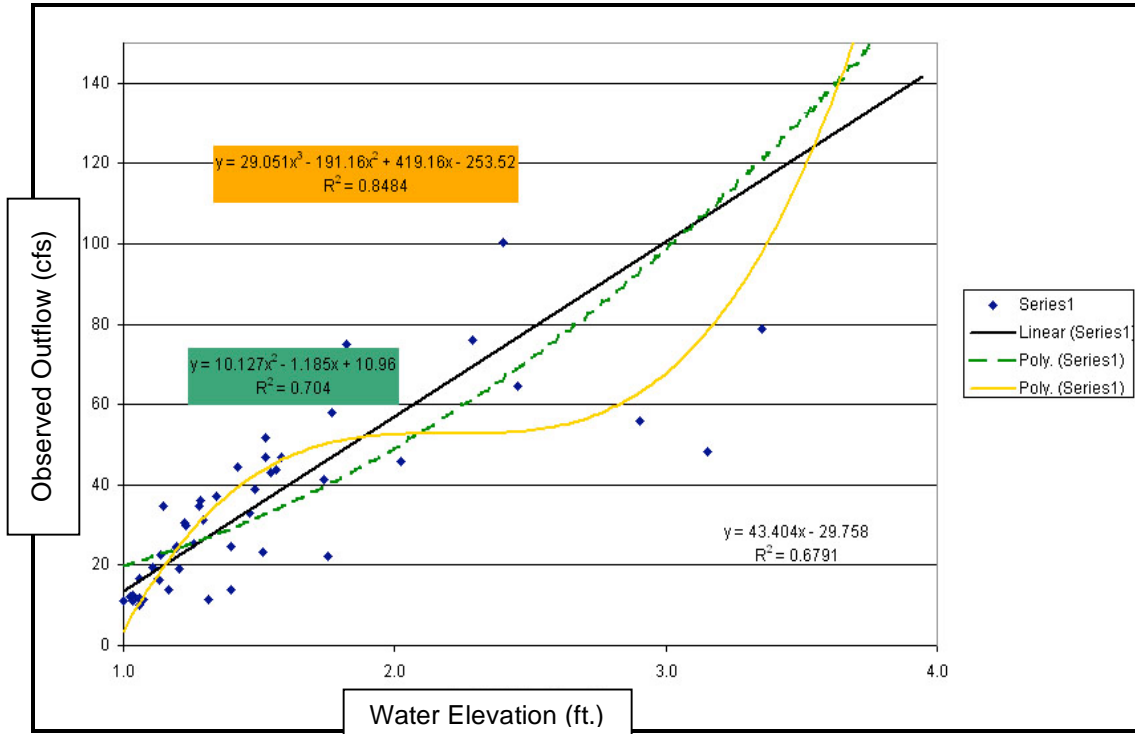
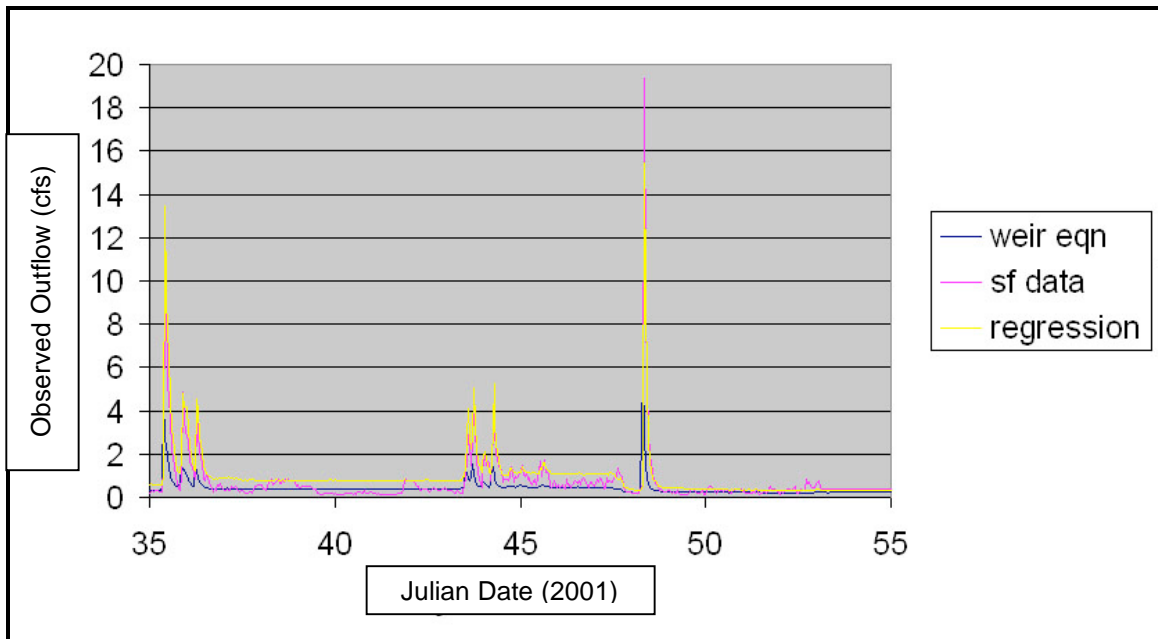


**Exhibit 2J.8: Catchment K3 Hydrograph from Three Sources (2001).** The purpose of this demonstration is to display the regression equations predicted flows in comparison to the observed flows during several storm events.



**Appendix 2K:** Cherry Point Observed Precipitation Data

**Exhibit 2K.1: Observed Rainfall File (2000).** The following information is the downloaded rainfall dataset that would eventually be inserted into the hydrologic model. The rain gauge is located near the outlet of catchment K1.

Date	Time	1/100 (in.)	
12/15/2000	44:32.0	0	Start
12/16/2000	04:13.0	1	
12/16/2000	06:28.0	2	
12/16/2000	22:50.5	3	
12/16/2000	28:59.5	4	
12/16/2000	50:58.0	5	
12/16/2000	49:09.5	6	
12/16/2000	24:35.0	7	
12/16/2000	25:04.5	8	
12/16/2000	26:09.0	9	
12/16/2000	27:29.5	10	
12/16/2000	29:26.0	11	
12/16/2000	37:14.5	12	
12/16/2000	41:03.0	13	
12/16/2000	47:34.0	14	
12/16/2000	54:20.0	15	
12/16/2000	50:50.0	16	
12/16/2000	51:02.0	17	
12/17/2000	01:14.0	18	
12/17/2000	29:37.5	19	
12/17/2000	22:35.0	20	
12/17/2000	33:58.0	21	
12/17/2000	35:04.5	22	
12/17/2000	35:35.5	23	
12/17/2000	37:45.5	24	
12/17/2000	43:09.5	25	
12/17/2000	44:35.5	26	
12/17/2000	49:06.5	27	
12/17/2000	50:05.5	28	
12/17/2000	50:53.5	29	
12/17/2000	52:06.0	30	
12/17/2000	52:50.0	31	
12/17/2000	53:20.5	32	
12/17/2000	53:51.0	33	
12/17/2000	54:32.0	34	
12/17/2000	57:10.0	35	
12/17/2000	00:07.0	36	
12/17/2000	04:09.0	37	

**Exhibit 2K.1 Continued**

12/17/2000	10:24.5	38	
12/17/2000	11:50.5	39	
12/19/2000	07:29.5	40	
12/19/2000	49:34.0	41	
12/27/2000	33:43.5	42	
12/27/2000	23:10.0	43	
12/27/2000	36:50.5	44	
12/27/2000	01:35.5	45	
12/27/2000	24:51.5	46	
12/27/2000	45:19.5	47	
12/27/2000	55:53.5	48	
12/27/2000	11:43.0	49	
12/27/2000	26:42.0	50	
12/27/2000	49:01.5	51	
12/27/2000	01:02.5	52	
12/27/2000	36:55.0	53	
12/27/2000	52:53.5	54	
12/28/2000	16:00.0	55	
12/28/2000	33:01.0	56	
12/28/2000	05:05.0	57	
12/28/2000	19:28.0	58	
12/28/2000	47:44.5	59	
12/28/2000	56:14.0	60	
12/28/2000	26:39.5	61	
12/28/2000	44:37.0	62	
12/28/2000	02:27.5	63	
12/28/2000	28:47.5	64	
12/28/2000	02:56.5	65	
1/5/2001	38:29.0	65	End

**Exhibit 2K.2: Manual Rain Gauge Comparison for Cherry Point (2000).** The below table is a collection of rainfall amounts as recorded by the three manual rain gauge located throughout the research area at Cherry Point, NC.

date	gauge no.	rain (in.)	gauge no.	rain (in.)	gauge no.	rain (in.)
1/5/2001	1	0.93	2	0.9	3	0.82
2/16/2001	1	1.07	2	1.03	3	1.09
3/1/2001	1	1.79	2	1.72	3	1.91
3/22/2001	1	2.51	2	2.62	3	2.53
4/12/2001	1	0.91	2	0.91	3	0
5/7/2001	1	0.82	2	0.9	3	1.97
5/24/2001	1	1.45	2	1.24	3	0.73
6/19/2001	1	8.47	2	7.15	3	6.43
7/3/2001	1	0.88	2	1.12	3	1.91
7/12/2001	1	1.91	2	0.98	3	0.84
8/2/2001	1	3.54	2	2.88	3	3.9
8/22/2001	1	4.9	2	4.46	3	4.25
9/26/2001	1	0	2	0	3	0
11/2/2001	1	0.63	2	0.63	3	0.02
12/19/2001	1	2.42	2	2.35	3	0.02
	sums	<b>32.23</b>		<b>28.89</b>		<b>26.42</b>
NOAA sum: <b>33.58 in.</b> tipping bucket: <b>27.37in.</b>  measured avg. <b>29.18</b> difference: <b>1.81 in.</b>						

**Exhibit 2K.3: Cherry Point Cumulative Rainfall for Year 2001.** The cumulative precipitation depths from the NOAA downloads and the tipping bucket recorder have been projected in the below figure.

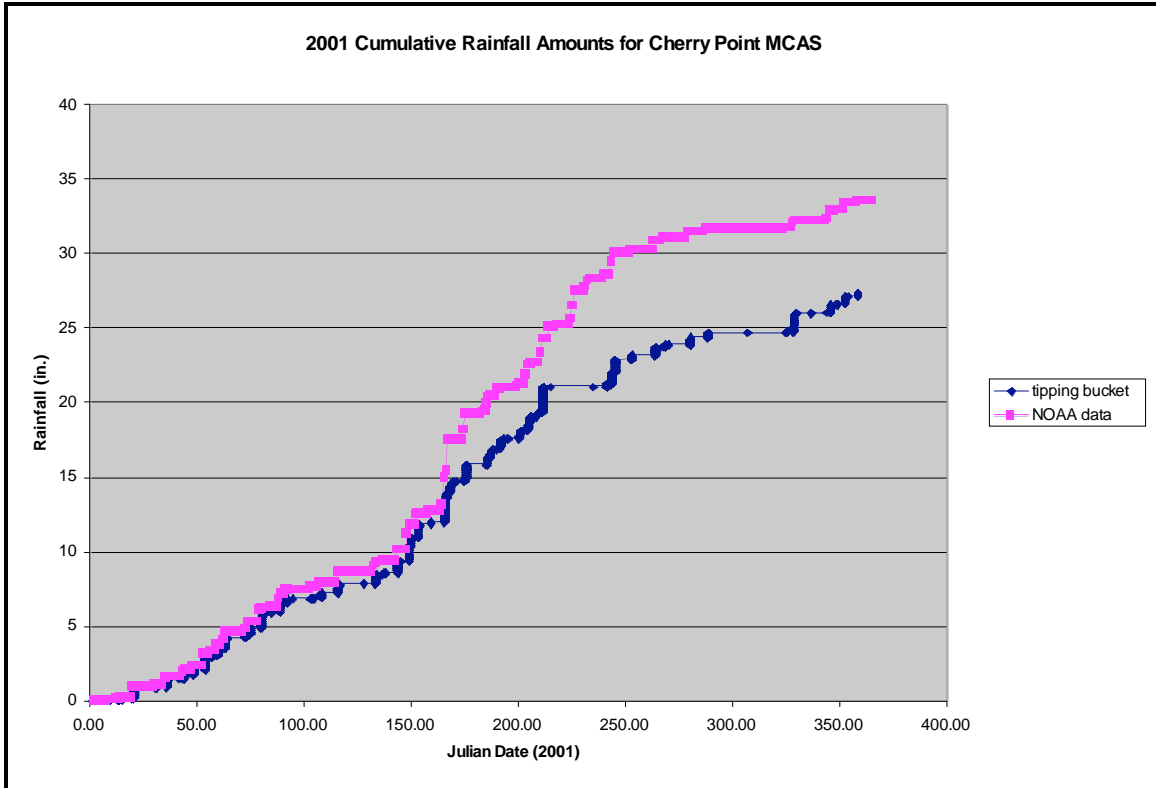


**Exhibit 2K.4: Cherry Point Cumulative Rainfall for Year 2002.** This chart contains rainfall information from two sources and attempts to graphically display the associated differences.

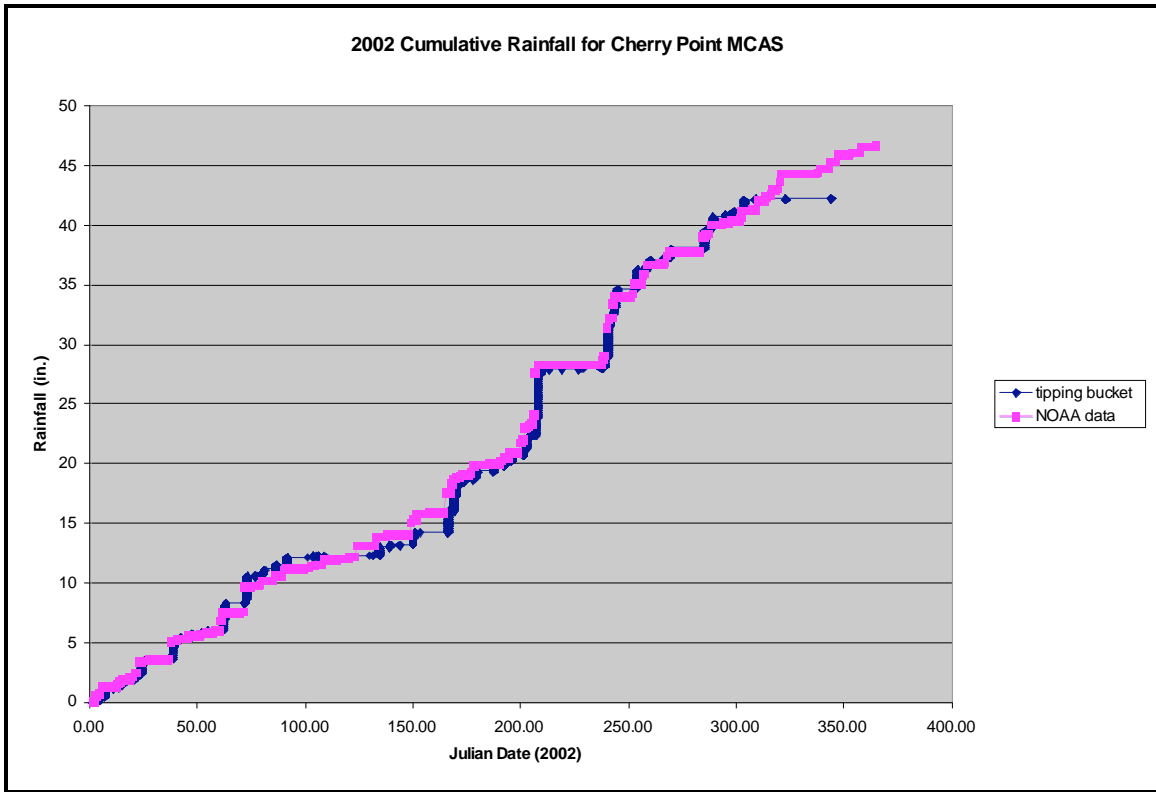


**Exhibit 2K.5: 2001 Rainfall Distribution Using the Anderson-Darling Method.** The below graph is the results acquired after applying a normal distribution analysis for the 2001 precipitation data for Cherry Point.

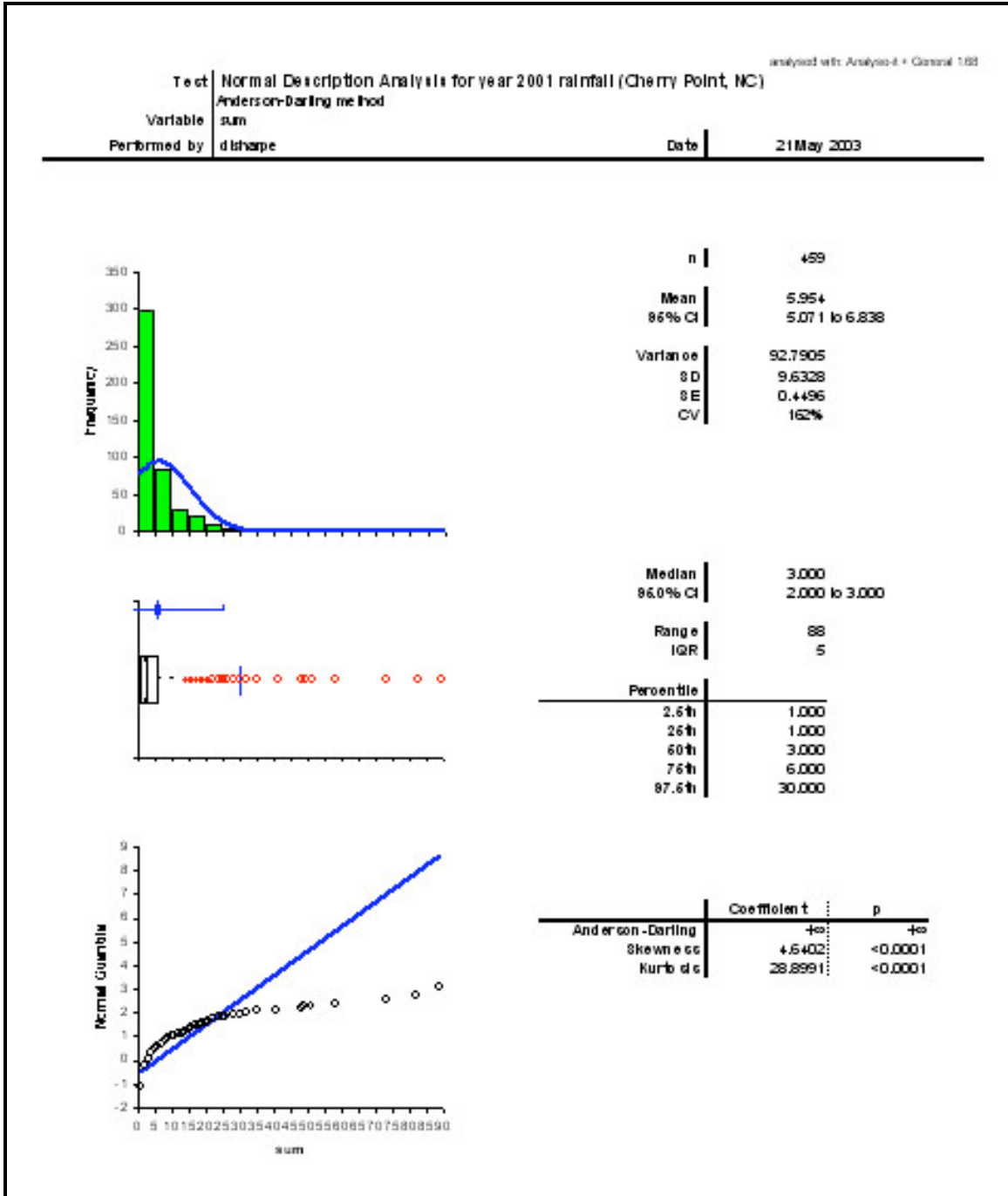


**Exhibit 2K.6: 2001 Rainfall Distribution Using the Shapiro-Wilk Method.** The below graph is the results acquired after applying a normal distribution analysis for the 2001 precipitation data for Cherry Point.

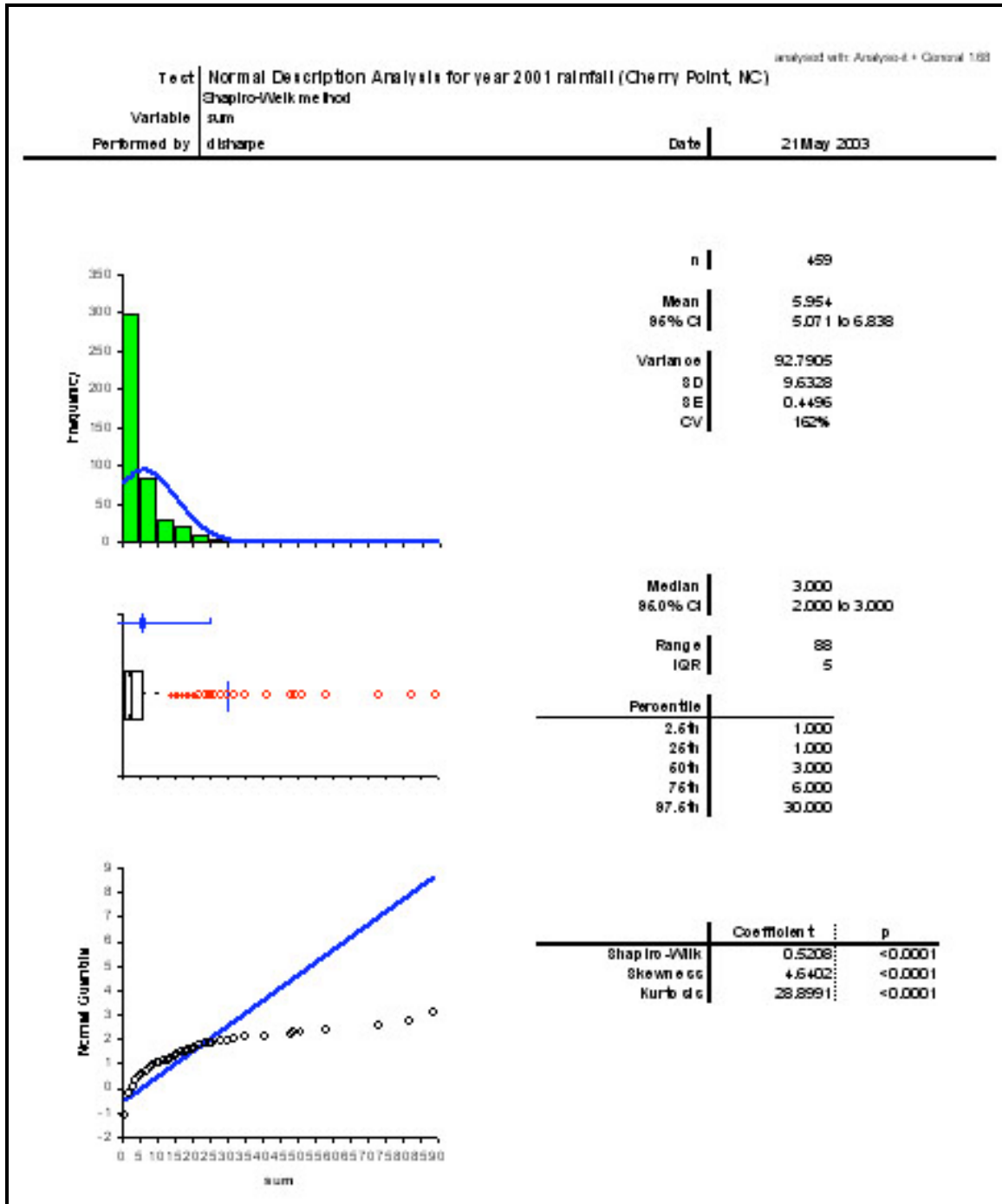


**Exhibit 2K.7: 2002 Rainfall Distribution Using the Anderson-Darling Method.** The following results were received after applying a normal distribution analysis for the Cherry Point precipitation data in 2002.

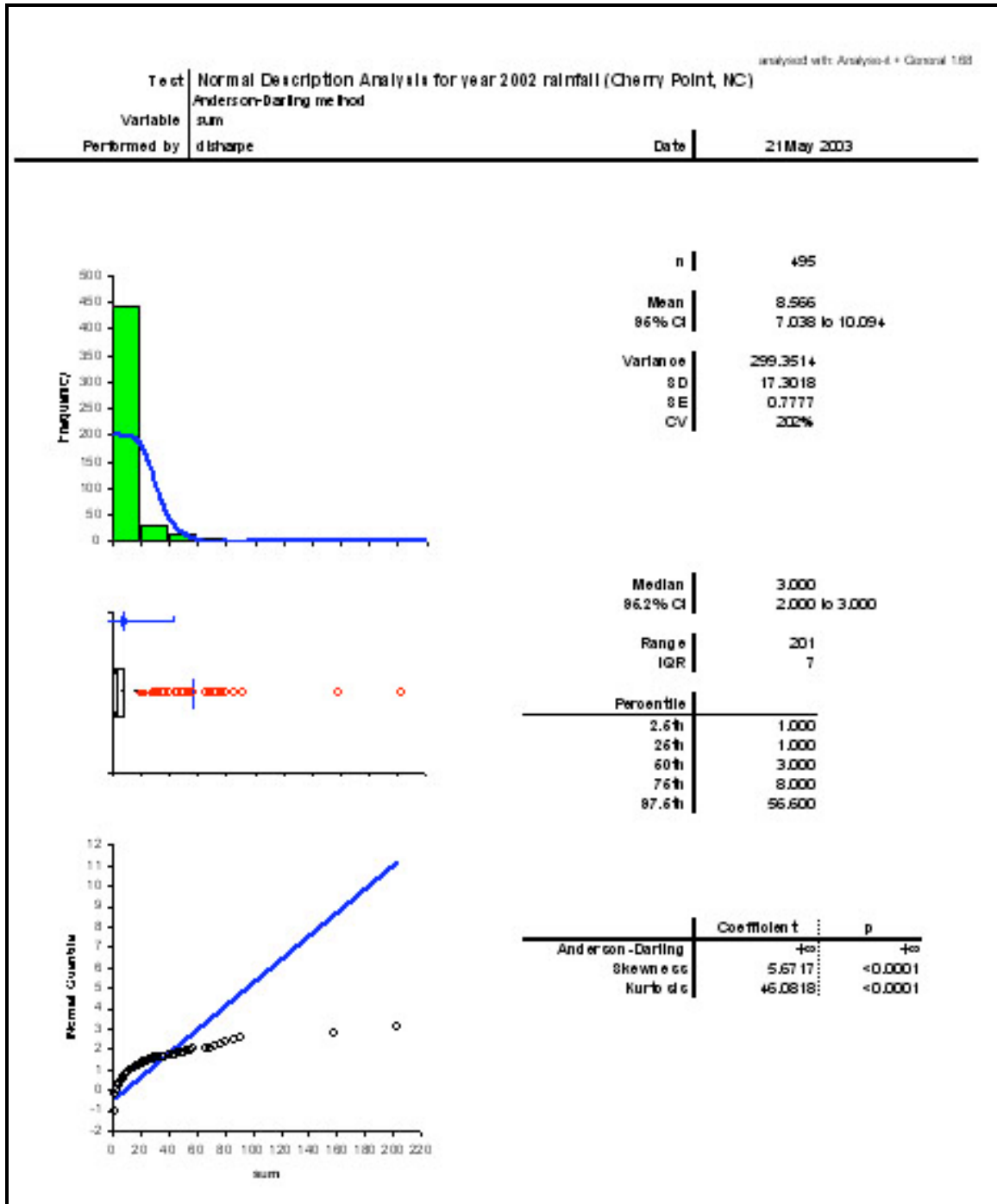


**Exhibit 2K.8: 2002 Rainfall Distribution Using the Shapiro-Wilk Technique.** The following results were received after applying a normal distribution analysis for the Cherry Point precipitation data in 2002.

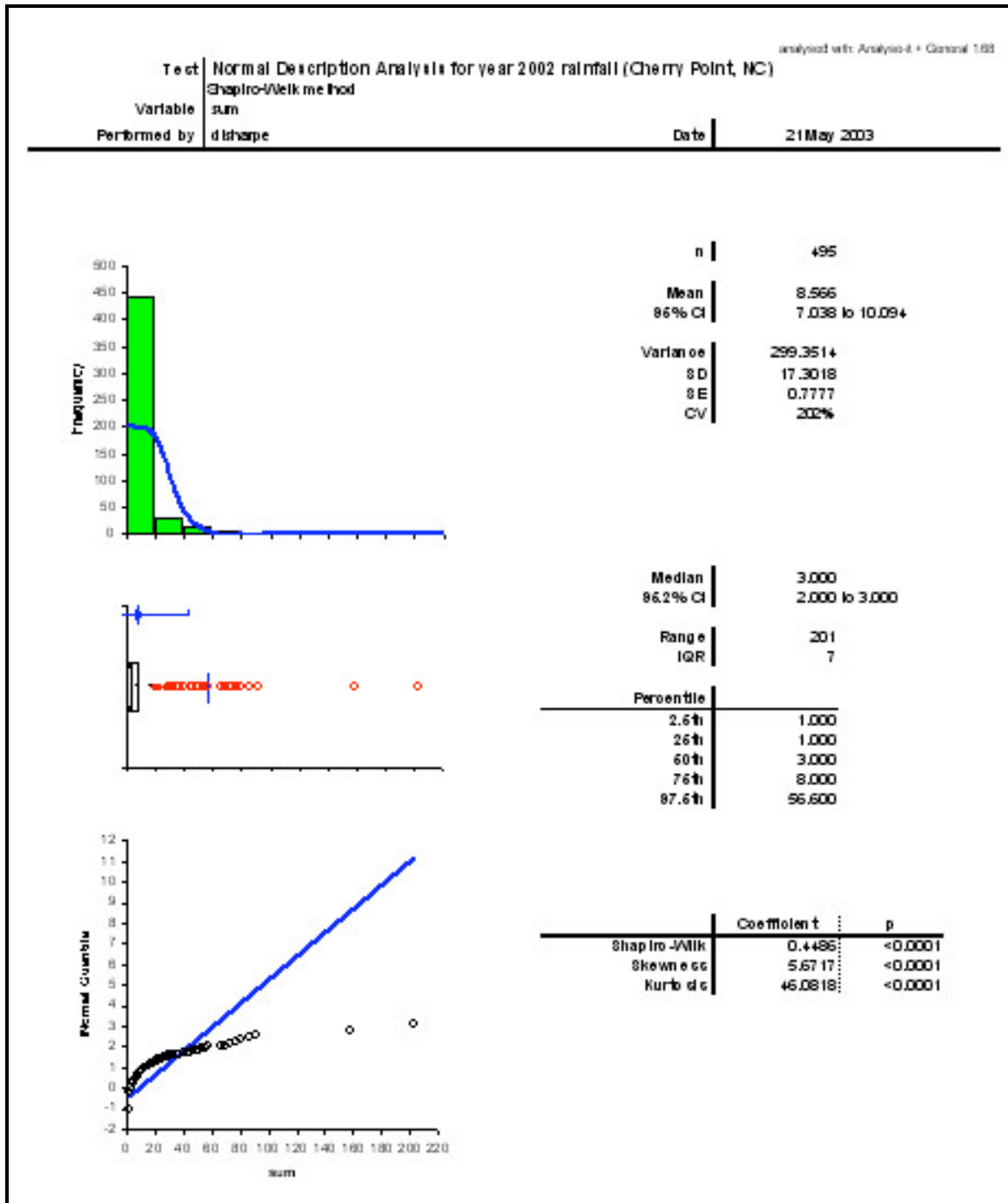


**Exhibit 2K.9: 2001 Cherry Point Lognormal Rainfall Distribution Results.** The following information was acquired after investigating if the Cherry Point precipitation exhibited the likeness of a lognormal distribution.

XLSTAT version 6.1 - Distribution Fitting		
Data: workbook = 2001 distro.xls / sheet = Sheet1 / range = \$G\$2:\$G\$460 / 459 rows and 1 column		
Estimation by the method of moments		
Probability distribution fitted to the data: Lognormal LogN(1.125 , 1.139)		
Comparison between the parameters estimated from the data and those of the fitted distribution:		
	Estimated	Theoretical
Expected value	5.954	5.445
Variance	92.790	62.940
Skewness	4.610	7.464
Kurtosis	28.435	179.259
Kolmogorov-Smirnov test / two-tailed test:		
Kolmogorov-Smirnov's D statistic observed value	0.196	
p-value	< 0.0001	
Alpha/2	0.025	
Decision:		
At the level of significance $\alpha=0.050$ the decision is to reject the null hypothesis of no difference between empirical and theoretical cumulative distributions.		
In other words, the difference between empirical and theoretical cumulative distributions is significant .		
Chi-square goodness of fit test between observed frequencies and theoretical frequencies:		
Number of classes: 20		
Number of estimated parameters: 2		

**Exhibit 2K.9 Continued**

<p>Chi-square observed value                      66.723  p-value    &lt; 0.0001  Chi-square Critical value  (df = 17)    27.587  Alpha    0.050</p>						
<p>Decision:  At the level of significance <math>\alpha=0.050</math> the decision is to reject the null hypothesis of goodness of fit between observed frequencies and theoretical frequencies. In other words, the difference between observed frequencies and theoretical frequencies is significant .</p> <p>Chi-square goodness of fit without highest contribution:</p> <p>Number of classes: 19  Number of estimated parameters: 2</p>						
<p>Chi-square observed value                      46.129  p-value    &lt; 0.0001  Chi-square Critical value  (df = 16)    26.296  Alpha    0.050</p>						
<p>Decision:  At the level of significance <math>\alpha=0.050</math> the decision is to reject the null hypothesis of goodness of fit between observed frequencies and theoretical frequencies. In other words, the difference between observed frequencies and theoretical frequencies is significant .</p> <p>Comparison between observed and theoretical frequencies:</p>						
						Chi-square
Class	Lower bound	Upper bound	Observed frequency	Theoretical frequency		contr.
1	1.000	5.400	327	254.590		<b>20.595</b>
2	5.400	9.800	55	73.626		4.712

**Exhibit 2K.9 Continued**

3	9.800	14.200	30	28.928	0.040
4	14.200	18.600	18	13.808	1.273
5	18.600	23.000	12	7.444	2.788
6	23.000	27.400	4	4.365	0.031
7	27.400	31.800	3	2.723	0.028
8	31.800	36.200	2	1.782	0.027
9	36.200	40.600	0	1.211	1.211
10	40.600	45.000	1	0.849	0.027
11	45.000	49.400	2	0.611	3.158
12	49.400	53.800	1	0.450	0.674
13	53.800	58.200	1	0.337	1.304
14	58.200	62.600	0	0.257	0.257
15	62.600	67.000	0	0.199	0.199
16	67.000	71.400	0	0.156	0.156
17	71.400	75.800	1	0.124	6.215
18	75.800	80.200	0	0.099	0.099
19	80.200	84.600	1	0.080	10.564
20	84.600	89.000	1	0.065	13.367

*In bold, maximum contribution to Chi-square*

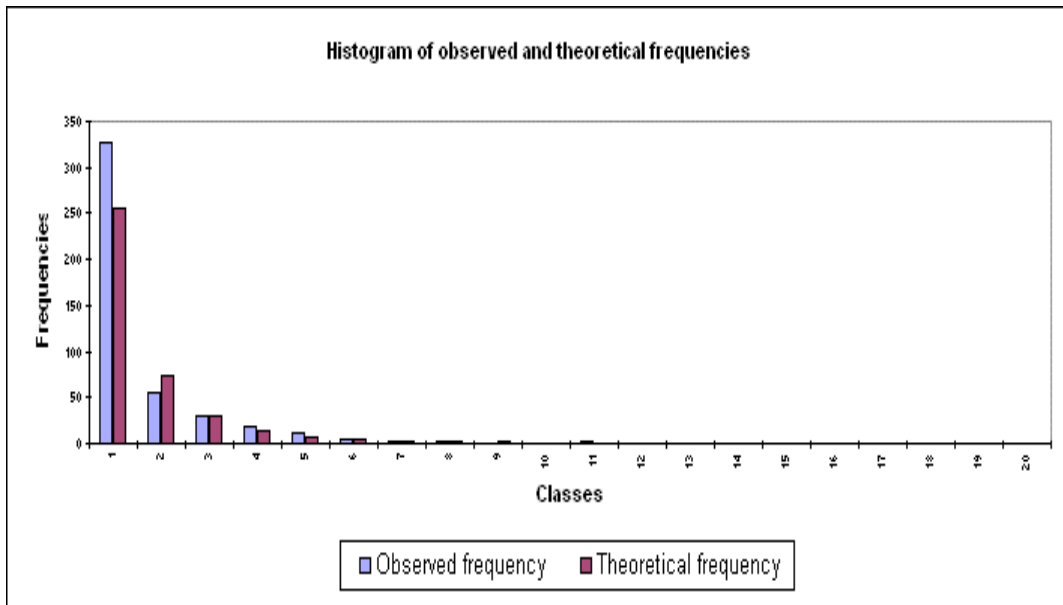


**Exhibit 2K.10: 2002 Cherry Point Lognormal Rainfall Distribution Results.** The 2002 rainfall data for the study site was also examined to determine if a lognormal distribution effectively characterized the observed data.

XLSTAT version 6.1 - Distribution Fitting - 5/27/2003 at 11:09:29 AM		
Data: workbook = 2002 distro .xls / sheet = Sheet2 / range = \$A\$2:\$A\$496 / 495 rows and 1 column		
Estimation by the method of moments		
Probability distribution fitted to the data: Lognormal LogN(1.256 , 1.491)		
Comparison between the parameters estimated from the data and those of the fitted distribution:		
	Estimated	Theoretical
Expected value	8.566	7.403
Variance	299.351	188.751
Skewness	5.637	11.958
Kurtosis	45.409	618.633
Kolmogorov-Smirnov test / two-tailed test:		
Kolmogorov-Smirnov's D statistic observed value	0.182	
p-value	< 0.0001	
Alpha/2	0.025	
Decision:		
At the level of significance $\alpha=0.050$ the decision is to reject the null hypothesis of no difference between empirical and theoretical cumulative distributions.		
In other words, the difference between empirical and theoretical cumulative distributions is significant .		
Chi-square goodness of fit test between observed frequencies and theoretical frequencies:		
Number of classes: 20		
Number of estimated parameters: 2		

**Exhibit 2K.10 Continued**

<p>Chi-square observed value            80.836 p-value                      &lt; 0.0001 Chi-square Critical value (df = 17)                        27.587 Alpha                         0.050</p>						
<p>Decision: At the level of significance <math>\alpha=0.050</math> the decision is to reject the null hypothesis of goodness of fit between observed frequencies and theoretical frequencies. In other words, the difference between observed frequencies and theoretical frequencies is significant .</p>						
<p>Chi-square goodness of fit without highest contribution:</p>						
<p>Number of classes: 19 Number of estimated parameters: 2</p>						
<p>Chi-square observed value            55.028 p-value                      &lt; 0.0001 Chi-square Critical value (df = 16)                        26.296 Alpha                         0.050</p>						
<p>Decision: At the level of significance <math>\alpha=0.050</math> the decision is to reject the null hypothesis of goodness of fit between observed frequencies and theoretical frequencies. In other words, the difference between observed frequencies and theoretical frequencies is significant .</p>						
<p>Comparison between observed and theoretical frequencies:</p>						
	Class	Lower bound	Upper bound	Observed frequency	Theoretical frequency	Chi-square contr.
	1	1.000	11.050	405	333.724	15.223
	2	11.050	21.100	45	50.963	0.698
	3	21.100	31.150	17	16.864	0.001
	4	31.150	41.200	6	7.456	0.284
	5	41.200	51.250	8	3.864	4.427

**Exhibit 2K.10 Continued**

6	51.250	61.300	3	2.219	0.275
7	61.300	71.350	2	1.370	0.289
8	71.350	81.400	5	0.893	18.881
9	81.400	91.450	2	0.607	3.192
10	91.450	101.500	0	0.427	0.427
11	101.500	111.550	0	0.309	0.309
12	111.550	121.600	0	0.229	0.229
13	121.600	131.650	0	0.173	0.173
14	131.650	141.700	0	0.133	0.133
15	141.700	151.750	0	0.104	0.104
16	151.750	161.800	1	0.082	10.218
17	161.800	171.850	0	0.066	0.066
18	171.850	181.900	0	0.053	0.053
19	181.900	191.950	0	0.044	0.044
20	191.950	202.000	1	0.036	<b>25.808</b>

*In bold, maximum contribution to Chi-square*

**Appendix 2L:** Excerpts of CPEC Inc. Metadata File for CP-MCAS

**DIRECTORY: 1GIS/drainage/CP Hydrology – NCSU**

FILE NAME	DESCRIPTION	SOURCE
cp industrialized zonef.apr	<b>ArcVIEW Project file</b>	Cpec
Buildings_cp.shp [POLYGON]	Buildings	MCAS-CP
contour_major (indust).shp [LINE]	topography: contour interval = 5 feet	MCAS-CP
contour_minor (indust).shp [LINE]	topography: contour interval = variable (1 foot; 0.5 foot)	MCAS-CP
cp soils (prelim).shp [POLYGON]	Soils (preliminary)	USDA- NRCS and Cpec
ephemeral channels (indust).shp [LINE]	ephemeral channels	Cpec
HywetInd.shp [POLYGON]	Jurisdictional wetlands	MCAS-CP
impervious surface (indust).shp [POLYGON]	Approximate impervious surface area	Cpec
Industrialized zone.shp [POLYGON]	Area of data coverage	Cpec
mcas .shp [POLYGON]	MCAS Cherry Point political boundary	MCAS-CP
ponded wetland (indust).shp [POLYGON]	Wetland area with ponded or standing water during Winter 2000	Cpec
retention ponds.shp [POLYGON]	retention ponds (permitted)	Cpec
roads.shp [LINE]	Roads (outline)	MCAS-CP
sheet-flow direction (indust).shp [LINE]	Approximate direction of sheet-flow	Cpec
stormwater open drainage network (indust).shp [LINE]	Stormwater system-open drainage network (ditches). Open drainage system includes the landscaped or perennially managed areas only! Excludes the woodland areas.	Cpec

**Appendix 2L Continued**

stormwater piped system (indust).shp [LINE]	Stormwater system-piped or subsurface drainage network	MCAS-CP
stormwater structures (indust).shp [POINT]	Stormwater system structures	MCAS-CP and Cpec
stream bed (indust).shp [POLYGON]	Approximate stream bed area	Cpec
stream centerline (indust).shp [LINE]	Centerline of streams	Cpec
stream points (indust).shp [POINT]	Cross-sectional midpoint of stream.	Cpec
water bodiescp.shp [POLYGON]	Water bodies of Cherry Point	MCAS-CP
watershed cpecf (indust).shp [POLYGON]	watersheds	Cpec

**Appendix 2L Continued**

**DIRECTORY: 1GIS/drainage/CP Hydrology – NCSU/Drgs**

FILE NAME	DESCRIPTION	SOURCE
catfish_lk.tif	<b><i>USGS 7.5' Quadrangle-Catfish Lake Quad (Digital Raster Graphics)</i></b>	USGS
hadnot_ck.tif	<b><i>USGS 7.5' Quadrangle-Hadnot Creek Quad (Digital Raster Graphics)</i></b>	USGS
masontown.tif	<b><i>USGS 7.5' Quadrangle-Masontown Quad (Digital Raster Graphics)</i></b>	USGS
newport.tif	<b><i>USGS 7.5' Quadrangle-Newport Quad (Digital Raster Graphics)</i></b>	USGS
Havelock.tif	<b><i>USGS 7.5' Quadrangle-Havelock Quad (Digital Raster Graphics)</i></b>	USGS
CherryPt.tif	<b><i>USGS 7.5' Quadrangle-Cherry Point Quad (Digital Raster Graphics)</i></b>	USGS

**Appendix 2L Continued**

**DIRECTORY: 1GIS/drainage/CP Hydrology – NCSU/Legends**

SHAPE FILE MATCH	LEGEND FILE (*.avl)	SOURCE
Buildings_cp.shp	buildings_cp.avl	MCAS-CP
contour_major (indust).shp	contour_major.avl	MCAS-CP
contour_minor (indust).shp	contour_minor.avl	MCAS-CP
cp soils (prelim).shp	general soil groups (a).avl (A-horizon soil textures) general soil groups (b).avl (B-horizon soil textures)	USDA- NRCS and Cpec
ephemeral channels (indust).shp	ephemeral channels.avl	Cpec
impervious surface (indust).shp	impervious surface .avl	Cpec
ponded wetland (indust).shp	ponded wetland.avl	Cpec
retention ponds.shp	retention ponds.avl	Cpec
roads.shp	roads.avl	MCAS-CP
sheet-flow direction (indust).shp	estimated sheet-flow direction.avl	Cpec
stormwater open drainage network (indust).shp]	stormwater open drainage network (indust).avl	Cpec
stormwater piped system (indust).shp	stormwater piped system (indust).avl	MCAS-CP
stormwater structures (indust).shp	stormwater structures (indust).avl	MCAS-CP and Cpec
stream bed (indust).shp	stream bed (indust).avl	Cpec
stream centerline (indust).shp	stream centerline (indust).avl	Cpec
stream points (indust).shp	stream points (indust).avl	Cpec
water bodiescp.shp	water bodiescp.avl	MCAS-CP
watershed cpecf (indust).shp	watershed cpecff.avl	Cpec

Appendix 2L Continued

**DIRECTORY:** 1GIS/drainage/CP Hydrology – NCSU/Plots

FILE NAME	EXPLANATION	SOURCE
stormindf.prn	Title: "Comprehensive Stormwater Conveyance Network Within the Industrialized Areas of Marine Corps Air Station, Cherry Point, NC"	Cpec

**4.0 DATABASE FIELD (\*.DBF) EXPLANATION**

**Buildings\_cp.dbf**

DBASE FIELD NAME	DESCRIPTION	SOURCE
FACNUM	<b>Facility number</b>	MCAS-CP
FAC_TYPE1	Structure or Building	MCAS-CP
FAC_TYPE2	Minor or major	MCAS-CP
DESC	Description	MCAS-CP
SOURCE	Unknown	MCAS-CP

**contour\_major (indust).dbf and contour\_minor (indust).dbf**

DBASE FIELD NAME	DESCRIPTION	SOURCE
LABEL	<b>Contour label to 1 decimal place</b>	MCAS-CP
ELEVATION	Contour elevation	MCAS-CP
LABEL2	Contour label	MCAS-CP

**Appendix 2L Continued**

**CP soils (prelim).dbf**

DBASE FIELD NAME	DESCRIPTION	SOURCE
SOIL_TYPE	<b>Soil Series identification</b>	USDA-NRCS
A_TEXTURE	A horizon soil texture (USDA Classification)	USDA-NRCS
B_TEXTURE	B horizon soil texture (USDA Classification)	USDA-NRCS
A_TEXTURE2	A horizon soil texture (abbreviated)	USDA-NRCS
B_TEXTURE2	B horizon soil texture (abbreviated)	USDA-NRCS
HYDRIC	Hydric soil classification	USDA-NRCS
AREA	Soil unit area (sq.ft.)	Cpec

**ephemeral channels (indust).dbf - (self explanatory)**

**HywetInd.db - (self explanatory)**

**impervious surface (indust).dbf**

DBASE FIELD NAME	DESCRIPTION	SOURCE
ID	<b>Cpec ID number</b>	Cpec
TYPE	Roads, Filght line, and Parking lots	Cpec
AREA	Area (sq.ft.)	Cpec

**industrialized zone.dbf - (self explanatory)**

**mcas.dbf - (self explanatory)**

**ponded wetland (indust).dbf - (self explanatory)**

**Appendix 2L Continued**

**retention ponds.dbf**

DBASE FIELD NAME	DESCRIPTION	SOURCE
CPECID	<b><i>Cpec ID number</i></b>	Cpec
WATERSHED_	Watershed location	Cpec

**roads.dbf - (self explanatory)**

**sheet-flow direction (indust).dbf - (self explanatory)**

**stormwater open drainage network (indust).dbf**

DBASE FIELD NAME	DESCRIPTION	SOURCE
FIELDID	<b><i>Cpec ID number</i></b>	Cpec
LENGTH	Length of ditch segment	Cpec
COVER	Ditch cover (vegetated, concrete, bare, riprap)	Cpec
E_SAT	biological evidence of saturation	Cpec
V_SAT	visual signs of saturation	Cpec
IN_FILL	ditch in-fill	Cpec
C_WIDTH	Width of ditch channel (ft). Measured in feet between ditch banks or slope break. If asymmetry is present, measured from lowest side.	Cpec
C_DEPTH	Depth of ditch channel (ft). Measured in feet below ditch bank.	Cpec
B_WIDTH	Width of ditch base (ft)	Cpec
COMMENTS	Field observations or comments	Cpec
SRVY_PRD	Survey period	Cpec
WATERSHED_	Watershed location	Cpec

Appendix 2L Continued

stormwater piped system (indust).dbf

DBASE FIELD NAME	DESCRIPTION	SOURCE
LENGTH	Length of piped segment	MCAS-CP
WATERSHED_	Watershed location	Cpec

stormwater structures (indust).dbf

DBASE FIELD NAME	DESCRIPTION	SOURCE
TYPE	<p><b>Structure type: mostly self-explanatory.</b>            Excluding:</p> <ul style="list-style-type: none"> <li>- Headwall: inlet or outlet end of a stormwater structure with permanent structural support (e.g., pipe encased in concrete, cast or molded water-conveyance structure).</li> <li>- Pipe (Inlet/Outlet): inlet or outlet end of a stormwater structure without permanent structural support.</li> <li>- Flared End Section: inlet or outlet end of a stormwater structure (with or without permanent structural support) that is flared-out at the base.</li> </ul>	variable
X_COORD	X coordinate (NC State Plane)	GIS
Y_COORD	Y coordinate (NC State Plane)	GIS
CPECNUM	Field Identification number assigned by Cpec Environmental, Inc.	variable
SYMNUM	Cherry Point MCAS-Identification number (alphanumeric code based on Air Station Grid)	MCAS-CP
CPNUM	Modified SYMNUM or Final CPECNUM	variable
RIM_ELEV	RIM elevation. (exclusive source: Gannett Flemming – NOTE: be careful with these data; NOT confirmed)	variable
EFF_INV	Effective Invert elevation. (exclusive source: Gannett Flemming – NOTE: be careful with these data; NOT confirmed)	variable

**Appendix 2L Continued**

D_SOURCE	Data sources: FED-Facilities Engineering Dept CPEC-Cpec Environmental, Inc. GF-Gannett Flemming	Variable
SIZE	opening diameter or width.	variable
BASAL_POS	basal position (ft): Relative elevation of adjacent ditch bottom (base) to inlet or outlet lip (feet). Positive values indicate aperture obstruction.	Cpec field verified
A_CONDITION	Aperture Condition: Qualitative flow-obstruction evaluation of the inlet or outlet opening only!. Example: If basal position is +0.75 and remaining aperture is free of additional obstructions, the aperture condition would be recorded as a 5. 0 - completely obscured or blocked 1 - 75% to 100% obstructed 2 - 50% to 75% obstructed 3 - 25% to 50% obstructed 4 - 1% to 25% obstructed 5 - completely unobscured	Cpec field verified
C_SKIRT	concrete skirt (0=No/1=Yes); Concrete skirt attached to base of inlet or outlet end of a stormwater structure.	Cpec field verified
S_GRATE	steel grate (0=No/1=Yes); Steel grate or mesh attached to inlet or outlet end of a stormwater structure.	Cpec field verified
COMMENTS	Field observations or comments	Cpec field verified
MULTIPLES	No entry means – typical or standard size (see SIZE field for diameter) 1 – atypical; generally single large structure > 3.0 ft diameter or width (see COMMENTS field for specifications) 2+ – means multiple inlet/outlet (see COMMENTS field for specifications)	Cpec field verified
MATERIAL	Construction material	Cpec field verified
SRVY_PRD	Survey period	Cpec

**Appendix 2L Continued**

STATUS	Active or abandoned	Variable
ORDERF	Cpec code	Cpec
WATERSHED_	Watershed location	Cpec

**stream bed (indust).dbf**

DBASE FIELD NAME	DESCRIPTION	SOURCE
WATERSHED_	Watershed location	Cpec

**stream centerline (indust).dbf**

DBASE FIELD NAME	DESCRIPTION	SOURCE
WATERSHED_	Watershed location	Cpec
LENGTH	Length of ditch segment	Cpec

**stream points (indust).dbf**

DBASE FIELD NAME	DESCRIPTION	SOURCE
ID	<b><i>Cpec ID number</i></b>	Cpec
X_CL_POINT	X coordinate (NC State Plane)	Cpec
Y_CL_POINT	Y coordinate (NC State Plane)	Cpec
TYPE	Type of point: <ul style="list-style-type: none"> <li>- stream center point or</li> <li>- stream end point (intermittent- ephemeral boundary)</li> </ul>	Cpec
C_WIDTH	Stream channel width (ft): horizontal distance across the estimated primary channel at right angle to flow direction.	Cpec
S_DEPTH	Stream depth (ft): vertical difference between the top of the estimated average high water flow and the base of the channel.	Cpec

**Appendix 2L Continued**

ORDERF	Cpec code	Cpec
WATERSHED_	Watershed location	Cpec

**water bodiescp.dbf (self explanatory)**

**watershed cpecf (indust).dbf (self explanatory)**

## Chapter Three Appendix

**Appendix 3A: Additional Chapter Three Figures**

```

* Enter GUTTER information on line G1. If weir is present also use G2.
* GUTTER NGTO NPG GWIDTH GLEN G3 GS1 GS2 G6 DFULL GDEPTH
G1 103 101 1 10.0 133 0.0005 0.30 0.30 0.030 8.0 1.0
G1 302 103 1 10.0 794 0.0063 0.60 0.60 0.030 3.0 0
G1 102 302 1 75.0 160 0.0190 0.15 0.15 0.040 3.0 0
G1 107 102 1 2.5 294 0.0034 0.33 0.33 0.030 2.0 0
G1 108 107 1 6.0 26 0.077 0.17 0.17 0.040 0.5 0
G1 106 302 1 75.0 144 0.0005 0.026 0.026 0.040 1.0 0
G1 104 103 3 0 0 0 0 0 0 0 0
G1 105 104 1 10.0 623 0.0005 0.60 0.60 0.030 3.0 0
G1 310 105 1 9.0 403 0.0050 0.015 0.015 0.075 1.5 0
G1 110 310 3 6.0 60 0.033 0.17 0.17 0.030 0.5 0
G1 312 310 1 53 363 0.0005 0.16 0.16 0.075 4.0 0
G1 309 312 1 15 305 0.0033 0.067 0.067 0.075 1.0 0
G1 112 312 3 0 0 0 0 0 0 0 0
G1 109 309 1 5 270 0.0037 0.01 0.01 0.030 1.0 0
G1 111 311 2 1.0 145 0.034 0 0 0.012 0 0
G1 311 109 1 8.0 213 0.0047 0.20 0.20 0.030 1.5 0
G1 113 311 2 4.0 56 0.161 0 0 0.012 0 0
G1 114 113 3 0 0 0 0 0 0 0 0
G1 115 114 2 3.5 933 0.0005 0 0 0.012 0 0
G1 117 115 2 3.0 872 0.0034 0 0 0.012 0 0
G1 116 117 2 1.5 183 0.0055 0 0 0.012 0 0
G1 118 116 3 0 0 0 0 0 0 0 0
* Enter SUBCATCHMENT Data on line H1.
* JK NAME NGTO WIDTH AREA %IMP SLP IMPN PERVN IDS PDS SUCT HYCOND MSTDEF
H1 1 1 101 321 6.27 71.3 0.0207 0.010 0.023 0.05 0.10 2.41 1.18 0.437
H1 1 2 102 259 6.66 65.1 0.0114 0.010 0.023 0.05 0.10 12.45 0.012 0.475
H1 1 3 103 464 7.86 53.1 0.0189 0.010 0.023 0.05 0.10 4.33 0.429 0.453
H1 1 4 104 270 3.04 25.0 0.0032 0.010 0.023 0.05 0.10 4.33 0.429 0.453
H1 1 5 105 178 3.27 25.0 0.0038 0.010 0.023 0.05 0.10 4.33 0.429 0.453
H1 1 6 106 467 9.72 50.9 0.0149 0.010 0.023 0.05 0.10 4.33 0.429 0.453
H1 1 7 107 125 2.02 44.8 0.0194 0.010 0.023 0.05 0.10 12.45 0.012 0.475
H1 1 8 108 170 2.67 63.8 0.0171 0.010 0.023 0.05 0.10 12.45 0.012 0.475
H1 1 9 109 463 8.95 97.0 0.0100 0.010 0.023 0.05 0.10 12.45 0.012 0.475
H1 1 10 110 499 4.33 74.3 0.0162 0.010 0.023 0.05 0.10 4.33 0.429 0.453
H1 1 11 111 318 2.30 97.3 0.0386 0.010 0.023 0.05 0.10 12.45 0.012 0.475
H1 1 12 112 528 7.66 76.8 0.0064 0.010 0.023 0.05 0.10 12.45 0.012 0.475
H1 1 13 113 188 9.38 97.4 0.0018 0.010 0.023 0.05 0.10 12.45 0.012 0.475
H1 1 14 114 264 8.19 68.5 0.0030 0.010 0.023 0.05 0.10 12.45 0.012 0.475
H1 1 15 115 550 16.1 82.8 0.0054 0.010 0.023 0.05 0.10 12.45 0.012 0.475
H1 1 16 116 283 6.23 74.1 0.0014 0.010 0.023 0.05 0.10 12.45 0.012 0.475
H1 1 17 117 128 3.25 90.8 0.0020 0.010 0.023 0.05 0.10 12.45 0.012 0.475
H1 1 18 118 327 6.72 93.0 0.0022 0.010 0.023 0.05 0.10 12.45 0.012 0.475
* Enter data for Channel/Inlet Print Control M lines.
* NO water quality simulations
* NPRNT INTERV
M1 1 1
* NDET STARTP(1) STOPPR(1) IPRNT(1)
M2 1 0 0
M3 101
* End your input data set with a $ENDPROGRAM.
$ENDPROGRAM

```

**Figure 3A.1: A Text-based SWMM Input Dataset, Excluding Rainfall Data.** The above collection of information in one dataset used to test early model predictions of SWMM at Cherry Point MCAS. Gutter and subcatchment attributes were collected from the GIS and inserted into input datasets in efforts to generate outflow at the catchment outlet

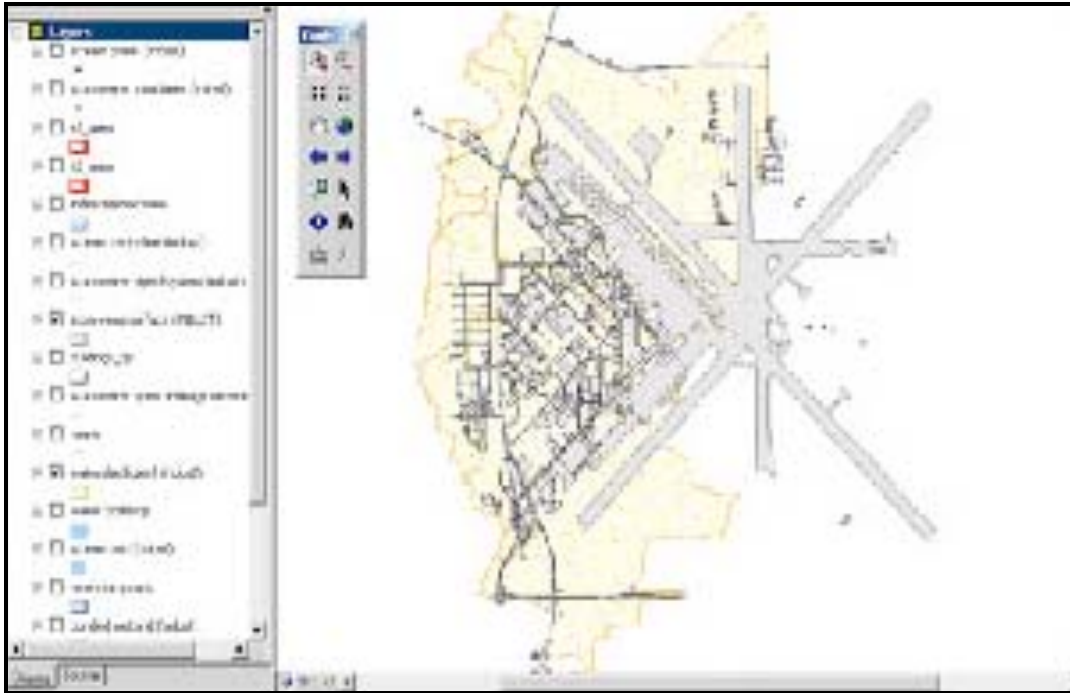


**Figure 3A.2: Impervious Surface Map for Industrialized Area of MCAS**

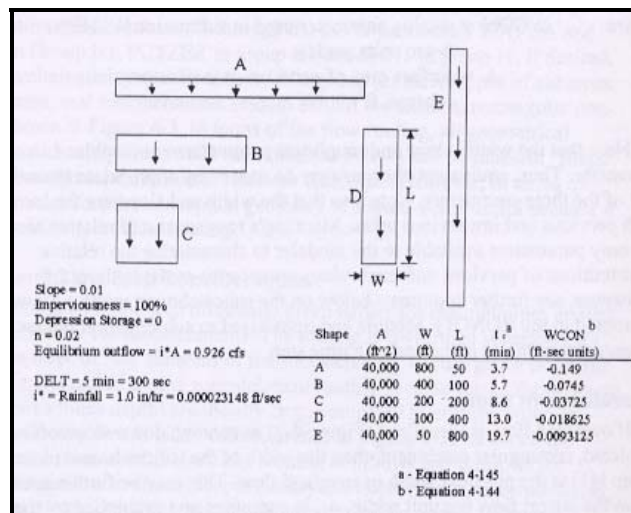


**Figure 3A.3: Importance of Technique when Measuring Catchment Width (USEPA SWMM4 User's Manual, 1999).**

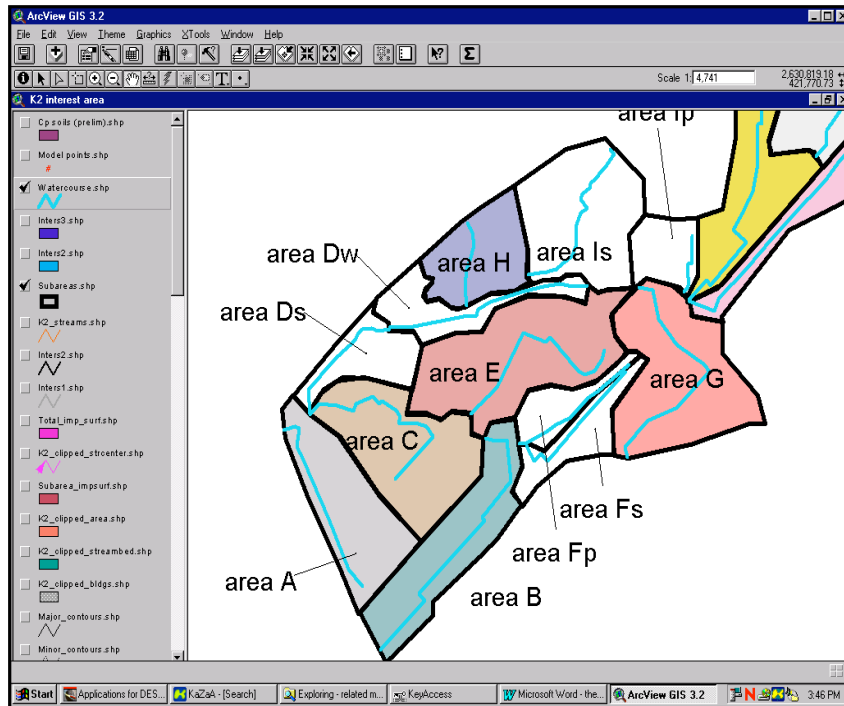


**Figure 3A.4: ArcVIEW 3.2 Window showing Catchment K2 Watercourses for Several Subcatchments**

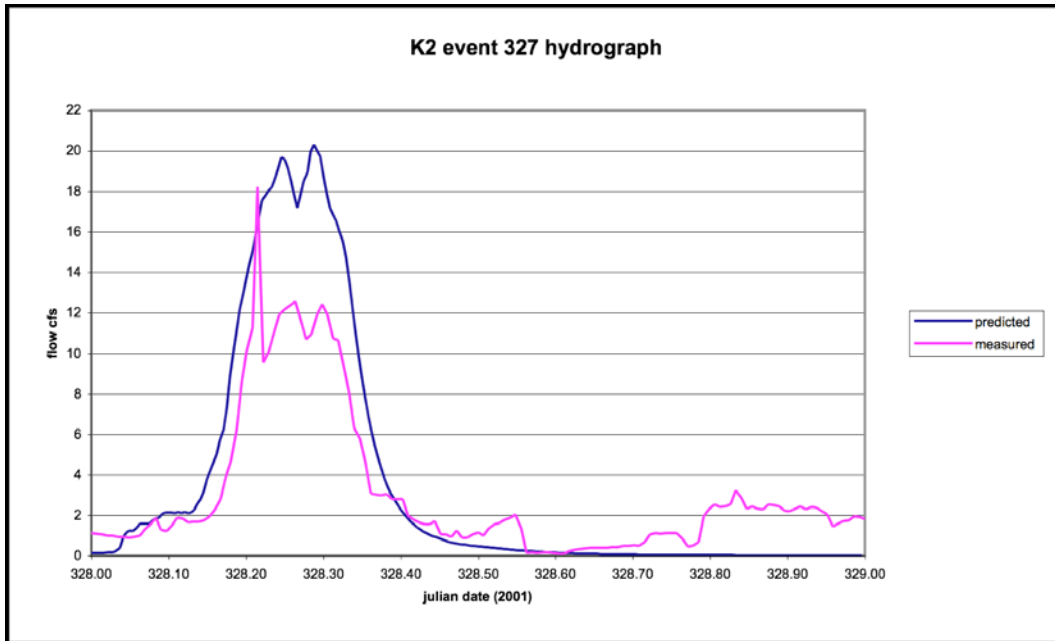


**Figure 3A.5: SWMM Over-prediction Example.** This is an example of an earlier hydrograph comparison effort using a single storm event in catchment K2.

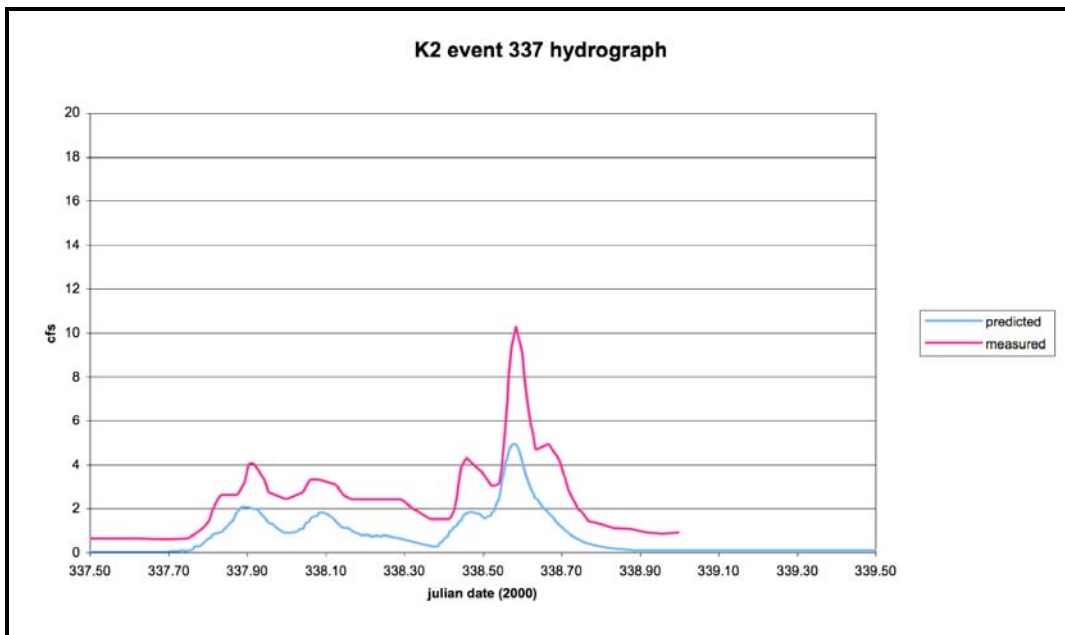


**Figure 3A.6: SWMM Under-prediction Example.** The graphic shows the situation where SWMM is underpredicting the outflow as compared to the measured data. This data is for catchment K3 in 2000.

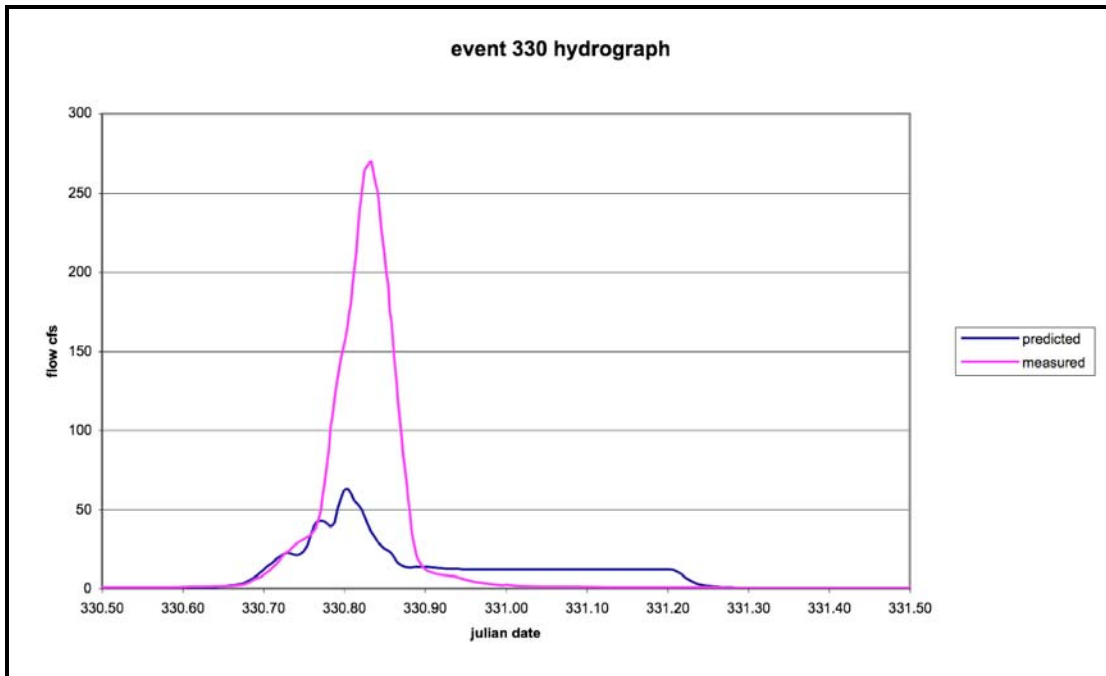


**Figure 3A.7: SWMM Plateau Example due to a Timing Issue**

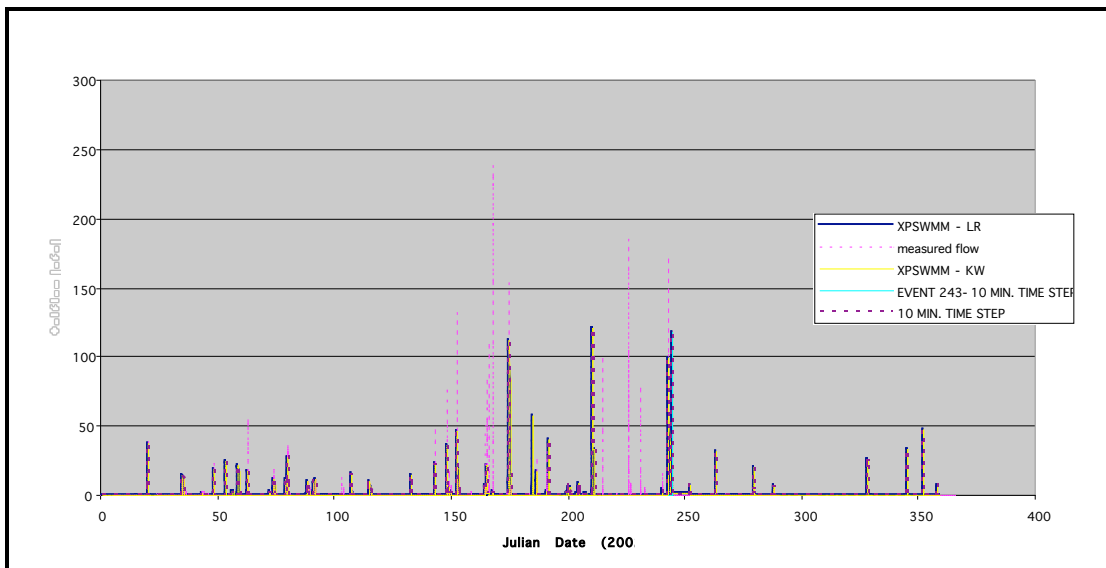


**Figure 3A.8: Catchment K3 Calibration Hydrograph, 2001.** This hydrograph contains all observed and measured points for catchment K3 in 2001.

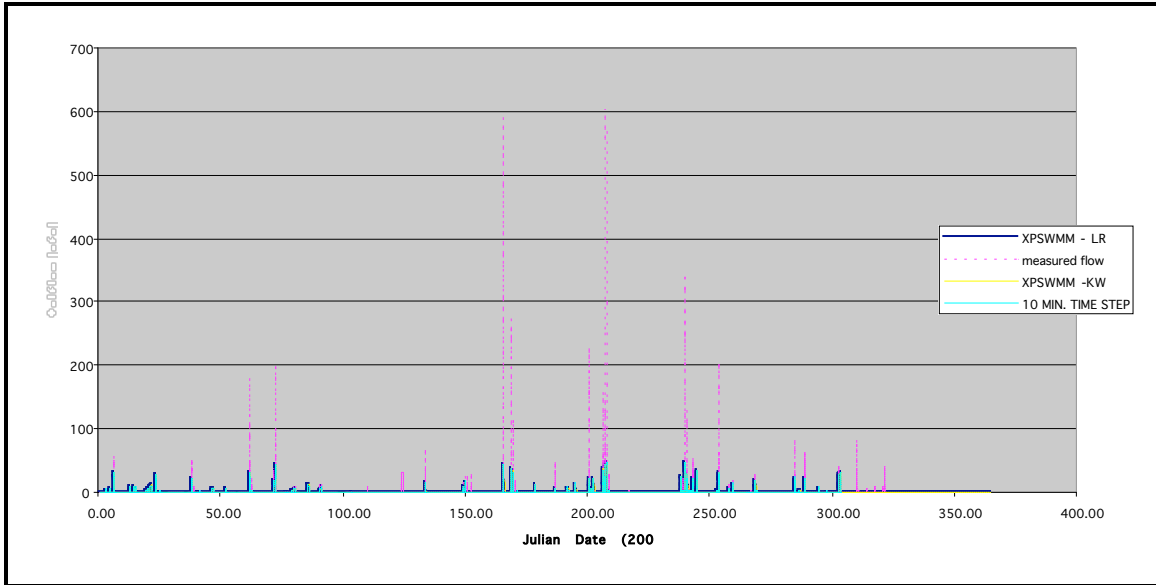


**Figure 3A.9: Catchment K3 Annual Calibration Hydrograph, 2002**

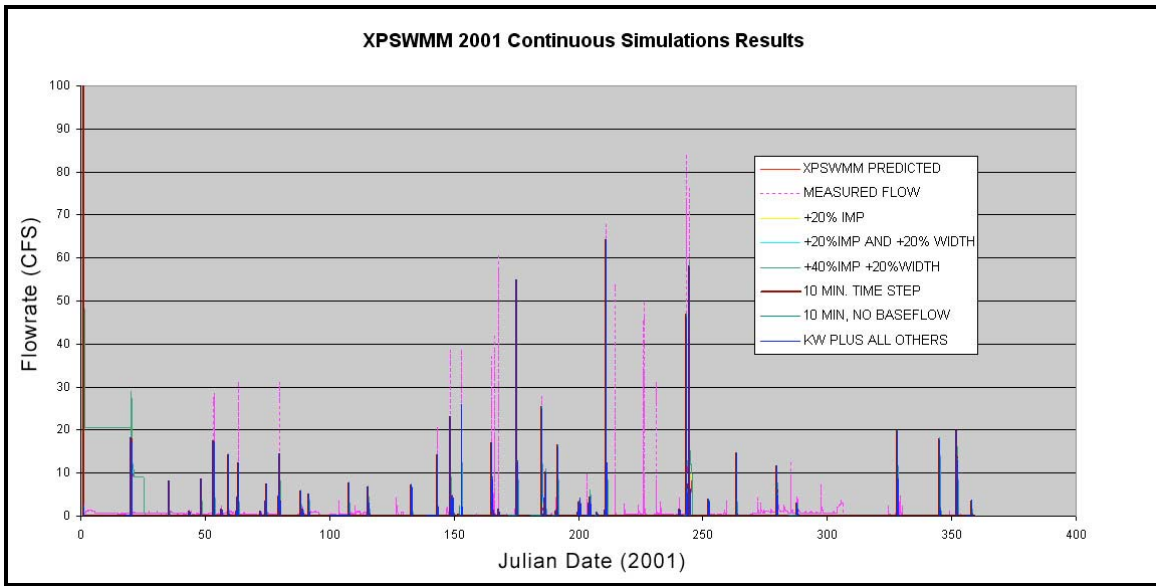


**Figure 3A.10: Catchment K2 Annual Calibration Hydrograph, 2001**

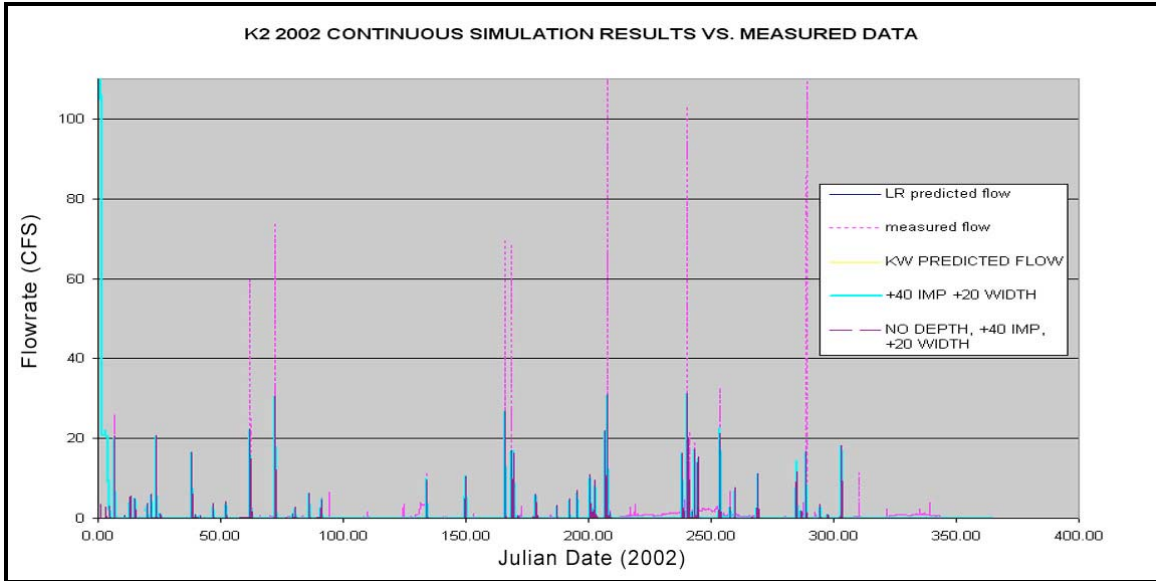


**Figure 3A.11: Catchment K2 Calibration Hydrograph, 2002**

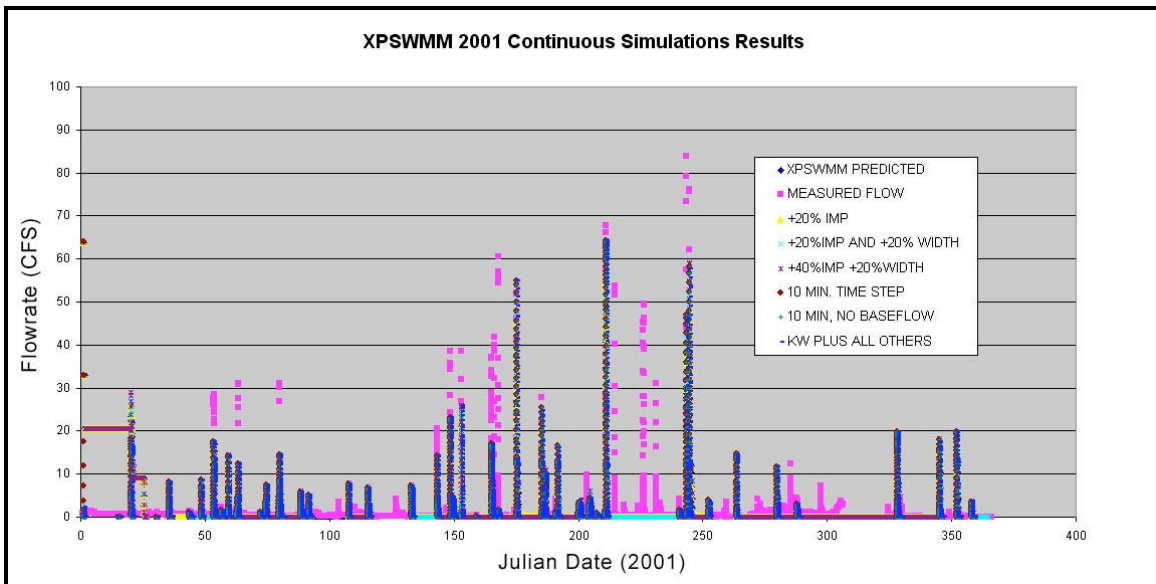


**Figure 3A.12: Catchment K2 2001 Continuous Hydrograph to Display Outliers**

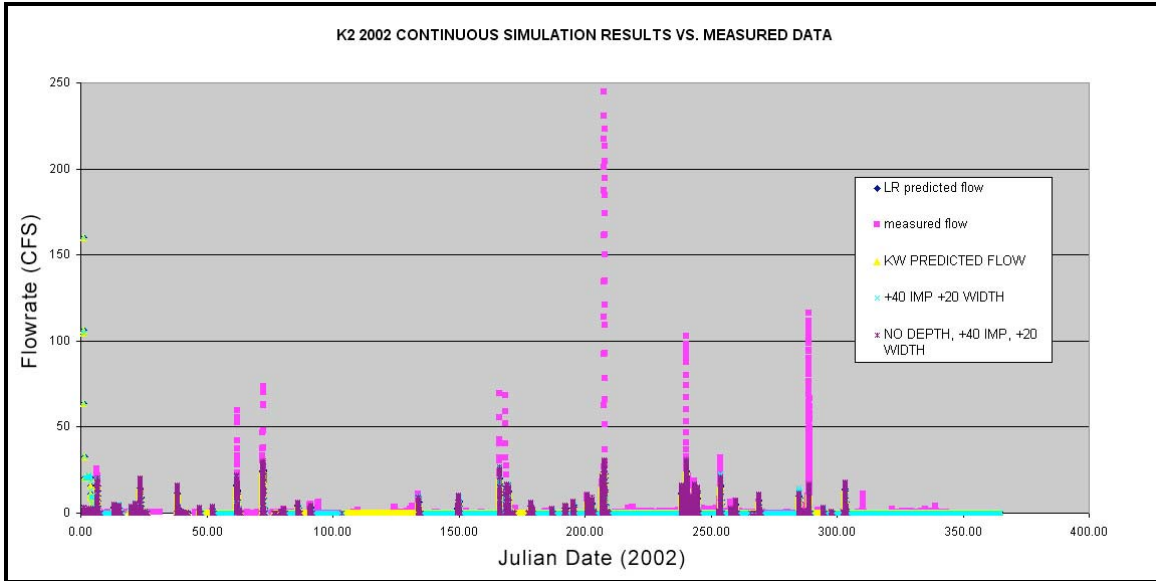


**Figure 3A.13: K2 2002 Continuous Hydrograph to Display Outliers**

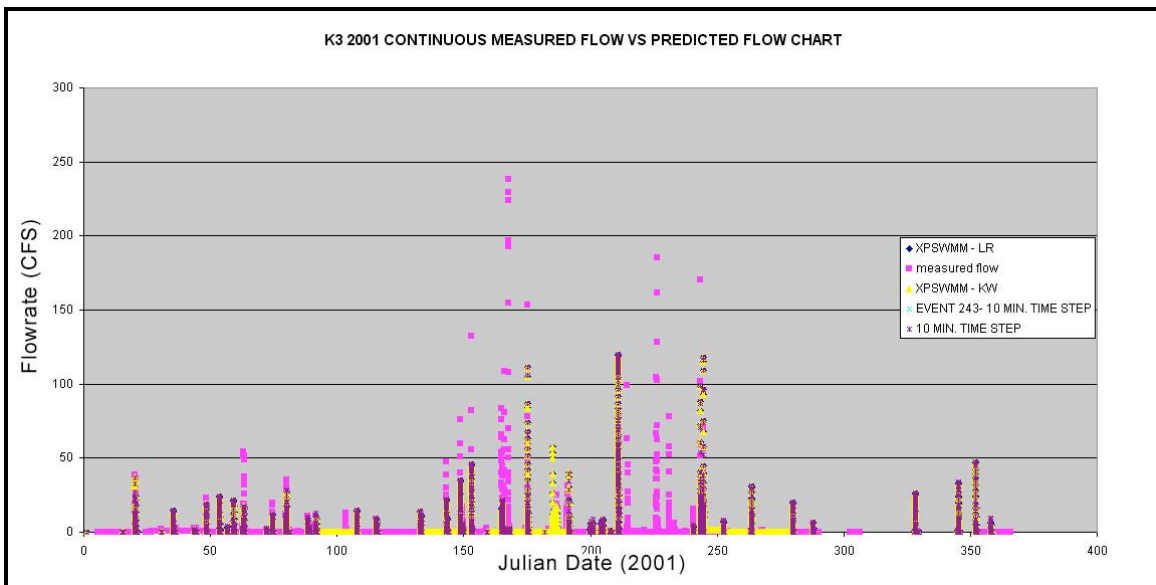


**Figure 3A.14: K3 2001 Continuous Hydrograph to Display Outliers**

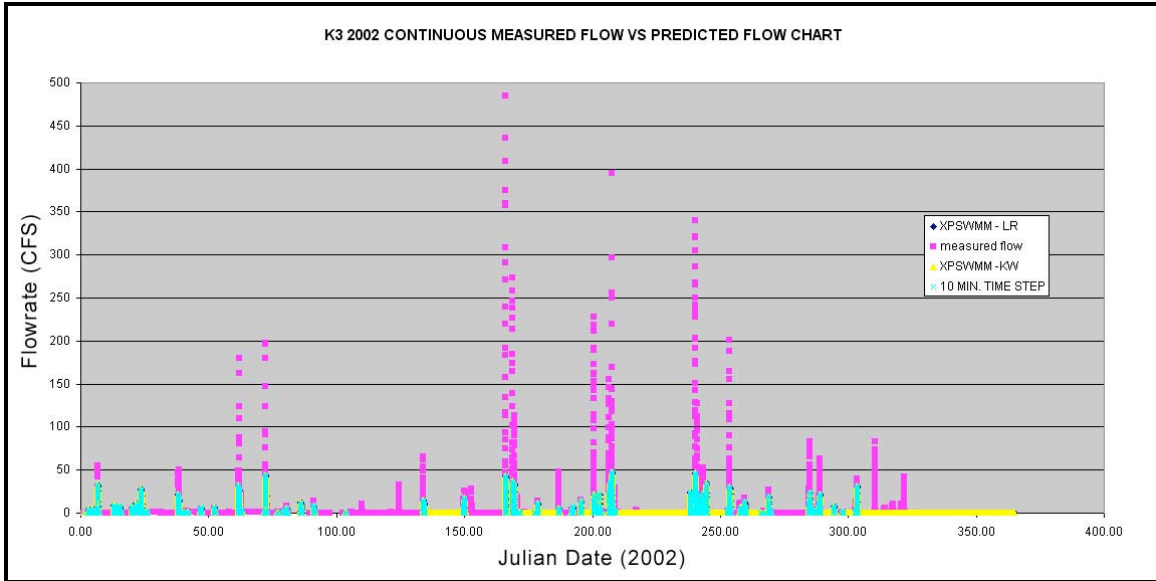


**Figure 3A.15: K3 2002 Continuous Hydrograph to display Outliers**

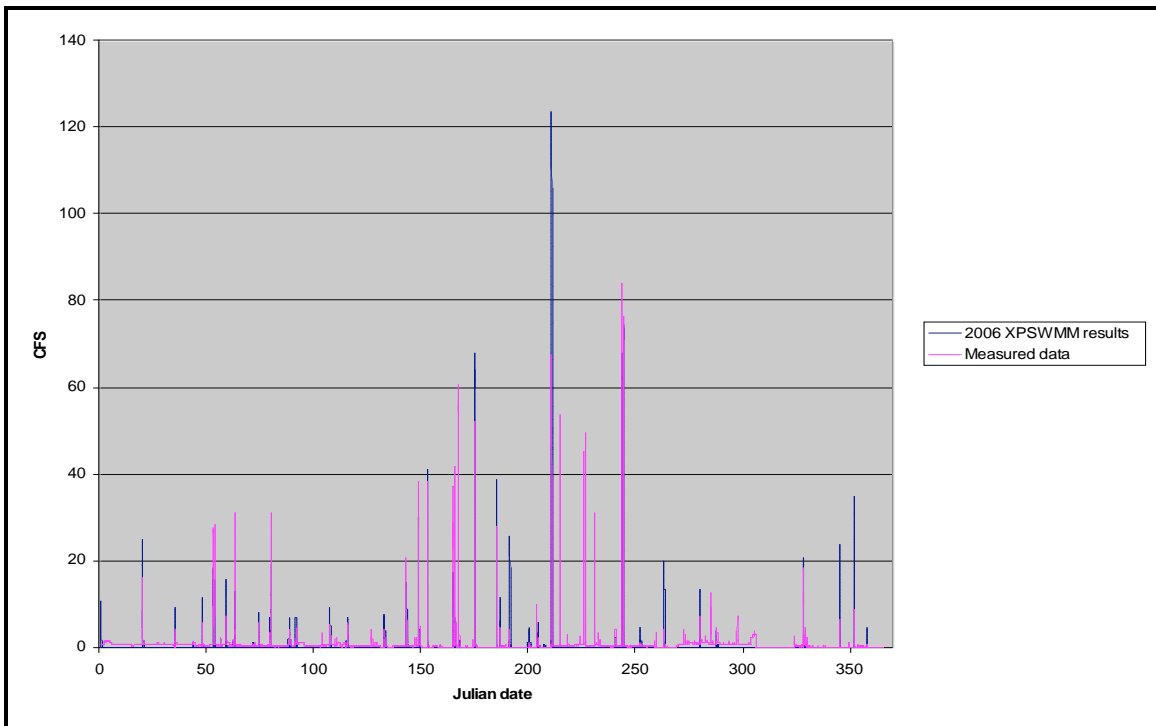


**Figure 3A.16: Catchment K2 2001 XPSWMM Outflow Hydrograph without Wetlands**

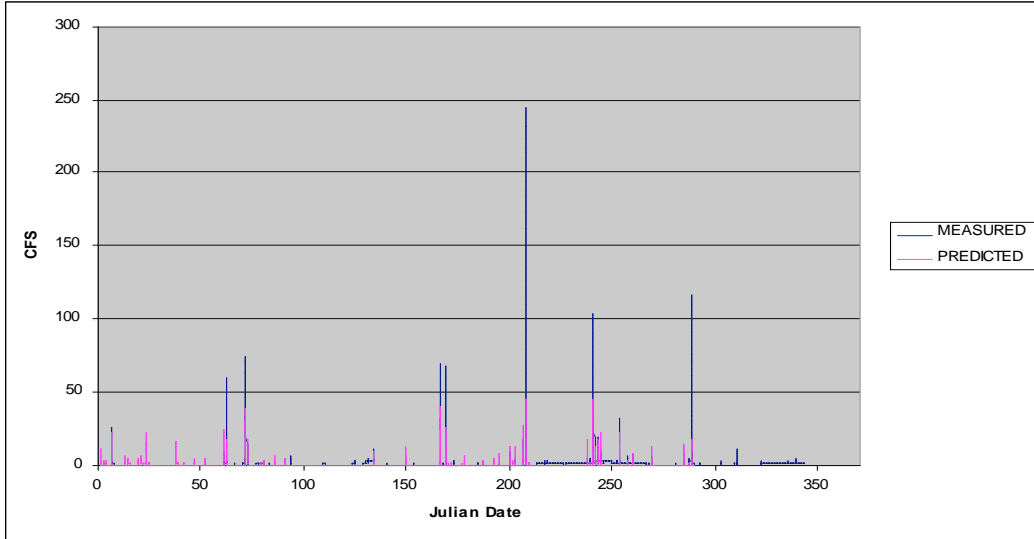


**Figure 3A.17: Catchment K2 2002 XPSWMM Outflow Hydrograph without Wetlands**

Appendix 3B: Additional Chapter Three Tables

**Table 3B.1: Sample Subcatchment Curve Numbers used for the Cherry Point MCAS Rainfall Runoff Simulations (Catchment K3)**

Sub-area	Area	Soils	Hyd. Soil Group	Soil Area	CN	Sub-area CN
0	7.454	NuB	B	1.384	69	69
		NoB	B	6.059	69	
1	7.28	NuB	B	0.697	69	69
		NoB	B	6.582	69	
		Ud	A	3.82?	?	
2	9.611	GuA	B	3.912	61	65.7
		NoB	B	5.696	69	
		Ud	A	0.544	?	
3	5.464	NuB	B	0.01	69	69
		NoB	B	5.454	69	
		Ud	A	2.684?	0	
4	5.702	NuB	B	0.002	69	65.4
		GuA	B	2.56	61	
		NoB	B	3.14	69	
5	22.14	GuA	B	0.158	61	90.6
		Lc	C	1.506	79	
		NoB	B	4.557	69	
		Ur	D	15.956	98	
6	16.778	Lc	C	6.335	79	90.7
		Ur	D	10.422	98	
7	27.934	GuA	B	26.94	61	61.3
		NoB	B	0.99	69	
8	25.203	GuA	B	11.29	61	80.2
		Ur	D	12.26	98	
		Lc	C	1.648	79	
9	20.448	GuA	B	12.9	61	71.3
		Ur	D	3.969	98	
		Lc	C	3.572	79	
10	11.631	GuA	B	11.631	61	61
11	11.947	Lc	C	11.947	79	79
12	12.551	GuA	B	9.666	61	65.14
		Lc	C	2.885	79	
13	15.48	GuA	B	1.874	61	76.8
		Lc	C	13.606	79	
14	15.735	Lc	C	15.735	79	79
15	16.633	GuA	B	3.475	61	75.23
		Lc	C	13.157	79	
16	19.337	GuA	B	6.725	61	71.11
		Lc	C	9.464	79	
		NoB	B	3.148	69	

**Table 3B.2: B1 Data Group Descriptions for SWMM4 (adapted from James, 1999)**

<i>NAME</i>	<i>Description</i>
IYBEG	Starting date of rainfall in YR/MO/DY format
IYEND	Ending date of rainfall in YR/MO/DY format
IYEAR	Echo print of the rainfall values
ISUM	Print control for storm event summary
MIT	Minimum intermittent time to separate storm events
NPTS	Controls number of points printed in the return period table
IFILE	Control to save storm event data
A	Plotting position parameter
NOSTAT	Control for storm event statistics printout

**Table 3B.3: Summary of Soil Types and Associated Areas from ArcVIEW for CPMCAS.** The below soil types are all the of the mapped soil units found at the air station as reported by CPEC, Inc. Using ArcVIEW, this soil information was reduced to only include the soils located within the research area.

<b>SOIL_TYPE</b>	<b>AREA (sq.ft.)</b>	<b>SOIL_TYPE</b>	<b>AREA (sq.ft.)</b>
<b>Ag</b>	658329.5	<b>NoB</b>	94060285.4
<b>Ap</b>	1600714.3	<b>NuB</b>	29517917.5
<b>AuB</b>	53963485	<b>On</b>	39393075.5
<b>BrB</b>	34359594.8	<b>Ra</b>	84454395.3
<b>CnB</b>	2174663.9	<b>Rc</b>	15812644.4
<b>CrB</b>	3047137.5	<b>Se</b>	7884175.9
<b>GoA</b>	68129082.1	<b>SuD</b>	50888238.1
<b>GuA</b>	31793553.3	<b>TaB</b>	725602.1
<b>Lc</b>	8794630	<b>Tc</b>	511977.8
<b>Le</b>	11447407.2	<b>To</b>	8608344.8
<b>Lf</b>	8363976.4	<b>Ud</b>	4616966.6
<b>Ly</b>	27686253.6	<b>Ud (B.A.)</b>	11638586
<b>MM</b>	32905424.6	<b>Ur</b>	45057437.5
<b>NoA</b>	30453889.7	<b>W</b>	947263.9

**Table 3B.4: XPSWMM Calibration and Validation Storm Events for Cherry Point (2000-2002)**

Year	Catchment Name	Calibration Storm Event (Julian Date)	Peak Outflow (cfs)	Cumulative Rainfall (in.)	Rainfall to Outflow Ratio	Validation Storm Event (Julian Date)	Peak Outflow (cfs)	Cumulative Rainfall (in.)	Rainfall to Outflow Ratio
2000	K2								
		319		0.51		330		2.69	
	K3	337		0.6		352		0.36	
		319		0.51		330		2.69	
2001	K2	324		0.6		345		0.28	
						348		0.23	
						351		0.16	
		48	8.54	0.31	0.04	152	25.89	0.89	0.03
		143	14.27	0.75	0.05	327	19.56	1.13	0.06
	K3	185	9.93	0.43					
		91	12.6	0.25	0.02	88	10.26	0.61	0.06
2002	K2	175	111.63	0.88	0.01	143	22.54	0.75	0.03
		186	n/a	0.43					
		6	20.41	0.68	0.03	71	30.15	2.24	0.07
						165	26.75	1.81	0.07
						168			
	K3	6	32.52	0.68	0.02	61	32.23	2.02	0.06
		38	21.68	1.66	0.08	72	44.31	2.16	0.05
						90	8.88	0.61	0.07
						133	14.77	0.65	0.04
						148.5	17.46	1	0.06

**Table 3B.5: 2002 SWMM Rainfall Sensitivity on a Percentage Basis**

<b>parameter name</b>	<b>2002 storm event</b>	<b>Max. peak outflow (cfs)</b>	<i>Negative max. difference</i>	<i>Negative percent change</i>	<i>Positive max. difference</i>	<i>Positive percent change</i>
<i>rain</i>	Day 06	53.8	23.4	43.49	24.8	46.10
<i>rain</i>	Day 61	128.2	63.2	49.30	63.8	49.77
<i>rain</i>	Day 133	54.1	27.3	50.46	34.5	63.77
<i>rain</i>	Day 148	25.7	14.4	56.03	10	38.91

**Table 3B.6: Z-Test Statistics for Several Calibration Storms (Event Based)**

<b>Z-Statistic</b>					
<i>area</i>	<i>year</i>	<i>storm date</i>	<i>value</i>	<i>z-critical (two-tail)</i>	<i>z-critical (one-tail)</i>
<b>K2</b>	2000	319	5.29	1.96	1.64
		337	-2.06	1.96	1.64
	2001	48	-1.07	1.96	1.64
		143	0.433	1.96	1.64
		185	-1.72	1.96	1.64
	2002	6	0.248	1.96	1.64
<b>K3</b>	2000	319	-3.6	1.96	1.64
		324	-0.904	1.96	1.64
	2001	91	-0.409	1.96	1.64
		175	-0.217	1.96	1.64
		186	-1.51	1.96	1.64
	2002	6	-0.75	1.96	1.64
		38	1.73	1.96	1.64

**Table 3B.7.1: Coefficient of Efficiency, E, Statistical Results from Calibration Storms (Event based)**

<b>E values</b>			
<i>area</i>	<i>year</i>	<i>storm date</i>	<i>value</i>
K2	2000	319	-2.03
		337	0.167
	2001	48	0.076
		143	0.777
		185	-0.515
	2002	6	0.879
K3	2000	319	-2.98
		324	0.701
	2001	91	0.244
		175	-3.271
		186	-0.568
	2002	6	0.64
		38	0.752

**Table 3B.7.2: Coefficient of Determination, R-Square, Results from Calibration Storms (Event Based)**

<b>R-Square values</b>			
<i>area</i>	<i>year</i>	<i>storm date</i>	<i>value</i>
K2	2000	319	0.67
		337	0.86
	2001	48	0.81
		143	0.78
		185	0.24
	2002	6	0.88
K3	2000	319	0.39
		324	0.72
	2001	91	0.64
		175	0.53
		186	0.14
	2002	6	0.69
		38	0.84

**Table 3B.7.3: Pearson Statistical Results from Calibration Storms (Event Based)**

Pearson values			
<i>area</i>	<i>year</i>	<i>storm date</i>	<i>value</i>
K2	2000	319	0.82
		337	0.93
	2001	48	0.9
		143	0.89
		185	0.51
	2002	6	0.94
K3	2000	319	0.93
		324	0.85
	2001	91	0.8
		175	0.73
		186	0.41
	2002	6	0.83
		38	0.92

**Table 3B.8.1: Validation Storms Z-Test Results (Event Based)**

<b>Z -Test Statistic</b>					
<i>Area</i>	<i>Year</i>	<i>Storm Date</i>	<i>Z-value</i>	<i>Z-critical Value (two-tail)</i>	<i>Z-critical Value (one-tail)</i>
<b>K2</b>	2000	330	n/a	n/a	n/a
		352	2.46	1.64	1.96
	2001	152	-0.702	1.64	1.96
		327	1.59	1.64	1.96
	2002	71	0.08	1.64	1.96
		165	-0.581	1.64	1.96
<b>K3</b>	2000	330	3.25	1.64	1.96
		345	6.71	1.64	1.96
		348	4.56	1.64	1.96
		351	-0.959	1.64	1.96
	2001	88	0.46	1.65	1.96
		143	0.73	1.64	1.96
	2002	72	2.09	1.64	1.96
		90	-1.98	1.64	1.96
		133	-0.929	1.64	1.96

**Table 3B.8.2: Validation Storms Coefficient of Efficiency Results (Event Based)**

<b>Nash-Sutcliffe values</b>			
<i>Area</i>	<i>Year</i>	<i>Storm Date</i>	<i>Value</i>
<b>K2</b>	2000	330	-0.0059
		352	0.403
	2001	152	-1.94
		327	0.82
	2002	71	0.65
		165	0.582
		168	0.0848
<b>K3</b>	2000	330	0.244
		345	0.164
		348	0.426
		351	-0.0829
	2001	88	0.262
		143	0.296
	2002	72	0.485
		90	-6.73
		133	-0.574

**Table 3B.8.3: Validation Storm R-square Results (Event Based)**

<b>R-square values</b>			
<i>Area</i>	<i>Year</i>	<i>Storm Date</i>	<i>Value</i>
<b>K2</b>	2000	330	0.343
		352	0.684
	2001	152	0.007
		327	0.904
	2002	71	0.724
		165	0.602
		168	0.243
<b>K3</b>	2000	330	0.581
		345	0.581
		348	0.872
		351	0.604
	2001	88	0.473
		143	0.32
	2002	72	0.692
		90	0.386
		133	0.204

**Table 3B.9: Measured and Predicted Continuous Hydrograph Dataset Sizes and the Related XPSWMM time controls**

Area	Year	Source	dry time step (sec)	transition time step (sec)	wet time step (sec)	number of hydrograph pts.
K2	2001	XPSWMM	600	172	172	15000
		Measured				17000
	2002	XPSWMM	1200	644	644	9600
		Measured				10000
K3	2001	XPSWMM	7200	600	600	7000
		Measured				7000
	2002	XPSWMM	7200	600	600	7000
		Measured				8000

**Table 3B.10: Correlation Statistics Results for Annual Continuous Hydrographs**

Catchment	Year	Statistical Test Method		
		Pearson Product Moment	Coefficient of Efficiency	Index of Agreement
K2	2001	0.607	0.33	0.75
	2002	0.502	0.19	0.43
K3	2001	0.419	-0.05	0.61
	2002	0.327	0.05	0.29

**Table 3B.11: Catchment K2 Rainfall Intensity Table for Cherry Point MCAS**

Catchment year event name			HOBO rainfall						NOAA rainfall			
			start date	end date	start rain depth (in.)	end rain depth (in.)	storm duration (hr)	rainfall amount (in.)	rainfall intensity (in/hr)	storm duration (hr)	rainfall amount (in.)	rainfall intensity (in/hr)
<b>Calibration Storms</b>												
K2	2000	319	319.44	319.55	0.51	1.02	2.64	0.51	0.19	24	0.54	0.02
		337	337.68	338.63	4.63	5.23	22.80	0.60	0.03	48	1.39	0.03
	2001	48	47.42	48.32	1.82	2.13	21.60	0.31	0.01	48	0.29	0.01
		143	143.20	143.71	8.62	9.37	12.24	0.75	0.06	24	0.78	0.03
		186	186.14	186.72	16.39	16.8 2	13.92	0.43	0.03	24	0.42	0.02
	2002	6	6.49	6.59	0.53	1.21	2.40	0.68	0.28	24	0.6	0.03
<b>Validation Storms</b>												
K2	2000	330	330.29	331.29	1.93	4.62	24.00	2.69	0.11	48	3.51	0.07
		352	351.47	352.30	6.02	6.38	19.92	0.36	0.02	48	0.58	0.01
	2001	152	152.93	153.23	11.00	11.8 9	7.20	0.89	0.12	48	0.72	0.02
		327	327.76	328.44	24.81	25.9 4	16.32	1.13	0.07	48	0.37	0.01
	2002	71	71.57	72.83	2.33	4.57 16.0	30.24	2.24	0.07	48	2.1	0.04
		165	165.46	166.03	14.27	8	13.68	1.81	0.13	48	1.65	0.03

**Table 3B.12: Catchment K3 Rainfall Intensity Table**

Catchment	year	event name	HOBO rainfall						NOAA rainfall			
			start date	end date	start rain depth (in.)	end rain depth (in.)	storm duration (hr)	rainfall amount (in.)	rainfall intensity (in/hr)	storm duration (hr)	rainfall amount (in.)	rainfall intensity (in/hr)
<b>Calibration Storms</b>												
K3	2000	319	319.44	319.55	0.51	1.02	2.64	0.51	0.19	24.00	0.54	0.02
		337	337.68	338.63	4.63	5.23	22.80	0.60	0.03	48.00	1.39	0.03
2001		91	91.59	91.84	6.64	6.89	6.00	0.25	0.04	24.00	0.29	0.01
		175	175.20	175.36	14.98	15.86	3.84	0.88	0.23	24.00	1.01	0.04
		186	186.14	186.72	16.39	16.82	13.92	0.43	0.03	24.00	0.42	0.02
2002		6	6.49	6.59	0.53	1.21	2.40	0.68	0.28	24.00	0.60	0.03
		38	37.80	40.41	3.66	5.32	62.64	1.66	0.03	96.00	1.59	0.02
<b>Validation Storms</b>												
K3	2000	330	330.29	331.29	1.93	4.62	24.00	2.69	0.11	24.00	3.51	0.15
		345	345.06	345.67	5.41	5.69	14.64	0.28	0.02	24.00	0.40	0.02
		348	348.97	349.32	5.76	5.99	8.40	0.23	0.03	48.00	0.34	0.01
		351	351.09	351.95	6.00	6.16	20.64	0.16	0.01	24.00	0.26	0.01
2001		88	88.16	89.25	6.02	6.63	26.16	0.61	0.02	48.00	0.83	0.02
		143	143.20	143.71	8.62	9.37	12.24	0.75	0.06	24.00	0.78	0.03
2002		61	61.59	62.13	6.13	8.15	12.96	2.02	0.16	48.00	1.54	0.03
		72	72.00	72.83	8.43	10.59	19.92	2.16	0.11	24.00	2.02	0.08
		90	90.97	91.21	11.59	12.20	5.76	0.61	0.11	48.00	0.65	0.01
		133	133.97	134.07	12.39	13.04	2.40	0.65	0.27	48.00	0.76	0.02
		148.5	149.40	150.79	13.26	14.26	33.36	1.00	0.03	48.00	1.21	0.03

**Table 3B.13: 2006 XPSWMM9.0 Return Period Simulation Results for Catchment K2.** The below tables displays the simulated maximum outflow rates for the Cherry Point project using the return period precipitation for Morehead City, NC. Outflows have been reported at all nodes. The outlet for catchment K2 is node 1.

ELEMENT NUMBER	PREDICTED FLOWRATE (CFS) FOR INDICATED PERIOD					
	2 YR	5 YR	10 YR	25 YR	50 YR	100 YR
<b>1 (OUTLET)</b>	<b>83.3</b>	<b>94.2</b>	<b>125.4</b>	<b>144.9</b>	<b>161.1</b>	<b>180.5</b>
2	9.9	10.8	14.6	16.9	18.9	21.2
3	80.0	88.7	117.7	135.1	150.2	168.4
4	54.9	62.9	82.9	95.3	105.6	117.9
5	55.6	63.6	83.5	95.9	106.2	118.5
6	7.0	7.7	10.3	12.0	13.4	15.0
7	3.7	4.1	5.5	6.4	7.1	8.0
8	2.4	2.7	3.6	4.2	4.6	5.2
9	43.4	50.1	64.5	73.4	80.9	89.7
10	54.9	62.9	82.3	94.4	104.5	116.4
11		3.2	4.3	5.0	5.6	6.3
12						
13	33.3	35.7	44.6	50.0	54.6	60.0
14	26.2	26.2	26.2	26.2	26.2	26.2
15	32.1	34.3	43.1	48.6	53.2	58.7
16	15.1	16.5	22.3	25.8	28.8	32.4
17	13.2	13.6	15.2	16.1	17.0	17.9
18						
1001	16.8	18.4	24.9	28.9	32.2	36.3
1003	51.4	58.8	76.4	87.4	96.5	107.4
1005	50.9	58.4	76.0	87.0	96.1	107.0
1006	32.4	37.9	48.0	54.2	59.4	65.5

**Table 3B.14: 2006 XPSWMM9.0 Return Period Simulation Results for Catchment K3.** The expected precipitation for several design storms was inserted into XPSWMM9.0 and simulated. The following table presents the outflows at each node where node 18 is the K3 catchment outlet.

ELEMENT NUMBER	PREDICTED FLOWRATE (CFS) FOR INDICATED PERIOD					
	2 YR	5 YR	10 YR	25 YR	50 YR	100 YR
1	7.8	8.5	11.5	13.3	14.9	16.7
2	1.5	1.7	2.2	2.6	2.9	3.3
3	3.2	3.5	4.8	5.5	6.2	6.9
4	20.9	22.9	30.9	35.9	40.0	45.0
5	4.4	4.8	6.5	7.5	8.4	9.4
6	6.8	7.4	10.0	11.6	13.0	14.6
7	11.1	11.6	13.5	14.8	15.8	17.0
8	7.4	8.1	11.0	12.7	14.2	16.0
9	5.2	5.8	7.8	9.0	10.0	11.3
10	29.7	32.2	42.5	46.8	49.8	53.5
11	6.0	6.6	8.9	10.3	11.5	12.9
12	39.5	41.6	50.0	55.3	59.7	65.0
13	63.3	67.6	85.2	96.1	105.3	116.2
14	30.6	32.8	41.6	47.1	51.7	57.3
15	11.7	12.8	17.2	20.0	22.3	25.1
16	9.2	10.1	13.7	15.9	17.7	19.9
17	15.1	16.5	22.3	25.9	28.9	32.5
<b>18 (OUTLET)</b>	<b>93.3</b>	<b>100.5</b>	<b>129.6</b>	<b>147.7</b>	<b>162.8</b>	<b>181.0</b>
19	83.2	89.5	114.6	130.3	143.4	159.1
20	0.2	0.2	0.3	0.4	0.4	0.5
21	3.7	4.1	5.5	6.4	7.2	8.1
22	5.0	5.5	7.4	8.6	9.6	10.8
1001	1.5	1.65	2.23	2.59	2.89	3.25
1002	90.9	97.9	126.1	143.6	158.3	175.9
1003	78.3	84.2	107.5	122	134.1	148.7
1004	20.9	22.9	30.9	35.9	40	45
1005	2.7	2.74	2.74	2.73	2.74	2.74

## Appendix 3C: HEC-HMS Materials

### Exhibit 3C.1: HMS Results using First Level Catchment Discretization

Extracting the display graphics directly from HEC-HMS version 3.0.0 (downloaded in February 2006) created the following screenshots. The actual HMS project and its associated attributes were determined in 2000. Specific results were not presented in the Chapter Three text because the area discretization had been updated years after the initial HMS project was created. Therefore, a comparison of the HMS to the XPSWMM results would not have been useful. The HMS simulation results are included for informational purposes solely.

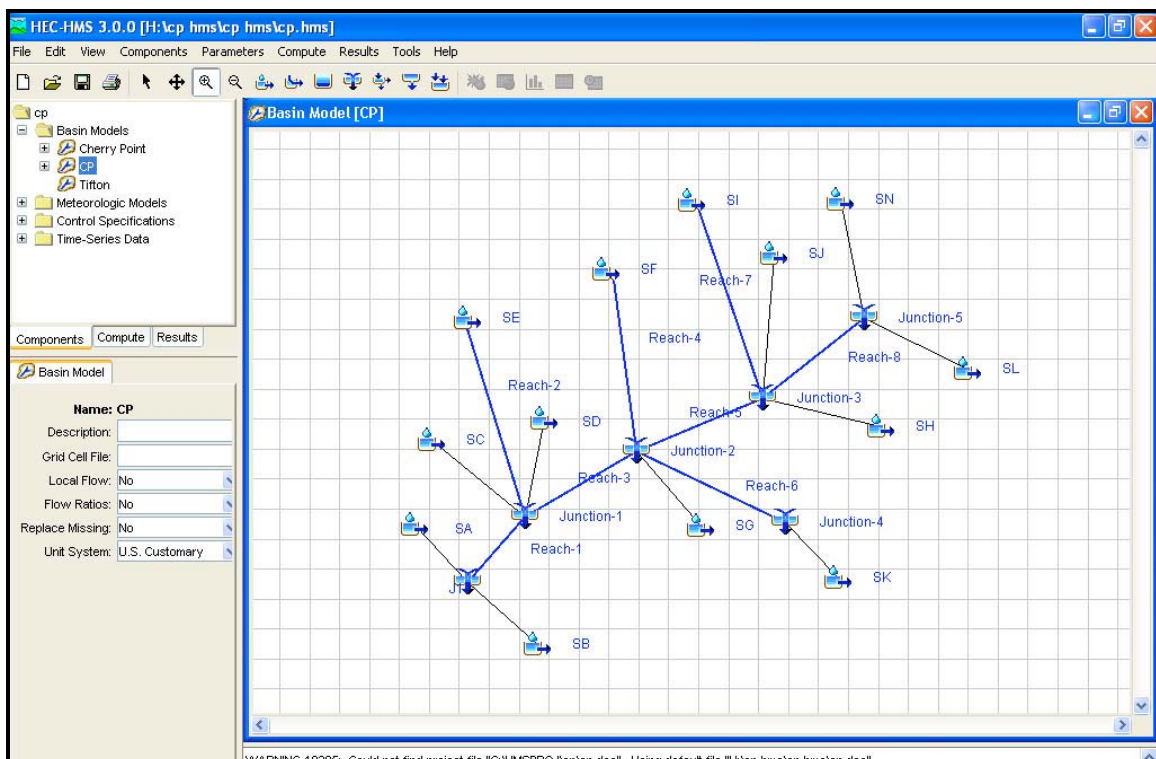


Figure 3C.1.1: HEC HMS screenshot of the Catchment K3 Basin Model

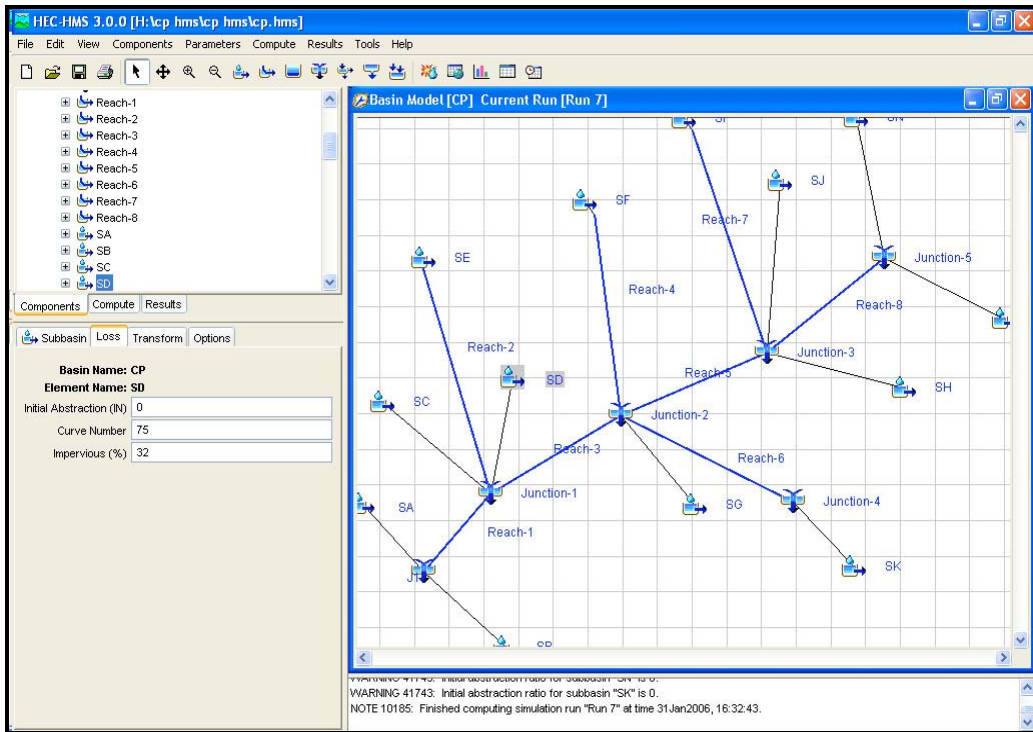


Figure 3C.1.2: HEC HMS screenshot of the K3 Catchment showing the Basin Loss Options

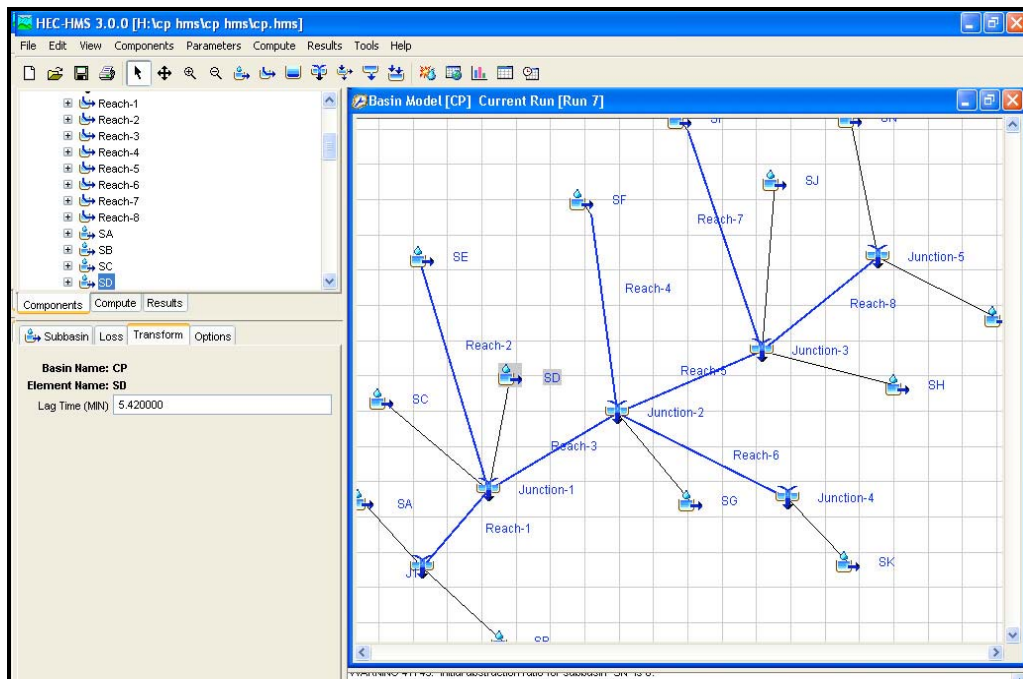


Figure 3C.1.3: HEC HMS screenshot of the K3 Catchment Displaying the Basin Transform Options Menu

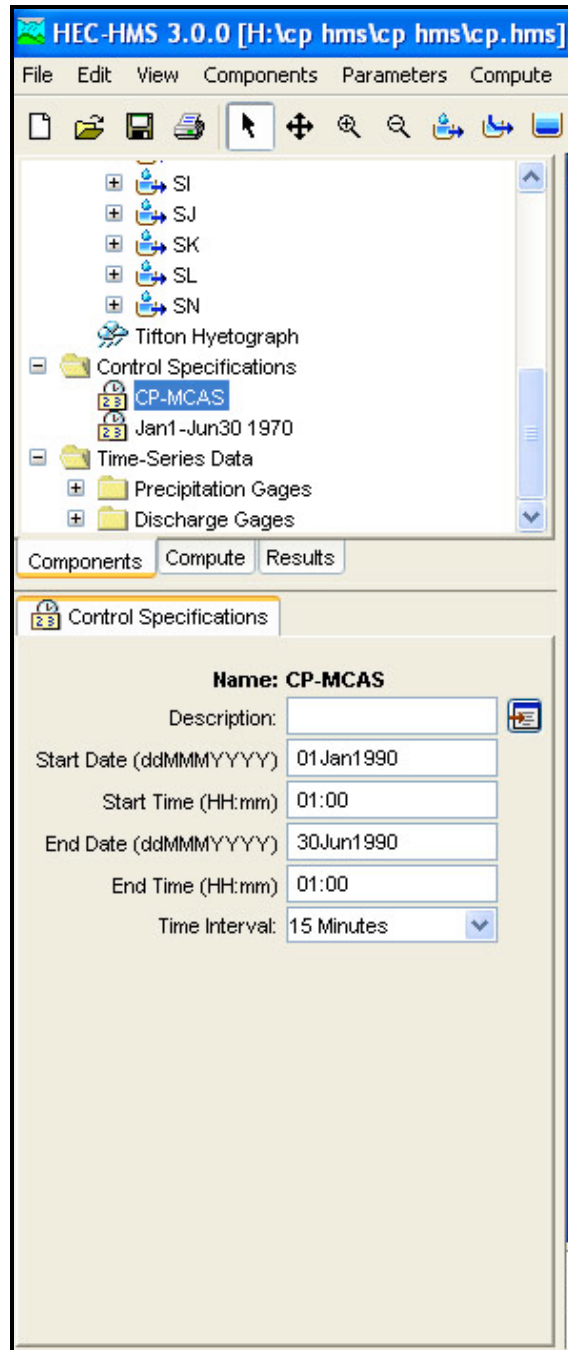
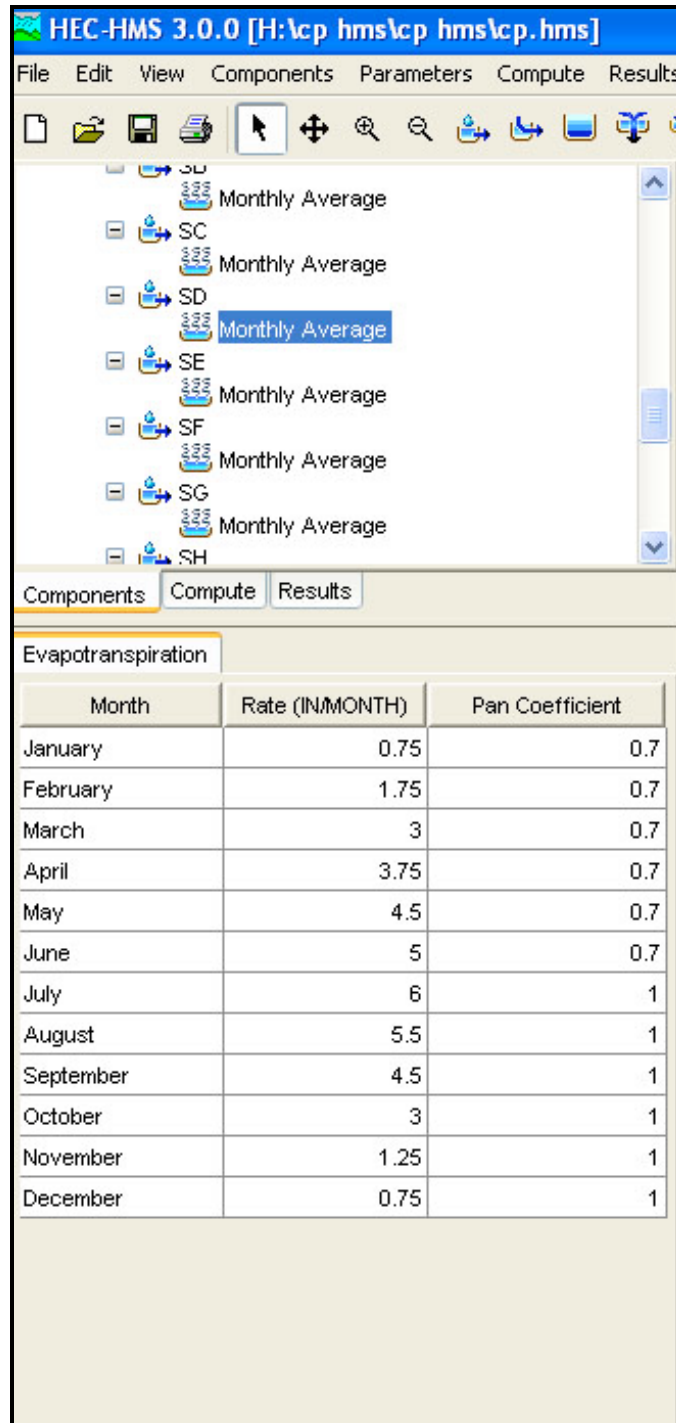


Figure 3C.1.4: HEC HMS screenshot of the K3 Catchment showing the Project Control Specifications



**Figure 3C.1.5: HEC HMS screenshot of a Typical Subcatchment Evapotranspiration Input Screen**

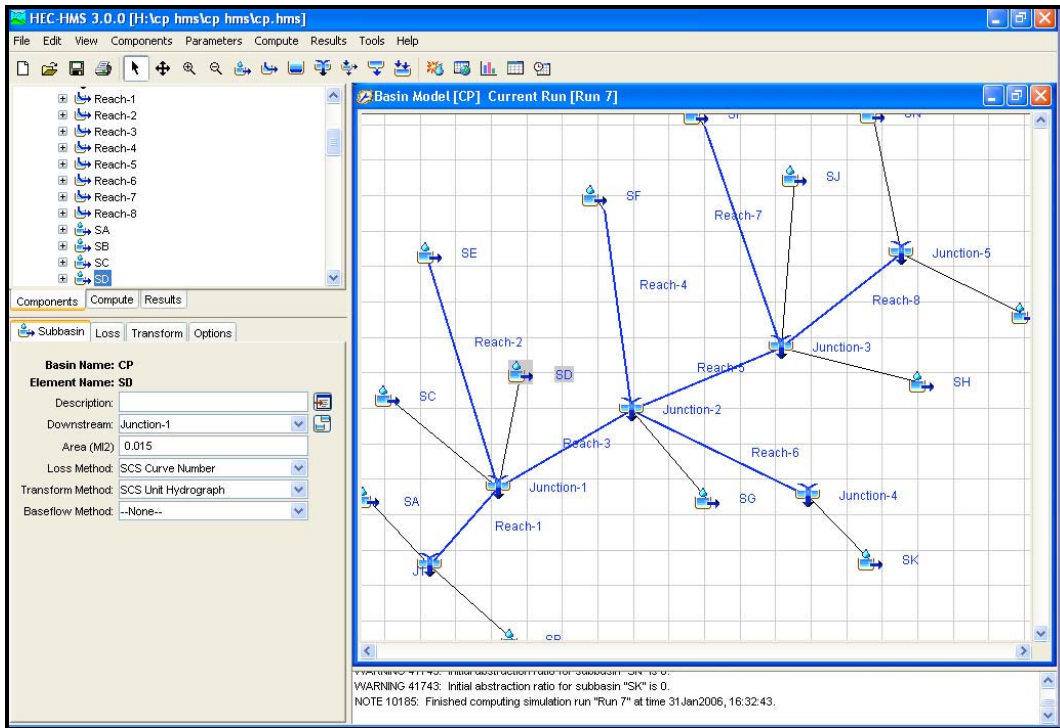


Figure 3C.1.6: HEC HMS screenshot displaying the General Basin Options page

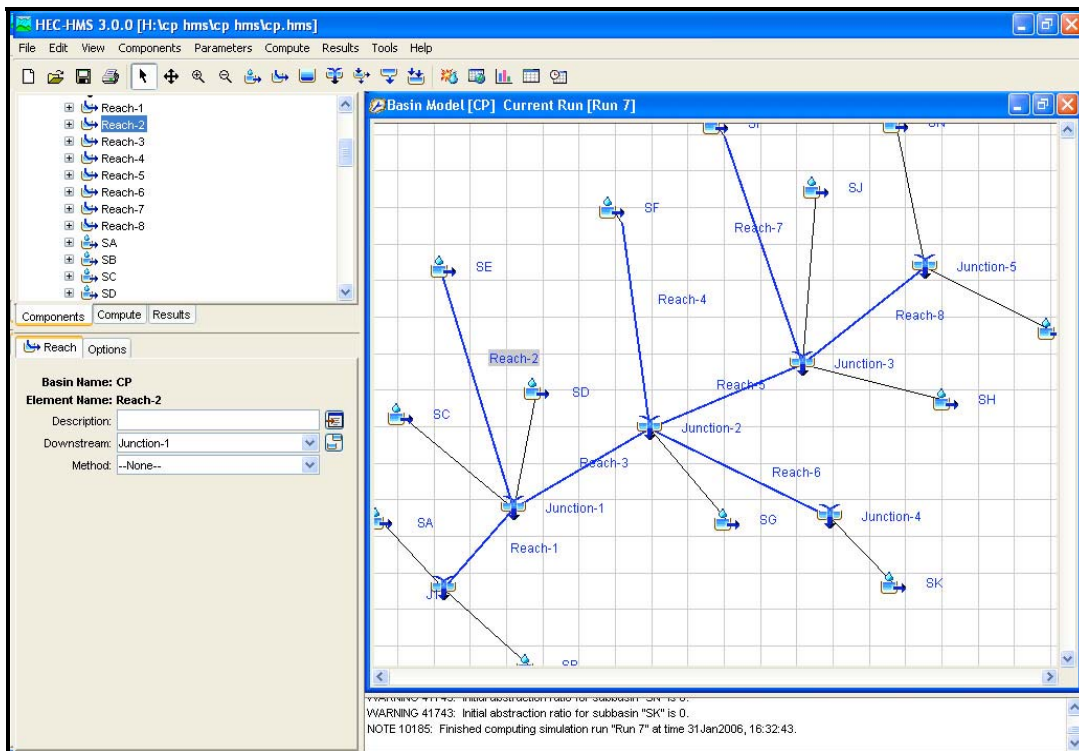


Figure 3C.1.7: HEC HMS screenshot of Catchment K3 displaying the Reach Options Menu

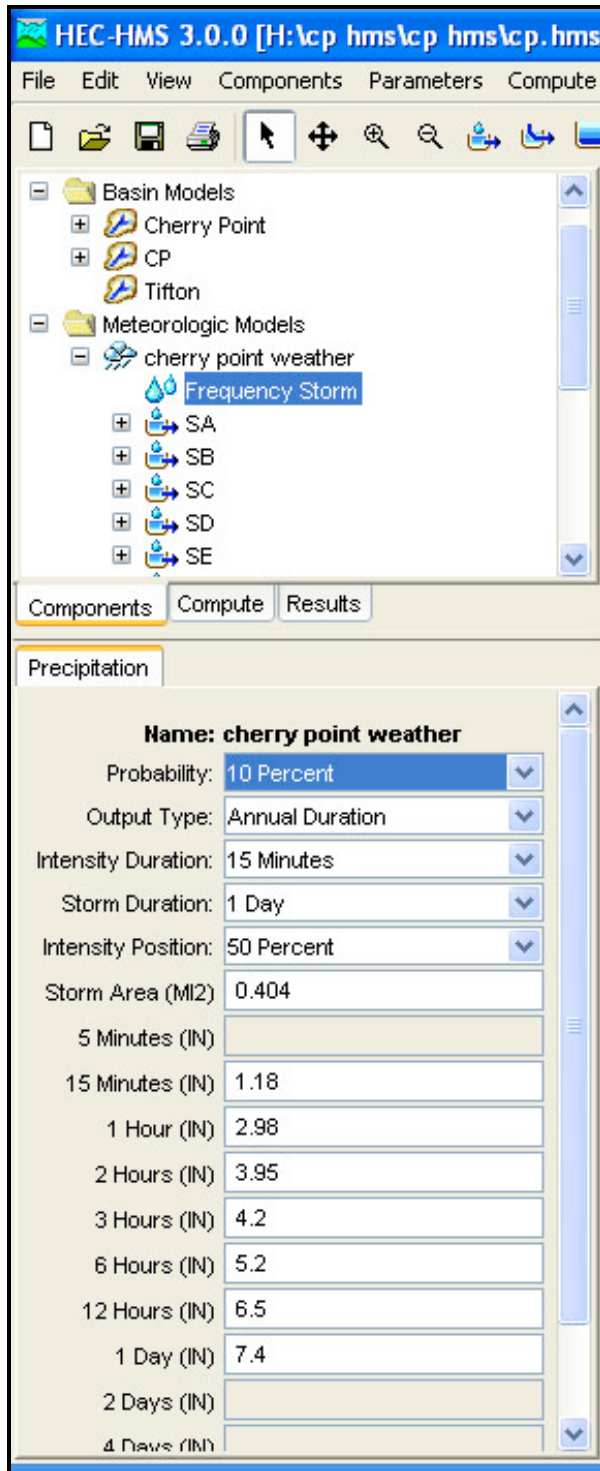


Figure 3C.1.8: *HEC HMS screenshot of the Precipitation Options Menu using User inputted values.*

**Exhibit 3C.2:** HEC HMS 3.0.0. General Results for the K3 Catchment

Hydrologic Element	Drainage Area (sq. mi.)	Area (ac.)	Peak Discharge (cfs)	Time to Peak	Volume (in)
J1	0.3051	195.264	636.52	01Jan1990, 13:15	6.15
Junction-1	0.2825	180.8	588.82	01Jan1990, 13:15	6.17
Junction-2	0.2501	160.064	512.51	01Jan1990, 13:15	6.21
Junction-3	0.1451	92.864	290.91	01Jan1990, 13:15	6.17
Junction-4	0.026	16.64	50.54	01Jan1990, 13:15	6.31
Junction-5	0.049	31.36	84.61	01Jan1990, 13:30	6.2
Reach-1	0.2825	180.8	588.82	01Jan1990, 13:15	6.17
Reach-2	0.0089	5.696	21.27	01Jan1990, 13:15	5.97
Reach-3	0.2501	160.064	512.51	01Jan1990, 13:15	6.21
Reach-4	0.044	28.16	105.04	01Jan1990, 13:15	6.2
Reach-5	0.1451	92.864	290.91	01Jan1990, 13:15	6.17
Reach-6	0.026	16.64	50.54	01Jan1990, 13:15	6.31
Reach-7	0.04	25.6	87.38	01Jan1990, 13:15	6.34
Reach-8	0.049	31.36	84.61	01Jan1990, 13:30	6.2
SA	0.0116	7.424	22.17	01Jan1990, 13:15	5.92
SB	0.011	7.04	25.53	01Jan1990, 13:15	6.02
SC	0.0085	5.44	20.01	01Jan1990, 13:15	5.83
SD	0.015	9.6	35.03	01Jan1990, 13:15	5.76
SE	0.0089	5.696	21.27	01Jan1990, 13:15	5.97
SF	0.044	28.16	105.04	01Jan1990, 13:15	6.2
SG	0.035	22.4	67.4	01Jan1990, 13:30	6.34
SH	0.0301	19.264	70.9	01Jan1990, 13:15	5.99
SI	0.04	25.6	87.38	01Jan1990, 13:15	6.34
SJ	0.026	16.64	49.75	01Jan1990, 13:15	6.04
SK	0.026	16.64	50.54	01Jan1990, 13:15	6.31
SL	0.025	16	51.83	01Jan1990, 13:15	5.83
SN	0.024	15.36	41.83	01Jan1990, 13:30	6.59

Note: The highlighted rows correspond to the subcatchments of interest. These simulation results were created before the subcatchments were given numeric names and positioned using the GPS coordinates. The purpose of the HEC HMS predictions was to generate surface runoff using minimal inputs to determine possible maximum peak discharge rates at the catchment and subcatchment levels.

**Appendix 3D: RAIN Module**

**Exhibit 3D.1: Sample RAIN Module Dataset for 2000**

```
SW 1 8 9
MM 4 1 2 3 4
@ 8 'TIPPING BUCKET.TXT'
@ 9 '2000 RAIN.DNT'
*=====
*   SWMM 4.4 RAIN DATA FILE
*=====
$RAIN
*=====
*   Create title lines for the simulation.
*=====
A1 'CHERRY POINT RAIN MODULE INPUT FILE'
A1 'YEAR 2000'
*=====
*   The 'B' lines are for program control purposes.
*=====
* IFORM ISTA IDECID IYBEG IYEAR ISUM MIT NPTS IFILE A NOSTAT
B1 3   1   1 001010 0   1 12 50 1 0.4 1111
* THISTO METRIC KUNIT FIRMAT   CONV F1 F2 F3 F4 F5 F6 F7
B2 6   0   1 (I6,513,F10) 1 0 2 3 4 5 6 7
*=====
*   Line D1 is the first rainfall control line.
*=====
* YEAR MONTH DAY  HR  MIN  SEC  RAIN
20001010      05   17   38   0.00
20001010      05   18   56   0.01
20001010      05   20   12   0.01
20001011      12   47   21   0.01
20001011      12   47   29   0.01
$ENDPROGRAM
```

**Exhibit 3D.2:** Tipping Bucket Rain Gauge Textfile Excerpt used for Continuous XPSWMM Simulations (2002)

<u>Date</u>	<u>time</u>	<u>01/100 in.</u>
01/02/2002	19:37:00	1
01/02/2002	21:22:00	1
01/02/2002	22:03:00	1
01/02/2002	22:53:00	1
01/02/2002	23:08:00	1
01/03/2002	00:00:00	1
01/03/2002	00:07:00	1
01/03/2002	00:55:00	1
01/03/2002	01:05:00	1
01/03/2002	01:10:00	1
01/03/2002	01:13:00	1
01/03/2002	01:16:00	1
01/03/2002	01:19:00	1
01/03/2002	01:24:00	1
01/03/2002	01:45:00	1
01/03/2002	03:17:00	1
01/03/2002	03:25:00	1
01/03/2002	03:30:00	1
01/03/2002	03:39:00	1
01/03/2002	03:48:00	1
01/03/2002	03:54:00	1
01/03/2002	03:59:00	1
01/03/2002	04:04:00	1
01/03/2002	04:27:00	1
01/03/2002	14:21:00	1
01/03/2002	15:20:00	1
01/03/2002	15:32:00	1
01/03/2002	16:04:00	1
01/04/2002	09:20:00	1
01/04/2002	11:46:00	1
01/04/2002	11:48:00	1
01/04/2002	11:59:00	1
01/04/2002	12:04:00	1
01/04/2002	12:08:00	1
01/04/2002	13:12:00	1
01/04/2002	13:31:00	1
01/04/2002	13:38:00	1
01/04/2002	13:44:00	1
01/04/2002	13:51:00	1
01/04/2002	13:58:00	1
01/04/2002	14:05:00	1
01/04/2002	14:12:00	1
01/04/2002	14:19:00	1
01/04/2002	14:28:00	1
01/04/2002	14:40:00	1
01/04/2002	14:53:00	1
01/04/2002	15:06:00	1
01/04/2002	15:18:00	1

### Exhibit 3D.2 Continued

01/04/2002	15:37:00	1
01/05/2002	10:04:00	1
01/05/2002	11:24:00	1
01/06/2002	11:51:00	1
01/06/2002	11:54:00	1
01/06/2002	11:57:00	1
01/06/2002	12:00:00	1
01/06/2002	12:03:00	1
01/06/2002	12:04:00	1
01/06/2002	12:05:00	1
01/06/2002	12:07:00	1
01/06/2002	12:08:00	1
01/06/2002	12:10:00	1
01/06/2002	12:14:00	1
01/06/2002	12:16:00	1
01/06/2002	12:18:00	1
01/06/2002	12:20:00	1
01/06/2002	12:23:00	1
01/06/2002	12:25:00	1
01/06/2002	12:27:00	1
01/06/2002	12:29:00	1
01/06/2002	12:30:00	1
01/06/2002	12:31:00	1
01/06/2002	12:31:00	1
01/06/2002	12:32:00	1
01/06/2002	12:32:00	1
01/06/2002	12:32:00	1
01/06/2002	12:33:00	1
01/06/2002	12:34:00	1
01/06/2002	12:35:00	1
01/06/2002	12:36:00	1
01/06/2002	12:38:00	1
01/06/2002	12:40:00	1
01/06/2002	12:43:00	1
01/06/2002	12:45:00	1
01/06/2002	12:47:00	1
01/06/2002	12:49:00	1
01/06/2002	12:50:00	1
01/06/2002	12:50:00	1
01/06/2002	12:51:00	1
01/06/2002	12:52:00	1
01/06/2002	12:53:00	1
01/06/2002	12:53:00	1
01/06/2002	12:53:00	1
01/06/2002	12:54:00	1
01/06/2002	12:54:00	1
01/06/2002	12:54:00	1
01/06/2002	12:55:00	1
01/06/2002	12:55:00	1
01/06/2002	12:56:00	1
01/06/2002	12:56:00	1

**Exhibit 3D.2 Continued**

01/06/2002	12:56:00	1
01/06/2002	12:57:00	1
01/06/2002	13:01:00	1
01/06/2002	13:05:00	1
01/06/2002	13:11:00	1
01/06/2002	13:17:00	1
01/06/2002	13:20:00	1
01/06/2002	13:25:00	1

**Appendix 3E: RUNOFF Module Exhibits**

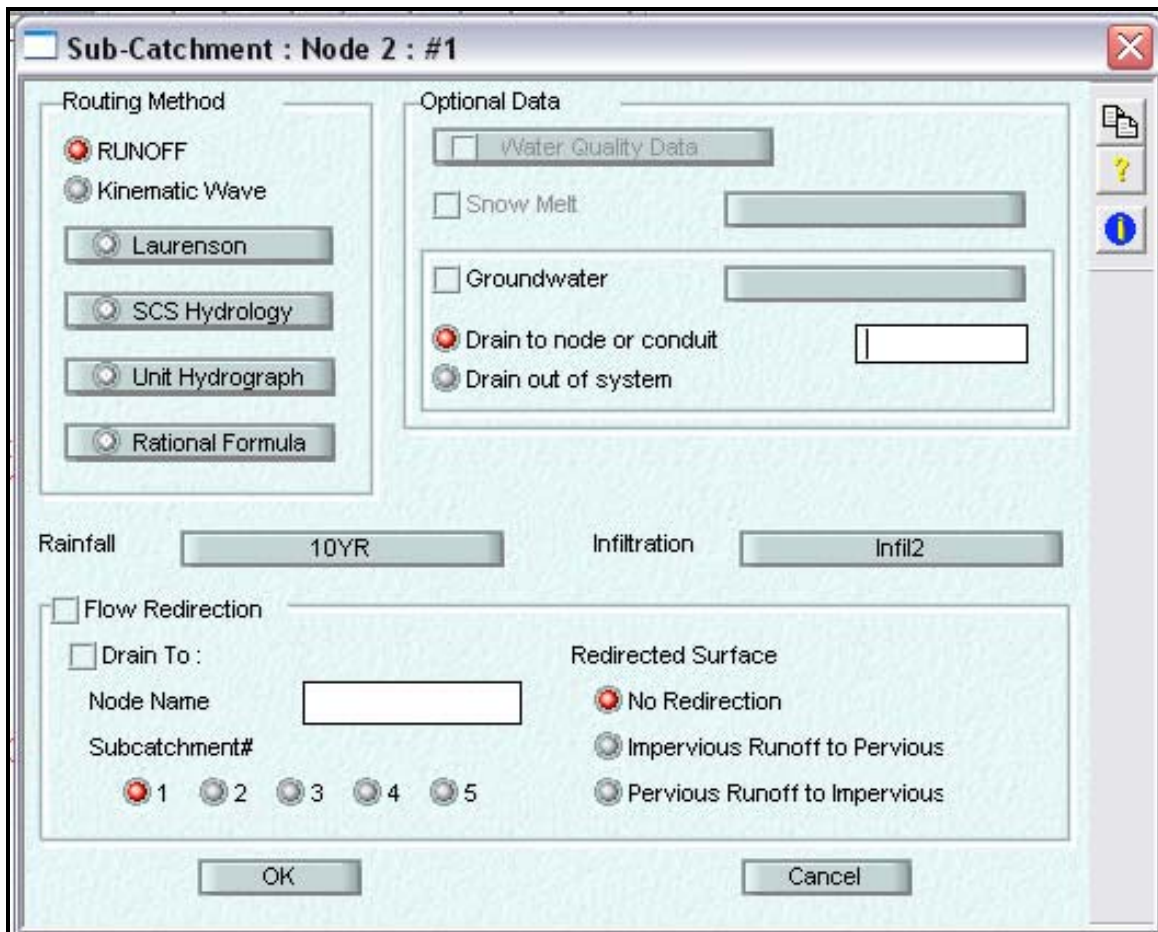


**Figure 3E.1: XPSWMM Screenshot of the Node Options Menu in the Runoff Block.** This menu allows the user to specify a routing method, rainfall file and infiltration method per model point.



**Figure 3E.2: The Import Screen in XPSWMM.** This input screen is where the modeler specifies the location of either exported XPSWMM files or older SWMM4.2 files to be imported into the current XPSWMM project.

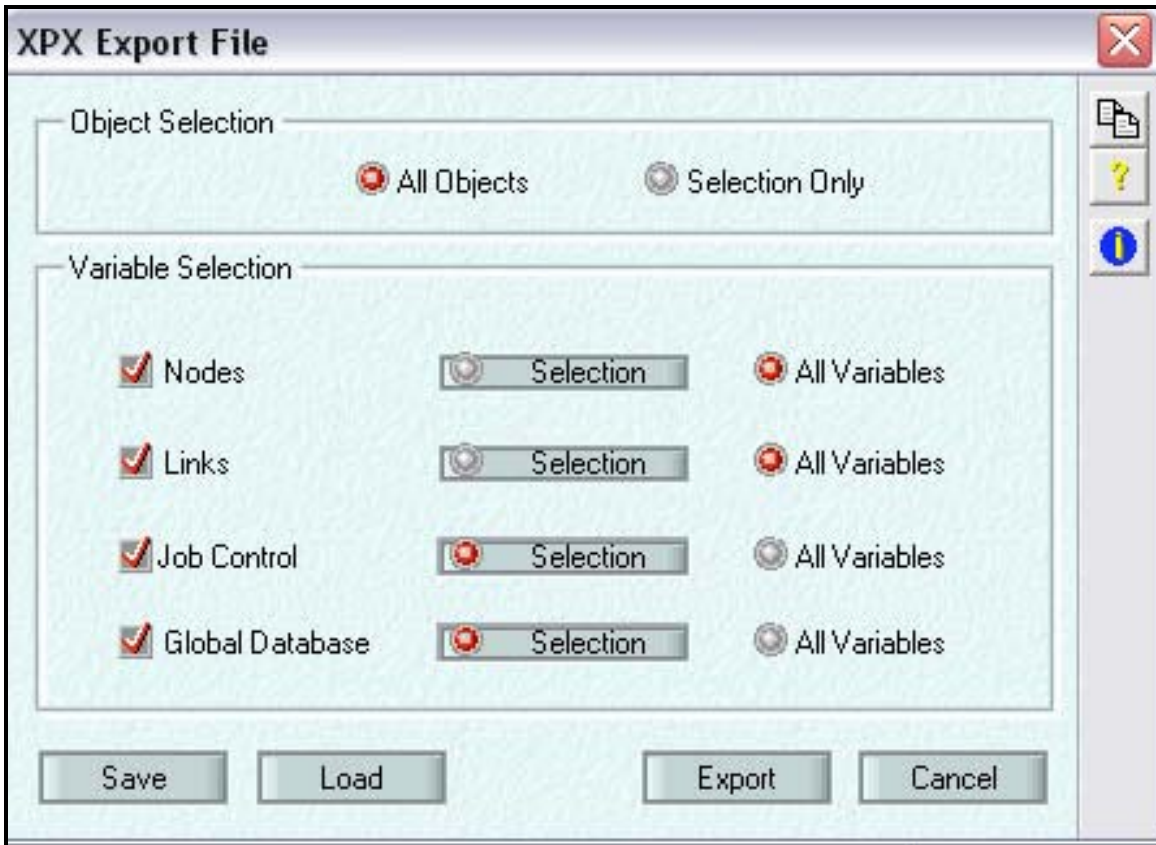


**Figure 3E.3: The Export Screen for creating .xpx Files.** The exportation wizard was used to create the various calibrations and design storm modeling scenarios that were saved individually. By exporting the entire XPSWMM project, a simple project rename created a cloned project file.

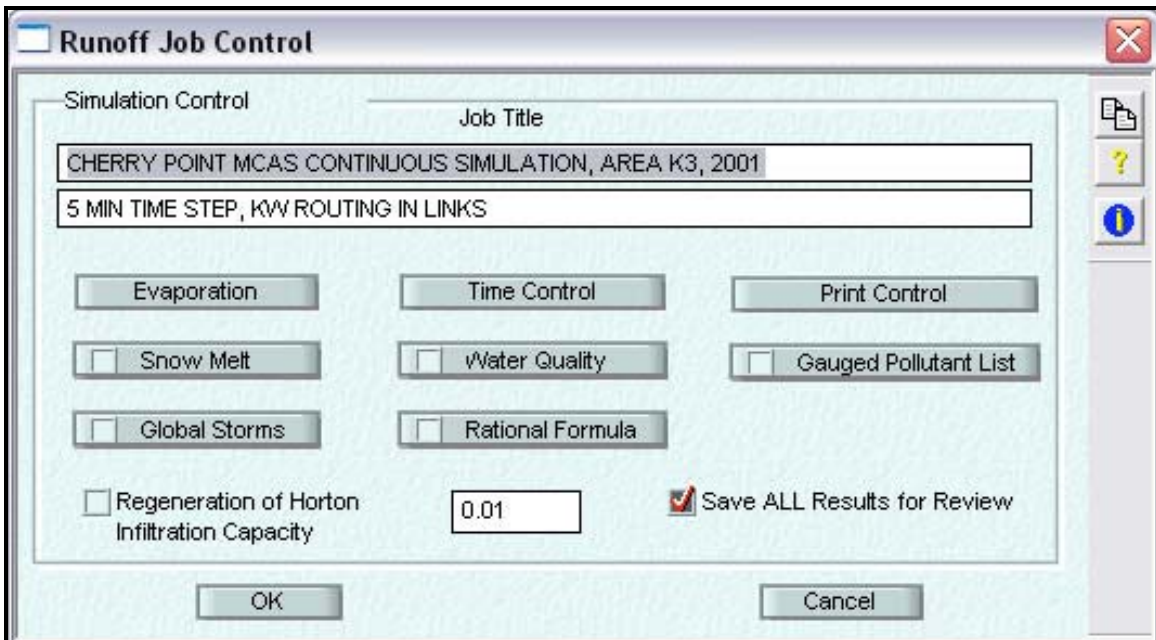


**Figure 3E.4: XPSWMM Runoff Block Job Control Options Screen.** The Job Controls screen was used to name the simulation and to access various submenus used to customize the inputs and outputs of the SPWMM simulation.

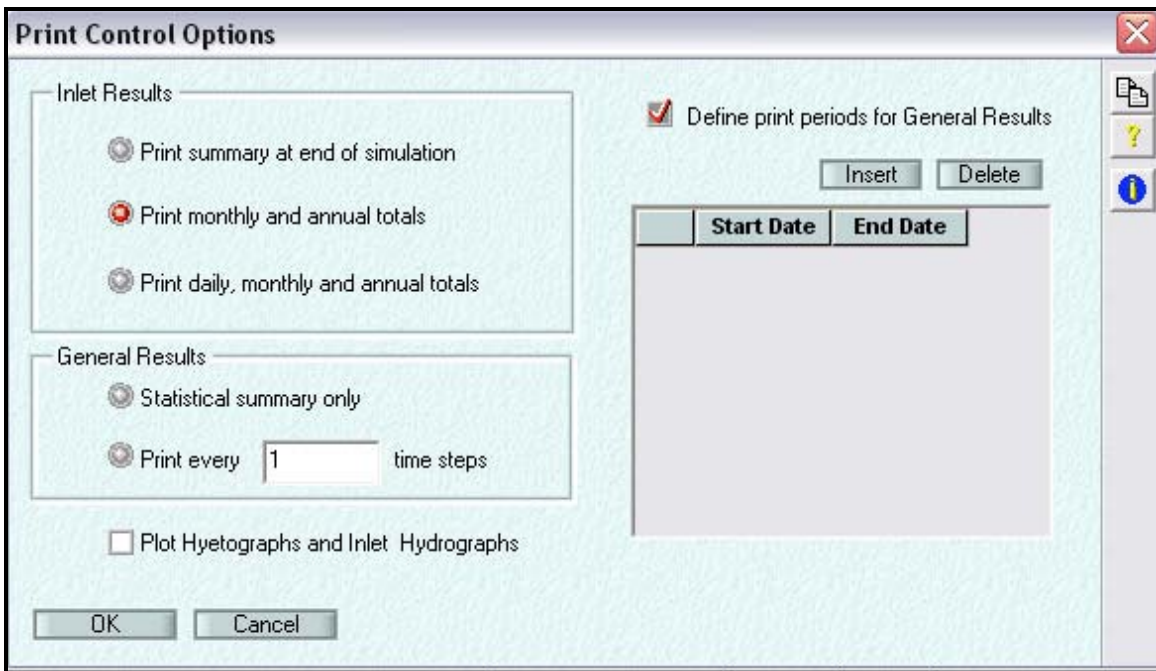


**Figure 3E.5: XPSWMM Print Control Options.** This screenshot is a graphic of how XPSWMM handles the user-determined print options for the simulations.

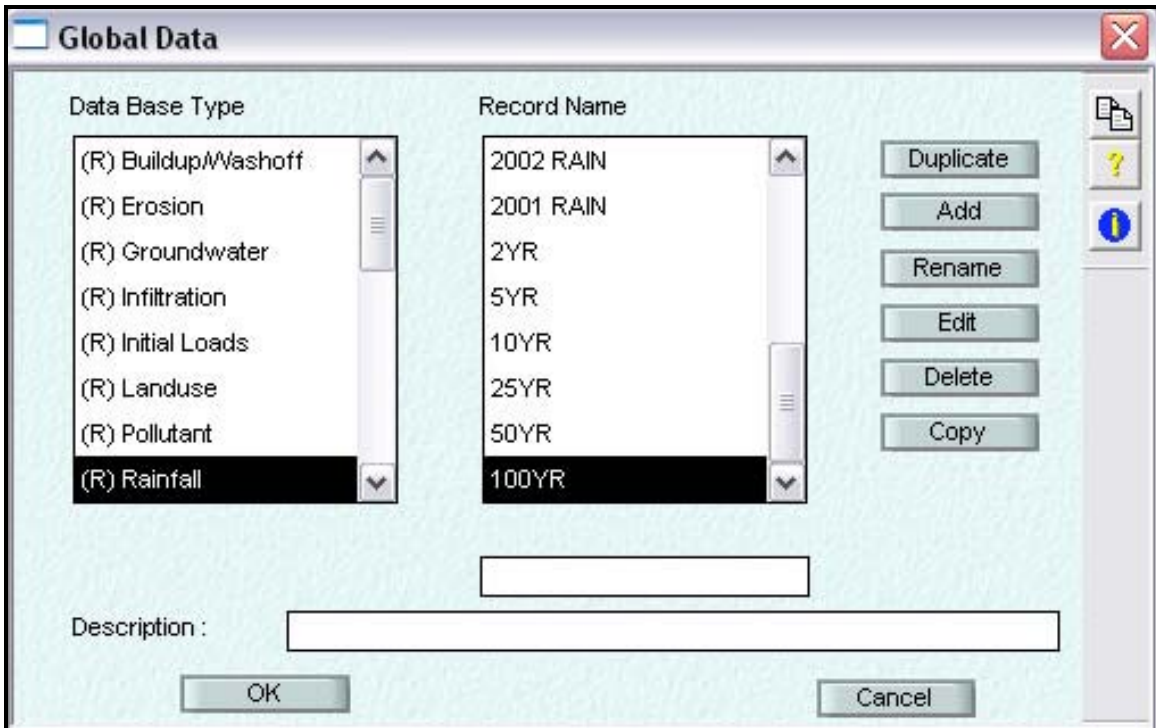


**Figure 3E.6: XPSWMM Global Data Screen.** This screenshot is used to link the various databases including rainfall, pollutant, and infiltration information to XPSWMM project. Therefore, the user only needs to create the dataset once, and then uses this screen to access the created data.

**Table 3E.7: SWMM 4.4 Event 88 RUNOFF file for Catchment K3 (2001)**

```

SW 1 0 3
MM 4 1 2 3 4
*=====
===
*   SWMM 4.4 RUNOFF DATA FILE
*=====
===
$RUNOFF
*=====
===
*   Create title lines for the simulation.
*=====
===
A1 'Cherry Point Test run'
A1 '2001 Storm Event on Day 88 in area k3.'
*=====
===
*   The 'B' lines are for program control purposes.
*=====
===
* METRIC ISNOW NRGAG INFILM KWALTY IVAP NHR NMN NDAY MONTH IYRSTR
B1 0 0 1 0 0 1 00 00 29 03 01
* IPRN(1) IPRN(2) IPRN(3) IRPNGW
B2 0 0 1
* WET WET/DRY DRY LUNIT LONG
B3 900. 3600. 7200. 3 2
*=====
===
*   Line D1 is the first rainfall control line.
*=====
===
*   ROPT
D1 0
*=====
===
*   Paste rainfall data (E lines) here.
*=====
===
* KTYPE KINC KPRINT KTHIS KTIME KPREP NHISTO THISTO TZRAIN
E1 1 1 0 0 0 1 481 6 0
E3 0 0.00
E3 6 0.00
E3 12 0.00
E3 18 0.00
E3 24 0.00
E3 30 0.00
E3 36 0.00
E3 42 0.00
E3 48 0.00
E3 54 0.00
E3 60 0.00

```

**Table 3E.7 Continued**

E3	66	0.00
E3	72	0.00
E3	78	0.00
E3	84	0.00
E3	90	0.00
E3	96	0.00
E3	102	0.00
E3	108	0.00
E3	114	0.00
E3	120	0.00
E3	126	0.00
E3	132	0.00
E3	138	0.00
E3	144	0.00
E3	150	0.00
E3	156	0.00
E3	162	0.00
E3	168	0.00
E3	174	0.00
E3	180	0.00
E3	186	0.00
E3	192	0.00
E3	198	0.00
E3	204	0.00
E3	210	0.00
E3	216	0.00
E3	222	0.00
E3	228	0.00
E3	234	0.00
E3	240	0.01
E3	246	0.00
E3	252	0.00
E3	258	0.00
E3	264	0.00
E3	270	0.00
E3	276	0.00
E3	282	0.00
E3	288	0.00
E3	294	0.01
E3	300	0.01
E3	306	0.01
E3	312	0.01
E3	318	0.01
E3	324	0.00
E3	330	0.01
E3	336	0.00
E3	342	0.01
E3	348	0.00
E3	354	0.01
E3	360	0.01
E3	366	0.00

**Table 3E.7 Continued**

E3	372	0.01
E3	378	0.01
E3	384	0.01
E3	390	0.01
E3	396	0.01
E3	402	0.01
E3	408	0.01
E3	414	0.00
E3	420	0.01
E3	426	0.01
E3	432	0.00
E3	438	0.01
E3	444	0.00
E3	450	0.01
E3	456	0.00
E3	462	0.00
E3	468	0.01
E3	474	0.00
E3	480	0.00
E3	486	0.00
E3	492	0.00
E3	498	0.00
E3	504	0.00
E3	510	0.00
E3	516	0.01
E3	522	0.01
E3	528	0.02
E3	534	0.04
E3	540	0.03
E3	546	0.00
E3	552	0.00
E3	558	0.01
E3	564	0.00
E3	570	0.00
E3	576	0.00
E3	582	0.01
E3	588	0.01
E3	594	0.00
E3	600	0.00
E3	606	0.00
E3	612	0.00
E3	618	0.01
E3	624	0.00
E3	630	0.00
E3	636	0.00
E3	642	0.00
E3	648	0.01
E3	654	0.00
E3	660	0.00
E3	666	0.00
E3	672	0.00

**Table 3E.7 Continued**

E3	678	0.00
E3	684	0.00
E3	690	0.00
E3	696	0.00
E3	702	0.00
E3	708	0.00
E3	714	0.00
E3	720	0.00
E3	726	0.00
E3	732	0.00
E3	738	0.00
E3	744	0.00
E3	750	0.00
E3	756	0.00
E3	762	0.00
E3	768	0.01
E3	774	0.00
E3	780	0.00
E3	786	0.00
E3	792	0.01
E3	798	0.00
E3	804	0.00
E3	810	0.00
E3	816	0.00
E3	822	0.00
E3	828	0.00
E3	834	0.00
E3	840	0.00
E3	846	0.00
E3	852	0.00
E3	858	0.00
E3	864	0.00
E3	870	0.00
E3	876	0.00
E3	882	0.00
E3	888	0.00
E3	894	0.00
E3	900	0.00
E3	906	0.00
E3	912	0.00
E3	918	0.00
E3	924	0.00
E3	930	0.00
E3	936	0.00
E3	942	0.00
E3	948	0.00
E3	954	0.00
E3	960	0.00
E3	966	0.00
E3	972	0.00
E3	978	0.00

**Table 3E.7 Continued**

E3	984	0.00
E3	990	0.00
E3	996	0.00
E3	1002	0.00
E3	1008	0.00
E3	1014	0.00
E3	1020	0.00
E3	1026	0.00
E3	1032	0.00
E3	1038	0.00
E3	1044	0.00
E3	1050	0.00
E3	1056	0.00
E3	1062	0.00
E3	1068	0.00
E3	1074	0.00
E3	1080	0.00
E3	1086	0.00
E3	1092	0.00
E3	1098	0.00
E3	1104	0.01
E3	1110	0.02
E3	1116	0.00
E3	1122	0.01
E3	1128	0.00
E3	1134	0.00
E3	1140	0.01
E3	1146	0.00
E3	1152	0.00
E3	1158	0.00
E3	1164	0.00
E3	1170	0.00
E3	1176	0.00
E3	1182	0.00
E3	1188	0.00
E3	1194	0.00
E3	1200	0.00
E3	1206	0.00
E3	1212	0.00
E3	1218	0.00
E3	1224	0.00
E3	1230	0.00
E3	1236	0.00
E3	1242	0.00
E3	1248	0.00
E3	1254	0.00
E3	1260	0.00
E3	1266	0.00
E3	1272	0.00
E3	1278	0.00
E3	1284	0.00

**Table 3E.7 Continued**

E3	1290	0.00
E3	1296	0.00
E3	1302	0.00
E3	1308	0.00
E3	1314	0.00
E3	1320	0.00
E3	1326	0.00
E3	1332	0.00
E3	1338	0.00
E3	1344	0.00
E3	1350	0.00
E3	1356	0.00
E3	1362	0.00
E3	1368	0.00
E3	1374	0.00
E3	1380	0.00
E3	1386	0.00
E3	1392	0.00
E3	1398	0.00
E3	1404	0.00
E3	1410	0.00
E3	1416	0.00
E3	1422	0.00
E3	1428	0.00
E3	1434	0.00
E3	1440	0.01
E3	1446	0.00
E3	1452	0.00
E3	1458	0.00
E3	1464	0.00
E3	1470	0.00
E3	1476	0.00
E3	1482	0.00
E3	1488	0.00
E3	1494	0.00
E3	1500	0.00
E3	1506	0.00
E3	1512	0.00
E3	1518	0.00
E3	1524	0.00
E3	1530	0.00
E3	1536	0.00
E3	1542	0.01
E3	1548	0.00
E3	1554	0.00
E3	1560	0.00
E3	1566	0.00
E3	1572	0.01
E3	1578	0.00
E3	1584	0.00
E3	1590	0.00

**Table 3E.7 Continued**

E3	1596	0.01
E3	1602	0.00
E3	1608	0.00
E3	1614	0.00
E3	1620	0.00
E3	1626	0.00
E3	1632	0.00
E3	1638	0.00
E3	1644	0.01
E3	1650	0.00
E3	1656	0.00
E3	1662	0.00
E3	1668	0.00
E3	1674	0.00
E3	1680	0.00
E3	1686	0.00
E3	1692	0.00
E3	1698	0.00
E3	1704	0.02
E3	1710	0.00
E3	1716	0.03
E3	1722	0.00
E3	1728	0.00
E3	1734	0.01
E3	1740	0.00
E3	1746	0.00
E3	1752	0.01
E3	1758	0.01
E3	1764	0.00
E3	1770	0.00
E3	1776	0.01
E3	1782	0.00
E3	1788	0.00
E3	1794	0.01
E3	1800	0.01
E3	1806	0.01
E3	1812	0.00
E3	1818	0.00
E3	1824	0.00
E3	1830	0.00
E3	1836	0.00
E3	1842	0.00
E3	1848	0.00
E3	1854	0.00
E3	1860	0.00
E3	1866	0.00
E3	1872	0.00
E3	1878	0.00
E3	1884	0.00
E3	1890	0.00
E3	1896	0.00

**Table 3E.7 Continued**

E3	1902	0.00
E3	1908	0.00
E3	1914	0.00
E3	1920	0.00
E3	1926	0.00
E3	1932	0.00
E3	1938	0.00
E3	1944	0.00
E3	1950	0.00
E3	1956	0.00
E3	1962	0.00
E3	1968	0.00
E3	1974	0.00
E3	1980	0.00
E3	1986	0.00
E3	1992	0.00
E3	1998	0.00
E3	2004	0.00
E3	2010	0.00
E3	2016	0.00
E3	2022	0.00
E3	2028	0.00
E3	2034	0.00
E3	2040	0.00
E3	2046	0.00
E3	2052	0.00
E3	2058	0.00
E3	2064	0.00
E3	2070	0.00
E3	2076	0.00
E3	2082	0.00
E3	2088	0.00
E3	2094	0.00
E3	2100	0.00
E3	2106	0.00
E3	2112	0.00
E3	2118	0.00
E3	2124	0.00
E3	2130	0.00
E3	2136	0.00
E3	2142	0.00
E3	2148	0.00
E3	2154	0.00
E3	2160	0.00
E3	2166	0.00
E3	2172	0.00
E3	2178	0.00
E3	2184	0.00
E3	2190	0.00
E3	2196	0.00
E3	2202	0.00

**Table 3E.7 Continued**

E3	2208	0.00
E3	2214	0.00
E3	2220	0.00
E3	2226	0.00
E3	2232	0.00
E3	2238	0.00
E3	2244	0.00
E3	2250	0.00
E3	2256	0.00
E3	2262	0.00
E3	2268	0.00
E3	2274	0.00
E3	2280	0.00
E3	2286	0.00
E3	2292	0.00
E3	2298	0.00
E3	2304	0.00
E3	2310	0.00
E3	2316	0.00
E3	2322	0.00
E3	2328	0.00
E3	2334	0.00
E3	2340	0.00
E3	2346	0.00
E3	2352	0.00
E3	2358	0.00
E3	2364	0.00
E3	2370	0.00
E3	2376	0.00
E3	2382	0.00
E3	2388	0.00
E3	2394	0.00
E3	2400	0.00
E3	2406	0.00
E3	2412	0.00
E3	2418	0.00
E3	2424	0.00
E3	2430	0.00
E3	2436	0.00
E3	2442	0.00
E3	2448	0.00
E3	2454	0.00
E3	2460	0.00
E3	2466	0.00
E3	2472	0.00
E3	2478	0.00
E3	2484	0.00
E3	2490	0.00
E3	2496	0.00
E3	2502	0.00
E3	2508	0.00

**Table 3E.7 Continued**

E3	2514	0.00
E3	2520	0.00
E3	2526	0.00
E3	2532	0.00
E3	2538	0.00
E3	2544	0.00
E3	2550	0.00
E3	2556	0.00
E3	2562	0.00
E3	2568	0.00
E3	2574	0.00
E3	2580	0.00
E3	2586	0.00
E3	2592	0.00
E3	2598	0.00
E3	2604	0.00
E3	2610	0.00
E3	2616	0.00
E3	2622	0.00
E3	2628	0.00
E3	2634	0.00
E3	2640	0.00
E3	2646	0.00
E3	2652	0.00
E3	2658	0.00
E3	2664	0.00
E3	2670	0.00
E3	2676	0.00
E3	2682	0.00
E3	2688	0.00
E3	2694	0.00
E3	2700	0.00
E3	2706	0.00
E3	2712	0.00
E3	2718	0.00
E3	2724	0.00
E3	2730	0.00
E3	2736	0.00
E3	2742	0.00
E3	2748	0.00
E3	2754	0.00
E3	2760	0.00
E3	2766	0.00
E3	2772	0.00
E3	2778	0.00
E3	2784	0.00
E3	2790	0.00
E3	2796	0.00
E3	2802	0.00
E3	2808	0.00
E3	2814	0.00

**Table 3E.7 Continued**

E3 2820 0.00  
 E3 2826 0.00  
 E3 2832 0.00  
 E3 2838 0.00  
 E3 2844 0.00  
 E3 2850 0.00  
 E3 2856 0.00  
 E3 2862 0.00  
 E3 2868 0.00  
 E3 2874 0.00  
 E3 2880 0.00  
 F1 0.1 0.2 0.2 0.2 0.3 0.4 0.5 0.5 0.4 0.3 0.2 0.1

\*=====

===  
 \* Enter gutter information on line G1. If weir is present also use G2.

\* NAMEG NGTO NPG GWIDTH GLEN G3 GS1 GS2 G6 DFULL GDEPTH

G1 301 118 1 21.0 398 0.0005 0.57 0.57 0.030 6 0  
 G1 302 101 2 2.5 512 0.0039 0.0 0.0 0.012 0 0  
 G1 101 301 1 9.0 545 0.0183 0.44 0.44 0.035 2 0  
 G1 102 302 1 17.0 288 0.0139 0.17 0.17 0.030 3 0  
 G1 119 301 1 21.0 316 0.0016 0.48 0.48 0.030 5 0  
 G1 317 119 1 21.0 477 0.0105 0.48 0.48 0.030 5 0  
 G1 117 317 2 3.0 396 0.0151 0.0 0.0 0.012 0 0  
 G1 122 117 2 2.5 276 0.0091 0.0 0.0 0.012 0 0  
 G1 121 122 2 2.0 194 0.0026 0.0 0.0 0.012 0 0  
 G1 116 117 2 2.5 1053 0.0047 0.0 0.0 0.012 0 0  
 G1 113 317 1 21.0 127 0.0552 0.48 0.48 0.030 5 0  
 G1 304 113 2 3.5 113 0.0354 0 0 0.012 0 0  
 G1 104 304 1 13.0 472 0.0053 0.77 0.77 0.030 5 0  
 G1 103 104 2 2.0 359 0.0223 0 0 0.012 0 0  
 G1 106 104 2 3.0 801 0.0081 0 0 0.012 0 0  
 G1 105 106 2 2.5 647 0.0015 0 0 0.012 0 0  
 G1 120 105 2 2.5 35 0.0005 0 0 0.012 0 0  
 G1 112 113 1 21.0 526 0.0038 0.48 0.48 0.030 5 0  
 G1 107 112 1 15.0 1295 0.0023 0.40 0.40 0.030 3 0  
 G1 108 107 2 2.0 290 0.0005 0 0 0.012 0 0  
 G1 114 112 2 2.0 1322 0.0019 0 0 0.012 0 0  
 G1 110 114 2 2.0 1195 0.0008 0 0 0.012 0 0  
 G1 309 110 1 15.0 282 0.0071 0.13 0.13 0.030 3 0  
 G1 109 309 2 1.5 234 0.0005 0 0 0.012 0 0  
 G1 111 110 1 15.0 297 0.0067 0.13 0.13 0.030 3 0  
 G1 115 110 2 2.0 656 0.0046 0 0 0.012 0 0

\* Enter Subcatchment Data on line H1.

\* JK NAMEW NGTO WIDTH AREA %IMP SLP IMPN PERVN IDS PDS SUCT  
 HYCOND MSTDEF

H1 1 1 101 690 11.4 43.3 0.0196 0.013 0.030 0.05 0.10 4.33 0.429 0.453  
 H1 1 2 102 392 3.67 32.5 0.0063 0.013 0.030 0.05 0.10 2.41 1.18 0.437  
 H1 1 3 103 323 5.20 48.9 0.0013 0.013 0.030 0.05 0.10 2.41 1.18 0.437  
 H1 1 4 104 693 16.3 52.8 0.0057 0.013 0.030 0.05 0.10 2.41 1.18 0.437  
 H1 1 5 105 534 7.50 43.8 0.0049 0.013 0.030 0.05 0.10 2.41 1.18 0.437  
 H1 1 6 106 335 3.30 57.8 0.0070 0.013 0.030 0.05 0.10 2.41 1.18 0.437

**Table 3E.7 Continued**

H1	1	7	107	402	7.60	53.8	0.0046	0.013	0.030	0.05	0.10	12.45	0.012	0.475
H1	1	8	108	456	9.20	63.7	0.0053	0.013	0.030	0.05	0.10	12.45	0.012	0.475
H1	1	9	109	641	7.80	53.1	0.0060	0.013	0.030	0.05	0.10	12.45	0.012	0.475
H1	1	10	110	362	14.7	49.8	0.0035	0.013	0.030	0.05	0.10	2.41	1.18	0.437
H1	1	11	111	818	10.8	43.8	0.0037	0.013	0.030	0.05	0.10	2.41	1.18	0.437
H1	1	12	112	769	28.9	46.2	0.0032	0.013	0.030	0.05	0.10	12.45	0.012	0.475
H1	1	13	113	618	7.93	28.8	0.0092	0.013	0.030	0.05	0.10	4.33	0.429	0.453
H1	1	14	114	1107	36.0	50.7	0.0019	0.013	0.030	0.05	0.10	12.45	0.012	0.475
H1	1	15	115	654	25.1	36.7	0.0025	0.013	0.030	0.05	0.10	12.45	0.012	0.475
H1	1	16	116	485	16.4	44.5	0.0032	0.013	0.030	0.05	0.10	12.45	0.012	0.475
H1	1	17	117	234	4.53	14.3	0.0029	0.013	0.030	0.05	0.10	4.33	0.429	0.453
H1	1	18	118	663	10.1	18.7	0.0085	0.013	0.030	0.05	0.10	2.41	1.18	0.437
H1	1	19	119	524	12.8	29.9	0.0095	0.013	0.030	0.05	0.10	4.33	0.429	0.453
H1	1	20	120	193	2.63	6.30	0.0015	0.013	0.030	0.05	0.10	2.41	1.18	0.437
H1	1	21	121	463	8.80	33.6	0.0067	0.013	0.030	0.05	0.10	12.45	0.012	0.475
H1	1	22	122	318	5.30	19.0	0.0059	0.013	0.030	0.05	0.10	12.45	0.012	0.475

\*=====

===

\* Enter data for Channel/Inlet Print Control M lines.

\*=====

===

\* NO water quality simulations

\* NPRNT INTERV

M1 1 1

\* NDET STARTP(1) STOPPR(1) IPRNT(1)

M2 1 0 0

M3 118

\*=====

===

\* End your input data set with a \$ENDPROGRAM.

\*=====

===

\$ENDPROGRAM

**Table 3E.8: SWMM Runoff Block Input Descriptions**

(values taken from SWMM input data file for catchment K2 for storm 020102)

Group	Name	Value	Description
<b>Inter-facing Files</b>	<b>SW</b>		The SW card creates or specifies which interface files SWMM will reference
	NBLOCK	1	block number
	JIN(1)	0	input interface file number
	JOUT(1)	3	output interface file number
	<b>MM</b>		The MM card opens the files to be used by the various subroutines
	NITCH	4	Number of scratch files
	NSCRAT(1)	1	Scratch file reference number
	NSCRAT(2)	2	"
	NSCRAT(3)	3	"
	NSCRAT(4)	4	"
<b>A</b>	<b>A1</b>		This area is used to create title lines for the simulation (2-line maximum). All comments must be enclosed in single quotation marks
<b>B</b>	<b>B1</b>		Control Parameters
	METRIC	0	Metric input/output: use U.S. customary units
	ISNOW	0	snowmelt parameter: no snowmelt simulated
	NRGAG	1	number of hyetographs/rain gages (10 max.)
	INFILM	1	infiltration equation: Green-Ampt equation selected
	KWALTY	0	water quality simulated: no
	IVAP	1	evaporation parameter: read monthly evaporation data in group F1, units: in/day
	NHR	0	hour of day of start of storm, using a 24-hour clock
	NMN	0	minute of hour of start of storm, (0-59 minutes)
	NDAY	2	day of month of start of storm (1-31)
	MONTH	1	month of start of simulation (1-12)
	IYRSTR	2	year of start of simulation (0-99)
	<b>B2</b>		
	IPRN(1)	0	print control for SWMM input: print all input data
	IPRN(2)	0	print control for Runoff Block graphs: plot all graphs
	IPRN(3)	1	print control for SWMM output: print monthly and annual totals only, one year per page
	IRPNGW		optional parameter
	<b>B3</b>		
	WET	900	Wet time step (seconds)
	WET/DRY	3600	Transition time between Wet and Dry time steps (seconds)

**Table 3E.8 Continued**

	DRY	7200	Dry time step (seconds)
	LUNIT	3	simulation length units: days
	LONG	5	simulation length: 5 days
<b>D</b>	<b>D1</b>		Precipitation Controls
	ROPT	0	Precipitation input option: read hyetograph data on lines E1-E3
<b>E</b>	<b>E1</b>		Precipitation Controls
	KTYPE	1	precipitation input: read KINC time and precipitation pairs per line
	KINC	1	number of precipitation pairs per line
	KPRINT	0	print control for precipitation input: print all data
	KTHIS	0	precipitation interval: constant
	KTIME	0	precipitation time units: minutes
	KPREP	1	precipitation unit type: total volume over interval (inches)
	NHISTO	1201	number of data points for each hyetograph
	THISTO	6	time interval between values in units of KTIME
	TZRAIN	0	initial time of day of precipitation input in units of KTIME
	<b>E3</b>		Precipitation Data
<b>F</b>	<b>F1</b>		Evaporation Data
		various	Evaporation rates for months 1-12 (in/day)
<b>G</b>	<b>G1</b>		Channel/Pipe Data
	NAMEG	various	channel/pipe number or name
	NGTO	various	channel/pipe or inlet number or name for drainage
	NPG		channel/pipe type:
		1	trapezoidal channel
		2	circular pipe
		3	dummy channel/pipe where inflow=outflow
	GWIDTH	various	bottom width of channel or diameter of pipe (ft)
	GLEN	various	channel/pipe length (ft)
	G3	various	invert slope (ft/ft)
	GS1	various	left-hand side slope (ft/ft)
	GS2	various	right-hand side slope (ft/ft)
	G6		Manning's roughness coefficient
		0.012	concrete pipe
		0.03	stream channel
		0.04	stream channel
		0.075	overland flow
	DFULL	various	channel depth when full (ft)
	GDEPTH	various	starting depth of pipe/channel (ft)
<b>H</b>	<b>H1</b>		Subcatchment Surface Data
	JK	1	hyetograph number

**Table 3E.8 Continued**

<b>M</b>	NAMEW	various	subcatchment number
	NGTO	various	channel/pipe inlet number for drainage
	WIDTH	various	subcatchment width
	AREA	various	subcatchment area
	%IMP	various	percent imperviousness of subcatchment
	SLP	various	ground slope (ft/ft)
	IMPV	0.01	impervious area Manning's roughness
	PERV	0.023	pervious area Manning's roughness
	IDS	0.05	impervious area depression storage (in)
	PDS	0.1	pervious area depression storage (in)
	SUCT	various	average capillary suction (in)
	HYCOND	various	saturated hydraulic conductivity, similar to porosity (in/hr)
	MSTDEF	various	initial soil moisture deficit=volume air/ volume voids (fraction)
	<b>M1</b>		Print Control Input
	NPRINT	1	total number of channels/inlets for which non-zero flows will be printed
	INTERV	1	print control: print every time step
	<b>M2</b>		Print Control Input
	NDET	1	number of detailed printout periods
	STARTP(1)	0	first starting printout date: total simulation printed as default
	STOPPR(1)	0	first stopping printout date
<b>M3</b>		Print Control Input	
IPRNT(1)	101	first channel/pipe number for which flows will be printed	

**Table 3E.9: Sample SWMM 4.4 Input File with Functional Routing Elements**

```

SW 1 0 3
MM 4 1 2 3 4
*=====
=====
*      SWMM 4.4 RUNOFF DATA FILE
*=====
=====
$RUNOFF
*=====
=====
*      Create title lines for the simulation.
*=====
=====
A1 'Cherry Point Test run'
A1 '2002 Storm Event on Day 090 in area K3.'
*=====
=====
*      The 'B' lines are for program control purposes.
*=====
=====
* METRIC ISNOW NRGAG INFILM KWALTY IVAP NHR NMN NDAY MONTH IYRSTR
B1 0      1  0      1 00  31 03 02
* IPRN(1) IPRN(2) IPRN(3) IRPNGW
B2  0  0  1
* WET  WET/DRY DRY LUNIT LONG
B3 900. 3600. 7200. 3 2
*=====
=====
*      Line D1 is the first rainfall control line.
*=====
=====
*      ROPT
D1 0
*=====
=====
*      Paste rainfall data (E lines) here.
*=====
=====
* KTYPE KINC KPRINT KTHIS KTIME KPREP NHISTO THISTO TZRAIN
E1 1 1 0 0 0 1 481 6 0
E3 data group is not included in this example

F1 0.1 0.2 0.2 0.2 0.3 0.4 0.5 0.5 0.4 0.3 0.2 0.1
*=====
=====
*      Enter gutter information on line G1.  If weir is present also use G2.
* NAMEG NGTO NPG GWIDTH GLEN  G3  GS1 GS2  G6  DFULL GDEPTH
G1 315 313 2 2.5 648 0.0039 0.00 0.00 0.014 0 0
G1 311 305 2 2.0 72 0.0139 0.00 0.00 0.014 0 0

```

**Table 3E.9 Continued**

G1	318	311	2	4.5	959	0.0026	0.00	0.00	0.014	0	0								
G1	309	302	1	2.0	2165	0.0069	0.20	0.20	0.023	1	0								
G1	314	315	2	1.5	36	0.0001	0.00	0.00	0.014	0	0								
G1	308	302	1	2.0	1305	0.0092	0.20	0.20	0.023	1	0								
G1	307	308	2	2.5	409	0.0073	0.00	0.00	0.014	0	0								
G1	312	305	3	0	100	0.0000	0.00	0.00	0.014	0	0								
G1	320	319	2	1.5	519	0.0137	0.00	0.00	0.014	0	0								
G1	305	302	1	6	895	0.0095	0.75	0.75	0.023	6	1								
G1	306	308	2	2.0	273	0.0073	0.00	0.00	0.014	0	0								
G1	303	302	1	1	543	0.0190	0.22	0.22	0.023	1	0								
G1	304	312	2	2.0	342	0.0130	0.00	0.00	0.014	0	0								
G1	313	312	2	3.5	1359	0.0059	0.00	0.00	0.014	0	0								
G1	302	300	1	6	398	0.0001	0.75	0.75	0.023	6	1								
G1	301	300	2	4.0	769	0.0001	0.00	0.00	0.014	0	0								
G1	322	318	2	4.0	1873	0.0010	0.00	0.00	0.014	0	0								
G1	321	319	2	1.5	367	0.0109	0.00	0.00	0.014	0	0								
G1	317	316	2	1.5	35	0.0140	0.00	0.00	0.014	0	0								
G1	316	311	1	2.0	1413	0.0021	0.43	0.43	0.023	3	1								
G1	319	318	2	2.5	144	0.0001	0.00	0.00	0.014	0	0								
G1	310	314	3	0.1	100	0.0001	0.00	0.00	0.001	0	0								
* Enter Subcatchment Data on line H1.																			
* JK NAMEW NGTO WIDTH AREA %IMP SLP IMPN PERVN IDS PDS MAX MIN DECAY																			
H1	1	1	201	690	11.4	43.3	0.0196	0.013	0.25	0.05	0.15	1.0	1.00	0.001					
H1	1	2	202	392	3.67	32.5	0.0063	0.013	0.25	0.05	0.15	1.0	1.00	0.001					
H1	1	3	203	323	5.20	48.9	0.0013	0.014	0.25	0.05	0.15	1.0	1.00	0.001					
H1	1	4	204	693	16.3	52.8	0.0057	0.013	0.25	0.05	0.15	1.0	1.00	0.001					
H1	1	5	205	534	7.50	43.8	0.0049	0.013	0.25	0.05	0.15	1.0	1.00	0.001					
H1	1	6	206	335	3.30	57.8	0.0070	0.013	0.25	0.05	0.15	1.0	1.00	0.001					
H1	1	7	207	402	7.60	53.8	0.0046	0.013	0.25	0.05	0.15	1.0	1.00	0.001					
H1	1	8	208	456	9.20	63.7	0.0053	0.013	0.25	0.05	0.15	1.0	1.00	0.001					
H1	1	9	209	641	7.80	53.1	0.0060	0.013	0.25	0.05	0.15	1.0	1.00	0.001					
H1	1	10	210	362	14.7	49.8	0.0035	0.013	0.25	0.05	0.15	1.0	1.00	0.001					

**Table 3E.9 Continued**

H1	1	11	211	818	10.8	43.8	0.0037	0.013	0.25	0.05	0.15	1.0	1.00	0.001
H1	1	12	212	769	28.9	46.2	0.0032	0.013	0.25	0.05	0.15	1.0	1.00	0.001
H1	1	13	213	618	7.93	28.8	0.0092	0.013	0.25	0.05	0.15	1.0	1.00	0.001
H1	1	14	214	1107	36.0	50.7	0.0019	0.013	0.25	0.05	0.15	1.0	1.00	0.001
H1	1	15	215	654	25.1	36.7	0.0025	0.013	0.25	0.05	0.15	1.0	1.00	0.001
H1	1	16	216	485	16.4	44.5	0.0032	0.013	0.25	0.05	0.15	1.0	1.00	0.001
H1	1	17	217	234	4.53	14.3	0.0029	0.013	0.25	0.05	0.15	1.0	1.00	0.001
H1	1	18	218	663	10.1	18.7	0.0085	0.013	0.25	0.05	0.15	1.0	1.00	0.001
H1	1	19	219	524	12.8	29.9	0.0095	0.013	0.25	0.05	0.15	1.0	1.00	0.001
H1	1	20	220	193	2.63	6.30	0.0015	0.013	0.25	0.05	0.15	1.0	1.00	0.001
H1	1	21	221	463	8.80	33.6	0.0067	0.013	0.25	0.05	0.15	1.0	1.00	0.001
H1	1	22	222	318	5.30	19.0	0.0059	0.013	0.25	0.05	0.15	1.0	1.00	0.001
*=====														
=====														
*       Enter data for Channel/Inlet Print Control M lines.														
*=====														
=====														
* NO water quality simulations														
M1 23 1														
* NDET STARTP(1) STOPPR(1) IPRNT(1)														
M2 1 0 0														
M3 300														
*=====														
=====														
*       End your input data set with a \$ENDPROGRAM.														
*=====														
=====														
ENDPROGRAM														

**Appendix 3F: Catchment K2 & K3 GIS Values**

**Table 3F.1: Roughness Coefficients for the Cherry Point Study Site**

<i>Channel Type</i>	<i>Manning's n</i>		
	<i>min.</i>	<i>normal</i>	<i>max.</i>
<b>concrete culvert</b> with bends connections and some debris	0.011	0.013	0.014
<b>finished concrete culvert</b>	0.011	0.012	0.014
<b>concrete sewer</b> with manholes, inlets, etc., straight	0.013	0.015	0.017
<b>natural stream</b> on plain, straight, full stage, no rifts or deep pools	0.025	0.03	0.033
<b>natural stream</b> on plain, clean, winding, some pools and shoals	0.033	0.04	0.045

(adapted from Chow ,1959)

**Table 3F.2: Catchment K2 Surface Measurements**

<b>subarea</b>	<b>total ac</b>	<b>max elev</b>	<b>min elev</b>	<b>length (ft)</b>	<b>slope(ft/ft)</b>	<b>width (ft)</b>
a	6.3	23	2	1012	0.020751	321
b	6.7	23.5	8	1360	0.011397	259
c	7.9	22	2	1060	0.018868	464
d	6.2	14	4	636	0.015723	218
d-wetland		8	5	1024	0.00293	181
e	9.7	22	7	1010	0.014851	467
f	4.7	23	10	708	0.018362	313
g	9	22	10	1192	0.010067	463
h	4.3	15	8	430	0.016279	499
l	9.9	18.5	9	861	0.011034	745
j	9.4	24	20	2250	0.001778	188
k	8.2	24.5	20	1494	0.003012	264
l	16.1	24.5	19	1013	0.005429	550
m	16.1	26	22	1300	0.003077	642

**Table 3F.3: Catchment K3 Surface Measurements**

sub area	Type	area (ac)	% of area	c - value	weighted C	sub-area c-value	% imp	length (ft)	slope (ft/ft)	width (ft)	CN
0	roads	1.05	14.1	0.8	0.113	0.430	43.0	980.95	0.0112 13619	187	69
	buildings	0.67	9.0	0.8	0.072						
	parking lots	1.13	15.2	0.8	0.121						
	Open area	4.6	61.7	0.2	0.123						
1	parking lots	0.67	6.0	0.8	0.048	0.259	25.9	680	0.0235 29412	536	69
	buildings	0.43	3.9	0.8	0.031						
	Open area	10	90.1	0.2	0.180						
2	roads	0.42	4.1	0.8	0.033	0.328	32.8	741.56	0.0229 24645	705	65.7
	parking lots	1.23	12.1	0.8	0.097						
	buildings	0.51	5.0	0.8	0.040						
	Open area	8	78.7	0.2	0.157						
3	roads	0	0.0	0.8	0.000	0.350	35.0	673.43	0.0200 46627	563	69
	parking lots	1.85	22.7	0.8	0.182						
	buildings	0.19	2.3	0.8	0.019						
	Open area	6.11	75.0	0.2	0.150						
4	roads	0.36	6.3	0.8	0.050	0.409	40.9	584.29	0.0128 36092	706	65.4
	parking lots	1.08	18.9	0.8	0.151						
	buildings	0.55	9.6	0.8	0.077						
	Open area	3.72	65.1	0.2	0.130						
5	roads	3.23	14.6	0.8	0.117	0.567	56.7	1795.3 4	0.0069 6247	1305	90.6
	parking lots	9.01	40.6	0.8	0.325						
	buildings	1.31	5.9	0.8	0.047						
	Open area	8.62	38.9	0.2	0.078						
6	roads	1.43	8.5	0.8	0.068	0.563	56.3	1426	0.0049 08836	954	90.7
	parking lots	4.78	28.5	0.8	0.228						
	buildings	3.93	23.4	0.8	0.187						
	open area	6.63	39.5	0.2	0.079						
7	roads	1.47	5.3	0.8	0.042	0.508	50.8	955.5	0.0115 12297	1332	61.3

**Table 3F.3 Continued**

	parking lots	10.14	36.3	0.8	0.290						
	buildings	2.72	9.7	0.8	0.078						
	open area	13.6	48.7	0.2	0.097						
8	roads	1.96	7.8	0.8	0.062	0.572	57.2	1193.7 3	0.0071 20538	1038	80.2
	parking lots	9.6	38.1	0.8	0.305						
	buildings	4.08	16.2	0.8	0.129						

	open area	9.57	38.0	0.2	0.076						
9	roads	1.15	5.6	0.8	0.045	0.491	49.1	1380.9 1	0.0054 31201	963	71.3
	parking lots	5.87	28.7	0.8	0.230						
	Buildings	2.9	14.2	0.8	0.114						
	open area	10.52	51.5	0.2	0.103						
10	roads	1	8.6	0.8	0.069	0.446	44.6	1080	0.0050 92593	489	61
	parking lots	3.4	29.2	0.8	0.234						
	buildings	0.38	3.3	0.8	0.026						
	open area	6.86	58.9	0.2	0.118						
11	roads	0.28	2.3	0.8	0.019	0.395	39.5	828.67	0.0018 10129	615	79
	parking lots	2.72	22.8	0.8	0.182						
	buildings	0.89	7.4	0.8	0.060						
	open area	8.06	67.4	0.2	0.135						
12	roads	0.51	4.1	0.8	0.033	0.335	33.5	1100.0 6	0.0054 54248	653	65.14
	parking lots	2.31	18.4	0.8	0.147						
	buildings	0	0.0	0.8	0.000						
	open area	9.73	77.5	0.2	0.155						
13	roads	0.18	1.2	0.8	0.009	0.680	68.0	1532	0.0013 05483	815	76.8
	parking lots	9.17	59.2	0.8	0.474						
	buildings	3.03	19.6	0.8	0.157						
	open area	3.1	20.0	0.2	0.040						
14	roads	0.47	3.0	0.8	0.024	0.354	35.4	868	0.0040 32258	840	79
	parking lots	3.08	19.6	0.8	0.157						
	buildings	0.49	3.1	0.8	0.025						
	open area	11.7	74.3	0.2	0.149						
15	roads	0.38	2.3	0.8	0.018	0.445	44.5	1131.5	0.0035 3513	990	75.23

**Table 3F.3 Continued**

	parking lots	2.8	16.8	0.8	0.135						
	buildings	3.61	21.7	0.8	0.174						
	open area	9.84	59.2	0.2	0.118						
16	roads	0.72	3.7	0.8	0.030	0.424	42.4	931.8	0.0123 41704	1078	71.11
	parking lots	4.48	23.2	0.8	0.185						
	buildings	2.02	10.4	0.8	0.084						
	open area	12.12	62.7	0.2	0.125						

In SWMM4.4 the user is able to define the infiltration method. Either the Horton or Green-Ampt technique may be applied. The below samples are SWMM4.4 input files. Figure 3F.4 is an actual SWMM file that was used during the earlier model testing. The second figure is an example from the user's manual. The text files have been truncated to only display information pertaining to infiltration and its associated parameters. Figure 3F.4 corresponds to using the Horton equation, while Figure 3F.5 utilizes the Green-Ampt equation.

```

*      The 'B' lines are for program control purposes.
*      METRIC ISNOW NRGAG  INFILM  KWALTY IVAP NHR NMN NDAY
MONTH IYRSTR
B1 0  0  1  0  0  1  10  00  13  06  01
*      IPRN(1) IPRN(2) IPRN(3) IRPNGW
*=====
=====
*      Enter Subcatchment Data on line H1.
*      JK NAMEW NGTO WIDTH AREA  %IMP    SLP    IMPN  PERVN
IDS PDS  MAX  MIN  DECAY
H1 1  1  200  321  6.27  57.4  0.0207  0.013  0.25  0.05  0.10  4.0
1.00  0.43
*=====
=====
*      End your input data set with a $ENDPROGRAM.
*=====
=====
$ENDPROGRAM

```

**Figure 3F.4: SWMM Input File using Horton's Equation.** When INFILM is set equal to 0, the Horton equation is used, requiring information regarding the maximum and minimum infiltration rates (in/hr). The values are then specified using the H1 line under the subcatchment data section. The decay value is the decay rate of infiltration in Horton's equation (1/sec).

```

*=====
=====
*       The 'B' lines are for program control purposes.
*=====
=====
*  METRIC ISNOW NRGAG  INFILM  KWALTY IVAP NHR NMN NDAY
MONTH IYRSTR
B1 0   0   1   1   0   1  10  00  13  06  01
*  IPRN(1) IPRN(2) IPRN(3) IRPNGW
*=====
=====
*  Enter Subcatchment Data on line H1.
*  JK NAMEW NGTO WIDTH AREA  %IMP   SLP   IMPN   PERVN
IDS PDS  SUCT  HYDCON  IMD
H1 1   1  200  321  6.27 57.4  0.0207  0.013  0.25 0.05  0.10  0.16
0.04  0.30
*=====
=====
*       End your input data set with a $ENDPROGRAM.
*=====
=====
$ENDPROGRAM

```

**Figure 3F.5: SWMM Input File using the Green-Ampt Equation at Cherry Point MCAS.** The inputs needed for the SWMM 4.4 simulations using the Green-Ampt equation are defined by the SUCT, HYDCON, and IMD parameters. SUCT represents the average capillary suction (in). The HYDCON value is the saturated hydraulic conductivity of the soil (in/hr). The initial moisture deficit for the soil (volume air divided by the volume of voids) is the IMD value.

**Appendix 3G:** XPSWMM Single Event Simulation Results, Completed in 2005

**Exhibit 3G.1:** Catchment K2 Selected Storm Selected Hydrographs

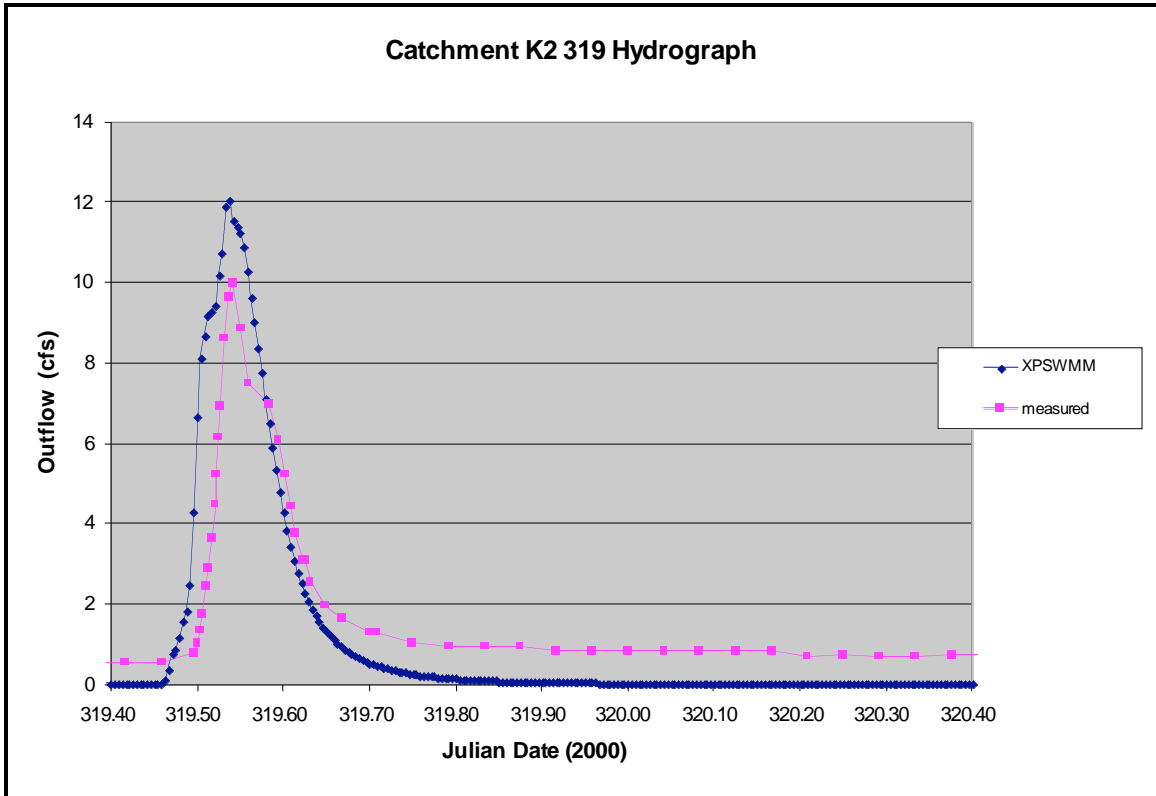


**Figure 3G.1.1:** Catchment K2 Event 319 Outflow Hydrograph (2000 Rainfall)

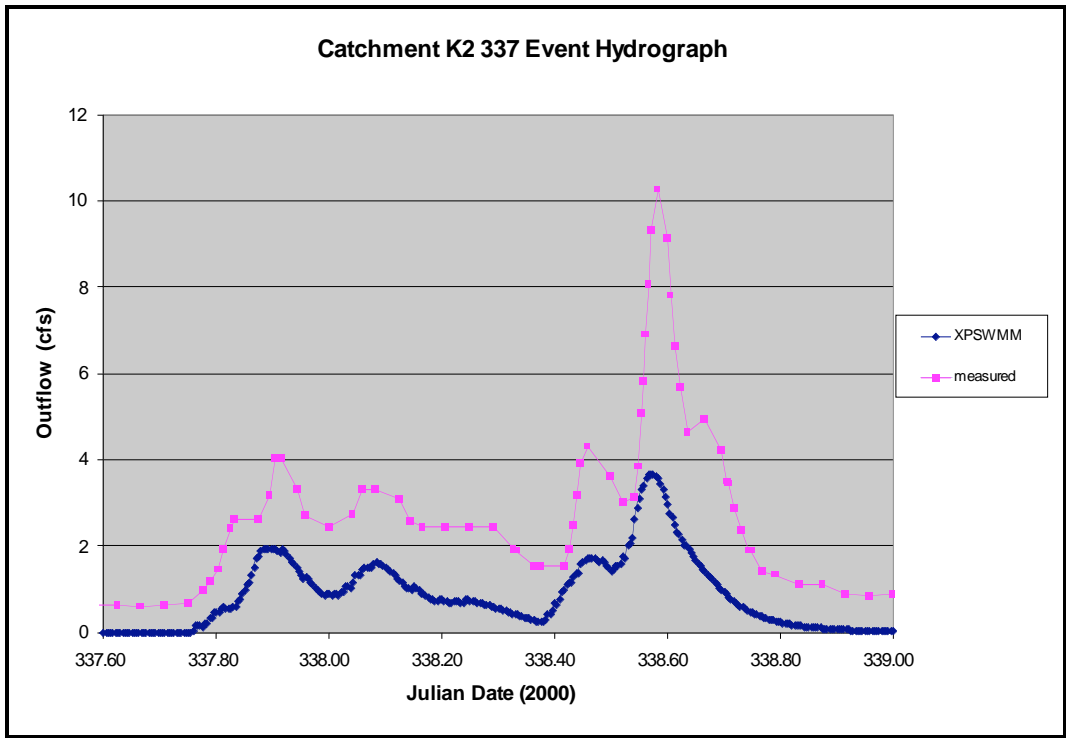


Figure 3G.1.2: *Catchment K2 Event 337 Outflow Hydrograph (2000 Rainfall)*

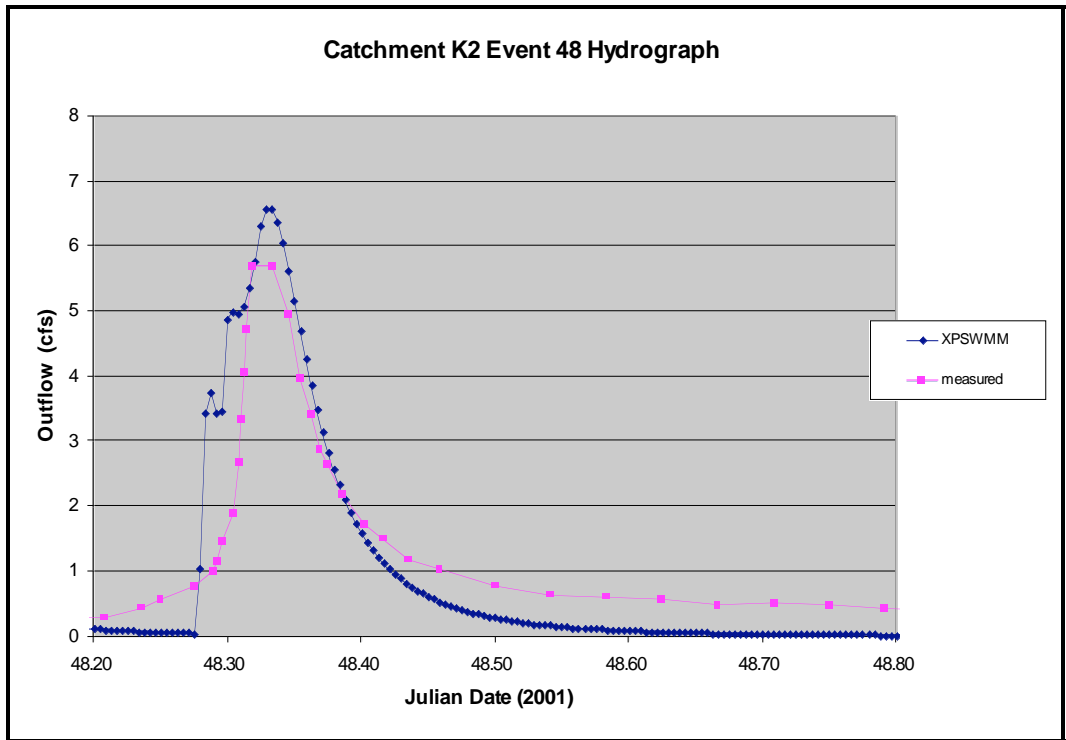
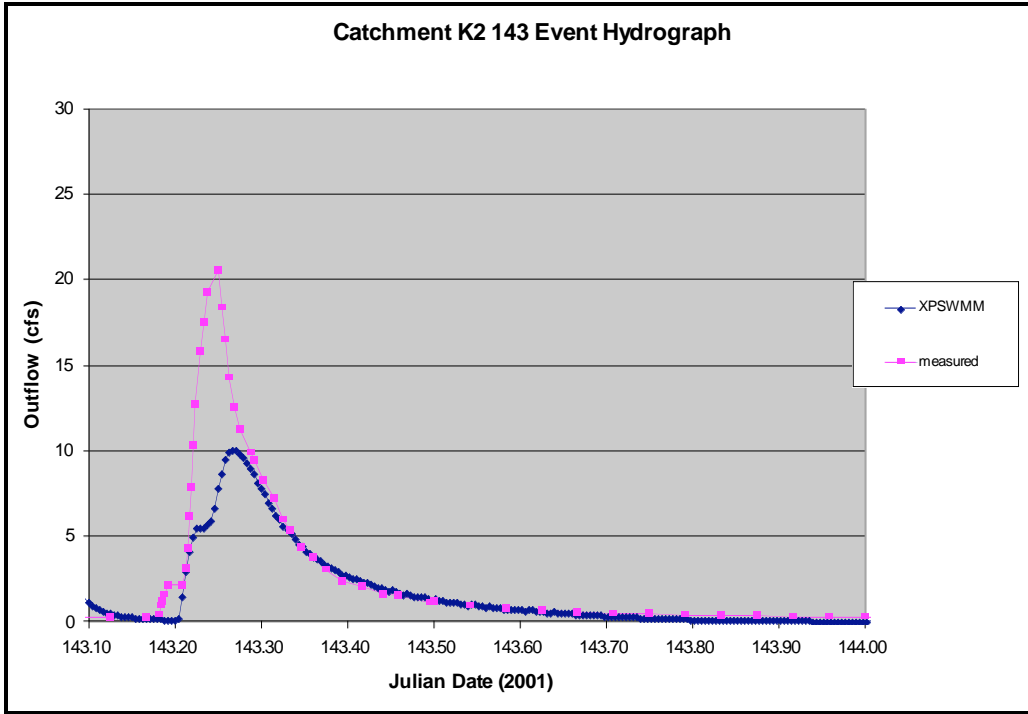
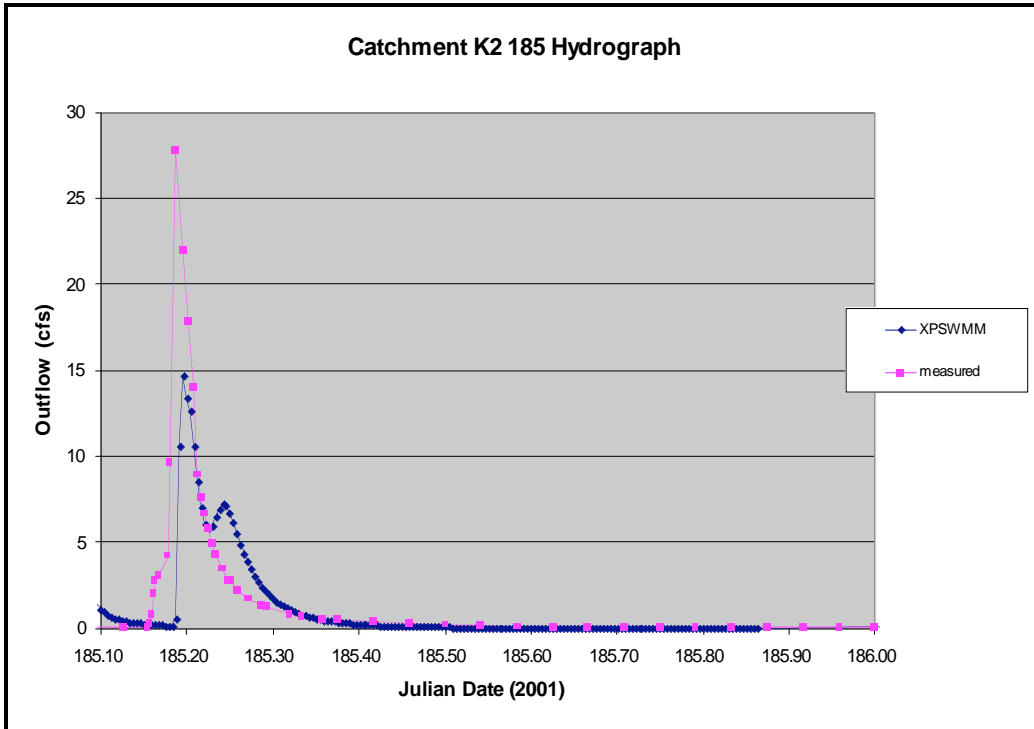


Figure 3G.1.3: *Catchment K2 Event 48 Outflow Hydrograph (2001 Rainfall)*



**Figure 3G.1.4: Catchment K2 Event 143 Outflow Hydrograph (2001 Rainfall)**



**Figure 3G.1.5: Catchment K2 Event 185 Outflow Hydrograph (2001 Rainfall)**

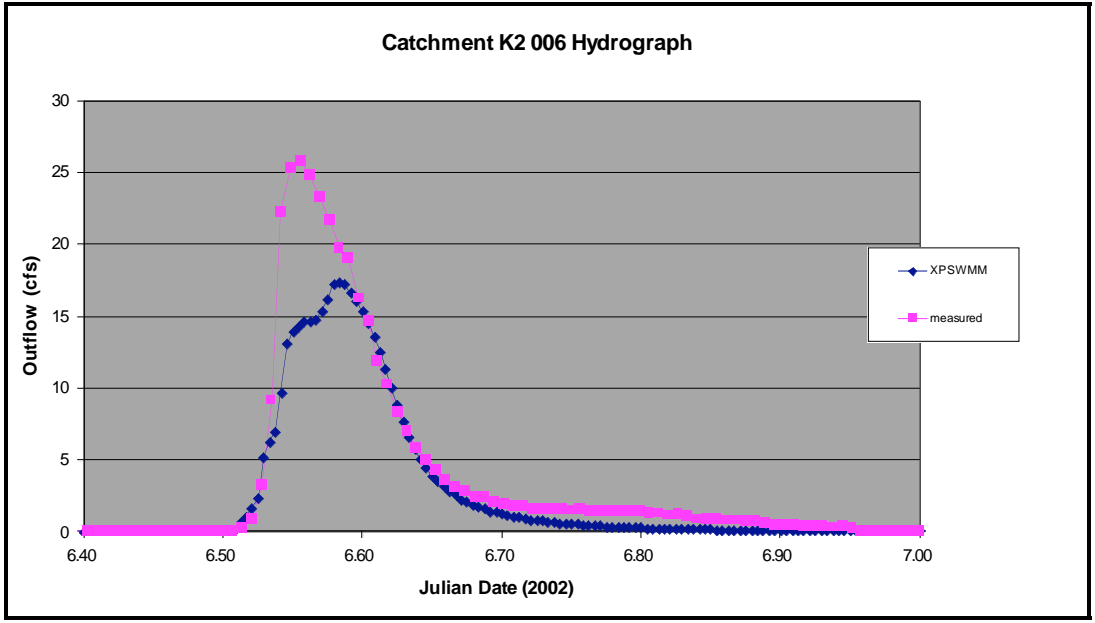


Figure 3G.1.6: Catchment K2 Event 006 Outflow Hydrograph (2002 Rainfall)

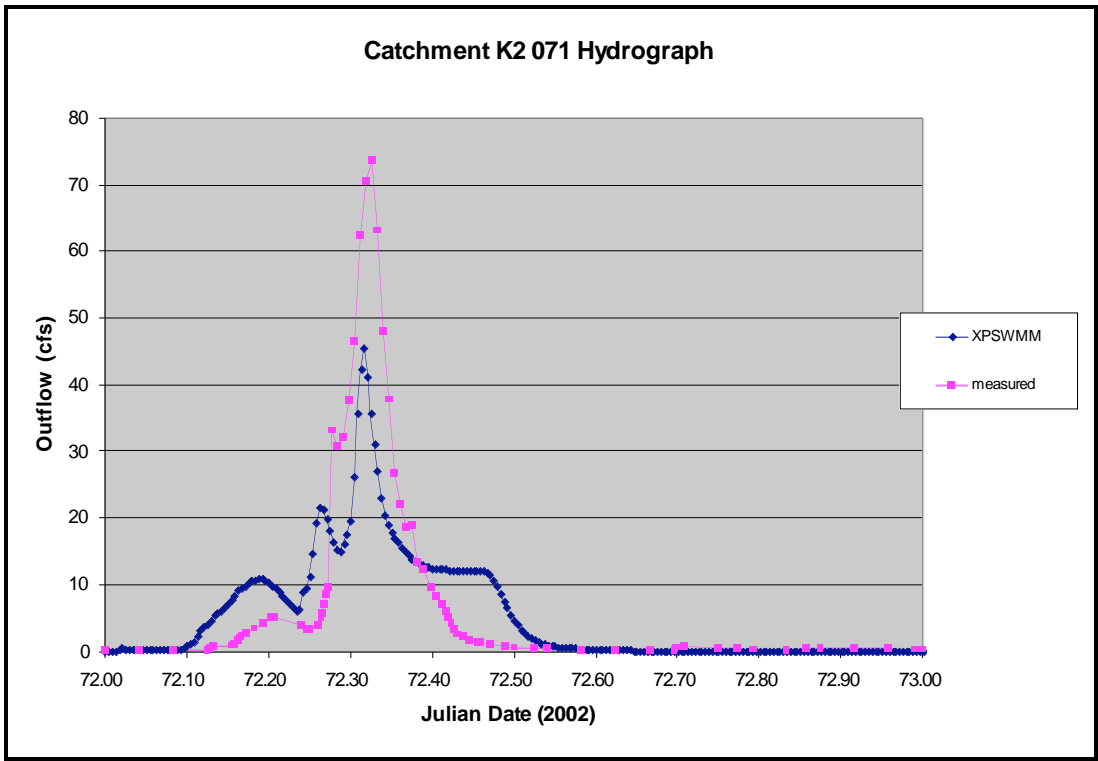
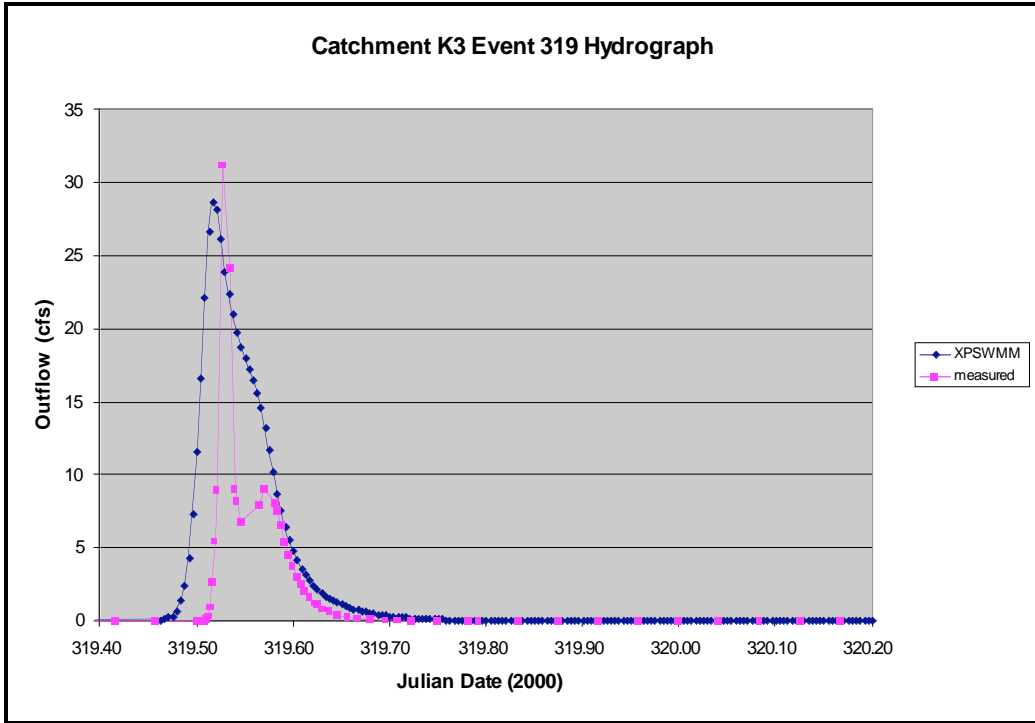


Figure 3G.1.7: Catchment K2 Event 71 Outflow Hydrograph (2002 Rainfall)

**Exhibit 3G.2: Catchment K2 2001 Selected Storms T-test Statistic Results**

t-Test: Paired Two Sample for Means	CATCHMENT K2 PEAK OUTFLOWS	
	<i>MEASURED PEAK OUTFLOW (CFS)</i>	<i>PREDICTED PEAK OUTFLOW (CFS)</i>
Mean	24.79857143	15.71571429
Variance	533.038581	194.6953286
Observations	7	7
Pearson Correlation	0.97292586	
Hypothesized Mean Difference	0	
df	6	
t Stat	2.39260218	
P(T<=t) one-tail	0.026917461	
t Critical one-tail	1.943180274	
P(T<=t) two-tail	0.053834922	
t Critical two-tail	2.446911846	

**Exhibit 3G.3: Catchment K3 Selected Event Hydrographs**



**Figure 3G.3.1: Catchment K3 Event 319 Outflow Hydrograph (2000)**

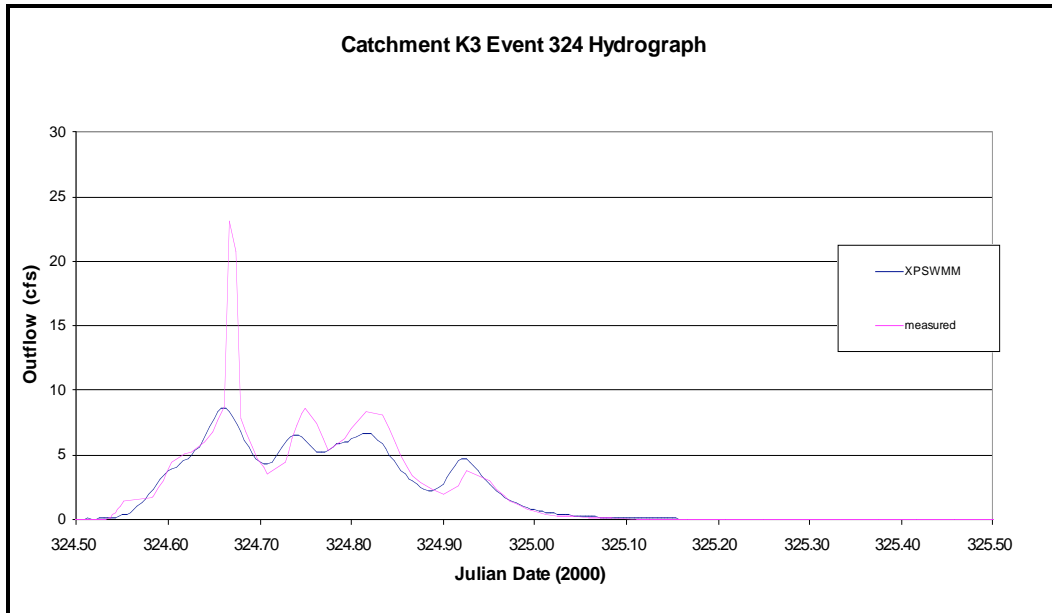


**Figure 3G.3.2: Catchment K3 Event 324 Outflow Hydrograph (2000)**

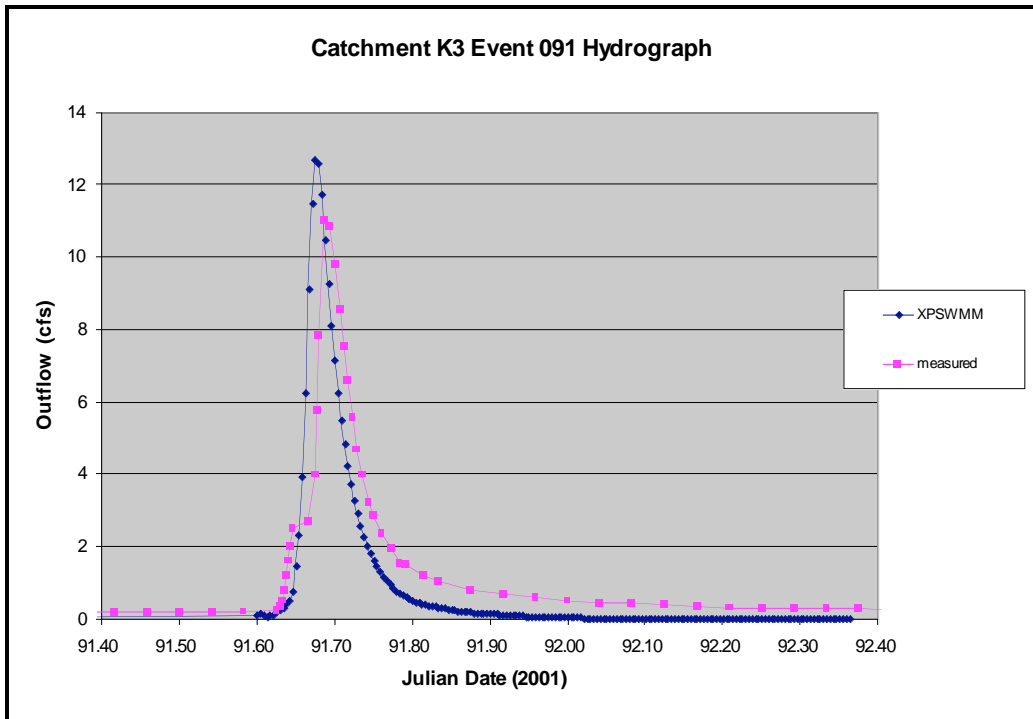


Figure 3G.3.3: *Catchment K3 Event 91 Outflow Hydrograph (2001)*

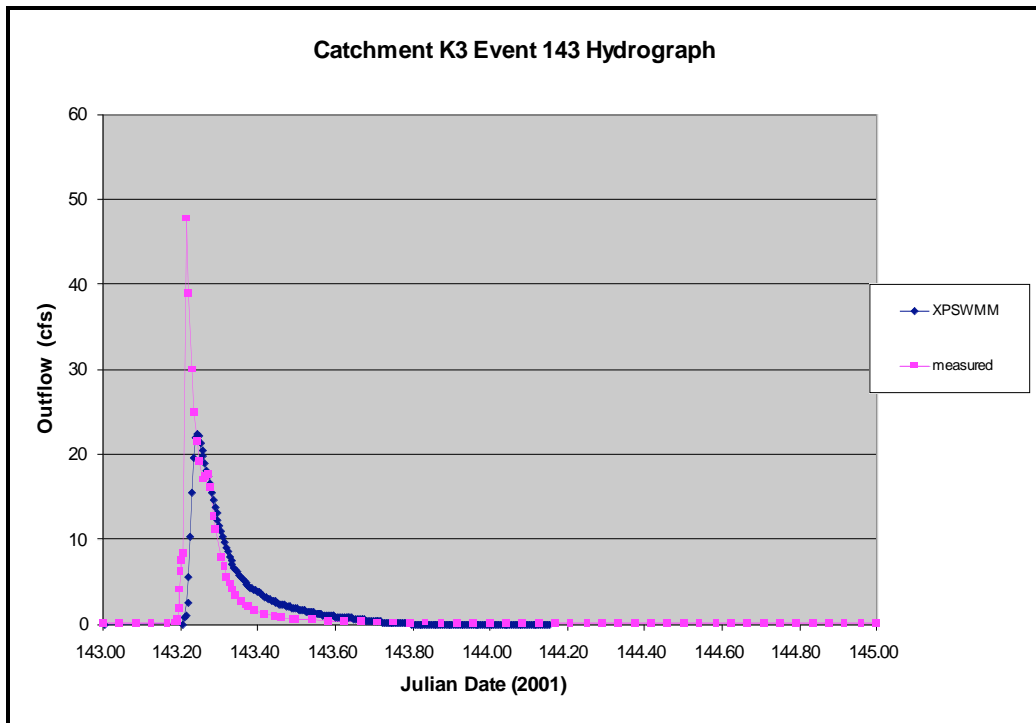


Figure 3G.3.4: *Catchment K3 Event 143 Outflow Hydrograph (2001)*

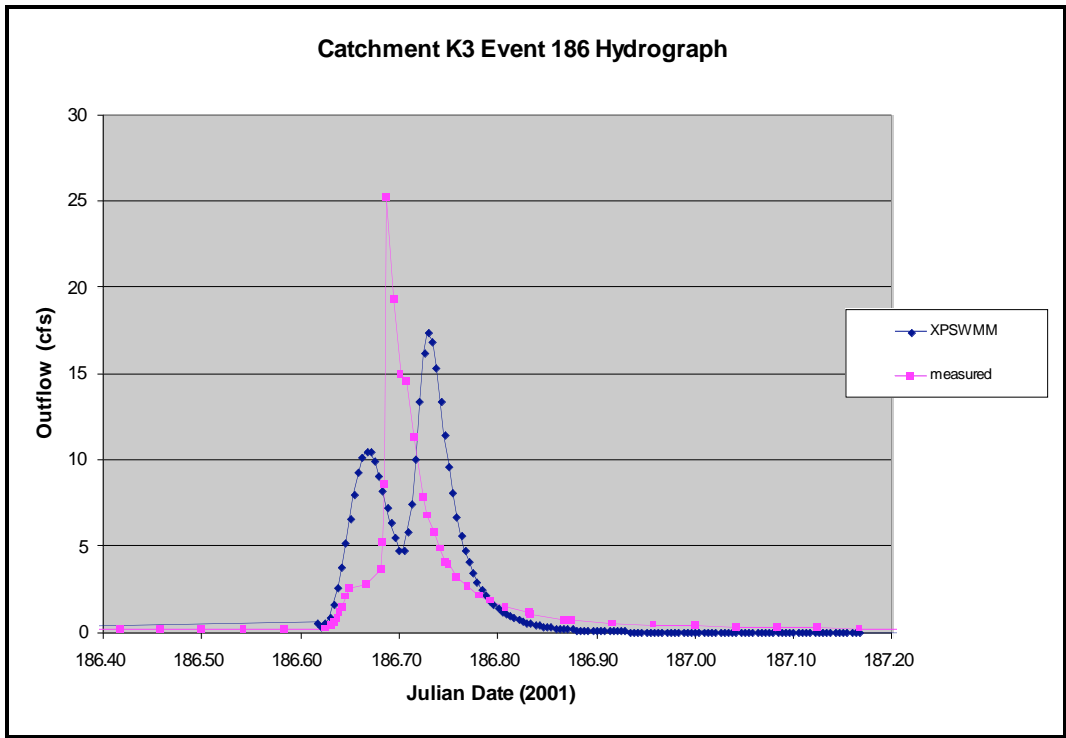


Figure 3G.3.5: *Catchment K3 Event 186 Outflow Hydrograph (2001)*

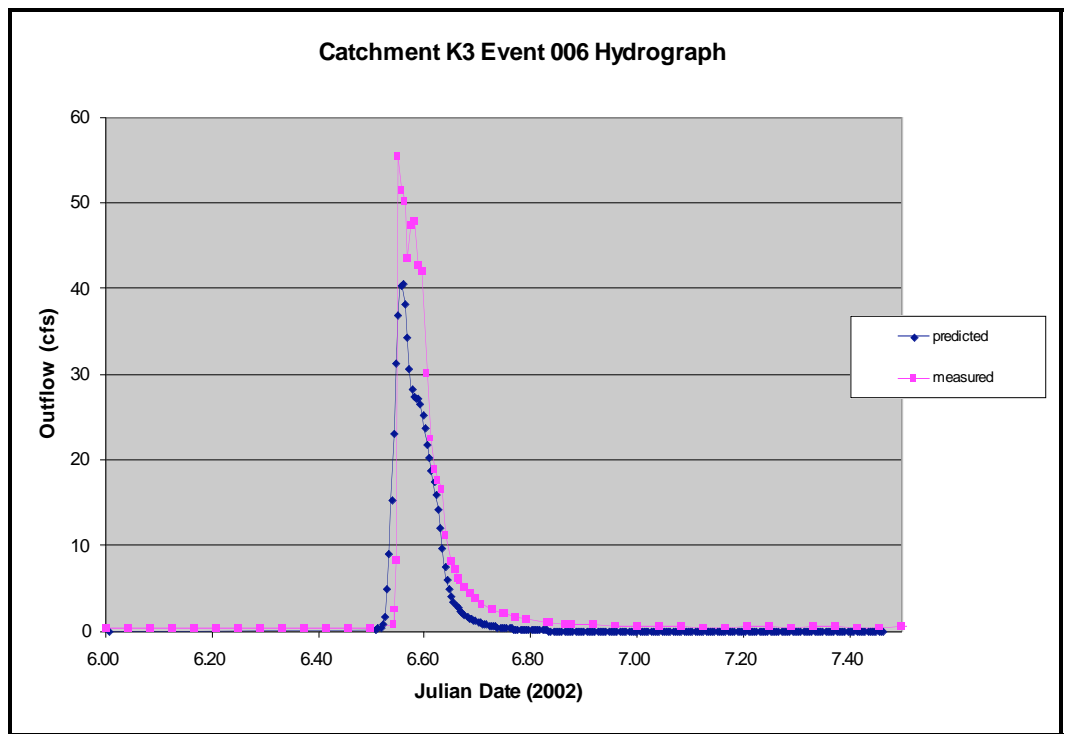


Figure 3G.3.6: *Catchment K3 Event 06 Outflow Hydrograph (2002)*

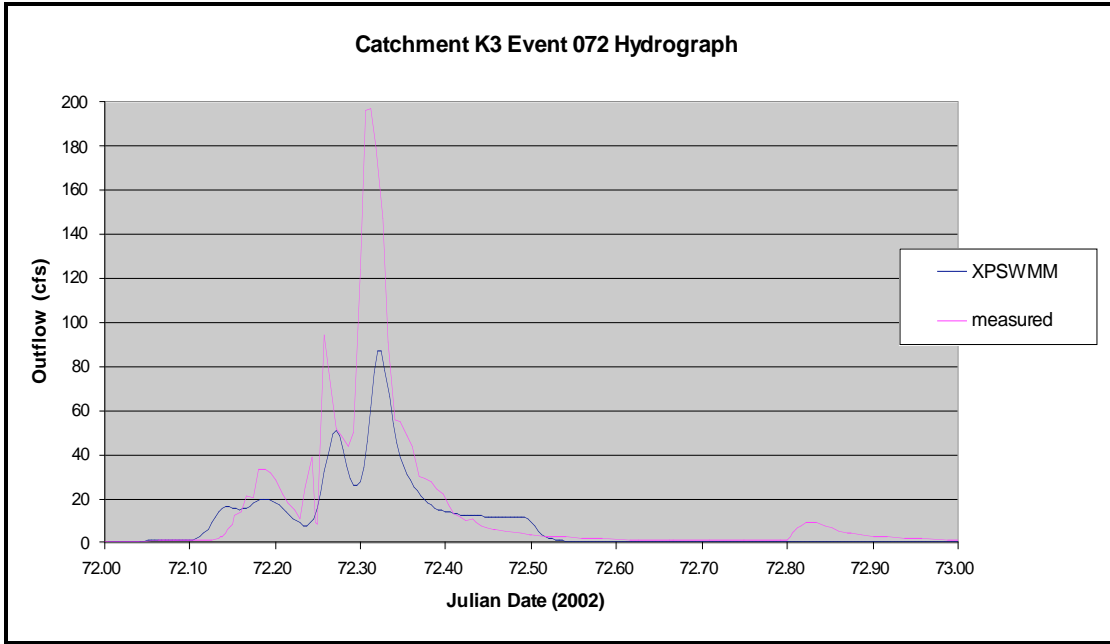


Figure 3G.3.7: Catchment K3 Event 72 Outflow Hydrograph (2002)

**Exhibit 3G.4: Catchment K3 T-Test Statistics for Selected Storms**

t-Test: Paired Two Sample for Means	CATCHMENT K3 OUTFLOWS	
	<i>MEASURED PEAK OUTFLOW (CFS)</i>	<i>PREDICTED PEAK OUTFLOW (CFS)</i>
Mean	55.79857143	25.96
Variance	4097.402648	235.2063
Observations	7	7
Pearson Correlation	0.835010481	
Hypothesized Mean Difference	0	
df	6	
t Stat	1.521236818	
P(T<=t) one-tail	0.089509751	
t Critical one-tail	1.943180274	
P(T<=t) two-tail	0.179019501	
t Critical two-tail	2.446911846	

### Appendix 3H: Calibration and Validation Hydrographs

The following figures are a collection of SWMM and XPSWMM predicted hydrographs for the hydrologic study conducted at Cherry Point MCAS between the years 2000 and 2002. The hydrographs reflect the calibration efforts using the model for selected storms. Calibration curve number five was the final calibration attempt for study area.

#### Exhibit 3H.1: Catchment K2 Calibration Outflow Hydrographs

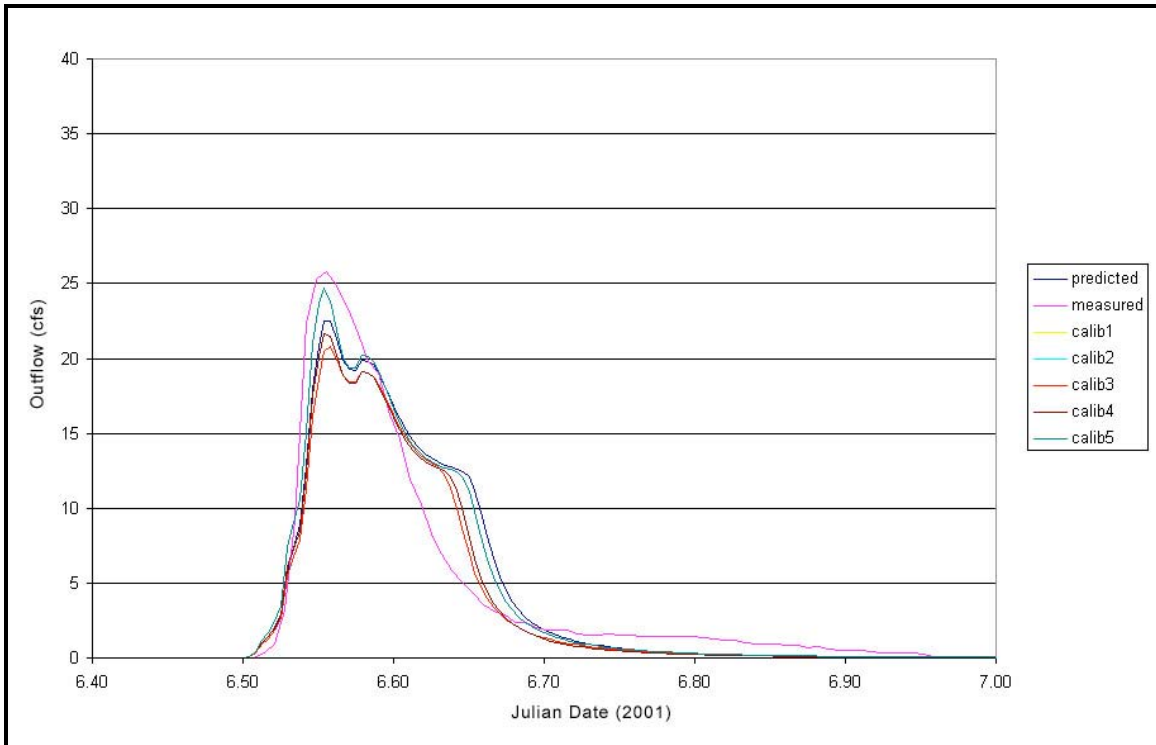


**Figure 3H.1.1: Catchment K2 Event 006 Calibration Hydrograph (2002).** This figure is a collection of hydrographs that represent several calibration attempts plus the observed flow data for a single storm event using SWMM. The final calibration hydrograph is named “Calib 5” which has a blue color. The observed data has been plotted using the purple color. The observed data for the calibration hydrograph was extracted directly from the composite flow information measured by the STARFLOW and the application of the weir equation using the Blue Earth stage measurements.

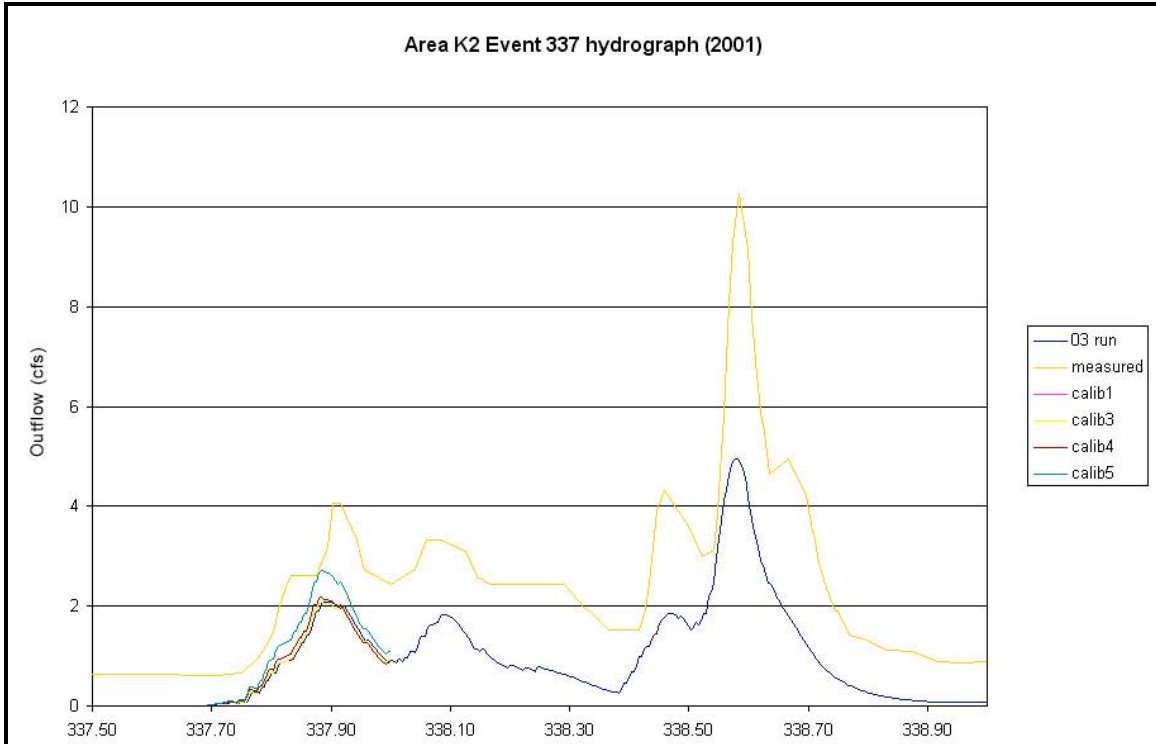


**Figure 3H.1.2: Catchment K2 Event 337 Calibration Hydrograph (2000).** These hydrographs represent the observed and predicted outflow for the outlet of catchment K2 during a single storm event in 2000 at Cherry Point. SWMM generated the predicted outflow, and apparently was having difficulties predicting flows after Julian day 338. The blue line represents the calibration completed in 2003, conveniently named “03 runs”. The Calib 5 line could contain some of the final settings used to validate SWMM’s prediction power as compared to the observed data.

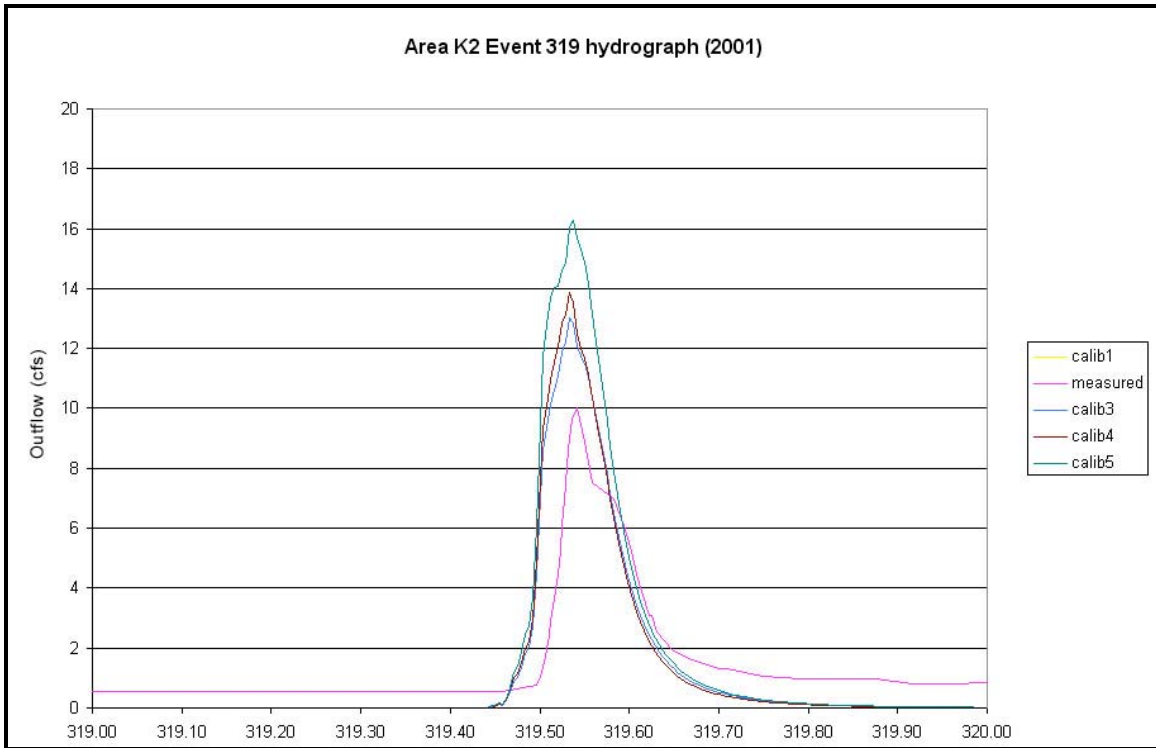


**Figure 3H.1.3: Catchment K2 Event 319 Calibration Hydrograph (2000).** This figure depicts several calibration attempts where the catchment width and percent imperviousness were adjusted to align the peak flow rates between the observed and predicted datasets. The Calib 5 hydrograph contains the final settings that would be used to validate the SWMM and XPSWMM outflow predictions. The measured data is represented by the purple line. During this storm event, it appears as though SWMM is over-predicting the outflow for Catchment K2 by 6 cfs. The time to peak between the measured and predicted hydrographs appears relatively consistent.

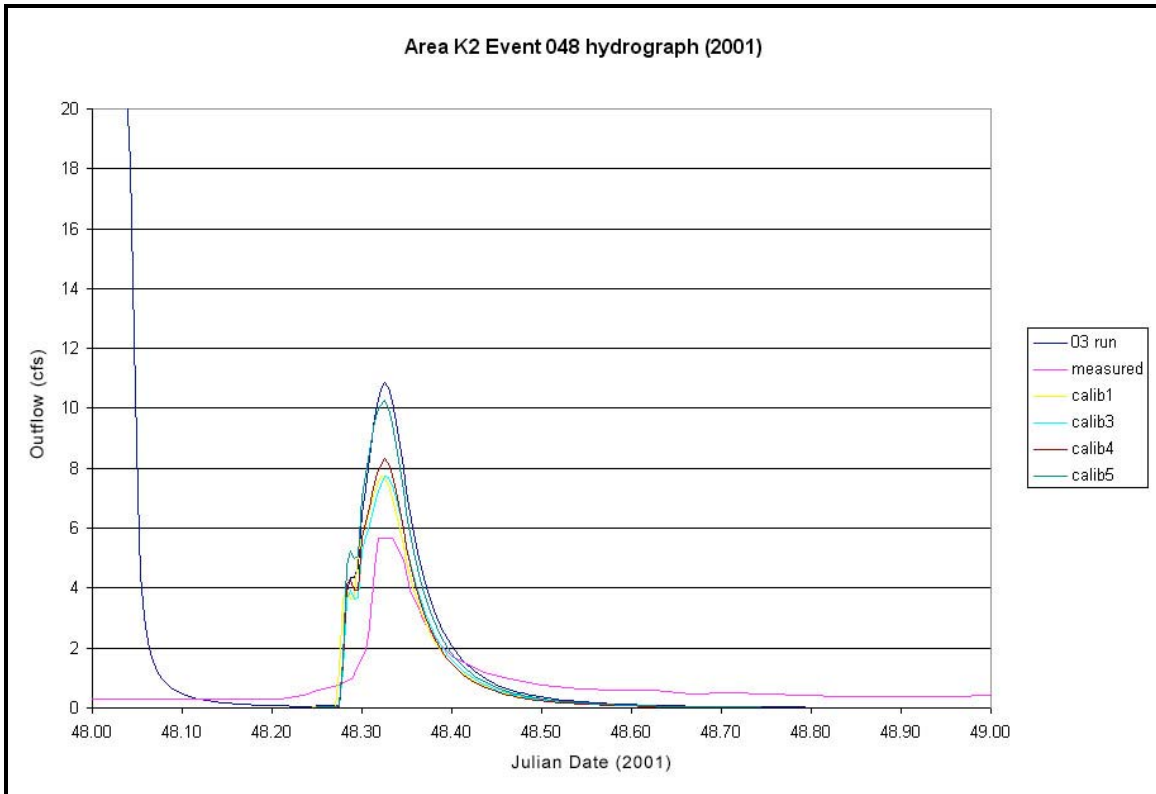


**Figure 3H.1.4: Catchment K2 Event 048 Calibration Hydrograph (2001).** This figure displays several calibration attempts using the measured hydrograph and the SWMM predicted hydrograph for a 24-hour time span. The erroneous, predicted flow data in the beginning of the “03 run” curve was generated by excessive baseflow present in several SWMM upstream routing elements. The problem was addressed and the baseflow was reduced, as demonstrated by the remaining four calibration curves. The Calib 5 line contained the information used to validate SWMM. The measured data is presented as a purple line. Apparently, the difference between the measured and predicted peak outflow rates for this storm event was approximately 2 cfs.

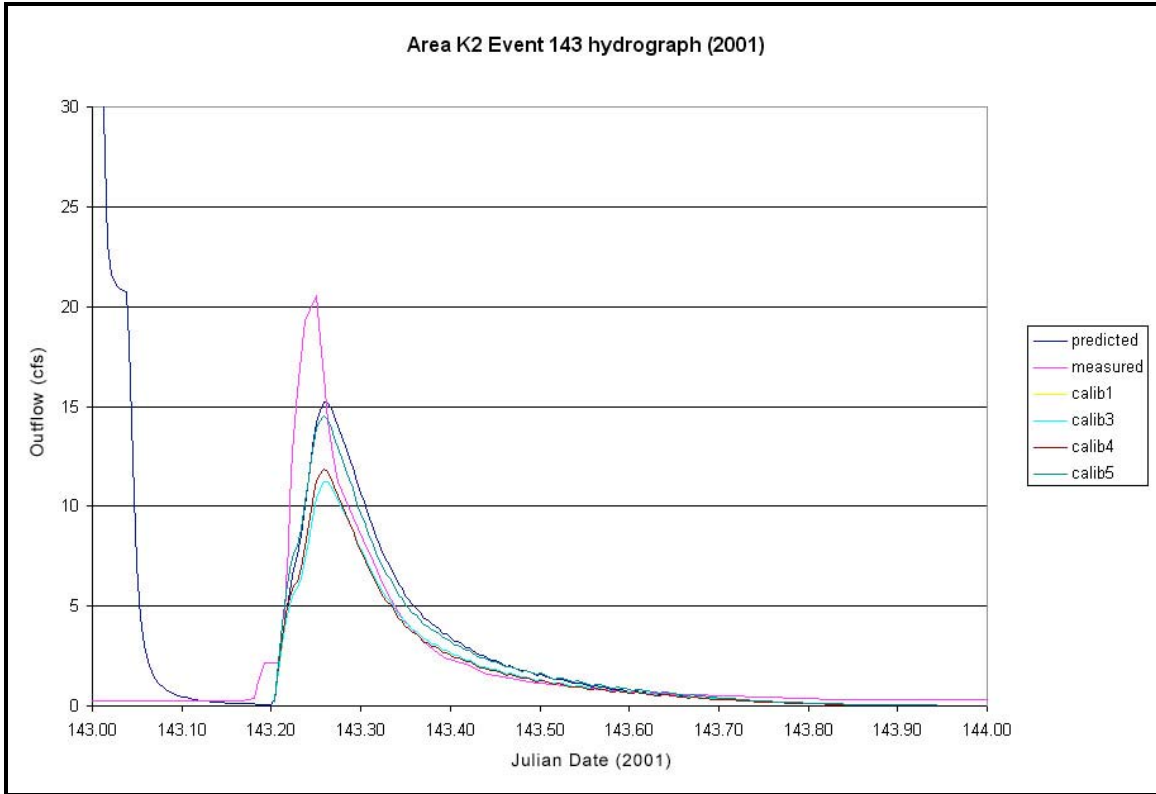


**Figure 3H.1.5: Catchment K2 Event 143 Calibration Hydrograph (2001).** This figure is a collection of six, single-event hydrographs, comparing the observed flow data to the SWMM predicted flow rates at the K2 catchment outflow in 2001. The measured data has been graphed using the purple line. The “predicted” hydrograph was the prediction attempt using SWMM. Calib 1 through Calib 5, represent the calibration curves. The setting associated with the Calib 5 curve were finally inserted into XPSWMM for validation purposes. In this case, SWMM was under predicting the peak outflow rate by approximately 9 cfs and the timing of the predicted peak was predicted after the occurrence of the observed peak.

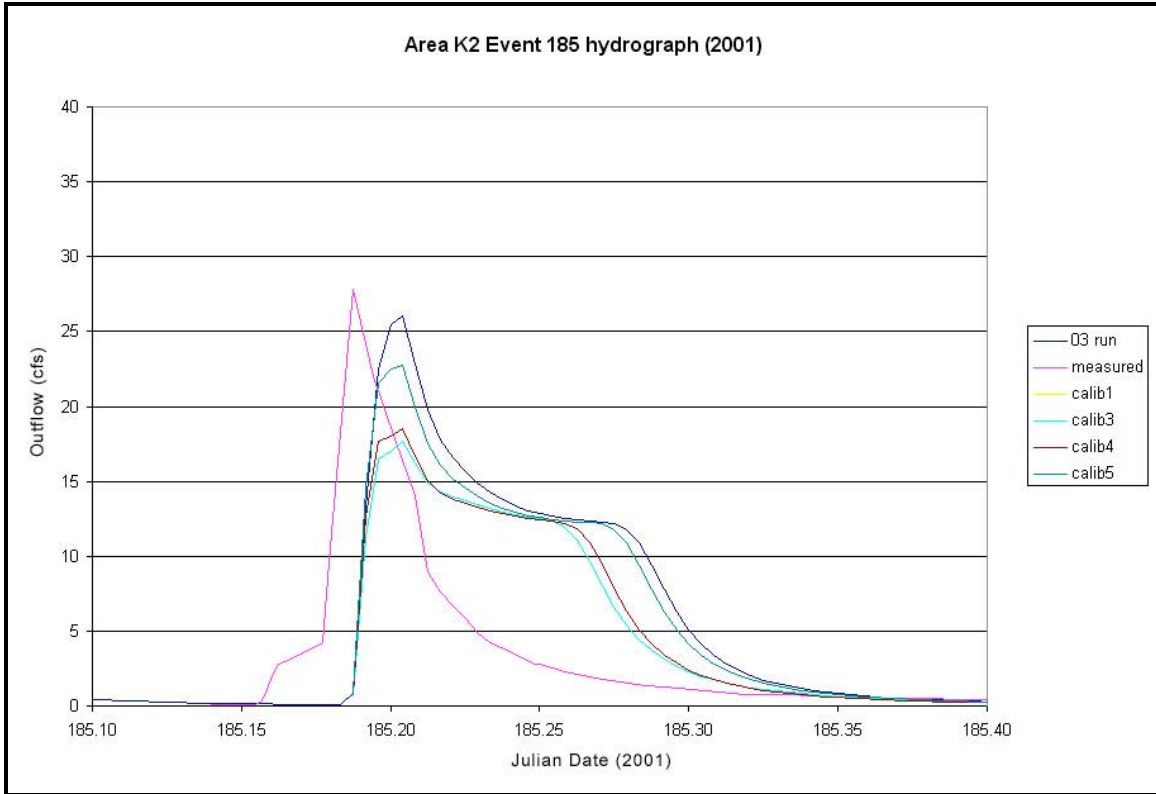


**Figure 3H.1.6: Catchment K2 Event 185 Calibration Hydrograph (2001).** This figure presents the observed and predicted outflow information for storm 185 at the K2 outlet in 2001. Using the 2001 rainfall, SWMM predicted the “03 run”, which represents the original predicted hydrograph prior to any calibration attempts. The remaining four calibration curves resulted from alterations with the catchment width and the catchment imperviousness. The Calib 5 dataset contained the settings that would be used in XPSWMM to validate the prediction hydrographs. From this figure, it is seen that the timing of the peak rate differs between the measured and simulated graphs. Likewise, SWMM is slightly under predicting the peak outflow rate by roughly 4 cfs.

**Exhibit 3H.2: Catchment K3 Calibration Hydrographs for Cherry Point, NC**

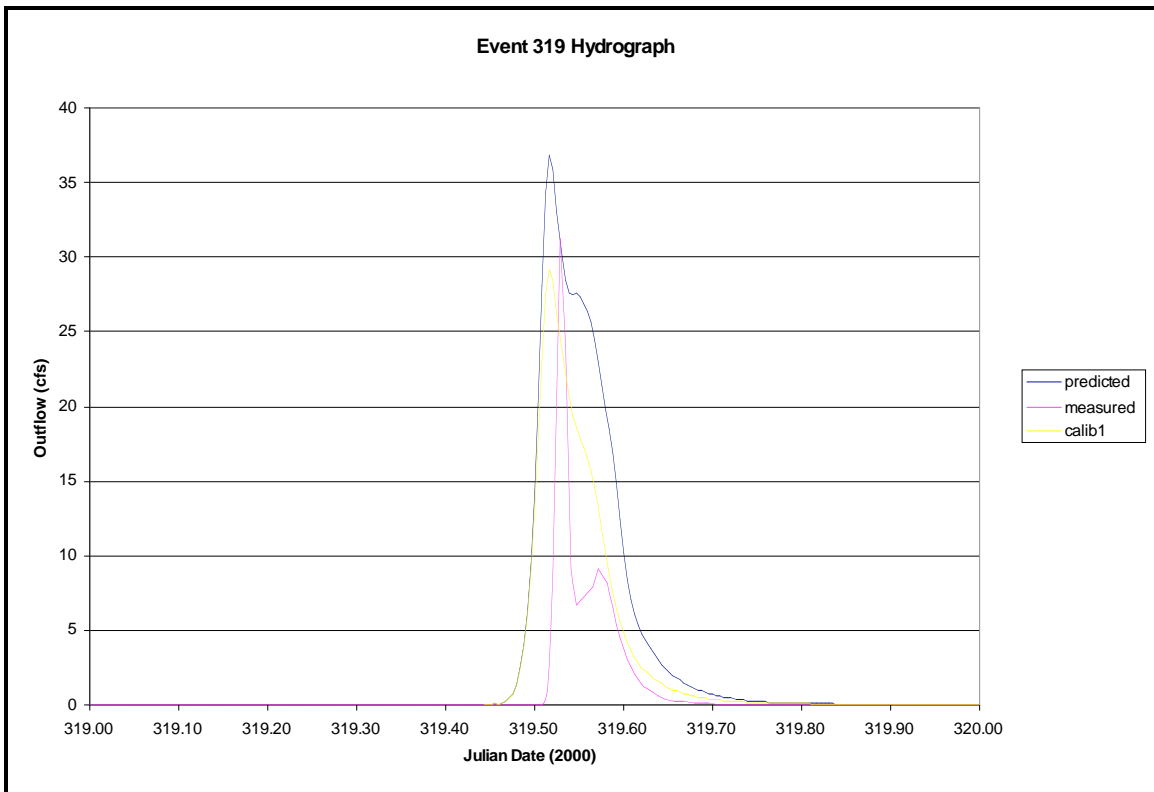


**Figure 3H.2.1: Catchment K3 Event 319 Calibration Hydrograph (2000).** This figure contains three hydrographs that were used to calibrate the predicted hydrograph for storm event 319 in catchment K3. The blue line represents the originally simulated SWMM hydrograph prior to any calibration attempts, while the purple line is the measured data. A majority of the adjustment procedures were understood from the catchment K2 calibration procedures, and were therefore adapted to catchment K3. The Calib 1 curve is the resulting calibration hydrograph which contained the settings used to validate the SWMM results. There exists a slight timing difference between the observed and predicted time-to-peak. In addition, SWMM under predicted the observed peak flow rate by approximately 2cfs.

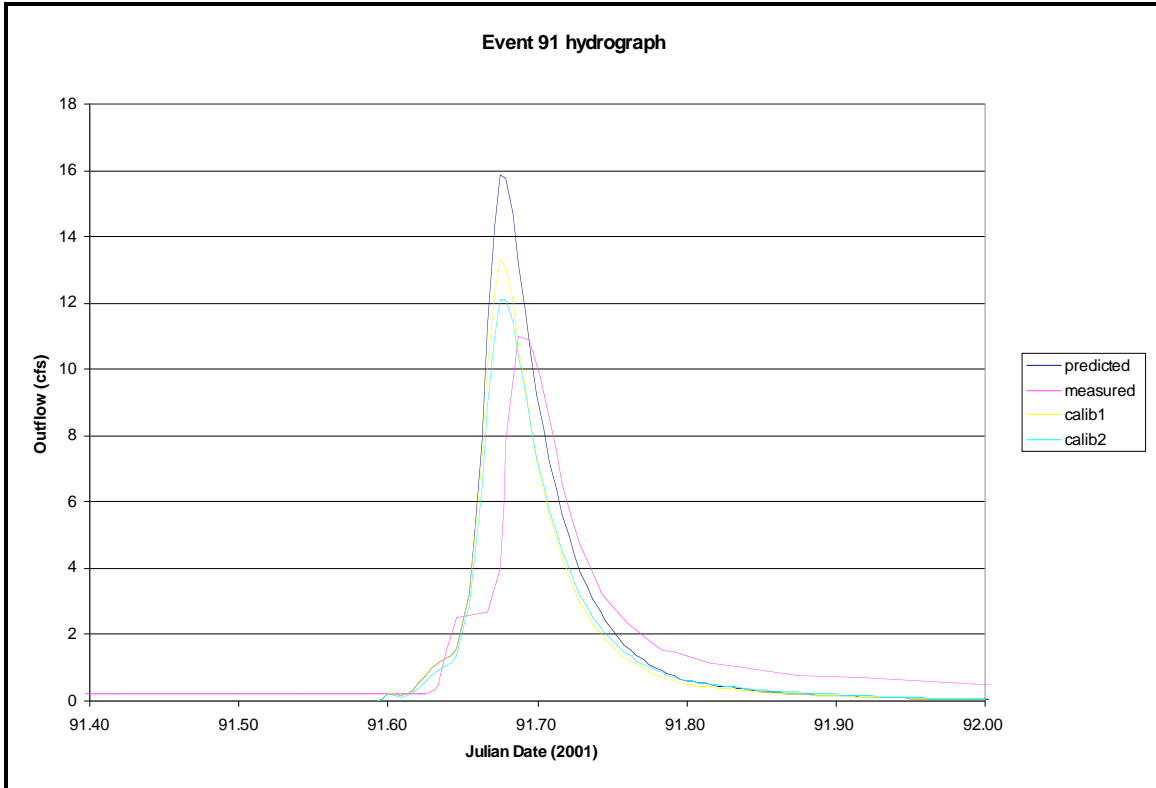


**Figure 3H.2.2: Catchment K3 Storm Event 091 Hydrograph (2001).** This figure contains two calibration curves, plus the original predicted and observed hydrographs for storm event 91 in 2001. The blue curve represents the originally simulated SWMM outflow hydrograph for this storm event. The purple curve is the observed, composite flow data, extracting from the weir and flow meter information. The Calib 2 curve contains the settings that were inserted into SWMM and XPSWMM to validate the model predictions. For this event, the timing of the peak is being predicted slightly earlier than the measured time-to-peak. In addition, the SWMM generated outflow is less than 2cfs greater than the observed peak outflow rate.

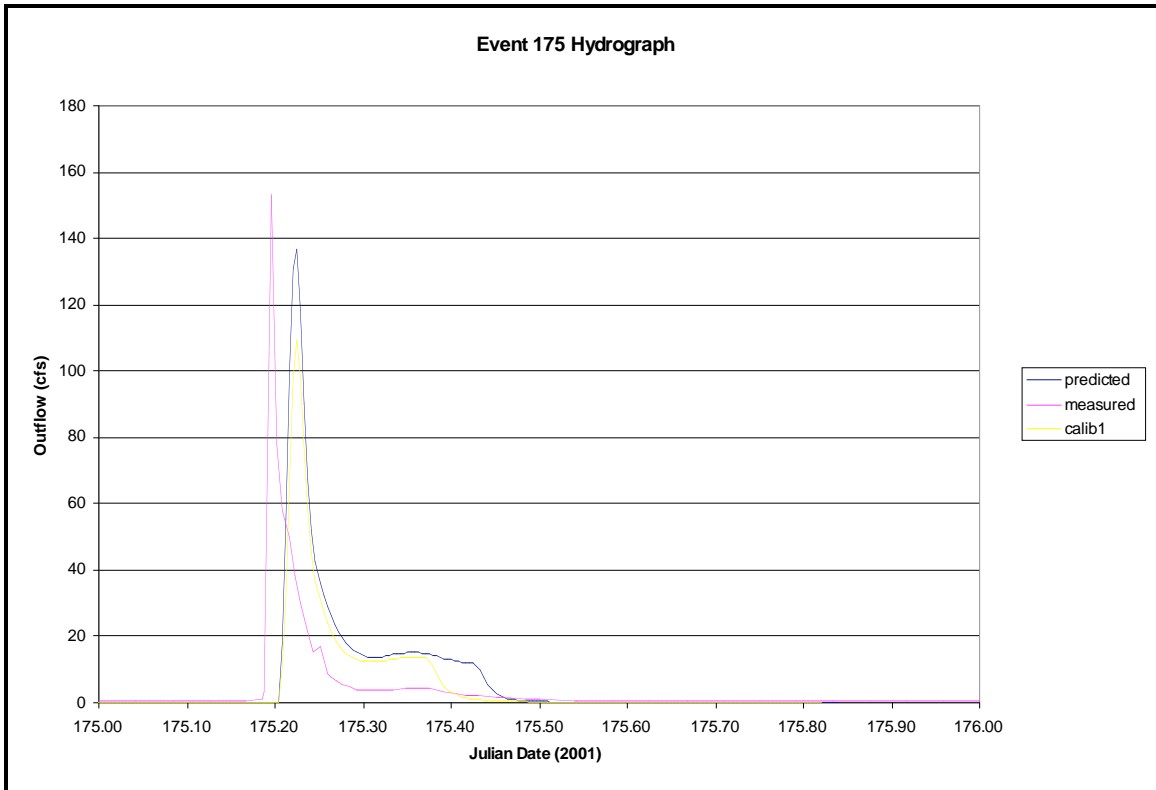


**Figure 3H.2.3: Catchment K3 Storm Event 175 Hydrograph (2001).** This figure displays several curves that were used to calibrate the simulated hydrograph for storm event 175 at the K3 catchment outflow. The purple line represents the observed flow data, which was collected from the calculated, composite flow data. The blue line is the first SWMM simulation attempt and the yellow line is the calibration curve resulting from altering the catchment and catchment imperviousness. For this situation, the timing of the observed peak flow rate occurs prior to the SWMM generated time-to-peak. SWMM predicted nearly 110 cfs of outflow, while more than 150 cfs of outflow was reported in the measured data.

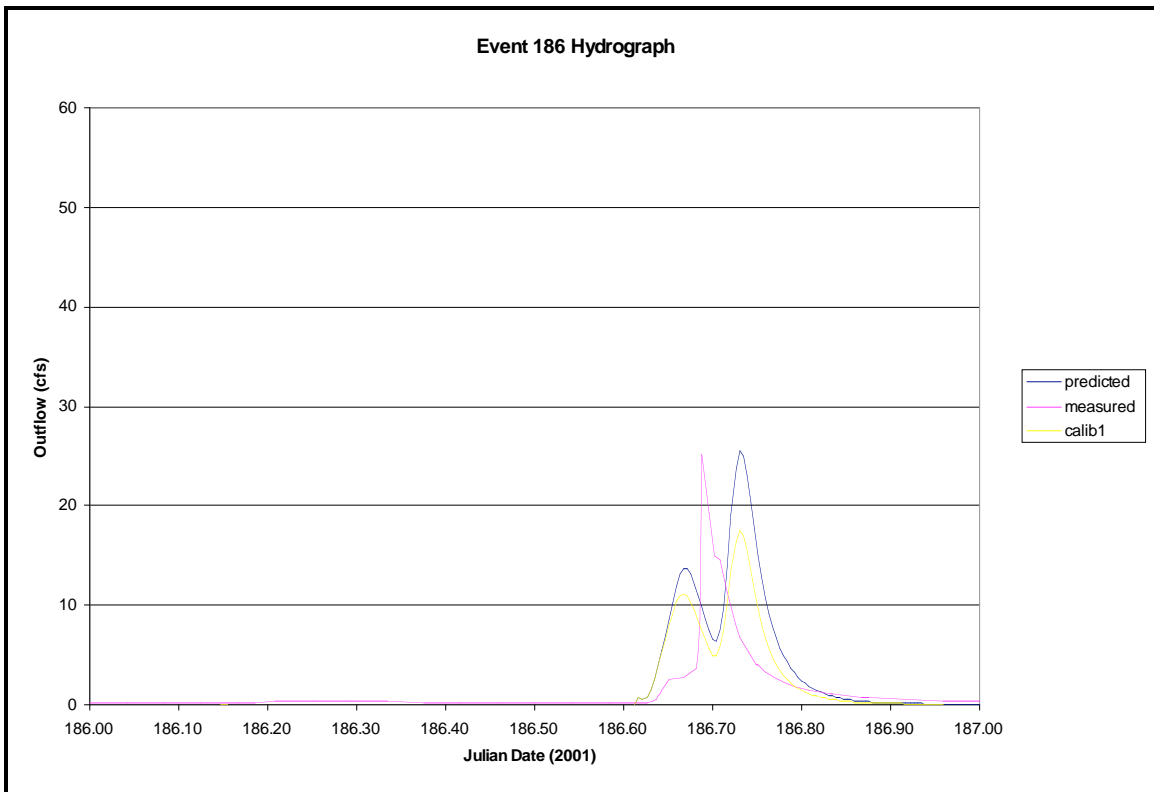


**Figure 3H.2.4: Catchment K3 Storm Event 186 Calibration Hydrograph (2001).** This figure presents three hydrographs that were used to calibrate the SWMM predicted curve to the observed flow data at the K3 catchment outlet for a single storm event. The purple line depicts the reported outflows at the monitoring location. The blue line is the original SWMM prediction curve prior to calibration. The yellow curve is the calibration hydrograph containing the information that would be used to validate the model's performance. The shapes of the measured and predicted hydrographs differ greatly. Recall that the SWMM information is directly dependent upon the rainfall acquired during the modeling duration. Apparently, the rainfall file contained a trend which created the two-peak formation presented above. The measured data does not demonstrate this same trend. Nonetheless, the observed peak flow rate was approximately 25 cfs. SWMM predicted nearly 18 cfs of outflow for the same storm event. The difference between the measured and simulated time-to-peak is less than 2 hrs.

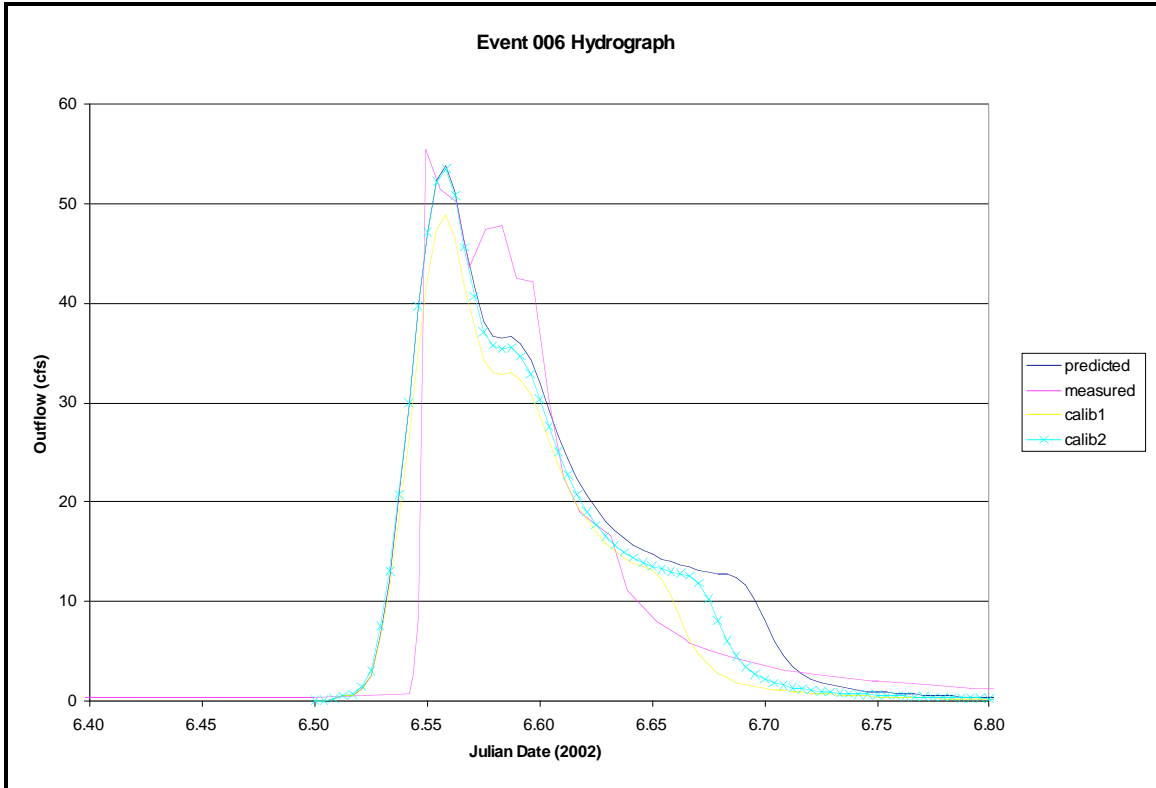


**Figure 3H.2.5: Catchment K3 Storm Event 006 Calibration Hydrograph (2002).** This figure is a collection of hydrographs used to calibrate the SWMM simulated curves to the data observed at the outlet of catchment K3 for storm event 006 in 2002. The blue line is the original SWMM predicted hydrograph prior to calibration. The purple line is the observed outflow data. The yellow and light blue lines correspond to the two calibration attempts using SWMM. The final SWMM settings were determined during the Calib 2 procedure, and were used to model the storms during the validation process. The shapes of the predicted and measured hydrographs are slight difference, since the second peak is more distinct in the measured data. The difference between the observed and simulated peak flow rates is approximately 2 cfs.

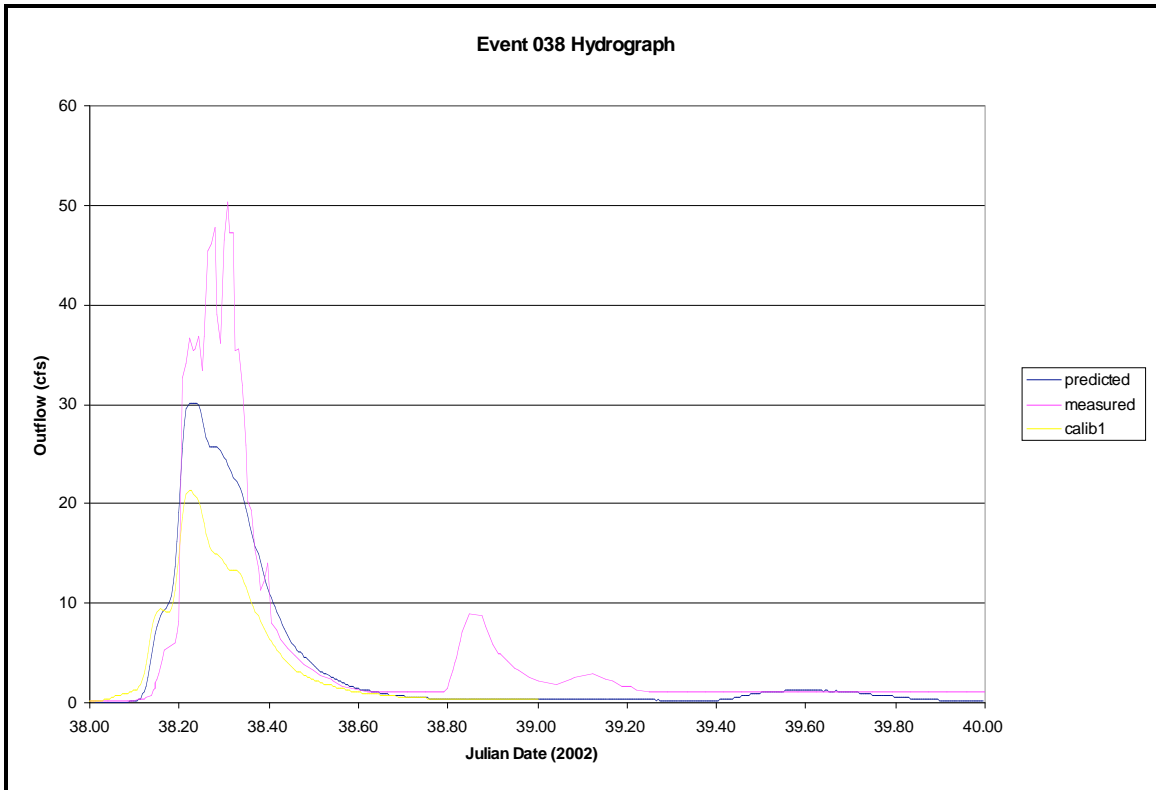


**Figure 3H.2.6: Catchment K3 Storm Event 038 Calibration Hydrograph (2002).** This figure is associated with the hydrographs used to calibrate a single storm event in catchment K3 in 2002. The purple curve represents the observed data, whose shape differs from the two SWMM simulated hydrographs. The blue line is the original SWMM prediction before the alterations were made to the catchment width and imperviousness. The yellow curve is the hydrograph used for the calibration, containing the set of values used to validate the SWMM estimates. The observed, peak outflow is nearly 50 cfs, while the simulated peak rate only achieves a maximum value of 30 cfs. The shapes of the observed and predicted hydrographs differ, plus the time-to-peak for each hydrograph fails to match. In addition, the failing tail of the measured data indicates that another surge in outflow was recorded that did not coincide with the rainfall data. The second peak is either incorrect, or probably resulted from some random upstream activity that was not connected to rainfall runoff.

**Exhibit 3H.3:** Catchment K2 Validation Hydrographs for Cherry Point, NC.

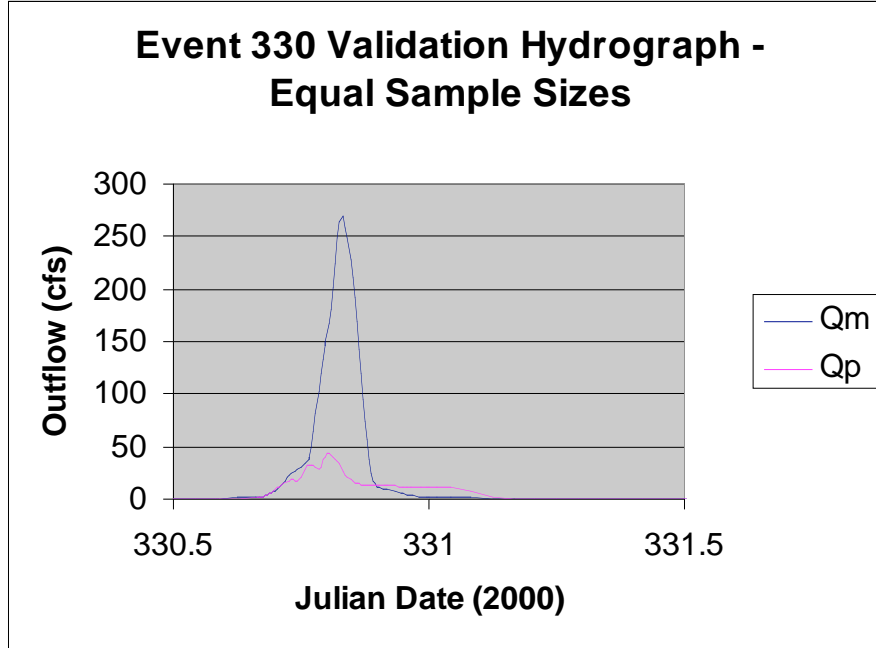


**Figure 3H.3.1: Event 330 Validation Hydrograph for Catchment K2 (2000).** These two hydrographs are from datasets used to compare the correlation between the observed outflow and the SWMM predicted outflows. For comparative purposes, the same sizes were adjusted to create equally sized datasets. The blue line is the observed data, and the purple line is the SWMM simulation results following calibration. SWMM severely under-predicts the measured data by over 200 cfs, but the certainty of the high observed flow rate is also questionable. During day 330, only the Blue Earth water stage information was recorded, therefore yielding the high flow rates. Unfortunately, the weir equation used to calculate the higher flows becomes invalid during submergence, and the STARFLOW data was unavailable during this event. Thus, only the Blue Earth's flow calculations have been plotted for the measured data hydrograph. Due to the large difference in the peak outflow rate, the associated R-square value for this correlation is 0.34.

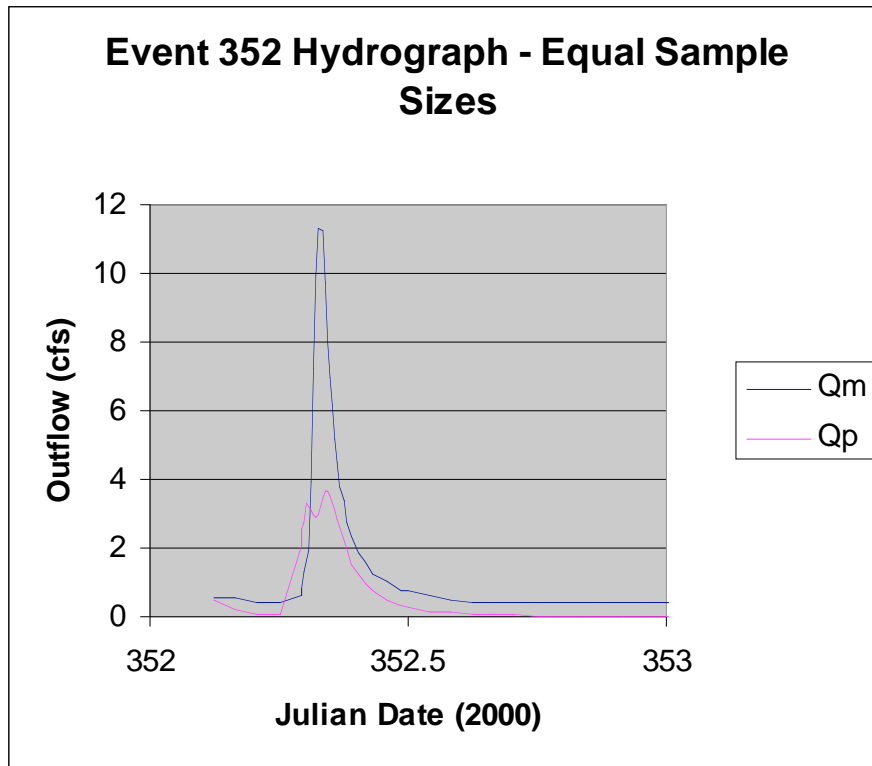


**Figure 3H.3.2: Catchment K2 Storm Event 352 Validation Hydrograph (2000).** This figure presents the observed and simulated hydrographs for a single storm event in catchment K2. The blue line is the measured hydrograph that reaches a peak outflow rate of more than 11 cfs. The purple is the SWMM predicted hydrograph for the same time period, which obtains a maximum flow value of nearly 4 cfs. The Nash Sutcliffe correlation statistic associated with this hydrograph is 0.40 and the adjusted R-square value is 0.68.

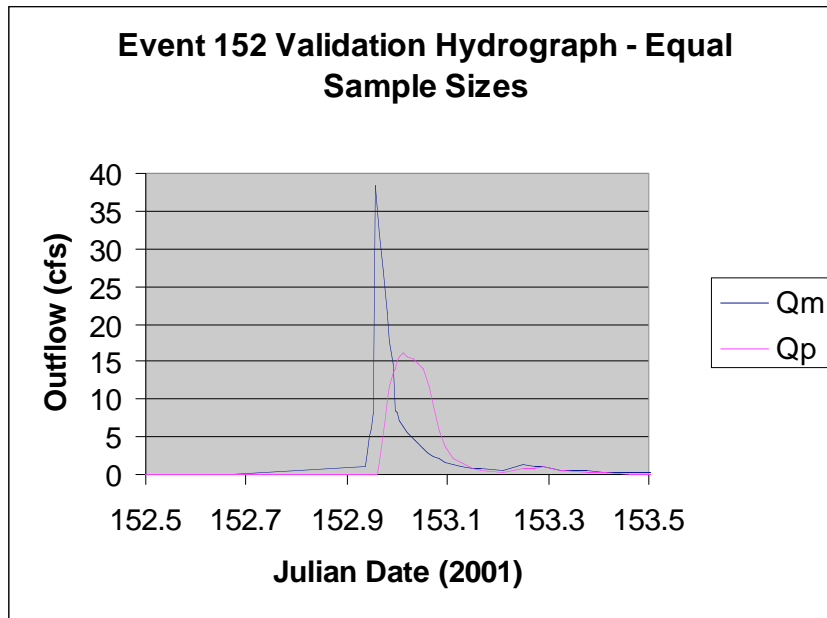


**Figure 3H.3.3: Catchment K2 Storm Event 152 Validation Hydrograph (2001).** The two hydrographs presented in this figure are associated with the measured and predicted datasets for storm even 152 during the validation period. The blue line represents the observed flow information, having a peak flow rate of approximate 37 cfs. The purple line is the SWMM simulated hydrograph whose peak flow rate only achieves a maximum value near 15 cfs. As suspected from the hydrograph shapes, the calculated correlation statistics reported minimal similarities between the two datasets.

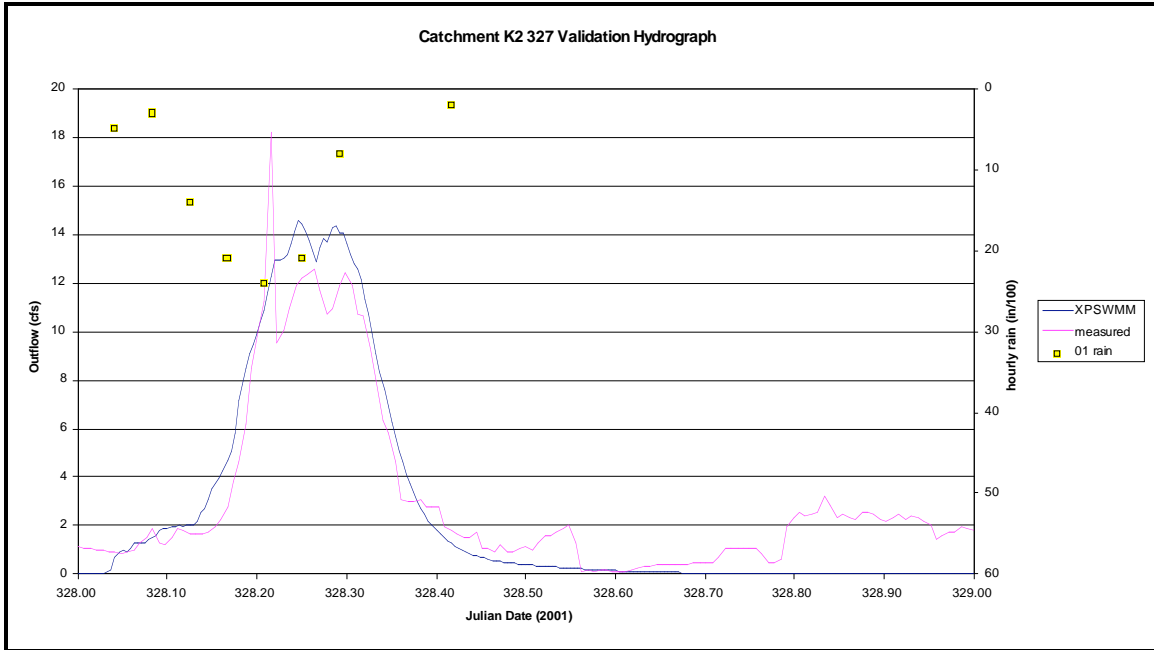


**Figure 3H.3.4: Validation Hydrograph for Event 327 in Catchment K2.** This figure presents the outflow data from the XPSWMM simulations and the measured flow data for storm event 327 in catchment K2. The blue line is the XPSWMM continuous outflow data that has been truncated to a 24-hour time period. The purple curve represents the measured data and the yellow dots are the corresponding hyetograph points plotted on a secondary axis. The maximum, measured flow rate was nearly 18 cfs, which compares favorably to the 14.25 outflow rate generated by the model. The overall trends of the hydrographs are similar and the test statistics verify this assumption. The calculated Nash-Sutcliffe statistic for this graph is 0.82 and the adjusted R-square value is 0.90.

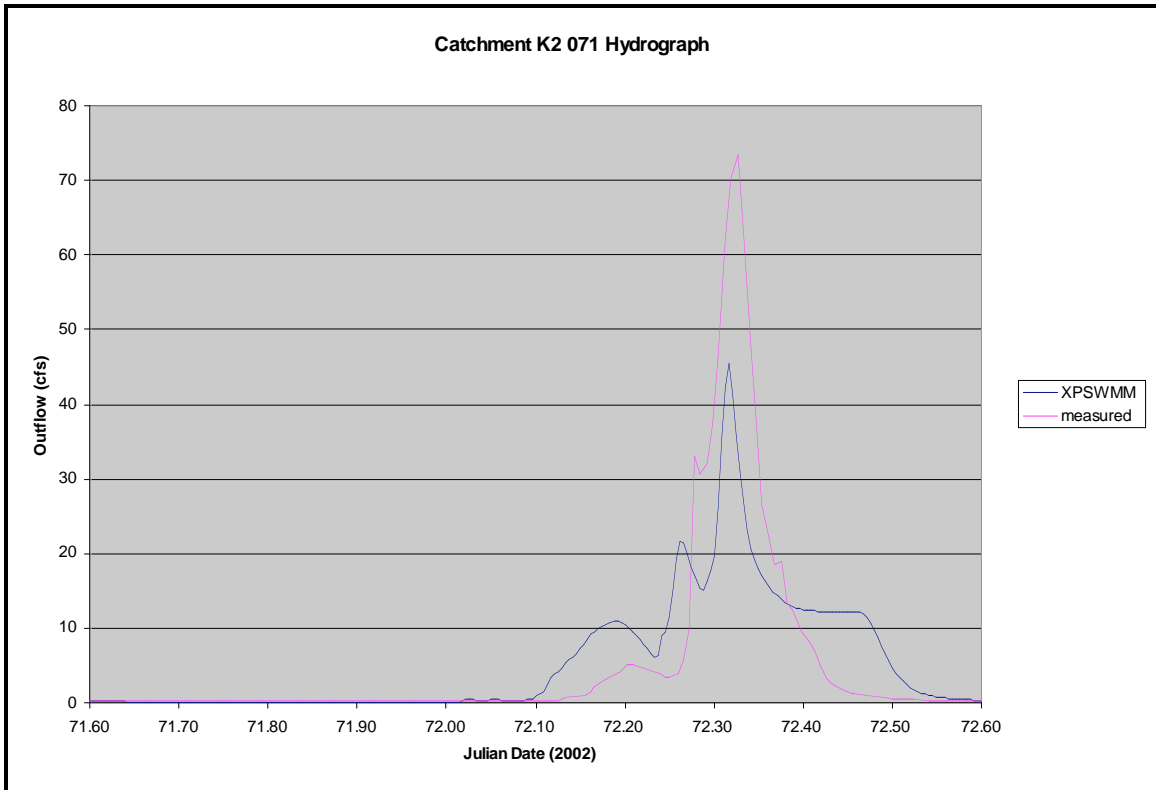


**Figure 3H.3.5: Event 71 (2002) Validation Hydrograph for Catchment K2 at Cherry Point.** This graph was created from the combination of the XPSWMM continuous outflow predictions and the measured flow data from event 71 in catchment K2. The purple line is the observed flow information and the blue line is the XPSWMM, continuous, simulation results using a one-day display span. The observed maximum outflow for this event was approximately 73 cfs while XPSWMM under predicted the observed maximum by less than 30 cfs. The hydrograph shapes share some resemblances but lack high correlation. The resulting R-square value for this figure is 0.72 and the Nash-Sutcliffe value is 0.65.

**Exhibit 3H.4:** Catchment K3 Validation Hydrographs for Cherry Point, NC

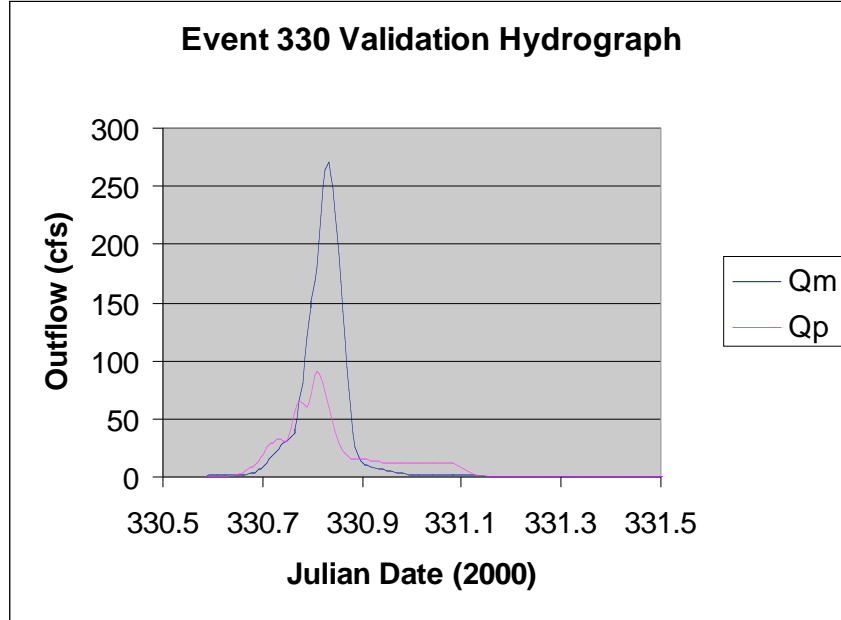


**Figure 3H.4.1: Event 330 (2000) Validation Storm for Catchment K3.** These two hydrographs were created from the observed, Blue Earth stage data and the SWMM predicted information for storm event 330 in catchment K3. The STARFLOW information for the storm event was unavailable; therefore the Blue Earth data was graphed, which relies solely upon the weir equation. The high flow rates were calculated using the v-notch weir elevation which is not reliable during weir submergence, thus the high flow rates are probably incorrect. SWMM predicted a maximum flow rate of nearly 90 cfs, which is far less than the more than 250 cfs value resulting from the weir equation. Using the regression equation to augment the observed dataset would have possibly increased the correlation between the two hydrograph. Nonetheless, the test statistics report little similarities between the two curves having calculated R-square and Nash-Sutcliffe values of 0.58 and 0.25, respectively.

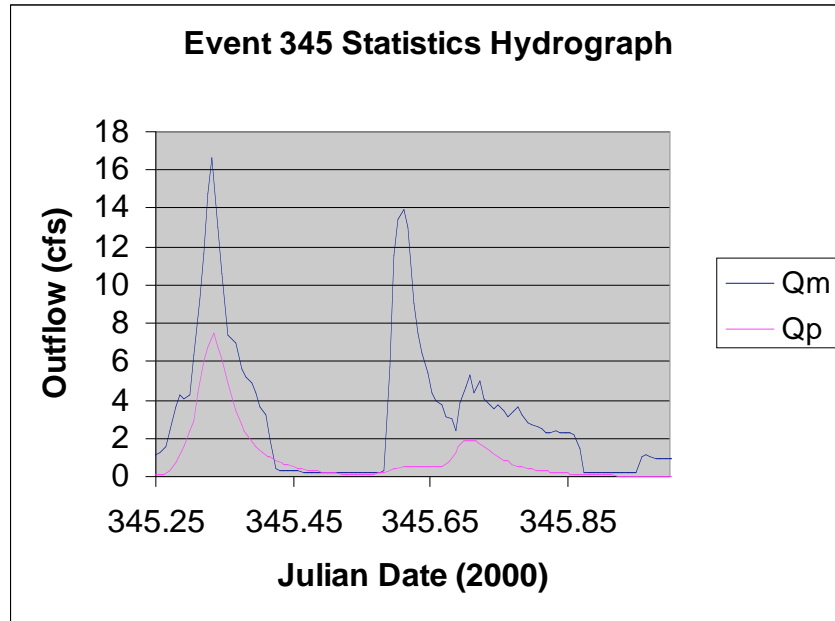


**Figure 3H.4.2: Event 345 Validation Hydrograph for Catchment K3.** The two hydrographs presented in this figure represent the observed and predicted outflow values for storm event 345 at the outlet of catchment K3 in 2000. The blue curve is the observed data for this time period. The purple line is the SWMM simulation results. The observed data achieves a maximum outflow rate of less than 17cfs during the earlier portion of the event. The corresponding, predicted maximum is about 7cfs. The shapes of the two hydrographs are similar, but the predicted hydrograph has less runoff volume. The reported Nash-Sutcliffe and adjusted R-square statistics for this figure are 0.16 and 0.58, respectively.

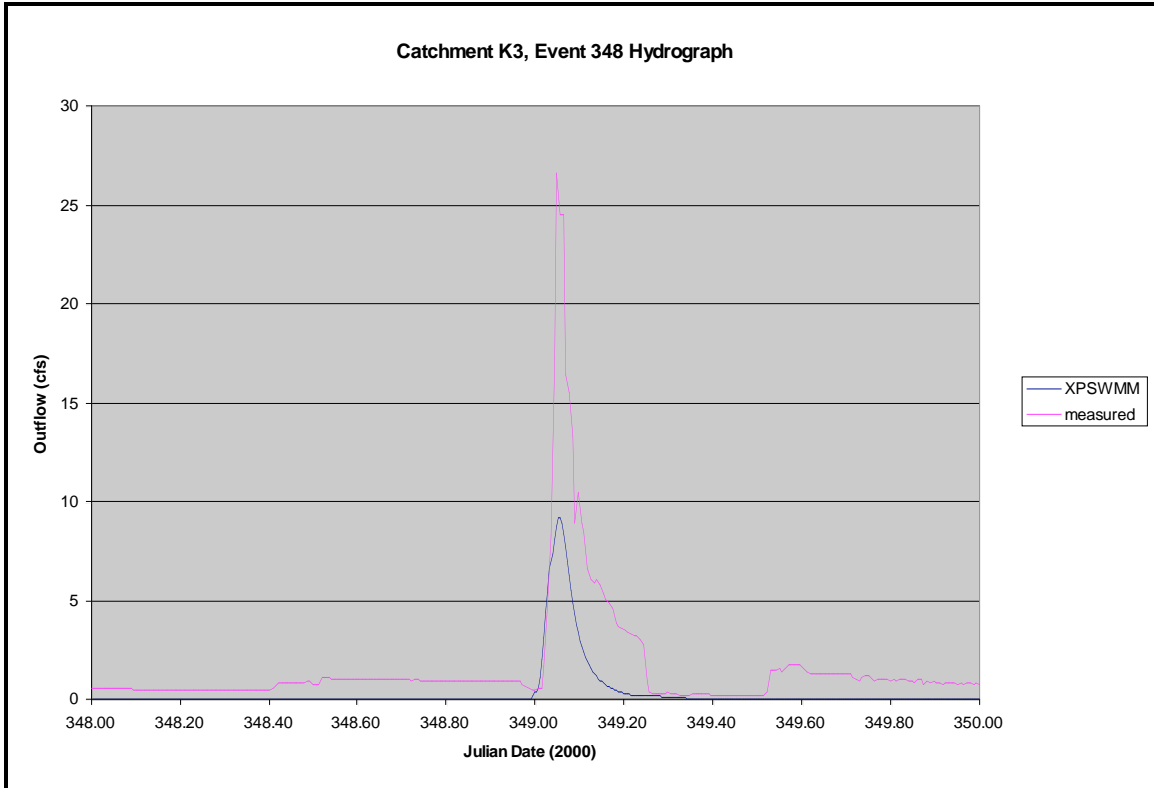


**Figure 3H.4.3: Event 348 (2000) Validation Hydrograph used for Statistical Correlation.** This hydrograph was generated using points predicted by XPSWMM from the 2000 precipitation data. The observed data, graphed as the purple line, achieves a maximum outflow rate of nearly 27 cfs during day 349. The corresponding XPSWMM prediction only reaches a maximum value of 9 cfs. The measured data also indicates the presence of baseflow preceding and following the storm event. The simulated hydrograph fails to demonstrate this same detail. The associated R-square and Nash-Sutcliffe correlation statistics for this figure are 0.87 and 0.43, respectively.

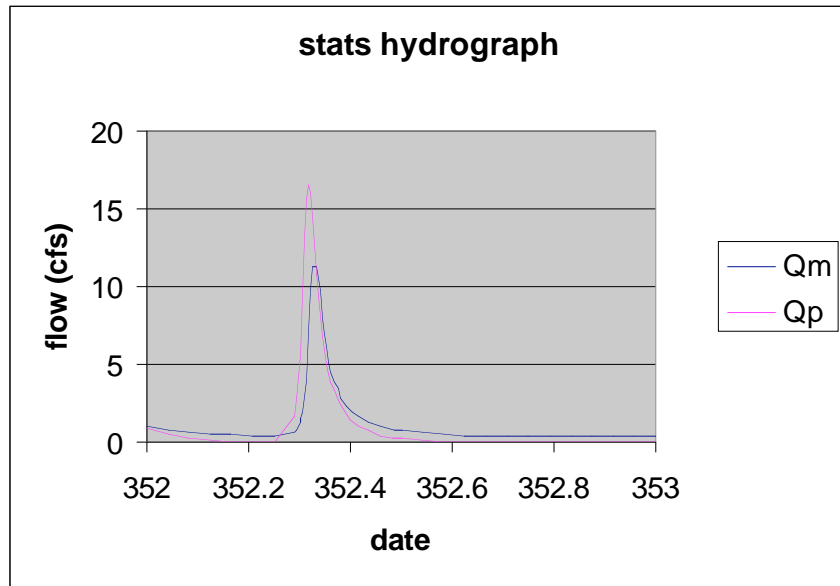


**Figure 3H.4.4: Event 351 (2000) Validation Hydrograph for Statistical Interpretation.** The above figure is the collection of outflow data used to statistically validate the correlation between the measure and predicted outflows for the catchment K3 outlet during a single rainfall event. The purple curve is the SWMM predicted hydrograph for event 351. The blue line represents the observed outflow rates at the catchment outlet. The measured, maximum outflow rate was approximately 11 cfs, which was nearly 6 cfs less than the predicted peak outflow. Seemingly, the hydrographs share comparable trends, although the statistics do not support this assumption. The resulting R-square and Nash-Sutcliffe values for this hydrograph are 0.59 and -0.08, respectively.

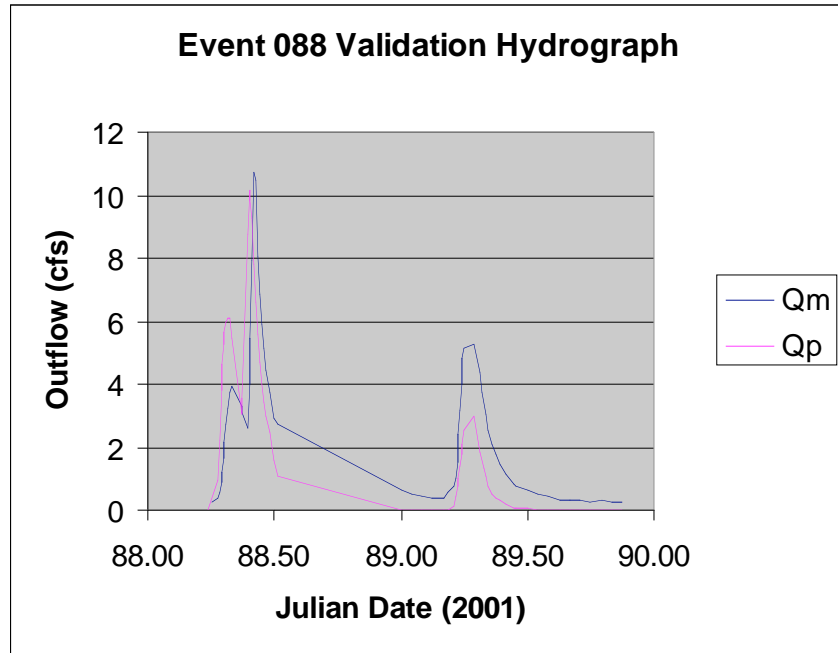


**Figure 3H.4.5: Catchment K3 Validation Hydrograph for Event 88 (2001).** These hydrographs were completed using the observed flow data and the predicted SWMM outflows for event 88 during 2001. The blue curve presents the measured flow as recorded at the catchment K3 outlet. The purple curve is the collection of simulated hydrograph points using the text based version of SWMM. The maximum flow value for the measured data exceeds 10 cfs. Likewise, predicted peak flow rate for this storm event barely surpasses the 10 cfs mark. From visual inspection, the hydrographs have similar trends, but this assumption is not supported by the correlation tests. The associated R-square and Nash Sutcliffe test statistics for this hydrograph are 0.47 and 0.26, respectively.

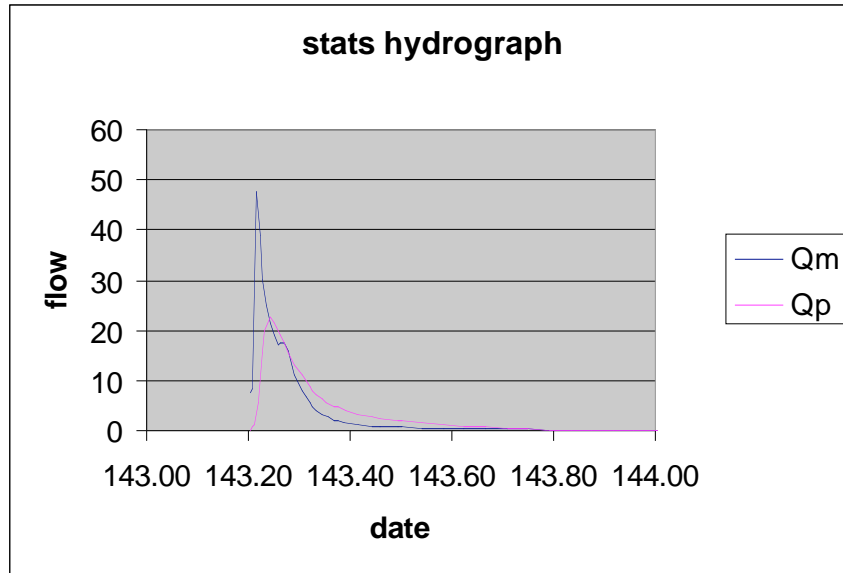


**Figure 3H.4.6: Catchment K3 Validation Hydrograph for Event 143 (2001).** Various test statistics were completed to describe the similarities between the measure and observed data for event 143 in 2001. The blue curve is the measure data as collected by the Blue Earth and STARFLOW meter. The purple line represents the SWMM predicted hydrograph resulting from the HOBO rainfall for year 2001. The measured maximum flow rate is approximately 46 cfs, while the SWMM estimate only reaches a maximum near 20 cfs. The missing, observed data is due to the correlation procedure which requires the samples to have equal sizes. Since the STARFLOW only records flow measurements in 10-min increment, the flow information for day 143.2 is the starting point of the hydrograph. The reported Nash-Sutcliffe and R-square values for this hydrograph are 0.30 and 0.31, respectively.

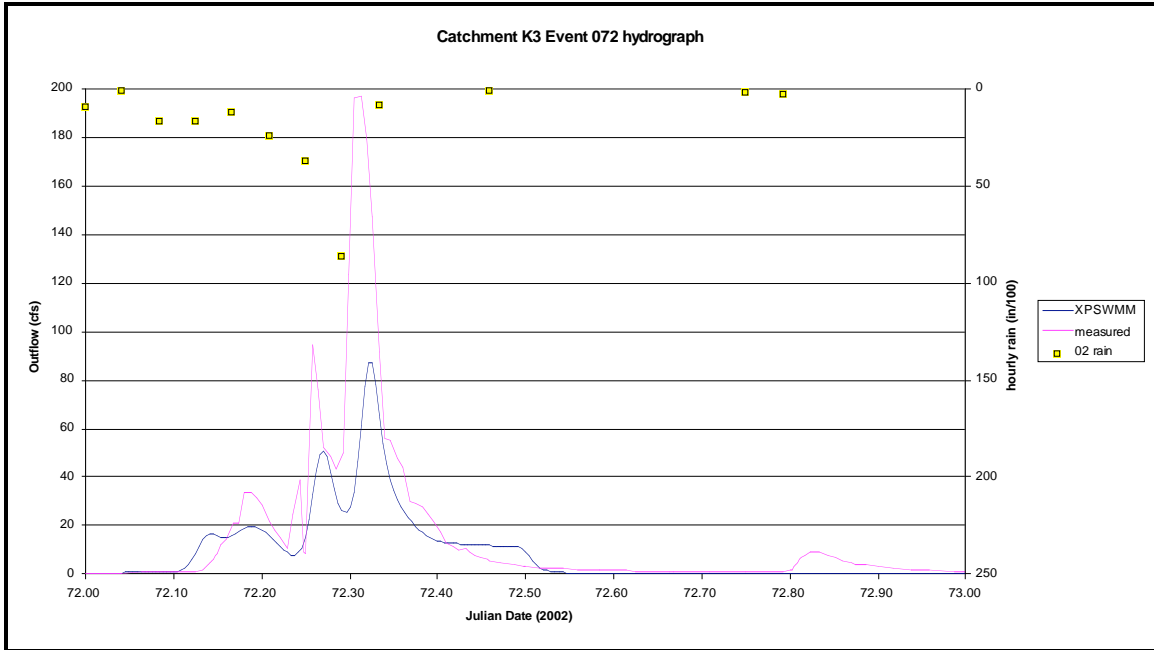


**Figure 3H.4.7: Catchment K3 Event 72 Hydrograph (2002).** This comparative hydrograph was created by extracting portions of the continuous XPSWMM predicted outflows and the observed flow measurements for the same time period. The purple curve represents the measure flow data, which reached a maximum outflow value of nearly 200 cfs around Julian date 72.30. The blue line is the truncated XPSWMM simulated hydrograph that displays the same trends as the observed data, but only achieves a peak outflow rate of approximately 85 cfs. The rainfall hyetograph points were plotted on the secondary axis, indicated by the yellow squares. The Nash-Sutcliffe and R-square values for this hydrograph are 0.49 and 0.69, respectively.

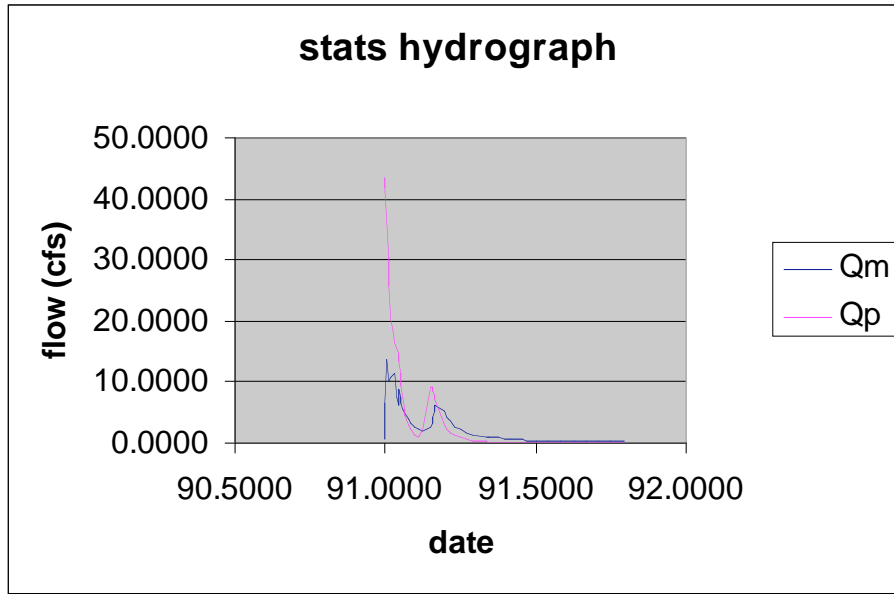


**Figure 3H.4.8: Catchment K3 Event 90 Validation Hydrograph (2002).** These two hydrographs were collected from the observed and predicted datasets for storm 090 in 2002. The purple curve represents the SWMM predicted hydrograph and appears to be missing data due to timing differences. When aligning the observed and simulated hydrograph points, no observed data corresponded to the simulated data, within a given tolerance, during that time span since the STARFLOW's recording interval is every ten minutes. Therefore, the resulting predicted hydrograph seems to be missing data, but in actuality, simply no observed data had been recorded. The blue curve represents the measured data and achieves a maximum outflow rate in excess of 10 cfs. The predicted hydrograph surpasses the measured peak rate by approximately 30 cfs. The correlation statistics for these hydrograph are -6.73 and 0.37 using the Nash-Sutcliffe and R-square techniques. A negative Nash-Sutcliffe value represents unfavorable agreement between the observed and predicted flow values.

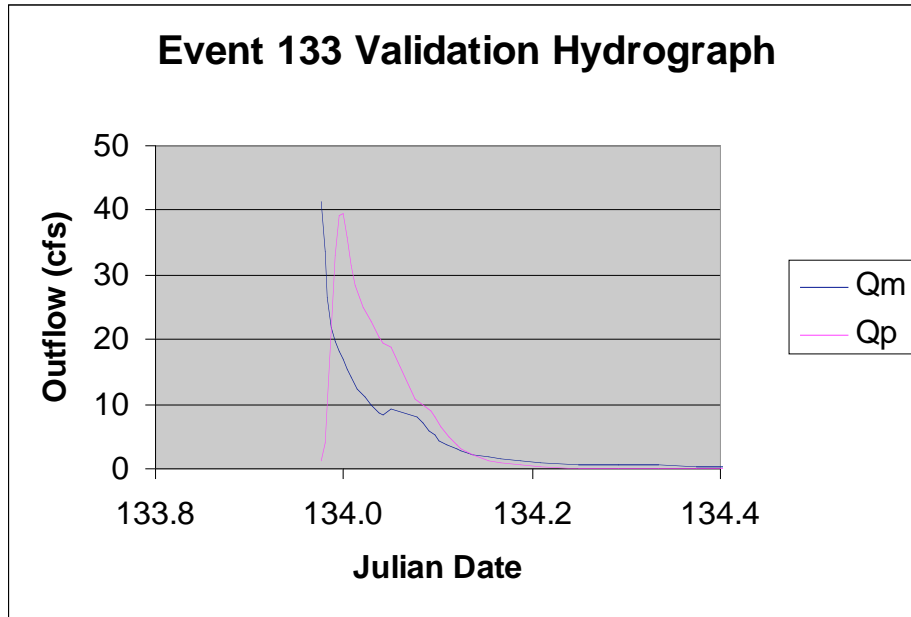


**Figure 3H.4.9: Catchment K3 Event 133 Validation Hydrograph (2002).** This hydrograph represents the SWMM predicted and observed outflow data for a single storm at Cherry Point. The measured data is presented as a blue curve, and the SWMM predicted hydrograph is colored purple. Similar to the situation presented in the previous chart, the seemingly missing data from the observed data is due to timing differences and the correlation efforts. Both hydrographs yield a maximum flow rate of nearly 40 cfs. Visually speaking, the hydrographs fail to share any noticeable similarity which is substantiated by the resulting correlation statistics. The associated test statistics used to describe the correlation between the two datasets are -0.57 and 0.18 for the Nash-Sutcliffe and R-square methods.

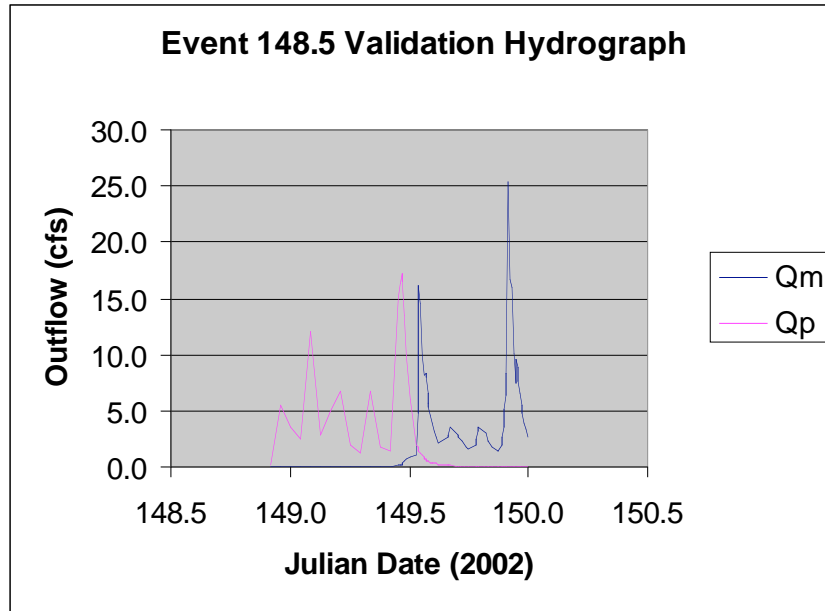


**Figure 3H.4.10: Catchment K3 Event 148.5 Validation Hydrograph (2002).** This hydrograph displays a discrepancy in the timing between the observed and predicted data for storm event 148.5 in 2002. The blue curve is the observed data and the predicted hydrograph is presented in purple. There appears to be a 24-hour timing difference between the two graphs. The observed hydrograph reports a maximum outflow value of over 15 cfs while the predicted data demonstrates a 25 cfs outflow at the monitoring location. The calculated statistics verify little agreement between the two datasets, reporting correlation values of -1.68 and 0.11 for the Nash-Sutcliffe and adjusted R-square methods.

**Appendix 3I: XPSWMM9.0 Simulation Results, Completed in 2006**

**Exhibit 3I.1: Catchment K2 Selected Storm Selected Hydrographs (2001)**

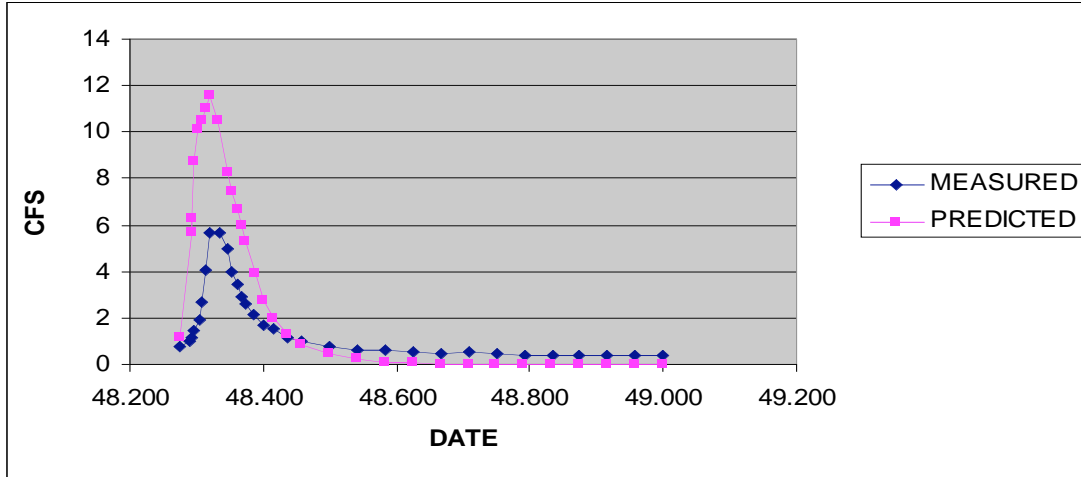


**Figure 3I.1.1: Catchment K2 Event 48 Outflow Hydrograph (2001 Rainfall)**

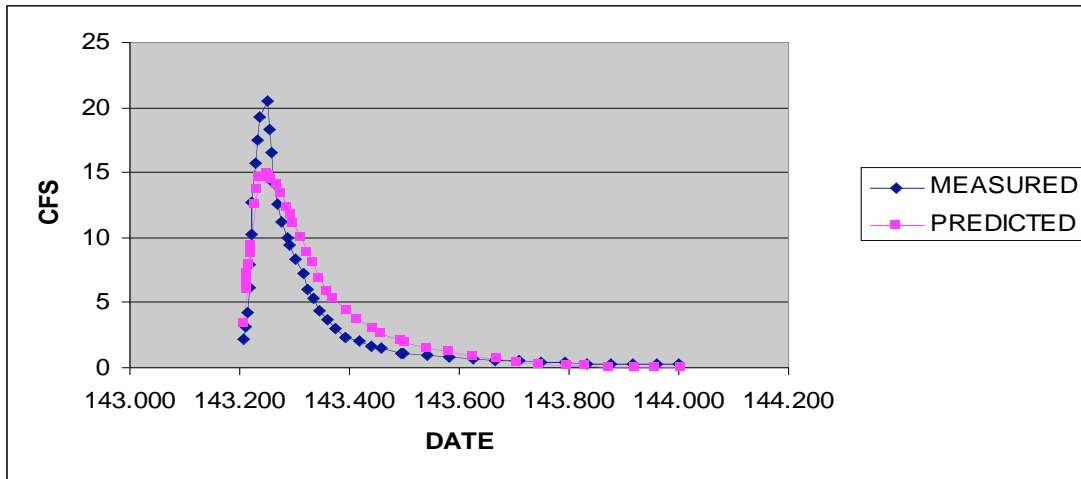


**Figure 3I.1.2: Catchment K2 Event 143 Outflow Hydrograph (2001 Rainfall)**

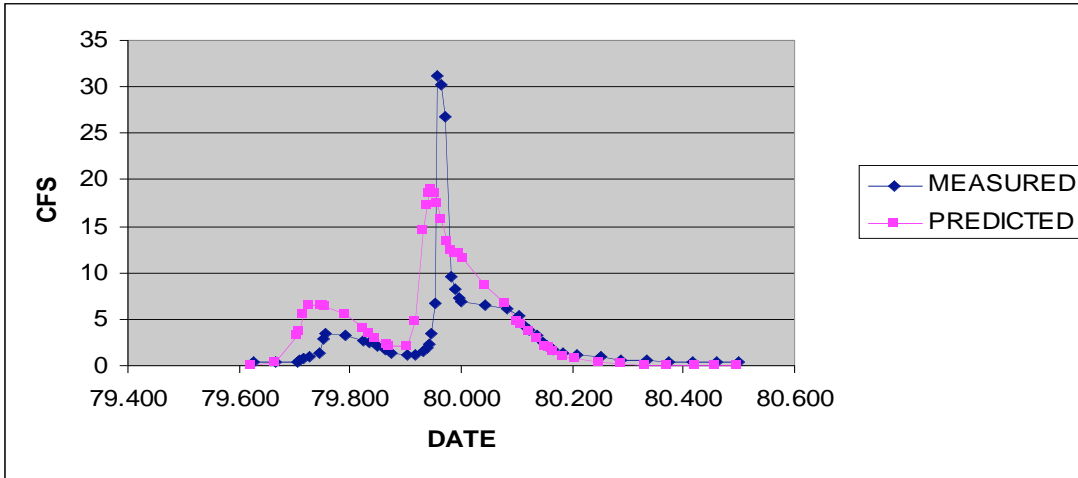


**Figure 31.1.3: Catchment K2 Event 79 Outflow Hydrograph (2001 Rainfall)**

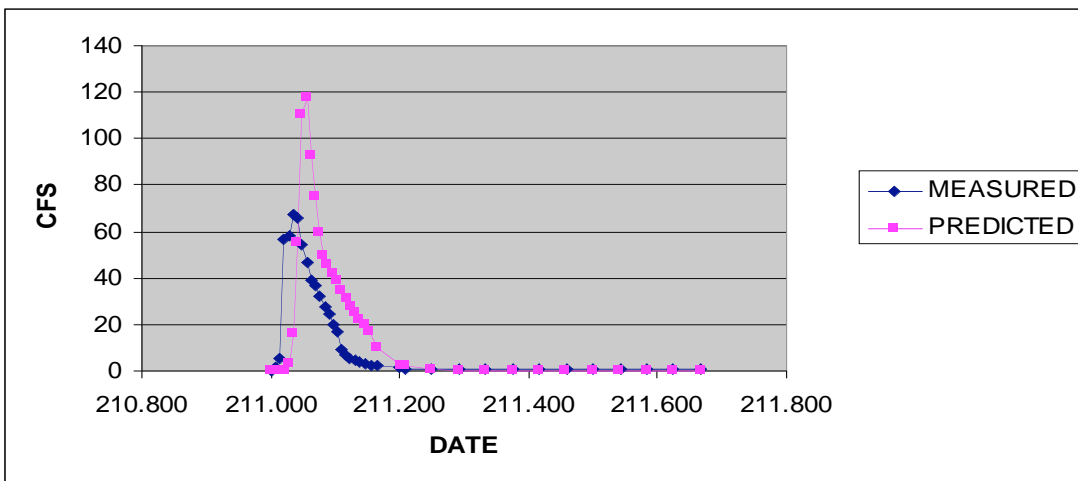


**Figure 31.1.4: Catchment K2 Event 211 Outflow Hydrograph (2001 Rainfall)**

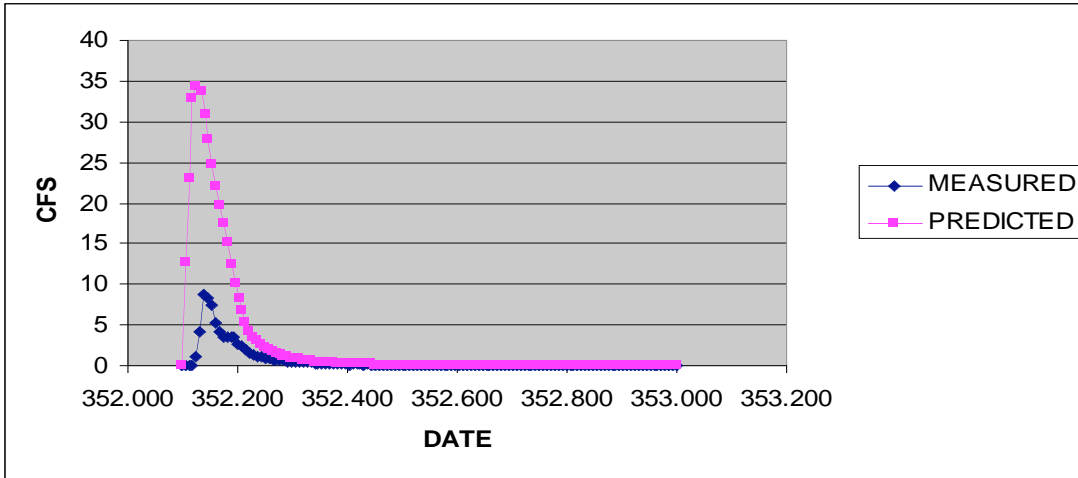


Figure 31.1.5: *Catchment K2 Event 352 Outflow Hydrograph (2001 Rainfall)*

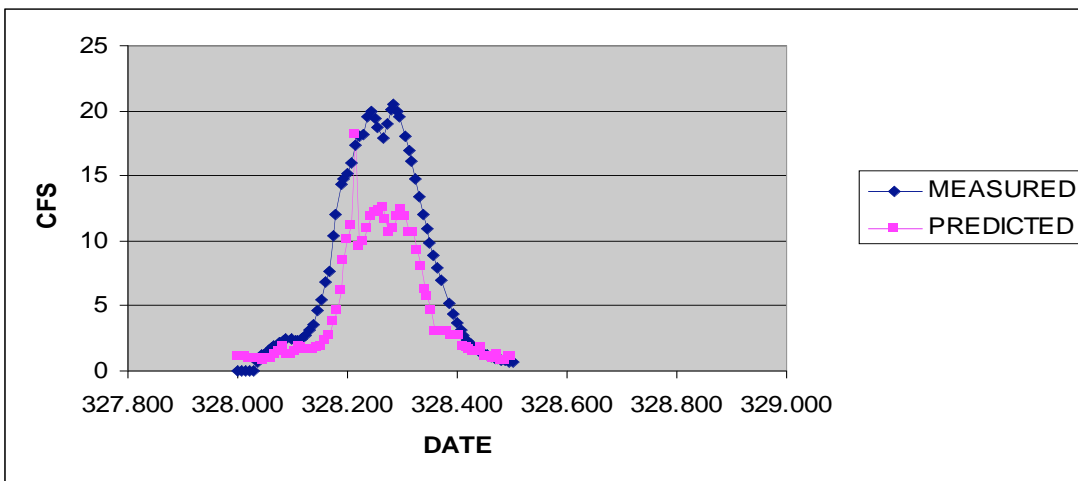


Figure 31.1.6: *Catchment K2 Event 328 Outflow Hydrograph (2001 Rainfall)*

**Exhibit 31.2: Catchment K2 2001 Selected Storms T-test Statistic Results**

t-Test: Paired Two Sample for Means

**event 48**

	<i>MEAS.</i> <i>FLOW(CFS)</i>	<i>PRED.</i> <i>VALUE</i> <i>(CFS)</i>
Mean	1.75	3.77
Variance	2.60	17.15
Observations	32.00	32.00
Pearson Correlation	0.84	
Hypothesized Mean Difference	0.00	
df	31.00	
t Stat	-3.92	
P(T<=t) one-tail	0.00	
t Critical one-tail	1.70	
P(T<=t) two-tail	0.00	
t Critical two-tail	2.04	

conclusion: absolute value of T stat is greater than the T crit value, so reject the null, so the means are different  
alpha =.05

### Exhibit 3I.2 Continued

t-Test: Paired Two Sample for Means  
**event 143**

	<i>MEAS. FLOW(CFS)</i>	<i>PRED. VALUE (CFS)</i>
Mean	6.18	6.50
Variance	39.04	28.03
Observations	43.00	43.00
Pearson Correlation	0.94	
Hypothesized Mean Difference	0.00	
df	42.00	
t Stat	-0.98	
P(T<=t) one-tail	0.17	
t Critical one-tail	1.68	
P(T<=t) two-tail	0.33	
t Critical two-tail	2.02	

conclusion: Absolute value of T stat is less than T crit for two tail, so accept null hypothesis, the samples have equal means  
alpha = .05

### Exhibit 3I.2 Continued

t-Test: Paired Two Sample for Means  
**event 79**

	<i>MEAS. FLOW(CFS)</i>	<i>PRED. VALUE (CFS)</i>
Mean	4.35	6.11
Variance	49.35	35.48
Observations	47.00	47.00
Pearson Correlation	0.57	
Hypothesized Mean Difference	0.00	
df	46.00	
t Stat	-1.98	
P(T<=t) one-tail	0.03	
t Critical one-tail	1.68	
P(T<=t) two-tail	0.05	
t Critical two-tail	2.01	

conclusion: the Absolute value of T stat  
is greater than the T crit value, so the  
reject the null, and the two samples  
have unequal means  
alpha=.05

### Exhibit 3I.2 Continued

t-Test: Paired Two Sample for Means  
**event 211**

	<i>MEAS. FLOW(CFS)</i>	<i>PRED. VALUE (CFS)</i>
Mean	16.17	24.34
Variance	475.36	1052.55
Observations	37.00	37.00
Pearson Correlation	0.59	
Hypothesized Mean Difference	0.00	
df	36.00	
t Stat	-1.90	
P(T<=t) one-tail	0.03	
t Critical one-tail	1.69	
P(T<=t) two-tail	0.07	
t Critical two-tail	2.03	

Conclusion: The absolute value of the T stat is greater than T crit, so reject the null, and sample have unequal means  
alpha = .05

### Exhibit 3I.2 Continued

t-Test: Paired Two Sample for Means  
**event 352**

	<i>MEAS. FLOW(CFS)</i>	<i>PRED. VALUE (CFS)</i>
Mean	0.58	2.84
Variance	2.29	55.54
Observations	131.00	131.00
Pearson Correlation	0.76	
Hypothesized Mean Difference	0.00	
df	130.00	
t Stat	-4.05	
P(T<=t) one-tail	0.00	
t Critical one-tail	1.66	
P(T<=t) two-tail	0.00	
t Critical two-tail	1.98	

Conclusion: The absolute value of T  
stat is greater than T crit, so reject the  
null, the samples have different means  
alpha = .05

### Exhibit 3I.2 Continued

t-Test: Paired Two Sample for Means  
**event 328**

	<i>MEAS. FLOW(CFS)</i>	<i>PRED. VALUE (CFS)</i>
Mean	4.68	7.69
Variance	20.04	52.18
Observations	73.00	73.00
Pearson Correlation	0.95	
Hypothesized Mean Difference	0.00	
df	72.00	
t Stat	-7.91	
P(T<=t) one-tail	0.00	
t Critical one-tail	1.67	
P(T<=t) two-tail	0.00	
t Critical two-tail	1.99	

Conclusion: The absolute value of T  
stat is greater than T crit, so reject the  
null, the sample have different means  
alpha = .05

**Exhibit 3I.3:** Catchment K2 Selected Storm Hydrographs (2002)

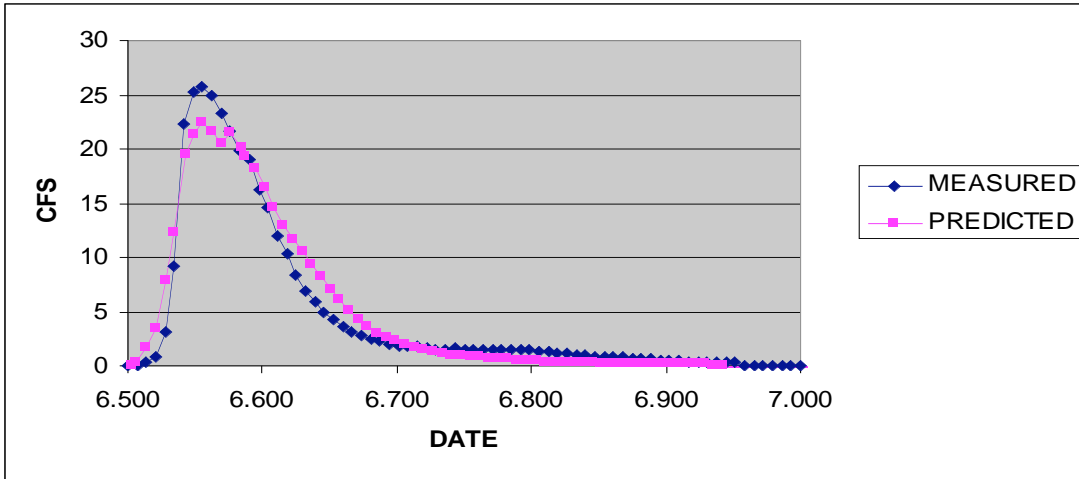


**Figure 3I.3.1:** Catchment K2 Event 06 Outflow Hydrograph (2002)

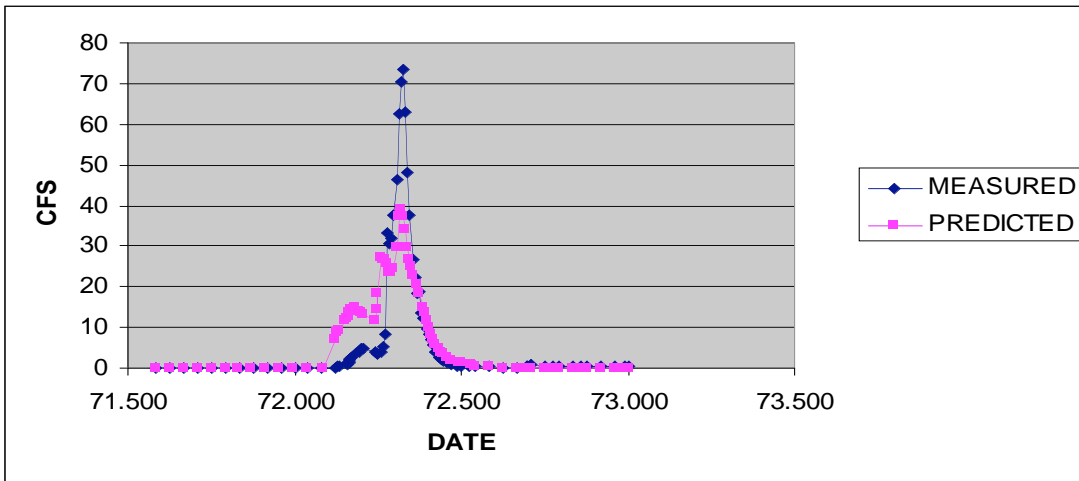


**Figure 3I.3.2:** Catchment K2 Event 71 Outflow Hydrograph (2002)

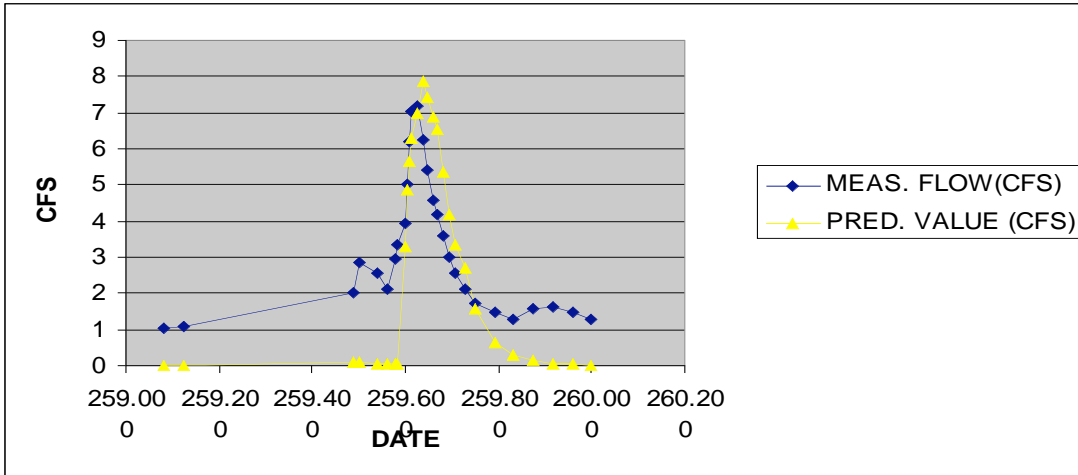


Figure 31.3.3: Catchment K2 Event 259 Outflow Hydrograph (2002)

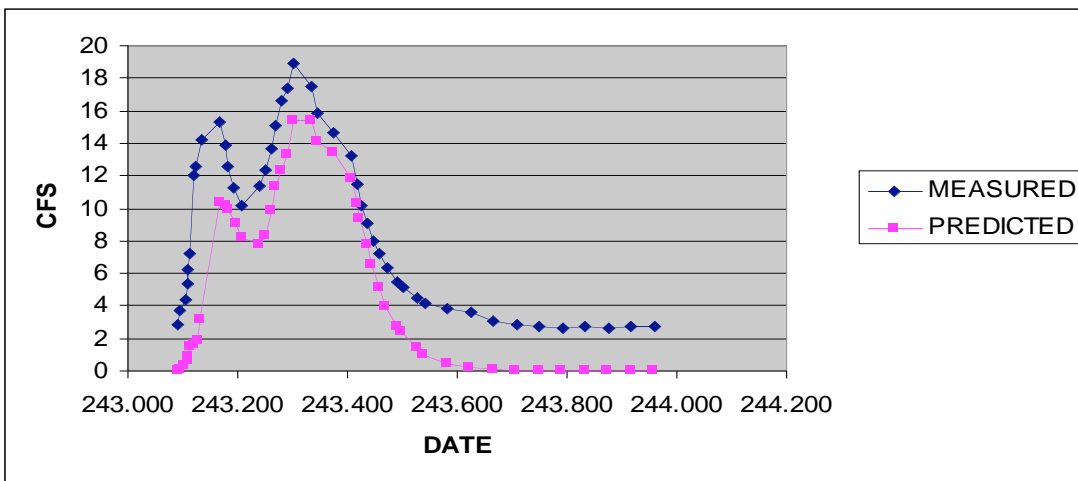


Exhibit 31.3.4: Catchment K2 Event 243 Outflow Hydrograph (2002)



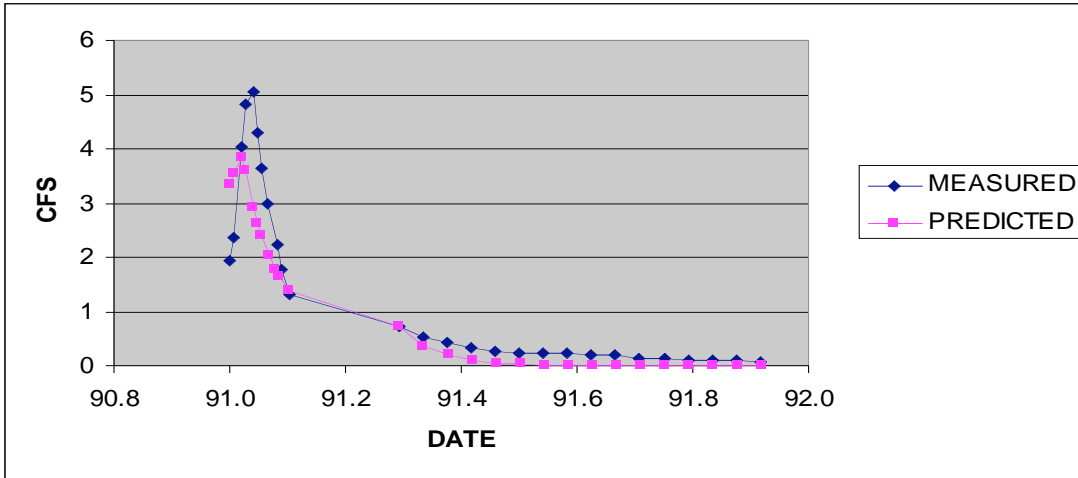


Figure 31.3.7: *Catchment K2 Event 91 Outflow Hydrograph (2002)*

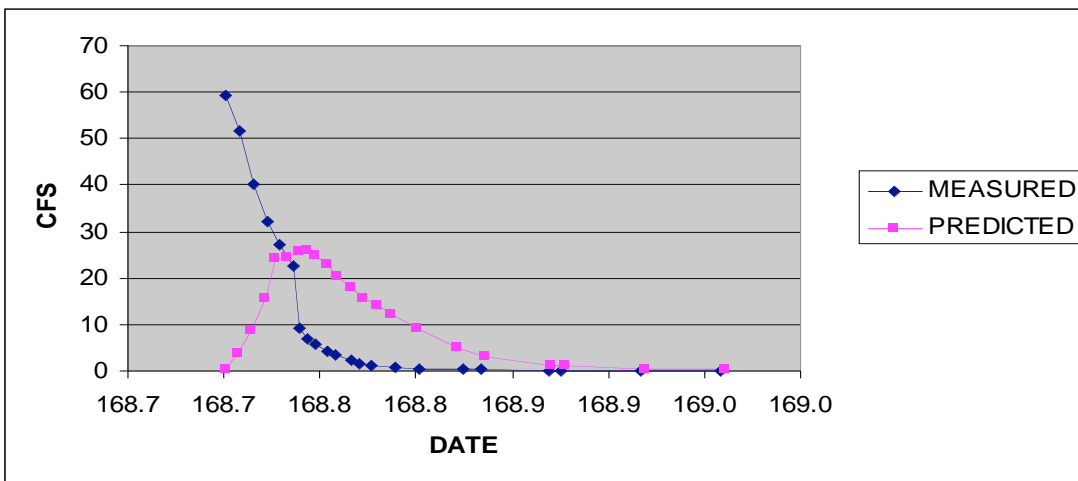


Figure 31.3.8: *Catchment K2 Event 168 Outflow Hydrograph (2002)*

**Exhibit 3I.4: Catchment K2 T-Test Statistics for Selected Storms (2002)**

t-Test: Paired Two Sample  
for Means

**event 06**

	<i>MEAS. FLOW(CFS)</i>	<i>PRED. VALUE (CFS)</i>
Mean	4.5892507	4.74529726
Variance	52.22881619	50.21074482
Observations	73	73
Pearson Correlation	0.974058896	
Hypothesized Mean Difference	0	
df	72	
	-	
t Stat	0.814912436	
P(T<=t) one-tail	0.20890492	
t Critical one-tail	1.666294338	
P(T<=t) two-tail	0.41780984	
t Critical two-tail	1.99346232	

Conclusion: The Absolute  
value of T stat is less than  
the one-tail T crit, so  
accept the null, and the  
two samples have equal  
means  
alpha = 0.05

**Exhibit 3I.4 Continued**

t-Test: Paired Two Sample  
for Means

**event 71**

	<i>MEAS. FLOW(CFS)</i>	<i>PRED. VALUE (CFS)</i>
Mean	9.573541084	10.05109494
Variance	308.7226697	126.856695
Observations	79	79
Pearson Correlation	0.843108868	
Hypothesized Mean Difference	0	
df	78	
t Stat	0.420523402	
P(T<=t) one-tail	0.337629727	
t Critical one-tail	1.664625415	
P(T<=t) two-tail	0.675259454	
t Critical two-tail	1.990847522	

Conclusion: The absolute  
value of T stat is less than  
the one-tailed T crit, so  
accepth the null, the  
sample means are equal.  
alpha = 0.05

**Exhibit 3I.4 Continued**

t-Test: Paired Two Sample  
for Means

**event 259**

	<i>MEAS. FLOW(CFS)</i>	<i>PRED. VALUE (CFS)</i>
Mean	3.192393468	2.658075
Variance	3.532551097	8.594219299
Observations	28	28
Pearson Correlation	0.865318651	
Hypothesized Mean Difference	0	
df	27	
t Stat	1.756472247	
P(T<=t) one-tail	0.045172941	
t Critical one-tail	1.703288035	
P(T<=t) two-tail	0.090345881	
t Critical two-tail	2.051829142	

Conclusion: The absolute  
value of T stat is greater  
than the one-tailed T crit,  
so decline the null, and the  
samples have different  
means  
alpha = 0.05

**Exhibit 3I.4 Continued**

t-Test: Paired Two Sample  
for Means

**event 243**

	<i>MEAS. FLOW(CFS)</i>	<i>PRED. VALUE (CFS)</i>
Mean	8.869459603	5.395231111
Variance	26.62121602	27.48160479
Observations	45	45
Pearson Correlation	0.908154861	
Hypothesized Mean Difference	0	
df	44	
t Stat	10.4485311	
P(T<=t) one-tail	8.48294E-14	
t Critical one-tail	1.680230071	
P(T<=t) two-tail	1.69659E-13	
t Critical two-tail	2.0153675	

Conclusion: The absolute  
value of the T stat is  
greater than the one-tailed  
T crit, so decline the null,  
the samples have unequal  
means  
alpha = 0.05

**Exhibit 3I.4 Continued**

t-Test: Paired Two Sample  
for Means

**event 186**

	<i>MEAS. FLOW(CFS)</i>	<i>PRED. VALUE (CFS)</i>
Mean	1.370935547	2.240275
Variance	0.144265546	0.783573319
Observations	8	8
Pearson Correlation	0.532611484	
Hypothesized Mean Difference	0	
df	7	
t Stat	-3.25772544	
P(T<=t) one-tail	0.006954008	
t Critical one-tail	1.894577508	
P(T<=t) two-tail	0.013908015	
t Critical two-tail	2.36462256	

Conclusion: The absolute  
value of T stat is greater  
than the one-tailed T crit,  
so deny the null, the  
samples have unequal  
means.  
alpha = 0.05

**Exhibit 3I.4 Continued**

t-Test: Paired Two Sample  
for Means

**event 165**

	<i>MEAS. FLOW(CFS)</i>	<i>PRED. VALUE (CFS)</i>
Mean	10.29057261	11.777375
Variance	316.3654755	183.2427303
Observations	36	36
Pearson Correlation	0.408437069	
Hypothesized Mean Difference	0	
df	35	
t Stat	0.512549219	
P(T<=t) one-tail	0.305743186	
t Critical one-tail	1.689572855	
P(T<=t) two-tail	0.611486372	
t Critical two-tail	2.030110409	

Conclusion: The absolute  
value of T stat is less than  
the one-tailed T crit, so  
accept the null, the  
samples have equal  
means.  
alpha = 0.05

**Exhibit 3I.4 Continued**

t-Test: Paired Two Sample  
for Means

**event 91**

	<i>MEAS. FLOW(CFS)</i>	<i>PRED. VALUE (CFS)</i>
Mean	1.425421779	1.131359259
Variance	2.733352338	1.941474437
Observations	27	27
Pearson Correlation	0.907445357	
Hypothesized Mean Difference	0	
df	26	
t Stat	2.17403405	
P(T<=t) one-tail	0.019496714	
t Critical one-tail	1.705616341	
P(T<=t) two-tail	0.038993427	
t Critical two-tail	2.055530786	

Conclusion: The absolute  
value of T stat is greater  
than the one-tailed T crit,  
so deny the null, the  
sample means are not  
equal.  
alpha = 0.05

**Exhibit 3I.4 Continued**

t-Test: Paired Two Sample  
for Means

**event 168**

	<i>MEAS. FLOW(CFS)</i>	<i>PRED. VALUE (CFS)</i>
Mean	12.2238785	12.60051364
Variance	332.3408211	92.79102056
Observations	22	22
	-	
Pearson Correlation	0.080223115	
Hypothesized Mean Difference	0	
df	21	
	-	
t Stat	0.082972794	
P(T<=t) one-tail	0.467329498	
t Critical one-tail	1.720743512	
P(T<=t) two-tail	0.934658995	
t Critical two-tail	2.079614205	

Conclusion: The absolute  
value of T stat is less than  
the one-tailed T crit, so  
accept the null, the  
samples have equal  
means.  
alpha = 0.05

**Exhibit 31.5:** K3 Catchment Selected Storm Hydrographs (2001)

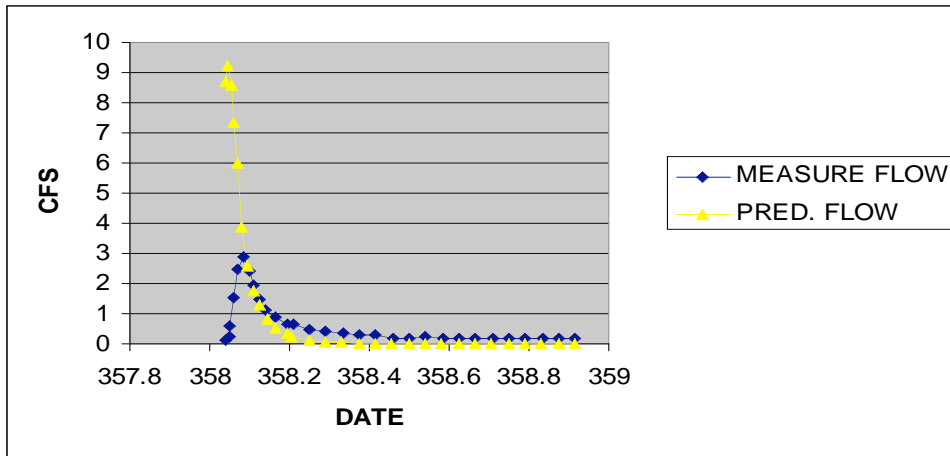


**Figure 31.5.1:** Catchment K3 Event 358 Outflow Hydrograph (2001)

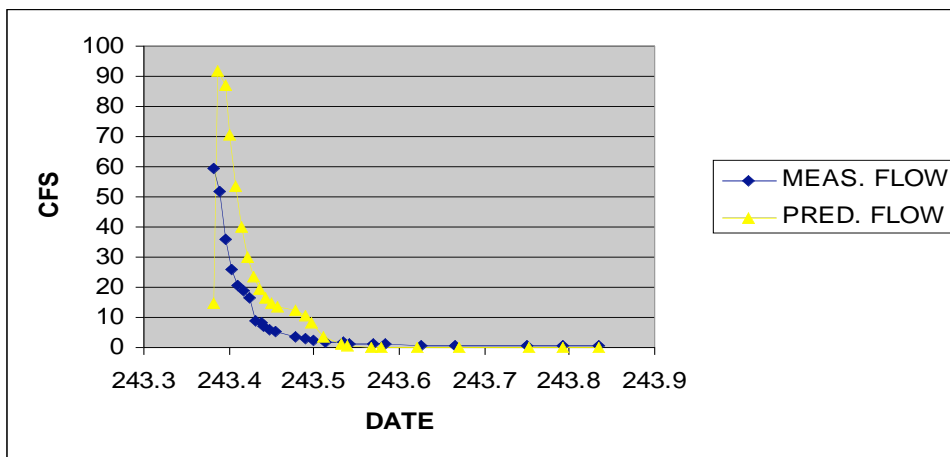


**Figure 31.5.2:** Catchment K3 Event 243 Outflow Hydrograph (2001)

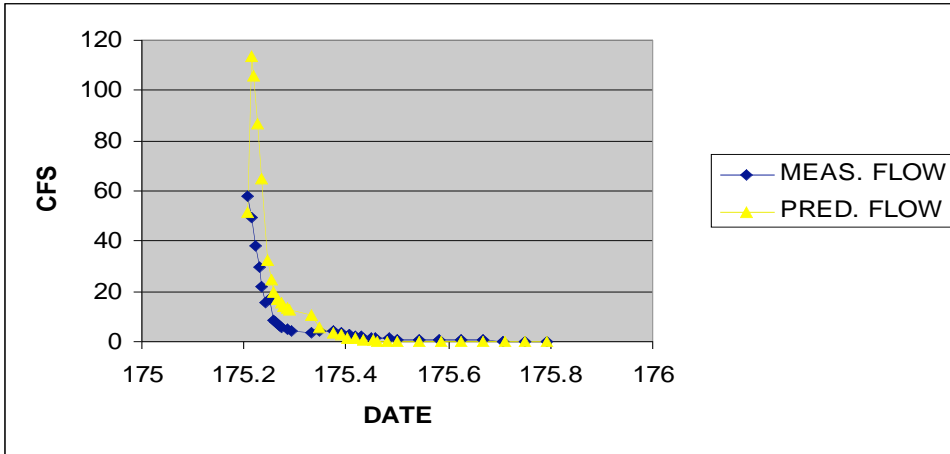


Figure 31.5.3: *Catchment K3 Event 175 Outflow Hydrograph (2001)*

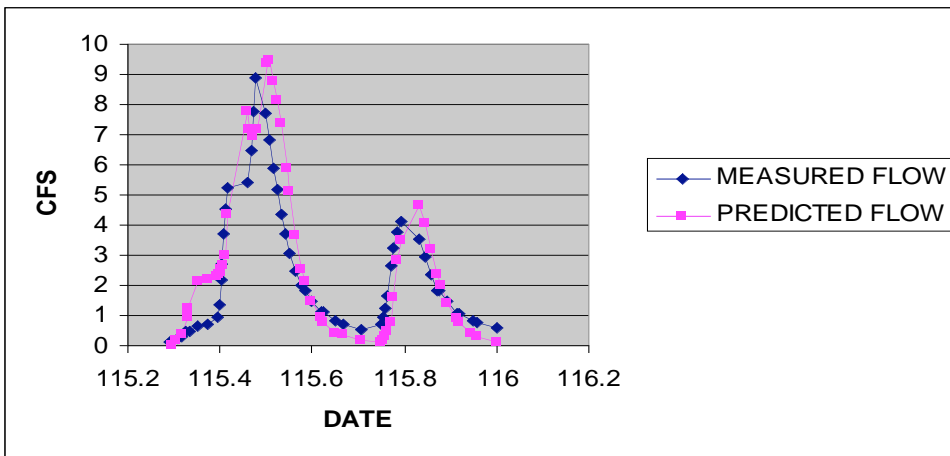


Figure 31.5.4: *Catchment K3 Event 115 Outflow Hydrograph (2001)*

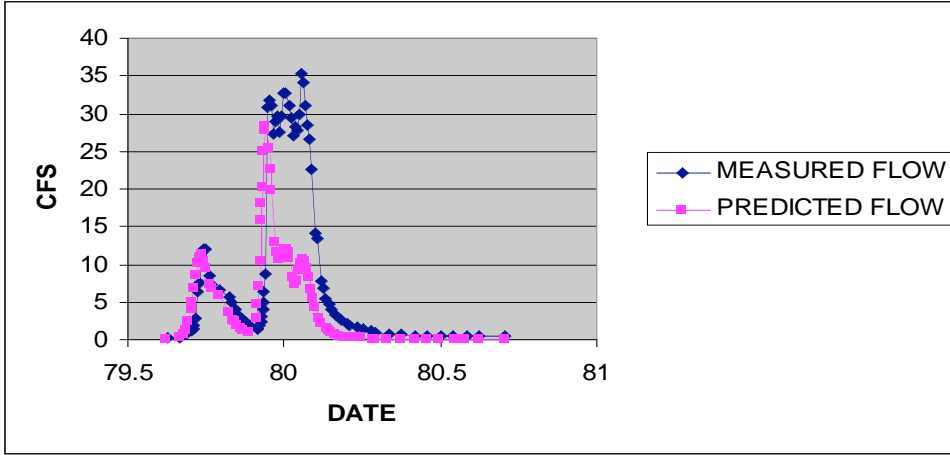


Figure 31.5.5: *Catchment K3 Event 80 Outflow Hydrograph (2001)*

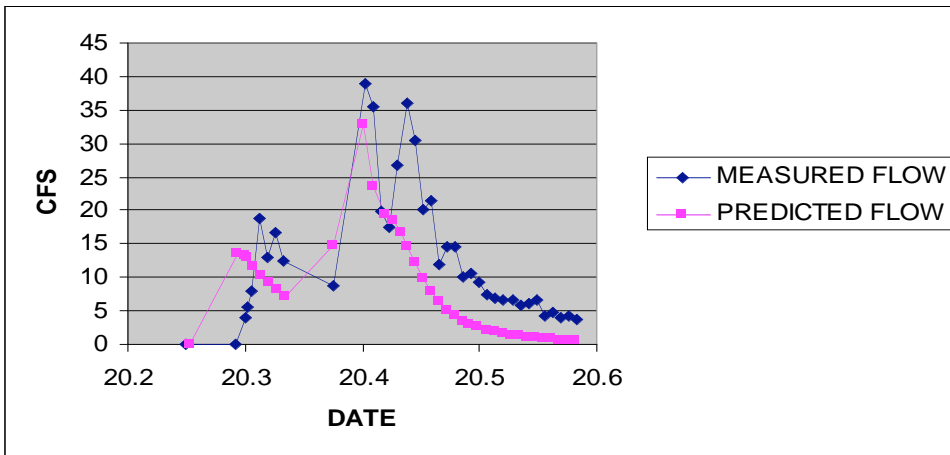


Figure 31.5.6: *Catchment K3 Event 20 Outflow Hydrograph (2001)*

**Exhibit 31.6: Catchment K3 T-Test Statistics Results (2001)**

t-Test: Paired  
Two Sample for  
Means

**event 358**

	MEAS. FLOW	PRED. FLOW
Mean	0.70803005	1.7249
Variance	0.623474905	9.126731348
Observations	30	30
Pearson Correlation	0.333503295	
Hypothesized Mean Difference	0	
df	29	
t Stat	-1.94986581	
P(T<=t) one-tail	0.030459793	
t Critical one-tail	1.699127097	
P(T<=t) two-tail	0.060919585	
t Critical two-tail	2.045230758	

Conclusion: The absolute value of T stat is greater than the one-tailed T crit, so reject the null, there is a difference between the two sample means.  
Alpha = 0.05

**Exhibit 3I.6 Continued**

t-Test: Paired  
Two Sample for  
Means

**event 243**

	MEAS. FLOW	PRED. FLOW
Mean	11.23962807	20.487724
Variance	263.1821881	748.8579118
Observations	25	25
Pearson Correlation	0.74013361	
Hypothesized Mean Difference	0	
df	24	
t Stat	2.454588476	
P(T<=t) one-tail	0.01086841	
t Critical one-tail	1.710882316	
P(T<=t) two-tail	0.021736821	
t Critical two-tail	2.063898137	

Conclusion: The absolute value of T stat is greater than the one-tailed T crit value, so reject the null, the means are not equal.  
alpha = 0.05

**Exhibit 3I.6 Continued**

t-Test: Paired  
Two Sample for  
Means

**event 175**

	MEAS. FLOW	PRED. FLOW
Mean	9.594479831	19.38035484
Variance	222.7707521	1008.363752
Observations	31	31
Pearson Correlation	0.883838795	
Hypothesized Mean Difference	0	
df	30	
t Stat	2.747260948	
P(T<=t) one-tail	0.005033284	
t Critical one-tail	1.697260359	
P(T<=t) two-tail	0.010066569	
t Critical two-tail	2.042270353	

Conclusion: The absolute value of the T stat is greater than the one-tailed T crit value, so reject the null, the means are not equal.  
alpha = 0.05

**Exhibit 3I.6 Continued**

t-Test: Paired  
Two Sample for  
Means

**event 115**

	<i>MEAS. FLOW</i>	<i>PRED. FLOW</i>
Mean	2.593031981	2.8721
Variance	4.874686327	7.561544291
Observations	53	53
Pearson Correlation	0.896921472	
Hypothesized Mean Difference	0	
df	52	
t Stat	1.634310609	
P(T<=t) one-tail	0.054117063	
t Critical one-tail	1.674688974	
P(T<=t) two-tail	0.108234126	
t Critical two-tail	2.006645445	

Conclusion: The  
absolute value of  
T stat is less  
than the one-  
tailed T crit  
value, so accept  
the null, the  
means are  
equal.  
alpha = 0.05

**Exhibit 3I.6 Continued**

t-Test: Paired  
Two Sample for  
Means

**event 80**

	<i>MEAS. FLOW</i>	<i>PRED. FLOW</i>
Mean	11.04184841	6.883851899
Variance	148.1765411	50.94564965
Observations	79	79
Pearson Correlation	0.583860087	
Hypothesized Mean Difference	0	
df	78	
t Stat	3.739622713	
P(T<=t) one-tail	0.000174961	
t Critical one-tail	1.664625415	
P(T<=t) two-tail	0.000349923	
t Critical two-tail	1.990847522	

Conclusion: The absolute value of T stat is greater than the one-tailed T crit value, so reject the null, the means are different.  
alpha = 0.05

**Exhibit 3I.6 Continued**

t-Test: Paired  
Two Sample for  
Means

**event 20**

	<i>MEAS. FLOW</i>	<i>PRED. FLOW</i>
Mean	12.73965821	7.974743243
Variance	101.8728855	58.90033954
Observations	37	37
Pearson Correlation	0.731385051	
Hypothesized Mean Difference	0	
df	36	
t Stat	4.207001495	
P(T<=t) one-tail	8.20307E-05	
t Critical one-tail	1.688297289	
P(T<=t) two-tail	0.000164061	
t Critical two-tail	2.02809133	

Conclusion: The  
absolute value of  
the T stat is  
greater than the  
one-tailed T crit,  
so reject the null,  
the means are  
not equal.  
alpha =0.05

**Exhibit 31.7:** K3 Catchment Selected Storm Hydrographs (2002)

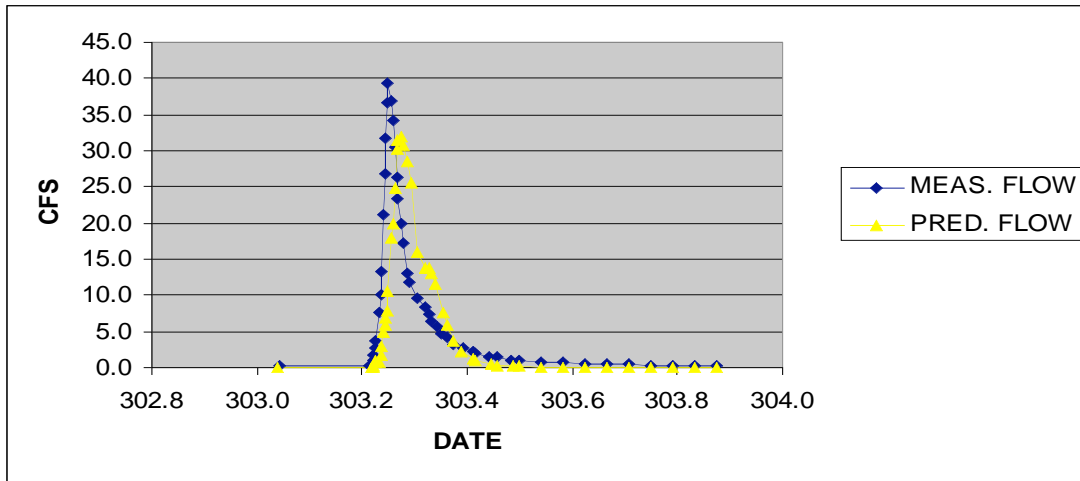


**Figure 31.7.1:** *Catchment K3 Event 303 Outflow Hydrograph (2002)*

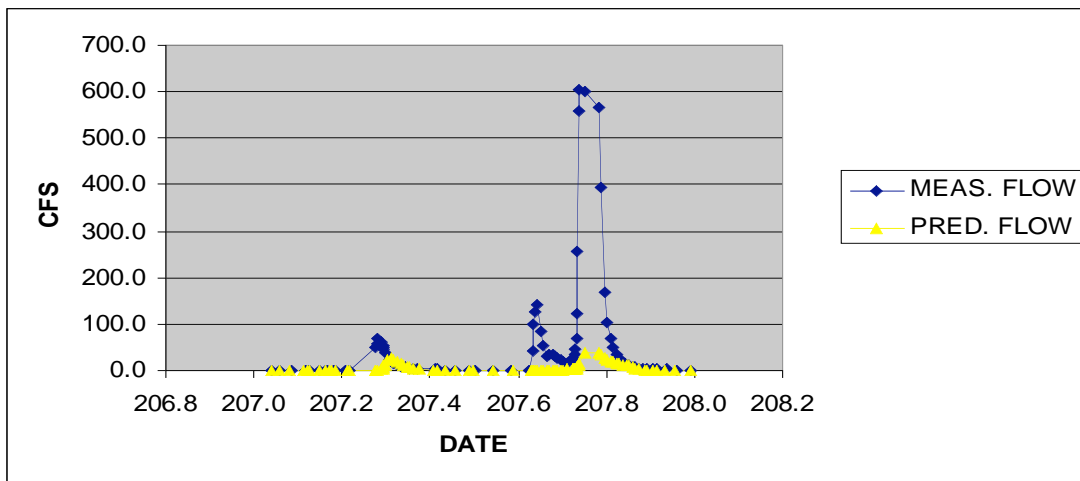


**Figure 31.7.2:** *Catchment K3 Event 207 Outflow Hydrograph (2002)*

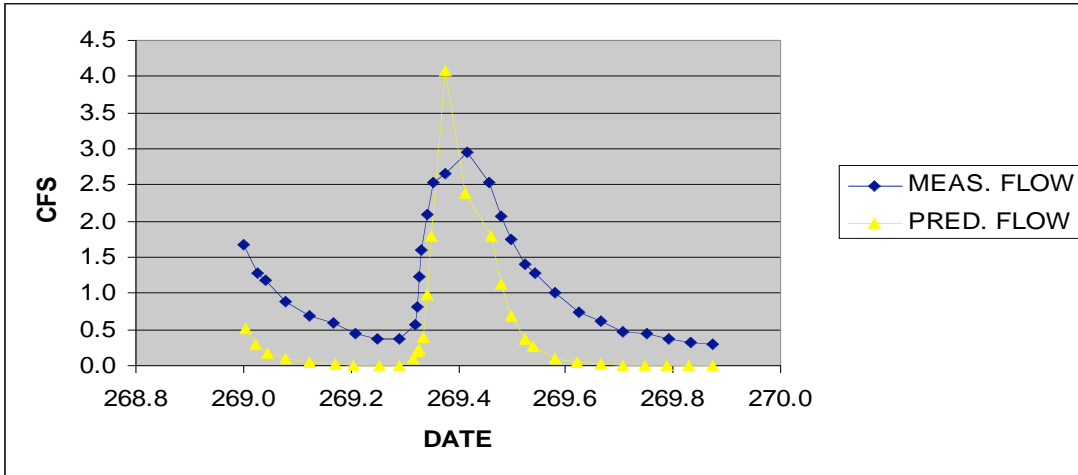


Figure 31.7.3: Catchment K3 Event 269 Outflow Hydrograph (2002)

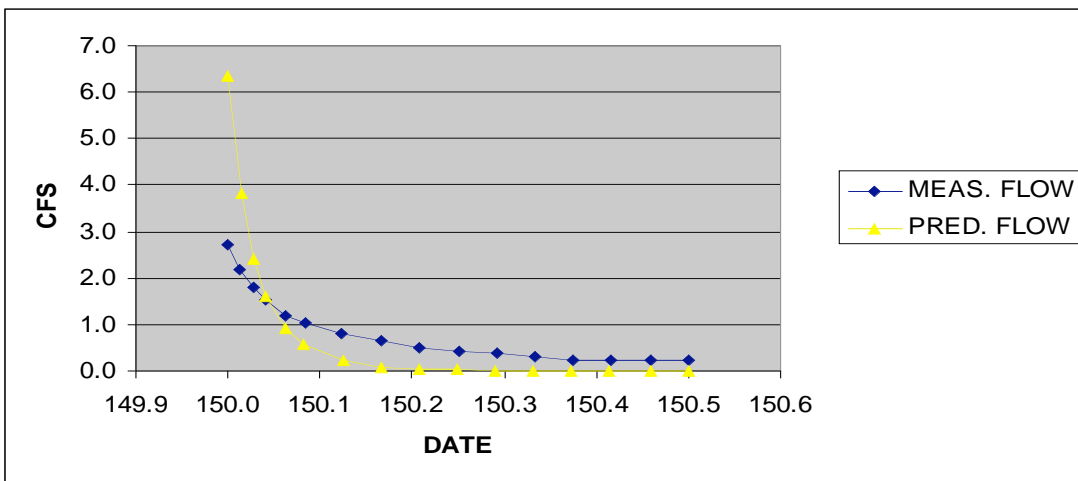


Figure 31.7.4: Catchment K3 Event 150 Outflow Hydrograph (2002)

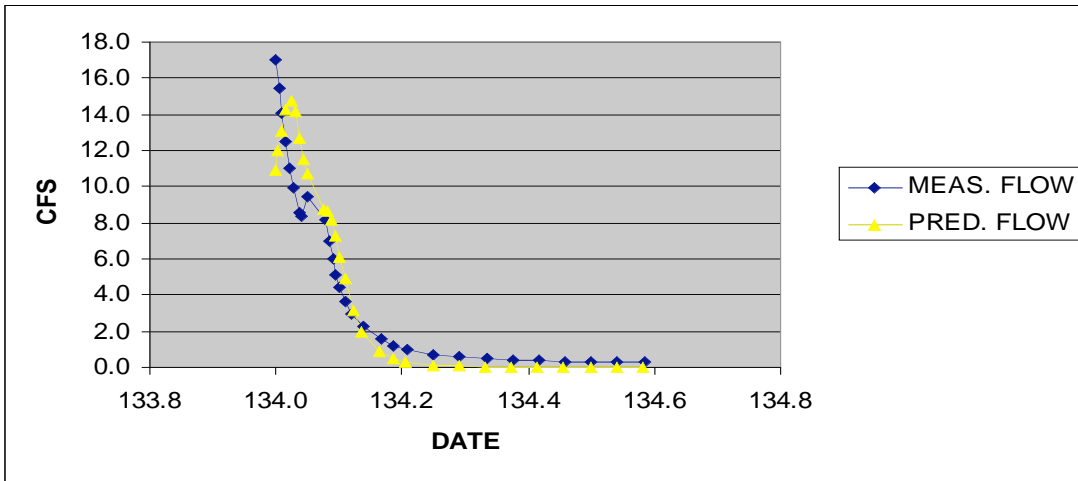


Figure 31.7.5: Catchment K3 Event 134 Outflow Hydrograph (2002)

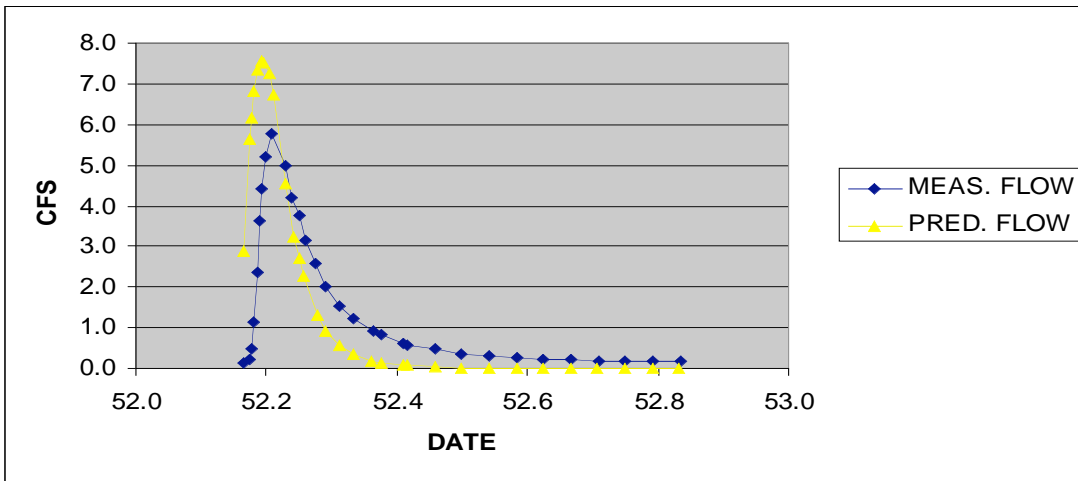


Figure 31.7.6: Catchment K3 Event 52 Outflow Hydrograph (2002)

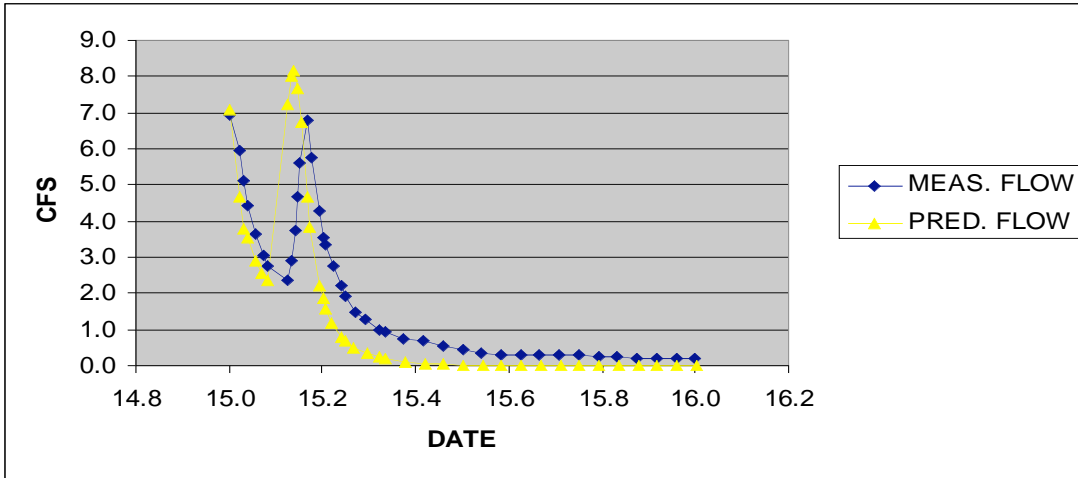


Figure 31.7.7: Catchment K3 Event 15 Outflow Hydrograph (2002)

**Exhibit 31.8: Catchment K3 T-test Statistics for Selected Storms (2002)**

t-Test: Paired Two  
Sample for Means

**event 330**

	<i>MEAS. FLOW</i>	<i>PRED. FLOW</i>
Mean	10.0988133	7.990595745
Variance	145.3956473	108.622709
Observations	47	47
Pearson Correlation	0.609672037	
Hypothesized Mean Difference	0	
df	46	
t Stat	1.439704054	
P(T<=t) one-tail	0.078361134	
t Critical one-tail	1.678658919	
P(T<=t) two-tail	0.156722268	
t Critical two-tail	2.012893674	

Conclusion: The  
absolute value of T Stat  
is less than the one-  
tailed T crit, so accept  
the null, the samples  
have equal means.  
alpha = 0.05

**Exhibit 3I.8 Continued**

t-Test: Paired Two  
Sample for Means  
**event 207**

	<i>MEAS. FLOW</i>	<i>PRED. FLOW</i>
Mean	60.5676301	6.203032941
Variance	17050.60912	88.27495647
Observations	85	85
Pearson Correlation	0.571794603	
Hypothesized Mean Difference	0	
df	84	
t Stat	3.995582585	
P(T<=t) one-tail	6.89532E-05	
t Critical one-tail	1.663197509	
P(T<=t) two-tail	0.000137906	
t Critical two-tail	1.988610165	

Conclusion: The  
absolute value of t Stat  
is greater than the one-  
tailed T crit, so reject  
the null, the sample  
means are not equal.  
alpha = 0.05

**Exhibit 3I.8 Continued**

t-Test: Paired Two  
Sample for Means  
**event 269**

	<i>MEAS. FLOW</i>	<i>PRED. FLOW</i>
Mean	1.175540927	0.526183333
Variance	0.622957813	0.831386495
Observations	30	30
Pearson Correlation	0.84939101	
Hypothesized Mean Difference	0	
df	29	
<b>t Stat</b>	<b>7.387508373</b>	
P(T<=t) one-tail	1.93189E-08	
<b>t Critical one-tail</b>	<b>1.699127097</b>	
P(T<=t) two-tail	3.86378E-08	
t Critical two-tail	2.045230758	

Conclusion: The  
absolute value of T stat  
is greater than the one-  
tailed T crit, so reject  
the null, the sample  
means are not equal.  
alpha = 0.05

**Exhibit 3I.8 Continued**

t-Test: Paired Two  
Sample for Means  
**event 150**

	<i>MEAS. FLOW</i>	<i>PRED. FLOW</i>
Mean	0.90271659	1.0069625
Variance	0.616185207	3.23745386
Observations	16	16
Pearson Correlation	0.94586455	
Hypothesized Mean Difference	0	
df	15	
t Stat	-0.38357818	
P(T<=t) one-tail	0.353336573	
t Critical one-tail	1.753051038	
P(T<=t) two-tail	0.706673145	
t Critical two-tail	2.131450856	

Conclusion: The  
absolute value of T stat  
is less than the one-  
tailed T crit, so accept  
the null, the sample  
means are equal.  
alpha = 0.05

**Exhibit 3I.8 Continued**

t-Test: Paired Two  
Sample for Means  
**event 134**

	<i>MEAS. FLOW</i>	<i>PRED. FLOW</i>
Mean	5.281775468	5.692603448
Variance	26.92455315	31.2319386
Observations	29	29
Pearson Correlation	0.923301616	
Hypothesized Mean Difference	0	
df	28	
t Stat	-1.03063098	
P(T<=t) one-tail	0.15576738	
t Critical one-tail	1.701130259	
P(T<=t) two-tail	0.31153476	
t Critical two-tail	2.048409442	

Conclusion: The  
absolute value of T stat  
is less than the one-  
tailed T crit number, so  
accept the null, the  
samples have like  
means.  
alpha = 0.05

**Exhibit 3I.8 Continued**

t-Test: Paired Two  
Sample for Means

**event 52**

	<i>MEAS. FLOW</i>	<i>PRED. FLOW</i>
Mean	1.690127854	2.401525806
Variance	3.192699374	8.615521521
Observations	31	31
Pearson Correlation	0.647531621	
Hypothesized Mean Difference	0	
df	30	
t Stat	1.768536387	
P(T<=t) one-tail	0.043569881	
t Critical one-tail	1.697260359	
P(T<=t) two-tail	0.087139762	
t Critical two-tail	2.042270353	

Conclusion: The  
absolute value of T stat  
is greater than the one-  
tailed T crit value, to  
reject the null, the  
sample means are  
different.

alpha = 0.05

**Exhibit 3I.8 Continued**

t-Test: Paired Two  
Sample for Means  
**event 15**

	<i>MEAS. FLOW</i>	<i>PRED. FLOW</i>
Mean	2.298351151	2.0767075
Variance	4.480303224	7.290546503
Observations	40	40
Pearson Correlation	0.778429842	
Hypothesized Mean Difference	0	
df	39	
<b>t Stat</b>	<b>0.827017343</b>	
P(T<=t) one-tail	0.206629422	
<b>t Critical one-tail</b>	<b>1.684875315</b>	
P(T<=t) two-tail	0.413258845	
t Critical two-tail	2.022688932	

Conclusion: The  
absolute value of T stat  
is less than the one-  
tailed T Crit value, so  
accept the null, the  
sample means are  
equal.  
alpha = 0.05

**Exhibit 31.9:** Sample "03" Simulation Results for Catchment K2 (2001)

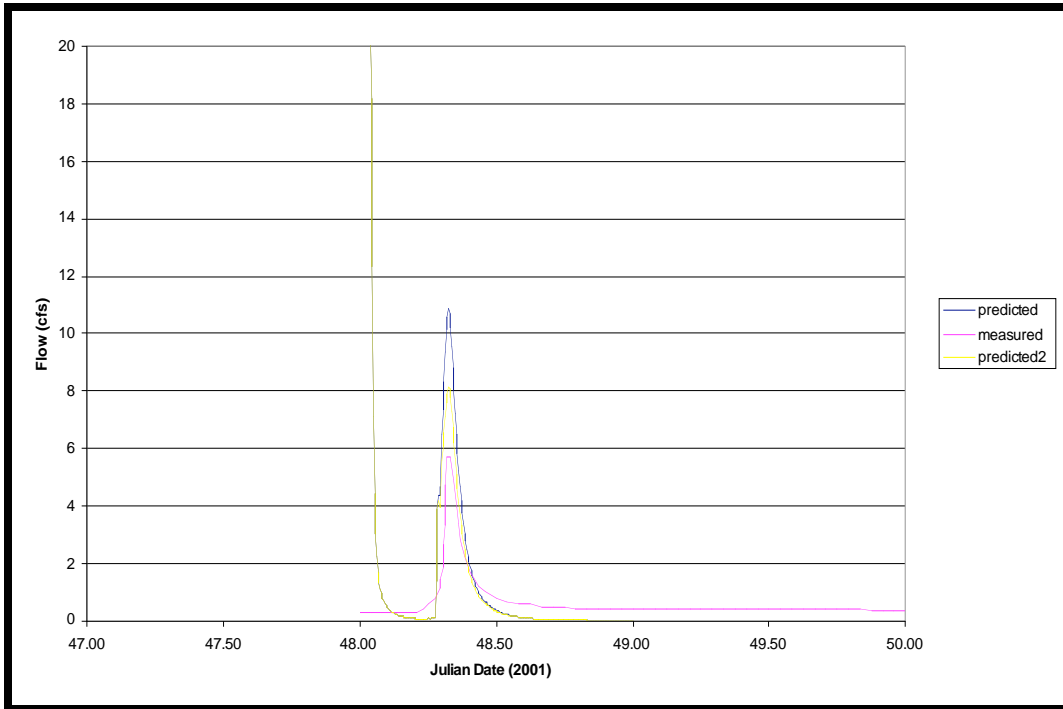


**Figure 31.9.1:** Event 48, "03" Simulation, Outflow Hydrograph for Catchment K2 (2001)

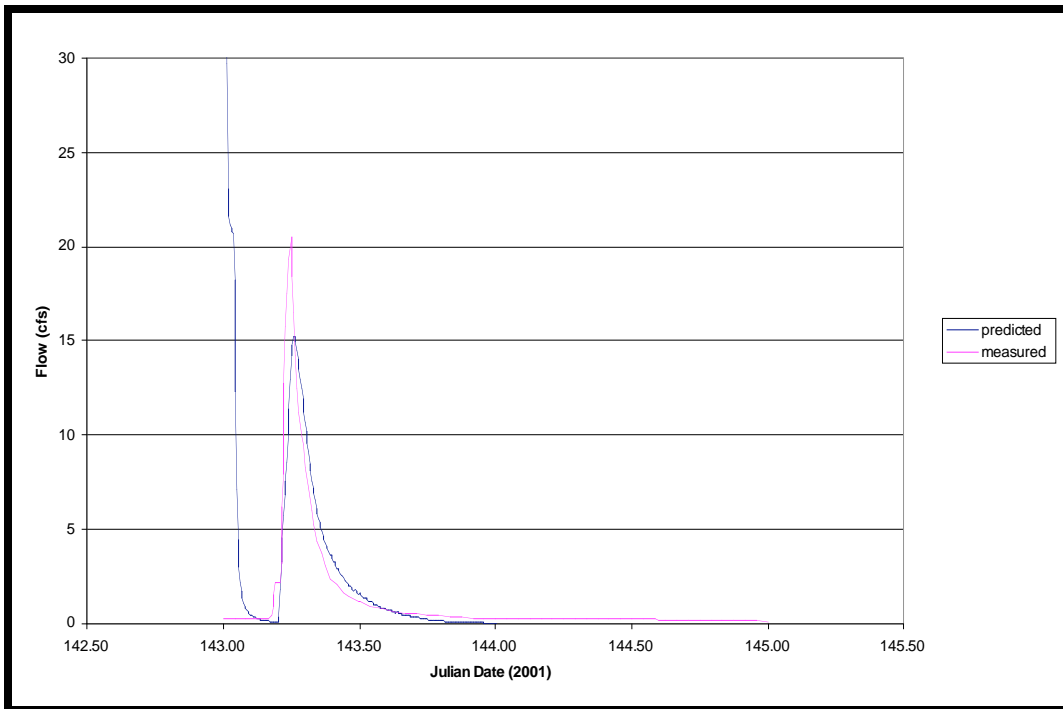


**Figure 31.9.2:** Event 143, "03" Simulation, Outflow Hydrograph for Catchment K2 (2001)

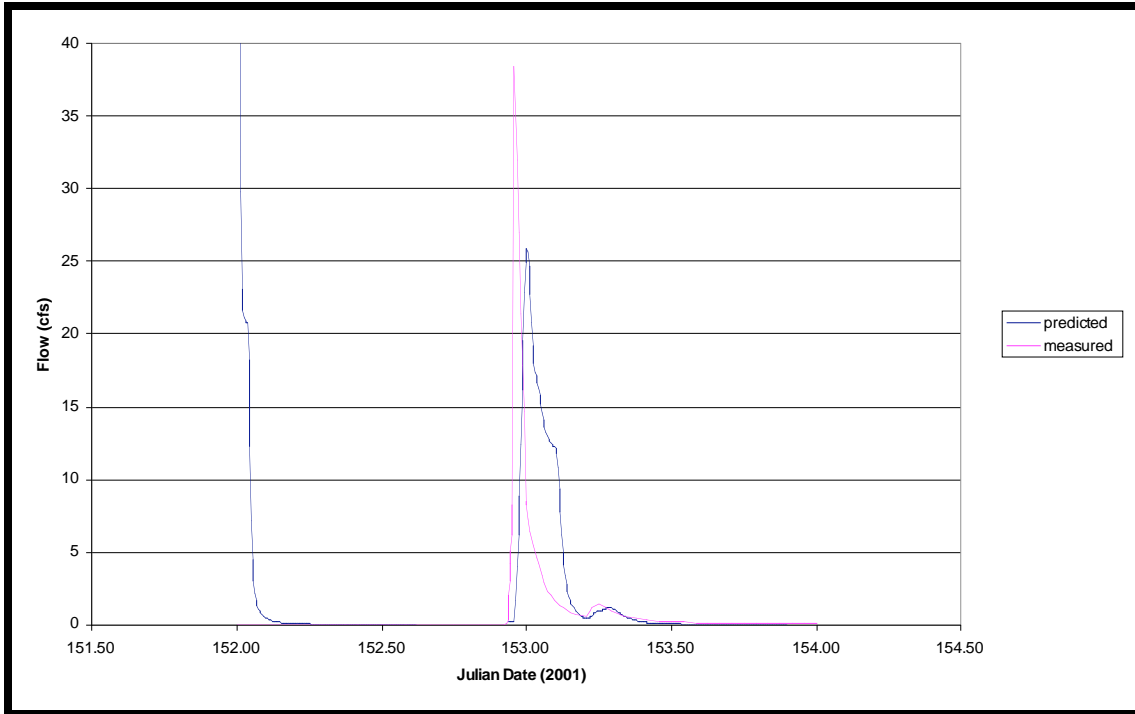


**Figure 31.9.3: Event 153, 03” Simulation, Outflow Hydrograph for Catchment K2 (2001)**

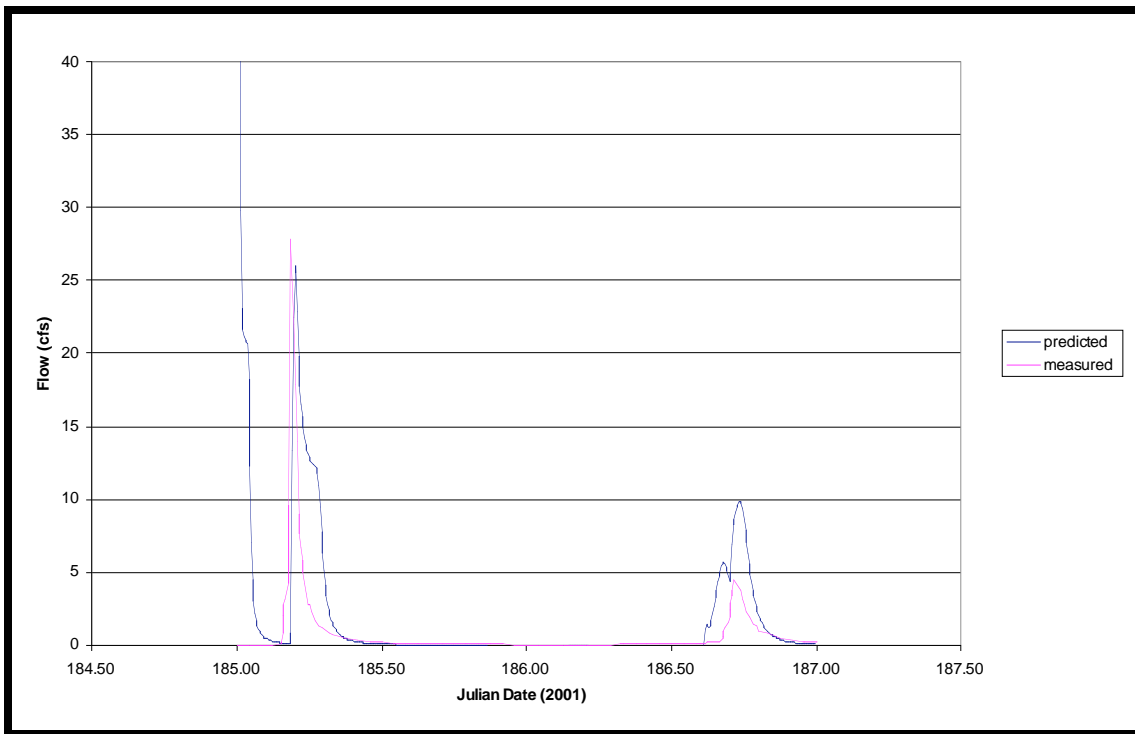


**Figure 31.9.4: Event 185, 03” Simulation, Outflow Hydrograph for Catchment K2 (2001)**

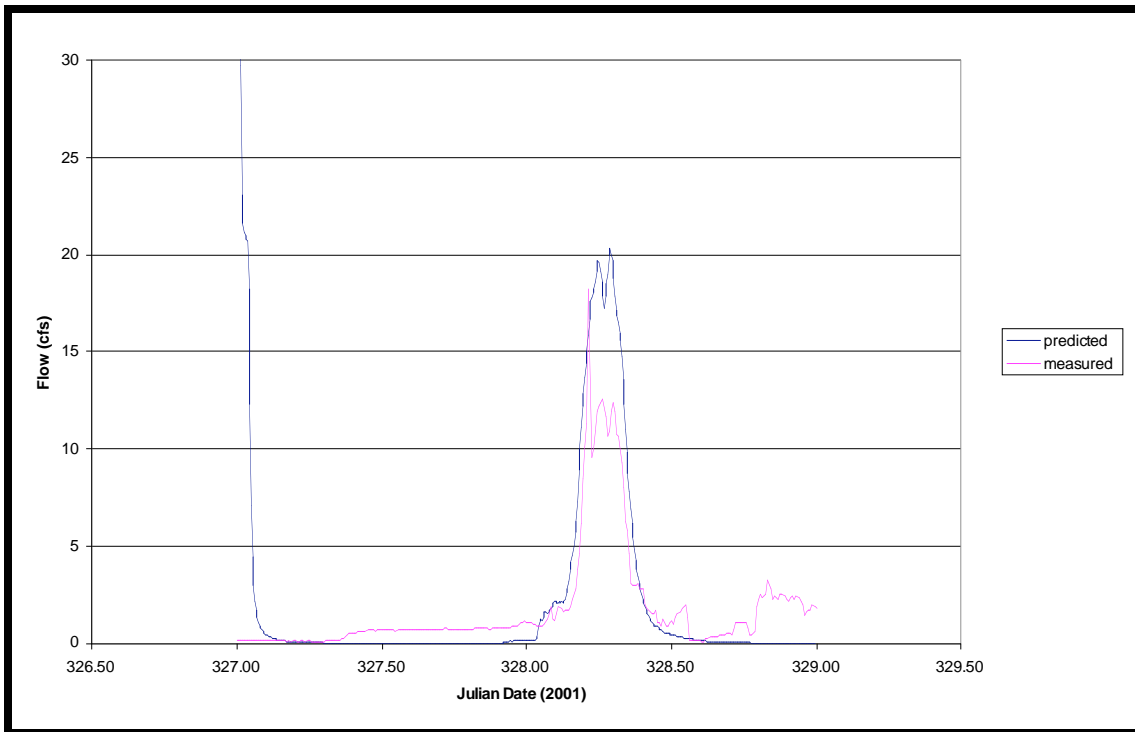


Figure 31.9.5: *Event 327, "03" Simulation, Outflow Hydrograph for Catchment K2 (2001)*

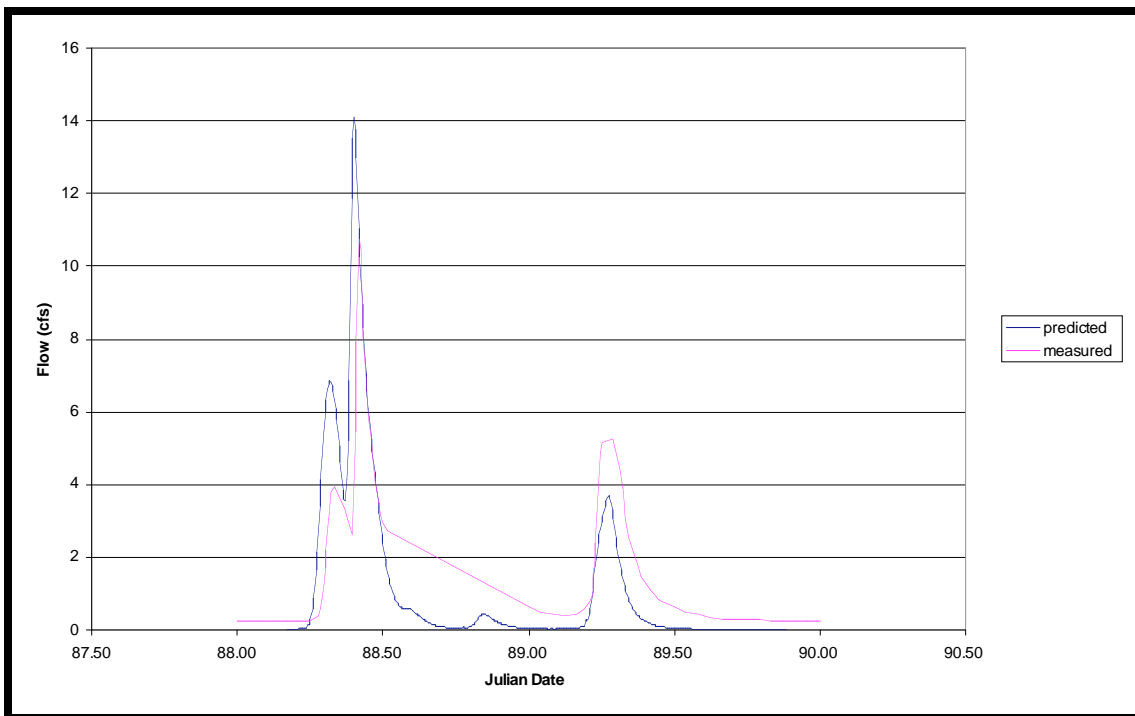


Figure 31.9.6: *Event 88, "03" Simulation, Outflow Hydrograph for Catchment K3 (2001)*

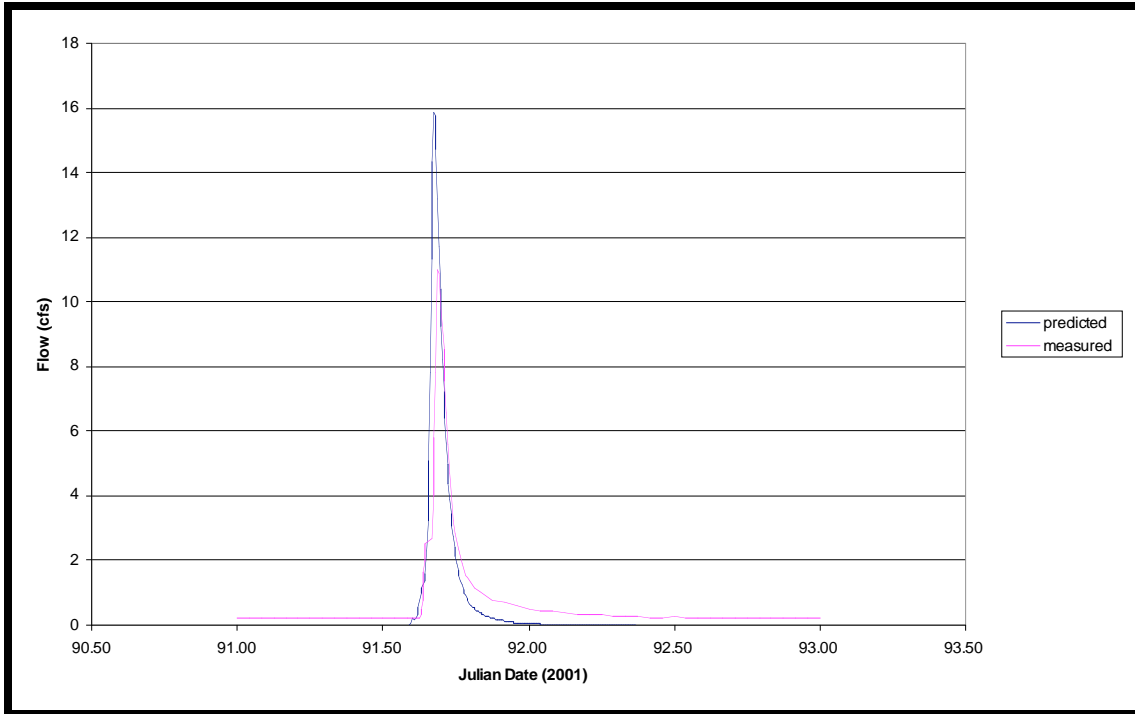


Figure 31.9.7: Event 88, "03" Simulation, Outflow Hydrograph for Catchment K3 (2001)

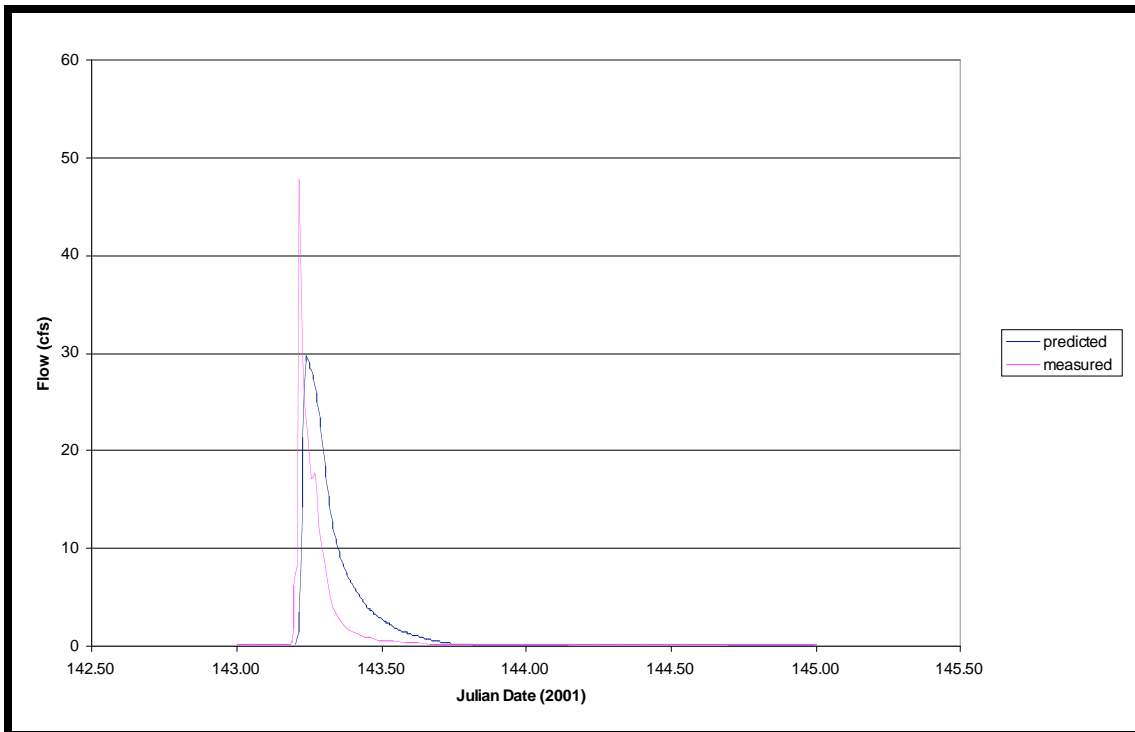
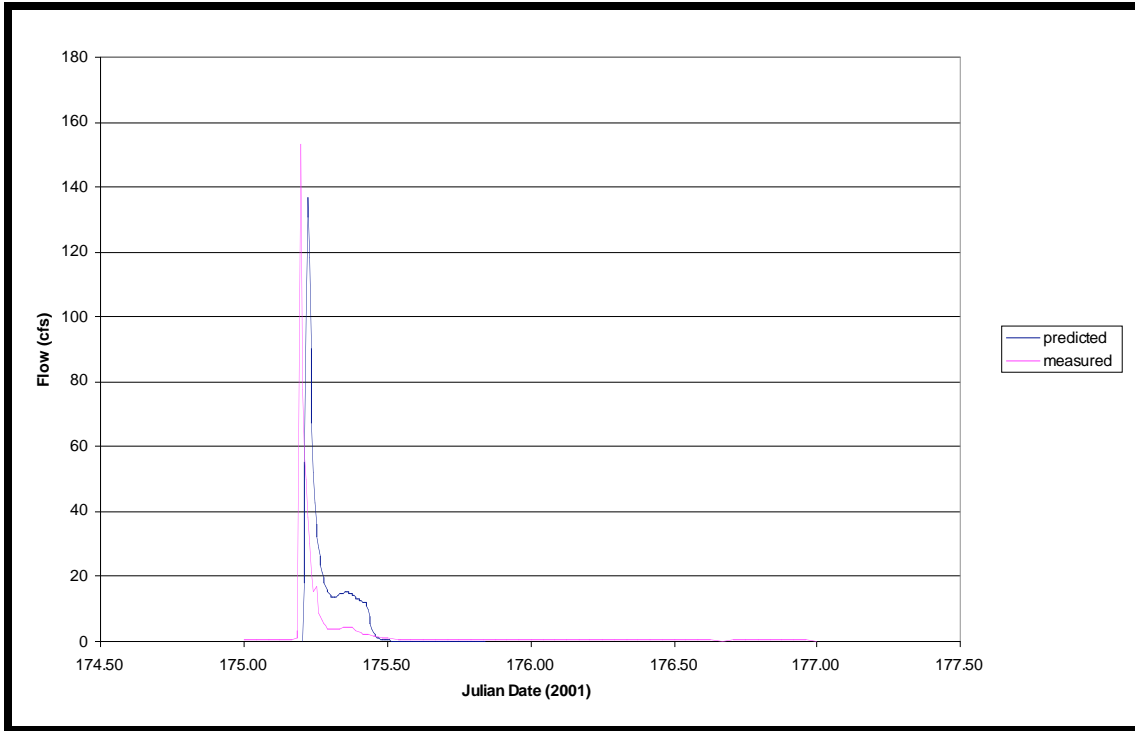
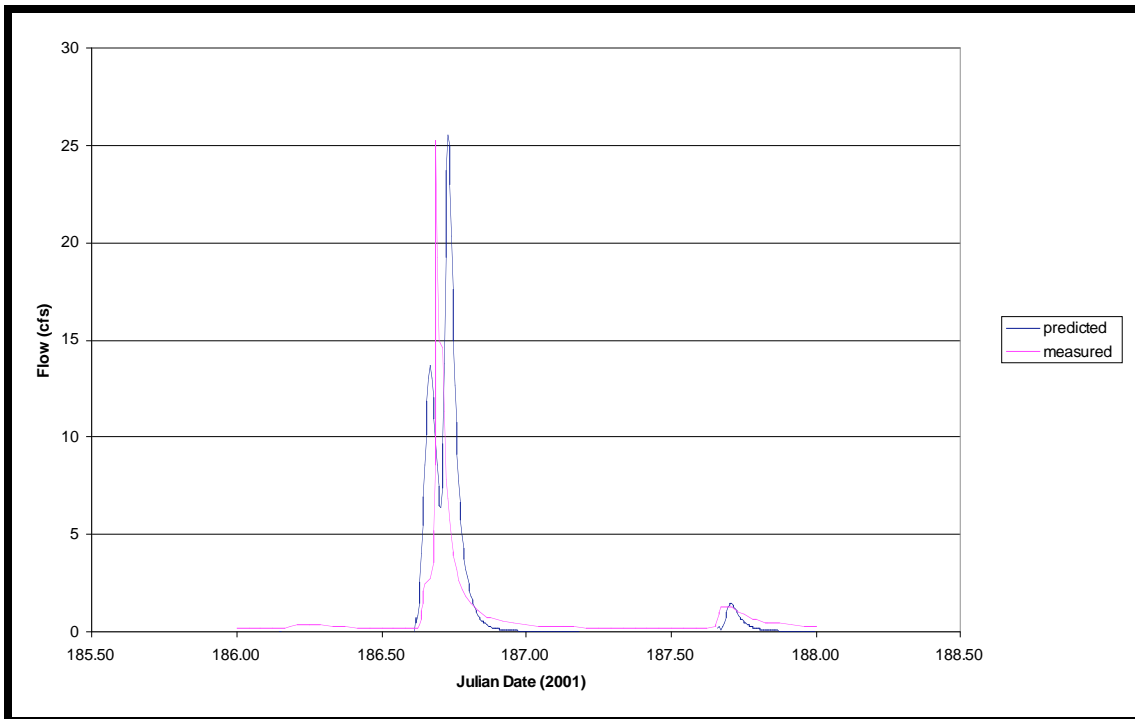


Figure 31.9.8: Event 143, "03" Simulation, Outflow Hydrograph for Catchment K3 (2001)



**Figure 31.9.9: Event 175, "03" Simulation, Outflow Hydrograph for Catchment K3 (2001)**



**Figure 31.9.10: Event 186, "03" Simulation, Outflow Hydrograph for Catchment K3 (2001)**

Appendix 3J: Catchment K2 Event-based Sensitivity Analyses (2002)

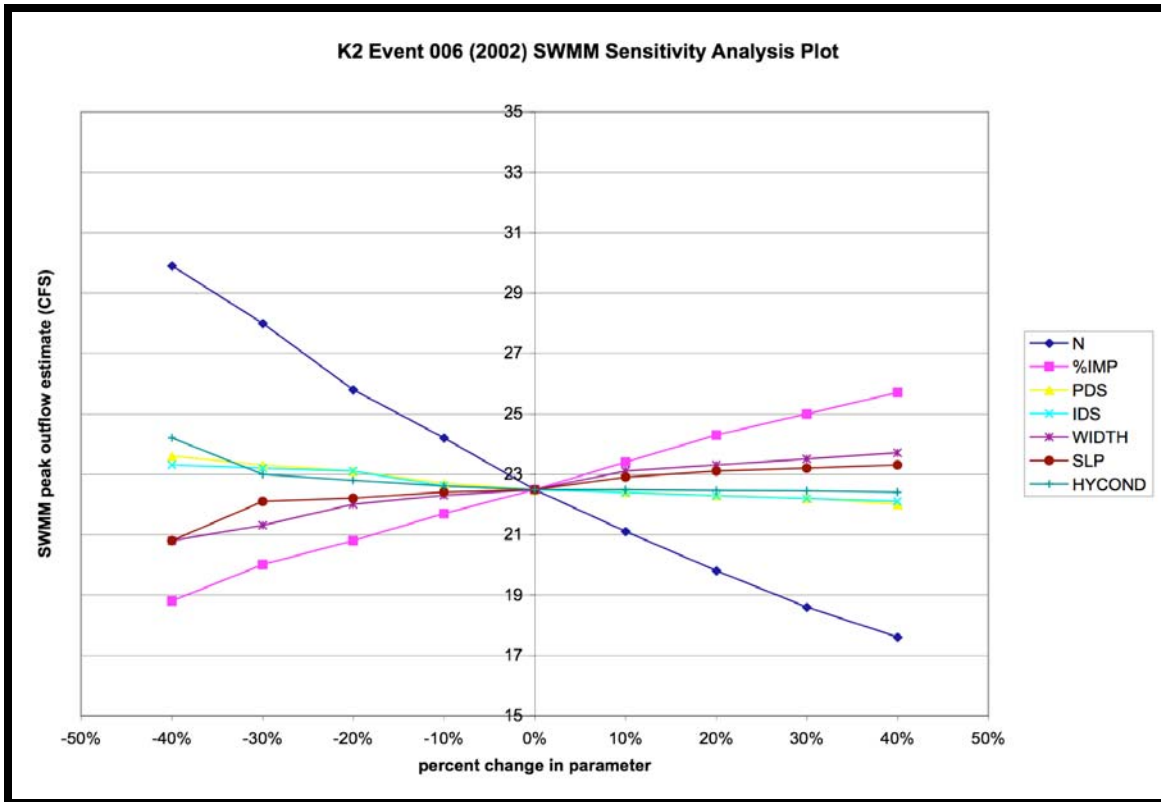


Figure 3J.1.1: Catchment K2 Sensitivity Analysis, Storm 06 (2002)

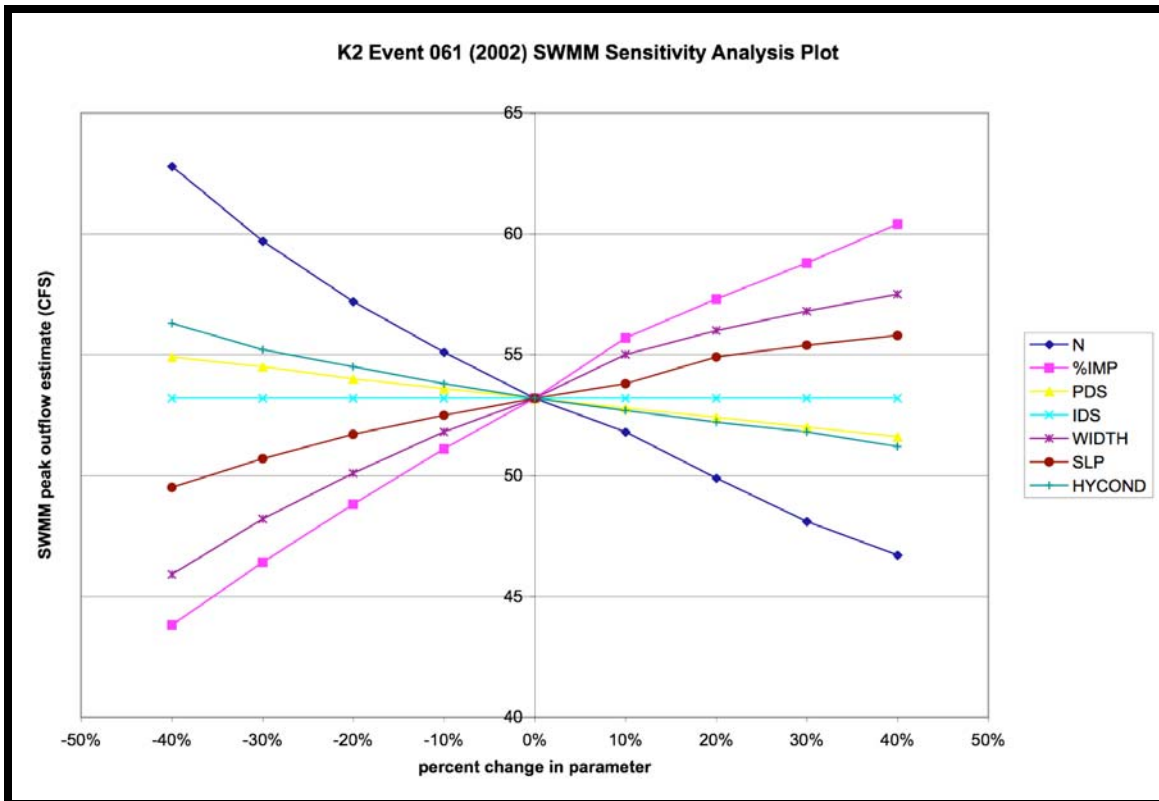


Figure 3J.1.2: Catchment K2 Sensitivity Analysis, Storm 61 (2002)

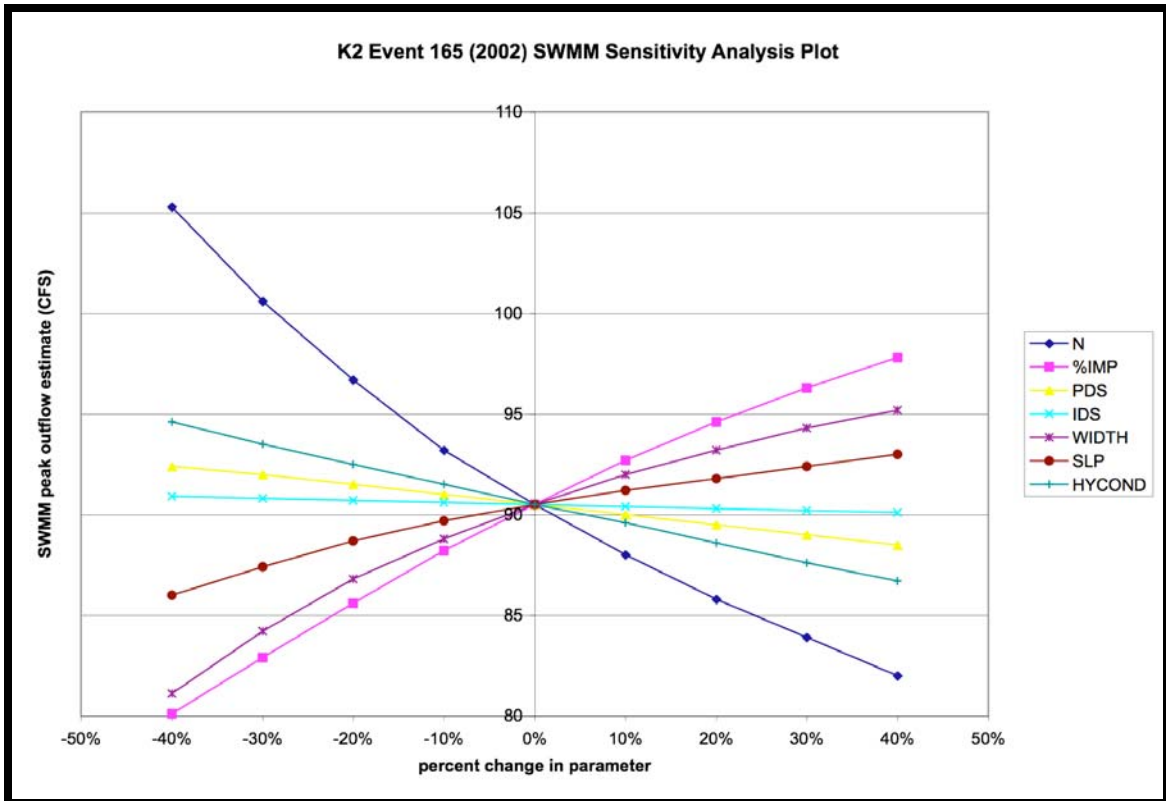


Figure 3J.1.3: Catchment K2 Sensitivity Analysis, Storm 165 (2002)

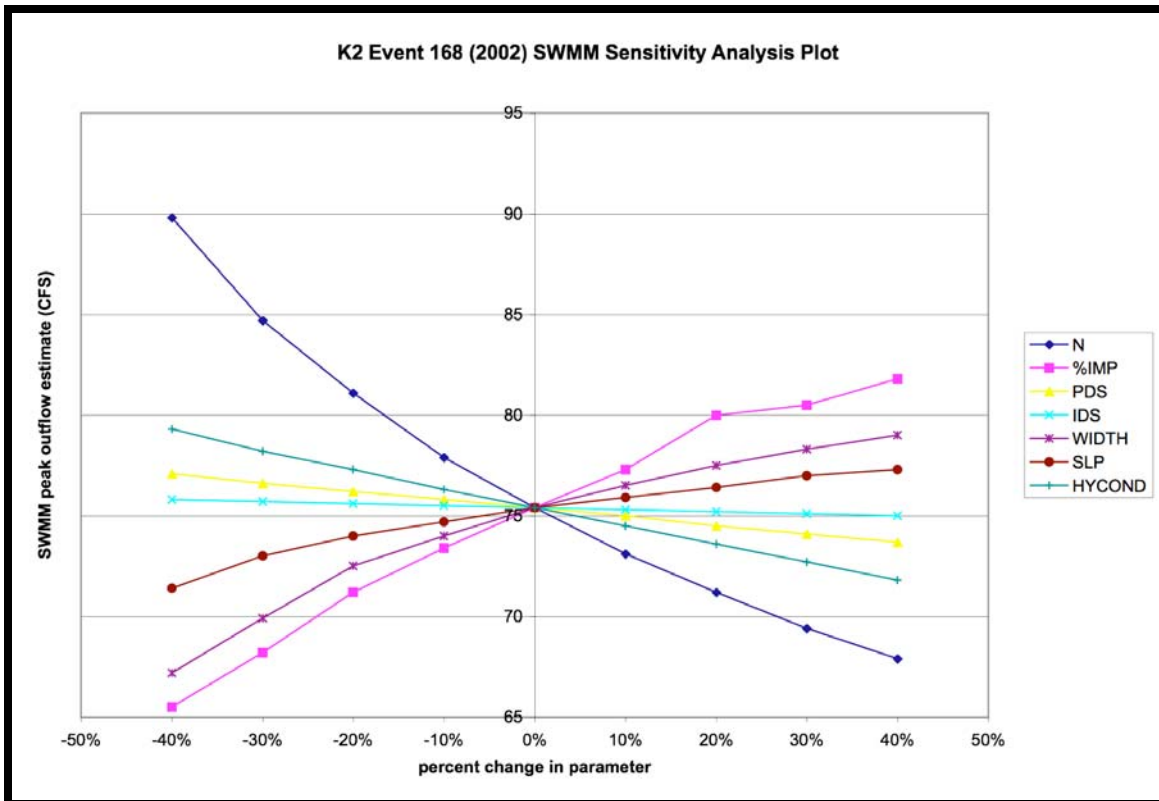


Figure 3J.1.4: Catchment K2 Sensitivity Analysis, Storm 168 (2002)

**Table 3J.1.5: Catchment K2 Parameter Sensitivity Rankings**

<b>2002 SWMM Parameter Rankings for Catchment K2</b>		
<b>event 06</b>	<b>Positive change</b>	<b>negative change</b>
<i>most sensitive</i>	N	N
	%imp	%imp
	Hycond	width
	Width	slp
	Slp	pds
	Pds	ids
<i>least sensitive</i>	Ids	hycond

<b>event 61</b>	<b>Positive change</b>	<b>negative change</b>
<i>most sensitive</i>	N	%imp
	%imp	N
	Width	width
	Slp	slp
	Hycond	hycond
	Pds	pds
<i>least sensitive</i>	Ids	ids

<b>event 165</b>	<b>Positive change</b>	<b>negative change</b>
<i>most sensitive</i>	N	%imp
	%imp	N
	Width	width
	Slp	hycond
	Hycond	slp
	Pds	pds
<i>least sensitive</i>	Ids	ids

<b>event 168</b>	<b>Positive change</b>	<b>negative change</b>
<i>most sensitive</i>	N	N
	%imp	%imp
	Width	width
	Hycond	hycond
	Slp	slp
	Pds	pds
<i>least sensitive</i>	Ids	ids

Exhibit 3J.2: Catchment K3 Sensitivity Analyses (2002)

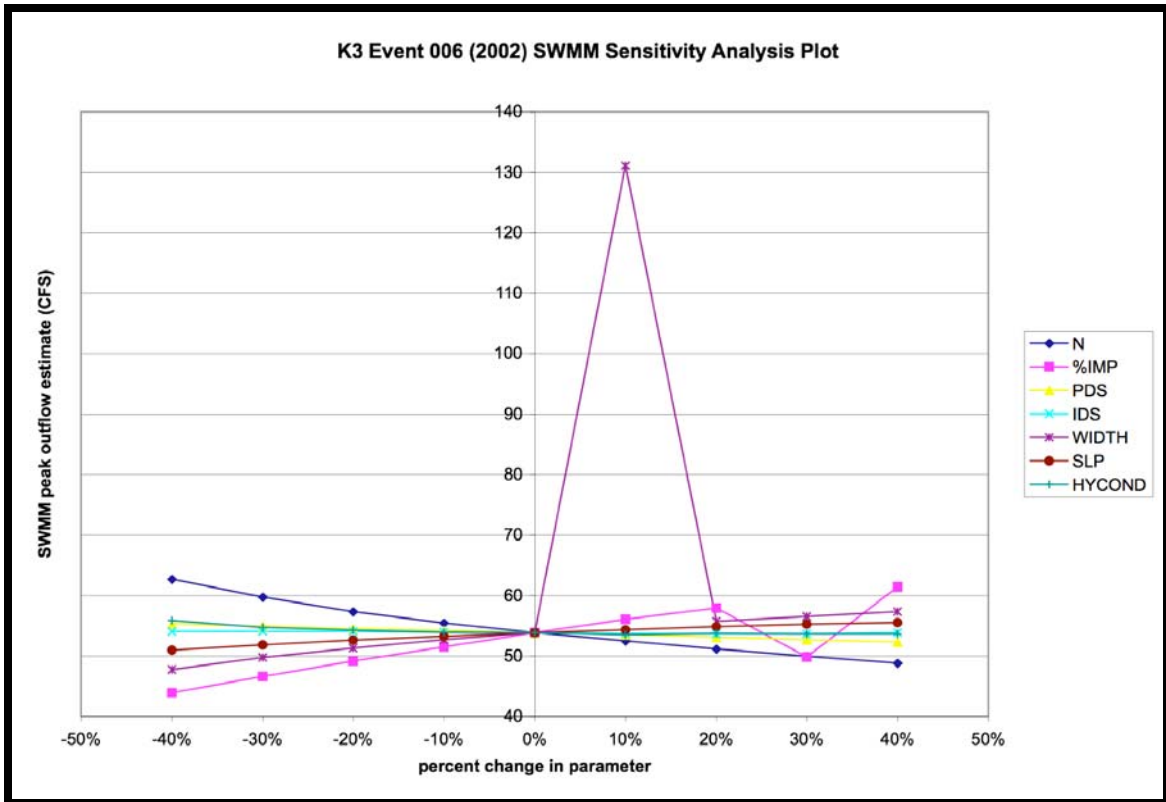


Figure 3J.2.1: Catchment K3 Sensitivity Analysis, Storm 06 (2002)

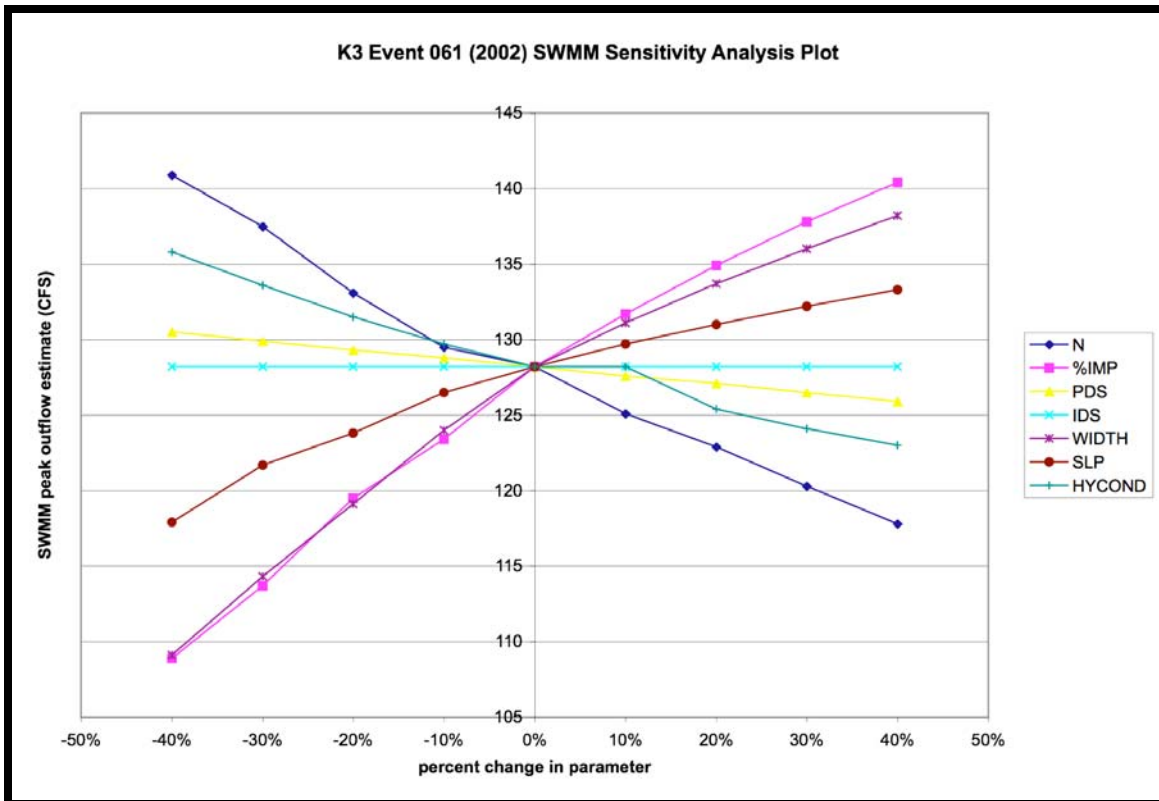


Figure 3J.2.2: Catchment K3 Sensitivity Analysis, Storm 61 (2002)

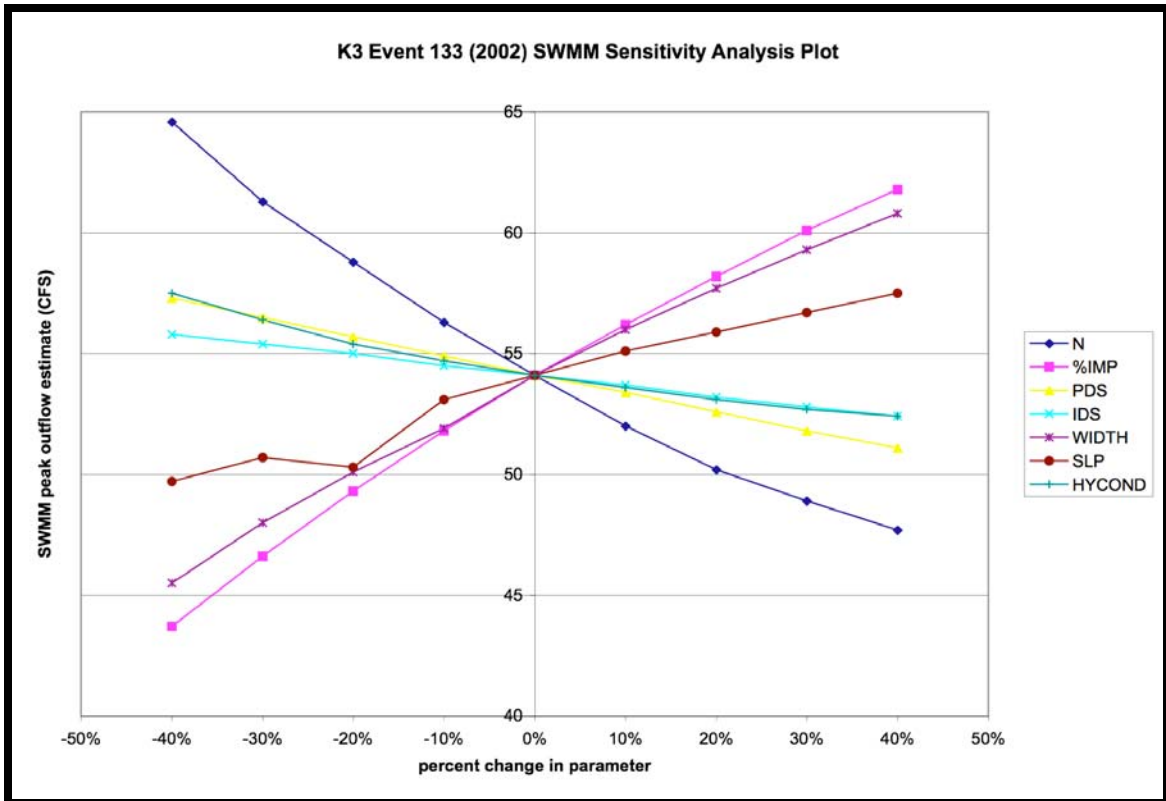


Figure 3J.2.3: Catchment K3 Sensitivity Analysis, Storm 133 (2002)

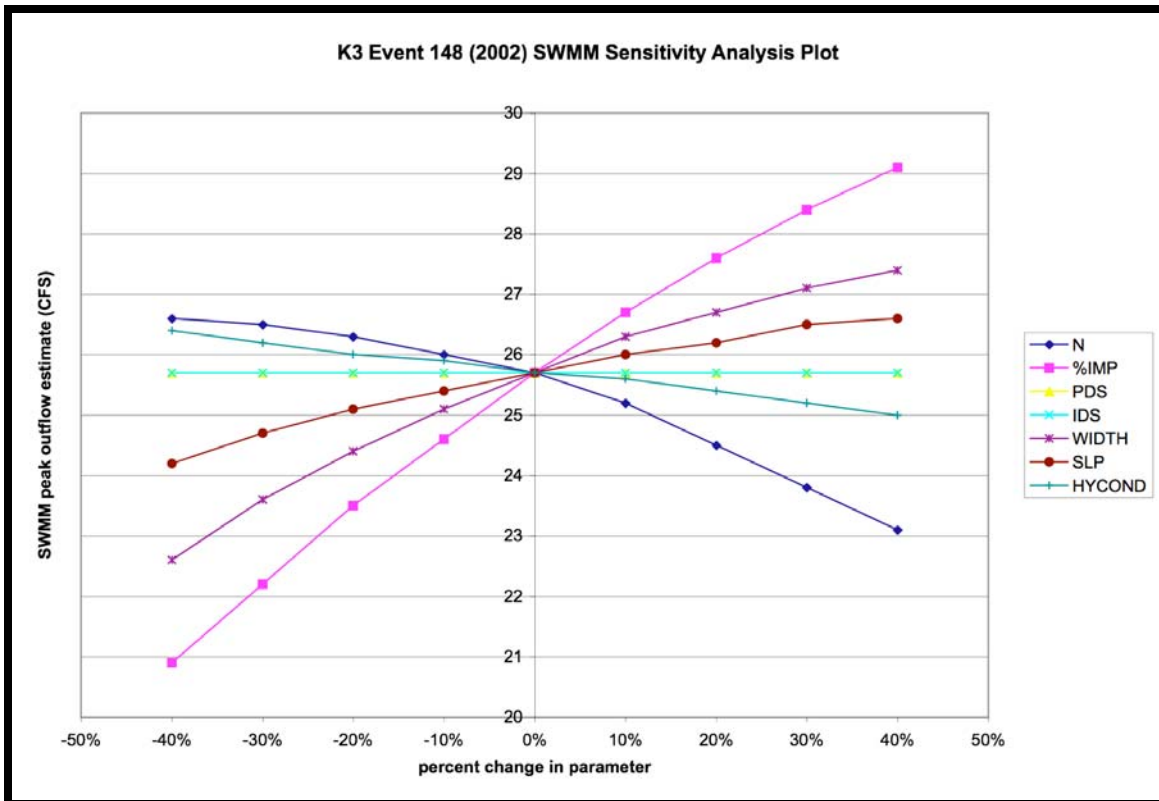


Figure 3J.2.4: Catchment K3 Sensitivity Analysis, Storm 148 (2002)

**Table 3J.2.5: Catchment K3 Parameter Sensitivity Rankings**

<b>2002 SWMM Parameter Rankings for Area K3</b>		
<b>event 06</b>	<b>positive change</b>	<b>negative change</b>
<i>Most sensitive</i>	%imp	%imp
	n	n
	width	width
	slope	slope
	hycond	pds
<i>least sensitive</i>	pds	hycond
	ids	ids

<b>event 61</b>	<b>positive change</b>	<b>negative change</b>
<i>most sensitive</i>	%imp	%imp
	width	n
	n	width
	slope	hycond
	hycond	slope
<i>least sensitive</i>	pds	pds
	ids	ids

<b>event 133</b>	<b>positive change</b>	<b>negative change</b>
<i>most sensitive</i>	n	%imp
	%imp	width
	width	n
	slope	slp
	hycond	pds
<i>least sensitive</i>	pds	hycond
	ids	ids

<b>event 148</b>	<b>positive change</b>	<b>negative change</b>
<i>most sensitive</i>	%imp	%imp
	width	n
	slope	width
	n	slope
	hycond	hycond
<i>least sensitive</i>	pds	pds
	ids	ids

## Chapter Four Appendix

**Appendix 4A: XPSWMM Sanitary Block Graphics**

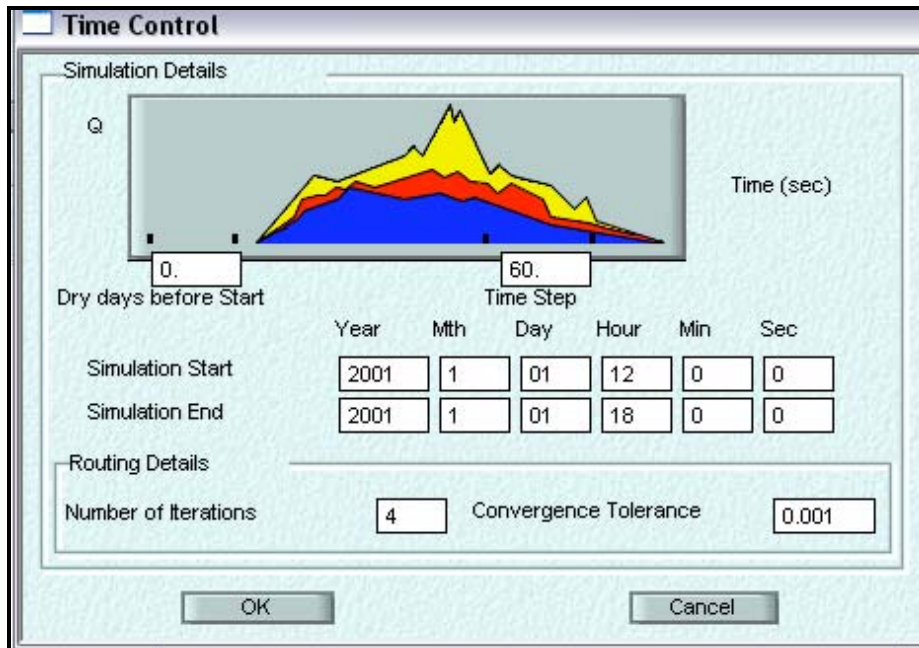


**Figure 4A.1: XPSWMM Sanitary Block Time Controls.** This screenshot is an example of the XPSWMM time control screen used to designate the simulation time functions in the Sanitary Block. This input screen is very similar to the Runoff Block screen, but includes user selections including iteration number and convergence tolerance.

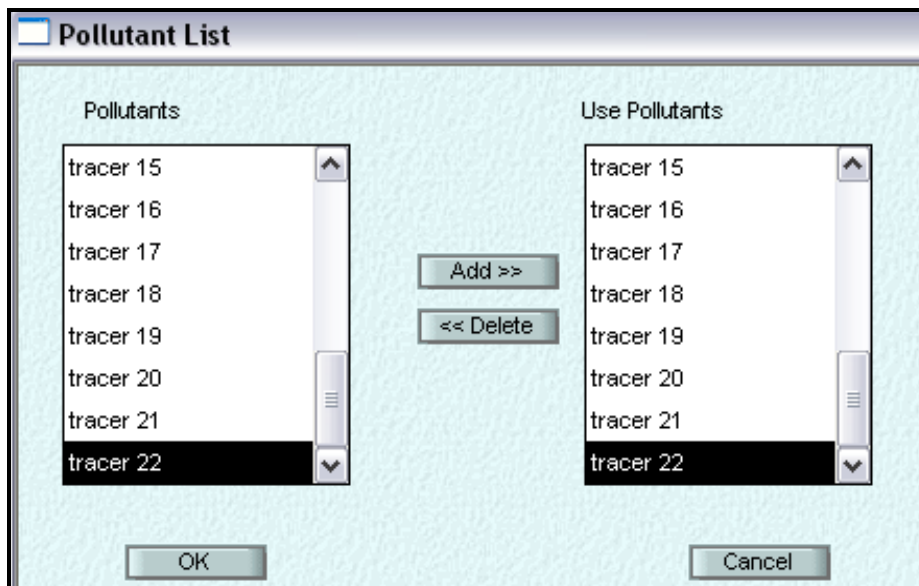


**Figure 4A.2: Sanitary Block Pollutant List.** This XPSWMM screenshot displays the imaginary tracers created to route pollutants during the Cherry Point study. The tracer numbers correspond to the individual subcatchments of either catchment K2 or K3 depending upon the interest area.

Pollutant	Initial Conc.	Conc.	Removal Fraction
tracer 1	IC01	C01	RF01
tracer 2	IC02	C02	RF02
tracer 3	IC03	C03	RF03
tracer 4	IC04	C04	RF04
tracer 5	IC05	C05	RF05
tracer 6	IC06	C06	RF06
tracer 7	IC07	C07	RF07
tracer 8	IC08	C08	RF08

OK Cancel

**Figure 4A.3: Pollutant Removal Equation Parameters.** This screen was used to assign pollutant properties in XPWMM. In the Sanitary Block, for every assigned pollutant a unique removal equation is used to decay the substance over time. The initial concentration, concentration and removal fraction parameters are user-defined and can be individually unique.

(T) Pollutant : tracer 20

Unit  
 mg/l     'other'/l     Other

Unit Label: none

Sanitary  
 Decay: 0.0  
 Scour/Deposition

Dry Weather Flow Generation  
 Use volume rate  
 Use per-capita rate

OK Cancel

**Figure 4A.4: Tracer Decay Specification Screen in XPSWMM.** This screen displays the additional options available for each pollutant. In this example, tracer 20 has not been assigned concentration units nor was decay included in the Cherry Point simulations.

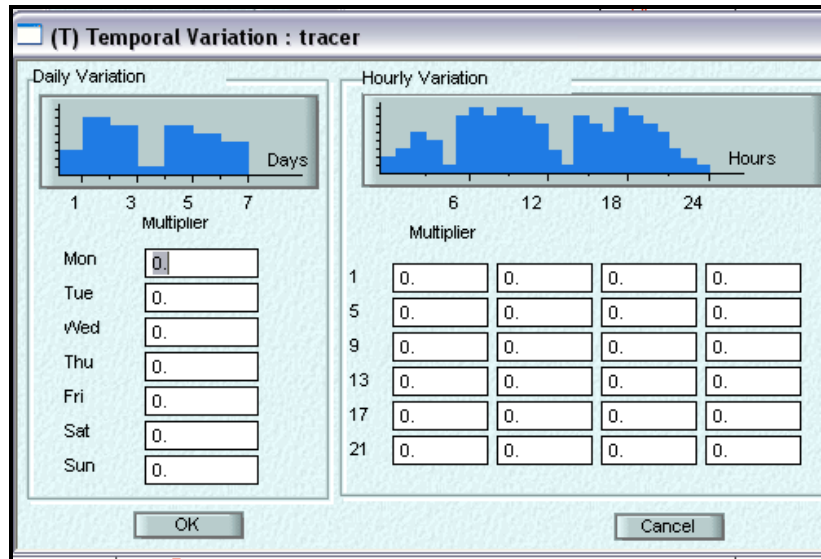


**Figure 4A.5: Pollutant Temporal Variation Screen in XPSWMM.** This input screen can be used to assign temporal variations in pollutant concentration for a period of one week. The multipliers are used to positively and negatively adjust the concentrations depending upon the modeled conditions in hourly intervals.

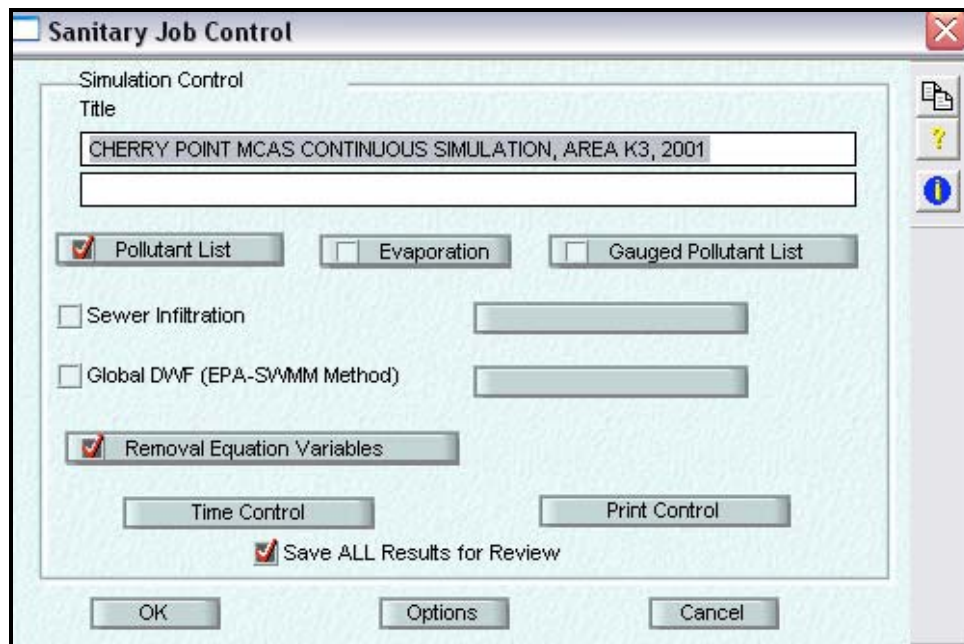


**Figure 4A.6: General Sanitary Job Control Screen.** This XPSWMM input screen is used to link the various options needed to fully simulate pollutant movement in the Sanitary Block. Only the created tracers and their associated removal rates were selected for the Cherry Point study. All simulation results were saved and exported into a spreadsheet for later analysis.

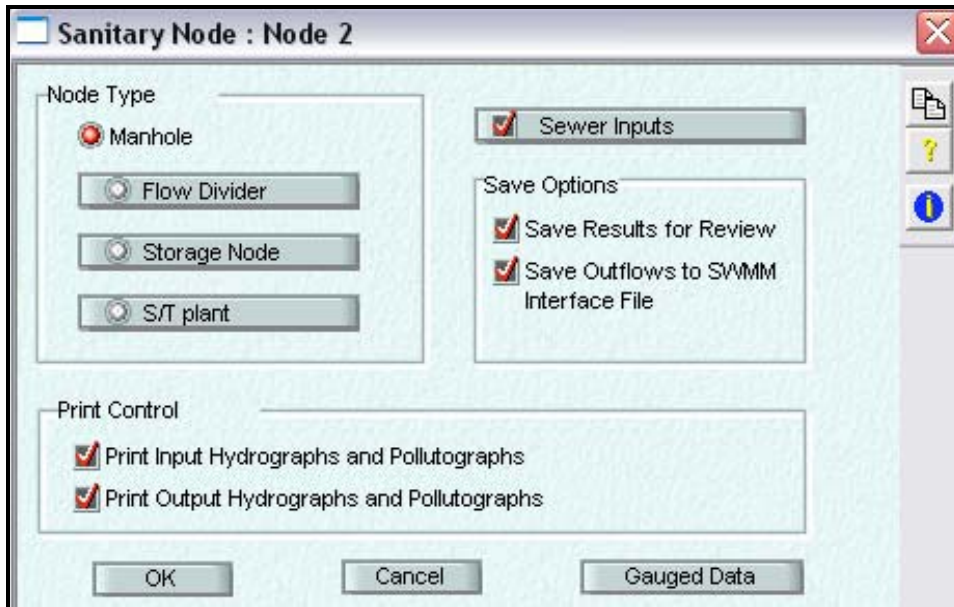


**Figure 4A.7: General Sewer Options Screen.** Each XPSWMM node has user-selected options in the Sanitary Block that control the routing of pollutants via pipes and surface channels. For Cherry Point, each modeling point (node) was considered a manhole without storage and the imaginary tracers were routed through the system. All predicted hydrographs and pollutographs were either examined within XPSWMM or exported.

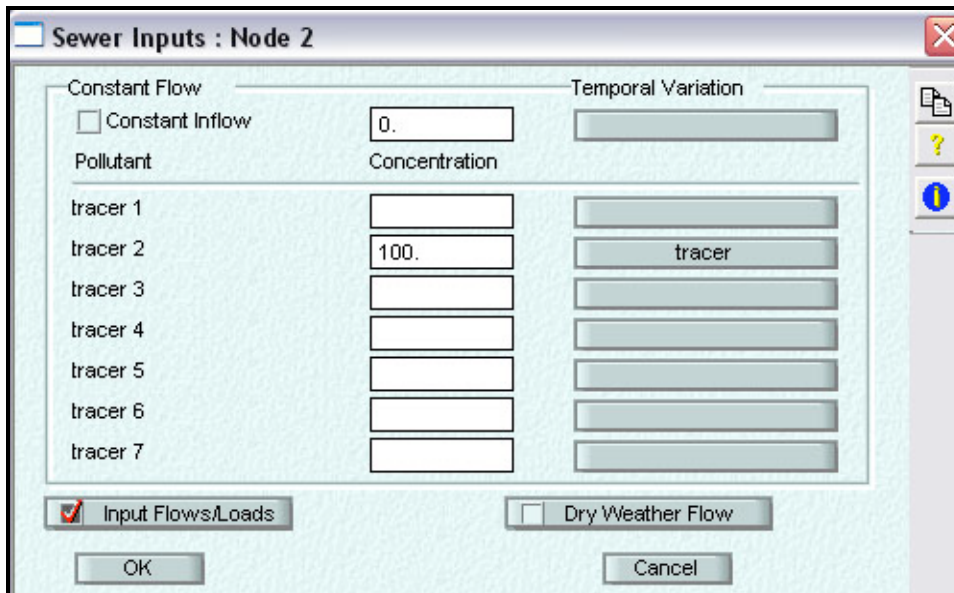


**Figure 4A.8: Tracer Input Main Menu, under the General Sewer Input Screen.** This screen is the submenu opened when the user selects the “Sewer Inputs” toggle button displayed in Figure 4A.7. For the Cherry Point study, information concerning the individual tracer for each subcatchment was entered into XPSWMM. Meaning, for node 2, only concentration information describing tracer 2 was considered. The concentration column refers to the initial pollutant concentration using the user-defined units.

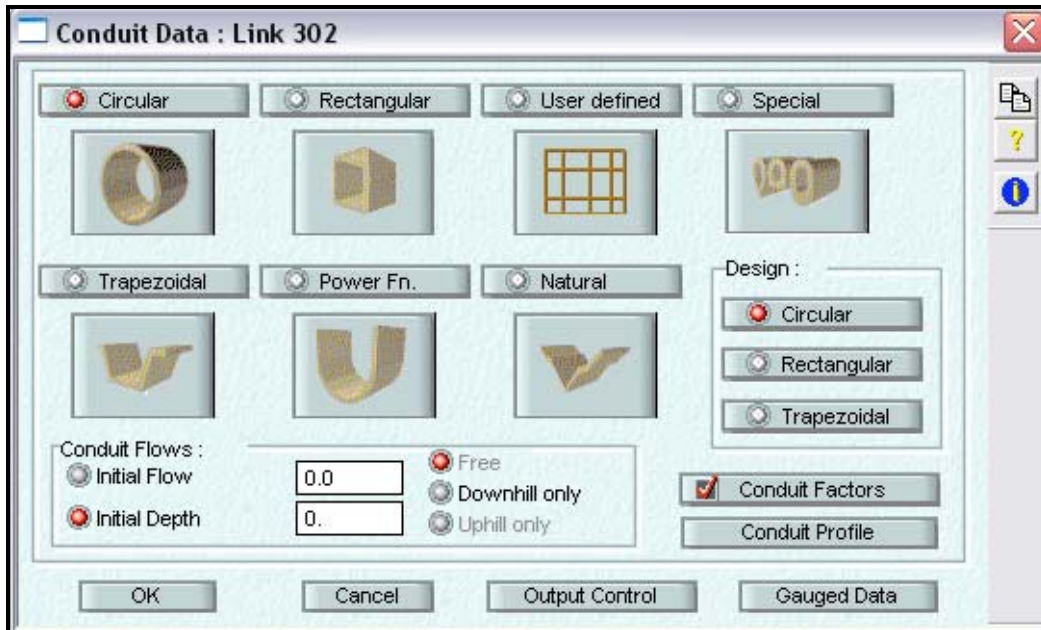


**Figure 4A.9: Conduit Information Screen in the Sanitary Block.** The input screen in XPSWMM was used to associate conduit shape and flow for the routing elements.

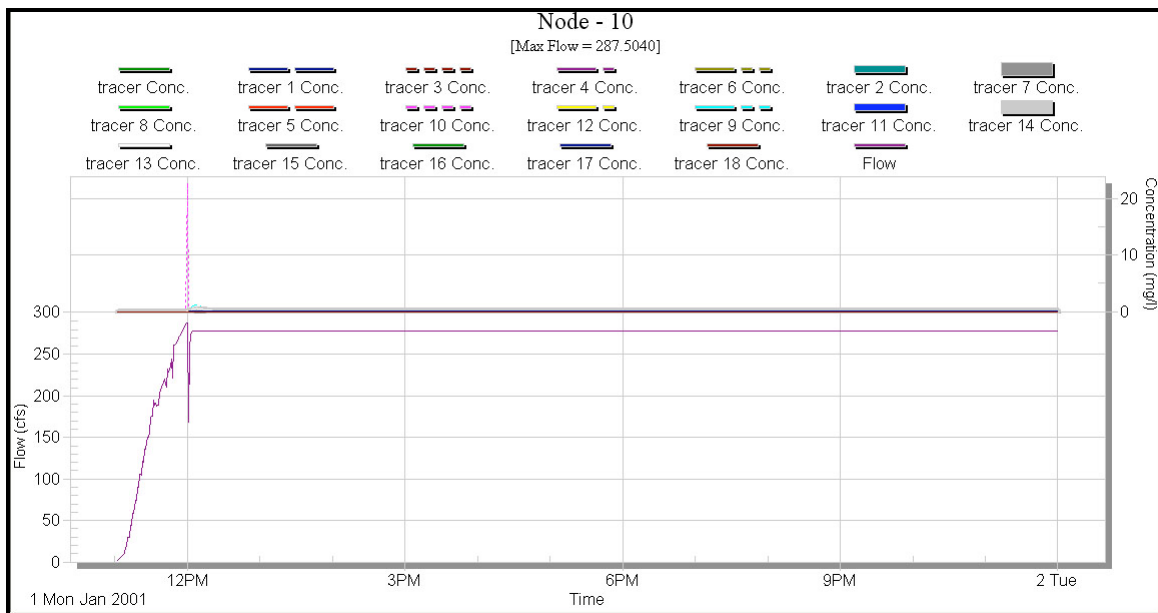


**Exhibit 4A.10: Sample Sanitary Block Tracer Results.** This is the simulated XPSWMM pollutograph using 5-yr return period rainfall. The results were examined at the main catchment outlet. Therefore, this figure shows the time needed for tracer 10 to exit subcatchment 10 and to be observed at the K2 catchment outlet.

**Appendix 4B:** Return Period Graphics in the Runoff Block



**Figure 4B.1:** XPSWMM Import Screen Used for Return Period Rainfall Transfer.

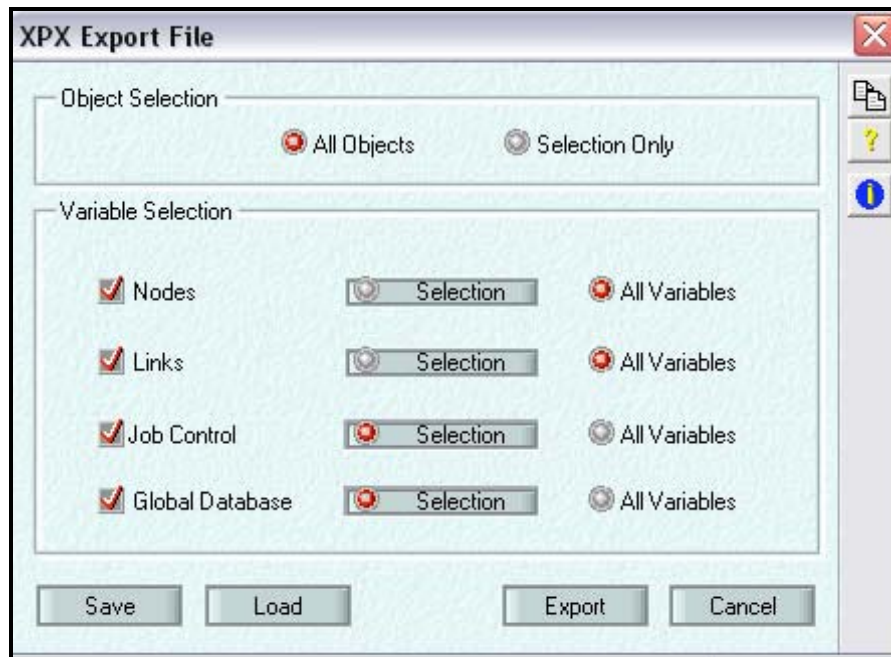


**Figure 4B.2:** XPSWMM Export Menu

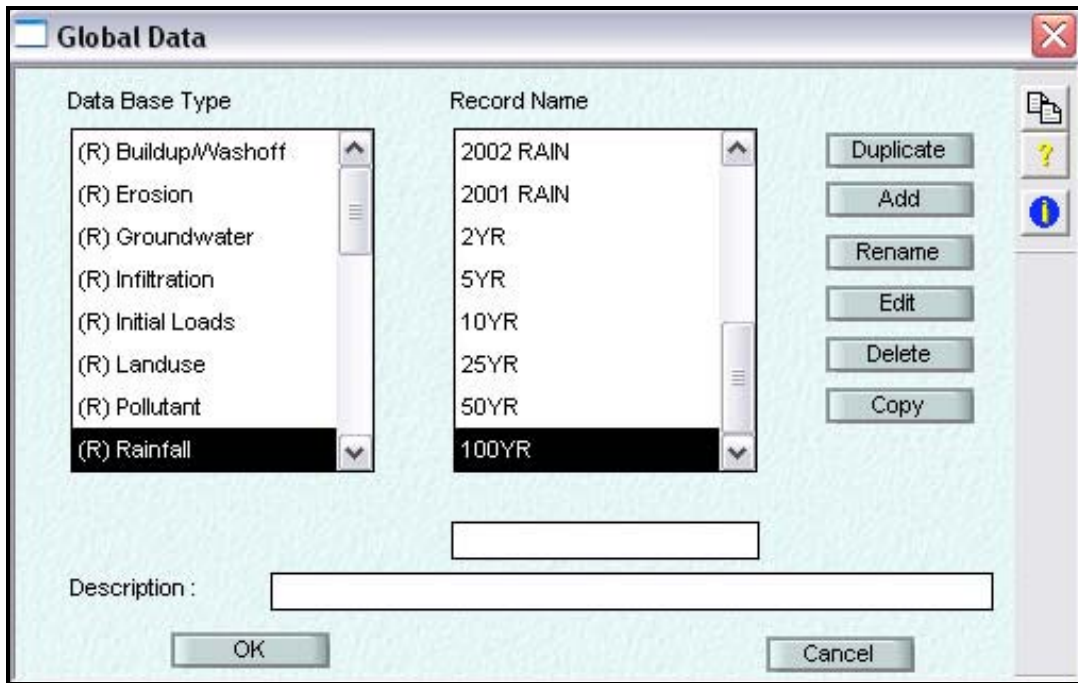


**Figure 4B.3: XPSWMM Runoff Block Global Data Screen.** The XPSWMM Global Data screen is where the modeler links rainfall to each node.

**Appendix 4C:** ArcMAP Travel Time Results

**Exhibit 4C.1:** Catchment K2 Travel Time Maps for Various Return Period Rainfall

Note: The indicated Travel Time predictions are the amount of time required for runoff exiting the subcatchment to be viewed at the catchment outlet, in minutes. Hourly Rainfall data, synthesized from standard storm data for Morehead City, North Carolina, was used to generate these graphs.

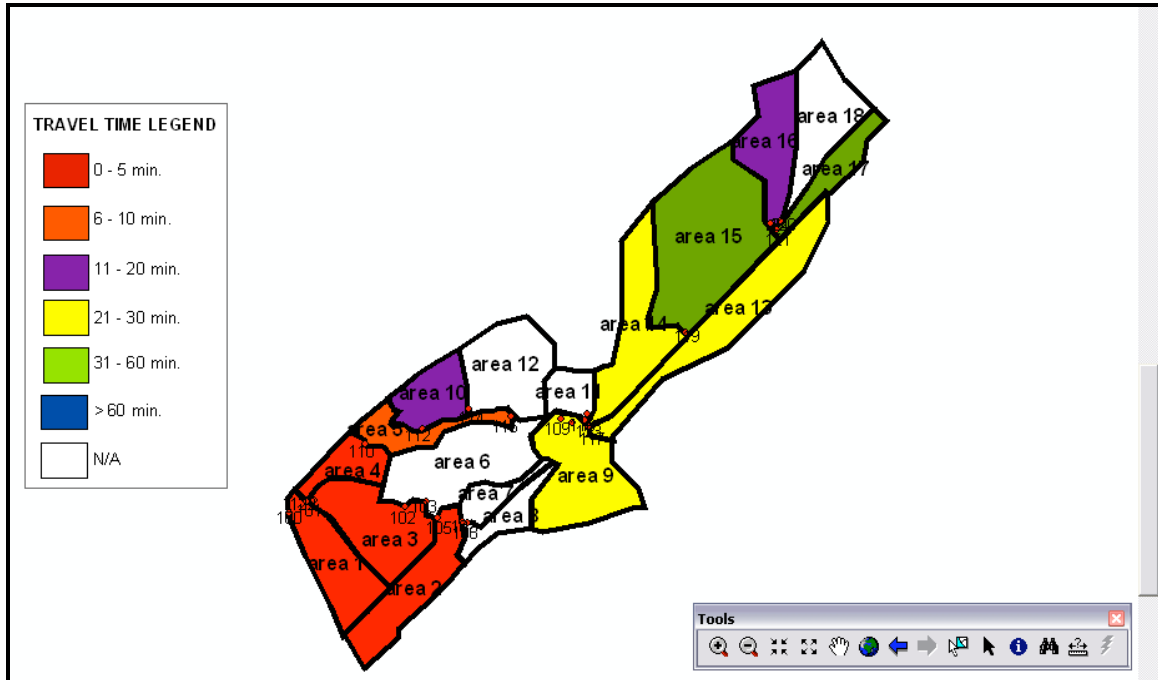


**Figure 4C.1.1:** Catchment K2 2yr Return Period Travel Time Map

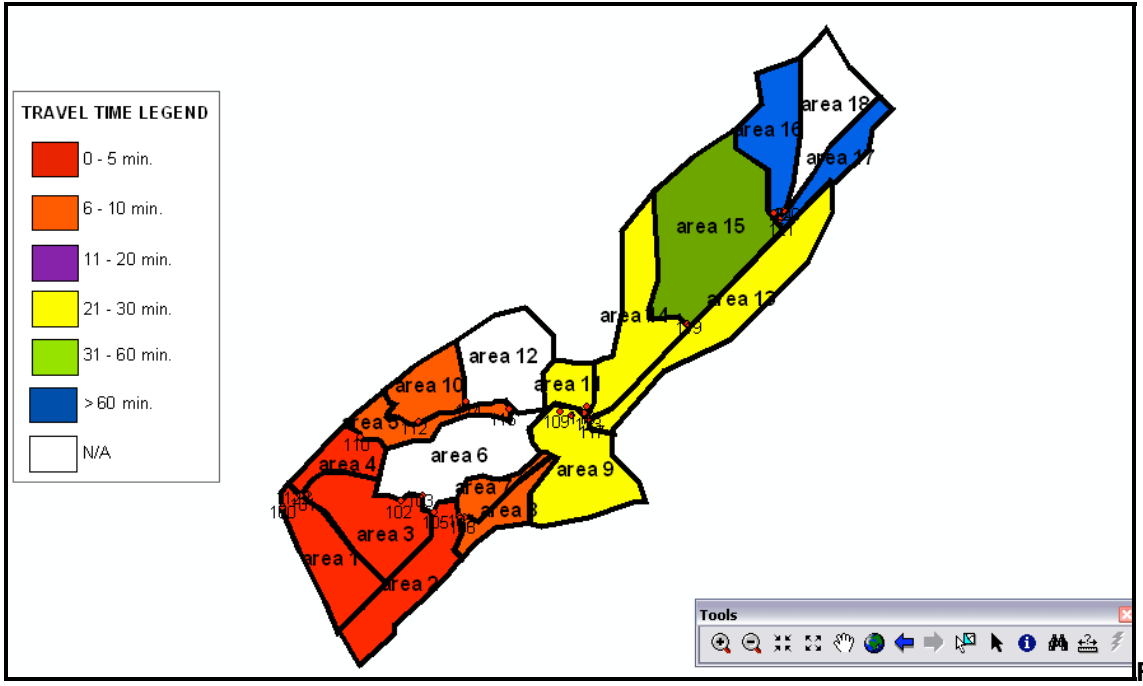


Figure 4C.1.2: Catchment K2 5yr Return Period Travel Time Map

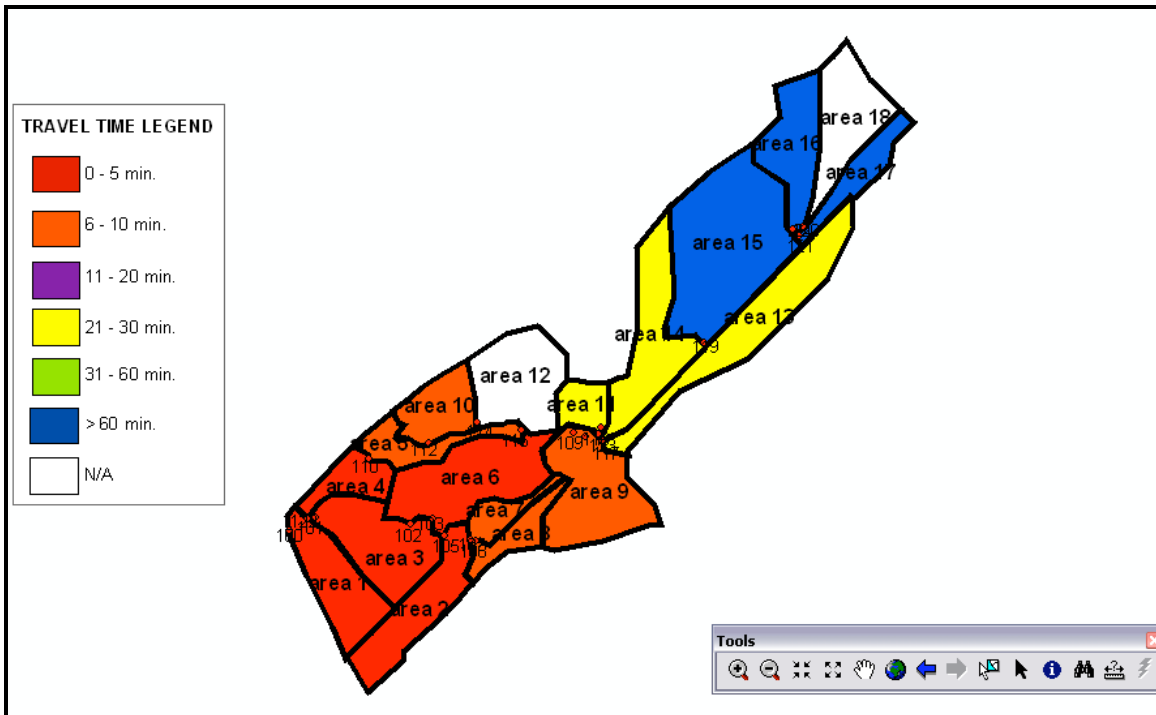


Figure 4C.1.3: Catchment K2 10yr Return Period Travel Time Map

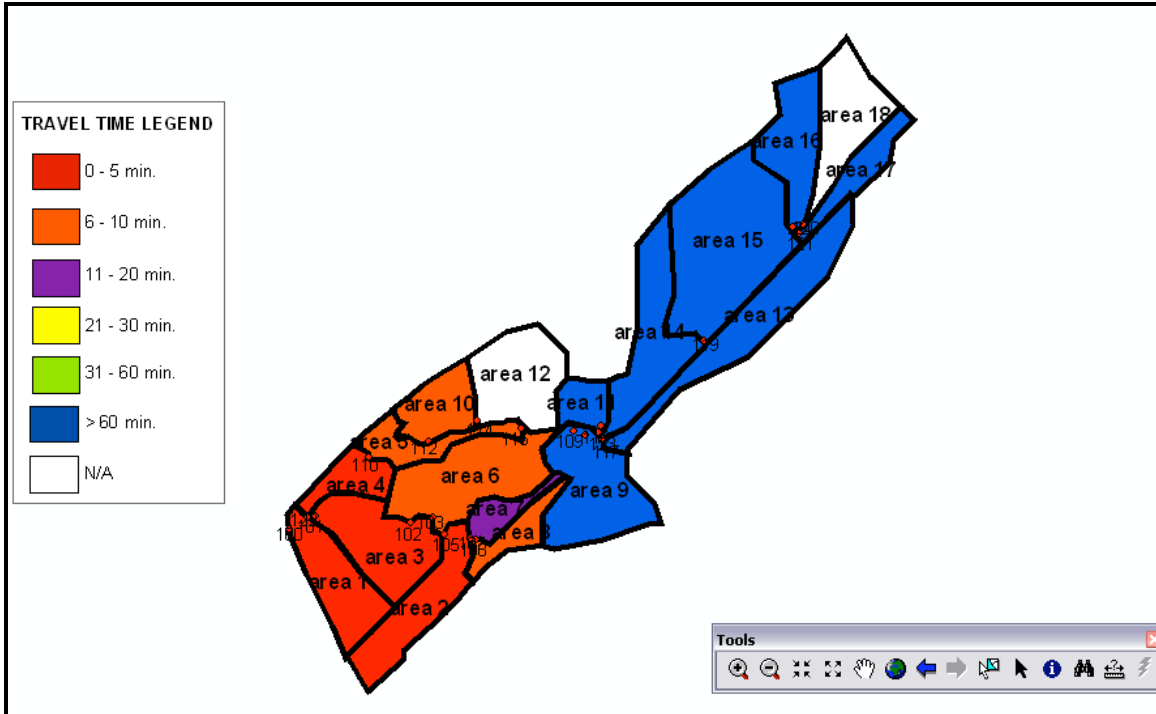


Figure 4C.1.4: Catchment K2 25yr Return Period Travel Time Map

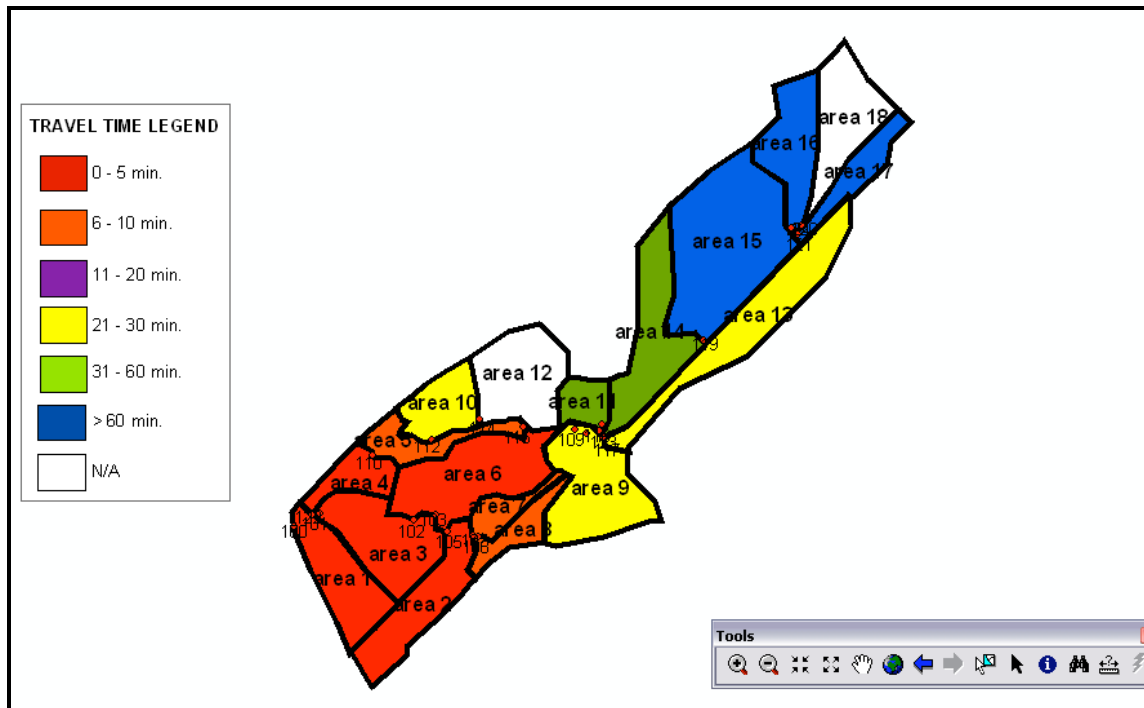


Figure 4C.1.5: Catchment K2 50yr Return Period Travel Time Map

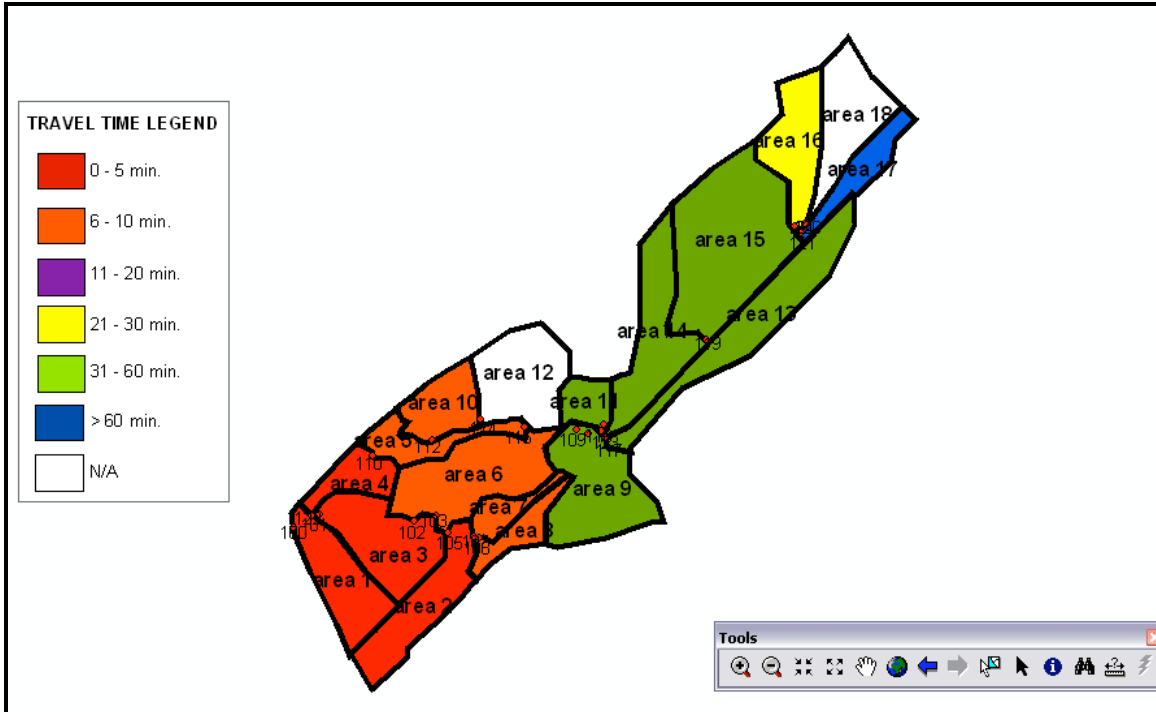
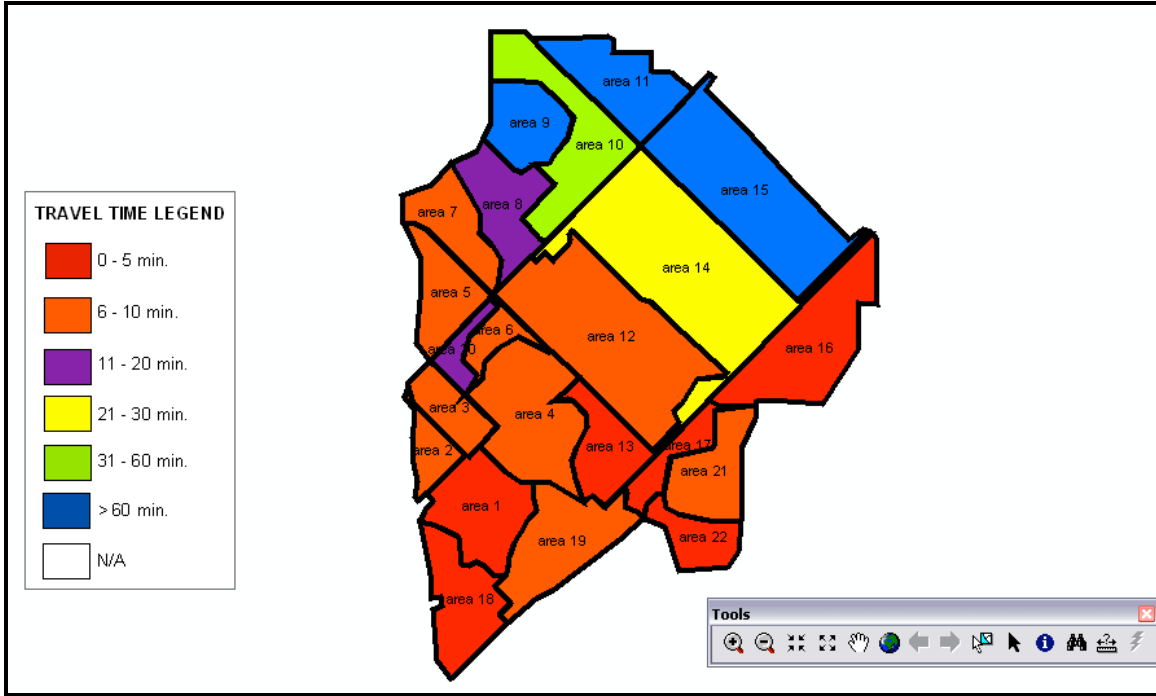


Figure 4C.1.6: Catchment K2 100yr Return Period Travel Time Map

**Exhibit 4C.2:** Catchment K3 Travel Time Maps for Various Return Period Rainfall

Note: The indicated Travel Time predictions are the amount of time required for runoff exiting the subcatchment to be viewed at the catchment outlet, in minutes. Hourly rainfall for Morehead City, North Carolina, was used to generate these graphs.



**Figure 4C.2.1:** Catchment K3 2yr Return Period Travel Time Map

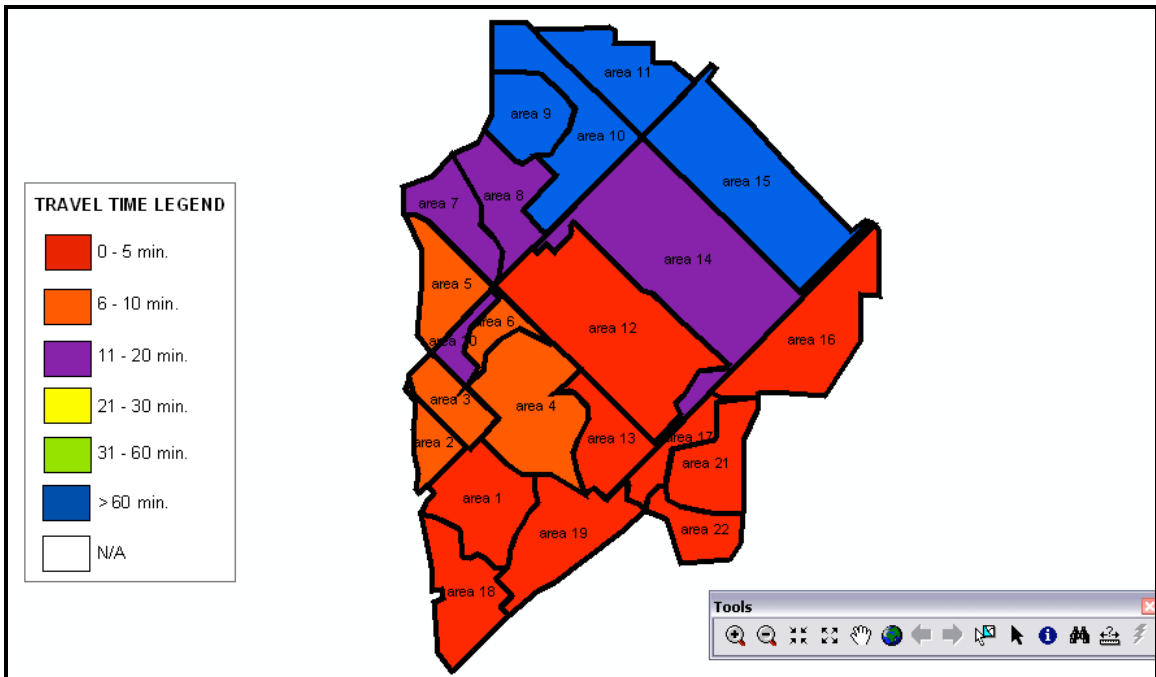


Figure 4C.2.2: Catchment K3 5yr Return Period Travel Time Map

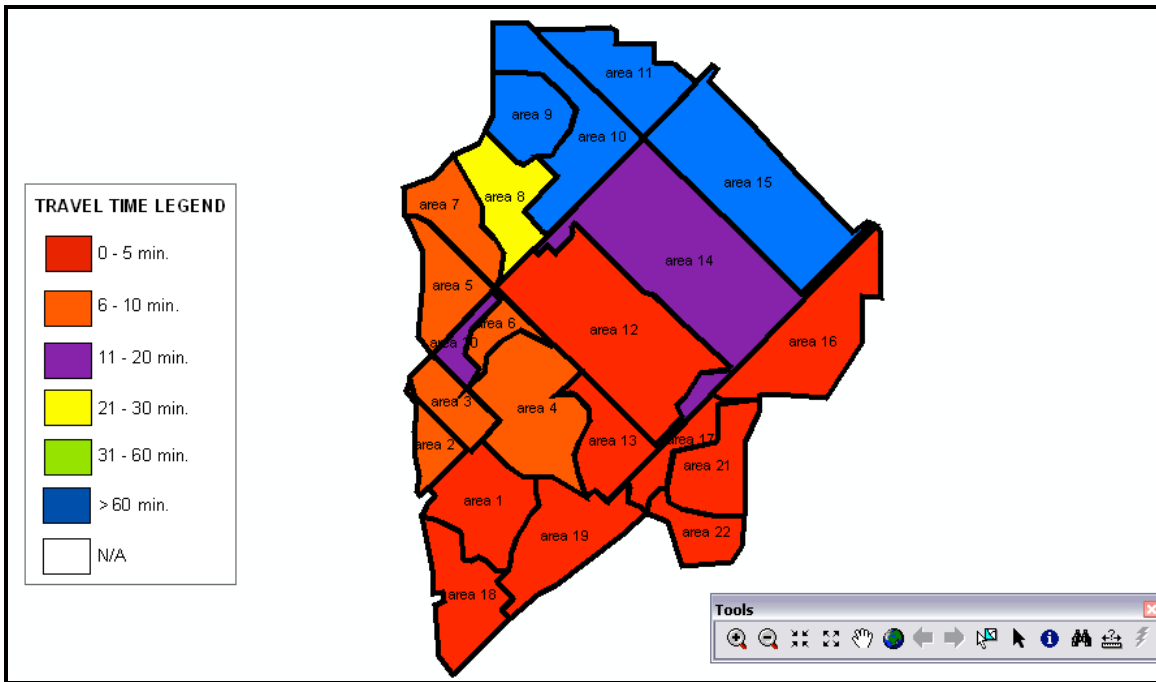


Figure 4C.2.3: Catchment K3 10yr Return Period Travel Time Map

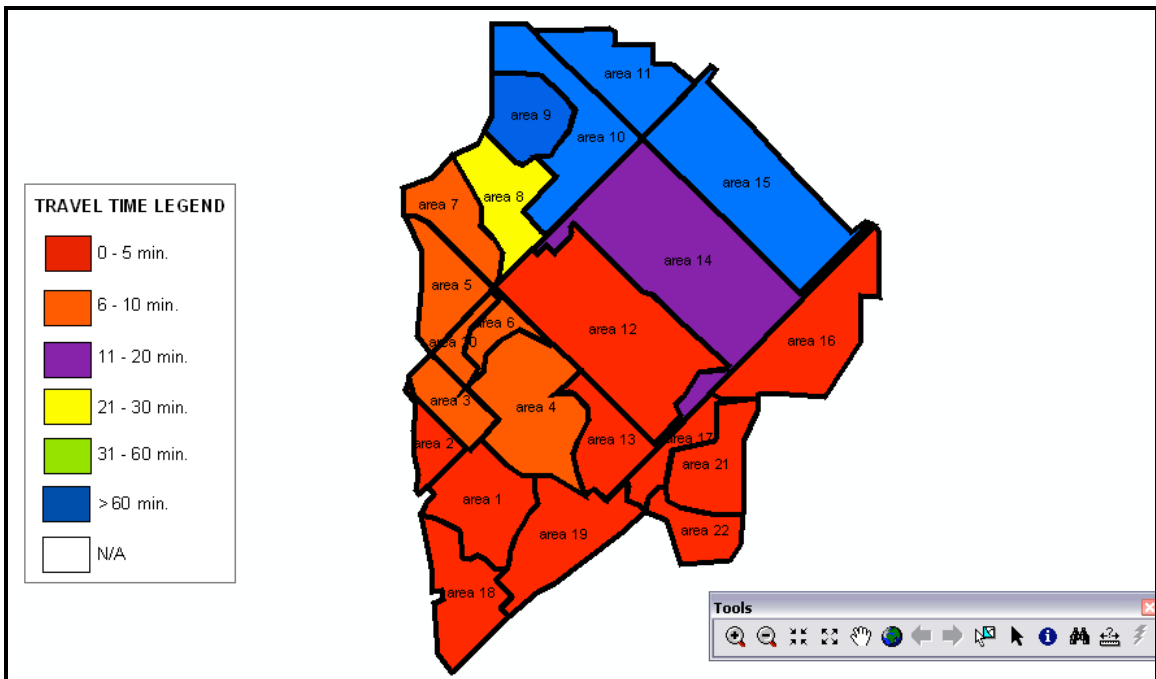


Figure 4C.2.4: Catchment K3 25yr Return Period Travel Time Map

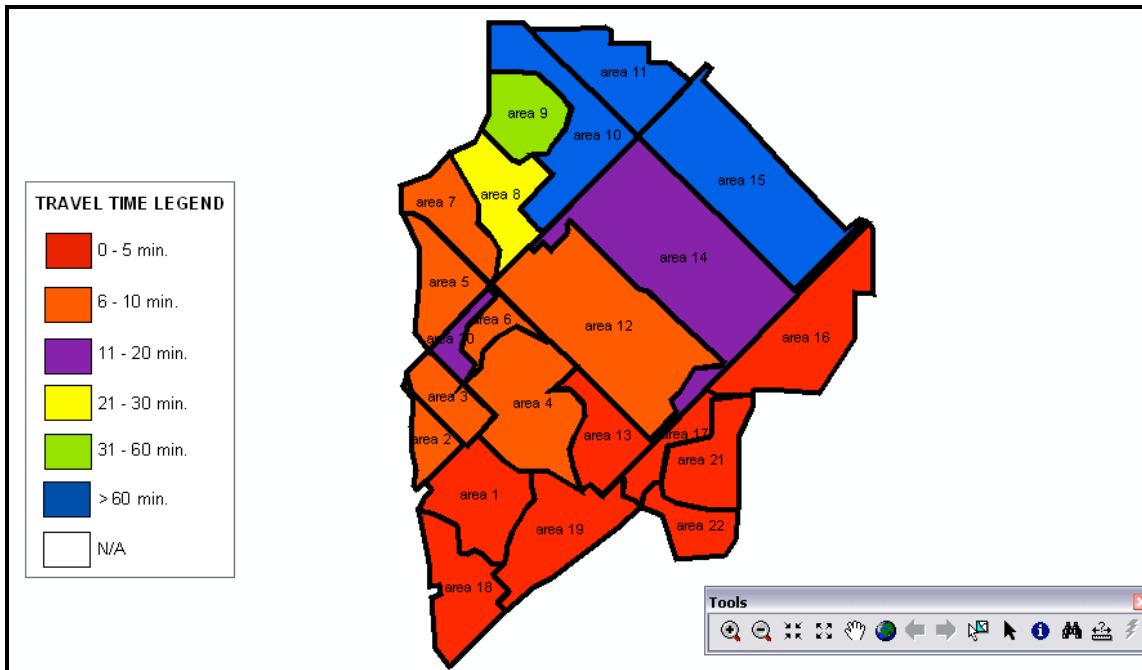


Figure 4C.2.5: Catchment K3 50yr Return Period Travel Time Map

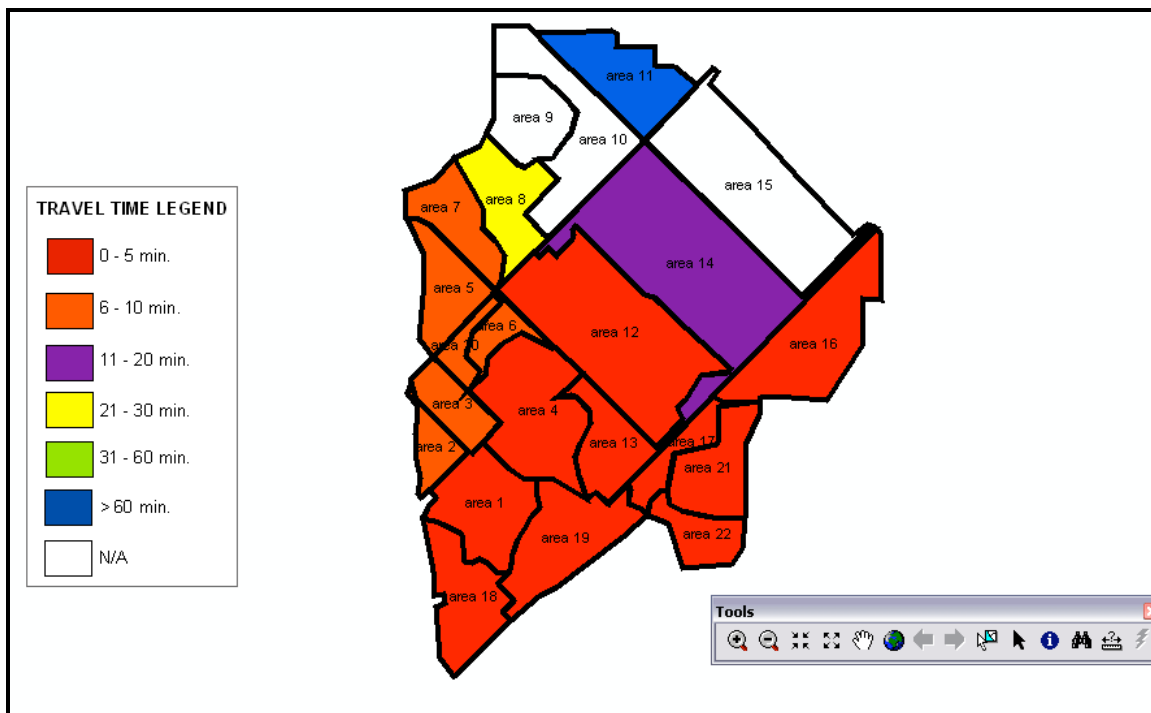
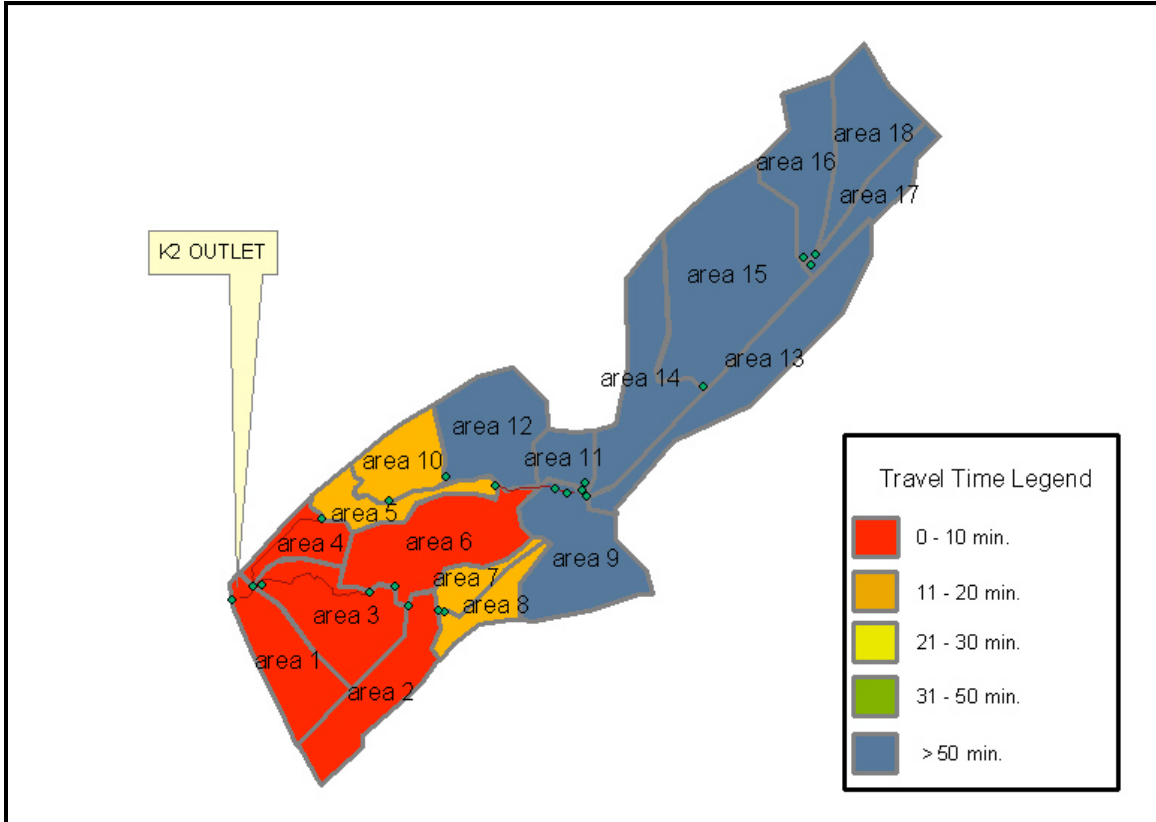


Figure 4C.2.6: Catchment K3 100yr Return Period Travel Time Map

**Exhibit 4C.3:** Catchment K2 Travel Time Maps for Various Return Period Rainfall, using 5-minute Precipitation Increments.

Note: These graphs are similar to the charts in Exhibits One but use 5-minute rainfall data.



**Figure 4C.3.1:** Catchment K2 2yr Return Period Travel Time Map

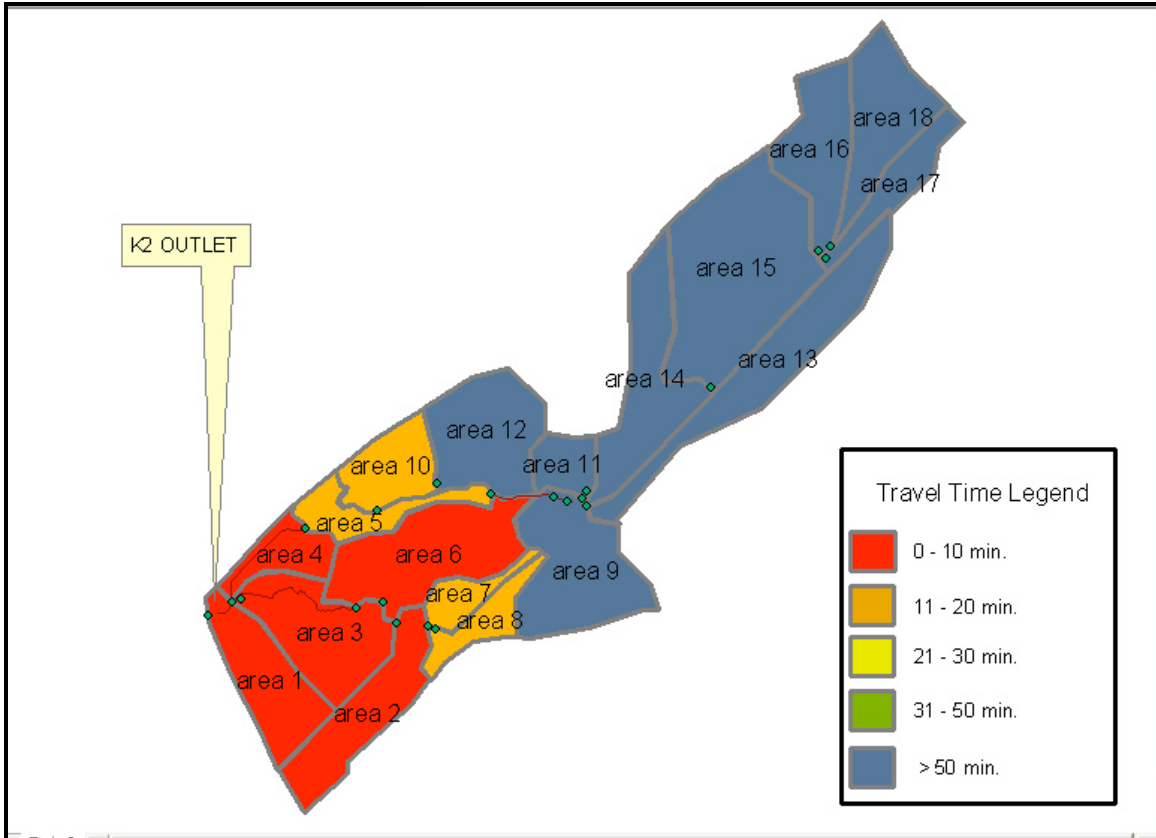
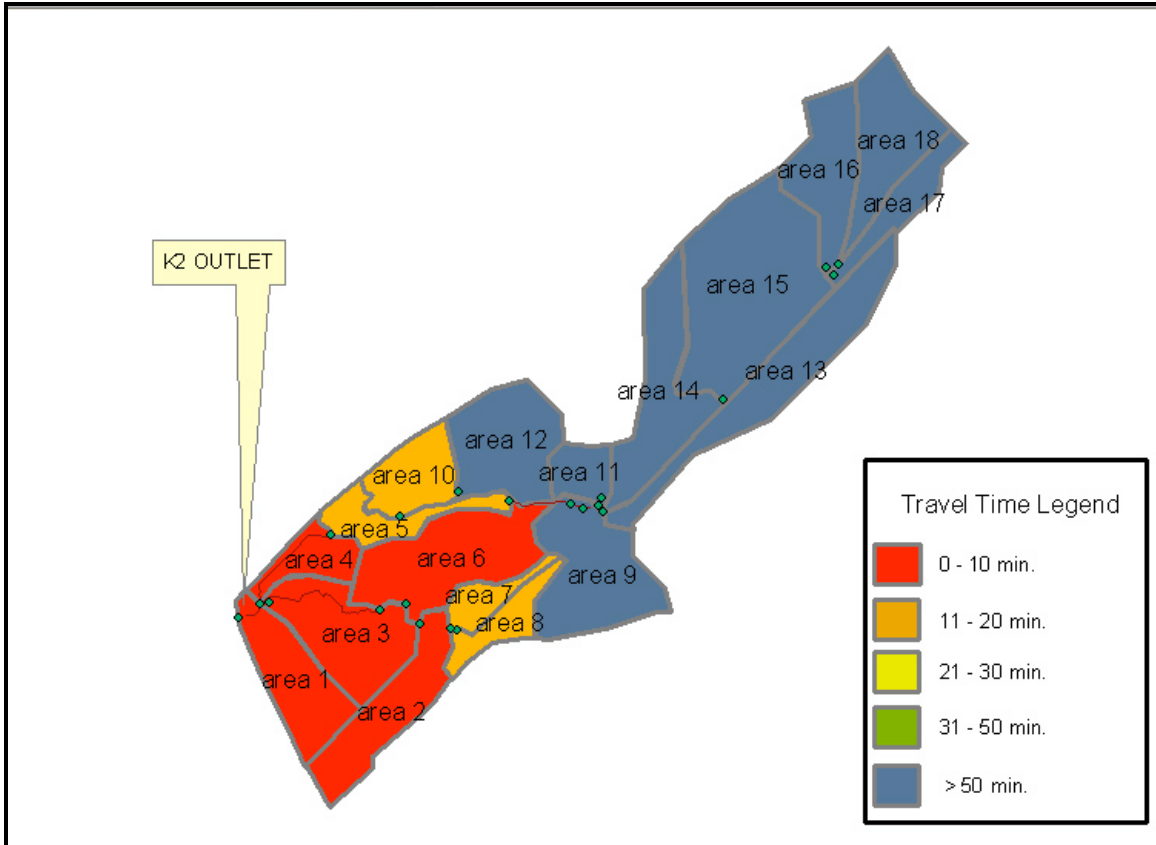


Figure 4C.3.2: Catchment K2 5yr Return Period Travel Time Map



**Figure 4C.3.3: Catchment K2 10yr Return Period Travel Time Map**

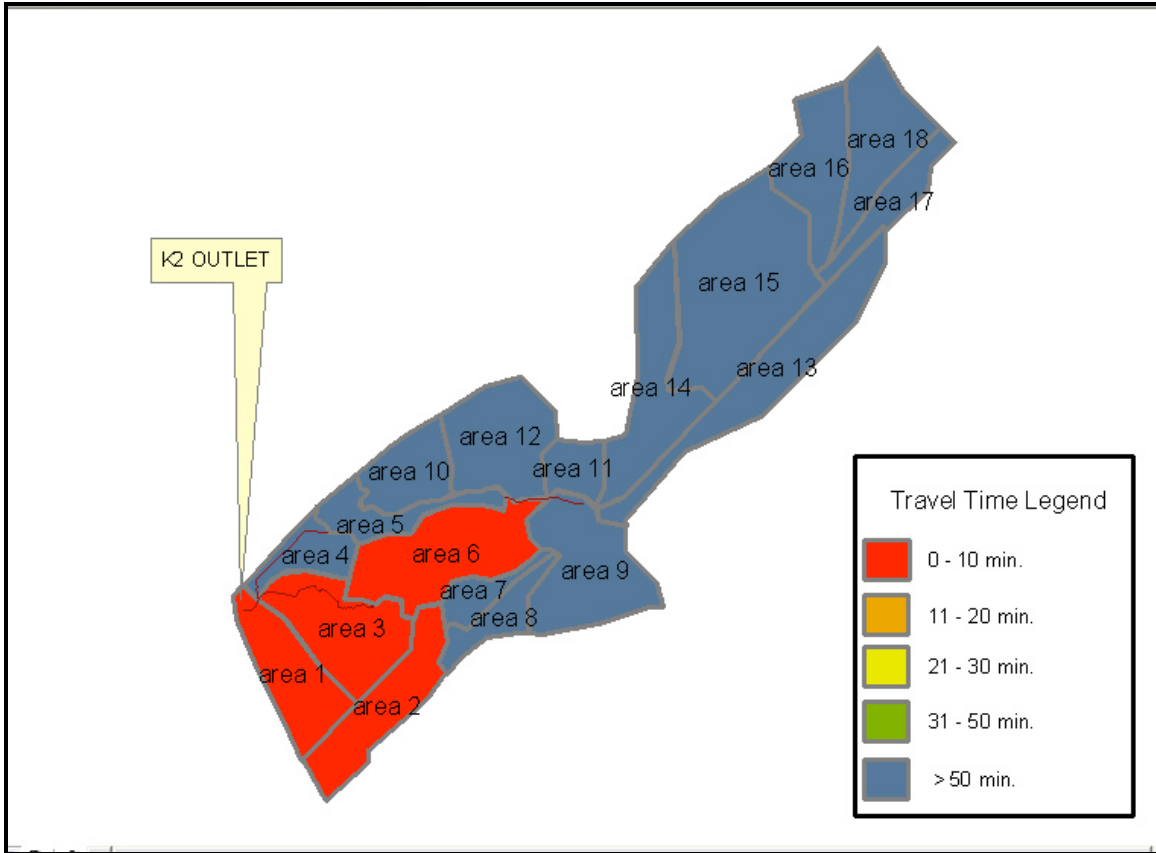


Figure 4C.3.4: Catchment K2 25yr Return Period Travel Time Map

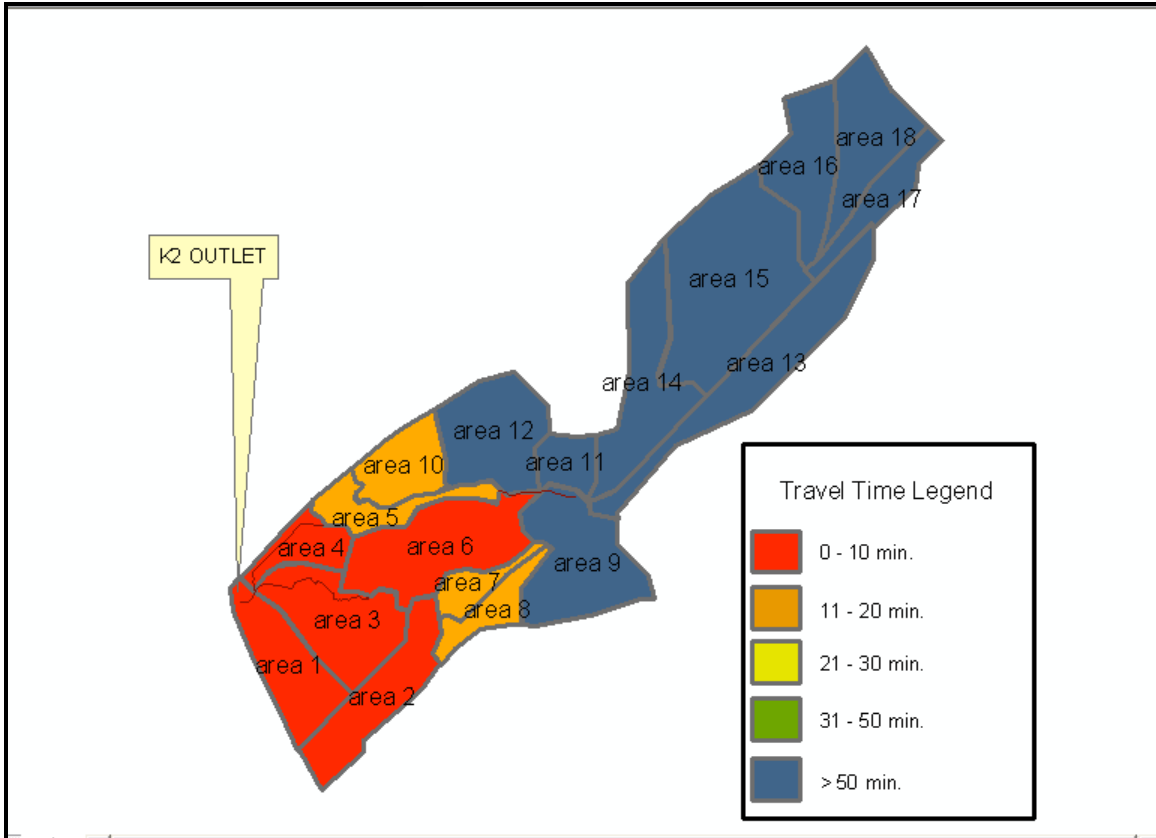


Figure 4C.3.5: *Catchment K2 50yr Return Period Travel Time Map*

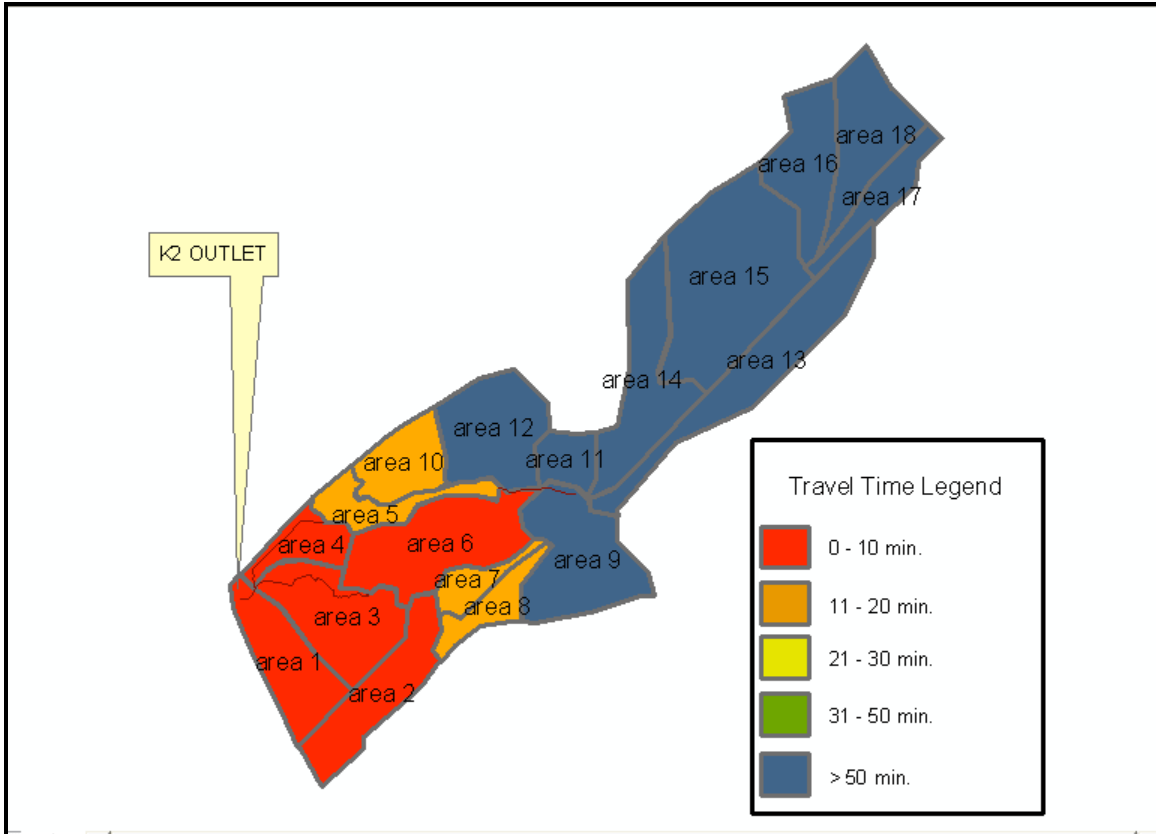
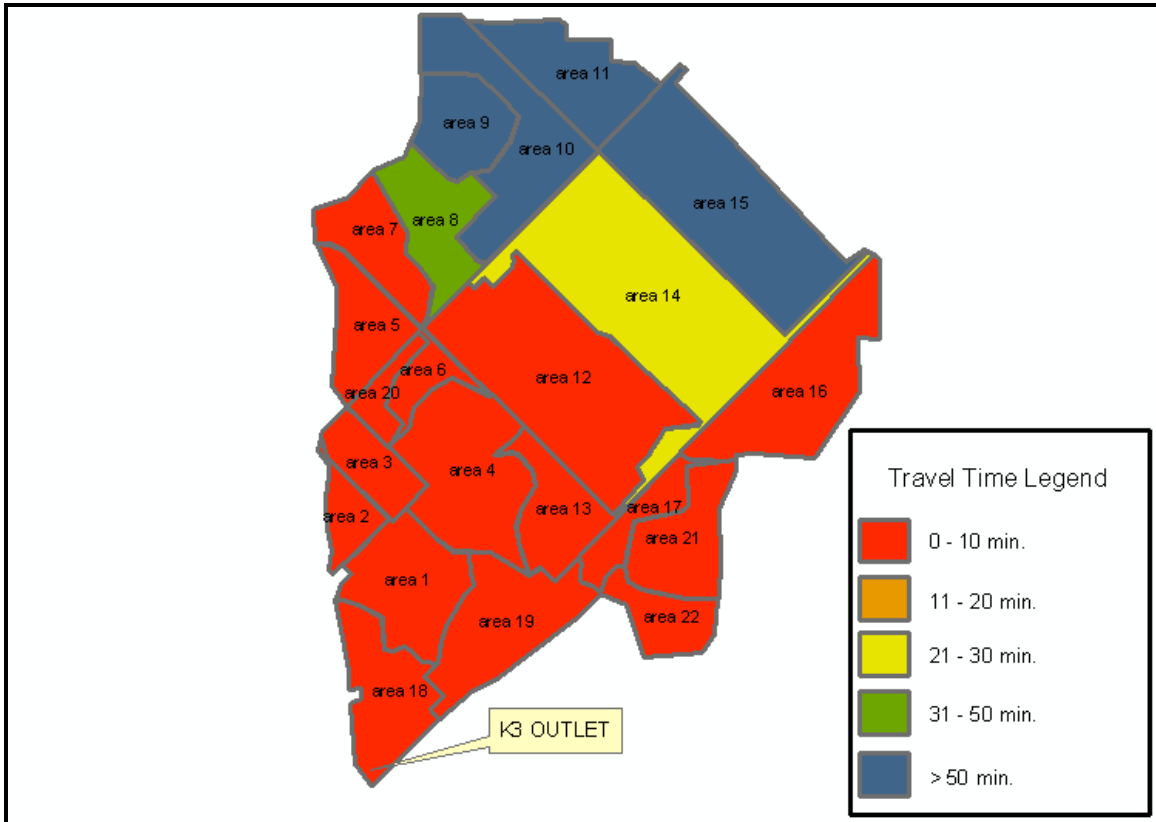


Figure 4C.3.6: Catchment K2 100yr Return Period Travel Time Map

**Exhibit 4C.4:** Catchment K3 Travel Time Maps for Various Return Period Rainfall, using 5-Minute Precipitation Increments.

Note: These graphs are similar to the charts in Exhibits Two but use 5-minute rainfall data.



**Figure 4C.4.1:** Catchment K3 2yr Return Period Travel Time Map

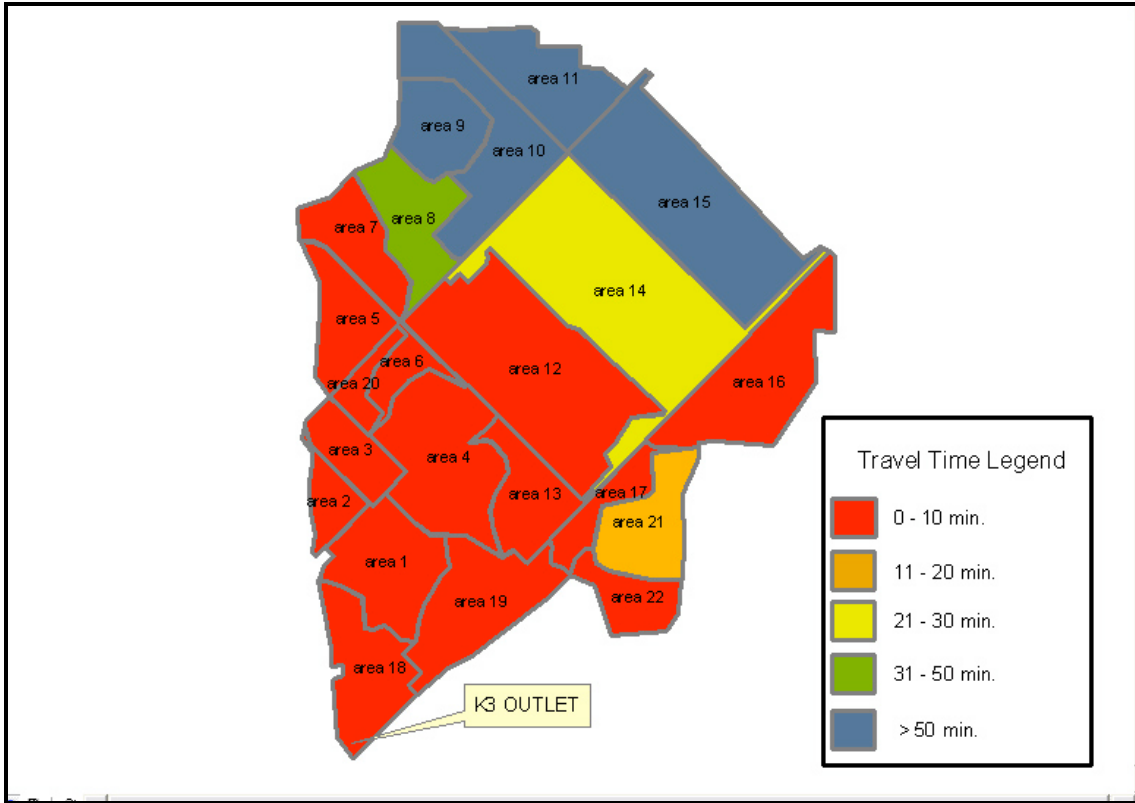


Figure 4C.4.2: Catchment K3 5yr Return Period Travel Time Map

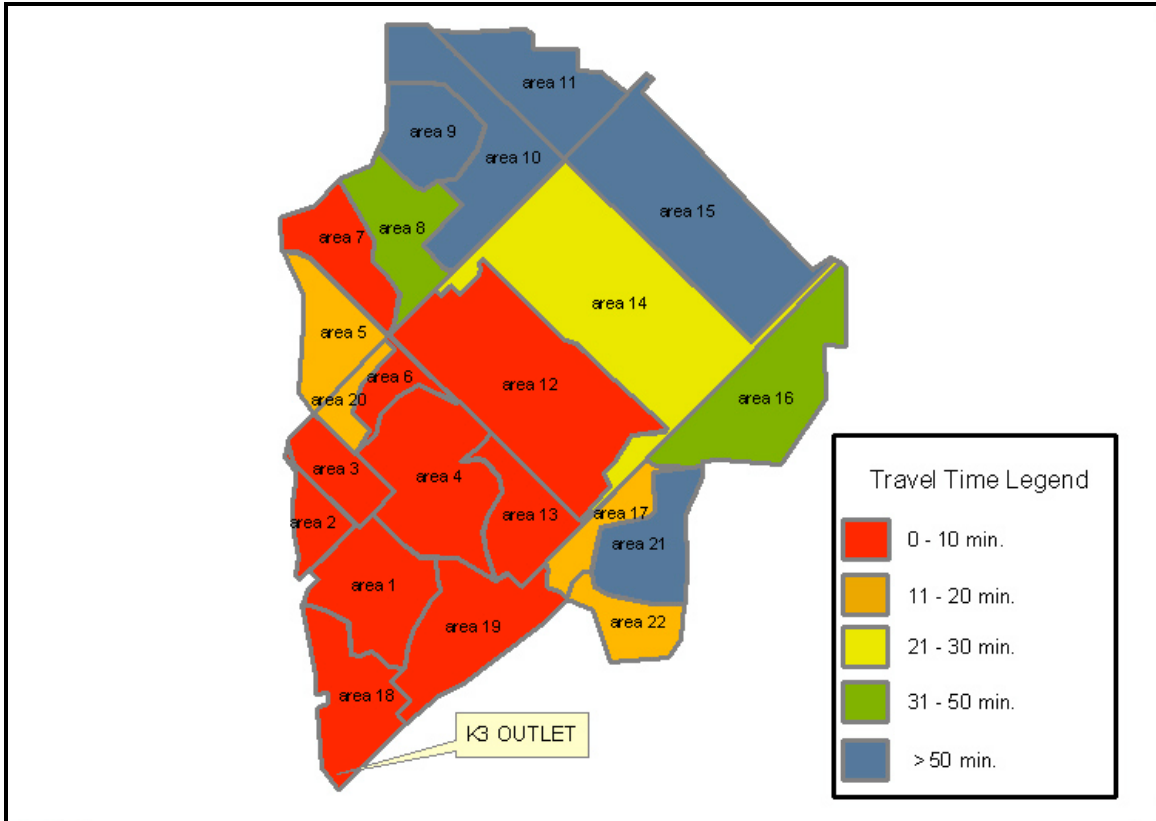


Figure 4C.4.3: Catchment K3 10yr Return Period Travel Time Map

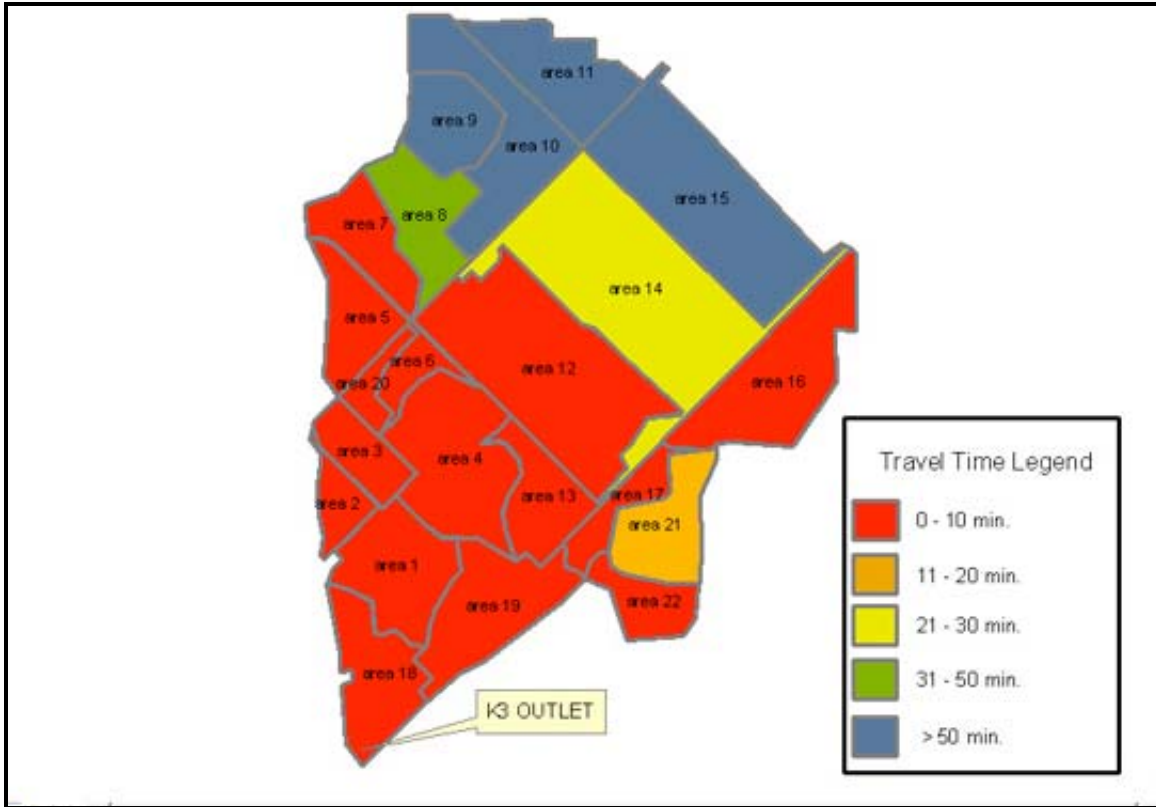


Figure 4C.4.4: Catchment K3 25yr Return Period Travel Time Map

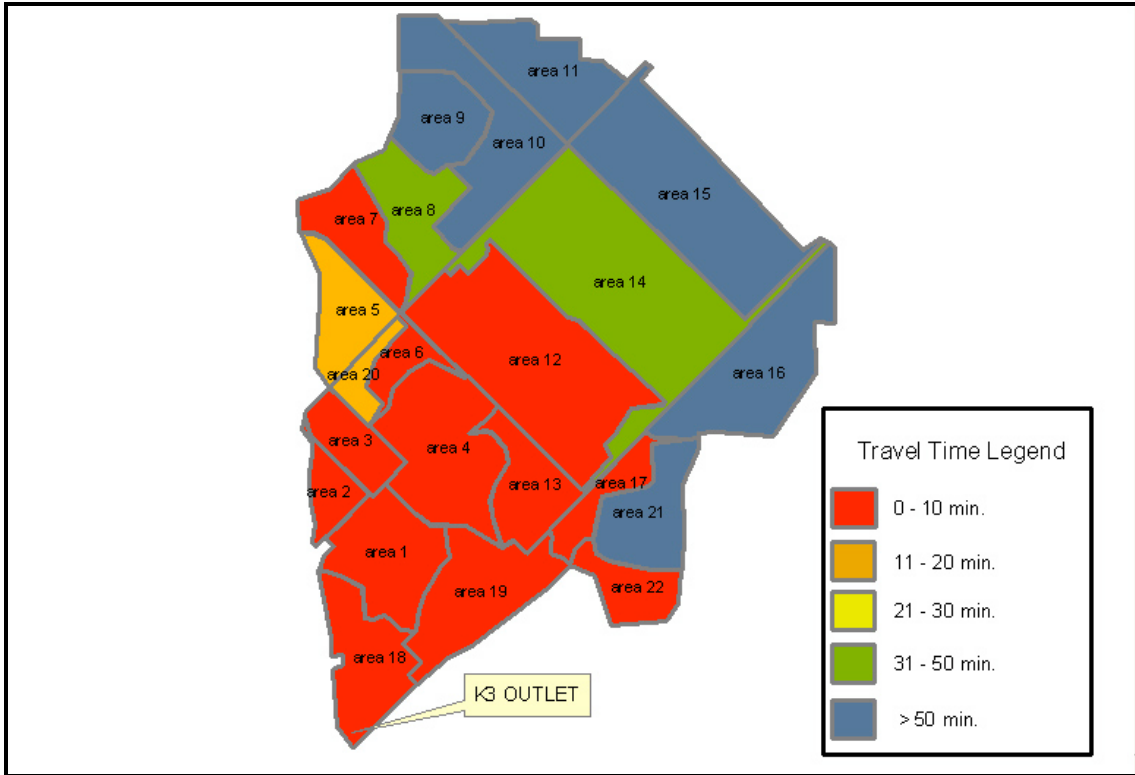


Figure 4C.4.5: *Catchment K3 50yr Return Period Travel Time Map*

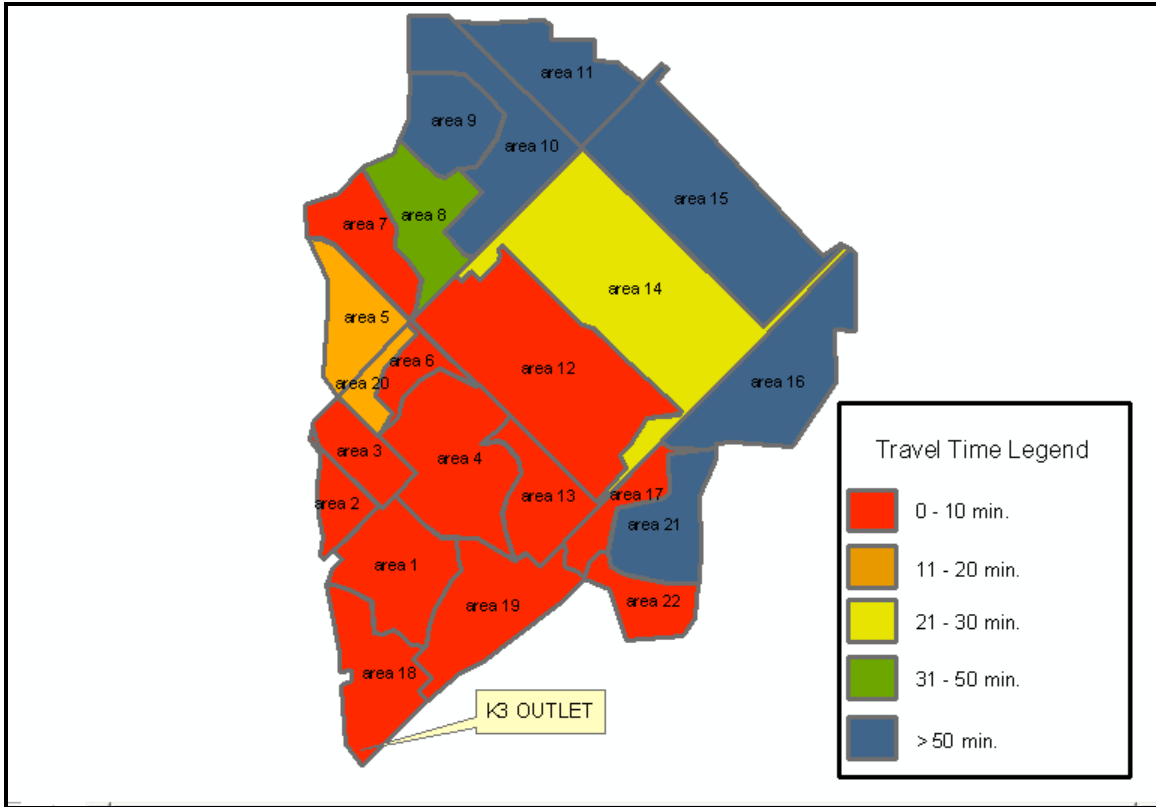


Figure 4C.4.6: Catchment K3 100yr Return Period Travel Time Map

**Appendix 4D:** Travel Time Comparison between the 60-minute and 5-minute XPSWMM simulations using Return Period Rainfall

**Exhibit 4D.1:** Catchment K2 Simulated Travel Time Comparison for Various Return Period Storms

**Table 4D.1.1: 2-Yr Travel Time Comparison**

Element Number	60 minute		5 minute		2 Yr Comparison	
	2 YR		2 YR		runoff % increase (CFS)	travel time % change (min)
	Runoff (CFS)	Travel time (min)	Runoff (CFS)	Travel time (min)		
<b>1(outlet)</b>	<b>83.3</b>	<b>0</b>	<b>135.55</b>	<b>0</b>	<b>62.7</b>	<b>0</b>
2	9.9	5	30.74	2	212.1	-60
3	80.0	1	125.18	1	56.5	0
4	54.9	3	82.78	3	50.8	0
5	55.6	7	84.32	12	51.7	71
6	7.0		23.39	2	235.1	
7	3.7	7	12.15	16	228.4	129
8	2.4	7	8.16	16	237.2	129
9	43.4	24	77.22	>1HR	77.9	
10	54.9	11	83.97	13	53.0	18
11			9.99	>1HR		
12			26.97	>1HR		
13	33.3	24	45.22	>1HR	35.8	
14	26.2	24	47.68	>1HR	82.0	
15	32.1	52	71.09	>1HR	121.5	
16	15.1	20	22.1	>1HR	46.4	
17	13.2	56	19.38	>1HR	46.8	
18			22.90	>1HR		
				mean	88.8	15.9

**Table 4D.1.2: 5-Yr Travel Time Comparison**

Element Number	60 minute		5 minute		5 Yr Comparison	
	5 YR		5 YR			
	Runoff (CFS)	Travel time (min)	Runoff (CFS)	Travel time (min)	runoff % increase (CFS)	travel time % change (min)
	<b>1(outlet)</b>	<b>94.2</b>	<b>0</b>	<b>148.62</b>	<b>0</b>	<b>57.8</b>
2	10.8	3	33.11	2	<b>206.6</b>	<b>-33</b>
3	88.7	1	137.61	1	<b>55.1</b>	<b>0</b>
4	62.9	2	89.2	3	<b>41.8</b>	<b>50</b>
5	63.6	7	90.59	12	<b>42.4</b>	<b>71</b>
6	7.7		26.08	2	<b>240.9</b>	
7	4.1	6	13.56	16	<b>234.0</b>	<b>167</b>
8	2.7	6	9.09	16	<b>243.0</b>	<b>167</b>
9	50.1	22	84.68	>1HR	<b>69.0</b>	
10	62.9	9	90.33	13	<b>43.6</b>	<b>44</b>
11	3.2	24	11.11	>1HR	<b>248.3</b>	
12			30.16	>1HR		
13	35.7	24	49.41	>1HR	<b>38.4</b>	
14	26.2	28	50.43	>1HR	<b>92.5</b>	
15	34.3	56	79	>1HR	<b>130.3</b>	
16	16.5	0	24.33	>1HR	<b>47.5</b>	
17	13.6	0	20.73	>1HR	<b>52.4</b>	
18			25.84	>1HR		
				mean	102.4	25.9

**Table 4D.1.3: 10-Yr Travel Time Comparison**

Element Number	60 minute		5 minute		10 Yr Comparison	
	10 YR		10 YR			
	Runoff (CFS)	Travel time (min)	Runoff (CFS)	Travel time (min)	runoff % increase (CFS)	travel time % change (min)
	<b>1(outlet)</b>	<b>125.4</b>	<b>0</b>	<b>199.49</b>	<b>0</b>	<b>59.1</b>
2	14.6	4	41.37	2	183.4	-50
3	117.7	1	183.64	1	56.0	0
4	82.9	4	112.89	3	36.2	-25
5	83.5	8	114.01	11	36.5	38
6	10.3	4	35.5	3	244.7	-25
7	5.5	6	18.55	16	239.1	167
8	3.6	6	12.36	17	245.3	183
9	64.5	8	112.75	>1HR	74.8	
10	82.3	9	114.12	12	38.7	33
11	4.3	29	15.01	>1HR	249.1	
12			41.40	>1HR		
13	44.6	30	65.81	>1HR	47.6	
14	26.2	30	60.46	>1HR	130.8	
15	43.1	0	107.74	>1HR	150.0	
16	22.3	0	32.45	>1HR	45.5	
17	15.2	0	25.71	>1HR	69.1	
18			36.56	>1HR		
				mean	105.9	17.8

**Table 4D.1.4: 25-Yr Travel Time Comparison**

Element Number	60 minute		5 minute		25 Yr Comparison	
	25 YR		25 YR			
	Runoff (CFS)	Travel time (min)	Runoff (CFS)	Travel time (min)	runoff % increase (CFS)	travel time % change (min)
	<b>1(outlet)</b>	<b>144.9</b>	<b>0</b>	<b>232.63</b>	<b>0</b>	<b>60.5</b>
2	16.9	4	46.74	3	176.6	-25
3	135.1	1	213.97	1	58.4	0
4	95.3	3	122.54	>1HR	28.6	
5	95.9	8	123.27	>1HR	28.5	
6	12.0	6	41.56	4	246.3	-33
7	6.4	18	21.79	>1HR	242.6	
8	4.2	6	14.46	>1HR	244.3	
9	73.4	0	130.85	>1HR	78.3	
10	94.4	9	121.81	>1HR	29.0	
11	5.0	0	17.52	>1HR	250.4	
12			48.68	>1HR		
13	50.0	0	76.59	>1HR	53.2	
14	26.2	0	67.13	>1HR	156.2	
15	48.6	0	126.84	>1HR	161.0	
16	25.8	0	37.86	>1HR	46.7	
17	16.1	0	29.05	>1HR	80.4	
18			43.68	>1HR		
				mean	107.8	-3.2

**Table 4D.1.5: 50-Yr Travel Time Comparison**

Element Number	60 minute		5 minute		50 Yr Comparison	
	50 YR		50 YR			
	Runoff (CFS)	Travel time (min)	Runoff (CFS)	Travel time (min)	runoff % increase (CFS)	travel time % change (min)
	<b>1(outlet)</b>	<b>161.1</b>	<b>0</b>	<b>256.6</b>	<b>0</b>	<b>59.3</b>
2	18.9	5	50.89	2	<b>169.3</b>	<b>-60</b>
3	150.2	1	235.2	1	<b>56.6</b>	<b>0</b>
4	105.6	2	129.59	2	<b>22.7</b>	<b>0</b>
5	106.2	7	128.49	12	<b>21.0</b>	<b>71</b>
6	13.4	5	46.26	2	<b>245.2</b>	<b>-60</b>
7	7.1	7	24.29	16	<b>242.6</b>	<b>129</b>
8	4.6	7	16.09	15	<b>246.8</b>	<b>114</b>
9	80.9	30	145.08	>1HR	<b>79.3</b>	
10	104.5	9	123.77	13	<b>18.4</b>	<b>44</b>
11	5.6	31	19.47	>1HR	<b>248.9</b>	
12			54.32	>1HR		
13	54.6	30	84.84	>1HR	<b>55.4</b>	
14	26.2	33	72.34	>1HR	<b>176.1</b>	
15	53.2	0	141.75	>1HR	<b>166.4</b>	
16	28.8	0	42.1	>1HR	<b>46.2</b>	
17	17.0	0	31.67	>1HR	<b>86.3</b>	
18			49.25	>1HR		
				mean	107.8	13.3

**Table 4D.1.6: 100-Yr Travel Time Comparison**

Element Number	60 minute		5 minute		100 Yr Comparison	
	100 YR		100 YR		runoff % increase (CFS)	travel time % change (min)
	Runoff (CFS)	Travel time (min)	Runoff (CFS)	Travel time (min)		
	<b>1(outlet)</b>	<b>180.5</b>	<b>0</b>	<b>282.52</b>		
2	21.2	3	56.22	2	165.2	-33
3	168.4	1	257.87	1	53.1	0
4	117.9	3	138.36	4	17.4	33
5	118.5	8	137.73	11	16.2	38
6	15.0	6	52.29	3	248.6	-50
7	8.0	8	27.52	17	244.9	113
8	5.2	8	18.18	17	248.3	113
9	89.7	34	162.07	>1HR	80.7	
10	116.4	8	134.53	13	15.6	63
11	6.3	35	21.97	UNSTABLE	249.8	
12			61.54	>1HR		
13	60.0	35	94.67	UNSTABLE	57.8	
14	26.2	38	78.93	UNSTABLE	201.3	
15	58.7	38	160.6	>1HR	173.6	
16	32.4	30	47.46	>1HR	46.5	
17	17.9	>1HR	34.98	>1HR	95.4	
18			56.30	>1HR		
				mean	109.5	15.3

**Exhibit 4D.2:** Catchment K3 Travel Time Comparisons using Various Return Period Rainfall Data

**Table 4D.2.1: 2-Yr Travel Time Comparison**

Element Number	60 minute		5 minute		2 YR comparison	
	2 YR		2 YR			
	Runoff (CFS)	Travel time (min)	Runoff (CFS)	Travel time (min)	runoff % increase (CFS)	travel time % change (min)
	1	7.8	2	25.65	1	228.8
2	1.5	9	5.17	7	244.7	-22
3	3.2	7	9.69	7	202.8	0
4	20.9	6	62.44	5	198.8	-17
5	4.4	10	14.59	9	231.6	-10
6	6.8	8	21.53	7	216.6	-13
7	11.1	10	22.37	9	101.5	-10
8	7.4	15	23.1	43	212.2	187
9	5.2	>1hr	17.55	>1HR	237.5	
10	29.7	0:00	64.69	>1HR	117.8	
11	6	>1hr	19.88	>1HR	231.3	
12	39.5	6	75.72	5	91.7	-17
13	63.3	4	136.07	3	115.0	-25
14	30.6	21	69.09	30	125.8	43
15	11.7	>1hr	33.4	>1HR	185.5	
16	9.2	5	26.79	5	191.2	0
17	15.1	4	41.27	4	173.3	0
<b>18 (outlet)</b>	<b>93.3</b>	<b>0</b>	<b>189.38</b>	<b>0</b>	<b>103.0</b>	<b>0</b>
19	83.2	6	178.62	1	114.7	-83
20	0.2	13	0.72	10	260.0	-23
21	3.7	6	12.57	5	239.7	-17
22	5	5	16.35	5	227.0	0
mean					184.1	-3.1

**Table 4D.2.2: 5-Yr Travel Time Comparison**

Element Number	60 minute		5 minute		5 YR comparison	
	5 YR		5 YR			
	Runoff (CFS)	Travel time (min)	Runoff (CFS)	Travel time (min)	runoff % increase (CFS)	travel time % change (min)
	1	8.5	2	28.56	1	236.0
2	1.7	8	5.75	6	238.2	-25
3	3.5	7	10.88	6	210.9	-14
4	22.9	7	69.95	5	205.5	-29
5	4.8	19	16.27	8	239.0	-58
6	7.4	8	24.03	7	224.7	-13
7	11.6	11	24.33	8	109.7	-27
8	8.1	19	25.9	42	219.8	121
9	5.8	>1hr	19.57	>1HR	237.4	
10	32.2	>1hr	70.17	>1HR	117.9	
11	6.6	>1hr	22.18	>1HR	236.1	
12	41.6	5	83.3	5	100.2	0
13	67.6	4	150.22	3	122.2	-25
14	32.8	20	77.04	29	134.9	45
15	12.8	>1hr	37.6	>1HR	193.8	
16	10.1	5	30.14	8	198.4	60
17	16.5	4	46.12	8	179.5	100
<b>18 (outlet)</b>	<b>100.5</b>	<b>0</b>	<b>209.36</b>	<b>0</b>	<b>108.3</b>	<b>0</b>
19	89.5	2	197.7	1	120.9	-50
20	0.2	12	0.8	10	300.0	-17
21	4.1	5	14.01	12	241.7	140
22	5.5	5	18.25	8	231.8	60
mean					191.2	12.2

**Table 4D.2.3: 10-Yr Travel Time Comparison**

Element Number	60 minute		5 minute		10 YR comparison	
	10 YR		10 YR			
	Runoff (CFS)	Travel time (min)	Runoff (CFS)	Travel time (min)	runoff % increase (CFS)	travel time % change (min)
	1	11.5	2	38.77	1	237.1
2	2.2	6	7.77	5	253.2	-17
3	4.8	6	15.14	6	215.4	0
4	30.9	6	95.67	5	209.6	-17
5	6.5	10	22.17	16	241.1	60
6	10	7	30.85	6	208.5	-14
7	13.5	10	31.29	7	131.8	-30
8	11	23	35.82	45	225.6	96
9	7.8	>1hr	26.64	>1HR	241.5	
10	42.5	>1hr	89.88	>1HR	111.5	
11	8.9	>1hr	30.27	>1HR	240.1	
12	50	5	110.73	5	121.5	0
13	85.2	4	200.66	3	135.5	-25
14	41.6	20	106	29	154.8	45
15	17.2	>1hr	52.73	>1HR	206.6	
16	13.7	5	42.19	44	208.0	780
17	22.3	4	56.88	11	155.1	175
<b>18 (outlet)</b>	<b>129.6</b>	<b>0</b>	<b>276.4</b>	<b>0</b>	<b>113.3</b>	<b>0</b>
19	114.6	2	259.34	1	126.3	-50
20	0.3	11	1.08	17	260.0	55
21	5.5	5	19.06	51	246.5	920
22	7.4	5	20	11	170.3	120
mean					191.5	113.8

**Table 4D.2.4: 25-Yr Travel Time Comparison**

Element Number	60 minute		5 minute		25 YR comparison	
	25 YR		25 YR			
	Runoff (CFS)	Travel time (min)	Runoff (CFS)	Travel time (min)	runoff % increase (CFS)	travel time % change (min)
	1	13.3	2	45.38	1	241.2
2	2.6	2	9.08	5	249.2	150
3	5.5	6	17.94	6	226.2	0
4	35.9	6	111.62	5	210.9	-17
5	7.5	9	25.97	18	246.3	100
6	11.6	7	32.95	6	184.1	-14
7	14.8	10	35.81	7	142.0	-30
8	12.7	23	42.29	42	233.0	83
9	9	>1hr	31.2	>1HR	246.7	
10	46.8	>1hr	102.87	>1HR	119.8	
11	10.3	>1hr	35.49	>1HR	244.6	
12	55.3	5	128.96	5	133.2	0
13	96.1	4	233.51	3	143.0	-25
14	47.1	19	125.28	29	166.0	53
15	20	>1hr	62.72	>1HR	213.6	
16	15.9	5	50.13	>1HR	215.3	
17	25.9	4	58.69	8	126.6	100
<b>18 (outlet)</b>	<b>147.7</b>	<b>0</b>	<b>317.16</b>	<b>0</b>	<b>114.7</b>	<b>0</b>
19	130.3	1	294.3	1	125.9	0
20	0.4	10	1.26	18	215.0	80
21	6.4	5	22.31	>1HR	248.6	
22	8.6	4	21.1	8	145.3	100
mean					190.5	24.1

**Table 4D.2.5: 50-Yr Travel Time Comparison**

Element Number						
	60 minute		5 minute		50 YR comparison	
	50 YR		50 YR			
	Runoff (CFS)	Travel time (min)	Runoff (CFS)	Travel time (min)	runoff % increase (CFS)	travel time % change (min)
1	14.9	2	50.49	1	238.9	-50
2	2.9	6	10.09	5	247.9	-17
3	6.2	6	20.1	5	224.2	-17
4	40	6	122.67	5	206.7	-17
5	8.4	10	28.91	18	244.2	80
6	13	7	34.57	6	165.9	-14
7	15.8	9	39.31	7	148.8	-22
8	14.2	25	47.3	48	233.1	92
9	10	58	34.74	>1HR	247.4	
10	49.8	>1hr	112.97	>1HR	126.8	
11	11.5	>1hr	39.53	>1HR	243.7	
12	59.7	6	143.15	5	139.8	-17
13	105.3	3	257.34	3	144.4	0
14	51.7	20	140.36	33	171.5	65
15	22.3	>1hr	70.48	>1HR	216.1	
16	17.7	5	56.3	>1HR	218.1	
17	28.9	4	60.1	7	108.0	75
<b>18 (outlet)</b>	<b>162.8</b>	<b>0</b>	<b>347.6</b>	<b>0</b>	<b>113.5</b>	<b>0</b>
19	143.4	2	319.74	1	123.0	-50
20	0.4	12	1.4	19	250.0	58
21	7.2	5	24.84	>1HR	245.0	
22	9.6	4	21.96	8	128.8	100
mean					190.3	12.1

**Table 4D.2.6: 100-Yr Travel Time Comparison**

Element Number	60 minute		5 minute		100 YR comparison	
	100 YR		100 YR		runoff % increase (CFS)	travel time % change (min)
	Runoff (CFS)	Travel time (min)	Runoff (CFS)	Travel time (min)		
1	16.7	2	57.03	1	241.5	-50
2	3.3	7	11.39	4	245.2	-43
3	6.9	7	22.86	5	231.3	-29
4	45	5	136.8	5	204.0	0
5	9.4	9	32.69	19	247.8	111
6	14.6	7	36.66	6	151.1	-14
7	17	8	43.79	6	157.6	-25
8	16	25	53.71	39	235.7	56
9	11.3	UNSTABLE	39.27	>1HR	247.5	
10	53.5	UNSTABLE	125.82	>1HR	135.2	
11	12.9	>1hr	44.71	>1HR	246.6	
12	65	4	161.1	4	147.8	0
13	116.2	3	287.31	3	147.3	0
14	57.3	20	159.44	28	178.3	40
15	25.1	UNSTABLE	80.36	>1HR	220.2	
16	19.9	5	64.15	>1HR	222.4	
17	32.5	3	61.91	7	90.5	133
<b>18 (outlet)</b>	<b>181</b>	<b>0</b>	<b>384.46</b>	<b>0</b>	<b>112.4</b>	<b>0</b>
19	159.1	1	351.24	1	120.8	0
20	0.5	10	1.58	19	216.0	90
21	8.1	5	28.07	>1HR	246.5	
22	10.8	4	23.06	8	113.5	100
mean					<b>189.0</b>	<b>16.8</b>

**Appendix 4E:** Catchment K2 Travel Time Maps for Various Return Period Rainfall, using 5-Minute Precipitation and Overland Flow Elements

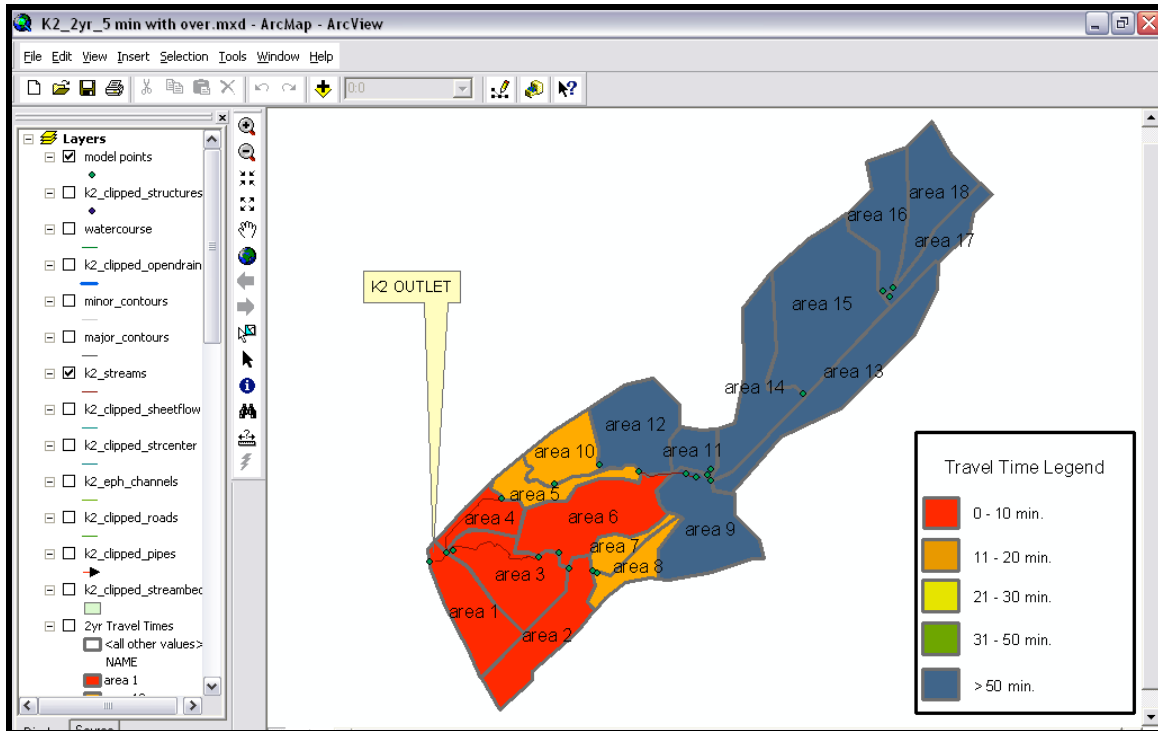


**Figure 4E.1:** Catchment K2 2-yr Return Period Travel Time Map including Overland Flow Elements.

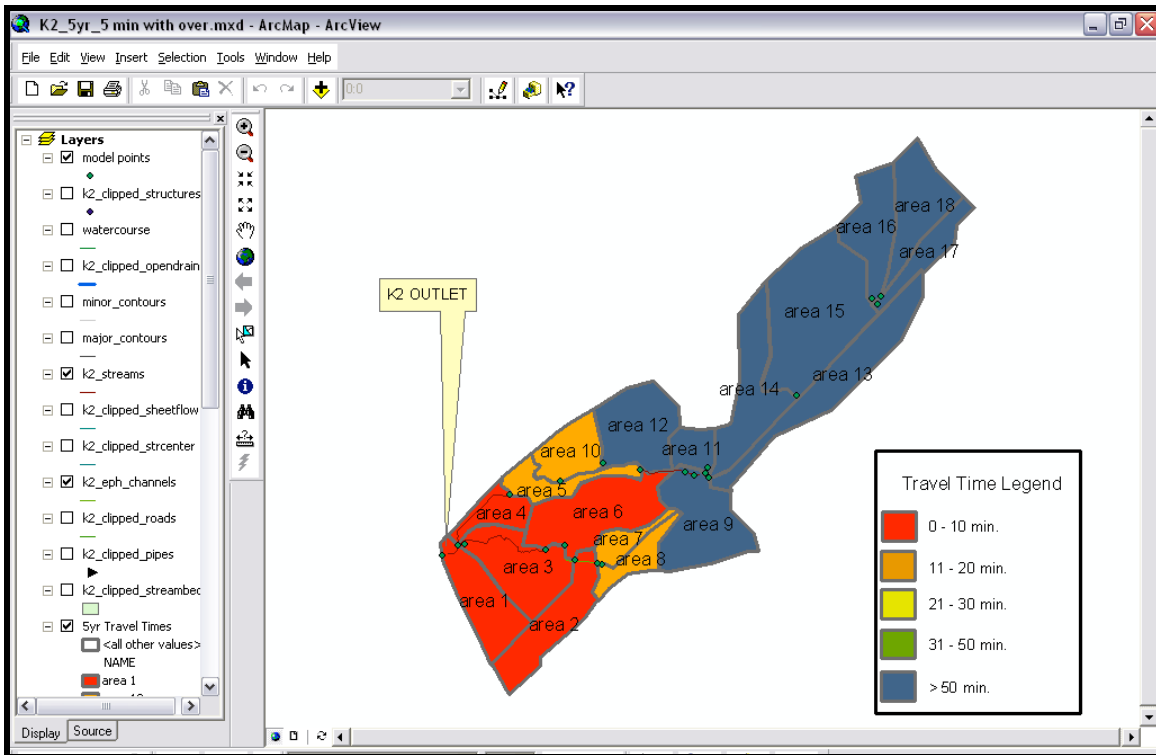


**Figure 4E.2: Catchment K2 5-yr Return Period Travel Time Map including Overland Flow Elements.**

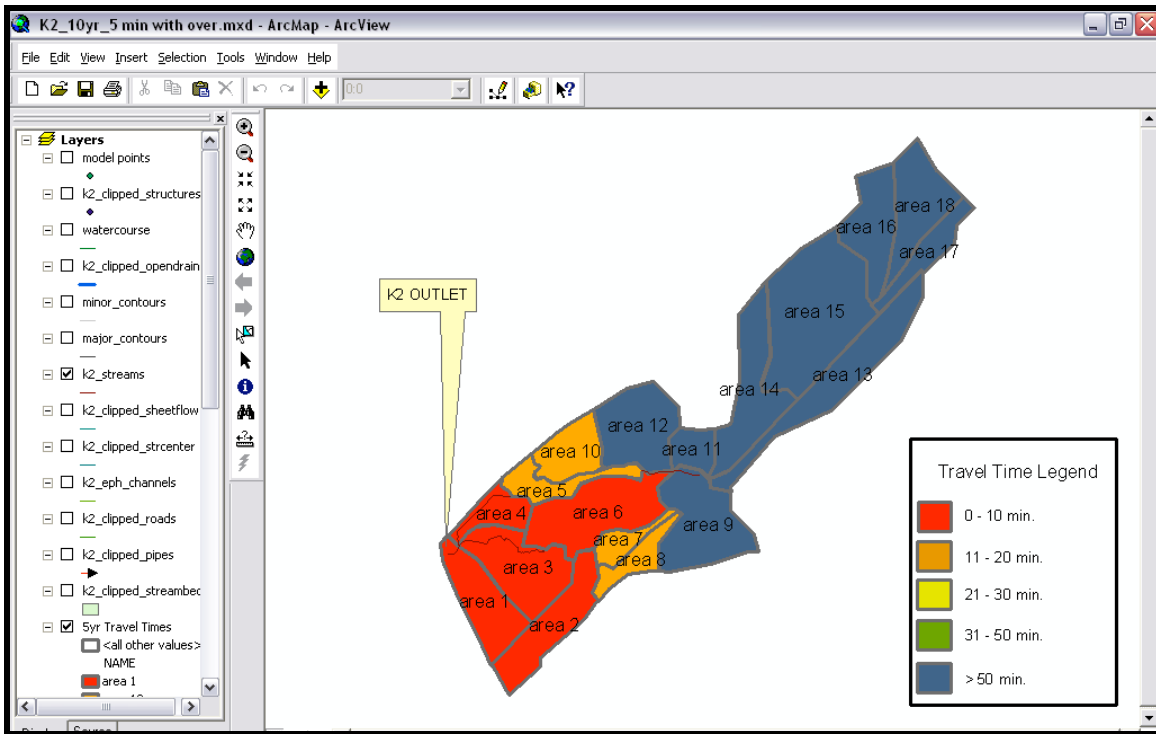


**Figure 4E.3: Catchment K2 10-yr Return Period Travel Time Map including Overland Flow Elements.**

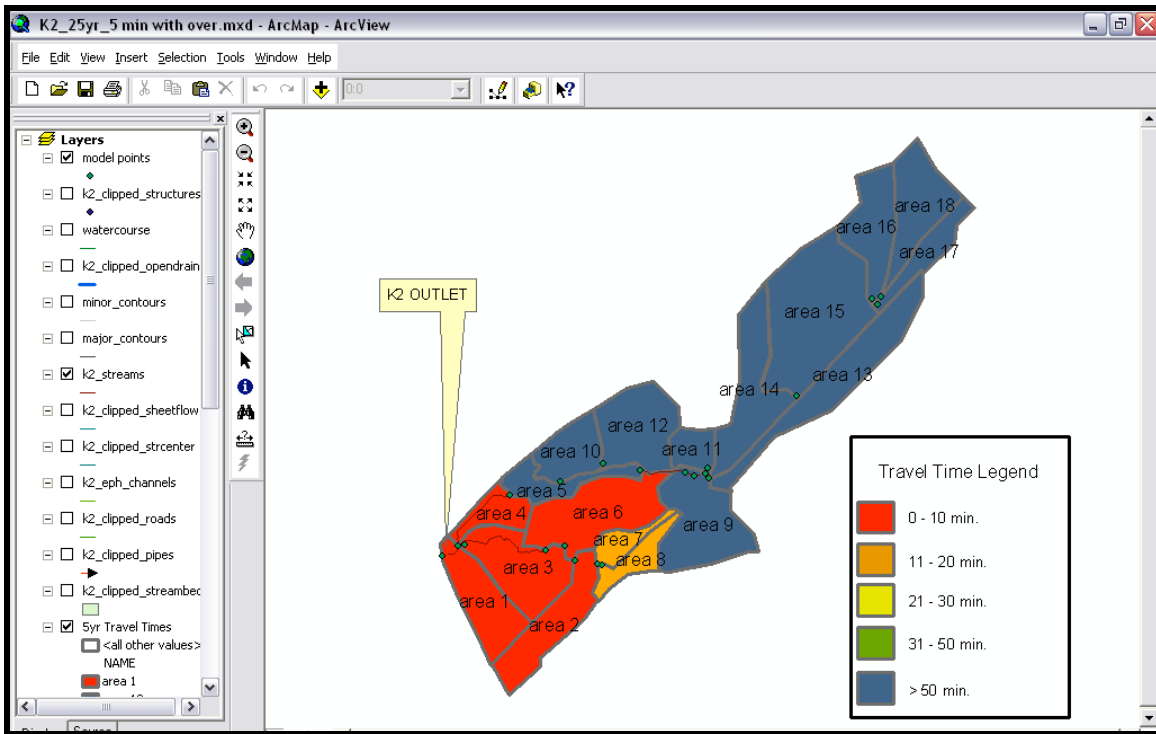


**Figure 4E.4: Catchment K2 25-yr Return Period Travel Time Map including Overland Flow Elements.**

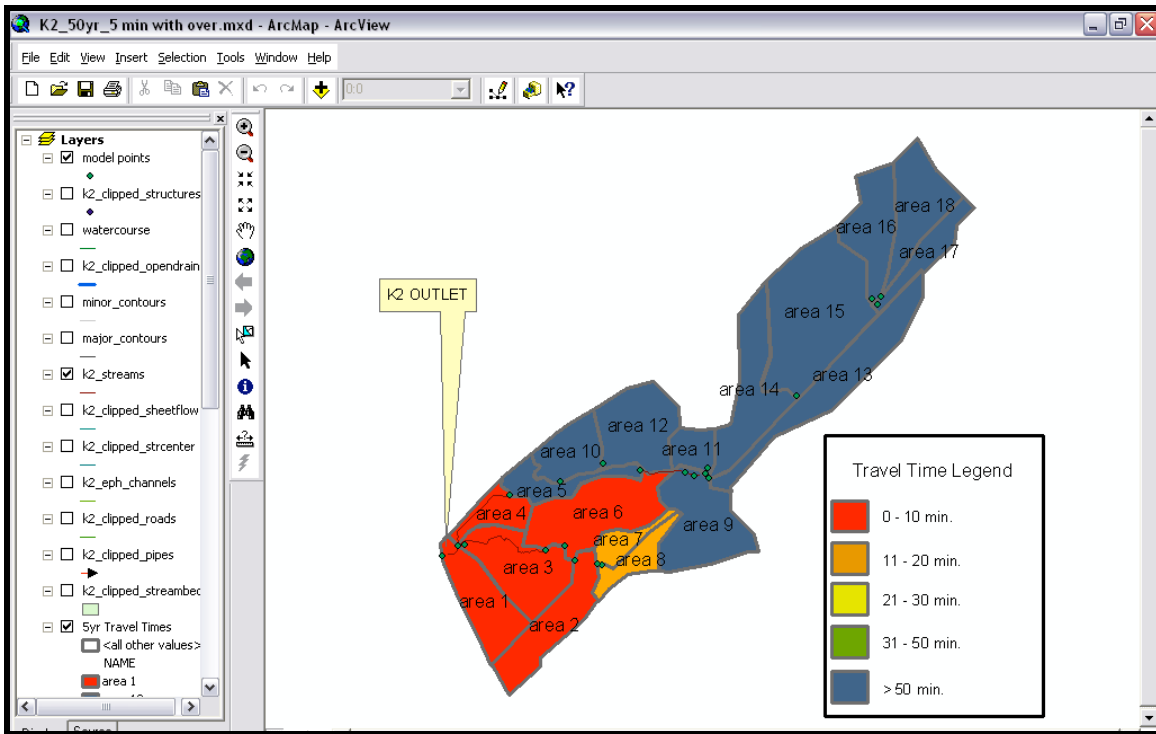


**Figure 4E.5: Catchment K2 50-yr Return Period Travel Time Map including Overland Flow Elements.**

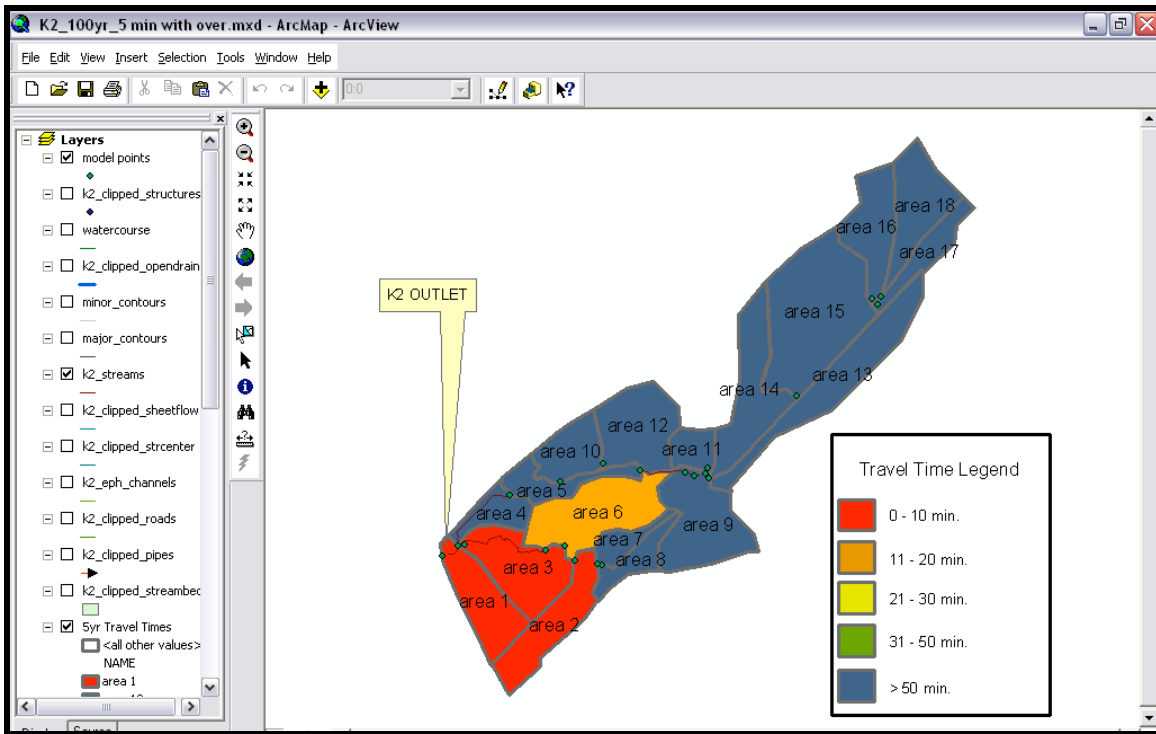


**Figure 4E.6: Catchment K2 100-yr Return Period Travel Time Map including Overland Flow Elements.**